EVALUATION OF THE GEOLOGIC RELATIONS AND SEISMOTECTONIC STABILITY OF THE YUCCA MOUNTAIN AREA NEVADA NUCLEAR WASTE SITE INVESTIGATIONS (NNWSI)

PROGRESS REPORT

SEPTEMBER 30, 1992

CENTER FOR NEOTECTONIC STUDIES
MACKAY SCHOOL OF MINES
UNIVERSITY OF NEVADA, RENO

INDEX TO YUCCA MOUNTAIN PROGRESS REPORT

OCTOBER 1, 1991 - SEPTEMBER 30, 1992

I. GENERAL TASK

Introduction and summary of activities conducted during the contract period

II. TASK 1: QUATERNARY TECTONICS

Summary of activities conducted during the contract period

Appendix A:

- Chemical Analyses of Rock Varnish Samples

Appendix B:

- Petrographic and Chemical Analyses of Volcanic Tephra

Appendix C:

- Paper and Field Guide Presented at Geological Society of Nevada, Symposium on Walk Lane

III. TASK 3: EVALUATION OF MINERAL RESOURCE POTENTIAL, CALDERA GEOLOGY, AND VOLCANO-TECTONIC FRAMEWORK AT AND NEAR YUCCA MOUNTAIN

Introduction and summary of activities conducted during the contract period

Appendix A:

- The initial gold contents of silicic volcanic rocks

Appendix B:

- Contrasting styles of epithermal precious-metal mineralization in the southwestern Nevada volcanic field, USA

IV. TASK 4: SEISMOLOGY

Summary of activities conducted during the contract period

Publications:

- *Seismicity in Nevada Apparently Triggered by the Landers, California, Earthquake, June 28, 1992*
- *Remote Seismicity Triggered by the M7.5 Landers, California, Earthquake of June 28, 1992*
- *Microearthquakes at Yucca Mountain, Nevada*

V. TASK 5: TECTONICS, NEOTECTONICS

Highlights and summary of activities conducted during the contract period

Appendix A:

- Abstracts and published papers

VI. TASK 8: BASINAL STUDIES

Report of investigations conducted during the contract period

Appendix A:

- Three core-to-rim analyses

Appendix B:

- Table of samples processed by Task 8

Appendix C:

- Table of sample processing in progress

Annual Progress Report—General Task
Prepared by C. H. Jones

1 October 1991 to 30 September 1992

Introduction

This report provides a summary of progress for the project "Evaluation of the Geologic Relations and Seismotectonic Stability of the Yucca Mountain Area, Nevada Nuclear Waste Site Investigation (NNWSI)." This progress report was preceded by the progress report for the year from 1 October 1990 to 30 September 1991. Initially the report will cover progress of the General Task, followed by sections describing progress of the other ongoing Tasks which are listed below.

Task 1 — Quaternary Tectonics
Task 3 — Mineral Deposits, Volcanic Geology
Task 4 — Seismology
Task 5 — Tectonics, Neotectonics
Task 8 — Basinal Studies

General Task
Staff

Steven G. Wesnousky, Project Director, Craig H. Jones, Research Associate, Ingrid Ramos and Gloria Sutherland, Secretaries.

The General task continued to coordinate project activities to meet general deadlines and responsibilities. The central office provided general secretarial support and network and computer support. Computer capabilities continued to expand. Dr. Wesnousky has also represented NWPO at a number of meetings with the NRC and other federal agencies during the year.

Technical Activities

Research activities conducted by the general task have focused on the tectonics of the Yucca Mountain region. Research conducted by Dr. Jones has focused on the seismological and tectonic framework of the entire lithosphere. Because Yucca Mountain lies near the boundary between two very different extensional regimes to the north and south, general tectonic study of both regions will improve understanding of the Yucca Mountain site.

The first project represents the completion of a project by Dr. Jones; work during the past year has centered about satisfying peer review for publication. In this experiment, seismometers were deployed in the high Sierra Nevada of southern California in 1988. Teleseisms and regional earthquake arrival times recorded by this network were used to examine the crustal and upper mantle structure beneath the southern Sierra. The results, presently in a manuscript in review, have proven quite controversial: While extension in the upper crust has accommodated over 250 km of motion in the Basin and Range, it appears from this work (when placed in context for the entire region) that the downward continuation of that deformation actually lies under the Sierra Nevada to the west. This deformation is inferred to have warmed and thinned the anti-buoyant mantle lithosphere, thus causing the Sierra Nevada to rise. Such a model has important implications in the Yucca Mountain area, because Death Valley's deformation lies only a few miles to the southwest. Understanding the lithosphere-scale tectonics of the region should improve the framework for systematically examining the Yucca Mountain site; this work complements the earlier study of Dr. Zhang, who described, without providing a tectonic explanation, the evolution of faulting in the Death Valley area through time.

The second project is something of an outgrowth of the first; Dr. Jones combined with other scientists representing other subdisciplines (Wernicke, Farmer, and Walker) to write a single paper that attempts to integrate geological, geochemical, and geophysical observation. This paper was completed during the past year and is in press in *Tectonophysics* at the present writing. Dr. Jones has been responsible for the geophysical study and the overall compilation and preparation of the manuscript. Although the paper contains considerable review, new work in the geophysical section explores the variation in the style of deformation through the Basin and Range by taking seismic velocity profiles of the crust that have been obtained in the past few years and converting them into density structures. Armed with the density of the crust, one can infer how much of the variation in elevation seen through the Basin and Range is due to variations in density in the crust; what remains is probably due to variations in the mantle. Results of this study that bear on Yucca Mountain directly are that to the north, extensional deformation in the mantle probably lies under the central part of the Basin and Range, while to the south, deformation in the upper mantle lies under the western flank of the Basin and Range. This implies that a major lithospheric boundary lies near the Yucca Mountain area; this boundary might be responsible for the diffuse band of seismicity that crosses the Basin and Range at this latitude. These results will be important when interpreting results from a 3-d velocity structure study discussed below. Some additional work might be started in the coming year to expand this analysis to the entire western U.S. and quantify the uncertainties in the techniques used will be quite useful in evaluating the inferences from this study.

A third project is a continuation of work undertaken at Caltech with Drs. Leslie Sonder (Dartmouth College) and Steven Salyards (New Mexico State University), which in turn was inspired by earlier work of Nelson and Jones (1987). Paleomagnetic samples have been gathered in Miocene sediments near Lake Mead in order to understand the mechanics that accompany the creation of "oroflexes," which are great bends in the earth's crust adjacent to large strike-slip faults. These bends are best understood through paleomagnetic work, which can constrain the exact amount of bending. Earlier work by Nelson and Jones documented the presence of an oroflex in the Las Vegas Range northwest of Las Vegas; that study lacked the spatial resolution to understand the mechanical underpinnings of the deformation and also could not constrain the age of deformation. The present study should solve both problems, for the young sediments in the Lake Mead area are well exposed and have not been as deformed as the sedimentary rocks in the Las Vegas Range. Although the study is still proceeding, data to date do clearly show that the oroflex does extend to the southeast and formed within the past 15-20 m.y.. This same structure or one analogous to it might extend into Yucca Mountain, where similar paleomagnetic rotations have been observed by USGS scientists over the past few years. Completion of this work should provide insight into structures that might be present in Yucca Mountain itself, including, possibly, the presence of large, subhorizontal decollements. Data collected in the past year have led to the presentation of this work at professional meetings and a manuscript is in preparation for submission early in 1993.

A fourth project conducted by Dr. Wesnousky and Dr. Jones investigates the physical parameters that control the partitioning of slip between a vertical fault and an adjacent dipping fault through the use of a simple model. The model was improved and expanded for use on fault systems within continents from models originally developed to understand analogous phenomena observed at plate boundaries. This model was initially applied to the San Andreas fault and it indicates that the slip rate along the San Andreas should vary as a function of the geometry of the adjacent dipping faults. It also provides some insights into the variation of physical characteristics of the faults that control the strength of the fault. A manuscript was published *Science*. Continuation of this work into the Basin and Range has begun and some initial results are to be presented at the fall meeting of the American Geophysical Union. Within the Basin and Range, several faults exhibit similar behavior: one large, vertical fault will tend to be strike-slip, while an adjacent fault might have oblique-slip on its dipping surface. Such fault systems include the Death Valley and Owens Valley fault systems. The latter fault system has been inferred to have slipped in different ways at different times in the past because of changes in the stress field in the Owens Valley area. We have found by extending our analysis to this area that this conclusion is unwarranted; this style of faulting is compatible with a single stress system. Implications from this work include evaluating the likely amount of variation in the stress field both in space and time; as such, it will have implications for evaluating the potential for changes in the stress regime and changes in the activity of faulting in the Yucca Mountain area.

A fifth project represents a collaboration of Dr. Jones with Dr. Steven Roecker (Rensselaer Polytechnic Institute) and Dr. Joan Gomberg (USGS Golden) on the seismic velocity structure of southern Nevada. During this year a new collection of arrival times were picked by a student of Roecker's with guidance from Gomberg. In the coming year this dataset will be used to determine a 3-dimensional velocity structure for southern Nevada. In addition, the Little Skull Mountain earthquake sequence from the summer of 1992 should provide additional constraints on the velocity structure in the immediate vicinity of Yucca Mountain. Dr. Jones assisted in deployment of portable seismometers from UNR after the mainshock and is beginning to gather data necessary for 3-d inversions from this earthquake sequence. Overall, the determination of the lateral variations in seismic velocity both improve the locations of earthquakes in the area and provide insight into lateral changes in earth structure reflecting subsurface geology.

Papers and preprints:

Jones, C. H., and S. G. Wesnousky, Variations in strength and slip rate along the San Andreas Fault system, *Science, 256,* 83-86, 1992.

Magistrale, H., H. Kanamori, and C. H. Jones, Forward and inverse three-dimensional P-wave velocity models of the southern California crust, *J. Geophys. Res., 97,* 14115-14135, 1992.

Jones, C. H., B. P. Wernicke, G. L. Farmer, J. D. Walker, D. S. Coleman, L. W. McKenna, and F. V. Perry, Variations across and along a major continental rift: An interdisciplinary study of the Basin and Range Province, western USA, *Tectonophysics* (part II of the Proceedings of the Geodynamics of Rifting Symposium held in Glion-sur-Montreux, Switzerland, 4-11 November 1990), *213*(?) in press, 1992.

Jones, C. H., H. Kanamori, and S. W. Roecker, Missing Roots and Mantle "Drips:" Regional P_n and Teleseismic Arrival Times in the Southern Sierra Nevada and Vicinity,

California, resubmitted to *J. Geophys. Res.*, August 1992; (in review).

Review and Meeting Activities

Date	Investigator	Meeting or Review
12-4-91	Wesnousky	Provided Review if NRC Staff technical position on investigations to identify fault displacement and seismic hazards at a geologic repository.
12-17-91	Wesnousky	Attended ACNW working group meeting in Bethesda, MD on concerns related to seismic and faulting investigations for a geologic repository
1-22-92	Wesnousky	Attended NWTRB meeting of the Panel on Structural Geology & Geoengineering in Irvine, CA.
12-28-92	Wesnousky	Provided detailed review of DOE study plan for effects of Local site Geology on Surface and Subsurface Motions (Study Plan 8.3.2.27.3.4)
3-1-92	Wesnousky	Provide NWPO a review of the DOE sponsored 'peer-reviewed' reports regarding the hypothesis that hydrologic and tectonic processes are coupled and responsible for carbonate deposits in and around Yucca Mountain
4-2-92	Wesnousky	Present summary of ongoing NWPO-supported Seismology and Neotectonic studies at Yucca Mountain to the Nevada Commission on Nuclear Projects- in Las Vegas
9-14 to 19-92	Wesnousky	Attend meetings in Las Vegas sponsored by the NWTRB and NRC concerning issues and progress in studies on Volcanism and Neotectonics at Yucca Mountain

PROGRESS REPORT

Task 1 Quaternary Tectonics

1 October 1991 to 30 September 1992

John W. Bell
Principal Investigator

Craig M. dePolo
Co-Investigator

SUMMARY OF ACTIVITIES CONDUCTED DURING THE CONTRACT PERIOD

During the contract period, the following activities were conducted by Task 1:

* J.W. Bell reviewed the final draft of the Nuclear Regulatory Commission Staff Technical Position (STP) on "The Identification of Fault Displacement and Seismic Hazards at a Geologic Repository" and submitted a two-page report to the Nevada Nuclear Waste Project Office.

* J.W. Bell and C.M. dePolo reviewed the Department of Energy Study Plan 8.3.1.17.3.1 "Relevant Earthquake Sources" and submitted a five-page report to the Nevada Nuclear Waste Project Office.

* J.W. Bell reviewed the Department of Energy "Outline for Topical Report on Erosion Rates at Yucca Mountain Geologic Setting: Methodology and Results" and submitted a three-page report to the Nevada Nuclear Waste Project Office.

* J.W. Bell participated in a three-day field review related to the Technical Review Board review of the volcanic hazard issue and the DOE/NRC site visit to Midway Valley.

* J.W. Bell and F.F. Peterson revised the manuscript "Late Quaternary Geomorphology and Soils in Crater Flat, Next to Yucca Mountain, Southern Nevada: A Reinterpretation" for resubmission to *Quaternary Research*.

* A.R. Ramelli completed the manuscript "Quaternary Fault Interconnection and Possible Distributive Behavior at Yucca Mountain, Southern Nevada" and submitted it to *Geology*.

* R. I. Dorn of Arizona State University provided a new rock varnish data set for previously analyzed Crater Flat samples and performed alkalinity analyses of rock varnish microlaminations on Crater Flat samples.

* A. Sarna-Wojcicki of the U.S. Geological Survey submitted the results of petrographic and microprobe chemical analyses for volcanic tephra samples from the Cedar Mountain area.

* J.W. Bell presented the paper "Tephras and Late Holocene Alluvial-fan Deposition in West-central Nevada: Is There a Connection?" at the 1991 Annual Meeting of the Geological Society of America in San Diego.

* C.M. dePolo presented the paper "The 1932 Cedar Mountain Earthquake: An Example of Active Tectonism in the Walker Lane" and led a one-day field trip at a symposium on the Structure, Tectonics, and Mineralization of the Walker Lane sponsored by the Geological Society of Nevada.

* C.M. dePolo investigated the surface faulting associated with the June 28, 1992 Landers earthquake (M7.4) in southern California.

* The geologic map of the Crater Flat 7½-minute quadrangle was completed by UNLV and NBMG investigators (J. Faulds, E.I. Smith, A.R. Ramelli, and J.W. Bell). The lower portion of the adjoining quadrangle to the north (East of Beatty 7½-minute) will be added and the composite map published by the Nevada Bureau of Mines and Geology.

* The bedrock geology of the Mina 7½-minute quadrangle was received from John Oldow of Rice University. The surficial geology (already completed) will be added by J.W. Bell and the map will be published by the Nevada Bureau of Mines and Geology.

* The causative fault(s) associated with the June 29, 1992 Little Skull Mountain earthquake (M5.6) was analyzed by J.W. Bell and C.M. dePolo. Based on focal mechanisms, either the Mine Mountain or Cane Springs fault systems are likely sources for the earthquake, and a low-sun-angle aerial photographic mission over the epicentral area was planned; the photography will be flown during the early part of the next contract period.

* J.W. Bell reviewed trenches excavated by M. Machette of the U.S. Geological Survey across the 1915 Pleasant Valley earthquake (M7.6) fault zone, including the evidence for temporal clustering on the fault zone.

* J.W. Bell led a one-day field trip for about 15 DOE and Woodward-Clyde personnel to trenches excavated across the Genoa fault in northern Nevada.

TECHNICAL REPORT

Crater Flat Allostratigraphy

Refinement and revision of Crater Flat Quaternary stratigraphy continued during the contract period and consisted of several activities: revision of the rock varnish (RV) cation-leaching curve; sample comparison of RV manganese:iron microlaminations; correlation of Crater Flat allostratigraphic units with regional chronologies.

Rock Varnish Chemistry Data

A complete compilation of all previous RV analytical data was prepared by Dr. Ronald I. Dorn for all Crater Flat samples and is attached as Appendix A. Recent criticism of Dr. Dorn's Crater Flat data by Bierman and Gillespie (1991) is addressed in our study in two ways. First, the Bierman and Gillespie (1991) conclusion that the U.C. Davis cation-ratio (CR) data set (analyses of Dorn's samples) is flawed has no merit based on both analytical procedure and on duplicate data sets. Cahill (1992) states that the Bierman and Gillespie (1991) data set was produced on entirely different laboratory equipment than Dorn's data, thus making the Bierman and Gillespie (1991) conclusions irrelevant. Second, only some of the early Crater Flat samples were analyzed by the PIXE system, and all samples were additionally analyzed by wavelength dispersive microprobe (Dorn, 1992). In order to address the Bierman and Gillespie (1992) comment that Dr. Dorn has not published all specific chemical analysis data, a complete compilation of this data is provided here (Table 1; Appendix A).

Rock Varnish Cation-leaching Curve

The cation-leaching curve for Crater Flat (Figure 1) has evolved since Dorn (1988a); revised calibration points have been added by Dr. Dorn during this contract period. The Lathrop Wells basalt flow K-Ar calibration point was dropped because recent studies (e.g., Wells *et al.*, 1990a; Zreda *et al.*, 1991; Wells *et al.*, 1992; Zreda *et al.*, in press) indicate the history of the eruptive center still needs to be resolved. The CR of $<2\mu m$ dust was viewed as unnecessary, because a ^{14}C age of $\sim$1300 yr BP is available for calibrating all but the youngest site; CFP-41 with the youngest CR is $<<$1300 yr BP, with a provisional age of $\sim 300\pm200$ yr BP based on an extension of the curve. We also use the most recent K-Ar dating results for basalt flows in Crater Flat from Smith *et al.*(1990). We note that CR's for the Early Black Cone, Yucca, and Solitario allostratigraphic units fall between the ^{14}C and K-Ar calibration points. The CR's used as calibration points in Table 1 are averages (with 1 standard deviation) of four or more individual measurements. The CR ages reported for each site in Table 1 are averages (with 1 standard deviation) of four to fifteen separate CR ages. (The complete PIXE and microprobe analyses data sets are attached as Appendix A).

Table 1. Results of Rock Varnish Analyses

Allostratigraphic Unit (This Study)	Sample	^{14}C AMS Date (yr B.P.; lab #)	K+Ca/Ti (Avg ±1σ)	Calculated Cation Ratio Age (yrs B.P.)
Crater Flat	CFP-41	–	9.17±0.25	300±200
	JWB-36	1,320±70 (ETH 5264)	7.94±0.17	1,100±400
Little Cones	CFP-2	6,645±245 (ETH 3197)	6.47±0.13	
	JWB-38	8,425±70 (ETH 5268)	6.37±0.13	
	CFP-26	10,180±270 (ETH 3187)	6.13±0.09	
	JWB-41	11,135±105 (ETH 5270)	5.99±0.13	
Late Black Cone	CFP-33	17,280±370 (ETH 3191)	5.75±0.06	
	CFP-31	–	5.67±0.15	19,000±4,000
	JWB-39	19,660±240 (ETH 4483)	5.68±0.15	
	CFP-27	25,700±360 (ETH 3188)	5.42±0.12	
	CFP-35	26,970±375 (ETH 3192)	5.34±0.15	
	CFP-36	28,920±400 (ETH 3190)	5.32±0.07	
	CFP-32	30,320±460 (ETH 3189)	5.14±0.07	
Early Black Cone	CFP-37	–	3.98±0.19	159,000±38,000
	CFP-29	>40,120 (ETH 5259)	3.98±0.32	168,000±75,000
	JWB-42	–	3.90±0.11	176,000±25,000
	JWB-20	–	3.79±0.11	200,000±29,000
Yucca	CFP-39	–	3.29±0.11	375,000±53,000
	CFP-38	–	3.29±0.11	373,000±50,000
Solitario	JWB-43	–	3.17±0.10	433,000±54,000
	CFP-40	–	2.95±0.10	572,000±66,000
	JWB-40	–	2.84±0.09	660,000±71,000
Little Cones basalt	Smith *et al.*, 1990	770,000±40,000	2.63±0.08	
Red Cone basalt	•	950,000±80,000	2.62±0.12	
Black Cone basalt	•	1,090,000±120,000	2.53±0.06	

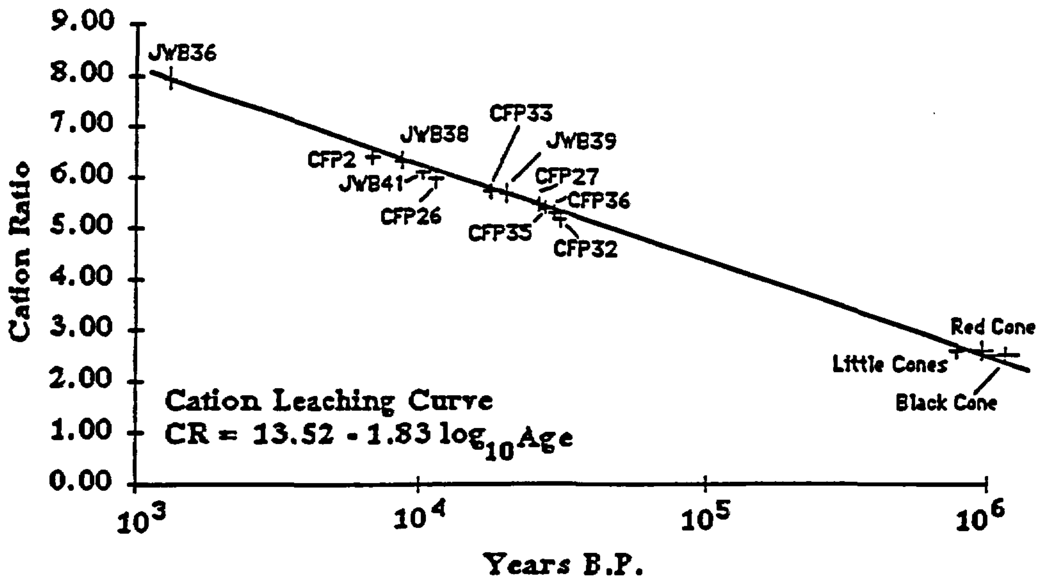

Figure 1. Rock varnish cation leaching curve for Crater Flat. Calibration is based on ^{14}C rock varnish dates on allostratigraphic surfaces and on K/Ar dates on basaltic cones (Smith *et al.*, 1990).

Microlamination Alkalinity Data

During the contract period, Dr. Dorn provided new RV alkalinity data that support correlation of samples and corroborate previously estimated numerical ages. Manganese:iron ratios on microlaminations are indicators of alkalinity fluctuations during the late Quaternary (Dorn, 1988b, 1990; Jones, 1991). The sequence of microlaminations observed in Crater Flat samples is consistent with other evidence when evenly layered subaerial varnishes are used (*cf.*, Dorn, 1990; Krinsley *et al.*, 1990). Selected Crater Flat samples were examined by wavelength dispersive microprobe, and several trends are evident on Figure 2. Younger varnishes have fewer Mn:Fe layers than older varnishes. Crater Flat and Little Cones varnishes are only Mn-poor, reflecting a period of enhanced alkalinity (Jones, 1991) during the Holocene. Late Black Cone varnishes show a basal layer of reduced alkalinity, probably corresponding with a more moist late Pleistocene period in the Nevada Test Site area (Spaulding, 1985; Claassen, 1986). Early Black Cone, Yucca, and Solitario varnishes show progressively more complex sequences.

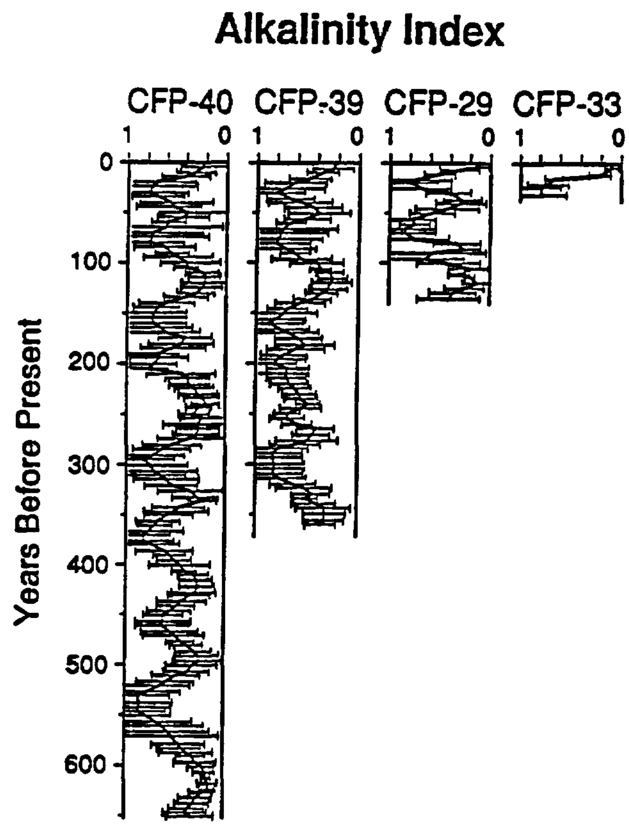

Figure 2. Averaged electron microprobe analyses (wavelength dispersive mode) of Mn:Fe microlaminations on the different Crater Flat stratigraphic units. As in Dorn (1990) the alkalinity index represents normalized Mn:Fe values. Zero is the lowest ratio (highest alkalinity) and 1 is the highest ratio (lowest alkalinity). Years before present (in 10^3) is derived by normalizing depth to the ^{14}C or cation ratio age. Alkalinity index values were regressed for every 5,000 years. The central line indicates the average alkalinity index values of 20 transects across layered varnishes from five different rocks, and bars represent 2 standard deviations.

Regional Correlation of Quaternary Stratigraphic Units

Similar Quaternary stratigraphic sequences have been described in the southern Nevada, Colorado River, Death Valley, and Mojave Desert regions. Although the Crater Flat units are more limited in extent and restricted to a single piedmont, a correlation of these sequences based on stratigraphic order and similarities in reported distinguishing characteristics, such as geomorphic character, soils, and estimated numerical age (Table 2), provides supporting evidence for the concept of regional climatic control of arid alluvial deposition (Bull, 1991) and an additional test of the Hoover *et al.* (1981) chronology.

TABLE 2. Comparison of Crater Flat Alluvial Chronology With Other Chronologies in the Region (Listed ages are ka).

Crater Flat (this study)	Lower Colorado River (Bull,1991)	Las Vegas and Indian Springs Valleys (Quade, 1986; Quade and Pratt, 1989)	S. Death Valley (Dorn, 1988b)	East-central Mojave (Wells *et al.*, 1990b)
Modern 0	Q4b 0	Modern 0	Modern 0	Modern (Qf9) 0
Crater Flat <.4->1.5	Q4a 0.1-2 Q3c 2-4 Q3b 4-8	Unit G 0.4.0 Unit F 4.0-8.0	Q3b3 0.5-2.5 Q3b2 2.0-4.5	Qf8 <0.3->0.7 Qf6,7 2-8
Little Cones 7-11	Q3a 8-12	Unit E 8.6-14.0	Q3b1 6-11	Qf5 8-15
Late Black Cone 17-30	Q2c 12-70	Unit D 15-30	Q3a 13-50	Qf4 <34->45
Early Black Cone 130-190	Q2b 70-200	Unit C >30 Unit B >40	Q2b 110-130 Q2a 140-190	Qf3 >47->130 Qf2 <160->320
Yucca >360-370	Q2a 400-740	Unit A	Q1b 400-650	
Solitario >450->740	Q1 >1200	Unit A	Q1 >650->800	Qf1 <3800

Most striking in this regional correlation is the evidence for widespread alluviation in the southern Basin and Range during the late Wisconsin pluvial (interstadial) and during the transition from the late Wisconsin maximum pluvial to the arid Holocene-- a concept discussed in detail by Bull (1991). Our Late Black Cone unit in Crater Flat is similar in stratigraphic order and soil morphology to unit Q2c (12-70 ka) of Bull (1991) in the lower Colorado River region; in both cases, the units contain the youngest well-developed Bt (argillic) and Bk (stage II-III) horizons in the stratigraphic section, a characteristic indicative of development under the more moist conditions of the late Wisconsin pluvial period (Nettleton *et al.*, 1975). We note that the Hoover *et al.* (1981) chronology *does not include* a similar late Wisconsin unit.

Cedar Mountain Allostratigraphy

As discussed in previous reports (Bell *et al.*, 1990, 1991), allostratigraphic relations in the 1932 Cedar Mountain earthquake area consist of seven units (Fig. 3). Studies conducted during this contract period included the refinement of the numerical ages of these units based on chemical microprobe analyses of 16 volcanic ashes and on 15 radiocarbon dates collected during the period. The results of the microprobe and radiocarbon analyses (Tables 3,4) indicate that additional age constraints can be placed both on recency and recurrence of faulting associated with the Cedar Mountain and adjacent fault zones.

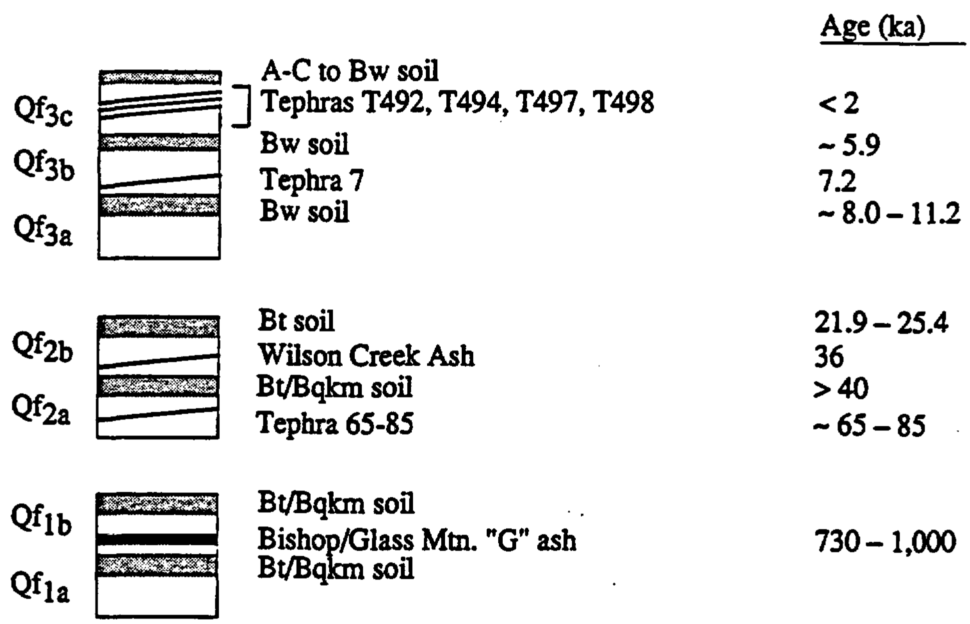

Figure 3. Cedar Mountain area allostratigraphy showing units, soil stratigraphic relations, tephras, and estimated numerical ages.

Volcanic ash analyses

The sixteen volcanic ash samples were submitted to Andrei Sarna-Wojcicki of the U.S. Geological Survey in December 1990, and the written report containing the analytical results and identifications were received in June 1992 (Appendix B). Three sets of Mono Craters ashes are identified here on the basis of glass shard chemistry: a Holocene set, a latest Pleistocene set, and an older Pleistocene set. Positive identification and differentiation of a number of the Holocene

Table 3. Identification and age of tephras from the Cedar Mountain and related areas; results from report of Andrei Sarna-Wojcicki (Appendix B).

Ash sample	Unit	Best Age Estimate (yrs)	Remarks
BS-1	Qf3c	1950±110, or 890±40	Similar to BS-9, -11, -12, -16
BS-2	Qf3c	~900, or 1950±110	Very similar to BS-7, -11, -12
BS-3	Qf2a	60,000-100,000	Previously reported as 65-85 ka
BS-4	Qf3c	1000-2000	Similar to BS-5
BS-5	Qf3c	1780-1960, possibly 7200	Similar to BS-1
BS-6	Qf2b	36,000	Wilson Creek Bed 19
BS-7	Qf3c	900 or 1780	Similar to BS-1, -5
BS-9	Qf3b	7200	Good match with Mono Lake ash
BS-11	Qf3c	900-3750	BS-11 through BS-16 all similar
BS-12	Qf3c	900-3750	"
BS-13	Qf3c	900-3750	"
BS-14	Qf3c	900-3750	"
BS-15	Qf3c	900-3750	"
BS-16	Qf3c	900-3750	"
BS-16	Qf3c	900-3750	"
BS-17	Qf2b	36,000	Wilson Creek Bed 19
Wassuk 1	Qfy	900-3750	Similar to BS-11

Table 4. Cedar Mountain Area ^{14}C Results

Sample	Date (yrs)	Lab #	Stratigraphic position
BS-1	995±110	GX-17250	6 cm below ash BS-23
BS-2	535±150	GX-17251	6 cm above ash BS-23
BS-3	1260±145	GX-17252	Disturbed zone
BS-4	435±110	GX-17253	30 cm above ash BS-25
BS-5	790±105	GX-17254	6 cm above ash BS-25
BS-6	1025±65	GX-17255	6 cm below ash BS-25
BS-7	1110±110	GX-17256	6 cm above ash BS-24
BS-8	1550±110	GX-17257	15 cm below ash BS-24
BS-9	1605±120	GX-17566	Immediately below ash BS-2
WR-3	Modern	GX-17568	
WR-4	685±135	GX-18127	Immediately below ash WR-6
WR-5	Modern	GX-18128	
WR-6	1230±125	GX-18129	60 cm below ash WR-7
WR-7	440±130	GX-18130	1 m above ash WR-7
11-Mile-1	2585±165	GX-17567	Av below Turupah Flat ash

ashes are problematic because of the close similarity in glass shard chemistry and variable degrees of hydration. Nevertheless, general groupings of the Holocene tephras are possible.

The Holocene age tephras can be divided into those of mid-Holocene (~7200 yrs) and late Holocene age (900-3750 yrs) based on correlation with other dated tephras in the western U.S.

(Sarna-Wojcicki *et al.*, 1988). In each case, however, several previously dated Mono Craters ashes are similar enough in composition to result in more than one possible correlation and age. This is large part due to the multiple eruptive sequences at Mono Craters all of which had generally similar glass chemistry. The late Holocene set, in particular, has significant uncertainties not resolved by the chemical comparisons. Many of these ashes are similar in composition to both the mid- and late Holocene Mono Craters sets.

Previous measurements of refractive indices of these ashes (Bell *et al.*, 1991) indicates that seven of the ashes analyzed here have refractive indices similar to that of the Turupah Flat ash (1.5-1.6 ka) of Davis (1978): BS-1, -4, -5, -11, -13, -15, -16. Bracketing radiocarbon ages at the Weber Dam locale of Davis (1978) were listed in previous reports (Bell *et al.*, 1991): 1455$\pm$140 and 1550$\pm$130 yrs. The age estimates for these samples in Table 3 are thus consistent with correlation to the Turupah Flat ash. In addition, a radiocarbon date of 1605$\pm$120 yrs was obtained from charcoal immediately beneath ash BS-2, an age also consistent with Sarna-Wojcicki's estimate of 900-1950 yrs.

Since submission of these original 16 samples, an additional 13 tephras from the Cedar Mountain area and 7 samples from the Walker Lake area have been collected. Although these have not been analyzed for glass chemistry, many have been examined for refractive index and glass morphology properties, and several have been dated by radiocarbon (Table 4). The ^{14}C results suggest that most, if not all, of these additional tephras are similar in age to those discussed above. During the next contract period, a more comprehensive analysis of trace element chemistry will be undertaken utilizing xray fluorescence (XRF) in order to develop more positive evidence for differentiations and correlations.

Two older, pre-Holocene tephras can be positively identified in the Cedar Mountain area. Samples BS-6 and -17 are chemically similar to the Wilson Creek Beds 16, 17 and 19, with the closest match being bed 19 which is about 36 ka old (Benson *et al.*, 1990). This ash is present in unit Qf2b in the Cedar Mountain region (Fig. 3), and it is overlain by geomorphic surfaces which have yielded ^{14}C AMS rock varnish ages ranging between about 21-25 ka (Bell *et al.*, 1991). An older Pleistocene tephra is present within Qf2a deposits (Fig. 3) that is correlative with an unnamed Mono Craters ash found in the Mono and Walker Lake areas (Sarna-Wojcicki *et al.*, 1988). This ash is on the order of 60-100 ka based on extrapolated sedimentation rates; it was previously estimated to be on the order of 65-85 ka (Sarna-Wojcicki, verbal communication, 1988).

Radiocarbon analyses

Fifteen samples were submitted for ^{14}C analysis during the contract period, and the results are listed in Table 4. Nine of the samples were from the immediate Cedar Mountain region and six of the samples were from outcrops of volcanic ash in the Walker Lake and Dixie Valley areas. The latter ashes are likely correlative with some or all of the Cedar Mountain ashes and provide additional constraints on the Cedar Mountain allostratigraphy. All of the samples either closely underlie or overlie a tephra, and thus provide tight constraints on tephra ages. All of the ages are latest Holocene, consistent with the results of Sarna-Wojcicki discussed above.

Refined ages of allostratigraphic units

Figure 3 lists the revised ages of the previously defined allostratigraphic units in the Cedar Mountain region; revisions are based on incorporation of tephra analyses conducted during this contract period. The principal differences in these refined ages compared to those reported in Bell *et al.* (1991) are related to the occurrence of the sequence of late Holocene tephras in unit Qf3c, the unnamed mid-Holocene 7.2 ka tephra in unit Qf3b, and the Wilson Creek Bed 19 (36 ka) in unit Qf2b. Of particular importance is the observation that the independently derived tephra ages are very consistent with the rock varnish ages estimated for the geomorphic surfaces of the same units. For example, a series of ^{14}C AMS varnish dates from four Qf2b surfaces range in age from 21.9-25.4 ka, ages which are younger (as expected) than the underlying volcanic ash. Additional rock varnish dating during the next contract period will provide further verification of these age relationships and the rock varnish dating procedure.

1932 Cedar Mountain Earthquake

Research continued on the 1932 Cedar Mountain earthquake, the principal relative comparison earthquake for the Yucca Mountain site. A surface rupture map was completed at a scale of 1:24,000, seismicity of the Cedar Mountain region was examined, a new kinematic model for the earthquake is being developed, surface rupturing from a large strike-slip earthquake in California (1992 Landers Earthquake, M7.5) was examined for similarities with the ground rupture associated with the Cedar Mountain event, and a working model for earthquakes along the Walker Lane was developed in light of these two earthquakes.

Surface rupture studies

A new surface rupture map has been completed and digitized (Fig. 4). This effort consisted of enlarging surface rupture maps from Gianella and Callaghan (1934) to 1:24,000 scale and transferring them to the topographic maps. New ruptures mapped by dePolo were transferred from various scale aerial photographs to these maps as well. The result gives us a better picture of the actual geometry and location of the surface breaks. This in turn has allowed a better estimate of the cross-strike width of faulting and emphasizes the northerly trends of surface ruptures in northern Monte Cristo and southern Stewart Valleys. This latter point has strongly influenced the formation of a new kinematic model for the southern part of this event.

Gianella's and Callaghan's field notes have been scrutinized as part of this process as well.

There are surface breaks mentioned in these notes that never made it to their final published maps, some which have important tectonic significance. For example, ruptures are reported in Gianella's notes just north of Stewart Springs (eastern Stewart Valley on the flank of Cedar Mountain) and through the springs itself. The rupture through the springs extends distinctly beyond the springs, suggesting that it was indeed a tectonic surface rupture, and not just a liquefaction or other effect of saturated ground. This becomes even more significant when considered along with a rupture mentioned in a letter from Gianella the Mr. Spencer (who I believe lived in the town of Gilbert in southern Monte Cristo Valley at the time), dated January 13, 1933. This paragraph is so significant that we reproduce it in its entirety here:

> "I learned today that Norman Annette found a crack south of Stewart Springs. He went up a wash about a mile or so beyond the Simon road and said that he traced it to within half a mile of the springs while the man with him, who owns a prospect out there, traced it in the other direction for a distance of a mile. This runs nearly N-S and may be a continuation of the ones we found on the Simon Road."

The Simon road is roughly 3 1/4 miles south of Stewart Springs. The breaks mentioned in this letter never made the map (with exception of the small break in the Simon road itself. This opens the possibility that there was intermittent, but semicontinuous rupture from Gianella and Callaghan's rupture numbers "17" and "18", through rupture "16", near rupture "13" and possibly beyond to the north. This will become an important consideration for the kinematic modeling.

Unmapped ruptures are now suspected to have occurred south of Gianella and Callaghan's rupture number "20" and north of new strike-slip breaks mapped during this project. A field trip is planned to investigate this area for ground disturbance. If breaks are found, this will extend the main surface rupture zone in Monte Cristo Valley to the north. At this point in their field work, Gianella and Callaghan were overwhelmed with surface breaks and were only noting those that crossed the roads, and were not walking them out to any extent.

Unfortunately, neither original photographs or originally sketched maps have been recovered from Gianella's or Callaghan's archives. This is a bit surprising. Sketch maps from the event must have existed, or it would have been hard to produce the maps presented in their published papers, unless they simply "faked" the details. The details are so realistic looking, however, that this is unlikely the case. Perhaps a deeper dig into the archives is warranted. More photographs were taken than are presented in their publications according to their notes.

Seismicity

After the surface ruptures were digitized, Diane dePolo of the University of Nevada, Reno Seismological Laboratory searched the UNR catalog for seismicity surrounding the breaks (Figs. 5, 6). The towns of Gabbs, Luning, and Mina were added for reference. Two plots are shown

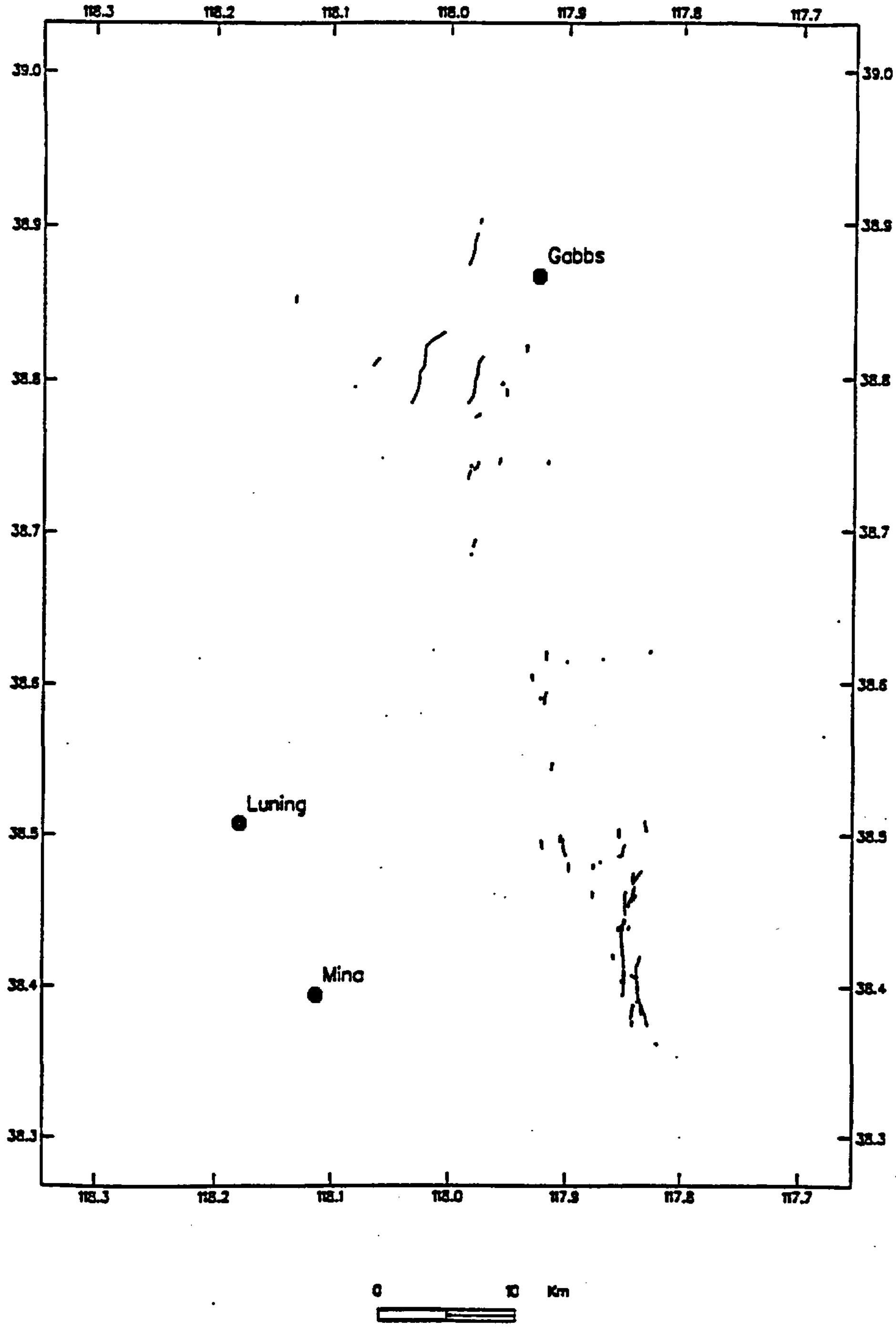

Figure 4. Digitized surface ruptures associated with the 1932 Cedar Mountain earthquake.

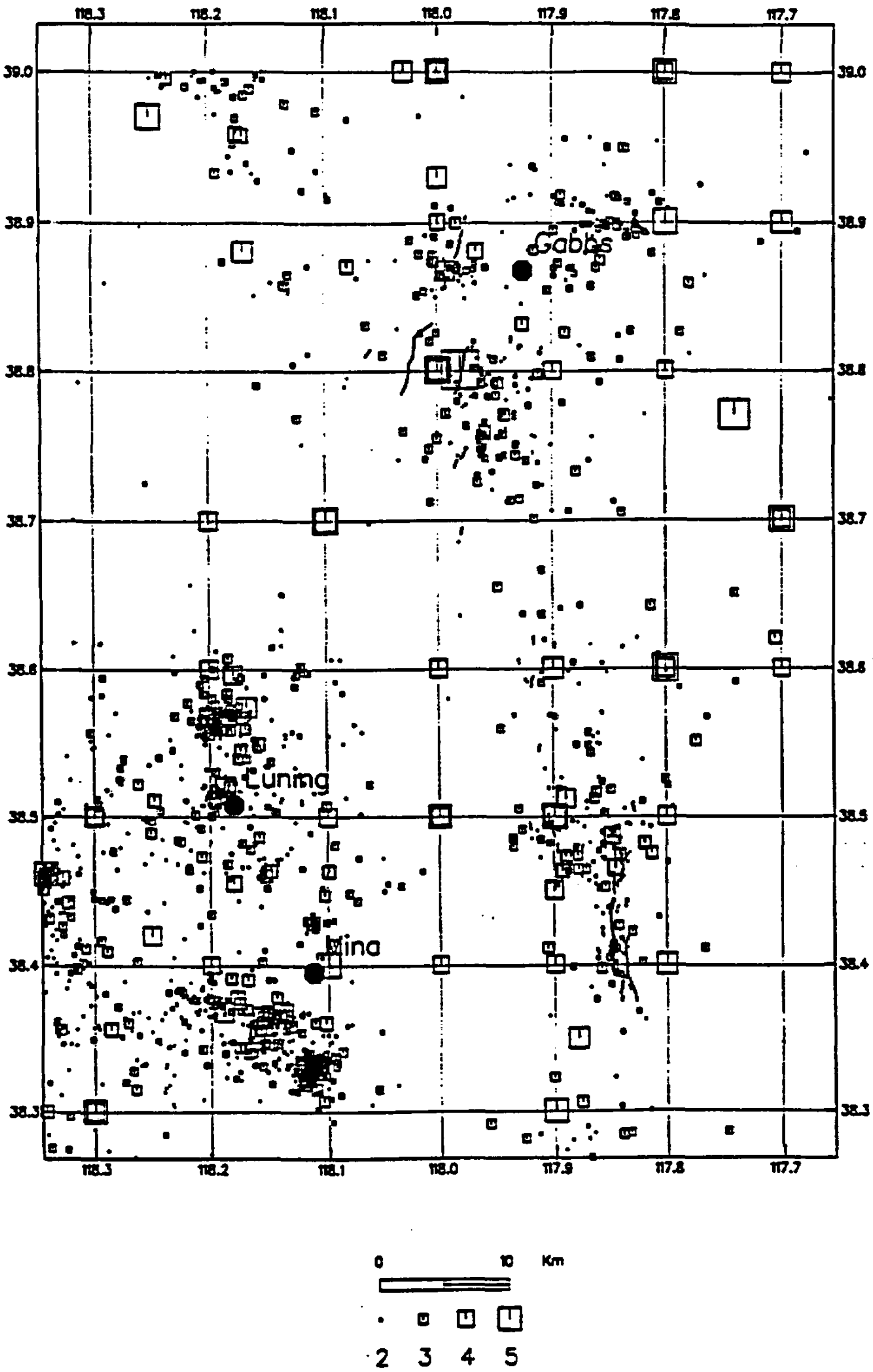

Figure 5. Seismicity catalogued in the 1932 Cedar Mountain earthquake area by the UNR Seismological Laboratory for the period 1932-June 1992. Surface ruptures are shown on the base map.

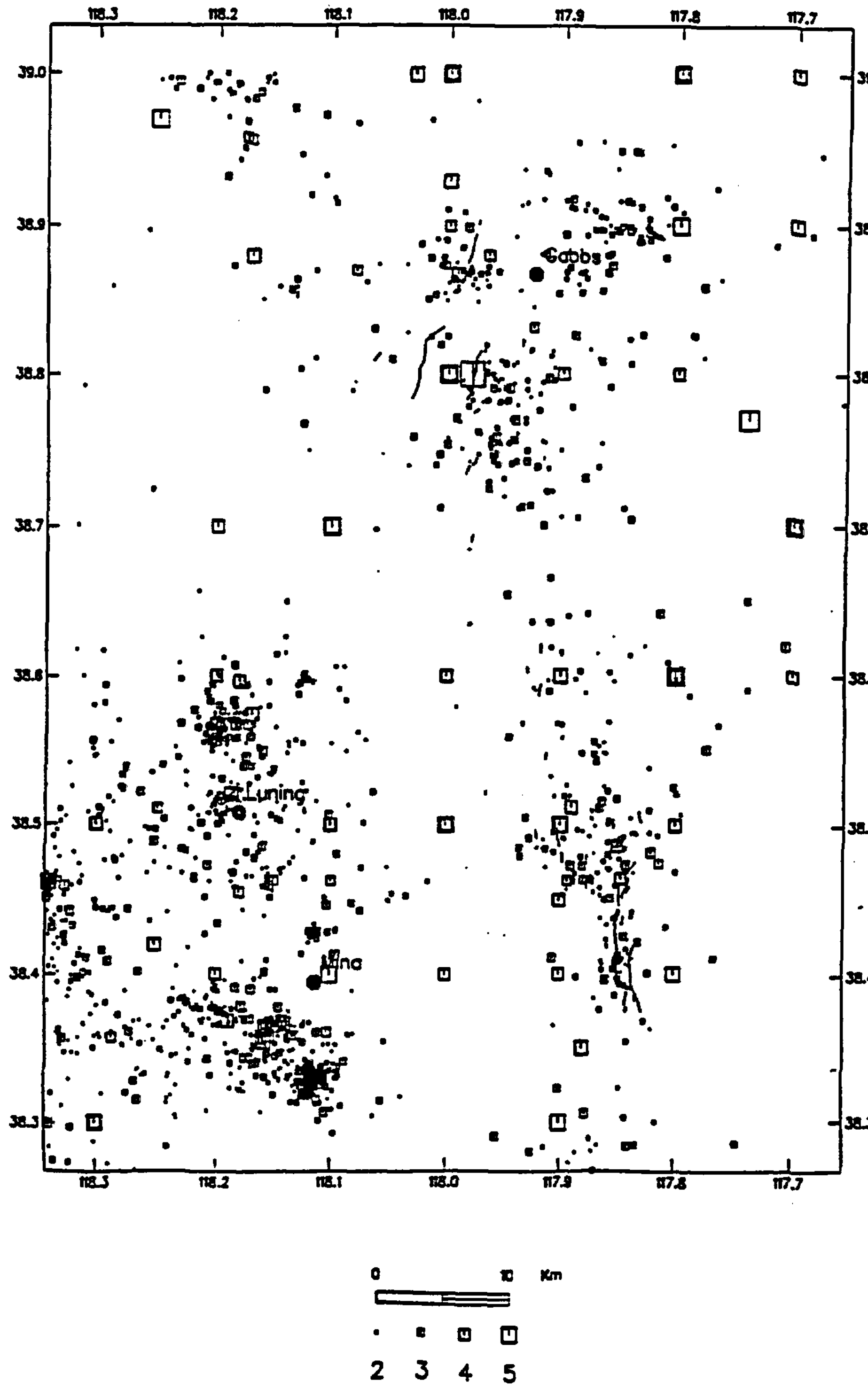

Figure 6. Seismicity catalogued in the 1932 Cedar Mountain earthquake area by the UNR Seismological Laboratory for the period 1970-June 1992. Some general groupings of seismicity can be seen. The surface ruptures are shown on the base map.

here, one for the time period 1932 to June 1992, and the other, for the time period that there has been more local monitoring, 1970 to June 1992.

Although the post-1932 seismicity map is clearly incomplete, it shows all the data that is available for the aftershocks in UNR's catalog. The difficulties of locating earthquakes in this area prior to 1970 is evident in the many magnitude 4 and 5 events located on the tenth of a degree latitude and longitude intersections. Contrasting the seismicity in the immediate area around the surface ruptures with the seismicity of small earthquake swarms near Mina and Luning, demonstrates that most of the aftershocks are missing. The areas around the surface breaks should be as black and much more extensive with earthquakes as these swarms.

The post-1970 data still must be viewed as somewhat fuzzy in the locations of the earthquakes, but offers the best opportunity to spatially associate earthquakes with the ruptures. Several groupings of seismicity are apparent on Figure 6. In general, as pointed out by Doser (1988), there are two groups of aftershocks, one associated with the northern ruptures, and one associated with the southern. The southern group of epicenters cluster around the surface ruptures rather tightly, several being located directly along rupture 23 A. There also seems to be a lot of activity in the northern part of Monte Cristo Valley and the southern part of Stewart Valley. In this region, there are several folds that were probably involved in the surface deformation. These folds are intimately associated with surface faulting and presently form small hills in the landscape. Most of the seismicity at the northern end is from the center of the surface ruptures, and to the east. There is some seismicity immediately southeast of the epicenter that is distributed in nature. A small pocket of seismicity is also located near rupture 3A in Gabbs Valley. Seismicity northwest of the surface rupture area is probably related to the 1954 Fairview Peak earthquake.

Kinematic models

A second kinematic model is being considered for the 1932 Cedar Mountain earthquake, although more work must be done to substantiate it. Initially, Gianella and Callaghan thought that the earthquake must be deep to give such a scattered pattern of surface ruptures. In its simplest form, this could involve a single, north-northwest-trending rupture at depth, that distributes and splays towards the surface. As discussed previously, however, Doser (1988) found evidence for multiple ruptures in the teleseismic P waves from this event, both located more toward the northern half of the surface rupture area. If the southern Stewart Valley and Monte Cristo Valley surface ruptures are interpreted to be primary surface ruptures, this might suggest that there were two other multiple events in addition to Doser's, both northerly trending. Such a model is consistent with the inferred regional stress regime. The consideration of this second kinematic model has come about from the new mapping of surface breaks by Task 1, plotting the breaks at a large scale, and incorporating Gianella and Callaghan' notes and correspondence.

Similarities with the 1992 Landers Earthquake

There are several similarities between the 1992 Landers earthquake and the 1932 Cedar Mountain earthquake including involvement of multiple faults, rupturing across valleys and along different ranges, rupturing multiple geometric and structural segments, and a dominant strike-slip nature.

Observations of the fresh surface ruptures from the Landers event are invaluable to the studies of the Cedar Mountain earthquake. Many of the same geomorphic features whose remnants can be seen from the 1932 earthquake occurred during the Landers earthquake. Of particular note are the occurrence of many swell features. These were almost always related to small left-steps between the main fault breaks. In the area of the Cedar Mountain surface breaks, we have delineated some ruptures based on the occurrence of an alignment of swells and disrupted pavement, and little else. Although these have always been fairly confidently interpreted as true indicators of surface rupture, there is no doubt now. Also in abundance along the Landers earthquake rupture were "moletracks", similar to the "molehill ridges" mentioned by Gianella and Callaghan (1934).

Implications for the Walker Lane

Commonly, a rather simplistic view of an earthquake along a single fault has been envisioned for the seismic hazard of the Walker Lane. Perhaps this is true for several cases. But earthquakes such as the 1923 Cedar Mountain earthquake and the more recent 1992 Landers earthquake in Mojave Desert, California remind us that these major earthquakes (magnitude 7+) can be complicated involving multiple geometric and structural segments of the same fault zone, or different fault zones.

An interesting aspect of the large strike-slip faults of the Walker Lane is that their activity, both in recency and geomorphic expression, is highly variable along their strike. What the previously mentioned earthquakes suggest as a possible explanation for this phenomenon is that parts of different strike-slip faults could be involved in the same major event. Such an event could either be characteristic, with some repeat history, or a random, triggered event. Such multiple fault events should be considered as a possible model for earthquake behavior in the contemporary Walker Lane.

References Cited

Bell, J.W., Ramelli, A.R., and dePolo, C.M., 1990, Progress report for the period 1 October 1989 to 30 September 1990, Task 1 Quaternary tectonics: Final project report submitted to the Nevada Nuclear Waste Project Office, 15 p.

Bell, J.W., Ramelli, A.R., and dePolo, C.M., 1991, Progress report for the period 1 October 1990 to 30 September 1991, Task 1, Quaternary tectonics: Final project report submitted to the Nevada Nuclear Waste Project Office, 10 p. with appendices.

Benson, L.V., and seven others, 1990, Chronology of expansion and contraction of four Great Basin lake systems during the past 35,000 years: Palaeogeography, Palaeoclimatology, Palaeoecology, v. 78, p. 241-286.

Bierman, P.R., and Gillespie, A.R., 1991, Accuracy of rock-varnish chemical analyses: implications for cation-ratio dating: Geology, v. 19, p. 196-199.

Bierman, P.R., and Gillespie, A.R., 1992, Reply to "Comment on 'Accuracy of rock-varnish chemical analyses: implications for cation-ratio dating'": Geology, v. 20, p. 471-472.

Bull, W.B., 1991, Geomorphic responses to climatic change: Oxford University Press, New York.

Cahill, T.A., 1992, Comment on "Accuracy of rock-varnish chemical analyses: implications for cation-ratio dating: Geology, v. 19, p. 469.

Claassen, H., 1986, Late-Wisconsin paleohydrology of the west-central Amargosa Desert, Nevada U.S.A.: Chemical Geology (Isotope Geosciences Section), v. 58, 311-323.

Davis, J.O., 1978, Quaternary tephrochronology of the Lake Lahontan area, Nevada and California, University of Nevada, Nevada Archeological Survey, Research Paper 7, 137 p.

Dorn, R.I., 1988a, A critical evaluation of cation-ratio dating of rock varnish, and an evaluation of its application to the Yucca Mountain repository by the Department of Energy and its subcontractors, *in* "Evaluation of the geologic relations and seismotectonic stability of the Yucca Mountain area, Nevada Nuclear Waste Site Investigation (NNWSI)." Center for Neotectonic Studies, University of Nevada, Reno.

Dorn, R.I., 1988b, A rock varnish interpretation of alluvial-fan development in Death Valley, California: National Geographic Research, v. 4, 56-73.

Dorn, R.I., 1990, Quaternary alkalinity fluctuations recorded in rock varnish microlaminations on western U.S.A. volcanics: Palaeogeography, Palaeoclimatology, Palaeoecology, v.

76, 291-310.

Dorn, R.I., 1992b, Comment on "Accuracy of rock-varnish chemical analyses: Implications for cation-ratio dating": Geology, v. 20, 470-471.

Doser, D.I., 1988, Source parameters of earthquakes in the Nevada seismic zone, 1915-1943: Journal of Geophysical Research, v. 93, no. B12, p. 15,001-15,015.

Gianella, V.P. and Callaghan, E., 1934, The Cedar Mountain, Nevada, earthquake of December 20, 1932: Seismological Society of America, Bulletin, v. 24, p. 345-377.

Hoover, D.L., Swadley, W.C., and Gordon, A.J., 1981, Correlation characteristics of surficial deposits with a description of surficial stratigraphy in the Nevada Test Site region: U.S. Geological Survey Open-File Report 81-512.

Jones, C.E., 1991, Characteristics and origin of rock varnish from the hyperarid coastal deserts of northern Peru: Quaternary Research, v. 35, 116-129.

Krinsley, D.H., Dorn, R.I., and Anderson, S., 1990, Factors that may interfere with the dating of rock varnish: Physical Geography, v. 11, 97-119.

Nettleton, W.D., Witty, J.E., Nelson, R.E., and Hawley, J.W., 1975, Genesis of argillic horizons in soils of desert areas of the southwestern United States: Soil Science Society of America Proceedings, v. 39, 919-926.

Quade, J., 1986, Late Quaternary environmental changes in the upper Las Vegas Valley, Nevada: Quaternary Research, v. 26, 340-357.

Quade, J. and Pratt, W.L., 1989, Late Wisconsin groundwater discharge environments of the southwestern Indian Springs Valley, southern Nevada: Quaternary Research, v. 31, 351-370.

Sarna-Wojcicki, A., Lajoie, K.R., Meyer, C.E., Adam, D.P., Robinson, S.W., and Anderson, R.S., 1988, Tephrochonologic studies of sediment cores from Walker Lake, Nevada: U.S. Geological Survey Open-file Report 88-548, 25 p.

Smith, E.I., Feuerbach, D., Naumann, T., Faulds, J.E., and Cascadden, T., 1990, Annual report for the period 10/189 to 9/30/90, submitted to the Nuclear Waste Project Office, State of Nevada, Report No. 41: Center for Volcanic and Tectonic Studies, Department of Geoscience, University of Nevada, Las Vegas.

Spaulding, W.G., 1985, Vegetation and climates of the last 45,000 years in the vicinity of the Nevada Test Site, south-central Nevada: U.S. Geological Survey Professional Paper

1329.

Wells, S.G., McFadden, L.D., Renault, C.E., and Crowe, B.M., 1990a, Geomorphic assessment of late Quaternary volcanism in the Yucca Mountain area, southern Nevada: Implications for the proposed high-level radioactive waste repository: Geology, v. 18, 549-553.

Wells, S.G., McFadden, L.D., and Harden, J., 1990b, Preliminary results of age estimations and regional correlations of Quaternary alluvial fans within the Mojave Desert of southern California, *in* "At the end of the Mojave: Quaternary studies in the eastern Mojave Desert" (R.E. Reynolds, S.G. Wells, and R.J. Brady, Eds.), Redlands: San Bernardino County Museum Association, p. 45-53.

Wells, S.G., Crowe, B.M., and McFadden, 1992, Measuring the age of the Lathrop Wells volcanic center at Yucca Mountain: Science, v. 257, p. 555-556.

Zreda, M.G., Phillips, F.M., Kubik, P.W., and Shamma, P., 1991, Cosmogenic chlorine-36 dates for a lava flow and volcanic bombs at Lathrop Wells, Nevada: EOS, v. 79, 577.

Zreda, M.G., Phillips, F.M., Kublik, P.W., Sharma, P., and Elmore, D., in press, Cosmogenic ^{36}Cl dating of a young basaltic eruption complex, Lathrop Wells, Nevada: Geology.

Appendix A

Chemical Analyses of Rock Varnish Samples

Appendix 1: Chemical analyses of rock varnish used in the paper. Electron microprobe measurements made by JEOL superprobe with wavelength dispersive mode. Samples were prepared and analyzed according to Dorn et al. (1990).
PIXE measurements have also been made on the some of the same samples analyzed by the electron microprobe. The PIXE results have been normalized to 100%. Zero is listed where PIXE values were not reported for an element or it was below limit of detection.

Site & Subsamples	CR	CR Age ± 1 Sigma	MgO	Al2O3	SiO2	P2O5	SO3	K2O	CaO	TiO2	MnO	Fe2O3	BaO	Total
Red Cone	2.62±0.12													
Red Cone_a	2.57	Used in Calibration	0.86	14.40	45.11	1.21	0.35	1.15	0.32	0.77	9.28	7.75	0.24	81.44
Red Cone_b	2.80	Used in Calibration	0.99	11.41	36.01	0.89	0.10	0.99	0.35	0.64	8.34	6.78	0.12	66.62
Red Cone_c	2.60	Used in Calibration	0.55	10.80	33.89	0.44	0.12	0.80	0.29	0.56	7.01	5.83	0.12	60.41
Red Cone_d	2.53	Used in Calibration	1.06	12.37	38.11	2.41	0.07	0.93	0.21	0.61	7.19	5.98	0.09	69.03
Little Cone	2.63±0.08													
Little_a	2.73	Used in Calibration	0.51	17.10	26.94	2.62	0.15	1.59	0.58	1.06	10.55	12.55	0.14	73.79
Little_b	2.55	Used in Calibration	0.35	13.45	22.19	3.60	0.24	1.00	0.40	0.73	6.85	8.00	0.26	57.07
Little_c	2.63	Used in Calibration	1.33	15.63	23.50	1.95	0.07	1.44	0.72	1.08	8.74	10.49	0.11	65.06
Little_d	2.67	Used in Calibration	0.50	13.66	23.15	3.62	0.05	1.41	0.63	1.01	8.80	10.09	0.07	62.99
Little_e	2.55	Used in Calibration	0.91	13.23	22.19	4.01	0.15	1.51	0.56	1.08	9.58	11.32	0.13	64.67
Black Cone	2.53±0.06													
Black_a	2.54	Used in Calibration	0.68	14.18	28.56	0.70	0.00	2.34	0.52	1.53	10.77	12.42	0.18	71.88
Black_b	2.60	Used in Calibration	0.43	19.10	37.17	0.25	0.02	2.69	0.54	1.69	12.48	13.12	0.13	87.62
Black_c	2.46	Used in Calibration	0.22	17.51	35.45	1.33	0.15	2.21	0.49	1.49	10.83	12.90	0.18	82.76
Black_d	2.51	Used in Calibration	0.33	17.11	32.44	1.05	0.05	2.13	0.41	1.38	8.92	9.76	0.07	73.65
CFP 2	6.47±0.13													
CFP_2_a	6.35	Used in Calibration	0.88	21.15	27.95	1.27	0.15	4.18	1.03	1.11	21.01	18.58	0.17	97.48
CFP_2_b	6.47	Used in Calibration	0.95	25.05	30.35	0.67	0.07	4.83	1.03	1.23	21.40	13.07	0.05	98.70
CFP_2_c	6.59	Used in Calibration	0.80	15.70	20.80	0.38	0.10	3.90	0.86	0.98	18.93	17.17	0.09	79.71
CFP_2_d	6.32	Used in Calibration	0.71	15.54	22.47	0.38	0.02	3.63	0.85	0.96	19.18	17.07	0.00	80.81
CFP_2_e	6.60	Used in Calibration	0.91	20.91	28.44	1.03	0.00	4.92	1.00	1.22	22.37	18.11	0.00	98.91

Site & Subsamples	CR	CR Age ± 1 Sigma	MgO	Al2O3	SiO2	P2O5	SO3	K2O	CaO	TiO2	MnO	Fe2O3	BaO	Total
CFP 26	6.13±0.09													
CFP_26_a	6.06	Used in Calibration	1.27	19.62	28.33	2.05	0.00	3.77	0.72	1.01	8.33	13.11	0.05	78.26
CFP_26_b	6.25	Used in Calibration	1.99	18.03	27.47	1.55	0.00	3.84	0.69	0.99	8.52	12.30	0.06	75.44
CFP_26_c	6.07	Used in Calibration	1.90	16.55	47.84	1.08	0.15	4.16	0.84	1.12	5.29	7.79	0.18	86.90
CFP_26_d	6.14	Used in Calibration	1.01	14.23	42.03	2.45	0.17	3.76	0.75	1.00	4.81	6.94	0.21	77.36
CFP 33	5.75±0.06													
CFP_33_a	5.74	Used in Calibration	0.91	9.32	52.60	2.09	0.15	2.79	0.64	0.81	4.00	8.05	0.15	81.51
CFP_33_b	5.82	Used in Calibration	1.94	9.88	46.73	1.12	0.00	2.48	0.98	0.79	3.16	7.09	0.00	74.17
CFP_33_c	5.69	Used in Calibration	1.66	12.66	54.81	1.55	0.00	2.12	1.13	0.75	2.91	6.64	0.06	84.29
CFP_33_d	5.73	Used in Calibration	1.96	13.38	57.21	1.83	0.15	2.70	1.15	0.89	3.50	7.32	0.17	90.26
CFP 27	5.42±0.12													
CFP_27_a	5.38	Used in Calibration	1.79	20.12	40.61	1.08	0.17	3.40	1.00	1.10	10.04	10.17	0.22	89.70
CFP_27_b	5.24	Used in Calibration	1.46	12.48	29.40	3.12	0.55	2.72	0.83	0.91	8.69	9.30	0.61	70.07
CFP_27_c	5.46	Used in Calibration	1.36	15.92	31.77	2.38	0.07	2.79	1.11	0.95	8.00	8.75	0.07	73.17
CFP_27_d	5.45	Used in Calibration	1.88	13.07	31.89	1.70	0.00	3.07	1.33	1.07	8.35	9.19	0.00	71.55
CFP_27_e	5.56	Used in Calibration	2.04	12.12	29.04	1.99	0.00	1.06	0.40	0.35	7.71	8.37	0.05	63.13
CFP 35	5.34±0.15													
CFP_35_a	5.26	Used in Calibration	1.06	14.66	27.51	2.98	0.10	3.49	1.89	1.34	17.76	13.13	0.14	84.06
CFP_35_b	5.27	Used in Calibration	1.39	14.13	22.66	1.79	0.10	3.86	1.35	1.32	17.38	12.55	0.17	76.70
CFP_35_c	5.21	Used in Calibration	0.81	16.51	25.38	2.57	0.22	3.92	1.57	1.40	17.49	15.36	0.32	85.55
CFP_35_d	5.58	Used in Calibration	1.28	16.78	22.46	2.73	0.40	3.36	1.20	1.09	14.08	10.11	0.41	73.90
CFP_35_e	5.37	Used in Calibration	1.74	15.83	22.25	0.99	0.00	3.72	1.31	1.25	15.54	10.50	0.17	73.30
CFP 36	5.32±0.07													
CFP_36_a	5.23	Used in Calibration	2.89	21.56	31.92	0.66	0.00	3.97	1.99	1.50	18.07	15.06	0.03	97.65
CFP_36_b	5.26	Used in Calibration	2.45	10.68	27.79	0.80	0.00	1.40	1.00	0.59	11.01	12.94	0.10	68.76
CFP_36_c	5.39	Used in Calibration	1.29	8.85	24.67	0.41	0.17	1.30	0.67	0.48	10.79	13.49	0.17	62.29
CFP_36_d	5.32	Used in Calibration	2.11	16.88	25.04	0.37	0.00	2.99	1.31	1.07	15.46	14.05	0.02	79.30
CFP_36_e	5.39	Used in Calibration	0.88	16.23	23.46	0.78	0.25	2.17	1.11	0.80	10.46	13.08	0.29	69.51

Site & Subsamples	CR	CR Age ± 1 Sigma	MgO	Al2O3	SiO2	P2O5	SO3	K2O	CaO	TiO2	MnO	Fe2O3	BaO	Total
CFP 32	5.14±0.07													
CFP_32_a	5.09	Used in Calibration	1.26	16.58	24.36	1.33	0.12	2.35	1.75	1.04	15.14	12.46	0.12	76.51
CFP_32_b	5.14	Used in Calibration	1.43	19.14	27.61	1.44	0.25	2.32	1.88	1.05	16.38	11.11	0.27	82.88
CFP_32_c	5.20	Used in Calibration	0.95	20.28	27.80	2.84	0.32	2.37	1.60	0.99	13.99	10.75	0.31	82.20
CFP_32_d	5.04	Used in Calibration	1.69	19.09	29.67	1.81	0.00	1.68	0.54	0.59	13.84	9.98	0.00	78.89
CFP_32_e	5.21	Used in Calibration	0.93	20.13	29.20	1.23	0.07	1.79	0.63	0.62	14.57	9.43	0.12	78.72
CFP 40	2.95±0.10	572,000 ± 66,000												
CFP_40_a	2.92	591,088	0.56	19.04	26.83	1.05	0.52	1.28	0.42	0.78	11.93	11.39	0.17	73.97
CFP_40_b	2.92	588,223	0.95	15.11	22.21	0.44	0.80	1.40	0.48	0.86	12.95	12.15	1.02	68.37
CFP_40_c	2.93	581,508	0.86	17.15	25.57	0.66	0.55	1.60	0.73	1.05	11.77	10.24	0.88	71.06
CFP_40_d	3.12	461,333	0.81	19.75	27.81	0.73	0.15	1.74	0.70	1.04	11.70	9.57	0.39	74.39
CFP_40_e	2.86	640,003	0.22	18.15	27.05	0.88	0.00	1.61	0.37	0.94	15.63	14.25	0.06	79.16
CFP 38	3.29±0.11	373,000 ± 50,000												
CFP_38_a	3.31	360,009	1.18	28.35	39.73	0.60	0.12	2.30	0.83	1.26	4.01	11.61	0.07	90.06
CFP_38_b	3.23	399,985	0.90	21.28	35.33	0.66	2.15	2.38	1.15	1.44	2.86	11.98	2.54	82.67
CFP_38_c	3.19	422,094	0.99	28.18	43.43	0.34	1.27	2.84	1.93	1.94	3.21	9.95	2.28	96.36
CFP_38_d	3.44	308,345	0.91	35.37	35.84	0.62	0.00	3.65	1.90	2.12	2.29	11.85	0.00	94.55
CFP 39	3.29±0.11	375,000 ± 53,000												
CFP_39_a	3.27	380,379	1.06	19.87	27.03	1.08	0.12	1.59	0.71	0.93	13.95	11.09	0.13	77.56
CFP_39_b	3.15	443,765	2.17	18.44	27.73	0.34	0.07	1.60	0.68	0.96	14.19	12.62	0.05	78.85
CFP_39_c	3.31	360,589	0.98	19.83	30.61	0.48	0.22	2.01	0.75	1.11	14.07	11.06	0.25	81.37
CFP_39_d	3.42	315,941	1.81	18.66	29.85	0.34	0.40	1.98	0.80	1.08	14.23	15.29	0.31	84.75
JWB 20	3.79±0.11	200,000 ± 29,000												
JWB_20_a	3.81	192,613	1.14	15.34	28.35	0.78	0.32	2.52	0.91	1.20	16.86	13.67	0.25	81.34
JWB_20_b	3.80	194,862	1.41	16.05	28.33	0.37	0.17	2.14	0.60	0.97	13.49	10.61	0.20	74.34
JWB_20_c	3.60	250,665	1.71	19.57	32.82	0.30	0.05	2.64	0.92	1.32	17.47	14.50	0.07	91.37
JWB_20_d	3.89	175,118	1.82	17.06	35.28	0.34	0.00	1.74	1.61	1.10	11.92	11.57	0.00	82.44
JWB_20_e	3.83	187,792	1.06	16.08	36.92	0.37	0.30	1.96	1.22	1.08	11.71	9.07	0.15	79.92

Site & Subsamples	CR	CR Age ± 1 Sigma	MgO	Al2O3	SiO2	P2O5	SO3	K2O	CaO	TiO2	MnO	Fe2O3	BaO	Total
CFP 29	3.98±0.32	168,000 ± 75,000												
CFP_29_a	4.22	116,299	0.93	17.04	38.22	0.48	0.05	2.77	1.43	1.31	7.76	16.80	0.00	86.79
CFP_29_b	4.22	115,732	1.26	20.84	36.98	0.69	0.17	2.59	0.84	1.09	5.30	15.09	0.12	84.97
CFP_29_c	4.12	130,592	1.92	23.34	33.95	2.18	0.12	2.28	0.66	0.96	4.90	15.84	0.11	86.26
CFP_29_d	3.86	182,798	0.81	23.87	33.50	1.42	0.07	2.33	0.68	1.05	5.07	10.30	0.15	79.25
CFP_29_e	3.48	292,089	1.08	17.66	25.29	0.76	0.00	2.35	0.52	1.12	8.03	19.82	0.07	76.70
CFP 37	3.98±0.19	159,000 ± 38,000												
CFP_37_a	4.12	131,924	0.85	14.00	22.54	0.89	0.00	2.25	1.02	1.05	16.31	13.85	0.00	72.76
CFP_37_b	4.12	130,625	1.34	23.11	29.93	1.19	0.15	2.36	1.00	1.08	16.59	13.94	0.21	90.90
CFP_37_c	4.12	131,845	0.90	15.50	30.38	0.92	0.15	2.45	0.70	1.03	13.91	10.34	0.16	76.44
CFP_37_d	3.75	208,203	1.24	17.17	30.21	0.57	0.20	2.41	0.65	1.10	14.37	12.08	0.12	80.12
CFP_37_e	3.81	192,630	0.83	15.04	29.50	0.66	0.20	2.29	0.59	1.02	13.01	10.22	0.12	73.48
JWB_YM36-V2	7.94±0.17													
a C-14 Calibration	8.19	Used in Calibration	1.18	14.85	22.85	0.55	0.10	1.35	1.41	0.43	21.00	13.87	0.07	77.66
b Site	8.19	Used in Calibration	0.86	15.66	25.37	0.50	0.25	1.65	1.06	0.43	25.93	14.53	0.15	86.39
c	8.07	Used in Calibration	0.95	15.80	24.39	0.78	0.10	1.65	1.47	0.50	19.68	13.45	0.05	78.82
d	8.09	Used in Calibration	1.16	14.85	22.81	0.60	0.75	1.41	0.97	0.38	16.75	15.22	0.45	75.35
e	7.82	Used in Calibration	2.52	18.61	27.83	0.66	0.00	1.75	0.73	0.42	17.03	18.89	0.00	88.44
f	7.82	Used in Calibration	1.36	17.50	25.31	1.01	0.00	1.53	1.97	0.56	15.65	19.55	0.00	84.44
g	7.65	Used in Calibration	0.99	20.63	30.06	0.57	0.12	2.00	0.99	0.52	15.32	13.75	0.00	84.95
h	7.95	Used in Calibration	1.33	16.95	23.88	1.17	0.02	2.24	1.62	0.63	15.40	10.77	0.00	74.01
i	7.86	Used in Calibration	0.78	17.59	24.77	0.73	0.55	1.67	1.25	0.48	22.00	13.85	0.45	84.12
j	7.77	Used in Calibration	2.60	15.09	29.05	0.48	0.25	1.52	1.50	0.50	19.25	18.34	0.19	88.77
k	7.88	Used in Calibration	1.24	17.46	22.57	1.26	0.05	1.99	1.33	0.55	18.96	18.96	0.07	84.44
l	8.00	Used in Calibration	1.06	16.51	25.52	0.64	0.32	1.73	1.79	0.57	18.68	14.76	0.25	81.83

Site & Subsamples	CR	CR Age ± 1 Sigma	MgO	Al2O3	SiO2	P2O5	SO3	K2O	CaO	TiO2	MnO	Fe2O3	BaO	Total
JWB_YM41	5.99±0.13													
a	5.83	Used in Calibration	0.91	17.29	27.17	0.53	0.22	1.61	1.22	0.63	20.69	13.25	0.26	83.78
b	5.92	Used in Calibration	1.86	17.61	22.44	1.26	0.00	1.83	1.02	0.63	18.96	12.17	0.00	77.78
c	6.10	Used in Calibration	1.06	16.02	34.70	2.18	0.11	1.74	1.34	0.65	13.87	11.19	0.14	83.00
d	6.02	Used in Calibration	1.08	15.61	21.24	1.28	0.00	1.70	1.71	0.72	22.13	13.60	0.00	79.07
e	5.90	Used in Calibration	2.59	19.39	27.64	0.76	0.00	1.88	0.69	0.58	16.08	13.94	0.11	83.66
f	5.75	Used in Calibration	1.09	15.78	24.90	0.78	0.00	1.87	1.23	0.70	20.00	13.19	0.00	79.54
g	6.11	Used in Calibration	2.42	19.12	26.76	0.87	0.10	1.67	0.73	0.52	17.38	13.72	0.13	83.42
h	6.20	Used in Calibration	0.63	17.19	23.70	1.01	0.27	1.20	0.97	0.45	21.10	15.28	0.47	82.27
i	6.01	Used in Calibration	1.23	18.21	29.29	0.57	0.07	1.65	1.13	0.60	17.76	14.46	0.05	85.02
j	6.06	Used in Calibration	1.04	13.26	16.02	1.67	0.25	0.98	1.72	0.55	19.51	12.20	0.22	67.42
k	5.98	Used in Calibration	0.85	13.83	33.78	0.94	0.92	1.47	1.06	0.55	17.39	12.67	0.97	84.43
l	5.94	Used in Calibration	1.09	14.98	26.64	1.83	0.10	0.95	1.18	0.45	20.93	12.48	0.11	80.74
JWB_YM38	6.37±0.13													
a	6.32	Used in Calibration	1.96	17.06	40.73	1.58	0.37	1.75	1.62	0.68	9.53	9.58	0.38	85.24
b	6.31	Used in Calibration	1.11	17.57	26.04	0.78	0.17	1.84	1.51	0.68	15.63	14.39	0.15	79.87
c	6.48	Used in Calibration	1.54	20.69	30.46	1.10	0.00	2.48	1.04	0.72	12.23	13.45	0.00	83.71
d	6.54	Used in Calibration	1.11	18.10	22.72	1.72	0.05	1.59	1.20	0.55	23.58	11.11	0.06	81.79
e	6.67	Used in Calibration	1.19	15.36	29.03	1.12	0.50	2.20	1.80	0.77	20.71	8.02	0.41	81.11
f	6.24	Used in Calibration	1.76	16.36	22.16	1.12	0.00	1.64	0.99	0.55	24.38	9.85	0.06	78.87
g	6.32	Used in Calibration	1.31	13.02	26.86	2.13	0.15	0.90	2.17	0.59	28.67	15.07	0.18	91.05
h	6.40	Used in Calibration	1.39	20.39	26.06	2.15	0.05	2.04	1.18	0.66	17.57	11.81	0.06	83.36
i	6.29	Used in Calibration	1.04	13.53	24.22	2.45	0.12	1.07	1.78	0.56	21.02	19.61	0.10	85.50
j	6.24	Used in Calibration	0.7	15.54	22.11	2.57	0.32	0.64	1.79	0.47	22.1	12.82	0.32	79.38
k	6.36	Used in Calibration	1.59	16.48	21.67	2.57	0.37	1.54	1.90	0.68	20.21	13.22	0.40	80.63
l	6.29	Used in Calibration	1.16	18.42	29.48	0.85	0.22	1.81	1.47	0.67	20.46	4.70	0.23	79.47

Site & Subsamples	CR	CR Age ± 1 Sigma	MgO	Al2O3	SiO2	P2O5	SO3	K2O	CaO	TiO2	MnO	Fe2O3	BaO	Total
JWB_YM39	5.68±0.15													
a ADJACENT TO	5.82	Used in Calibration	1.58	15.55	19.94	1.33	0.00	1.47	1.25	0.60	27.88	9.74	0.09	79.43
b TRENCH CF 8	5.44	Used in Calibration	1.21	15.30	19.02	1.86	0.07	0.99	1.60	0.59	27.80	9.15	0.12	77.71
c	5.49	Used in Calibration	1.48	15.66	19.60	1.19	0.00	1.42	1.05	0.58	27.50	9.65	0.00	78.13
d	5.90	Used in Calibration	1.71	15.89	20.71	1.26	0.00	1.48	1.29	0.60	26.56	9.69	0.00	79.19
e	5.85	Used in Calibration	0.91	9.92	16.34	0.89	0.15	1.60	1.78	0.73	37.61	2.53	0.18	72.64
f	5.74	Used in Calibration	1.67	15.80	20.32	1.33	0.00	1.46	1.12	0.58	26.34	10.02	0.00	78.64
g	5.48	Used in Calibration	1.19	15.04	23.68	0.89	0.35	1.70	1.61	0.77	30.18	4.70	0.41	80.52
h	5.55	Used in Calibration	1.74	16.25	21.37	1.19	0.12	1.57	1.09	0.62	25.17	9.62	0.16	78.90
i	5.67	Used in Calibration	1.79	17.27	26.06	2.41	0.30	1.88	1.67	0.80	16.19	13.41	0.34	82.12
j	5.57	Used in Calibration	1.96	16.44	23.92	1.22	0.00	1.19	1.22	0.55	17.51	14.67	0.00	78.68
k	5.61	Used in Calibration	2.32	16.74	23.02	0.92	0.00	2.28	1.28	0.83	22.74	9.12	0.00	79.25
l	5.71	Used in Calibration	0.95	11.79	12.92	2.34	0.10	0.65	1.46	0.45	32.54	12.34	0.15	75.69
m	5.74	Used in Calibration	1.14	14.47	26.96	0.41	0.50	1.94	1.74	0.82	28.39	4.12	0.31	80.80
n	5.77	Used in Calibration	1.34	14.70	19.40	1.99	0.25	1.13	1.81	0.63	25.72	14.61	0.30	81.88
o	5.89	Used in Calibration	1.81	16.99	21.82	1.26	0.00	1.78	1.17	0.65	19.91	11.64	0.00	77.03
JWB_YM36-V1		1,100 ± 400												
a NOT THE	8.33	672	1.34	18.80	27.70	0.39	0.10	1.61	1.82	0.52	25.61	3.97	0.07	81.93
b CALIBRATION S	8.23	762	0.86	12.77	20.39	0.69	0.15	1.54	1.50	0.47	37.03	3.52	0.17	79.09
c SWALE LOCALE	8.31	689	1.11	10.62	23.39	1.24	0.46	1.18	0.88	0.32	23.35	6.78	0.38	69.71
d	8.02	991	1.04	16.36	26.49	0.64	0.20	1.63	1.16	0.45	29.96	3.27	0.14	81.34
e	7.80	1,306	0.93	14.89	25.07	0.89	0.22	1.73	1.50	0.53	30.20	3.89	0.23	80.08
f	7.87	1,196	0.98	12.19	18.53	0.78	0.25	1.77	1.62	0.55	38.48	2.97	0.25	78.37
g	7.64	1,596	1.13	16.85	19.70	1.51	0.12	1.58	1.61	0.53	26.88	9.25	0.15	79.31
	7.74	1,408	0.90	12.41	19.23	0.50	0.15	1.48	1.85	0.54	36.45	2.30	0.15	75.96
i	7.89	1,167	1.31	17.52	21.35	1.72	0.00	1.78	1.41	0.52	24.11	10.18	0.00	79.90
j	8.03	979	1.36	17.70	23.75	1.26	0.05	2.29	1.62	0.63	21.65	10.84	0.07	81.22
CFP-41-V1	9.17±0.25	300 ± 200												
a PETERSON	9.25	212	1.19	16.19	20.88	1.40	0.05	1.93	1.90	0.53	15.74	17.58	0.00	77.39
b PEDON 13	8.68	434	0.88	12.77	21.37	0.60	0.17	1.70	1.43	0.47	12.92	17.29	0.14	69.74
c	9.36	185	1.04	15.79	26.43	0.32	0.12	1.57	1.85	0.47	12.33	13.24	0.15	73.31
d	9.23	218	1.13	18.56	24.61	0.34	0.07	1.54	2.08	0.50	12.73	14.64	0.07	76.27
e	9.36	185	0.83	15.87	24.15	0.50	0.27	1.70	1.30	0.42	12.92	19.26	0.25	77.47
f	9.15	241	1.21	16.61	20.77	1.26	0.15	1.71	1.47	0.45	18.35	17.28	0.12	79.38

Site & Subsamples	CR	CR Age ± 1 Sigma	MgO	Al2O3	SiO2	P2O5	SO3	K2O	CaO	TiO2	MnO	Fe2O3	BaO	Total
CFP-31-V1	5.67±0.15	19,000 ± 4,000												
a PETERSON	5.63	19,797	1.64	18.29	19.28	1.55	0.08	1.04	1.09	0.48	22.85	11.89	0.10	78.288
b PEDON 14	5.77	16,613	2.45	18.18	28.58	1.22	0	1.35	1.02	0.53	18.21	9.31	0.00	80.85
c	5.53	22,440	0.93	14.61	19.54	2.75	0.27	0.93	1.43	0.53	26.87	9.34	0.24	77.44
d	5.92	13,766	2.22	18.04	25.72	0.87	0.12	1.61	0.98	0.57	19.07	8.76	0.13	78.09
e	5.48	23,890	1.67	19.2	21.09	1.88	0.17	1.22	0.9	0.5	18.23	10.45	0.20	75.511
f	5.60	20,556	1.13	15.63	23.25	1.53	0.07	1.58	1.69	0.75	24.66	8.96	0.07	79.32
g	5.61	20,300	0.98	16.14	22.72	1.79	0.00	1.47	1.83	0.75	29.92	3.00	0.00	78.60
h	5.79	16,201	0.71	11.26	23.95	2.2	0.23	0.98	1.59	0.55	24.22	10.84	0.17	76.70
JWB_YM40	2.84±0.09	660,000 ± 71,000												
a ADJACENT TO	2.77	712,386	1.81	15.66	28.54	0.99	0.47	1.08	0.66	0.82	17.33	15.79	0.48	83.63
b TRENCH CF 1	2.87	628,501	2.22	19.05	34.27	0.34	0.25	0.73	0.69	0.63	15.07	13.05	0.22	86.52
c	2.95	568,563	0.85	15.81	25.03	1.31	0.05	0.74	1.01	0.74	19.80	14.06	0.09	79.49
d	2.75	730,461	1.09	11.47	22.04	0.94	0.07	0.82	0.41	0.59	24.86	13.63	0.13	76.05
e	2.77	712,386	0.27	12.64	24.37	1.05	0.36	0.88	0.55	0.67	18.99	14.56	0.29	74.63
f	2.93	582,989	1.01	19.18	29.81	1.28	0.00	0.83	0.73	0.68	15.32	9.81	0.00	78.65
g	2.72	758,438	1.43	18.46	25.12	0.99	0.00	0.75	0.46	0.58	23.07	12.14	0.04	83.04
h	2.92	590,339	0.61	16.67	24.73	1.56	0.12	0.84	0.58	0.63	23.83	12.66	0.15	82.38
i	2.84	652,573	1.96	17.86	29.61	0.44	0.05	1.02	0.67	0.77	17.59	17.12	0.07	87.16

Site & Subsamples	CR	CR Age ± 1 Sigma	MgO	Al2O3	SiO2	P2O5	SO3	K2O	CaO	TiO2	MnO	Fe2O3	BaO	Total
JWB_YM42	3.90±0.11	176,000 ± 25,000												
a EARLY BLACK	3.69	224,983	1.26	16.78	27.88	0.55	0.10	1.02	1.08	0.72	17.68	10.03	0.15	77.25
b CONE SURFACE	3.77	203,527	1.24	17.18	23.92	1.05	0.00	1.17	0.89	0.70	21.49	11.50	0.00	79.14
c NEAR	3.89	175,118	0.83	11.53	23.80	1.10	0.12	1.12	1.08	0.72	21.14	10.01	0.17	71.62
d	3.92	168,658	1.11	13.56	23.34	0.37	0.12	1.20	0.65	0.62	21.10	13.07	0.15	75.29
e	3.90	172,938	0.18	12.74	25.60	0.41	0.10	0.95	0.96	0.62	21.32	12.00	0.12	75.00
f	4.02	148,799	1.11	12.51	24.75	0.76	0.77	1.29	0.46	0.58	18.85	14.60	0.80	76.48
g	4.08	138,023	0.90	13.91	26.04	0.82	0.40	1.24	0.70	0.62	28.34	13.40	0.58	86.95
h	3.88	177,326	1.23	17.69	28.69	0.50	0.42	1.17	1.01	0.72	22.20	9.79	0.45	83.87
i	3.85	184,117	1.87	19.08	27.55	2.22	1.07	1.36	0.79	0.73	17.86	10.52	1.17	84.22
j	3.95	162,437	1.41	12.88	23.17	0.55	0.07	1.26	0.77	0.67	22.42	13.07	0.09	76.36
JWB_YM43	3.17±0.10	433,000 ± 54,000												
a	3.16	437,038	0.86	16.21	26.98	0.82	0.15	1.07	0.85	0.78	29.57	12.99	0.15	90.43
b	3.25	390,437	1.03	11.62	20.47	2.89	0.37	1.15	0.50	0.67	21.48	13.59	0.29	74.06
c	3.07	489,201	0.63	14.45	22.01	0.53	0.10	1.31	0.35	0.73	28.82	11.89	0.12	80.94
d	3.13	453,776	0.48	16.82	20.33	2.77	0.87	1.22	0.78	0.83	24.82	10.85	0.99	80.76
e	3.02	520,825	2.85	15.35	24.05	0.27	0.07	1.03	0.40	0.63	27.26	16.25	0.08	88.24
f	3.21	410,501	1.18	15.33	27.18	0.53	0.27	1.07	0.57	0.67	22.03	12.52	0.25	81.60
g	3.36	340,173	1.01	15.53	27.26	1.03	0.25	1.05	1.16	0.83	20.80	12.69	0.27	81.88
h	3.22	405,390	0.96	14.38	21.24	0.50	1.55	1.18	0.47	0.68	20.42	14.78	1.56	77.72
i	3.13	453,776	0.91	12.34	17.97	0.69	0.02	1.19	0.64	0.77	29.11	12.92	0.00	76.56

PIXE RESULTS

Sample	PIXE CR	Al	Si	Ca	K	Ti	V	Mn	Fe	Ni	Cu	Zn	Pb	Mg	Sr	Ba
Red Cone_a	2.61	12.89	50.48	1.95	0.90	1.09	0.25	17.40	14.13	0.10	0.00	0.11	0.69	0.00	0.00	0.00
Red Cone_b	2.68	12.21	47.81	1.84	1.16	1.12	0.27	18.84	15.80	0.06	0.07	0.12	0.69	0.00	0.00	0.00
Red Cone_c	2.48	13.06	50.43	1.65	0.98	1.06	0.24	17.17	14.37	0.05	0.00	0.11	0.88	0.00	0.00	0.00
Red Cone_d	2.54	13.82	51.63	1.92	0.77	1.06	0.19	16.20	13.62	0.10	0.04	0.09	0.56	0.00	0.00	0.00
Little_a	2.73	16.12	32.35	2.75	1.73	1.64	0.14	20.54	23.77	0.00	0.00	0.18	0.80	0.00	0.00	0.00
Little_b	2.55	16.40	33.45	2.30	1.53	1.50	0.15	18.15	21.11	0.18	0.00	0.15	0.75	4.32	0.00	0.00
Little_c	2.54	17.18	32.21	2.57	2.25	1.90	0.19	19.44	23.34	0.00	0.04	0.14	0.74	0.00	0.00	0.00
Little_d	2.66	14.29	30.25	2.68	2.05	1.78	0.16	20.04	23.78	0.04	0.06	0.26	0.84	3.77	0.00	0.00
Little_e	2.57	14.92	30.88	2.94	1.92	1.89	0.15	21.26	24.71	0.15	0.09	0.15	0.91	0.00	0.00	0.00
Black_a	2.56	13.53	33.48	4.13	1.62	2.25	0.18	20.75	22.87	0.19	0.04	0.22	0.73	0.00	0.00	0.00
Black_b	2.57	13.73	33.89	3.85	1.36	2.03	0.14	19.24	21.61	0.15	0.00	0.17	0.77	3.04	0.00	0.00
Black_c	2.49	14.70	36.27	3.48	1.37	1.95	0.11	18.04	20.06	0.04	0.05	0.14	0.00	3.77	0.00	0.00
Black_d	2.41	16.38	37.87	3.67	1.18	2.01	0.19	17.47	20.29	0.00	0.00	0.19	0.76	0.00	0.00	0.00
CFP_2_a	6.34	13.97	23.20	5.30	2.25	1.19	0.29	29.26	23.68	0.00	0.00	0.00	0.85	0.00	0.00	0.00
CFP_2_b	6.57	15.32	23.44	5.86	2.15	1.22	0.23	27.98	23.18	0.00	0.02	0.00	0.60	0.00	0.00	0.00
CFP_2_c	6.57	12.53	20.69	5.89	2.26	1.24	0.26	31.02	25.27	0.00	0.00	0.00	0.84	0.00	0.00	0.00
CFP_2_d	6.46	12.17	22.10	5.56	2.26	1.21	0.25	30.88	25.54	0.00	0.04	0.00	0.00	0.00	0.00	0.00
CFP_2_e	6.60	13.14	22.33	6.13	2.18	1.26	0.21	29.64	24.40	0.00	0.07	0.09	0.56	0.00	0.00	0.00

Sample	PIXE CR	Al	Si	Ca	K	Ti	V	Mn	Fe	Ni	Cu	Zn	Pb	Mg	Sr	Ba
CFP_26_a	6.02	16.84	30.26	6.25	2.06	1.38	0.17	14.96	24.35	0.00	0.00	0.00	0.64	3.10	0.00	0.00
CFP_26_b	6.24	15.53	29.53	6.37	1.99	1.34	0.11	15.21	23.34	0.00	0.04	0.00	0.71	5.84	0.00	0.00
CFP_26_c	6.08	13.57	48.23	6.55	2.32	1.46	0.00	8.83	18.29	0.00	0.00	0.12	0.63	0.00	0.00	0.00
CFP_26_d	6.12	13.02	47.47	6.66	2.27	1.46	0.09	9.02	19.32	0.00	0.00	0.00	0.68	0.00	0.00	0.00
CFP_33_a	5.79	8.47	59.38	4.86	1.92	1.17	0.07	7.51	16.08	0.00	0.00	0.11	0.43	0.00	0.00	0.00
CFP_33_b	5.82	10.03	58.23	4.53	3.04	1.30	0.10	6.69	15.45	0.00	0.00	0.10	0.54	0.00	0.00	0.00
CFP_33_c	5.65	11.46	62.81	3.26	2.95	1.10	0.00	5.47	12.90	0.00	0.00	0.06	0.00	0.00	0.00	0.00
CFP_33_d	5.67	11.31	60.17	3.89	3.03	1.22	0.08	6.04	13.85	0.00	0.00	0.08	0.33	0.00	0.00	0.00
CFP_27_a	5.40	15.25	38.76	4.78	2.51	1.35	0.17	15.72	16.15	0.00	0.06	0.15	0.68	4.42	0.00	0.00
CFP_27_b	5.20	12.66	36.41	4.96	2.69	1.47	0.16	18.20	18.27	0.00	0.00	0.10	0.00	5.09	0.00	0.00
CFP_27_c	5.46	15.27	38.05	4.64	3.27	1.45	0.13	15.90	16.32	0.00	0.05	0.12	0.00	4.81	0.00	0.00
CFP_27_d	5.33	13.53	40.21	5.24	3.82	1.70	0.00	17.25	17.59	0.00	0.00	0.17	0.49	0.00	0.00	0.00
CFP_27_e	5.51	13.39	39.86	5.22	3.27	1.54	0.00	17.48	18.52	0.00	0.00	0.22	0.49	0.00	0.00	0.00
CFP_35_a	5.28	11.63	27.80	4.72	4.15	1.68	0.00	29.43	19.56	0.00	0.04	0.19	0.80	0.00	0.00	0.00
CFP_35_b	5.28	11.80	22.96	5.33	3.43	1.66	0.32	29.08	22.35	0.00	0.06	0.15	0.00	2.86	0.00	0.00
CFP_35_c	5.19	12.77	24.00	5.16	3.56	1.68	0.35	27.41	21.65	0.00	0.02	0.15	0.00	3.25	0.00	0.00
CFP_35_d	5.42	15.41	25.81	5.55	3.40	1.65	0.30	26.96	20.74	0.00	0.06	0.13	0.00	0.00	0.00	0.00
CFP_35_e	5.35	13.77	24.16	5.85	3.52	1.75	0.29	28.23	22.24	0.00	0.03	0.16	0.00	0.00	0.00	0.00
CFP_36_a	5.27	14.17	26.54	4.49	3.78	1.57	0.22	24.84	19.99	0.00	0.00	0.15	0.50	3.75	0.00	0.00
CFP_36_b	5.27	10.34	33.81	2.03	2.71	0.90	0.17	22.22	27.08	0.00	0.00	0.11	0.64	0.00	0.00	0.00
CFP_36_c	5.17	9.56	32.53	2.13	1.90	0.78	0.16	23.33	29.51	0.00	0.00	0.10	0.00	0.00	0.00	0.00
CFP_36_d	5.22	14.58	26.54	4.36	3.26	1.46	0.32	27.28	21.98	0.00	0.08	0.15	0.00	0.00	0.00	0.00
CFP_36_e	5.39	15.19	27.28	3.39	3.02	1.19	0.27	20.32	25.77	0.00	0.02	0.13	0.00	3.41	0.00	0.00

Sample	PIXE CR	Al	Si	Ca	K	Ti	V	Mn	Fe	Ni	Cu	Zn	Pb	Mg	Sr	Ba
CFP_32_a	5.04	15.12	26.94	3.14	4.02	1.42	0.24	27.91	20.94	0.00	0.10	0.16	0.00	0.00	0.00	0.00
CFP_32_b	5.18	15.53	27.21	2.86	3.82	1.29	0.36	26.28	19.39	0.00	0.00	0.12	0.63	2.51	0.00	0.00
CFP_32_c	5.21	16.60	28.66	3.38	4.02	1.42	0.26	24.37	20.32	0.00	0.06	0.17	0.74	0.00	0.00	0.00
CFP_32_d	5.09	18.11	34.04	2.78	1.55	0.85	0.13	26.15	15.62	0.00	0.06	0.11	0.60	0.00	0.00	0.00
CFP_32_e	5.20	18.16	32.20	2.86	1.77	0.89	0.14	26.69	16.55	0.00	0.00	0.11	0.63	0.00	0.00	0.00
CFP_40_a	2.94	17.69	31.10	2.17	1.30	1.18	0.20	23.04	22.05	0.07	0.16	0.21	0.83	0.00	0.00	0.00
CFP_40_b	2.95	15.17	26.99	2.41	1.45	1.31	0.65	26.13	23.36	0.00	0.08	0.18	0.99	0.00	0.00	1.29
CFP_40_c	2.80	16.54	30.36	2.45	1.95	1.57	0.60	23.04	21.58	0.13	0.13	0.15	0.77	0.00	0.00	0.73
CFP_40_d	3.01	17.80	31.10	2.61	1.84	1.48	0.59	21.62	20.88	0.19	0.05	0.15	1.18	0.00	0.00	0.51
CFP_40_e	2.93	14.39	26.55	2.46	1.00	1.18	0.14	25.99	23.36	0.10	0.09	0.18	0.00	4.56	0.00	0.00
CFP_38_a	3.22	20.47	35.29	2.80	1.74	1.41	0.26	5.72	25.49	0.00	0.07	0.22	0.94	5.58	0.00	0.00
CFP_38_b	3.39	19.92	40.45	3.92	3.30	2.13	0.00	5.39	20.52	0.05	0.00	0.22	0.00	0.00	0.00	4.09
CFP_38_c	3.31	21.12	41.36	3.40	3.94	2.22	0.00	5.07	19.36	0.00	0.14	0.09	0.00	0.00	0.00	3.29
CFP_38_d	3.32	23.37	29.07	4.02	3.64	2.31	0.00	3.14	34.39	0.07	0.00	0.00	0.00	0.00	0.00	0.00
CFP_39_a	3.21	17.28	29.61	2.29	1.79	1.27	0.31	25.03	21.46	0.03	0.11	0.15	0.67	0.00	0.00	0.00
CFP_39_b	3.27	16.24	29.83	2.51	1.80	1.32	0.34	25.59	21.44	0.06	0.06	0.13	0.68	0.00	0.00	0.00
CFP_39_c	3.30	15.64	29.49	2.69	1.77	1.35	0.23	22.48	22.32	0.11	0.00	0.11	0.67	3.13	0.00	0.00
CFP_39_d	3.46	14.73	29.09	2.82	1.92	1.37	0.16	23.24	22.90	0.12	0.04	0.12	0.73	2.75	0.00	0.00
JWB_20_a	3.91	12.81	28.85	3.65	2.29	1.52	0.34	28.13	21.55	0.00	0.00	0.16	0.70	0.00	0.00	0.00
JWB_20_b	3.63	15.32	31.95	3.50	1.76	1.45	0.35	25.46	19.39	0.00	0.03	0.15	0.63	0.00	0.00	0.00
JWB_20_c	3.71	14.42	30.17	3.59	2.09	1.53	0.34	26.81	20.14	0.00	0.07	0.18	0.66	0.00	0.00	0.00
JWB_20_d	3.69	14.50	37.69	3.30	2.09	1.46	0.10	20.87	19.17	0.00	0.08	0.12	0.61	0.00	0.00	0.00
JWB_20_e	3.85	12.47	37.69	2.66	2.84	1.43	0.10	20.12	18.60	0.00	0.07	0.11	0.70	3.22	0.00	0.00

Sample	PIXE CR	Al	Si	Ca	K	Ti	V	Mn	Fe	Ni	Cu	Zn	Pb	Mg	Sr	Ba
CFP_29_a	4.09	14.09	39.48	3.74	3.34	1.73	0.00	13.23	23.55	0.05	0.00	0.13	0.66	0.00	0.00	0.00
CFP_29_b	4.03	15.41	32.81	3.15	1.77	1.22	0.00	7.80	29.29	0.00	0.00	0.15	0.00	8.40	0.00	0.00
CFP_29_c	3.95	20.24	34.86	3.29	1.65	1.25	0.00	8.28	29.71	0.03	0.00	0.16	0.52	0.00	0.00	0.00
CFP_29_d	3.82	20.59	34.36	3.18	1.60	1.25	0.00	8.25	30.58	0.00	0.06	0.13	0.00	0.00	0.00	0.00
CFP_29_e	3.80	16.72	29.82	4.58	1.76	1.67	0.27	15.87	29.01	0.00	0.09	0.19	0.00	0.00	0.00	0.00
CFP_37_a	4.10	12.15	23.44	3.17	2.45	1.37	0.27	28.00	24.75	0.00	0.00	0.19	0.97	3.24	0.00	0.00
CFP_37_b	4.02	16.82	28.00	2.95	2.16	1.27	0.33	25.52	22.06	0.00	0.00	0.12	0.77	0.00	0.00	0.00
CFP_37_c	3.99	14.07	33.97	3.96	1.94	1.48	0.17	25.08	18.55	0.00	0.00	0.15	0.63	0.00	0.00	0.00
CFP_37_d	3.90	14.75	32.00	3.81	1.73	1.42	0.16	25.70	19.72	0.00	0.00	0.11	0.61	0.00	0.00	0.00
CFP_37_e	3.92	13.97	33.58	3.95	1.77	1.46	0.18	24.59	18.44	0.00	0.00	0.09	0.64	1.33	0.00	0.00

Appendix B

Petrographic and Chemical Analyses of Volcanic Tephra

United States Department of the Interior

GEOLOGICAL SURVEY

Geologic Division; Branch of Western Regional Geology
Tephrochronology Project; MS 975; 345 Middlefield Road
Menlo Park, CA 94025; Tel. 415 329-4938; FTS 459-4938;
FAX: 415 329-4936 or FTS 459-4936

June 29, 1992

John Bell
Nevada Bureau of Mines and Geology
University of Nevada,
Reno, NV 89557

Dear John:

Here are the results of our analyses of your 16 tephra samples that you submitted to us in January of last year. Samples JB-BS-4 through -7 were analyzed last June, and samples JB-BS-9 through -17, and JB-WA-1, were analyzed last October. Samples JB-BS-1 through -3 somehow slipped through the cracks, and were not analyzed until last week. I have given you results of the earlier analyses on two different occasions via the telephone. This letter is a written evaluation of the analyses as a follow-up to our phone conversations, and for citation if you wish to publish the data, and a first report on samples -1 through 3. I'm sorry it has taken so long to finish these; part of the problem was that I was away out of the country for most of last summer and we lost some continuity in our work.

Petrographic Characteristics:

The samples were examined initially by Elmira Wan in our Tephrochronology Lab before any treatment was begun, to check if isotropic glass shards were present; a brief petrographic description was made at that time. Subsequent observations were made on the various processed fractions during sample preparation as warranted. Because the samples were small, all available material was processed (for future reference, you may want to collect larger samples, as this makes a big difference in ease of processing). Petrographic descriptions by Elmira are enclosed on copies of the lab notes. A few words of explanation about abbreviations used in the notes:

#212

WS - wet sieved

HCl - treated with 10% HCl (to get rid of carbonate coating or cement)

HF - treated with 8% HF (to etch outside of shard; get rid of hydrated or altered exterior)

Numbers below HCl or HF refer to number of seconds sample was treated with acid.

BW - bubble-wall shard.

BWJ - bubble-wall junction shard.

Mesh sizes used in sieving samples are for nylon screens. The sizes differ from metal screens.

100 mesh has openings of about 150 microns.

200 mesh has openings of about 80 microns.

325 mesh has openings of about 40 microns.

Chemistry of glass shards based on probe analysis:

JB-BS-1 contains very homogenous glass, as indicated by variations from shard to shard. Only silica seems somewhat variable, and that is probably a result of variation in hydration from shard to shard. The total for this sample is high, 97.4%, indicating that the glass is not very hydrated. Closest matches are with young, near surface layers erupted from the Mono Craters, and with pumice from the Panum tuff ring (material sampled 1.5 m below the surface - KRL82282A(P)). The chemically most similar dated tephra layer to -1 is OD-ML-65CM, a sample of Owen Davis' from Mono Lake, the uppermost of a sequence of Holocene ash layers; the date is essentially at the level of the ash, a radiocarbon age of 1950 ± 110. Samples of yours similar to this one are JB-BS-2, -4, -5, -7, -12, -15, and 16. Samples -2, -7, -11, and -12 have somewhat more iron than -1. Another similar sample, BL-RSA-4 of Scott Anderson from Barrett Lake, has an interpolated age from radiocarbon dates of about 950 yrs B.P. Yet another good match with -1 and several of your other samples in this batch (-9, -11, -12 through -16, and JB-WA-1) is sample 3-30-82-1 of Scott Stine's, a "proto Panum" ash overlying a radiocarbon date of 890 ±40 in Lee Vining Creek.

JB-BS-2 is likewise similar to late Holocene tephra layers erupted from the Mono Craters, including one of a sequence from Barrett Lake, BL-RSA-2, estimated to be about 900 yrs B.P. It totals a high 98%, thus is little hydrated. It is similar again to tephra from the Panum Crater tuff ring, the matrix ash from 1.5 m below the surface (KRL82282A), as opposed to the pumice, and a late Holocene ash layer in Yosemite Valley, in lake deposits formed behind a terminal or recessional moraine near Bridalvail Falls (YOS-1). Sample -2 is also chemically similar to an early Holocene tephra layer at Crooked Meadow, except that the latter is more hydrated than -2. Closest matches to -2 in this batch are -12, -7, -11 (all with slightly higher iron content), and -1.

JB-BS-3 is a moderately hydrated, homogenous tephra (K is slightly variable). The total of 94.9% indicates about 5 % water in the glass. This tephra, of probable early Mono Craters provenance, matches well with tephra layers in Walker Lake (WL 3-7-2.66, WLC-85-2(11.34M), WL-5-19-0.27M, WLC-85-2(13.65M),*WL5-19 78.19m, and in Mono Lake (KRL71082(CII), that are late Pleistocene in age and roughly bracketed between about 60 and 100 Ka. The age control is obtained from a sedimentation-rate curve in Walker Lake constrained by radiocarbon ages on the young end, uranium-series ages in the middle and lower parts, and some direct and indirect tephra correlations to dated source units (Sarna-Wojcicki and others, USGS OFR 88-548, and a later unpublished revision of this report).

JB-BS-4 is a fairly homogenous, poorly hydrated (about 3.5% water) tephra similar to -5 and other Mono Craters tephra layers in the age range of about 1000 to 2000 yrs. B.P. See notes to -1, above.

JB-BS-5 is a fairly homogenous tephra with about 3.5% water. It matches most closely with late Holocene tephra layers erupted from Mono Craters such as -1 (above), and SL-103 and SL-115.5 (Swamp Lake; about 1780 and 1960 yrs B.P., respectively), but also with KRL82182(A-1), an older but more hydrated Mono Craters tephra layer from Crooked Meadow, about 7200 yrs B.P.

JB-BS-6 is a very homogenous tephra layer that is moderately hydrated (about 6.5% water). This is more typical of late Pleistocene or older tephra layers. Closest matches are with the lowest tephra layers in the Wilson Creek Beds of Ken Lajoie, Ash Beds 16, 17, and 19. The closest match (similarity coefficient of 0.998 amd 0.991 for the six elements used) is to ash bed 19 (KRL7982-19B and 679-340), extrapolated to be about 36 Ka, according to Ken (see Benson and others, 1990, Paleo., Paleo., Paleo. v.78, 241-286). There are also correlative beds in Walker Lake, and your sample -17.

JB-BS-7 is another poorly hydrated (about 3.25%) fairly homogenous (except for K) tephra, similar to late Holocene Mono

Craters tephra layers. The closest match is to surface ash at Putnam Dome (North)(KRL-91882A') and Crater Mt (Russell), ash from the pit (KRL91882B), as well as dated late Holocene layers from Barrett Lake (BL-RSA-2, about 900 yrs. B.P., and SL-103, about 1780 yrs. B.P.).

Samples JB-BS-9, -11, -12, -13, -14, -15, -16, and JB-WA-1 are all very similar to one another. They are relatively homogenous, weakly hydrated (range from 1.5 to 2.5%), except for -9, which is moderately hydrated (4.7%). Closest matches fall into two categoried for these: 1) mostly late Holocene tephra layers of Mono Craters provenance, in the range of about 900 to 3750 yrs B.P., but 2) KRL82182(A1) shows-up as a persistant good match for many of these, and as the best for -9, the most hydrated one of the bunch. This is an early Holocene layer, interpolated from Ken Lajoie's radiocarbon dates to be about 7200 yrs. B.P.

JB-BS-17, as mentioned above, matches the oldest ash layers in the Wilson Creek Beds (see comments on your sample -6).

I compared your two samples from a previously submitted set, 1-JWB-1-CM-2 and -3, to see if any new good matches appeared since the last evaluation. The best match is (still) with KRL-71082(II-3), a tephra layer recently exposed on the causeway between Negit Island and the north shore during a recent anthropogenic lowstand of Mono Lake; this layer, according to Ken Lajoie who sampled it, is part of a sequence of about eight or more beds interbedded with "older", deformed lake beds. The set of beds are of two types, one set similar to your sample -6, a putative early Mono Craters set of tephra layers, the other similar to rhyolites erupted from Mammoth Mountain, in the age range of 50 to 100 Ka. These age constraints, plus additional ones from a sedimentation rate curve in Walker Lake based on various age constraints (Sarna-Wojcicki and others, 1988, revised, as above), suggest that these units are in the age range of 60 to 100 Ka. The manganese was not determined for the Mono causeway samples because one of the spectrometers was not working at the time.

Interpretation:

The differences among tephra layers derived from the Mono Craters are small. I think, however, that we can distinguish three sets of Mono Craters and Mono Craters-like ash layers without too much difficulty; these are a Holocene set, a latest Pleistocene set (13-

36 Ka)(some of your samples correlate with the oldest of these), and an older late Pleistocene set (about 60 to 100 Ka).

When we attempt to distinguish between Holocene Mono Craters tephra layers we are basically splitting hairs; I'm not sure such distinctions are valid--at least not on the basis of electron-probe analysis alone. I think we can safely say that the large group of your samples (all except -3, -6, and -17) are Holocene. I suspect that most of these, with the possible exception of -9, are late Holocene, and that the latter might be early Holocene, based on its greater degree of hydration. A problem I see here is that the more distal tephra layers, being finer grained, may hydrate more rapidly than the proximal coarse-grained tephra of equivalent age. Further analysis of the Holocene tephra of Mono Craters source by XRF and other techniques may help us to distinguish them with greater certainty. I was hoping that radiocarbon ages would help to sort these layers out, but it looks to me like there are systematic errors of about 1000 years in Holocene sets of layers sampled from different sites (for example, sets from peat deposits at Crooked Meadow, and from lake deposits in Barrett Lake and Walker Lake).

I hope these data are useful to you. I am sending a copy of this letter to Ken Lajoie, because he is closely involved in investigations of the Mono Craters tephra layers and has provided us with much of the age control and reference samples.

Sincerely,

Andrei Sarna-Wojcicki

Andrei M. Sarna-Wojcicki

P.S.: Your 1-st sample, CMT-3, submitted way back when, still matches best with Bishop-like tephra layers such as the Bishop ash bed, Mono Glass Mt. ash beds B and G, and the Bailey ash bed, all in the age range of 0.75 - 1.2 Ma. The iron is more like the older ash beds than like the Bishop.

A.

~~color~~ N8 - 5YR 8/1 — DISAGGREGATION
Very lt. gray - pinkish gray — H20 Spray

WS	HCl	HF
✓	60	15

(Benton Spring Ash #1, Dunlap Canyon, nr. mouth, NV, 38°24'48"N, 118°4'12" W.)
- Processed entire spl. Spl. is a fine-grained pumiceous ash dominated by blocky, subangular, hydrated, highly vesicular (elongated spindle, tubular & irreg. bubble-type), and ribbed shards (mostly straight, few slightly wavy). (There are a few % feldspars.) Compound grains are also abundant. Altered/heavily coated mat'l makes-up ~6-7% of spl. There is a slight surficial coating on most of the glass so first → ACIDS
* Upon examination of [-200+325], the decision to process this size fraction for probe also was made as most of the grains are less hydrated/vesicular and contain far fewer microliths/microphenocrysts than the [-100+200] size.
- Good clean-up of both fractions. [-100+200] has in addtn to mostly vesicular + compound shards, a fair # of acicular ones. The same can be said for the [-200+325] fraction albeit this size has a fair amt. of platy shards. Both portions contain a few % feldspars, altered mat'l, etc. However, because ~~of small~~ the remaining amts. of residue are so small (<.09 grams), processing was stopped at this pt. Samples are good enough for probe. → PROBE NEXT

✓ DONE FOR PROBE 5/1/91

· 380 JB-BS-2

COLOR NB DISAGGREGATION

~~white~~ Very lt. gray H2O spray

WS	HCl	HF
✓	60	20

(Benton Spring Ash #2. Dunlap Cyn., NV 38°24'54"N, 118°3'18"W.) Entire spl. processed.
- Spl. similar to JB-BS-1 a fine-grained, unconsolidated pumiceous ash.
Glass makes up ~85% of sample, altered mat'l, feldspars and heavies = the rest. Grains are slightly coated w/ FeO3. First step = ACIDS
~~+ +325~~ [-200 +325] fraction also similar to JB-BS-1. Shards make-up ~90%, feldspars ~ 5-6%, remaining grains (heavies [hornblende, biotite, pyroxene(?), dk. shards], altered ≤2%.) → ACIDS ALSO
— Nice clean-up of both portions. Still a fair amt. of grungy mat'l in each plus unwanted xtls but deemed by CEM as good enough for probe → PROBE NEXT

DONE FOR PROBE 5/1/91

Very L

WS
✓

(Be

~~Lxxx~~ N8 – 5YR 8/1
Very Lt. Pinkish ~~white~~ gray

DISAGGREGATION
H_2O spray

WS	HCl	HF	TUBE
✓	60	15	///

(Benton Spring Ash #3, NV, 38°25'36"N, 118°4'24"W.) Entire spl. processed. Another fine-grained, pumiceous tephra. At the [-100 +200] size, shards are highly vesicular (elongated conical, spindle and irreg. bubble-type), hydrated, mostly ribbed and blocky, sub & /or compound. Feldspars (~8%), Biotites (~8%) and hornblendes → zircons, pyroxene (<1%) make up ~17-18% of spl. At [200 +325] better glass is observed (i.e., most of the shards are ribbed, platy w/ few vesicles and little or no hydration). The % minerals is halved (~8-9%). Will process finer fraction for probing instead of [-100 +200]. To remove dirt → ACIDS 1ST

✓ Nice clean-up after acids. To drop unwanted xtls → TUBE NEXT

– Fair tubing. All of heavies removed, some of feldspars → TUBE AGAIN

– Good tubing. Many feldspars dropped out → TUBE AGAIN

– Spl. still has ~5% feldspars but good enough for probe for now → PROBE NEXT

✓ DONE FOR PROBE 5/2/91

JB-BS-4

COLOR 10 YR 8/2 DISAGGREGATION

VERY PALE ORANGE H2O Spray

WS	HCl	HF
√	60	10

(Benton Spring Ash #4, NV, 38°25'43"N, 118°4'24" W.) Entire spl. processed.

- A fair amt. of good glass in a very tiny spl. Mostly pumiceous + vesicular. Biotite, zircons, feldspars, pyroxene (?), and magnetite also present. Give a quick acid bath to clean up for probe → ACIDS 1ST *
- Acids removed most of coating, devitrified and altered mat'l. Still contains minerals but not enough spl. to process further. Good enough for probe. → PROBE NEXT

* med. + fine fractions wet-sieved together to make [-100+325]

DONE FOR PROBE 5/2/91

COLOR NG DISAGGREGATION

WHITE H2O Spray

WS	HCl	HF
✓	60	20

(Benton Spring Ash #5, NV 38°25'49"N, 118°3'54"W.) Processed entire spl.
– Mostly good glass, a fair amt. of grungies, few feldspars (~4%). Acid wash to remove surficial coating → ACIDS 1ST *.
– GOOD CLEAN-UP OF SPL. AFTER ACIDS, STILL A FEW % GRUNGIES AND MINERALS BUT NOT ENOUGH SPL. TO PROCESS ANY FURTHER SO SUBMITTED FOR PROBE
→ PROBE NEXT

* med. + fine fraction wet-sieved together to make [-100+325].

DONE FOR PROBE 5/2/91

JB-BS-6

COLOR ~5YR 8/1 DISAGGREGATION

~~white~~ Lt. Pinkish Gray H2O spray

WS	HCl	HF
√	60	10

(Benton Spring Ash #6, NV, 38°29'47"N, 118°3'29"W.) Entire spl. processed.
- Highly vesicular, pumiceous spl. that is moderately to heavily coated. Spl. also contains a few % compounds: feldspar, biotite, hornblende + magnetite; clean up w/ a short acid bath → ACIDS 1ST.
- Good clean-up of spl. Lots of good glass to work w/ even though spl. is diluted w/ a fair amt. of altered mat'l + xtls.* Good enough for probe → PROBE NEXT

* med + fine fractions combined to make [-100 +325].

DONE FOR PROBE 5/7/91

COLOR 5YR 8/1. DISAGGREGATION
Pinkish gray H2O Spray

WS	HCl	HF
✓	60	10

(Benton Spring Ash #7, Dunlap Cyn., NV, 38°24'54"N, 118°3'24"W.) Entire spl. processed.

- Mostly ribbed glass, some platy, some compound. Vesicular shards are hydrated, irregular bubble-type or elongated conical, spindly; a lot of dirty mat'l present → ACID 1ST.
- Good clean-up*. As described above w/ still a few coated/altered grains. In addtn, hornblende, biotite, etched pyroxene(?), and feldspar present in rel. small #'s. Too small a spl. to continue processing so → PROBE NEXT

- Combined med + fine fractions to make [−100 +325].

DONE FOR PROBE 5/7/91

JB-85-9

COLOR 5 YR 8/1 DISAGGREGATION

Pinkish gray H2O Spray

WS	HCl	HF
/	60	10

(Benton Spring Ash #9, NV, 38°26'48" N, 117°59'38" W.) Entire spl. processed.
Spl. contains an abundant amt. (~75%) good, strongly vesiculate, hydrated, ribbed &/or webby, and sometimes compound glass. A few microlitic shards were observed. BW's + BWJ's were also few in #. Shards containing vesicles have those that are cylindrical, conical, spindle and irreg. bubble-type. Minerals observed in ash were = feldspar, zircon, biotite, + hornblende. Lithic fragments are sparse, as are altered grains + brown shards. There is a slight to mod. coating on grains. A quick acid wash will render this spl. good enough for probe so → ACIDS 1ST
Nice clean-up. Spl. is too small to process any further. Submit to CEM at this point for analysis → PROBE NEXT

DONE FOR PROBE 10/1/91

Color 10 YR 8/2 DISAGGREGATION

Very pale orange H_2O spray

WS	HCl
✓	60

(Benton Spring Ash #11. NV, 38°27'18"N, 117°59'6"W.) Entire spl. processed. Vfg. Spl. contains abundant (~90%) good glass. Almost all of the shards contain microcrystallites. However, these vary in amt. from sparse to abundant. Vesicles w/in shards are mostly cylindrical, but spindle-shaped, conical and irreg. bubble-type are present also. Minerals observed incl. feldspar, hornblende, apatite, calcite, + biotite. Lithic fragments are rare. To clean off the slight surficial coating of $CaCO_3$ found on some of the grains, an HCl treatment will be given 1ST before submitting spl. to probe → HCl FIRST

Nice clean-up. All traces of $CaCO_3$ remove. Too small a spl. to process any further → PROBE NEXT

DONE FOR PROBE 10/1/91

189 JB-BS-12

COLOR 5YR 8/1 DISAGGREGATION

Pinkish gray H2O spray

WS	HCl	HF
✓	60	10

(Benton Spring Ash #12. NV. 38°26'16"N, 118°1'43" W.) Entire spl. processed.
- Another vfg spl. containing ~90% glass: 10% minerals + altered/lithic fragments.
Most of the shards are ribbed, a few are platy; bw's + bwjs are rare in either of these morphotypes. Shards w/ vesicles have those that are usu. hydrated/tubular, altho' spindle-shaped and irreg. bubble-types are commonly observed. Microxtlites + microphenocrysts are often found in a number of shards also. Minerals observed incl.: feldspar, biotite, magnetite, hornblende, ilmenite & hypersthene. $CaCO_3$ is present as a coating. To clean up → AG10S 1ST
- Decent acid wash. Still a small amt. of cement on grains but spl is clean enough for probe analysis. Too small to warrant any further processing. Submit for probe → PROBE NEXT

DONE FOR PROBE 10/1/91

JB-BS-13

COLOR 5YR 8/1

PINKISH GRAY

DISAGGREGATION

H2O Spray

WS	HCl	HF
✓	60	15

(Benton Spring Ash #13. NV, 38°26' 18" N, 118° 1' 43" W.) Entire spl. processed. – Vfg spl. containing ~ 90% mostly ribbed shards and ~ 10% minerals, etc. Platy/blocky shards are also common. Many of these shards are ~~also~~ moderately vesiculate, hydrated, and compound. Microxtllites + phenocrysts are common. The most prevalent vesicle shape is conical, followed by spindle, tubular + irreg. bubble-type. Minerals occurring incl. feldspar biotite, magnetite, poss. ilmenite, and calcite. $CaCO_3$ is found on many of ~~of~~ the surfaces. To remove the carbonate → ACIDS 1ST
– Still a trace of coating left but overall, a good clean-up. There is a fair amt. of good mat'l to work w/. Too small a spl. to continue processing further. Submit to PROBE → PROBE NEXT

DONE FOR PROBE 10/1/91

00002

JB-85-14

COLOR 5YR 8/1
Pinkish gray

DISAGGREGATION
H_2O spray

WS	HCl	HF
✓	60	10

(Benton Spring Ash #14, NV, 38°26'18"N, 118°1'43"W) Entire spl. processed
- Vfg spl contains ~95% good glass : ~5% misc. xtls, lithic frags., etc. However, much of this glass is compound and contains xtllites + microphenocrysts. Shards are commonly blocky, some are ribbed and very few are platy. Most are moderately vesiculate, and may or may not be hydrated. The most common vesicle morph is elongated spindle, though irreg. bubble-types are also prevalent. Minerals in spl. incl.: calcite, feldspar, magnetite, biotite, hornblende, and possibly apatite. There is a slight coating of $FeO_3 + CaCO_3$ on the grain surfaces so the 1st step will be acid washes → ACIDS 1ST
- Spl. completely cleaned. Percentages have changed to ~85-90% glass : 15% xtls. Oxyhornblende is the only new mineral observed. Sample can use more processing but not enough residue to warrant extra work - submit to CEM for probe analysis → PROBE NEXT

DONE FOR PROBE 10/1/91

JB-85-15

COLOR 5 YR 8/1
Pinkish gray

DISAGGREGATION
H_2O Spray

WS	HCl	HF
✓	60	10

(Benton Spring Ash #15, NV, 38°26'18" N, 118° 1' 27" W.) Entire spl. processed.
– Vfg spl. w/ mostly blocky, compound shards. Ribbed shards are relatively common tho'. Glass is moderately veciculate; vesicles may or may not be hydrated, and are predominantly spindle-shaped or conical. Irreg. b-t's were present in smaller numbers. Minerals make up ~5-6% of spl. and include mostly feldspars, some biotite and calcite. There is a slight coating on the grains so to remove this ⟶ ACIDS 1ST
– Spl. looks better after acid wash. No Δ's in %'s Altho' ilmenite (?) was observed after process. Again spl. is too small to continue w/ further processing; good enough for probe however so ⟶ PROBE NEXT

DONE FOR PROBE 10/1/91

00004.

JB-BS-16

COLOR 5YR 8/1
Pinkish gray

DISAGGREGATION
H20 spray

WS	HCl	HF
/	60	10

(Benton Spring Ash #16. NV, 38°27'36"N, 117°58'27" W). Entire spl. processed.
- Vfg, moderately to strongly vesiculate, blocky +/or ribbed shards dominate in this ash spl. Vesicles are mostly hydrated and spindle-shaped; a few tubular + irreg. b-t are present also. Additionally, there are sparse conical vesicles. Compound grains were commonly observed as were a few % shards w/ bw's + bwj's. Minerals incl.: feldspars, biotite, hornblende, magnetite, calcite and orthopx. To remove slight residual coating → ACIDS 1ST
- Nice clean-up. Spl. ratios are ~80% glass : ~15% xtls : ~5% altered grains. There is Not enough residue to continue w/ additional processing. However, enough good mat'l to probe so → PROBE NEXT

DONE FOR PROBE - 10/2/91

JB-BS-17

COLOR 5 YR 8/1
Pinkish gray

DISAGGREGATION
H2O spray

WS	HCl	HF
✓	60	10

(Benton Spring Ash #17. NV, 38°27'35"N, 117°58'24" W.) Entire spl. processed - vfg spl. is composed of mostly moderately to strongly vesiculate, ribbed + pumiceous shards. Vesicles are hydrated for the most part and are usu. spindle-shaped. (A few of these "spindles" are arcuate) The remaining vesicles are usu. irreg. bubble-type. A fair # of shards contain xllites and microphenocrysts. There is a slight surficial coating on many of the grains. Minerals observed: feldspars, calcite, hornblende, magnetite, and biotite. To clean-up spl. → Acids 1st

—

his

js.

.Thor

gh

DONE FOR PROBE 10/2/91

00006

JB-WA-1

COLOR 5 YR 8/1

Pinkish gray

DISAGGREGATION

H_2O spray

WS	HCl	HF
✓	60	15

(Wassuk Ash #1. Reese River Cyn., NV, 38°48'30"N, 118°47'30"W) Entire spl. processed.

DONE FOR PROBE 10/2/91

SAMPLE: T226-6 JB-BS-1

PT	BEAM COUNTS	NA COUNTS	9 SD	MG COUNTS	8 SD	AL COUNTS	3 SD	SI COUNTS	7 SD	K COUNTS	2 SD	CA COUNTS	6 SD	TI COUNTS	5 SD	MN COUNTS	1 SD	FE COUNTS	4 SD
1	14582	2516	50	159	13	14138	119	26910	164	8649	93	970	31	26	5	100	10	618	25
2	14589	2673	111	168	6	14923	555	28278	967	9147	352	933	26	37	8	90	7	575	31
3	14594	2627	81	142	13	14857	436	28015	726	9343	358	966	20	27	6	106	8	607	23
4	14600	2611	66	147	12	14824	367	27962	604	9245	309	985	22	21	7	110	9	653	32
5	14604	2616	57	152	10	14816	324	28420	594	9299	282	1016	30	19	7	87	10	626	29
6	14602	2640	53	172	12	14823	293	27985	532	9043	255	1025	34	24	6	102	9	605	26
7	14597	2708	60	171	12	14900	275	27924	485	9131	233	981	31	23	6	88	9	578	27
8	14587	2787	79	193	16	14941	263	27987	450	9119	216	964	29	16	6	91	9	659	31
9	14572	2631	74	157	16	14817	246	27415	455	8746	238	957	29	32	7	87	9	626	29
10	14565	2567	74	163	15	14574	241	26753	557	8972	227	968	27	30	6	106	9	603	28
11	14563	2550	75	164	14	14472	245	27186	557	9005	216	984	26	27	6	91	9	601	27
12	14555	2726	77	129	16	15022	248	27288	545	9069	206	959	25	26	6	81	9	633	26
13	14548	2622	74	184	17	14990	246	27509	524	9185	200	970	24	27	6	101	9	563	29
14	14546	2785	81	158	16	14939	240	27236	516	9031	192	1027	27	28	5	93	9	570	30
15	14550	2618	79	159	16	14671	233	27608	497	9148	187	958	27	31	5	91	9	595	29
16	14551	2637	76	181	16	14617	229	27731	481	9062	180	995	26	26	5	92	8	546	32
17	14548	2676	74	204	19	14905	224	28264	490	9171	176	967	25	36	6	99	8	555	33
18	14548	2639	72	166	18	15000	224	28522	515	9129	171	951	25	18	6	95	8	621	32
19	14547	2600	71	202	20	14838	218	28027	506	9008	167	997	25	22	6	94	8	624	32
20	14547	2628	69	188	20	15041	219	28269	506	9474	185	1181	52	23	6	96	8	526	35

LINES DELETED: 1

AVE. BEAM CURRENT/SEC = 728

DATA REDUCED USING $B-AL: $GL9M

ON SPECIMEN: T226-6 JB-BS-1

$B-AL VERSION 1.0

OXIDE FORM.	WEIGHT% (OXIDE)	STD.DEV. (%)	HOMO. INDEX	FORMULA	K-RATIO	UNKN PEAK (COUNTS)	UNKN BKGD (COUNTS)	COUNTING TIME(SEC)	STD PEAK (COUNTS)	STD BKGD (COUNTS)	COUNTING TIME(SEC)	STANDARD FILENAME
NA2O	3.953	2.84	1.236	0.000	1.02731	2649.5	46.8	20.00	2579.8	46.2	20.00	%RGSC
MGO	0.019	133.04	1.542	0.000	0.00500	168.4	154.9	20.00	2859.9	155.1	20.00	%RGSC
AL2O3	12.482	1.18	1.288	0.000	0.95526	14840.5	249.1	20.00	15523.8	249.1	20.00	%5831
SIO2	~~76.919~~ 74.138	0.86	2.863	0.000	1.04418	27809.3	87.9	20.00	26636.5	87.9	20.00	%5831
K2O	4.604	1.62	1.634	0.000	1.26169	9122.5	139.9	20.00	7267.9	148.4	20.00	%RGSC
CAO	0.527	4.39	1.681	0.000	0.10288	988.7	181.6	20.00	8037.0	192.7	20.00	%RGSC
TIO2	0.060	66.60	1.123	0.000	0.00055	26.2	16.4	20.00	17895.8	23.7	20.00	%TIO2
MNO	0.041	61.10	0.783	0.000	0.00041	95.0	73.7	20.00	52602.4	137.9	20.00	%MN20
FEO	0.933	5.63	1.478	0.000	0.14576	598.2	102.6	20.00	3509.7	109.8	20.00	%RGSC

97.406

TAL 99.537 NO. OXYGENS = 0 NO. ITERS. = 2 AVE. ATOMIC NO. = 11.18

SAMPLE ID: JB-BS-1 T226-6 Date of Analysis: 6/24/92

Raw Probe Data		Raw Probe Data (FeO to Fe2O3)		Recalculated to 100%	
SiO2	74.788			SiO2	76.70
Al2O3	12.482			Al2O3	12.80
FeO	0.933*1.1113=Fe2O3		1.037	Fe2O3	1.06
MgO	0.019			MgO	0.02
MnO	0.041			MnO	0.04
CaO	0.527			CaO	0.54
TiO2	0.060			TiO2	0.06
Na2o	3.953			Na2o	4.05
K2O	4.604			K2O	4.72
TOTAL(O)	97.406	TOTAL(N)	97.510	TOTAL(R)	99.99

20 Best Matches:

1	0.9966	6/8/91	SS-91-1-1 T232-2
2	0.9903		3-30-82-1, T43-3
3	0.9893	xx/xx/83	KRL82282A(P), T66-6
4	0.9891	5/2/85	WL CORE G 380cm T92-8
5	0.9890	8/7/91	SS-91-1-5 T232-6
6	0.9890	8/6/91	SS-91-1-SU T232-1
7	0.9889	6/13/91	JB-BS-4 T227-1
8	0.9888	8/7/91	SS-91-1-4 T323-5
9	0.9886	10/25/83	KRL-91882G, T66-11
10	0.9883		BO-16
11	0.9883	5/2/85	WL CORE G 370cm T92-7
12	0.9883	1/30/92	FLV-201-TO T249-5
13	0.9882	8/7/91	SS-91-1-Adgss
14	0.9878	6/24/87	OD-ML-65CM T143-7
15	0.9878	10/21/91	JB-BS-11 T241-2
16	0.9875	9/3/88	FLV-64-CS T170-7
17	0.9874	6/22/84	KRL-71082C (590) T58-1
18	0.9873	10/23/85	BL-RSA-4 T112-9
19	0.9860	11/25/86	KRL 860922 A T134-2
20	0.9859	12/20/90	FLV-159-CH T219-6

Elements used in the calculation are:

Na2o
Al2O3
SiO2
K2O
CaO
FeO

***** This sample has been added to the data base *****

Listing of 50 closest matches for COMP. NO. 2820 for elements: Na, Al, Si, K , Ca, Fe Date of Update: 6/25/92

	C.No	Sample Number	Date	SiO2	Al2O3	Fe2O3	MgO	MnO	CaO	TiO2	Na2O	K2O	Total,R	Sim. Co
1	2820	JB-BS-1 T226-6	6/24/92	76.70	12.80	1.06	0.02	0.04	0.54	0.06	4.05	4.72	99.99	1.0000
2	2557	SS-91-1-1 T232-2	6/8/91	76.57	12.92	1.07	0.02	0.04	0.54	0.06	4.05	4.72	99.99	0.9966
3	435	3-30-82-1, T43-3		76.62	12.93	1.06	0.02	0.05	0.54	0.07	4.13	4.59	100.01	0.9903
4	562	KRL82282A(P), T66-6	xx/xx/83	76.86	12.85	1.05	0.03	0.06	0.54	0.05	3.87	4.70	100.01	0.9893
5	1225	WL CORE G 380cm T92-8	5/2/85	76.82	12.79	1.06	0.04	0.04	0.56	0.06	4.00	4.65	100.02	0.9891
6	2562	SS-91-1-5 T232-6	8/7/91	76.97	12.65	1.08	0.03	0.04	0.54	0.07	3.98	4.65	100.01	0.9890
7	2558	SS-91-1-SU T232-1	8/6/91	76.74	12.86	1.09	0.04	0.04	0.54	0.05	3.95	4.68	99.99	0.9890
8	2567	JB-BS-4 T227-1	6/13/91	76.75	12.83	1.04	0.03	0.06	0.55	0.06	3.95	4.73	100.00	0.9889
9	2561	SS-91-1-4 T323-5	8/7/91	77.02	12.63	1.06	0.02	0.04	0.53	0.06	4.00	4.63	99.99	0.9888
10	682	KRL-91882G, T66-11	10/25/83	76.91	12.76	1.07	0.03	0.06	0.54	0.07	3.87	4.68	99.99	0.9886
11	760	BO-16		76.59	12.92	1.11	0.03	0.03	0.54	0.07	4.00	4.71	100.00	0.9883
12	1224	WL CORE G 370cm T92-7	5/2/85	76.83	12.82	1.09	0.04	0.04	0.54	0.05	3.95	4.65	100.01	0.9883
13	2717	FLV-201-TO T249-5	1/30/92	76.85	12.77	1.10	0.02	0.04	0.54	0.04	3.99	4.65	100.00	0.9883
14	2563	SS-91-1-Adgss	8/7/91	76.73	12.85	1.04	0.03	0.05	0.53	0.07	3.95	4.74	99.99	0.9882
15	1806	OD-ML-65CM T143-7	6/24/87	76.81	12.80	1.05	0.03	0.05	0.56	0.05	3.96	4.70	100.01	0.9878
16	2638	JB-BS-11 T241-2	10/21/91	76.55	12.80	1.10	0.02	0.08	0.54	0.06	4.16	4.68	99.99	0.9878
17	2060	FLV-64-CS T170-7	9/3/88	76.71	12.87	1.11	0.02	0.04	0.54	0.04	4.02	4.64	99.99	0.9875
18	1025	KRL-71082C (590) T58-1	6/22/84	76.91	12.71	1.08	0.02	0.00	0.53	0.05	3.95	4.74	99.99	0.9874
19	1418	BL-RSA-4 T112-9	10/23/85	76.83	12.79	1.08	0.04	0.04	0.55	0.06	3.96	4.65	100.00	0.9873
20	1680	KRL 860922 A T134-2	11/25/86	76.94	12.75	1.07	0.03	0.04	0.55	0.06	3.91	4.65	100.00	0.9860
21	2496	FLV-159-CH T219-6	12/20/90	77.01	12.76	1.08	0.03	0.03	0.54	0.05	3.94	4.57	100.01	0.9859
22	2570	JB-BS-7 T227-4	6/13/91	76.73	12.89	1.10	0.03	0.05	0.54	0.06	3.91	4.69	100.00	0.9859
23	2821	JB-BS-2 T226-7	6/24/92	76.56	12.91	1.12	0.02	0.04	0.53	0.08	4.04	4.72	100.02	0.9858
24	2716	FLV-200-LC T249-4	1/30/92	76.77	12.80	1.11	0.02	0.04	0.53	0.06	4.01	4.67	100.01	0.9858
25	2560	SS-91-1-3 t232-4	8/7/91	77.08	12.64	1.06	0.02	0.05	0.53	0.06	3.92	4.64	100.00	0.9858
26	681	KRL-91882A', T66-8	10/25/83	76.79	12.83	1.10	0.03	0.06	0.54	0.07	3.91	4.67	100.00	0.9858
27	1141	WL-2-3-1.94M T85-1	12/4/84	76.97	12.65	1.05	0.03	0.05	0.56	0.05	4.00	4.66	100.02	0.9858
28	2795	FLV-209-BC T254-6	4/14/92	76.36	13.11	1.09	0.03	0.06	0.55	0.07	4.01	4.73	100.01	0.9857
29	1034	WL 2-2-2.64, T78-7	08/18/84	77.06	12.62	1.06	0.03	0.05	0.55	0.06	3.86	4.71	100.00	0.9857
30	2568	JB-BS-5 T227-2	6/13/91	76.69	12.91	1.08	0.02	0.05	0.55	0.09	3.90	4.70	99.99	0.9856
31	431	YOS-1, T13-1		76.61	12.93	1.12	0.03	0.05	0.54	0.07	4.03	4.64	100.02	0.9856
32	1186	WALKER LAKE CORE G 380CM t89-1	2/28/85	76.98	12.79	1.08	0.02	0.05	0.54	0.05	3.86	4.64	100.01	0.9855
33	2643	JB-BS-16 T241-7	10/21/91	76.97	12.59	1.04	0.02	0.08	0.54	0.05	4.13	4.58	100.00	0.9854
34	2639	JB-BS-12 T241-3	10/21/91	76.51	12.85	1.11	0.03	0.08	0.54	0.05	4.16	4.67	100.00	0.9853
35	1142	WL-2-3-2.14M T85-2	12/4/84	76.97	12.69	1.06	0.03	0.05	0.56	0.06	3.96	4.63	100.01	0.9851
36	1310	WL 8-2B 172-174.5CM T99-10	7/1/85	76.90	12.74	1.05	0.02	0.05	0.56	0.07	3.91	4.71	100.01	0.9851
37	2236	SL-115.5 T186-3	2/28/89	76.76	12.91	1.07	0.03	0.04	0.55	0.06	3.84	4.73	99.99	0.9849
38	1409	KRL 82182 (A1) (599) T112-1	10/22/85	76.60	12.87	1.11	0.04	0.04	0.55	0.06	4.08	4.65	100.00	0.9846
39	2642	JB-BS-15 T241-6	10/21/91	76.59	12.83	1.08	0.03	0.07	0.54	0.04	4.23	4.59	100.00	0.9846
40	1948	WL-4-4 (12.25M) T162-2	5/14/88	76.87	12.86	1.09	0.02	0.05	0.54	0.06	3.80	4.72	100.01	0.9840
41	2493	FLV-156-SS T219-3	12/20/90	76.64	13.06	1.09	0.03	0.04	0.54	0.05	3.94	4.62	100.01	0.9839
42	2559	SS-91-1-2 T232-3	8/7/91	77.11	12.63	1.03	0.03	0.05	0.54	0.06	3.89	4.67	100.01	0.9838
43	570	KRL91982D, T66-10	xx/xx/83	76.81	12.89	1.08	0.03	0.05	0.53	0.06	3.90	4.65	100.00	0.9838
44	566	KRL91882B, T64-12	09/06/83	76.81	12.82	1.10	0.01	0.05	0.53	0.08	3.91	4.69	100.00	0.9835
45	680	KRL-82282B, T54-4	xx//xx/x	76.99	12.71	1.08	0.02	0.06	0.53	0.04	3.86	4.70	99.99	0.9835
46	1972	WL-4-58 (144.77m) T164-1	5/21/88	76.73	12.71	1.15	0.00	0.03	0.54	0.12	4.02	4.69	99.99	0.9834
47	1419	BL-RSA-5 T112-10	10/23/85	76.98	12.65	1.09	0.04	0.04	0.53	0.05	3.93	4.68	99.99	0.9834
48	2585	FLV-168-TC T229-3	6/14/91	76.89	12.90	1.05	0.03	0.05	0.54	0.06	3.74	4.74	100.00	0.9833
49	2718	FLV-202-D T249-6	1/30/92	76.79	12.79	1.06	0.02	0.04	0.58	0.07	3.96	4.68	99.99	0.9831
50	1757	OD-ML-10-405 CM T139-14	5/28/87	76.99	12.77	1.05	0.03	0.06	0.53	0.09	3.80	4.69	100.01	0.9830

SAMPLE: T226-7 [illegible]-2

	BEAM	[illegible]	9	MG	8	AL	3	SI	7	K	2	CA	6	TI	5	MN	1	FE	4
PT	COUNTS	COUNTS	SD	COUNTS	SD	COUNTS	SD	COUNTS	SD	COUNTS	SD	COUNTS	SD	COUNTS	SD	COUNTS	SD	COUNTS	SD
1	14564	2562	51	151	12	15320	124	27025	164	8959	95	1028	32	27	5	96	10	652	26
2	14563	2758	138	157	4	15294	19	27914	628	9064	74	932	68	24	2	108	9	652	0
3	14573	2672	98	181	15	15286	18	27290	456	9151	96	993	49	28	2	89	10	540	65
4	14577	2672	80	190	18	15043	129	27876	439	9363	172	988	40	31	3	96	8	602	53
5	14584	2670	69	150	18	14781	232	27748	393	9038	155	990	35	32	3	94	7	694	59
6	14591	2767	74	190	19	15100	208	27972	388	9195	142	966	32	24	3	88	7	596	54
7	14601	2735	71	162	18	15156	190	27985	378	9500	191	997	30	36	4	117	11	658	52
8	14602	2588	75	159	17	14718	231	27415	363	9147	177	941	32	30	4	101	10	654	49
9	14595	52	878	168	16	507	****	38607	****	142	****	170	271	16	6	62	15	92	185
10	14600	2612	831	160	15	15009	****	27732	****	9240	****	895	256	25	6	84	15	531	175
11	14593	2633	791	168	14	15078	****	28379	****	9219	****	989	245	34	6	90	14	636	167
12	14585	2708	759	171	14	15051	****	28402	****	9112	****	1012	235	38	6	108	14	639	161
13	14574	2649	729	166	13	14835	****	28608	****	9134	****	966	226	25	6	97	14	626	154
14	14564	2685	702	180	13	15089	****	28348	****	9198	****	998	218	19	6	87	13	601	149
15	14564	2634	678	162	13	14918	****	27903	****	9234	****	953	211	29	6	85	13	639	144
16	14555	2683	657	152	13	15073	****	27931	****	9216	****	959	204	30	6	89	13	641	140
17	14549	2644	637	187	13	15217	****	27790	****	8959	****	991	198	19	6	73	13	647	136
18	14541	2543	618	171	13	15171	****	28471	****	9036	****	973	192	23	6	85	13	619	132
19	14551	2717	602	167	13	15211	****	27944	****	9179	****	963	187	29	6	99	13	674	129
20	14544	2303	588	184	13	14617	****	26647	****	9323	****	988	182	27	6	105	13	432	131

LINES DELETED:

:

LINES DELETED: 2 9 20

AVE. BEAM CURRENT/SEC = 729

DATA REDUCED USING $B-AL: #GL9M

ON SPECIMEN: T226-7 JB-BS-2

$B-AL VERSION 1.0

OXIDE FORM.	WEIGHT% (OXIDE)	STD.DEV. (%)	HOMO. INDEX	FORMULA	K-RATIO	UNKN PEAK (COUNTS)	UNKN BKGD (COUNTS)	COUNTING TIME(SEC)	STD PEAK (COUNTS)	STD BKGD (COUNTS)	COUNTING TIME(SEC)	STANDARD FILENAME
NA2O	3.962	2.84	1.154	0.000	1.03044	2657.5	46.7	20.00	2579.8	46.2	20.00	%RGSC
MGO	0.019	130.45	1.001	0.000	0.00510	168.7	154.9	20.00	2859.9	155.1	20.00	%RGSC
AL2O3	12.665	1.17	1.380	0.000	0.96975	15062.2	249.5	20.00	15523.8	249.1	20.00	%5831
SIO2	77.270	0.86	2.567	0.000	1.04874	27930.5	87.9	20.00	26636.5	87.9	20.00	%5831
K2O	4.628	1.61	1.408	0.000	1.26822	9169.3	140.2	20.00	7267.9	148.4	20.00	%RGSC
CAO	0.519	4.44	0.978	0.000	0.10129	976.6	182.0	20.00	8037.0	192.7	20.00	%RGSC
TIO2	0.074	55.82	1.008	0.000	0.00067	28.5	16.5	20.00	17895.8	23.7	20.00	%TIO2
MNO	0.037	67.68	1.059	0.000	0.00036	93.0	73.9	20.00	52602.4	137.9	20.00	%MN2O
FEO	0.985	5.45	1.707	0.000	0.15397	626.4	102.9	20.00	3509.7	109.8	20.00	%RGSC

SAMPLE ID: JB-BS-2 T226-7 Date of Analysis: 6/24/92

Raw Probe Data		Raw Probe Data (FeO to Fe2O3)		Recalculated to 100%	
SiO2	75.129			SiO2	76.56
Al2O3	12.665			Al2O3	12.91
FeO	0.985*1.1113=Fe2O3		1.095	Fe2O3	1.12
MgO	0.019			MgO	0.02
MnO	0.037			MnO	0.04
CaO	0.519			CaO	0.53
TiO2	0.074			TiO2	0.08
Na2o	3.962			Na2o	4.04
K2O	4.628			K2O	4.72
TOTAL(O)	98.018	TOTAL(N)	98.128	TOTAL(R)	100.02

20 Best Matches:

1	0.9936	1/30/92	FLV-200-LC T249-4
2	0.9933		YOS-1, T13-1
3	0.9932		BO-16
4	0.9912	10/25/83	KRL82282A, T66-5
5	0.9909	9/3/88	FLV-64-CS T170-7
6	0.9907		DR-64
7	0.9907	1/30/92	FLV-199-BC T249-3
8	0.9889	6/8/91	SS-91-1-1 T232-2
9	0.9889	09/06/83	KRL91882B, T64-12
10	0.9889		HC-10
11	0.9886		BO-11
12	0.9885	10/23/85	BL-RSA-2 T112-7
13	0.9883		LD-12, T3,4
14	0.9880	10/21/91	JB-BS-12 T241-3
15	0.9877	10/22/85	KRL 82182 (A1) (599) T112-1
16	0.9877	5/21/88	WL-4-58 (144.77m) T164-1
17	0.9875		LD-12
18	0.9871		GS-32
19	0.9870	1/30/92	FLV-201-TO T249-5
20	0.9869	6/13/91	JB-BS-7 T227-4

Elements used in the calculation are:

Na2o
Al2O3
SiO2
K2O
CaO
FeO

***** This sample has been added to the data base *****

Listing of 50 closest matches for COMP. NO. 2821 for elements: Na, Al, Si, K , Ca, Fe Date of Update: 6/25/92

	C.No	Sample Number	Date	SiO2	Al2O3	Fe2O3	MgO	MnO	CaO	TiO2	Na2O	K2O	Total,R	Sim. Co
1	2821	JB-BS-2 T226-7	6/24/92	76.56	12.91	1.12	0.02	0.04	0.53	0.08	4.04	4.72	100.02	1.0000
2	2716	FLV-200-LC T249-4	1/30/92	76.77	12.80	1.11	0.02	0.04	0.53	0.06	4.01	4.67	100.01	0.9936
3	431	YOS-1, T13-1		76.61	12.93	1.12	0.03	0.05	0.54	0.07	4.03	4.64	100.02	0.9933
4	760	BO-16		76.59	12.92	1.11	0.03	0.03	0.54	0.07	4.00	4.71	100.00	0.9932
5	561	KRL82282A, T66-5	10/25/83	76.71	12.88	1.12	0.04	0.05	0.52	0.06	3.98	4.65	100.01	0.9912
6	2060	FLV-64-CS T170-7	9/3/88	76.71	12.87	1.11	0.02	0.04	0.54	0.04	4.02	4.64	99.99	0.9909
7	952	DR-64		76.57	13.01	1.13	0.03	0.05	0.53	0.07	3.90	4.70	99.99	0.9907
8	2721	FLV-199-BC T249-3	1/30/92	76.88	12.71	1.13	0.02	0.03	0.53	0.06	3.98	4.66	100.00	0.9907
9	2557	SS-91-1-1 T232-2	6/8/91	76.57	12.92	1.07	0.02	0.04	0.54	0.06	4.05	4.72	99.99	0.9889
10	566	KRL91882B, T64-12	09/06/83	76.81	12.82	1.10	0.01	0.05	0.53	0.08	3.91	4.69	100.00	0.9889
11	750	HC-10		76.27	13.21	1.15	0.03	0.03	0.53	0.07	4.00	4.70	99.99	0.9889
12	758	BO-11		76.35	13.11	1.12	0.03	0.04	0.55	0.09	4.00	4.70	99.99	0.9886
13	1416	BL-RSA-2 T112-7	10/23/85	76.78	12.85	1.12	0.04	0.03	0.54	0.06	3.90	4.68	100.00	0.9885
14	192	LD-12, T3,4		76.94	12.70	1.12	0.03	0.07	0.53	0.07	3.91	4.64	100.01	0.9883
15	2639	JB-BS-12 T241-3	10/21/91	76.51	12.85	1.11	0.03	0.08	0.54	0.05	4.16	4.67	100.00	0.9880
16	1409	KRL 82182 (A1) (599) T112-1	10/22/85	76.60	12.87	1.11	0.04	0.04	0.55	0.06	4.08	4.65	100.00	0.9877
17	1972	WL-4-58 (144.77m) T164-1	5/21/88	76.73	12.71	1.15	0.00	0.03	0.54	0.12	4.02	4.69	99.99	0.9877
18	701	LD-12		76.94	12.72	1.12	0.03	0.07	0.53	0.07	3.91	4.61	100.00	0.9875
19	788	GS-32		76.58	12.90	1.13	0.03	0.04	0.56	0.06	4.00	4.70	100.00	0.9871
20	2717	FLV-201-TO T249-5	1/30/92	76.85	12.77	1.10	0.02	0.04	0.54	0.04	3.99	4.65	100.00	0.9870
21	2570	JB-BS-7 T227-4	6/13/91	76.73	12.89	1.10	0.03	0.05	0.54	0.06	3.91	4.69	100.00	0.9869
22	1240	WL 4-2 3.29m T93-9	5/2/85	76.75	12.79	1.13	0.03	0.04	0.55	0.05	4.02	4.64	100.00	0.9869
23	560	KRL82282, T66-4	xx/xx/83	76.74	12.90	1.13	0.02	0.06	0.54	0.06	3.87	4.68	100.00	0.9865
24	1025	KRL-71082C (590) T58-1	6/22/84	76.91	12.71	1.08	0.02	0.00	0.53	0.05	3.95	4.74	99.99	0.9863
25	2558	SS-91-1-SU T232-1	8/6/91	76.74	12.86	1.09	0.04	0.04	0.54	0.05	3.95	4.68	99.99	0.9863
26	2638	JB-BS-11 T241-2	10/21/91	76.55	12.80	1.10	0.02	0.08	0.54	0.06	4.16	4.68	99.99	0.9863
27	972	DR-86		76.74	12.92	1.15	0.03	0.04	0.53	0.07	3.91	4.61	100.00	0.9859
28	2820	JB-BS-1 T226-6	6/24/92	76.70	12.80	1.06	0.02	0.04	0.54	0.06	4.05	4.72	99.99	0.9858
29	567	KRL91882-K-1, T64-13	09/06/83	76.93	12.82	1.11	0.01	0.05	0.53	0.07	3.88	4.60	100.00	0.9857
30	1419	BL-RSA-5 T112-10	10/23/85	76.98	12.65	1.09	0.04	0.04	0.53	0.05	3.93	4.68	99.99	0.9853
31	681	KRL-91882A', T66-8	10/25/83	76.79	12.83	1.10	0.03	0.06	0.54	0.07	3.91	4.67	100.00	0.9853
32	570	KRL91982D, T66-10	xx/xx/83	76.81	12.89	1.08	0.03	0.05	0.53	0.06	3.90	4.65	100.00	0.9850
33	2795	FLV-209-BC T254-6	4/14/92	76.36	13.11	1.09	0.03	0.06	0.55	0.07	4.01	4.73	100.01	0.9849
34	1224	WL CORE G 370cm T92-7	5/2/85	76.83	12.82	1.09	0.04	0.04	0.54	0.05	3.95	4.65	100.01	0.9845
35	757	BO-7		76.35	13.23	1.14	0.03	0.03	0.52	0.09	4.01	4.61	100.01	0.9843
36	783	GS-27		76.74	12.92	1.12	0.03	0.05	0.55	0.07	3.91	4.61	100.00	0.9842
37	753	BO-1		76.45	13.11	1.09	0.03	0.04	0.51	0.07	4.00	4.70	100.00	0.9841
38	1241	WL 4-2 3.31m T93-10	5/2/85	76.69	12.91	1.14	0.04	0.04	0.55	0.06	3.92	4.67	100.02	0.9840
39	971	DR-85		76.75	12.93	1.14	0.03	0.05	0.52	0.07	3.91	4.61	100.01	0.9840
40	2380	FLV-131-FC T203-4	4/16/90	77.18	12.43	1.12	0.01	0.04	0.54	0.06	3.93	4.68	99.99	0.9834
41	1029	KRL-99182K-1P (595) T58-6	6/22/84	76.79	12.72	1.13	0.03	0.00	0.54	0.05	3.91	4.83	100.00	0.9833
42	2493	FLV-156-SS T219-3	12/20/90	76.64	13.06	1.09	0.03	0.04	0.54	0.05	3.94	4.62	100.01	0.9827
43	2563	SS-91-1-Adgss	8/7/91	76.73	12.85	1.04	0.03	0.05	0.53	0.07	3.95	4.74	99.99	0.9825
44	2235	SL-103 T186-2	2/28/89	76.68	12.95	1.10	0.03	0.04	0.55	0.07	3.88	4.69	99.99	0.9825
45	1223	WL CORE G 180cm T92-6	5/2/85	76.64	12.88	1.11	0.04	0.05	0.57	0.06	3.99	4.67	100.01	0.9824
46	680	KRL-82282B, T54-4	xx//xx/x	76.99	12.71	1.08	0.02	0.06	0.53	0.04	3.86	4.70	99.99	0.9824
47	437	6A, T35-7		75.81	12.97	1.11	0.03	0.03	0.52	0.06	3.92	4.56	99.01	0.9824
48	564	KRL82782A, T64-11	09/06/83	76.99	12.75	1.09	0.01	0.06	0.53	0.08	3.90	4.59	100.00	0.9822
49	2562	SS-91-1-5 T232-6	8/7/91	76.97	12.65	1.08	0.03	0.04	0.54	0.07	3.98	4.65	100.01	0.9818
50	571	KRL91982F, T56-5	07/01/83	76.61	12.89	1.14	0.03	0.05	0.55	0.05	4.12	4.56	100.00	0.9818

SAMPLE: T226-8 JB-BS-3

	BEAM	NA	9	MG	8	AL	3	SI	7	K	2	CA	6	TI	5	MN	1	FE	4
PT	COUNTS	COUNTS	SD	COUNTS	SD	COUNTS	SD	COUNTS	SD	COUNTS	SD	COUNTS	SD	COUNTS	SD	COUNTS	SD	COUNTS	SD
1	14542	2318	48	180	13	14766	122	26450	163	9272	96	1358	37	33	6	88	9	459	21
2	14551	2319	0	218	27	15056	205	27215	541	9366	66	1367	6	25	6	84	3	531	52
3	14560	2215	60	227	25	14877	146	27058	404	9979	384	1381	11	31	4	92	4	472	39
4	14572	2289	49	181	25	14335	307	27830	567	9199	357	812	279	29	3	87	3	464	34
5	14571	2328	46	210	22	15218	336	26912	501	9398	310	1337	246	27	3	81	4	506	31
6	14571	2334	45	224	21	15235	339	27176	450	9596	284	1398	228	30	3	104	8	495	28
7	14545	2298	41	194	20	14833	311	26539	463	9509	260	1348	210	26	3	109	10	454	29
8	14539	2399	51	227	20	14970	289	26781	438	9306	248	1337	195	24	3	89	10	497	27

LINES DELETED: 4

AVE. BEAM CURRENT/SEC = 728

DATA REDUCED USING $B-AL: $GL9M

ON SPECIMEN: T226-8 JB-BS-3

$B-AL VERSION 1.0

OXIDE FORM.	WEIGHT% (OXIDE)	STD.DEV. (%)	HOMO. INDEX	FORMULA	K-RATIO	UNKN PEAK (COUNTS)	UNKN BKGD (COUNTS)	COUNTING TIME(SEC)	STD PEAK (COUNTS)	STD BKGD (COUNTS)	COUNTING TIME(SEC)	STANDARD FILENAME
NA2O	3.466	2.95	1.136	0.000	0.89556	2315.8	46.8	20.00	2579.8	46.2	20.00	%RGSC
MGO	0.079	33.82	1.254	0.000	0.02096	211.6	154.9	20.00	2859.9	155.1	20.00	%RGSC
AL2O3	12.627	1.17	1.508	0.000	0.96535	14993.4	248.1	20.00	15523.8	249.1	20.00	%5831
SIO2	72.201 74.429	0.87	1.835	0.000	1.00902	26876.0	87.9	20.00	26636.5	87.9	20.00	%5831
K2O	4.788	1.60	2.500	0.000	1.31331	9489.2	139.1	20.00	7267.9	148.4	20.00	%RGSC
CAO	0.769	3.52	0.618	0.000	0.15047	1360.9	180.6	20.00	8037.0	192.7	20.00	%RGSC
TIO2	0.074	55.68	0.639	0.000	0.00067	28.3	16.3	20.00	17895.8	23.7	20.00	%TIO2
MNO	0.037	66.45	1.062	0.000	0.00037	92.6	73.2	20.00	52602.4	137.9	20.00	%MN2O
FEO	0.727	6.54	1.254	0.000	0.11351	487.9	101.9	20.00	3509.7	109.8	20.00	%RGSC

94.945

TOTAL 96.995 NO. OXYGENS = 0 NO. ITERS. = 2 AVE. ATOMIC NO. = 11.12

24-JUN-92 14:15:23

SAMPLE ID: JB-BS-3 T226-8 Date of Analysis: 6/24/92

Raw Probe Data		Raw Probe Data (FeO to Fe2O3)		Recalculated to 100%	
SiO2	72.367			SiO2	76.16
Al2O3	12.627			Al2O3	13.29
FeO	0.727*1.1113=Fe2O3		0.808	Fe2O3	0.85
MgO	0.079			MgO	0.08
MnO	0.037			MnO	0.04
CaO	0.769			CaO	0.81
TiO2	0.074			TiO2	0.08
Na2o	3.466			Na2o	3.65
K2O	4.788			K2O	5.04
TOTAL(O)	94.933	TOTAL(N)	95.014	TOTAL(R)	100.00

20 Best Matches:

1	0.9886	12/3/84	WL-5-19-0.27M T84-13
2	0.9857		DR-14
3	0.9843	7/2/91	EL-1-M T230-5
4	0.9824	5/2/85	WL 3-7 17.51m T93-8
5	0.9824	6/14/91	FLV-176-TC T229-8
6	0.9806	8/18/86	WLC-85-2 (13.65M) T128-2
7	0.9750	07/01/83	KRL71082(CII), T56-3
8	0.9748	08/18/84	WL 3-7-2.66
9	0.9746	5/15/88	WL-4-27 (69.77M) T163-9
10	0.9721	5/22/88	WL-5-16 (73.40m) T164-12
11	0.9712	5/15/88	WL-4-27 (68.59M) T163-8
12	0.9688	8/18/86	WLC-85-2 (11.34M) T128-1
13	0.9681	5/15/88	WL-4-26 (66.50M) T163-7
14	0.9678	5/22/88	WL-5-16 (73.62m) T164-14
15	0.9678	08/18/84	WL 4-26-3.06, T78-12
16	0.9670	3/6/86	6VI84-1-5.5M T117-13
17	0.9662	11/25/83	KRL71082F, T55-5
18	0.9659	6/22/84	KRL-71082 (II-4) (593) T58-4
19	0.9638		DR-12
20	0.9632	07/18/84	DSDP 36-10-2 SSA, T78-5

Elements used in the calculation are:

Na2o
Al2O3
SiO2
K2O
CaO
FeO

***** This sample has been added to the data base *****

Listing of 50 closest matches for COMP. NO. 2822 for elements: Na, Al, Si, K , Ca, Fe Date of Update: 6/25/92

	C.No	Sample Number	Date	SiO2	Al2O3	Fe2O3	MgO	MnO	CaO	TiO2	Na2O	K2O	Total,R	Sim. Co
1	2822	JB-BS-3 T226-8	6/24/92	76.16	13.29	0.85	0.08	0.04	0.81	0.08	3.65	5.04	100.00	1.0000
2	1137	WL-5-19-0.27M T84-13	12/3/84	76.42	13.19	0.85	0.07	0.05	0.82	0.09	3.67	4.84	100.00	0.9886
3	909	DR-14		76.37	13.21	0.87	0.08	0.06	0.80	0.10	3.60	4.90	99.99	0.9857
4	2595	EL-1-M T230-5	7/2/91	76.61	13.14	0.85	0.06	0.04	0.79	0.08	3.64	4.79	100.00	0.9843
5	1239	WL 3-7 17.51m T93-8	5/2/85	76.22	13.30	0.89	0.10	0.03	0.83	0.10	3.61	4.92	100.00	0.9824
6	2590	FLV-176-TC T229-8	6/14/91	76.53	13.22	0.85	0.07	0.06	0.82	0.10	3.44	4.91	100.00	0.9824
7	1571	WLC-85-2 (13.65M) T128-2	8/18/86	76.71	13.06	0.84	0.06	0.06	0.81	0.09	3.43	4.94	100.00	0.9806
8	546	KRL71082(CII), T56-3	07/01/83	76.09	13.39	0.90	0.08	0.03	0.83	0.09	3.74	4.85	100.00	0.9750
9	1037	WL 3-7-2.66	08/18/84	76.74	13.00	0.82	0.06	0.03	0.83	0.08	3.51	4.92	99.99	0.9748
10	1965	WL-4-27 (69.77M) T163-9	5/15/88	76.69	13.07	0.87	0.09	0.05	0.80	0.11	3.38	4.94	100.00	0.9746
11	1983	WL-5-16 (73.40m) T164-12	5/22/88	76.37	13.29	0.81	0.05	0.04	0.75	0.10	3.70	4.89	100.00	0.9721
12	1964	WL-4-27 (68.59M) T163-8	5/15/88	76.85	13.06	0.85	0.04	0.06	0.75	0.06	3.64	4.69	100.00	0.9712
13	1570	WLC-85-2 (11.34M) T128-1	8/18/86	76.89	12.97	0.84	0.04	0.05	0.75	0.08	3.54	4.85	100.01	0.9688
14	1963	WL-4-26 (66.50M) T163-7	5/15/88	76.67	13.24	0.84	0.04	0.04	0.73	0.07	3.66	4.70	99.99	0.9681
15	1985	WL-5-16 (73.62m) T164-14	5/22/88	76.34	13.31	0.83	0.06	0.03	0.73	0.10	3.47	5.13	100.00	0.9678
16	1039	WL 4-26-3.06, T78-12	08/18/84	76.97	12.78	0.86	0.04	0.05	0.73	0.06	3.65	4.87	100.01	0.9678
17	1480	6VI84-1-5.5M T117-13	3/6/86	76.73	13.08	0.87	0.06	0.05	0.74	0.08	3.55	4.85	100.01	0.9670
18	549	KRL71082F, T55-5	11/25/83	76.59	13.26	0.86	0.05	0.05	0.71	0.07	3.59	4.82	100.00	0.9662
19	1033	KRL-71082 (II-4) (593) T58-4	6/22/84	76.44	13.18	0.88	0.05	0.00	0.70	0.07	3.69	4.98	99.99	0.9659
20	907	DR-12		76.27	13.53	0.73	0.09	0.03	0.81	0.12	3.61	4.81	100.00	0.9638
21	1045	DSDP 36-10-2 SSA, T78-5	07/18/84	76.90	12.80	0.85	0.04	0.04	0.72	0.09	3.73	4.83	100.00	0.9632
22	1966	WL-4-30 (78.72M) T163-10	5/15/88	76.62	13.09	0.89	0.09	0.05	0.87	0.09	3.49	4.82	100.01	0.9629
23	1242	WL 4-26 66.33m T93-11	5/2/85	76.65	13.16	0.87	0.05	0.04	0.71	0.05	3.69	4.78	100.00	0.9625
24	696	RSCS2		77.33	12.80	0.89	0.01	0.00	0.81	0.05	3.50	4.60	99.99	0.9624
25	1243	WL 4-26 66.40m T93-12	5/2/85	76.71	13.12	0.83	0.05	0.04	0.71	0.06	3.70	4.78	100.00	0.9613
26	1958	WL-4-17 (39.81M) T162-12	5/15/88	76.91	12.98	0.84	0.04	0.05	0.72	0.05	3.70	4.70	99.99	0.9605
27	1040	WL 4-30-28M, T78-13	07/18/84	76.80	12.82	0.92	0.07	0.03	0.85	0.10	3.44	4.97	100.00	0.9603
28	1982	WL-5-13 (64.49m) T164-11	5/22/88	76.59	13.19	0.83	0.03	0.05	0.70	0.07	3.73	4.80	99.99	0.9597
29	1262	*WL 5-19 78.91m	5/29/85	77.29	12.54	0.79	0.06	0.05	0.84	0.08	3.62	4.73	100.00	0.9588
30	1979	WL-5-12 (61.28m) T164-8	5/22/88	76.51	13.26	0.87	0.04	0.05	0.70	0.07	3.76	4.75	100.01	0.9579
31	1261	*WL 4-30 78.77m t95-10	5/29/85	77.12	12.57	0.89	0.08	0.04	0.86	0.11	3.50	4.83	100.00	0.9579
32	1260	*WL 4-26 6a7.04m t95-7	5/29/85	77.27	12.59	0.84	0.04	0.05	0.74	0.06	3.73	4.70	100.02	0.9576
33	1136	WL-5-13-1.11M T84-12	12/3/84	76.59	13.09	0.89	0.04	0.06	0.71	0.07	3.74	4.82	100.01	0.9572
34	183	KRL7982-19B, T45-4		76.37	13.29	0.83	0.04	0.02	0.71	0.07	3.88	4.79	100.00	0.9569
35	1569	WLC-85-2 (10.65M) T127-14	8/18/86	76.61	13.40	0.87	0.03	0.06	0.70	0.05	3.52	4.76	100.00	0.9560
36	1257	*WL 4-26 66.68m	5/29/85	76.78	12.82	0.88	0.05	0.05	0.75	0.07	3.86	4.73	99.99	0.9554
37	2569	JB-BS-6 T227-3	6/13/91	76.39	13.29	0.83	0.04	0.06	0.71	0.06	3.88	4.74	100.00	0.9552
38	1300	WL 5-13 64.51M T99-15	07/01/85	77.18	12.74	0.88	0.04	0.06	0.73	0.07	3.53	4.78	100.01	0.9547
39	454	679-340, T31-2		76.57	13.20	0.84	0.03	0.03	0.70	0.07	3.84	4.71	99.99	0.9542
40	1977	WL-5-7 (50.91m) T164-6	5/21/88	76.58	13.13	0.93	0.04	0.05	0.71	0.08	3.54	4.94	100.00	0.9538
41	1258	*WL 4-26 66.79m t95-5	5/29/85	76.94	12.84	0.81	0.05	0.04	0.73	0.07	3.77	4.75	100.00	0.9535
42	545	KRL7982-17, T50-4	02/01/83	76.61	13.14	0.87	0.03	0.04	0.68	0.05	3.77	4.79	99.98	0.9530
43	1238	WL 2-7 21.02m T93-7	5/1/85	76.85	13.15	0.89	0.05	0.04	0.71	0.05	3.48	4.78	100.00	0.9523
44	1962	WL-4-25 (62.76M) T164-6	5/15/88	76.91	12.91	0.79	0.05	0.05	0.70	0.09	3.62	4.87	99.99	0.9522
45	495	IIB, T32-1		76.58	13.16	0.87	0.03	0.06	0.71	0.05	3.87	4.68	100.01	0.9517
46	1259	*WL 4-26 66.87m t95-6	5/29/85	77.01	12.69	0.88	0.04	0.04	0.73	0.09	3.81	4.71	100.00	0.9506
47	1956	WL-4-13 (33.32M) T162-10	5/15/88	76.98	12.91	0.86	0.04	0.04	0.65	0.06	3.60	4.85	99.99	0.9500
48	2644	JB-BS-17 T241-8	10/21/91	76.22	13.28	0.84	0.04	0.08	0.70	0.05	4.04	4.76	100.01	0.9498
49	1959	WL-4-18 (43.53M) T162-13	5/15/88	77.01	12.97	0.82	0.04	0.04	0.67	0.06	3.63	4.77	100.01	0.9496
50	1951	WL-4-8B (21.275M) T162-5	5/14/88	76.67	13.13	0.82	0.06	0.07	0.65	0.12	3.47	5.01	100.00	0.9489

SAMPLE: T227-1 JB-BS-4

PT	BEAM COUNTS	NA COUNTS	9 SD	MG COUNTS	8 SD	AL COUNTS	3 SD	SI COUNTS	7 SD	K COUNTS	2 SD	CA COUNTS	6 SD	TI COUNTS	5 SD	MN COUNTS	1 SD	FE COUNTS	4 SD
1	13535	2663	52	144	12	14337	120	25821	161	8458	92	916	30	18	4	106	10	596	24
2	13539	2725	43	150	4	14289	34	26114	207	8513	39	966	35	29	8	110	3	595	1
3	13536	2449	145	149	3	13483	480	24604	801	7878	352	872	47	27	6	102	4	553	25
4	13548	2570	120	168	10	14493	454	26183	734	8830	397	937	40	33	6	126	10	496	47
5	13547	2513	111	177	14	14330	401	26395	712	9178	483	1039	62	23	6	76	18	447	65
6	13544	4187	662	152	13	29858	####	18422	####	955	####	13854	####	11	8	87	18	219	143
7	13538	44	####	131	15	443	####	36553	####	136	####	166	####	15	8	64	21	104	194
8	13543	2597	####	148	14	14349	####	25776	####	8749	####	980	####	22	7	95	20	576	187
9	13544	2451	####	147	13	13846	####	24737	####	8254	####	979	####	27	7	97	18	591	181
10	13552	2644	1000	145	13	14066	####	25378	####	8518	####	985	####	26	7	99	17	630	179
11	13546	2641	950	145	12	14027	####	25463	####	8555	####	993	####	23	6	105	17	645	177
12	13546	2698	907	145	12	14077	####	25971	####	8470	####	936	####	24	6	101	16	587	170
13	13543	2724	870	145	11	14254	####	26081	####	8504	####	973	####	19	6	101	15	595	165
14	13568	2647	837	151	11	14226	####	25895	####	8628	####	938	####	26	6	97	15	622	161
15	13559	36	####	147	11	445	####	36549	####	135	####	162	####	22	6	84	15	91	191
16	13571	5496	####	105	15	27302	####	19901	####	709	####	8949	####	14	6	94	14	121	206
17	13565	2611	####	169	16	14560	####	26058	####	8708	####	1066	####	20	6	98	14	441	200
18	13564	2485	####	154	15	13816	####	25311	####	9424	####	994	####	28	6	92	13	476	194
19	13559	6516	####	130	15	25230	####	20458	####	394	####	6127	####	11	6	69	14	107	205
20	13562	6534	####	136	15	25351	####	21060	####	332	####	5929	####	21	6	64	16	122	213

LINES DELETED: 3 6 7 15 16 19 20

AVE. BEAM CURRENT/SEC = 677

DATA REDUCED USING $B-AL; #GL9M

ON SPECIMEN: T227-1 JB-BS-4

$B-AL VERSION 1.0

OXIDE FORM.	WEIGHT% (OXIDE)	STD.DEV. (%)	HOMO. INDEX	FORMULA	K-RATIO	UNKN PEAK (COUNTS)	UNKN BKGD (COUNTS)	COUNTING TIME(SEC)	STD PEAK (COUNTS)	STD BKGD (COUNTS)	COUNTING TIME(SEC)	STANDARD FILENAME
NA2O	~~3.961~~ 3.811	2.86	1.717	0.000	1.02240	2613.0	47.6	20.00	2556.2	47.0	20.00	ZRGSC
MGO	0.030	93.66	0.891	0.000	0.00783	152.9	134.8	20.00	2448.4	135.3	20.00	ZRGSC
AL2O3	12.394	1.20	1.909	0.000	0.94468	14205.4	245.3	20.00	15024.3	246.7	20.00	Z5831
SIO2	74.118	0.88	2.808	0.000	1.00366	25783.3	52.8	20.00	25689.8	53.2	20.00	Z5831
K2O	4.564	1.66	2.481	0.000	1.25191	8599.4	135.2	20.00	6904.5	143.5	20.00	ZRGSC
CAO	0.531	4.37	1.337	0.000	0.10408	977.0	172.8	20.00	7912.2	185.5	20.00	ZRGSC
TIO2	0.055	69.11	0.863	0.000	0.00050	24.4	15.3	20.00	18243.6	25.1	20.00	ZTIO2
MNO	0.055	47.22	1.128	0.000	0.00055	100.1	70.0	20.00	55217.4	137.4	20.00	ZMN2O
FEO	0.905	5.79	2.975	0.000	0.14139	561.4	95.8	20.00	3397.2	104.0	20.00	ZRGSC

TOTAL ~~96.613~~ 96.471 NO. OXYGENS = 0 NO. ITERS. = 2 AVE. ATOMIC NO. = 11.10

Listing of 25 closest matches for COMP. NO. 2567 for elements: Na, Al, Si, K , Ca, Fe Date of Update: 06/18/92

	C.No	Sample Number	Date	SiO2	Al2O3	Fe2O3	MgO	MnO	CaO	TiO2	Na2O	K2O	Total,R	Sim. Co
1	2567	JB-BS-4 T227-1	6/13/91	76.75	12.83	1.04	0.03	0.06	0.55	0.06	3.95	4.73	100.00	1.0000
2	1806	OD-ML-65CM T143-7	6/24/87	76.81	12.80	1.05	0.03	0.05	0.56	0.05	3.96	4.70	100.01	0.9934
3	2563	SS-91-1-Adgss	8/7/91	76.73	12.85	1.04	0.03	0.05	0.53	0.07	3.95	4.74	99.99	0.9933
4	1310	WL 8-2B 172-174.5CM T99-10	7/1/85	76.90	12.74	1.05	0.02	0.05	0.56	0.07	3.91	4.71	100.01	0.9915
5	562	KRL82282A(P), T66-6	xx/xx/83	76.86	12.85	1.05	0.03	0.06	0.54	0.05	3.87	4.70	100.01	0.9905
6	1418	BL-RSA-4 T112-9	10/23/85	76.83	12.79	1.08	0.04	0.04	0.55	0.06	3.96	4.65	100.00	0.9899
7	2236	SL-115.5 T186-3	2/28/89	76.76	12.91	1.07	0.03	0.04	0.55	0.06	3.84	4.73	99.99	0.9896
8	2568	JB-BS-5 T227-2	6/13/91	76.69	12.91	1.08	0.02	0.05	0.55	0.09	3.90	4.70	99.99	0.9895
9	1680	KRL 860922 A T134-2	11/25/86	76.94	12.75	1.07	0.03	0.04	0.55	0.06	3.91	4.65	100.00	0.9894
10	1036	WL 2-3-2.01, T78-9	08/18/84	77.05	12.74	1.05	0.02	0.04	0.55	0.05	3.82	4.67	99.99	0.9890
11	1034	WL 2-2-2.64, T78-7	08/18/84	77.06	12.62	1.06	0.03	0.05	0.55	0.06	3.86	4.71	100.00	0.9890
12	1225	WL CORE G 380cm T92-8	5/2/85	76.82	12.79	1.06	0.04	0.04	0.56	0.06	4.00	4.65	100.02	0.9883
13	1141	WL-2-3-1.94M T85-1	12/4/84	76.97	12.65	1.05	0.03	0.05	0.56	0.05	4.00	4.66	100.02	0.9881
14	1142	WL-2-3-2.14M T85-2	12/4/84	76.97	12.69	1.06	0.03	0.05	0.56	0.06	3.96	4.63	100.01	0.9876
15	2559	SS-91-1-2 T232-3	8/7/91	77.11	12.63	1.03	0.03	0.05	0.54	0.06	3.89	4.67	100.01	0.9873
16	2558	SS-91-1-SU T232-1	8/6/91	76.74	12.86	1.09	0.04	0.04	0.54	0.05	3.95	4.68	99.99	0.9872
17	2557	SS-91-1-1 T232-2	6/8/91	76.57	12.92	1.07	0.02	0.04	0.54	0.06	4.05	4.72	99.99	0.9863
18	1224	WL CORE G 370cm T92-7	5/2/85	76.83	12.82	1.09	0.04	0.04	0.54	0.05	3.95	4.65	100.01	0.9862
19	682	KRL-91882G, T66-11	10/25/83	76.91	12.76	1.07	0.03	0.06	0.54	0.07	3.87	4.68	99.99	0.9859
20	1684	SCHURZ-1 T134-6	11/25/86	77.01	12.64	1.09	0.03	0.05	0.55	0.05	3.94	4.64	100.00	0.9857
21	1025	KRL-71082C (590) T58-1	6/22/84	76.91	12.71	1.08	0.02	0.00	0.53	0.05	3.95	4.74	99.99	0.9855
22	2110	KRL-82982-F T174-14	10/28/88	76.85	12.91	1.02	0.02	0.05	0.56	0.09	3.84	4.66	100.00	0.9855
23	2795	FLV-209-BC T254-6	4/14/92	76.36	13.11	1.09	0.03	0.06	0.55	0.07	4.01	4.73	100.01	0.9855
24	2718	FLV-202-D T249-6	1/30/92	76.79	12.79	1.06	0.02	0.04	0.58	0.07	3.96	4.68	99.99	0.9854
25	1472	KRL 82182 (A-1) T117-3	3/6/86	76.80	12.75	1.10	0.03	0.04	0.55	0.07	3.87	4.77	99.98	0.9850

SAMPLE: T227-2 JB-BS-5

PT	BEAM COUNTS	NA COUNTS	9 SD	MG COUNTS	8 SD	AL COUNTS	3 SD	SI COUNTS	7 SD	K COUNTS	2 SD	CA COUNTS	6 SD	TI COUNTS	5 SD	MN COUNTS	1 SD	FE COUNTS	4 SD
1	13546	2481	50	147	12	14541	121	26218	162	8586	93	1056	32	31	6	101	10	574	24
2	13542	2679	140	150	2	14623	58	26076	100	8486	71	1017	27	33	1	99	1	602	20
3	13540	2573	99	144	3	14415	105	25818	203	8617	69	988	34	19	8	111	6	625	26
4	13544	2303	160	135	6	12171	****	22558	****	7422	574	880	75	15	9	85	11	479	64
5	13546	2520	138	148	6	14452	****	25472	****	8563	513	1026	68	23	8	102	9	607	58
6	13542	2560	125	161	8	14309	944	25588	****	8679	480	970	61	29	7	127	14	571	52
7	13542	2472	116	133	9	13937	864	24794	****	8130	449	958	57	20	7	114	13	576	47
8	13545	2589	111	181	15	14450	811	25862	****	8377	416	998	53	28	6	104	12	592	44
9	13547	2608	107	164	15	14528	771	26053	****	8731	408	1018	51	83	20	98	12	678	53
10	13553	2545	101	138	15	13993	729	25351	****	8267	387	870	61	31	19	63	17	455	66
11	13557	2615	99	139	14	14581	704	25819	****	8838	392	941	59	27	18	104	16	570	62
12	13548	2597	96	123	16	14295	672	26015	997	8612	377	937	58	27	17	89	16	584	60
13	13545	2606	93	145	15	14262	644	25891	961	8614	365	980	55	26	17	96	15	563	57
14	13545	2592	91	150	15	14065	620	26057	936	8646	354	1016	54	34	16	108	15	612	56
15	13548	2660	91	154	14	14378	599	26114	914	8469	341	969	52	20	16	102	14	568	54
16	13547	2612	89	150	14	14056	580	25548	883	8671	333	986	51	24	15	97	14	608	53
17	13553	2576	87	141	13	14240	562	26006	861	8591	324	942	50	28	15	100	13	578	51
18	13553	2542	84	152	13	13669	559	25134	842	8175	323	855	56	24	14	106	13	418	62
19	13556	2532	82	156	13	14049	544	25459	819	8497	314	978	54	22	14	92	13	606	61
20	13552	2506	81	147	12	14099	529	25162	803	8461	305	869	57	34	14	91	13	435	67

LINES DELETED: 4 7 18

AVE. BEAM CURRENT/SEC = 677

DATA REDUCED USING $B-AL: #GL9M

ON SPECIMEN: T227-2 JB-BS-5

$B-AL VERSION 1.0

OXIDE FORM.	WEIGHT% (OXIDE)	STD.DEV. (%)	HOMO. INDEX	FORMULA	K-RATIO	UNKN PEAK (COUNTS)	UNKN BKGD (COUNTS)	COUNTING TIME(SEC)	STD PEAK (COUNTS)	STD BKGD (COUNTS)	COUNTING TIME(SEC)	STANDARD FILENAME
NA2O	~~3.910~~ 3.764	2.87	1.023	0.000	1.00911	2579.6	47.6	20.00	2556.2	47.0	20.00	%RGSC
MGO	0.024	116.25	1.020	0.000	0.00627	149.3	134.8	20.00	2448.4	135.3	20.00	%RGSC
AL2O3	12.487	1.20	1.714	0.000	0.95200	14313.8	245.4	20.00	15024.3	246.7	20.00	%5831
SIO2	74.158	0.88	1.920	0.000	1.00410	25794.6	52.9	20.00	25689.8	53.2	20.00	%5831
K2O	4.549	1.66	1.470	0.000	1.24769	8570.9	135.2	20.00	6904.5	143.5	20.00	%RGSC
CAO	0.529	4.38	1.637	0.000	0.10370	974.2	172.9	20.00	7912.2	185.5	20.00	%RGSC
TIO2	0.091	44.63	2.581	0.000	0.00083	30.5	15.3	20.00	18243.6	25.1	20.00	%TIO2
MNO	0.053	44.90	1.283	0.000	0.00053	99.0	70.0	20.00	55217.4	137.4	20.00	%MN2O
FEO	0.937	5.68	2.390	0.000	0.14641	578.0	95.9	20.00	3397.2	104.0	20.00	%RGSC

TOTAL ~~[illegible]~~ 96.597 NO. OXYGENS = 0 NO. ITERS. = 2 AVE. ATOMIC NO. = 11.10

Listing of 25 closest matches for COMP. NO. 2568 for elements: Na, Al, Si, K , Ca, Fe Date of Update: 06/18/92

	C.No	Sample Number	Date	SiO2	Al2O3	Fe2O3,	MgO	MnO	CaO	TiO2	Na2O	K2O	Total,R	Sim. Co
1	2568	JB-BS-5 T227-2	6/13/91	76.69	12.91	1.08	0.02	0.05	0.55	0.09	3.90	4.70	99.99	1.0000
2	2235	SL-103 T186-2	2/28/89	76.68	12.95	1.10	0.03	0.04	0.55	0.07	3.88	4.69	99.99	0.9952
3	2236	SL-115.5 T186-3	2/28/89	76.76	12.91	1.07	0.03	0.04	0.55	0.06	3.84	4.73	99.99	0.9947
4	1418	BL-RSA-4 T112-9	10/23/85	76.83	12.79	1.08	0.04	0.04	0.55	0.06	3.96	4.65	100.00	0.9938
5	1680	KRL 860922 A T134-2	11/25/86	76.94	12.75	1.07	0.03	0.04	0.55	0.06	3.91	4.65	100.00	0.9937
6	2570	JB-BS-7 T227-4	6/13/91	76.73	12.89	1.10	0.03	0.05	0.54	0.06	3.91	4.69	100.00	0.9928
7	1244	WL 8-3A ASH A 64-66cm T93-13	5/2/85	76.97	12.80	1.08	0.03	0.05	0.55	0.05	3.86	4.60	99.99	0.9927
8	2558	SS-91-1-SU T232-1	8/6/91	76.74	12.86	1.09	0.04	0.04	0.54	0.05	3.95	4.68	99.99	0.9919
9	570	KRL91982D, T66-10	xx/xx/83	76.81	12.89	1.08	0.03	0.05	0.53	0.06	3.90	4.65	100.00	0.9916
10	681	KRL-91882A', T66-8	10/25/83	76.79	12.83	1.10	0.03	0.06	0.54	0.07	3.91	4.67	100.00	0.9912
11	682	KRL-91882G, T66-11	10/25/83	76.91	12.76	1.07	0.03	0.06	0.54	0.07	3.87	4.68	99.99	0.9910
12	1186	WALKER LAKE CORE G 380CM t89-1	2/28/85	76.98	12.79	1.08	0.02	0.05	0.54	0.05	3.86	4.64	100.01	0.9910
13	1472	KRL 82182 (A-1) T117-3	3/6/86	76.80	12.75	1.10	0.03	0.04	0.55	0.07	3.87	4.77	99.98	0.9909
14	1684	SCHURZ-1 T134-6	11/25/86	77.01	12.64	1.09	0.03	0.05	0.55	0.05	3.94	4.64	100.00	0.9905
15	1034	WL 2-2-2.64, T78-7	08/18/84	77.06	12.62	1.06	0.03	0.05	0.55	0.06	3.86	4.71	100.00	0.9903
16	783	GS-27		76.74	12.92	1.12	0.03	0.05	0.55	0.07	3.91	4.61	100.00	0.9902
17	1224	WL CORE G 370cm T92-7	5/2/85	76.83	12.82	1.09	0.04	0.04	0.54	0.05	3.95	4.65	100.01	0.9901
18	1228	WL 8-2B 130-134cm T92-12	5/2/85	77.03	12.81	1.08	0.04	0.04	0.55	0.04	3.77	4.63	99.99	0.9899
19	1621	BO-18 JOD	09/12/86	76.98	12.70	1.10	0.03	0.05	0.55	0.07	3.83	4.68	99.99	0.9899
20	562	KRL82282A(P), T66-6	xx/xx/83	76.86	12.85	1.05	0.03	0.06	0.54	0.05	3.87	4.70	100.01	0.9899
21	2795	FLV-209-BC T254-6	4/14/92	76.36	13.11	1.09	0.03	0.06	0.55	0.07	4.01	4.73	100.01	0.9896
22	2567	JB-BS-4 T227-1	6/13/91	76.75	12.83	1.04	0.03	0.06	0.55	0.06	3.95	4.73	100.00	0.9895
23	1948	WL-4-4 (12.25M) T162-2	5/14/88	76.87	12.86	1.09	0.02	0.05	0.54	0.06	3.80	4.72	100.01	0.9894
24	1416	BL-RSA-2 T112-7	10/23/85	76.78	12.85	1.12	0.04	0.03	0.54	0.06	3.90	4.68	100.00	0.9893
25	1241	WL 4-2 3.31m T93-10	5/2/85	76.69	12.91	1.14	0.04	0.04	0.55	0.06	3.92	4.67	100.02	0.9893

SAMPLE: T2 JB-BS-6

PT	BEAM COUNTS	NA COUNTS	9 SD	MG COUNTS	8 SD	AL COUNTS	3 SD	SI COUNTS	7 SD	K COUNTS	2 SD	CA COUNTS	6 SD	TI COUNTS	5 SD	MN COUNTS	1 SD	FE COUNTS	4 SD
1	13550	2378	49	143	12	14240	119	24667	157	8400	92	1143	34	34	6	91	10	482	22
2	13555	2469	64	169	18	14234	4	24718	36	8417	12	1137	4	16	13	84	5	441	29
3	13559	2476	54	146	14	14027	121	24499	114	8305	60	1142	3	27	9	99	7	408	37
4	13557	2508	56	164	13	14190	99	24566	98	8490	76	1316	88	26	7	112	12	453	31
5	13561	2447	48	162	12	14458	154	24388	132	8873	220	1180	76	28	6	99	10	419	29
6	13564	2584	68	138	13	14209	138	25015	217	8466	197	1117	73	24	6	103	10	477	30
7	13560	2465	62	160	12	14341	133	24692	199	8380	185	1210	68	21	6	92	9	454	28
8	13565	2501	58	184	15	14443	142	25038	230	8382	175	1233	66	33	6	107	9	451	26
9	13561	2492	55	162	14	14465	148	24963	233	8304	172	1227	64	19	6	99	9	462	25
10	13561	2429	54	150	14	14155	146	24855	223	8189	181	1144	62	19	6	108	9	480	25
11	13565	2232	89	186	16	14391	143	24920	218	8956	236	1127	61	28	6	94	8	473	25
12	13567	2418	86	170	15	14070	150	25054	225	8386	226	1145	59	20	6	92	8	452	23
13	13567	2564	88	157	14	14339	145	24677	218	8422	217	1154	57	33	6	105	8	433	23
14	13562	2400	86	157	14	14369	141	25416	271	8706	219	1125	56	29	6	109	8	446	22
15	13564	2531	85	154	14	14206	138	25106	271	8207	222	1119	56	26	6	108	8	435	22
16	13559	2459	82	166	13	14165	136	24678	265	8404	215	1176	54	24	5	100	8	455	21
17	13564	2280	91	188	14	14219	132	25192	271	8845	228	1366	71	21	5	99	8	488	22
18	13564	2384	89	144	15	14247	128	24916	264	8294	226	1189	69	24	5	78	9	466	22
19	13564	2484	87	155	14	14200	125	24920	257	8377	220	1168	67	29	5	108	9	466	22
20	13564	2412	85	142	14	14059	130	24797	250	8466	214	1145	66	20	5	89	9	460	21

LINES DELETED:

LINES DELETED: 5 11 14 17

AVE. BEAM CURRENT/SEC = 678

DATA REDUCED USING $B-AL: #GL9M

ON SPECIMEN: T227-3 JB-BS-6

$B-AL VERSION 1.0

OXIDE FORM.	WEIGHT% (OXIDE)	STD.DEV. (%)	HOMO. INDEX	FORMULA	K-RATIO	UNKN PEAK (COUNTS)	UNKN BKGD (COUNTS)	COUNTING TIME(SEC)	STD PEAK (COUNTS)	STD BKGD (COUNTS)	COUNTING TIME(SEC)	STANDARD FILENAME
NA2O	~~3.745~~ 3.630	2.90	1.187	0.000	0.96623	2472.1	47.7	20.00	2556.2	47.0	20.00	%RGSC
MGO	0.035	78.94	0.996	0.000	0.00935	156.3	134.7	20.00	2448.4	135.3	20.00	%RGSC
AL2O3	12.443	1.20	1.046	0.000	0.94609	14224.5	243.6	20.00	15024.3	246.7	20.00	%5831
SIO2	71.499	0.89	1.184	0.000	0.96620	24822.5	52.4	20.00	25689.8	53.2	20.00	%5831
K2O	4.476	1.67	0.953	0.000	1.21788	8368.1	134.0	20.00	6904.5	143.5	20.00	%RGSC
CAO	0.660	3.84	1.521	0.000	0.12964	1172.8	171.1	20.00	7912.2	185.5	20.00	%RGSC
TIO2	0.057	66.17	1.103	0.000	0.00052	24.6	15.1	20.00	18243.6	25.1	20.00	%TIO2
MNO	0.053	44.49	0.990	0.000	0.00053	98.3	69.1	20.00	55217.4	137.4	20.00	%MN20
FEO	0.700	6.75	0.902	0.000	0.10934	454.8	94.7	20.00	3397.2	104.0	20.00	%RGSC

93.514

TOTAL ~~93.4[illegible]~~ NO. OXYGENS = 6 NO. ITERS = [illegible] AVE. ATOMIC NO. = 10.[illegible]

Listing of 25 closest matches for COMP. NO. 2569 for elements: Na, Al, Si, K , Ca, Fe Date of Update: 06/18/92

	C.No	Sample Number	Date	SiO2	Al2O3	Fe2O3	MgO	MnO	CaO	TiO2	Na2O	K2O	Total,R	Sim. Co
1	2569	JB-BS-6 T227-3	6/13/91	76.39	13.29	0.83	0.04	0.06	0.71	0.06	3.88	4.74	100.00	1.0000
2	183	KRL7982-19B, T45-4		76.37	13.29	0.83	0.04	0.02	0.71	0.07	3.88	4.79	100.00	0.9982
3	454	679-340, T31-2		76.57	13.20	0.84	0.03	0.03	0.70	0.07	3.84	4.71	99.99	0.9914
4	1243	WL 4-26 66.40m T93-12	5/2/85	76.71	13.12	0.83	0.05	0.04	0.71	0.06	3.70	4.78	100.00	0.9880
5	2644	JB-BS-17 T241-8	10/21/91	76.22	13.28	0.84	0.04	0.08	0.70	0.05	4.04	4.76	100.01	0.9879
6	495	IIB, T32-1		76.58	13.16	0.87	0.03	0.06	0.71	0.05	3.87	4.68	100.01	0.9878
7	1982	WL-5-13 (64.49m) T164-11	5/22/88	76.59	13.19	0.83	0.03	0.05	0.70	0.07	3.73	4.80	99.99	0.9874
8	182	KRL7982-16, T45-3		76.66	13.17	0.83	0.03	0.02	0.68	0.07	3.91	4.64	100.01	0.9861
9	1979	WL-5-12 (61.28m) T164-8	5/22/88	76.51	13.26	0.87	0.04	0.05	0.70	0.07	3.76	4.75	100.01	0.9838
10	1958	WL-4-17 (39.81M) T162-12	5/15/88	76.91	12.98	0.84	0.04	0.05	0.72	0.05	3.70	4.70	99.99	0.9815
11	1963	WL-4-26 (66.50M) T163-7	5/15/88	76.67	13.24	0.84	0.04	0.04	0.73	0.07	3.66	4.70	99.99	0.9814
12	572	KRL91982J, T64-14	09/06/83	76.90	12.98	0.83	0.02	0.05	0.67	0.06	3.85	4.65	100.01	0.9812
13	1242	WL 4-26 66.33m T93-11	5/2/85	76.65	13.16	0.87	0.05	0.04	0.71	0.05	3.69	4.78	100.00	0.9806
14	1258	*WL 4-26 66.79m t95-5	5/29/85	76.94	12.84	0.81	0.05	0.04	0.73	0.07	3.77	4.75	100.00	0.9795
15	2709	FLV-194-BC T246-3	12/12/91	76.50	12.97	0.88	0.05	0.05	0.72	0.06	4.00	4.75	99.98	0.9786
16	1974	WL-5-5 (36.93m) T164-3	5/21/88	76.69	13.09	0.83	0.03	0.05	0.66	0.06	3.79	4.82	100.02	0.9785
17	756	BO-5		76.29	13.42	0.90	0.04	0.06	0.70	0.08	3.80	4.71	100.00	0.9784
18	549	KRL71082F, T55-5	11/25/83	76.59	13.26	0.86	0.05	0.05	0.71	0.07	3.59	4.82	100.00	0.9782
19	1975	WL-5-6 (39.31m) T164-4	5/21/88	76.69	13.10	0.82	0.04	0.05	0.66	0.07	3.79	4.78	100.00	0.9780
20	1976	WL-5-6 (40.08m) T164-5	5/21/88	76.68	13.08	0.82	0.03	0.05	0.66	0.06	3.81	4.82	100.01	0.9772
21	1136	WL-5-13-1.11M T84-12	12/3/84	76.59	13.09	0.89	0.04	0.06	0.71	0.07	3.74	4.82	100.01	0.9770
22	1045	DSDP 36-10-2 SSA, T78-5	07/18/84	76.90	12.80	0.85	0.04	0.04	0.72	0.09	3.73	4.83	100.00	0.9770
23	545	KRL7982-17, T50-4	02/01/83	76.61	13.14	0.87	0.03	0.04	0.68	0.05	3.77	4.79	99.98	0.9765
24	2565	SS-91-1 high Ca SS	8/7/91	77.12	12.77	0.83	0.03	0.05	0.67	0.05	3.79	4.67	99.98	0.9762
25	1983	WL-5-16 (73.40m) T164-12	5/22/88	76.37	13.29	0.81	0.05	0.04	0.75	0.10	3.70	4.89	100.00	0.9742

SAMPLE: '-4 JB-BS-7

PT	BEAM COUNTS	NA COUNTS	9 SD	MG COUNTS	8 SD	AL COUNTS	3 SD	SI COUNTS	7 SD	K COUNTS	2 SD	CA COUNTS	6 SD	TI COUNTS	5 SD	MN COUNTS	1 SD	FE COUNTS	4 SD
1	13563	5054	71	131	11	26887	164	20293	142	2221	47	8479	92	20	4	83	9	218	15
2	13558	2561	****	164	23	14404	****	25712	****	8565	****	1007	****	22	1	98	11	590	264
3	13562	2652	****	136	18	14477	****	25987	****	8413	****	950	****	35	8	83	9	570	210
4	13562	2550	****	143	15	14295	****	25461	****	8290	****	968	****	22	7	91	7	582	182
5	13567	2560	****	173	18	14268	****	25875	****	8671	****	982	****	32	7	97	7	533	159
6	13561	2727	1000	155	16	14534	****	26217	****	8671	****	962	****	21	6	91	6	555	144
7	13581	2508	933	143	15	13981	****	25566	****	8235	****	890	****	28	6	95	6	609	137
8	13588	2595	873	154	14	14265	****	26298	****	8477	****	1002	****	31	6	110	9	579	128
9	13588	2673	820	127	15	14618	****	26486	****	8723	****	929	****	29	5	107	9	551	120
10	13585	3402	791	167	16	32138	****	18016	****	475	****	16859	****	27	5	81	10	225	149
11	13586	2624	756	177	17	14182	****	25345	****	8485	****	860	****	33	5	89	9	764	162
12	13577	47	****	121	19	605	****	35257	****	158	****	169	****	23	5	67	12	111	195
13	13588	2656	****	163	18	14403	****	25418	****	8640	****	951	****	27	5	103	12	602	190
14	13593	2651	****	148	18	14096	****	25386	****	8342	****	1011	****	22	5	103	12	594	184
15	13591	2448	972	137	17	13924	****	25212	****	8253	****	932	****	29	5	123	14	557	178
16	13594	2652	939	147	17	14366	****	26246	****	8405	****	949	****	19	5	99	13	604	173
17	13593	2558	909	143	16	14133	****	25781	****	8318	****	984	****	20	5	90	13	626	170
18	13595	2572	882	145	16	14414	****	26136	****	8718	****	1034	****	12	6	93	12	523	165
19	13592	4223	931	138	16	29612	****	19084	****	1397	****	12845	****	12	6	77	13	250	172
20	13593	2440	909	164	16	14602	****	26526	****	9731	****	1015	****	19	6	116	13	607	169

LINES DELETED: 1 10 12 19

AVE. BEAM CURRENT/SEC = 679

DATA REDUCED USING $B-AL: #GL9M

ON SPECIMEN: T227-4 JB-BS-7

$B-AL VERSION 1.0

OXIDE FORM.	WEIGHT% (OXIDE)	STD.DEV. (%)	HOMO. INDEX	FORMULA	K-RATIO	UNKN PEAK (COUNTS)	UNKN BKGD (COUNTS)	COUNTING TIME(SEC)	STD PEAK (COUNTS)	STD BKGD (COUNTS)	COUNTING TIME(SEC)	STANDARD FILENAME
NA2O	3.783 ~~3.929~~	2.87	1.579	0.000	1.01296	2589.3	47.6	20.00	2556.2	47.0	20.00	ZRGSC
MGO	0.027	102.80	1.144	0.000	0.00711	151.2	134.8	20.00	2448.4	135.3	20.00	ZRGSC
AL2O3	12.482	1.20	1.732	0.000	0.95175	14310.1	245.5	20.00	15024.3	246.7	20.00	Z5831
SIO2	74.320	0.88	2.674	0.000	1.00639	25853.2	52.9	20.00	25689.8	53.2	20.00	Z5831
K2O	4.542	1.66	3.837	0.000	1.24587	8558.6	135.3	20.00	6904.5	143.5	20.00	ZRGSC
CAO	0.523	4.42	1.508	0.000	0.10239	964.1	173.0	20.00	7912.2	185.5	20.00	ZRGSC
TIO2	0.058	65.85	1.265	0.000	0.00053	25.0	15.3	20.00	18243.6	25.1	20.00	ZTIO2
MNO	0.053	45.04	1.063	0.000	0.00052	93.9	70.1	20.00	55217.4	137.4	20.00	ZMN20
FEO	0.[illegible]1	5.59	2.242	0.000	0.15018	590.5	95.9	20.00	3397.2	104.0	20.00	ZRGSC

TOTAL 96.749 ~~96.[illegible]~~ NO. OXYGENS = 0 NO. ITERS. = 2 AVE. ATOMIC NO. = 11.11

[illegible]

Listing of 25 closest matches for COMP. NO. 2570 for elements: Na, Al, Si, K , Ca, Fe Date of Update: 06/18/92

	C.No	Sample Number	Date	SiO2	Al2O3	Fe2O3	MgO	MnO	CaO	TiO2	Na2O	K2O	Total,R	Sim. Co
1	2570	JB-BS-7 T227-4	6/13/91	76.73	12.89	1.10	0.03	0.05	0.54	0.06	3.91	4.69	100.00	1.0000
2	681	KRL-91882A', T66-8	10/25/83	76.79	12.83	1.10	0.03	0.06	0.54	0.07	3.91	4.67	100.00	0.9984
3	2558	SS-91-1-SU T232-1	8/6/91	76.74	12.86	1.09	0.04	0.04	0.54	0.05	3.95	4.68	99.99	0.9960
4	566	KRL91882B, T64-12	09/06/83	76.81	12.82	1.10	0.01	0.05	0.53	0.08	3.91	4.69	100.00	0.9958
5	1416	BL-RSA-2 T112-7	10/23/85	76.78	12.85	1.12	0.04	0.03	0.54	0.06	3.90	4.68	100.00	0.9956
6	2235	SL-103 T186-2	2/28/89	76.68	12.95	1.10	0.03	0.04	0.55	0.07	3.88	4.69	99.99	0.9948
7	1224	WL CORE G 370cm T92-7	5/2/85	76.83	12.82	1.09	0.04	0.04	0.54	0.05	3.95	4.65	100.01	0.9943
8	2717	FLV-201-TO T249-5	1/30/92	76.85	12.77	1.10	0.02	0.04	0.54	0.04	3.99	4.65	100.00	0.9934
9	560	KRL82282, T66-4	xx/xx/83	76.74	12.90	1.13	0.02	0.06	0.54	0.06	3.87	4.68	100.00	0.9934
10	760	BO-16		76.59	12.92	1.11	0.03	0.03	0.54	0.07	4.00	4.71	100.00	0.9933
11	2568	JB-BS-5 T227-2	6/13/91	76.69	12.91	1.08	0.02	0.05	0.55	0.09	3.90	4.70	99.99	0.9928
12	2493	FLV-156-SS T219-3	12/20/90	76.64	13.06	1.09	0.03	0.04	0.54	0.05	3.94	4.62	100.01	0.9924
13	1948	WL-4-4 (12.25M) T162-2	5/14/88	76.87	12.86	1.09	0.02	0.05	0.54	0.06	3.80	4.72	100.01	0.9920
14	570	KRL91982D, T66-10	xx/xx/83	76.81	12.89	1.08	0.03	0.05	0.53	0.06	3.90	4.65	100.00	0.9919
15	2060	FLV-64-CS T170-7	9/3/88	76.71	12.87	1.11	0.02	0.04	0.54	0.04	4.02	4.64	99.99	0.9919
16	1290	WL 8-1B 92-94cm T99-1	07/01/85	76.99	12.72	1.11	0.02	0.06	0.54	0.07	3.84	4.65	100.00	0.9913
17	1947	WL-4-4 (10.83M) T162-1	5/14/88	76.86	12.94	1.10	0.04	0.06	0.54	0.06	3.77	4.64	100.01	0.9913
18	682	KRL-91882G, T66-11	10/25/83	76.91	12.76	1.07	0.03	0.06	0.54	0.07	3.87	4.68	99.99	0.9913
19	1186	WALKER LAKE CORE G 380CM t89-1	2/28/85	76.98	12.79	1.08	0.02	0.05	0.54	0.05	3.86	4.64	100.01	0.9912
20	783	GS-27		76.74	12.92	1.12	0.03	0.05	0.55	0.07	3.91	4.61	100.00	0.9907
21	1419	BL-RSA-5 T112-10	10/23/85	76.98	12.65	1.09	0.04	0.04	0.53	0.05	3.93	4.68	99.99	0.9906
22	1472	KRL 82182 (A-1) T117-3	3/6/86	76.80	12.75	1.10	0.03	0.04	0.55	0.07	3.87	4.77	99.98	0.9905
23	1621	BO-18 JOD	09/12/86	76.98	12.70	1.10	0.03	0.05	0.55	0.07	3.83	4.68	99.99	0.9902
24	952	DR-64		76.57	13.01	1.13	0.03	0.05	0.53	0.07	3.90	4.70	99.99	0.9898
25	1241	WL 4-2 3.31m T93-10	5/2/85	76.69	12.91	1.14	0.04	0.04	0.55	0.06	3.92	4.67	100.02	0.9896

SAMPLE: [illegible]41-1   JB-RS-9

	BE	NA	9	MG	8	[illegible]	3	SI	7	K	[illegible]	CA	6	TI	5	MN	1	[illegible]	4
PT	COUNTS	COUNTS	SD	[illegible]	SD	COUNTS	SD	COUNTS	SD	COUNTS	SD	COUNTS	SD	COUNTS	SD	COUNTS	SD	[illegible]	SD
1	14122	2444	[illegible]	127	11	13627	117	25617	160	8386	92	960	31	29	5	127	11	594	24
2	[illegible]	2517	52	143	11	13867	170	26275	465	8611	159	923	[illegible]	32	2	89	27	654	42
3	14128	2383	67	154	14	14244	311	26090	339	9135	[illegible]	983	30	27	3	100	20	480	88
4	14127	5572	****	160	14	27140	****	20990	****	706	****	8050	****	11	9	85	19	123	238
5	14124	2467	****	153	13	[illegible]	[illegible]	26396	****	8671	****	947	****	24	8	114	17	602	[illegible]
6	14135	2514	****	[illegible]	[illegible]	14630	****	27034	****	9157	****	938	****	19	8	[illegible]	[illegible]	582	196
7	14138	[illegible]	[illegible]	152	12	14416	****	27299	****	8958	****	925	****	32	9	113	16	602	182
[illegible]	14138	2375	****	132	12	13646	****	26297	****	8644	****	960	****	32	8	105	15	587	171
9	14132	2450	****	163	13	14212	****	26801	****	[illegible]	****	918	****	30	7	109	14	580	161
10	14138	2474	983	141	13	14346	****	[illegible]	****	8834	****	979	****	23	7	101	13	604	153
11	14138	2466	937	161	13	[illegible]	****	25958	****	8799	****	911	****	22	7	99	13	595	146
12	14132	45	****	132	13	485	****	38274	****	161	****	162	****	12	7	74	15	89	192
13	[illegible]	2493	****	140	12	13960	****	26253	****	8505	****	919	****	21	7	102	14	569	184
14	14124	46	****	127	13	508	****	38075	****	152	****	189	****	16	7	86	15	99	209
15	14119	2554	****	147	13	14315	****	26790	****	8573	****	929	****	30	7	101	14	609	204
16	14123	2604	****	159	13	21407	****	23364	****	21540	****	496	****	19	7	83	14	130	217
17	14112	33	****	[illegible]	[illegible]	480	****	38450	****	137	****	177	****	14	7	101	[illegible]	91	229
18	14113	2331	****	134	13	13846	****	26132	****	9273	****	874	****	23	7	102	14	541	223
19	14098	6098	****	157	13	24089	****	22422	****	2965	****	4056	****	22	7	81	14	160	227
20	14099	2569	****	138	13	13955	****	26397	****	8464	****	939	****	29	7	113	14	573	223

LINES DELETED: 4 12 14 17 19 16 3

AVE. BEAM CURRENT/SEC =   706

DATA REDUCED USING $B-AL: $GL9M

ON SPECIMEN: T241-1 JB-RS-9

$B-AL VERSION 1.0

OXIDE FORM.	WEIGHT% (OXIDE)	STD.DEV. (%)	HOMO. INDEX	FORMULA	K-RATIO	UNKN PEAK (COUNTS)	UNKN BKGD (COUNTS)	COUNTING TIME(SEC)	STD PEAK (COUNTS)	STD BKGD (COUNTS)	COUNTING TIME(SEC)	STANDARD FILENAME
NA2O	4.024	2.95	1.580	0.000	1.03512	2483.5	50.5	20.00	2400.2	49.7	20.00	ZRGSC
MGO	0.011	236.92	0.943	0.000	0.00303	143.4	136.3	20.00	2469.5	136.9	20.00	ZRGSC
AL2O3	12.331	1.21	2.636	0.000	0.93784	14039.5	245.7	20.00	14955.9	247.8	20.00	Z5831
SIO2	72.929	0.87	3.110	0.000	0.98634	26501.7	53.5	20.00	26868.4	53.9	20.00	Z5831
K2O	4.436	1.64	2.914	0.000	1.21735	8759.2	143.6	20.00	7230.1	152.8	20.00	ZRGSC
CAO	0.524	4.57	0.862	0.000	0.10287	932.3	177.5	20.00	7528.9	191.2	20.00	ZRGSC
TIO2	0.046	79.80	0.911	0.000	0.00042	26.6	18.2	20.00	19938.2	26.6	20.00	ZTIO2
MNO	0.077	30.16	0.968	0.000	0.00077	107.2	63.8	20.00	56342.7	119.9	20.00	ZMN2O
FEO	0.946	5.71	1.074	0.000	0.14776	591.7	104.6	20.00	3409.3	112.6	20.00	ZRGSC

TOTAL   95.326   NO. OXYGENS = 0   NO. ITERS. = 2   AVE. ATOMIC NO. = 11.06

21-OCT-91 13:59:35

SAMPLE ID: JB-BS-9 T241-1 Date of Analysis: 10/21/91

Raw Probe Data		Raw Probe Data (FeO to Fe2O3)		Recalculated to 100%	
SiO2	72.929			SiO2	76.42
Al2O3	12.331			Al2O3	12.92
FeO	0.946*1.1113=Fe2O3		1.051	Fe2O3	1.10
MgO	0.011			MgO	0.01
MnO	0.077			MnO	0.08
CaO	0.524			CaO	0.55
TiO2	0.046			TiO2	0.05
Na2o	4.024			Na2o	4.22
K2O	4.436			K2O	4.65
TOTAL(O)	95.326	TOTAL(N)	95.431	TOTAL(R)	100.00

20 Best Matches:

1	0.9919	10/22/85	KRL 82182 (A1) (599) T112-1
2	0.9862	07/01/83	KRL91982F, T56-5
3	0.9859	9/3/88	FLV-64-CS T170-7
4	0.9856		YOS-1, T13-1
5	0.9849	5/2/85	WL 4-2 3.29m T93-9
6	0.9846		3-30-82-1, T43-3
7	0.9843		BD-16
8	0.9842	2/28/89	SL-103 T186-2
9	0.9841	10/23/85	BL-RSA-4 T112-9
10	0.9840		BD-11
11	0.9829	6/8/91	SS-91-1-1 T232-2
12	0.9827		GS-27
13	0.9826	5/2/85	WL CORE G 370cm T92-7
14	0.9823	8/6/91	SS-91-1-SU T232-1
15	0.9822	6/13/91	JB-BS-7 T227-4
16	0.9822	11/25/86	SCHURZ-1 T134-6
17	0.9820	10/25/83	KRL-91882A", T66-8
18	0.9819	5/2/85	WL CORE G 180cm T92-6
19	0.9818	6/13/91	JB-BS-5 T227-2
20	0.9815		GS-32

Elements used in the calculation are:

Na2o
Al2O3
SiO2
K2O
CaO
FeO

***** This sample has been added to the data base *****

Listing of 50 closest matches for COMP. NO. 2638 for elements: Na, Al, Si, K, Ca, Fe Date of Update: 10/22/91

No	Sample Number	Date	[illegible]	Al2O3	Fe2O3	MgO	MnO	CaO	TiO2	Na2O	K2O	Total,	. Cc
1	2638 JB-BS-9 T241-1	10/21/91	76.42	12.92	1.10	0.01	0.06	0.55	0.05	4.22	4.63	100.00	1.0000
2	2642 JB-BS-14 T241-5	10/21/91	76.55	12.82	1.11	0.02	0.07	0.55	0.06	4.20	4.62	100.00	0.9951
3	1439 KRL 82182 (A1) (599) T112-1	10/22/85	76.60	12.87	1.11	0.04	0.04	0.55	0.06	4.08	4.63	100.00	0.9915 -72m
4	2639 JB-BS-11 T241-2	10/21/91	76.55	12.80	1.10	0.02	0.08	0.54	0.06	4.16	4.68	99.99	0.9917
5	2640 JB-BS-12 T241-3	10/21/91	76.51	12.85	1.11	0.03	0.09	0.54	0.05	4.16	4.67	100.00	0.9912
6	2643 JB-BS-15 T241-6	10/21/91	76.59	12.83	1.08	0.03	0.07	0.54	0.04	4.13	4.59	100.00	0.9899
7	2641 JB-BS-13 T241-4	10/21/91	76.49	12.83	1.09	0.03	0.08	0.53	0.06	4.26	4.64	100.00	0.9877
8	571 KRL91982F, T56-5	07/01/83	76.61	12.89	1.14	0.03	0.05	0.55	0.05	4.12	4.56	100.00	0.9864
9	2050 FLV-64-CS T170-7	3/3/88	76.71	12.87	1.11	0.02	0.04	0.54	0.04	4.02	4.54	99.99	0.9859
10	431 YOS-1, T13-1		76.61	12.93	1.12	0.03	0.05	0.54	0.07	4.03	4.64	100.02	0.9858
11	1240 WL 4-2 3.29m T93-9	5/2/85	76.75	12.79	1.13	0.03	0.04	0.55	0.05	4.02	4.64	100.00	0.9845
12	2646 JB-WA-1 T242-1	10/21/91	76.77	12.70	1.09	0.02	0.07	0.53	0.06	4.15	4.57	100.00	0.9848
13	435 3-30-82-1, T43-3		76.62	12.93	1.06	0.02	0.05	0.54	0.07	4.13	4.59	100.01	0.9846
14	750 BO-16		76.59	12.92	1.11	0.03	0.03	0.54	0.07	4.00	4.71	100.00	0.9843
15	2236 SL-103 T186-2	2/28/89	76.68	12.95	1.10	0.03	0.04	0.55	0.07	3.68	4.69	99.99	0.9844 4726
16	1418 BL-RSA-4 T112-9	10/23/85	76.83	12.79	1.08	0.04	0.04	0.55	0.06	3.56	4.55	100.00	0.9841 -1600
17	758 BO-11		76.35	13.11	1.12	0.03	0.04	0.55	0.09	4.00	4.70	99.99	0.9840
18	2558 SS-91-1-1 T232-2	6/8/91	76.57	12.92	1.07	0.02	0.04	0.54	0.06	4.05	4.72	99.99	0.9829
19	783 GS-27		76.74	12.92	1.12	0.03	0.05	0.55	0.07	3.91	4.61	100.00	0.9827
20	1224 WL CORE G 370cm T92-7	5/2/85	75.83	12.82	1.09	0.04	0.04	0.54	0.05	3.55	4.65	100.01	0.9826
21	2559 SS-91-1-SU T232-1	8/6/91	76.74	12.86	1.09	0.04	0.04	0.54	0.05	3.55	4.68	99.99	0.9823
22	2571 JB-BS-7 T227-4	6/13/91	75.73	12.89	1.10	0.03	0.05	0.54	0.06	3.91	4.65	100.00	0.9822
23	1684 SCHURZ-1 T134-6	11/25/86	77.01	12.64	1.09	0.03	0.05	0.55	0.05	3.54	4.64	100.00	0.9822
24	681 KRL-91882A*, T66-8	10/25/83	76.79	12.83	1.10	0.03	0.06	0.54	0.07	3.91	4.67	100.00	0.9820
25	1223 WL CORE G 180cm T92-6	5/2/85	76.64	12.88	1.11	0.04	0.05	0.57	0.06	3.55	4.57	100.01	0.9819
26	2569 JB-BS-5 T227-2	6/13/91	76.69	12.91	1.08	0.02	0.05	0.55	0.09	3.50	4.70	99.99	0.9818
27	788 GS-32		76.58	12.90	1.13	0.03	0.04	0.56	0.06	4.00	4.70	100.00	0.9815
28	2494 FLV-156-SS T213-3	12/20/90	76.54	13.06	1.09	0.03	0.04	0.54	0.05	3.54	4.62	100.01	0.9811
29	1241 WL 4-2 3.31m T93-10	5/2/85	76.69	12.91	1.14	0.04	0.04	0.55	0.06	3.52	4.67	100.02	0.9809
30	1680 KRL 860922 A T134-2	11/25/86	76.94	12.75	1.07	0.03	0.04	0.55	0.06	3.53	4.65	100.00	0.9795
31	2170 KRL-82982-KP T178-5	12/6/88	76.70	13.01	1.11	0.02	0.06	0.55	0.06	3.81	4.67	99.99	0.9796
32	2563 SS-91-1-5 T232-6	8/7/91	76.97	12.65	1.08	0.03	0.04	0.54	0.07	3.98	4.65	100.01	0.9796
33	1225 WL CORE G 380cm T92-8	5/2/85	76.82	12.79	1.06	0.04	0.04	0.56	0.06	4.00	4.65	100.02	0.9797
34	1621 BO-16 JDO	09/12/86	76.98	12.70	1.10	0.03	0.05	0.55	0.07	3.83	4.68	99.99	0.9795
35	1672 KRL 82182 (A-1) T117-3	3/6/86	76.80	12.75	1.10	0.03	0.04	0.55	0.07	3.87	4.77	99.98	0.9790
36	1416 BL-RSA-2 T112-7	10/23/85	76.78	12.85	1.12	0.04	0.03	0.54	0.06	3.90	4.68	100.00	0.9786
37	1245 WL 8-3A ASH B 59.5-64.0cm T93-	5/2/85	77.00	12.70	1.10	0.03	0.06	0.56	0.04	3.85	4.61	99.99	0.9785
38	1244 WL 8-3A ASH A 64-66cm T93-13	5/2/85	76.97	12.80	1.08	0.03	0.05	0.55	0.05	3.66	4.60	99.99	0.9782
39	556 KRL91882B, T64-12	09/06/83	76.81	12.82	1.10	0.01	0.05	0.53	0.06	3.91	4.69	100.00	0.9781
40	1947 WL-4-4 (10.83M) T162-1	3/14/88	76.86	12.94	1.10	0.04	0.06	0.54	0.06	3.77	4.64	100.01	0.9776
41	551 KRL82282A, T66-5	10/25/83	76.71	12.88	1.12	0.04	0.05	0.52	0.06	3.58	4.65	100.01	0.9773
42	1229 WL 8-3A 14.5-20cm T92-13	5/2/85	77.03	12.78	1.09	0.03	0.04	0.55	0.06	3.78	4.63	99.99	0.9773
43	570 KRL91982D, T66-10	xx/xx/83	76.81	12.89	1.08	0.03	0.05	0.53	0.06	3.90	4.65	100.00	0.9770
44	1972 WL-4-58 (144.77m) T164-1	5/21/88	76.73	12.71	1.15	0.00	0.03	0.54	0.12	4.02	4.69	99.99	0.9770
45	1231 WL 8-1B 192-194cm T99-3	07/01/85	76.95	12.70	1.11	0.03	0.06	0.56	0.07	3.66	4.64	99.98	0.9770
46	1417 BL-RSA-3 T112-8	10/23/85	76.83	12.80	1.15	0.04	0.05	0.55	0.05	3.85	4.64	100.00	0.9765
47	1227 WL 8-2A 61-5-70.0cm T92-11	5/2/85	77.09	12.70	1.11	0.03	0.05	0.55	0.04	3.78	4.65	100.00	0.9768
48	2237 SL-115.5 T186-3	2/28/89	76.76	12.91	1.07	0.03	0.04	0.55	0.06	3.84	4.73	99.99	0.9768
49	550 KRL82282, T66-4	xx/xx/83	76.74	12.90	1.13	0.02	0.06	0.54	0.06	3.87	4.68	100.00	0.9767
50	2497 FLV-159-CH T219-6	12/20/90	77.01	12.76	1.08	0.03	0.03	0.54	0.05	3.94	4.57	100.01	0.9767

Listing of 25 closest matches for COMP. NO. 2637 for elements: Na, Al, Si, K , Ca, Fe Date of Update: 06/18/92

	C.No	Sample Number	Date	SiO2	Al2O3	Fe2O3	MgO	MnO	CaO	TiO2	Na2O	K2O	Total,R	Sim. Co
1	2637	JB-BS-9 T241-1	10/21/91	76.42	12.92	1.10	0.01	0.08	0.55	0.05	4.22	4.65	100.00	1.0000
2	2641	JB-BS-14 T241-5	10/21/91	76.55	12.82	1.11	0.02	0.07	0.55	0.06	4.20	4.62	100.00	0.9951
3	1409	KRL 82182 (A1) (599) T112-1	10/22/85	76.60	12.87	1.11	0.04	0.04	0.55	0.06	4.08	4.65	100.00	0.9919
4	2638	JB-BS-11 T241-2	10/21/91	76.55	12.80	1.10	0.02	0.08	0.54	0.06	4.16	4.68	99.99	0.9917
5	2639	JB-BS-12 T241-3	10/21/91	76.51	12.85	1.11	0.03	0.08	0.54	0.05	4.16	4.67	100.00	0.9913
6	2642	JB-BS-15 T241-6	10/21/91	76.59	12.83	1.08	0.03	0.07	0.54	0.04	4.23	4.59	100.00	0.9899
7	2682	JB-BS-9 T241-1	10/21/91	76.15	13.07	1.11	0.01	0.08	0.56	0.05	4.27	4.70	100.00	0.9893
8	2640	JB-BS-13 T241-4	10/21/91	76.49	12.83	1.08	0.03	0.08	0.53	0.06	4.26	4.64	100.00	0.9877
9	571	KRL91982F, T56-5	07/01/83	76.61	12.89	1.14	0.03	0.05	0.55	0.05	4.12	4.56	100.00	0.9862
10	2060	FLV-64-CS T170-7	9/3/88	76.71	12.87	1.11	0.02	0.04	0.54	0.04	4.02	4.64	99.99	0.9859
11	431	YOS-1, T13-1		76.61	12.93	1.12	0.03	0.05	0.54	0.07	4.03	4.64	100.02	0.9856
12	2717	FLV-201-TO T249-5	1/30/92	76.85	12.77	1.10	0.02	0.04	0.54	0.04	3.99	4.65	100.00	0.9850
13	1240	WL 4-2 3.29m T93-9	5/2/85	76.75	12.79	1.13	0.03	0.04	0.55	0.05	4.02	4.64	100.00	0.9849
14	2795	FLV-209-BC T254-6	4/14/92	76.36	13.11	1.09	0.03	0.06	0.55	0.07	4.01	4.73	100.01	0.9848
15	2645	JB-WA-1 T242-1	10/21/91	76.77	12.70	1.09	0.02	0.07	0.53	0.06	4.19	4.57	100.00	0.9848
16	435	3-30-82-1, T43-3		76.62	12.93	1.06	0.02	0.05	0.54	0.07	4.13	4.59	100.01	0.9846
17	760	BO-16		76.59	12.92	1.11	0.03	0.03	0.54	0.07	4.00	4.71	100.00	0.9843
18	2235	SL-103 T186-2	2/28/89	76.68	12.95	1.10	0.03	0.04	0.55	0.07	3.88	4.69	99.99	0.9842
19	1418	BL-RSA-4 T112-9	10/23/85	76.83	12.79	1.08	0.04	0.04	0.55	0.06	3.96	4.65	100.00	0.9841
20	758	BO-11		76.35	13.11	1.12	0.03	0.04	0.55	0.09	4.00	4.70	99.99	0.9840
21	2557	SS-91-1-1 T232-2	6/8/91	76.57	12.92	1.07	0.02	0.04	0.54	0.06	4.05	4.72	99.99	0.9829
22	783	GS-27		76.74	12.92	1.12	0.03	0.05	0.55	0.07	3.91	4.61	100.00	0.9827
23	1224	WL CORE G 370cm T92-7	5/2/85	76.83	12.82	1.09	0.04	0.04	0.54	0.05	3.95	4.65	100.01	0.9826
24	2558	SS-91-1-SU T232-1	8/6/91	76.74	12.86	1.09	0.04	0.04	0.54	0.05	3.95	4.68	99.99	0.9823
25	2570	JB-BS-7 T227-4	6/13/91	76.73	12.89	1.10	0.03	0.05	0.54	0.06	3.91	4.69	100.00	0.9822

Listing of 25 closest matches for COMP. NO. 2682 for elements: Na, Al, Si, K , Ca, Fe Date of Update: 06/18/92

	C.No	Sample Number	Date	SiO2	Al2O3	Fe2O3	MgO	MnO	CaO	TiO2	Na2O	K2O	Total,R	Sim. Co
1	2682	JB-BS-9 T241-1	10/21/91	76.15	13.07	1.11	0.01	0.08	0.56	0.05	4.27	4.70	100.00	1.0000
2	2637	JB-BS-9 T241-1	10/21/91	76.42	12.92	1.10	0.01	0.08	0.55	0.05	4.22	4.65	100.00	0.9893
3	2641	JB-BS-14 T241-5	10/21/91	76.55	12.82	1.11	0.02	0.07	0.55	0.06	4.20	4.62	100.00	0.9874
4	2639	JB-BS-12 T241-3	10/21/91	76.51	12.85	1.11	0.03	0.08	0.54	0.05	4.16	4.67	100.00	0.9851
5	1409	KRL 82182 (A1) (599) T112-1	10/22/85	76.60	12.87	1.11	0.04	0.04	0.55	0.06	4.08	4.65	100.00	0.9843
6	758	BO-11		76.35	13.11	1.12	0.03	0.04	0.55	0.09	4.00	4.70	99.99	0.9841
7	788	GS-32		76.58	12.90	1.13	0.03	0.04	0.56	0.06	4.00	4.70	100.00	0.9834
8	2638	JB-BS-11 T241-2	10/21/91	76.55	12.80	1.10	0.02	0.08	0.54	0.06	4.16	4.68	99.99	0.9832
9	2795	FLV-209-BC T254-6	4/14/92	76.36	13.11	1.09	0.03	0.06	0.55	0.07	4.01	4.73	100.01	0.9818
10	1223	WL CORE G 180cm T92-6	5/2/85	76.64	12.88	1.11	0.04	0.05	0.57	0.06	3.99	4.67	100.01	0.9816
11	760	BO-16		76.59	12.92	1.11	0.03	0.03	0.54	0.07	4.00	4.71	100.00	0.9803
12	2640	JB-BS-13 T241-4	10/21/91	76.49	12.83	1.08	0.03	0.08	0.53	0.06	4.26	4.64	100.00	0.9802
13	2642	JB-BS-15 T241-6	10/21/91	76.59	12.83	1.08	0.03	0.07	0.54	0.04	4.23	4.59	100.00	0.9801
14	571	KRL91982F, T56-5	07/01/83	76.61	12.89	1.14	0.03	0.05	0.55	0.05	4.12	4.56	100.00	0.9785
15	2060	FLV-64-CS T170-7	9/3/88	76.71	12.87	1.11	0.02	0.04	0.54	0.04	4.02	4.64	99.99	0.9784
16	431	YOS-1, T13-1		76.61	12.93	1.12	0.03	0.05	0.54	0.07	4.03	4.64	100.02	0.9783
17	2708	FLV-193-BC T246-2	12/12/91	76.75	12.61	1.16	0.04	0.06	0.56	0.06	4.11	4.65	100.00	0.9776
18	1240	WL 4-2 3.29m T93-9	5/2/85	76.75	12.79	1.13	0.03	0.04	0.55	0.05	4.02	4.64	100.00	0.9773
19	2235	SL-103 T186-2	2/28/89	76.68	12.95	1.10	0.03	0.04	0.55	0.07	3.88	4.69	99.99	0.9773
20	780	GS-21		76.41	13.12	1.13	0.03	0.05	0.58	0.06	4.01	4.61	100.00	0.9768
21	2169	KRL-82982-KP T178-5	12/6/88	76.70	13.01	1.11	0.02	0.06	0.55	0.06	3.81	4.67	99.99	0.9760
22	2557	SS-91-1-1 T232-2	6/8/91	76.57	12.92	1.07	0.02	0.04	0.54	0.06	4.05	4.72	99.99	0.9759
23	741	BC-1		76.76	12.83	1.11	0.02	0.03	0.58	0.06	3.91	4.71	100.01	0.9755
24	1291	WL 8-1B 192-194cm T99-3	07/01/85	76.95	12.70	1.11	0.03	0.06	0.56	0.07	3.86	4.64	99.98	0.9754
25	1225	WL CORE G 380cm T92-8	5/2/85	76.82	12.79	1.06	0.04	0.04	0.56	0.06	4.00	4.65	100.02	0.9752

Listing of 25 closest matches for COMP. NO. 2638 for elements: Na, Al, Si, K , Ca, Fe Date of Update: 06/18/92

	C.No	Sample Number	Date	SiO2	Al2O3	Fe2O3	MgO	MnO	CaO	TiO2	Na2O	K2O	Total,R	Sim. Co
1	2638	JB-BS-11 T241-2	10/21/91	76.55	12.80	1.10	0.02	0.08	0.54	0.06	4.16	4.68	99.99	1.0000
2	2639	JB-BS-12 T241-3	10/21/91	76.51	12.85	1.11	0.03	0.08	0.54	0.05	4.16	4.67	100.00	0.9974
3	2637	JB-BS-9 T241-1	10/21/91	76.42	12.92	1.10	0.01	0.08	0.55	0.05	4.22	4.65	100.00	0.9917
4	2641	JB-BS-14 T241-5	10/21/91	76.55	12.82	1.11	0.02	0.07	0.55	0.06	4.20	4.62	100.00	0.9915
5	2717	FLV-201-TO T249-5	1/30/92	76.85	12.77	1.10	0.02	0.04	0.54	0.04	3.99	4.65	100.00	0.9911
6	2642	JB-BS-15 T241-6	10/21/91	76.59	12.83	1.08	0.03	0.07	0.54	0.04	4.23	4.59	100.00	0.9905
7	2060	FLV-64-CS T170-7	9/3/88	76.71	12.87	1.11	0.02	0.04	0.54	0.04	4.02	4.64	99.99	0.9902
8	1409	KRL 82182 (A1) (599) T112-1	10/22/85	76.60	12.87	1.11	0.04	0.04	0.55	0.06	4.08	4.65	100.00	0.9902
9	760	BO-16		76.59	12.92	1.11	0.03	0.03	0.54	0.07	4.00	4.71	100.00	0.9894
10	2558	SS-91-1-SU T232-1	8/6/91	76.74	12.86	1.09	0.04	0.04	0.54	0.05	3.95	4.68	99.99	0.9889
11	681	KRL-91882A', T66-8	10/25/83	76.79	12.83	1.10	0.03	0.06	0.54	0.07	3.91	4.67	100.00	0.9887
12	431	YOS-1, T13-1		76.61	12.93	1.12	0.03	0.05	0.54	0.07	4.03	4.64	100.02	0.9886
13	2716	FLV-200-LC T249-4	1/30/92	76.77	12.80	1.11	0.02	0.04	0.53	0.06	4.01	4.67	100.01	0.9886
14	2645	JB-WA-1 T242-1	10/21/91	76.77	12.70	1.09	0.02	0.07	0.53	0.06	4.19	4.57	100.00	0.9885
15	1224	WL CORE G 370cm T92-7	5/2/85	76.83	12.82	1.09	0.04	0.04	0.54	0.05	3.95	4.65	100.01	0.9881
16	2570	JB-BS-7 T227-4	6/13/91	76.73	12.89	1.10	0.03	0.05	0.54	0.06	3.91	4.69	100.00	0.9881
17	2557	SS-91-1-1 T232-2	6/8/91	76.57	12.92	1.07	0.02	0.04	0.54	0.06	4.05	4.72	99.99	0.9880
18	2640	JB-BS-13 T241-4	10/21/91	76.49	12.83	1.08	0.03	0.08	0.53	0.06	4.26	4.64	100.00	0.9880
19	435	3-30-82-1, T43-3		76.62	12.93	1.06	0.02	0.05	0.54	0.07	4.13	4.59	100.01	0.9877
20	2562	SS-91-1-5 T232-6	8/7/91	76.97	12.65	1.08	0.03	0.04	0.54	0.07	3.98	4.65	100.01	0.9858
21	566	KRL91882B, T64-12	09/06/83	76.81	12.82	1.10	0.01	0.05	0.53	0.08	3.91	4.69	100.00	0.9857
22	1416	BL-RSA-2 T112-7	10/23/85	76.78	12.85	1.12	0.04	0.03	0.54	0.06	3.90	4.68	100.00	0.9855
23	1972	WL-4-58 (144.77m) T164-1	5/21/88	76.73	12.71	1.15	0.00	0.03	0.54	0.12	4.02	4.69	99.99	0.9852
24	1240	WL 4-2 3.29m T93-9	5/2/85	76.75	12.79	1.13	0.03	0.04	0.55	0.05	4.02	4.64	100.00	0.9849
25	1418	BL-RSA-4 T112-9	10/23/85	76.83	12.79	1.08	0.04	0.04	0.55	0.06	3.96	4.65	100.00	0.9841

Listing of 50 closest matches for COMP. NO. 2639 for elements: Na, Al, Si, K , Ca, Fe Date of Update: 10/22/91

	C.No	Sample Number	Date	[illegible]	Al2O3	Fe2O3	MgO	MnO	CaO	TiO2	Na2O	K2O	Total	. Co
1	2639	JB-BS-11 T241-2	10/21/91	76.55	12.80	1.10	0.02	0.08	0.54	0.06	4.16	4.68	99.99	1.0000
2	2640	JB-BS-12 T241-3	10/21/91	76.51	12.85	1.11	0.03	0.08	0.54	0.05	4.16	4.67	100.00	0.9974
3	2638	JB-BS-9 T241-1	10/21/91	76.42	12.92	1.10	0.01	0.08	0.55	0.05	4.22	4.65	100.00	0.9917
4	2642	JB-BS-14 T241-5	10/21/91	76.55	12.82	1.11	0.02	0.07	0.55	0.06	4.20	4.62	100.00	0.9912
5	2643	JB-BS-15 T241-6	10/21/91	76.59	12.83	1.08	0.03	0.07	0.54	0.04	4.23	4.59	100.00	0.9905
6	2060	FLV-64-CS T170-7	9/3/88	76.71	12.87	1.11	0.02	0.04	0.54	0.04	4.02	4.64	99.99	0.9902
7	1409	KRL 82182 (A1) (599) T112-1	10/22/85	76.60	12.87	1.11	0.04	0.04	0.55	0.06	4.08	4.65	100.00	0.9902
8	750	BD-16		76.59	12.92	1.11	0.03	0.03	0.54	0.07	4.00	4.71	100.00	0.9894
9	2559	SS-91-1-SU T232-1	8/6/91	76.74	12.86	1.09	0.04	0.04	0.54	0.05	3.95	4.68	99.99	0.9885
10	681	KRL-91882A', T66-8	10/25/83	76.79	12.83	1.10	0.03	0.06	0.54	0.07	3.91	4.67	100.00	0.9867
11	431	YOS-1, T13-1		76.61	12.93	1.12	0.03	0.05	0.54	0.07	4.03	4.64	100.02	0.9866
12	2646	JB-HA-1 T242-1	10/21/91	76.77	12.70	1.09	0.02	0.07	0.53	0.06	4.19	4.57	100.00	0.9865
13	1224	WL CORE G 370cm T92-7	5/2/85	76.83	12.82	1.09	0.04	0.04	0.54	0.05	3.99	4.65	100.01	0.9863
14	2571	JB-BS-7 T227-4	6/13/91	76.73	12.89	1.10	0.03	0.05	0.54	0.06	3.91	4.69	100.00	0.9863
15	2558	SS-91-1-1 T232-2	6/8/91	76.57	12.92	1.07	0.02	0.04	0.54	0.06	4.05	4.72	99.99	0.9860
16	2641	JB-BS-13 T241-4	10/21/91	76.49	12.83	1.08	0.03	0.08	0.53	0.06	4.26	4.64	100.00	0.9860
17	435	3-30-82-1, T43-3		76.62	12.93	1.06	0.02	0.05	0.54	0.07	4.13	4.59	100.01	0.9857
18	2563	SS-91-1-5 T232-6	8/7/91	76.97	12.65	1.08	0.03	0.04	0.54	0.07	3.98	4.65	100.01	0.9858
19	566	KRL91882B, T64-12	09/06/83	76.81	12.82	1.10	0.01	0.05	0.53	0.08	3.91	4.69	100.00	0.9857
20	1416	BL-RSA-2 T112-7	10/23/85	76.78	12.85	1.12	0.04	0.03	0.54	0.06	3.90	4.68	100.00	0.9855
21	1972	WL-4-58 (144.77m) T164-1	5/21/88	76.73	12.71	1.15	0.00	0.03	0.54	0.12	4.02	4.69	99.99	0.9852
22	1240	WL 4-2 3.29m T93-9	5/2/85	76.75	12.79	1.13	0.03	0.04	0.55	0.05	4.02	4.64	100.00	0.9849
23	1418	BL-RSA-4 T112-9	10/23/85	76.83	12.79	1.08	0.04	0.04	0.55	0.06	3.96	4.65	100.00	0.9843
24	2494	FLV-156-SS T219-3	12/20/90	76.64	13.06	1.09	0.03	0.04	0.54	0.05	3.94	4.62	100.01	0.9840
25	571	KRL91982F, T56-5	07/01/83	76.61	12.89	1.14	0.03	0.05	0.55	0.05	4.12	4.56	100.00	0.9840
26	1419	BL-RSA-5 T112-10	10/23/85	76.98	12.65	1.09	0.04	0.04	0.53	0.05	3.93	4.68	99.99	0.9833
27	2236	SL-103 T186-2	2/28/89	76.68	12.95	1.10	0.03	0.04	0.55	0.07	3.88	4.65	99.99	0.9832
28	2497	FLV-159-CH T219-6	12/20/90	77.01	12.76	1.08	0.03	0.03	0.54	0.05	3.54	4.57	100.01	0.9827
29	1230	WL 8-1B 92-94cm T99-1	07/01/85	76.99	12.72	1.11	0.02	0.06	0.54	0.07	3.64	4.65	100.00	0.9826
30	682	KRL-91882G, T66-11	10/25/83	76.91	12.76	1.07	0.03	0.06	0.54	0.07	3.87	4.68	99.99	0.9825
31	2644	JB-BS-16 T241-7	10/21/91	76.97	12.59	1.04	0.02	0.08	0.54	0.05	4.13	4.58	100.00	0.9825
32	758	BD-11		76.35	13.11	1.12	0.03	0.04	0.55	0.09	4.00	4.70	99.99	0.9825
33	1196	WALKER LAKE CORE G 380CM t89-1	2/28/85	76.98	12.79	1.08	0.02	0.05	0.54	0.05	3.86	4.64	100.01	0.9825
34	550	KRL82282, T66-4	xx/xx/83	76.74	12.90	1.13	0.02	0.06	0.54	0.06	3.87	4.68	100.00	0.9823
35	1684	SCHURZ-1 T134-6	11/25/86	77.01	12.64	1.09	0.03	0.05	0.55	0.05	3.94	4.64	100.00	0.9821
36	2381	FLV-131-FC T203-4	4/16/90	77.18	12.43	1.12	0.01	0.04	0.54	0.06	3.93	4.68	99.99	0.9816
37	1521	BD-18 JOD	09/12/86	76.98	12.70	1.10	0.03	0.05	0.55	0.07	3.83	4.68	99.99	0.9815
38	1025	KRL-71082C (590) T58-1	6/22/84	76.91	12.71	1.08	0.02	0.00	0.53	0.05	3.95	4.74	99.99	0.9814
39	1223	WL CORE G 180cm T92-6	5/2/85	76.64	12.88	1.11	0.04	0.05	0.57	0.06	3.95	4.67	100.01	0.9813
40	561	KRL82282A, T66-5	10/25/83	76.71	12.88	1.12	0.04	0.05	0.52	0.06	3.98	4.65	100.01	0.9812
41	1948	WL-4-4 (12.25M) T162-2	5/14/88	76.87	12.86	1.09	0.02	0.05	0.54	0.06	3.80	4.72	100.01	0.9812
42	788	GS-32		76.58	12.90	1.13	0.03	0.04	0.56	0.06	4.00	4.70	100.00	0.9811
43	2569	JB-BS-5 T227-2	6/13/91	76.69	12.91	1.08	0.02	0.05	0.55	0.09	3.90	4.70	99.99	0.9811
44	1472	KRL 82182 (A-1) T117-3	3/6/86	76.80	12.75	1.10	0.03	0.04	0.55	0.07	3.87	4.77	99.98	0.9810
45	570	KRL91982D, T66-10	xx/xx/83	76.81	12.89	1.08	0.03	0.05	0.53	0.06	3.90	4.65	100.00	0.9807
46	1947	WL-4-4 (10.83M) T162-1	5/14/88	76.86	12.94	1.10	0.04	0.06	0.54	0.06	3.77	4.64	100.01	0.9805
47	192	LD-12, T3,4		76.94	12.70	1.12	0.03	0.07	0.53	0.07	3.51	4.64	100.01	0.9803
48	567	KRL91882-K-1, T64-13	09/06/83	76.93	12.82	1.11	0.01	0.05	0.53	0.07	3.88	4.60	100.00	0.9803
49	564	KRL82782A, T64-11	09/06/83	76.99	12.75	1.09	0.01	0.06	0.53	0.08	3.90	4.59	100.00	0.9802
50	1680	KRL 860922 A T134-2	11/25/86	76.94	12.75	1.07	0.03	0.04	0.55	0.06	3.91	4.65	100.00	0.9796

SAMPLE ID: J8-BS-11 T241-2 Date of Analysis: 10/21/91

Raw Probe Data		Raw Probe Data (FeO to Fe2O3)		Recalculated to 100%	
SiO2	75.463			SiO2	76.55
Al2O3	12.620			Al2O3	12.80
FeO	0.977*1.1113=Fe2O3		1.086	Fe2O3	1.10
MgO	0.023			MgO	0.02
MnO	0.080			MnO	0.08
CaO	0.533			CaO	0.54
TiO2	0.056			TiO2	0.06
Na2o	4.101			Na2o	4.16
K2O	4.612			K2O	4.68
TOTAL(O)	98.465	TOTAL(N)	98.574	TOTAL(R)	99.99

20 Best Matches:

1	0.9917	10/21/91	J8-BS-9 T241-1
2	0.9902	9/3/88	FLV-64-CS T170-7
3	0.9902	10/22/85	KRL 82182 (A1) (599) T112-1
4	0.9894		80-16
5	0.9889	8/6/91	SS-91-1-SU T232-1
6	0.9887	10/25/83	KRL-91882A", T66-8
7	0.9886		YOS-1, T13-1
8	0.9881	5/2/85	WL CORE G 370cm T92-7
9	0.9881	6/13/91	J8-BS-7 T227-4
10	0.9880	6/8/91	SS-91-1-1 T232-2
11	0.9877		3-30-82-1, T43-3
12	0.9858	8/7/91	SS-91-1-5 T232-6
13	0.9857	09/06/83	KRL91882B, T64-12
14	0.9855	10/23/85	BL-RSA-2 T112-7
15	0.9852	5/21/88	WL-4-SB (144.77m) T164-1
16	0.9849	5/2/85	WL 4-2 3.29m T93-9
17	0.9841	10/23/85	BL-RSA-4 T112-9
18	0.9840	12/20/90	FLV-156-SS T219-3
19	0.9840	07/01/83	KRL91982F, T56-5
20	0.9833	10/23/85	BL-RSA-5 T112-10

Elements used in the calculation are:

Na2o
Al2O3
SiO2
K2O
CaO
FeO

***** This sample has been added to the data base *****

SAMPLE ·1-2 JB-BS-11

	BE	NA	9	MG	8	AL	3	SI	7	K		CA	6	TI	5	MN	1	FE	4
PT	COUNTS	COUNTS	SD	COUNTS	SD	COUNTS	SD	COUNTS	SD	COUNTS	SD	COUNTS	SD	COUNTS	SD	COUNTS	SD	COUNTS	SD
1	14133	2492	50	137	12	14368	120	27028	164	9171	96	919	30	27	5	91	10	604	25
2	14142	2515	17	164	19	13984	272	27208	127	8814	252	935	12	21	4	105	10	584	14
3	14143	2531	20	150	13	14404	233	26698	259	8819	205	926	8	39	9	95	7	540	33
4	14146	2608	50	149	11	14335	195	26927	213	8916	167	927	7	33	8	113	10	633	39
5	14148	2580	48	154	10	14399	178	27896	455	9098	163	960	16	11	11	127	14	673	50
6	14142	2615	51	133	11	14576	195	27592	445	9318	205	961	18	26	10	106	13	652	49
7	14139	2565	47	150	10	14505	188	27661	439	8923	191	939	17	21	9	141	18	629	45
8	14146	2301	101	153	10	14318	175	26923	426	10213	461	815	46	38	9	102	17	579	43
9	14139	41	834	130	11	515	****	38051	****	139	****	147	262	20	9	79	19	101	175
10	14139	2080	788	167	12	14152	****	26911	****	10965	****	854	247	30	9	102	18	436	169
11	14141	3255	809	200	19	31086	****	18585	****	1727	****	15598	****	42	9	84	18	411	165
12	14147	2680	778	151	18	14650	****	27473	****	9019	****	935	****	28	9	116	18	650	161
13	14146	2665	749	161	18	14807	****	27058	****	9185	****	946	****	37	9	106	17	608	156
14	14151	2680	725	146	17	14455	****	27893	****	8914	****	986	****	22	9	116	16	561	150
15	14149	2540	699	157	17	14183	****	28088	****	8978	****	952	****	21	9	121	16	589	145
16	14145	2471	676	144	16	14488	****	27780	****	9188	****	1023	****	27	8	113	16	592	140
17	14144	2556	655	163	16	14292	****	27289	****	8812	****	908	****	38	9	110	15	632	137
18	14148	2530	636	154	15	14434	****	27822	****	9126	****	990	****	34	8	82	16	610	134
19	14143	2484	618	148	15	14501	****	28006	****	9013	****	988	****	33	8	118	16	597	130
20	14143	2503	602	148	15	14406	****	27590	****	9110	****	942	****	30	8	104	15	621	127

LINES DELETED: 9 11 10

AVE. BEAM CURRENT/SEC = 707

DATA REDUCED USING $B-AL: $GL9M

ON SPECIMEN: T241-2 JB-BS-11

$B-AL VERSION 1.0

OXIDE FORM.	WEIGHT% (OXIDE)	STD.DEV. (%)	HOMO. INDEX	FORMULA	K-RATIO	UNKN PEAK (COUNTS)	UNKN BKGD (COUNTS)	COUNTING TIME(SEC)	STD PEAK (COUNTS)	STD BKGD (COUNTS)	COUNTING TIME(SEC)	STANDARD FILENAME
NA2O	4.101	2.93	1.826	0.000	1.06265	2548.2	50.4	20.00	2400.2	49.7	20.00	%RGSC
MGO	0.023	119.33	0.670	0.000	0.00609	150.6	136.4	20.00	2469.5	136.9	20.00	%RGSC
AL2O3	12.620	1.20	1.516	0.000	0.96344	14417.8	247.4	20.00	14955.9	247.8	20.00	%5831
SIO2	75.463	0.86	2.600	0.000	1.02232	27466.7	53.8	20.00	26868.4	53.9	20.00	%5831
K2O	4.612	1.62	3.396	0.000	1.26465	9095.1	144.7	20.00	7230.1	152.8	20.00	%RGSC
CAO	0.533	4.54	1.454	0.000	0.10427	944.3	179.2	20.00	7528.9	191.2	20.00	%RGSC
TIO2	0.056	67.45	1.450	0.000	0.00051	28.5	18.4	20.00	19938.2	26.6	20.00	%TIO2
MNO	0.080	29.32	1.316	0.000	0.00080	109.5	64.5	20.00	56342.7	119.9	20.00	%MN2O
FEO	0.977	5.61	1.389	0.000	0.15274	609.1	105.6	20.00	3409.3	112.6	20.00	%RGSC

TOTAL 98.465 NO. OXYGENS = 0 NO. ITERS. = 2 AVE. ATOMIC NO. = 11.16

21-OCT-91 14:15:28

SAMPLE: T JB-BS-12

	BEAM	NA	9	MG	8	AL	3	SI	7	K	2	CA	6	TI	5	MN	1	FE	4
PT	COUNTS	COUNTS	SD	COUNTS	SD	COUNTS	SD	COUNTS	SD	COUNTS	SD	COUNTS	SD	COUNTS	SD	COUNTS	SD	COUNTS	SD
1	14146	2489	50	168	13	14585	121	27408	166	10053	100	863	29	33	6	115	11	455	21
2	14146	2456	23	168	0	14511	52	27334	52	9979	759	920	40	22	8	103	8	633	126
3	14139	2632	94	145	13	21373	****	23547	****	21554	****	446	259	17	8	86	15	144	248
4	14142	2732	129	173	13	14843	****	27521	****	9114	****	986	244	27	7	111	13	573	218
5	14138	3611	476	201	20	31543	****	18570	****	851	****	15335	****	21	6	92	12	331	196
6	14150	2424	450	148	20	13822	****	26563	****	8064	****	957	****	27	6	102	11	565	184
7	14142	2645	412	143	21	14491	****	27400	****	9025	****	952	****	37	7	102	10	619	180
8	14136	2556	385	162	19	14392	****	27709	****	9112	****	916	****	21	7	133	14	606	173
9	14135	2641	361	151	18	14276	****	27936	****	9014	****	940	****	34	7	107	14	605	165
10	14132	2620	341	141	18	14308	****	27540	****	9076	****	984	****	32	7	108	13	625	161
11	14140	2216	352	143	18	14101	****	26773	****	8973	****	1047	****	27	6	103	12	513	153
12	14145	2499	338	148	18	14615	****	27555	****	8956	****	903	****	21	6	103	12	726	158
13	14146	2577	324	156	17	14619	****	27401	****	9193	****	933	****	27	6	125	12	657	155
14	14145	2562	312	136	17	14639	****	27589	****	9071	****	949	****	25	6	94	12	702	155
15	14150	2225	317	147	17	13678	****	26243	****	8967	****	736	****	20	6	95	12	441	152
16	14147	3135	325	158	16	18006	****	25486	****	12229	****	1040	****	28	6	110	12	405	151
17	14153	2598	325	155	16	14609	****	27729	****	9097	****	944	****	33	6	112	12	652	149
18	14156	2502	316	156	15	14678	****	27297	****	9885	****	840	****	30	6	123	12	594	145
19	14153	2541	308	161	15	14606	****	27424	****	9108	****	948	****	27	5	100	12	593	142
20	14150	2592	300	160	15	14373	****	27271	****	9087	****	943	****	23	5	105	11	653	140

LINES DELETED:
LINES DELETED: 3 5 16 15 18

AVE. BEAM CURRENT/SEC = 707

DATA REDUCED USING $B-AL: $GL9M

ON SPECIMEN: T241-3 JB-BS-12

$B-AL VERSION 1.0

OXIDE FORM.	WEIGHT% (OXIDE)	STD.DEV. (%)	HOMO. INDEX	FORMULA	K-RATIO	UNKN PEAK (COUNTS)	UNKN BKGD (COUNTS)	COUNTING TIME(SEC)	STD PEAK (COUNTS)	STD BKGD (COUNTS)	COUNTING TIME(SEC)	STANDARD FILENAME
NA2O	4.094	2.93	2.385	0.000	1.06053	2543.2	50.4	20.00	2400.2	49.7	20.00	%RGSC
MGO	0.029	96.33	0.892	0.000	0.00759	154.1	136.4	20.00	2469.5	136.9	20.00	%RGSC
AL2O3	12.453	1.20	2.103	0.000	0.96581	14452.5	247.3	20.00	14955.9	247.8	20.00	%5831
SIO2	75.324	0.86	2.103	0.000	1.02021	27410.2	53.9	20.00	26868.4	53.9	20.00	%5831
K2O	4.595	1.62	4.005	0.000	1.25990	9061.4	144.7	20.00	7230.1	152.8	20.00	%RGSC
CAO	0.534	4.54	1.347	0.000	0.10447	945.7	179.2	20.00	7528.9	191.2	20.00	%RGSC
TIO2	0.051	72.90	0.955	0.000	0.00047	27.7	18.4	20.00	19938.2	26.6	20.00	%TIO2
MNO	0.079	30.21	0.963	0.000	0.00077	108.0	64.5	20.00	56342.7	119.9	20.00	%MN2O
FEO	0.983	5.59	2.778	0.000	0.15357	611.8	105.5	20.00	3409.3	112.6	20.00	%RGSC

TOTAL 98.339 NO. OXYGENS = 0 NO. ITERS. = 2 AVE. ATOMIC NO. = 11.16

Listing of 25 closest matches for COMP. NO. 2639 for elements: Na, Al, Si, K , Ca, Fe Date of Update: 06/18/92

	C.No	Sample Number	Date	SiO2	Al2O3	Fe2O3	MgO	MnO	CaO	TiO2	Na2O	K2O	Total,R	Sim. Co
1	2639	JB-BS-12 T241-3	10/21/91	76.51	12.85	1.11	0.03	0.08	0.54	0.05	4.16	4.67	100.00	1.0000
2	2638	JB-BS-11 T241-2	10/21/91	76.55	12.80	1.10	0.02	0.08	0.54	0.06	4.16	4.68	99.99	0.9974
3	2641	JB-BS-14 T241-5	10/21/91	76.55	12.82	1.11	0.02	0.07	0.55	0.06	4.20	4.62	100.00	0.9931
4	2060	FLV-64-CS T170-7	9/3/88	76.71	12.87	1.11	0.02	0.04	0.54	0.04	4.02	4.64	99.99	0.9926
5	1409	KRL 82182 (A1) (599) T112-1	10/22/85	76.60	12.87	1.11	0.04	0.04	0.55	0.06	4.08	4.65	100.00	0.9926
6	2637	JB-BS-9 T241-1	10/21/91	76.42	12.92	1.10	0.01	0.08	0.55	0.05	4.22	4.65	100.00	0.9913
7	760	BO-16		76.59	12.92	1.11	0.03	0.03	0.54	0.07	4.00	4.71	100.00	0.9911
8	431	YOS-1, T13-1		76.61	12.93	1.12	0.03	0.05	0.54	0.07	4.03	4.64	100.02	0.9910
9	2716	FLV-200-LC T249-4	1/30/92	76.77	12.80	1.11	0.02	0.04	0.53	0.06	4.01	4.67	100.01	0.9897
10	2642	JB-BS-15 T241-6	10/21/91	76.59	12.83	1.08	0.03	0.07	0.54	0.04	4.23	4.59	100.00	0.9894
11	2717	FLV-201-TO T249-5	1/30/92	76.85	12.77	1.10	0.02	0.04	0.54	0.04	3.99	4.65	100.00	0.9892
12	681	KRL-91882A', T66-8	10/25/83	76.79	12.83	1.10	0.03	0.06	0.54	0.07	3.91	4.67	100.00	0.9876
13	2558	SS-91-1-SU T232-1	8/6/91	76.74	12.86	1.09	0.04	0.04	0.54	0.05	3.95	4.68	99.99	0.9876
14	435	3-30-82-1, T43-3		76.62	12.93	1.06	0.02	0.05	0.54	0.07	4.13	4.59	100.01	0.9872
15	1416	BL-RSA-2 T112-7	10/23/85	76.78	12.85	1.12	0.04	0.03	0.54	0.06	3.90	4.68	100.00	0.9872
16	2640	JB-BS-13 T241-4	10/21/91	76.49	12.83	1.08	0.03	0.08	0.53	0.06	4.26	4.64	100.00	0.9871
17	2557	SS-91-1-1 T232-2	6/8/91	76.57	12.92	1.07	0.02	0.04	0.54	0.06	4.05	4.72	99.99	0.9868
18	1224	WL CORE G 370cm T92-7	5/2/85	76.83	12.82	1.09	0.04	0.04	0.54	0.05	3.95	4.65	100.01	0.9868
19	2570	JB-BS-7 T227-4	6/13/91	76.73	12.89	1.10	0.03	0.05	0.54	0.06	3.91	4.69	100.00	0.9868
20	2645	JB-WA-1 T242-1	10/21/91	76.77	12.70	1.09	0.02	0.07	0.53	0.06	4.19	4.57	100.00	0.9866
21	571	KRL91982F, T56-5	07/01/83	76.61	12.89	1.14	0.03	0.05	0.55	0.05	4.12	4.56	100.00	0.9863
22	1240	WL 4-2 3.29m T93-9	5/2/85	76.75	12.79	1.13	0.03	0.04	0.55	0.05	4.02	4.64	100.00	0.9860
23	1972	WL-4-58 (144.77m) T164-1	5/21/88	76.73	12.71	1.15	0.00	0.03	0.54	0.12	4.02	4.69	99.99	0.9856
24	2682	JB-BS-9 T241-1	10/21/91	76.15	13.07	1.11	0.01	0.08	0.56	0.05	4.27	4.70	100.00	0.9851
25	758	BO-11		76.35	13.11	1.12	0.03	0.04	0.55	0.09	4.00	4.70	99.99	0.9844

Listing of 50 closest matches for COMP. NO. 2640 for elements: Na, Al, Si, K, Ca, Fe Date of Update: 10/22/91

	No	Sample Number	Date	SiO2	Al2O3	Fe2O3	MgO	MnO	CaO	TiO2	Na2O	K2O	Total	[illegible]
1	2640	JB-BS-12 T241-3	10/21/91	76.51	12.85	1.11	0.03	0.08	0.54	0.05	4.16	4.57	100.00	1.0000
2	2639	JB-BS-11 T241-2	10/21/91	76.55	12.80	1.10	0.02	0.08	0.54	0.06	4.16	4.68	99.99	0.9934
3	2642	JB-BS-14 T241-5	10/21/91	76.55	12.82	1.11	0.02	0.07	0.55	0.06	4.20	4.62	100.00	0.9931
4	2060	FLV-64-CS T170-7	9/3/88	76.71	12.87	1.11	0.02	0.04	0.54	0.04	4.02	4.64	99.99	0.9926
5	1439	KRL 82182 (A1) (599) T112-1	10/22/85	76.60	12.87	1.11	0.04	0.04	0.55	0.06	4.08	4.65	100.00	0.9926
6	2638	JB-BS-9 T241-1	10/21/91	76.42	12.92	1.10	0.01	0.08	0.55	0.05	4.22	4.65	100.00	0.9913
7	750	BD-16		76.59	12.92	1.11	0.03	0.03	0.54	0.07	4.00	4.71	100.00	0.9911
8	431	YOS-1, T13-1		76.61	12.93	1.12	0.03	0.05	0.54	0.07	4.03	4.64	100.02	0.9910
9	2643	JB-BS-15 T241-6	10/21/91	76.59	12.83	1.08	0.03	0.07	0.54	0.04	4.23	4.59	100.00	0.9894
10	681	KRL-91882A", T66-8	10/25/83	76.79	12.83	1.10	0.03	0.06	0.54	0.07	3.91	4.67	100.00	0.9876
11	2559	SS-91-1-SU T232-1	8/6/91	76.74	12.86	1.09	0.04	0.04	0.54	0.05	3.99	4.68	99.99	0.9876
12	435	3-30-82-1, T43-3		76.62	12.93	1.06	0.02	0.05	0.54	0.07	4.13	4.59	100.01	0.9872
13	1416	BL-RSA-2 T112-7	10/23/85	76.78	12.85	1.12	0.04	0.03	0.54	0.06	3.90	4.68	100.00	0.9872
14	2641	JB-BS-13 T241-4	10/21/91	76.49	12.83	1.08	0.03	0.08	0.53	0.06	4.26	4.64	100.00	0.9871
15	2558	SS-91-1-1 T232-2	6/8/91	76.57	12.92	1.07	0.02	0.04	0.54	0.06	4.05	4.72	99.99	0.9868
16	1224	WL CORE G 370cm T92-7	5/2/85	76.83	12.82	1.09	0.04	0.04	0.54	0.05	3.95	4.65	100.01	0.9868
17	2571	JB-BS-7 T227-4	6/13/91	76.73	12.89	1.10	0.03	0.05	0.54	0.06	3.91	4.69	100.00	0.9868
18	2646	JB-WA-1 T242-1	10/21/91	76.77	12.70	1.09	0.02	0.07	0.53	0.06	4.15	4.57	100.00	0.9866
19	571	KRL91982F, T56-5	07/01/83	76.61	12.89	1.14	0.03	0.05	0.55	0.05	4.12	4.56	100.00	0.9863
20	1240	WL 4-2 3.29m T93-9	5/2/85	76.75	12.79	1.13	0.03	0.04	0.55	0.05	4.02	4.64	100.00	0.9860
21	1972	WL-4-58 (144.77m) T164-1	5/21/88	76.73	12.71	1.15	0.00	0.03	0.54	0.12	4.02	4.69	99.99	0.9856
22	758	BD-11		76.35	13.11	1.12	0.03	0.04	0.55	0.09	4.00	4.70	99.99	0.9844
23	2563	SS-91-1-5 T232-6	8/7/91	76.97	12.65	1.08	0.03	0.04	0.54	0.07	3.98	4.65	100.01	0.9840
24	560	KRL82282, T66-4	xx/xx/83	76.74	12.90	1.13	0.02	0.06	0.54	0.06	3.87	4.68	100.00	0.9839
25	1223	WL CORE G 180cm T92-6	5/2/85	76.64	12.88	1.11	0.04	0.05	0.57	0.06	3.99	4.67	100.01	0.9837
26	1290	WL 8-1B 92-94cm T99-1	07/01/85	76.99	12.72	1.11	0.02	0.06	0.54	0.07	3.84	4.65	100.00	0.9837
27	566	KRL91882B, T64-12	09/06/83	76.81	12.82	1.10	0.01	0.05	0.53	0.08	3.91	4.69	100.00	0.9836
28	561	KRL82282A, T66-5	10/25/83	76.71	12.88	1.12	0.04	0.05	0.52	0.06	3.98	4.65	100.01	0.9836
29	2494	FLV-156-SS T219-3	12/20/90	76.64	13.06	1.09	0.03	0.04	0.54	0.05	3.94	4.62	100.01	0.9834
30	788	GS-32		76.58	12.90	1.13	0.03	0.04	0.56	0.06	4.00	4.70	100.00	0.9828
31	1418	BL-RSA-4 T112-9	10/23/85	76.83	12.79	1.08	0.04	0.04	0.55	0.06	3.96	4.65	100.00	0.9823
32	2381	FLV-131-FC T203-4	4/16/90	77.18	12.43	1.12	0.01	0.04	0.54	0.06	3.93	4.68	99.99	0.9820
33	783	GS-27		76.74	12.92	1.12	0.03	0.05	0.55	0.07	3.91	4.61	100.00	0.9815
34	557	KRL91882-K-1, T64-13	09/06/83	76.93	12.82	1.11	0.01	0.05	0.53	0.07	3.88	4.60	100.00	0.9815
35	2236	SL-103 T186-2	2/28/89	76.68	12.95	1.10	0.03	0.04	0.55	0.07	3.86	4.69	99.99	0.9815
36	1241	WL 4-2 3.31m T93-10	5/2/85	76.69	12.91	1.14	0.04	0.04	0.55	0.06	3.92	4.67	100.02	0.9816
37	192	LD-12, T3,4		76.94	12.70	1.12	0.03	0.07	0.53	0.07	3.91	4.64	100.01	0.9813
38	2497	FLV-159-CH T219-6	12/20/90	77.01	12.76	1.08	0.03	0.03	0.54	0.05	3.94	4.57	100.01	0.9809
39	1419	BL-RSA-5 T112-10	10/23/85	76.98	12.65	1.09	0.04	0.04	0.53	0.05	3.93	4.68	99.99	0.9807
40	2644	JB-BS-16 T241-7	10/21/91	76.97	12.59	1.04	0.02	0.08	0.54	0.05	4.13	4.56	100.00	0.9807
41	781	LD-12		76.94	12.72	1.12	0.03	0.07	0.53	0.07	3.91	4.61	100.00	0.9803
42	1136	WALKER LAKE CORE G 380CM t89-1	2/20/85	76.98	12.79	1.08	0.02	0.05	0.54	0.05	3.86	4.64	100.01	0.9806
43	2170	KRL-82982-KP T178-5	12/6/88	76.70	13.01	1.11	0.02	0.06	0.55	0.06	3.81	4.67	99.99	0.9805
44	952	DR-64		76.57	13.01	1.13	0.03	0.05	0.53	0.07	3.90	4.70	99.99	0.9803
45	1684	SCHURZ-1 T134-6	11/25/86	77.01	12.64	1.09	0.03	0.05	0.55	0.05	3.94	4.64	100.00	0.9803
46	570	KRL91982D, T66-10	xx/xx/83	76.81	12.89	1.08	0.03	0.05	0.53	0.06	3.90	4.65	100.00	0.9801
47	1226	WL 8-2A 28.5-33.0cm T92-10	5/2/85	77.00	12.77	1.12	0.03	0.05	0.54	0.06	3.76	4.66	99.99	0.9800
48	682	KRL-91882G, T66-11	10/25/83	76.91	12.76	1.07	0.03	0.06	0.54	0.07	3.87	4.68	99.99	0.9800
49	1848	WL-4-4 (12.25M) T162-2	5/14/88	76.87	12.86	1.09	0.02	0.05	0.54	0.06	3.80	4.72	100.01	0.9800
50	1947	WL-4-4 (10.83M) T162-1	5/14/88	76.86	12.94	1.10	0.04	0.06	0.54	0.06	3.77	4.64	100.01	0.9799

SAMPLE ID: JB-BS-12 T241-3 Date of Analysis: 10/21/91

Raw Probe Data		Raw Probe Data (FeO to Fe2O3)		Recalculated to 100%	
SiO2	75.324			SiO2	76.51
Al2O3	12.653			Al2O3	12.85
FeO	0.983*1.1113=Fe2O3		1.092	Fe2O3	1.11
MgO	0.029			MgO	0.03
MnO	0.078			MnO	0.08
CaO	0.534			CaO	0.54
TiO2	0.051			TiO2	0.05
Na2o	4.094			Na2o	4.16
K2O	4.595			K2O	4.67
TOTAL(O)	98.339	TOTAL(N)	98.448	TOTAL(R)	100.00

20 Best Matches:

1	0.9974	10/21/91	JB-BS-11 T241-2
2	0.9926	9/3/88	FLV-64-CS T170-7
3	0.9926	10/22/85	KRL 82182 (A1) (S99) T112-1
4	0.9913	10/21/91	JB-BS-9 T241-1
5	0.9911		BO-16
6	0.9910		YDS-1, T13-1
7	0.9876	10/25/83	KRL-91882A*, T66-8
8	0.9876	8/6/91	SS-91-1-SU T232-1
9	0.9872		3-30-82-1, T43-3
10	0.9872	10/23/85	BL-RSA-2 T112-7
11	0.9868	6/8/91	SS-91-1-1 T232-2
12	0.9868	5/2/85	WL CORE G 370cm T92-7
13	0.9868	6/13/91	JB-BS-7 T227-4
14	0.9863	07/01/83	KRL91982F, T56-5
15	0.9860	5/2/85	WL 4-2 3.29m T93-9
16	0.9856	5/21/88	WL-4-58 (144.77m) T164-1
17	0.9844		BO-11
18	0.9840	8/7/91	SS-91-1-5 T232-6
19	0.9839	xx/xx/83	KRL82282, T66-4
20	0.9837	5/2/85	WL CORE G 180cm T92-6

Elements used in the calculation are:

Na2o
Al2O3
SiO2
K2O
CaO
FeO

***** This sample has been added to the data base *****

SAMPLE: T241-4 JB-BS-13

PT	BEAM COUNTS	NA COUNTS	9 SD	MG COUNTS	8 SD	AL COUNTS	3 SD	SI COUNTS	7 SD	K COUNTS	2 SD	CA COUNTS	6 SD	TI COUNTS	5 SD	MN COUNTS	1 SD	FE COUNTS	4 SD
1	14162	2643	51	162	13	14575	121	27136	165	9039	95	922	30	28	5	100	10	619	25
2	14156	2628	11	142	14	14438	97	26921	152	9306	189	949	19	25	2	99	1	566	37
3	14153	2455	105	155	10	14094	248	25988	610	8747	280	928	14	46	11	108	5	593	26
4	14162	2579	85	170	12	14419	204	27003	523	9167	238	930	12	33	9	97	5	581	22
5	14171	2493	83	140	13	14240	188	27775	641	8909	218	893	21	43	9	112	6	613	22
6	14170	2580	74	163	12	14491	177	27407	601	9087	196	890	23	31	8	102	6	664	35
7	14173	2396	93	147	11	13646	320	25632	764	8500	272	901	22	25	8	101	5	578	33
8	14177	2574	87	133	13	14422	301	27272	724	8879	254	948	23	35	8	101	5	573	32
9	14167	2565	81	145	12	14333	292	27035	679	8896	228	904	23	36	7	119	7	610	31
10	14166	2570	77	165	12	14444	270	27823	702	9091	229	919	21	21	8	106	7	598	29
11	14167	2655	80	147	12	14208	258	27481	682	8936	219	938	21	34	8	105	6	580	28
12	14168	2624	78	160	12	13854	278	27016	650	8527	242	928	20	30	7	112	7	601	27
13	14161	39	704	153	11	503	****	39649	****	144	****	167	210	23	7	71	11	95	142
14	14169	2627	680	162	11	14316	****	27467	****	9050	****	936	203	19	8	131	13	625	137
15	14170	2628	659	160	11	14508	****	27143	****	8998	****	912	196	23	8	92	13	567	132
16	14165	2624	639	142	11	14472	****	27118	****	9046	****	936	190	29	8	120	13	582	128
17	14164	2580	620	149	10	14415	****	26989	****	8800	****	974	185	31	7	103	13	590	124
18	14159	46	822	150	10	531	****	38423	****	134	****	154	248	22	7	84	14	96	164
19	14174	2534	801	168	11	14061	****	27407	****	8922	****	929	242	30	7	110	13	558	159
20	14173	2567	782	166	11	14259	****	27375	****	8775	****	954	237	27	7	117	13	597	155

LINES DELETED: 13 18 3

AVE. BEAM CURRENT/SEC = 708

DATA REDUCED USING $B-AL: #GL9M

ON SPECIMEN: T241-4 JB-BS-13

$B-AL VERSION 1.0

OXIDE FORM.	WEIGHT% (OXIDE)	STD.DEV. (%)	HOMO. INDEX	FORMULA	K-RATIO	UNKN PEAK (COUNTS)	UNKN BKGD (COUNTS)	COUNTING TIME(SEC)	STD PEAK (COUNTS)	STD BKGD (COUNTS)	COUNTING TIME(SEC)	STANDARD FILENAME
NA2O	4.161	2.92	1.257	0.000	1.07662	2581.0	50.5	20.00	2400.2	49.7	20.00	ZRGSC
MGO	0.028	97.40	0.933	0.000	0.00750	153.8	136.3	20.00	2469.5	136.9	20.00	ZRGSC
AL2O3	12.533	1.20	2.055	0.000	0.95548	14300.0	246.8	20.00	14955.9	247.8	20.00	Z5831
SIO2	74.715	0.86	2.907	0.000	1.01150	27176.5	53.7	20.00	26868.4	53.9	20.00	Z5831
K2O	4.530	1.63	2.188	0.000	1.24234	8936.9	144.4	20.00	7230.1	152.8	20.00	ZRGSC
CAO	0.521	4.60	0.746	0.000	0.10201	927.1	178.7	20.00	7528.9	191.2	20.00	ZRGSC
TIO2	0.061	62.55	1.105	0.000	0.00055	29.4	18.3	20.00	19938.2	26.6	20.00	ZTIO2
MNO	0.077	30.55	0.982	0.000	0.00076	107.2	64.3	20.00	56342.7	119.9	20.00	ZMN20
FEO	0.949	5.70	1.087	0.000	0.14835	594.3	105.3	20.00	3409.3	112.6	20.00	ZRGSC

TOTAL 97.575 NO. OXYGENS = 0 NO. ITERS. = 2 AVE. ATOMIC NO. = 11.13

21-OCT-91 14:45:41

Listing of 50 closest matches for COMP. NO. 2641 [illegible]lements: Na, Al, Si, K , Ca, Fe Date of Update: 10/22/91

	Co.No	Sample Number	Date	[illegible]	Al2O3	Fe2O3	MgO	MnO	CaO	TiO2	Na2O	K2O	Total	[illegible]a. Co
1	2641	JB-BS-13 T241-4	10/21/91	76.49	12.83	1.08	0.03	0.08	0.53	0.06	4.26	4.64	100.00	1.0000
2	2643	JB-BS-15 T241-6	10/21/91	76.59	12.83	1.08	0.03	0.07	0.54	0.04	4.23	4.59	100.00	0.9937
3	2646	JB-WA-1 T242-1	10/21/91	76.77	12.70	1.09	0.02	0.07	0.53	0.06	4.19	4.57	100.00	0.9905
4	2639	JB-BS-11 T241-2	10/21/91	76.55	12.80	1.10	0.02	0.08	0.54	0.06	4.16	4.68	99.99	0.9880
5	2638	JB-BS-9 T241-1	10/21/91	76.42	12.92	1.10	0.01	0.08	0.55	0.05	4.22	4.65	100.00	0.9877
6	2640	JB-BS-12 T241-3	10/21/91	76.51	12.85	1.11	0.03	0.08	0.54	0.05	4.16	4.67	100.00	0.9871
7	2642	JB-BS-14 T241-5	10/21/91	76.55	12.82	1.11	0.02	0.07	0.55	0.06	4.20	4.62	100.00	0.9861
8	435	3-30-82-1, T43-3		76.62	12.93	1.06	0.02	0.05	0.54	0.07	4.13	4.59	100.01	0.9854
9	570	KRL91982D, T66-10	xx/xx/83	76.81	12.89	1.08	0.03	0.05	0.53	0.06	3.90	4.65	100.00	0.9841
10	2558	SS-91-1-1 T232-2	6/8/91	76.57	12.92	1.07	0.02	0.04	0.54	0.06	4.05	4.72	99.99	0.9830
11	2562	SS-91-1-4 T323-5	8/7/91	77.02	12.63	1.06	0.02	0.04	0.53	0.06	4.00	4.63	99.99	0.9826
12	2563	SS-91-1-5 T232-6	8/7/91	76.97	12.65	1.08	0.03	0.04	0.54	0.07	3.98	4.65	100.01	0.9822
13	1224	WL CORE G 370cm T92-7	5/2/85	76.83	12.82	1.09	0.04	0.04	0.54	0.05	3.95	4.65	100.01	0.9820
14	2060	FLV-64-CS T170-7	9/3/88	76.71	12.87	1.11	0.02	0.04	0.54	0.04	4.02	4.64	99.99	0.9820
15	1025	KRL-71082C (590) T58-1	6/22/84	76.91	12.71	1.08	0.02	0.00	0.53	0.05	3.95	4.74	99.99	0.9815
16	1409	KRL 82182 (A1) (599) T112-1	10/22/85	76.60	12.87	1.11	0.04	0.04	0.55	0.06	4.08	4.65	100.00	0.9813
17	2559	SS-91-1-SU T232-1	8/6/91	76.74	12.86	1.09	0.04	0.04	0.54	0.05	3.95	4.68	99.99	0.9809
18	1419	BL-RSA-5 T112-10	10/23/85	76.98	12.65	1.09	0.04	0.04	0.53	0.05	3.93	4.68	99.99	0.9807
19	566	KRL91882B, T64-12	09/06/83	76.81	12.82	1.10	0.01	0.05	0.53	0.08	3.91	4.69	100.00	0.9807
20	1418	BL-RSA-4 T112-9	10/23/85	76.83	12.79	1.08	0.04	0.04	0.55	0.06	3.96	4.65	100.00	0.9806
21	564	KRL82782A, T64-11	09/06/83	76.99	12.75	1.09	0.01	0.06	0.53	0.08	3.90	4.59	100.00	0.9805
22	431	YDS-1, T13-1		76.61	12.93	1.12	0.03	0.05	0.54	0.07	4.03	4.64	100.02	0.9804
23	2561	SS-91-1-3 t232-4	8/7/91	77.08	12.64	1.06	0.02	0.05	0.53	0.06	3.92	4.64	100.00	0.9799
24	2497	FLV-159-CH T219-6	12/20/90	77.01	12.76	1.08	0.03	0.03	0.54	0.05	3.94	4.57	100.01	0.9798
25	1196	WALKER LAKE CORE G 380CM t89-1	2/28/85	76.98	12.79	1.08	0.02	0.05	0.54	0.05	3.86	4.64	100.01	0.9797
26	680	KRL-82282B, T54-4	xx//xx/x	76.99	12.71	1.08	0.02	0.06	0.53	0.04	3.86	4.70	99.99	0.9796
27	2644	JB-BS-16 T241-7	10/21/91	76.97	12.59	1.04	0.02	0.08	0.54	0.05	4.13	4.58	100.00	0.9793
28	2494	FLV-156-SS T219-3	12/20/90	76.64	13.06	1.09	0.03	0.04	0.54	0.05	3.94	4.62	100.01	0.9785
29	681	KRL-91882A', T66-8	10/25/83	76.79	12.83	1.10	0.03	0.06	0.54	0.07	3.91	4.67	100.00	0.9785
30	551	KRL82282A, T66-5	10/25/83	76.71	12.88	1.12	0.04	0.05	0.52	0.06	3.98	4.65	100.01	0.9785
31	760	BD-16		76.59	12.92	1.11	0.03	0.03	0.54	0.07	4.00	4.71	100.00	0.9784
32	567	KRL91882-K-1, T64-13	09/06/83	76.93	12.82	1.11	0.01	0.05	0.53	0.07	3.88	4.60	100.00	0.9781
33	132	LD-12, T3,4		76.94	12.70	1.12	0.03	0.07	0.53	0.07	3.91	4.64	100.01	0.9777
34	2564	SS-91-1-Adgas	8/7/91	76.73	12.85	1.04	0.03	0.05	0.53	0.07	3.95	4.74	99.99	0.9774
35	2571	JB-BS-7 T227-4	6/13/91	76.73	12.89	1.10	0.03	0.05	0.54	0.06	3.91	4.69	100.00	0.9771
36	2488	FLV-149-CS T218-8	11/19/90	76.77	13.05	1.07	0.03	0.05	0.53	0.06	3.81	4.63	100.00	0.9771
37	701	LD-12		76.94	12.72	1.12	0.03	0.07	0.53	0.07	3.91	4.61	100.00	0.9765
38	682	KRL-91882G, T66-11	10/25/83	76.91	12.76	1.07	0.03	0.06	0.54	0.07	3.87	4.68	99.99	0.9765
39	1680	KRL 860922 A T134-2	11/25/86	76.94	12.75	1.07	0.03	0.04	0.55	0.06	3.91	4.65	100.00	0.9763
40	679	KRL-82182(A-4), T66-3	10/25/83	76.89	12.82	1.02	0.02	0.05	0.52	0.04	4.08	4.55	99.99	0.9763
41	1694	SCHURZ-1 T134-6	11/25/86	77.01	12.64	1.09	0.03	0.05	0.55	0.05	3.94	4.64	100.00	0.9763
42	2669	JB-BS-5 T227-2	6/13/91	76.69	12.91	1.08	0.02	0.05	0.55	0.09	3.90	4.70	99.99	0.9763
43	753	BD-1		76.45	13.11	1.09	0.03	0.04	0.51	0.07	4.00	4.70	100.00	0.9762
44	1225	WL CORE G 380cm T92-8	5/2/85	76.82	12.79	1.06	0.04	0.04	0.56	0.06	4.00	4.65	100.02	0.9762
45	1240	WL 4-2 3.29m T93-9	5/2/85	76.75	12.79	1.13	0.03	0.04	0.55	0.05	4.02	4.64	100.00	0.9761
46	571	KRL91982F, T56-5	07/01/83	76.61	12.89	1.14	0.03	0.05	0.55	0.05	4.12	4.56	100.00	0.9758
47	1244	WL 8-3A ASH A 64-66cm T93-13	5/2/85	76.97	12.80	1.08	0.03	0.05	0.55	0.05	3.86	4.60	99.99	0.9754
48	739	S-20		76.83	12.90	1.09	0.03	0.07	0.51	0.06	4.00	4.50	99.99	0.9753
49	684	KRL--92082D, T66-12	10/25/83	77.02	12.69	1.09	0.02	0.05	0.51	0.04	3.92	4.66	100.00	0.9752
50	559	KRL82182(bubble wall), T56-4	07/01/83	76.87	12.92	1.01	0.02	0.03	0.53	0.03	4.03	4.55	99.99	0.9750

Listing of 25 closest matches for COMP. NO. 2640 for elements: Na, Al, Si, K , Ca, Fe Date of Update: 06/18/92

	C.No	Sample Number	Date	SiO2	Al2O3	Fe2O3	MgO	MnO	CaO	TiO2	Na2O	K2O	Total,R	Sim. Co
1	2640	JB-BS-13 T241-4	10/21/91	76.49	12.83	1.08	0.03	0.08	0.53	0.06	4.26	4.64	100.00	1.0000
2	2642	JB-BS-15 T241-6	10/21/91	76.59	12.83	1.08	0.03	0.07	0.54	0.04	4.23	4.59	100.00	0.9937
3	2645	JB-WA-1 T242-1	10/21/91	76.77	12.70	1.09	0.02	0.07	0.53	0.06	4.19	4.57	100.00	0.9909
4	2638	JB-BS-11 T241-2	10/21/91	76.55	12.80	1.10	0.02	0.08	0.54	0.06	4.16	4.68	99.99	0.9880
5	2637	JB-BS-9 T241-1	10/21/91	76.42	12.92	1.10	0.01	0.08	0.55	0.05	4.22	4.65	100.00	0.9877
6	2639	JB-BS-12 T241-3	10/21/91	76.51	12.85	1.11	0.03	0.08	0.54	0.05	4.16	4.67	100.00	0.9871
7	2641	JB-BS-14 T241-5	10/21/91	76.55	12.82	1.11	0.02	0.07	0.55	0.06	4.20	4.62	100.00	0.9861
8	435	3-30-82-1, T43-3		76.62	12.93	1.06	0.02	0.05	0.54	0.07	4.13	4.59	100.01	0.9854
9	2707	FLV-192-BC T246-1	12/12/91	77.01	12.55	1.05	0.03	0.05	0.53	0.05	4.18	4.56	100.01	0.9846
10	570	KRL91982D, T66-10	xx/xx/83	76.81	12.89	1.08	0.03	0.05	0.53	0.06	3.90	4.65	100.00	0.9841
11	2716	FLV-200-LC T249-4	1/30/92	76.77	12.80	1.11	0.02	0.04	0.53	0.06	4.01	4.67	100.01	0.9836
12	2557	SS-91-1-1 T232-2	6/8/91	76.57	12.92	1.07	0.02	0.04	0.54	0.06	4.05	4.72	99.99	0.9830
13	2561	SS-91-1-4 T323-5	8/7/91	77.02	12.63	1.06	0.02	0.04	0.53	0.06	4.00	4.63	99.99	0.9826
14	2562	SS-91-1-5 T232-6	8/7/91	76.97	12.65	1.08	0.03	0.04	0.54	0.07	3.98	4.65	100.01	0.9822
15	1224	WL CORE G 370cm T92-7	5/2/85	76.83	12.82	1.09	0.04	0.04	0.54	0.05	3.95	4.65	100.01	0.9820
16	2060	FLV-64-CS T170-7	9/3/88	76.71	12.87	1.11	0.02	0.04	0.54	0.04	4.02	4.64	99.99	0.9820
17	1025	KRL-71082C (590) T58-1	6/22/84	76.91	12.71	1.08	0.02	0.00	0.53	0.05	3.95	4.74	99.99	0.9819
18	2717	FLV-201-TO T249-5	1/30/92	76.85	12.77	1.10	0.02	0.04	0.54	0.04	3.99	4.65	100.00	0.9814
19	1409	KRL 82182 (A1) (599) T112-1	10/22/85	76.60	12.87	1.11	0.04	0.04	0.55	0.06	4.08	4.65	100.00	0.9813
20	2558	SS-91-1-SU T232-1	8/6/91	76.74	12.86	1.09	0.04	0.04	0.54	0.05	3.95	4.68	99.99	0.9809
21	1419	BL-RSA-5 T112-10	10/23/85	76.98	12.65	1.09	0.04	0.04	0.53	0.05	3.93	4.68	99.99	0.9807
22	566	KRL91882B, T64-12	09/06/83	76.81	12.82	1.10	0.01	0.05	0.53	0.08	3.91	4.69	100.00	0.9807
23	1418	BL-RSA-4 T112-9	10/23/85	76.83	12.79	1.08	0.04	0.04	0.55	0.06	3.96	4.65	100.00	0.9806
24	564	KRL82782A, T64-11	09/06/83	76.99	12.75	1.09	0.01	0.06	0.53	0.08	3.90	4.59	100.00	0.9805
25	431	YOS-1, T13-1		76.61	12.93	1.12	0.03	0.05	0.54	0.07	4.03	4.64	100.02	0.9804

SAMPLE ID: JB-BS-13 T241-4 D[illegible] of Analysis: 10/21/91

Raw Probe Data		Raw Probe Data (FeO to Fe2O3)		[illegible]lculated to 100%	
SiO2	74.715			SiO2	76.49
Al2O3	12.533			Al2O3	12.83
FeO	0.949*1.1113=Fe2O3		1.055	Fe2O3	1.08
MgO	0.028			MgO	0.03
MnO	0.077			MnO	0.08
CaO	0.321			CaO	0.53
TiO2	0.061			TiO2	0.06
Na2o	4.161			Na2o	4.26
K2O	4.530			K2O	4.64
TOTAL(O)	97.575	TOTAL(N)	97.681	TOTAL(R)	100.00

20 Best Matches:

1	0.9880	10/21/91	JB-BS-11 T241-2
2	0.9877	10/21/91	JB-BS-9 T241-1
3	0.9871	10/21/91	JB-BS-12 T241-3
4	0.9854		3-30-82-1, T43-3
5	0.9841	xx/xx/83	KRL91982D, T66-10
6	0.9830	6/8/91	SS-91-1-1 T232-2
7	0.9826	8/7/91	SS-91-1-4 T323-5
8	0.9822	8/7/91	SS-91-1-5 T232-6
9	0.9820	5/2/85	WL CORE G 370cm T92-7
10	0.9820	9/3/88	FLV-64-CS T170-7
11	0.9819	6/22/84	KRL-71082C (590) T58-1
12	0.9813	10/22/85	KRL 82182 (A1) (599) T112-1
13	0.9809	8/6/91	SS-91-1-SU T232-1
14	0.9807	10/23/85	BL-RSA-5 T112-10
15	0.9807	09/06/83	KRL91882B, T64-12
16	0.9806	10/23/85	BL-RSA-4 T112-9
17	0.9805	09/06/83	KRL82782A, T64-11
18	0.9804		YOS-1, T13-1
19	0.9799	8/7/91	SS-91-1-3 t232-4
20	0.9798	12/20/90	FLV-159-CM T219-6

Elements used in the calculation are:

Na2o
Al2O3
SiO2
K2O
CaO
FeO

***** This sample has been added to the data base *****

SAMPLE: T2 JB-BS-14

	BEAM	NA	9	MG	8	AL	3	SI	7	K	2	CA	6	TI	5	MN	1	FE	4
PT	COUNTS	COUNTS	SD	COUNTS	SD	COUNTS	SD	COUNTS	SD	COUNTS	SD	COUNTS	SD	COUNTS	SD	COUNTS	SD	COUNTS	SD
1	14188	2553	51	148	12	14729	121	27530	166	9218	96	936	31	28	5	107	10	609	25
2	14182	2642	63	146	1	14335	278	27336	137	8917	212	928	6	24	3	95	9	614	4
3	14179	2548	53	156	5	14324	231	27451	98	9015	153	963	18	25	2	96	7	603	5
4	14178	45	****	134	9	473	****	38956	****	136	****	188	377	16	5	87	9	103	253
5	14181	2803	****	151	9	14946	****	27326	****	8771	****	1089	360	33	6	112	10	586	224
6	14185	2612	****	151	8	14344	****	27788	****	9090	****	969	327	25	6	90	10	644	208
7	14195	6479	****	146	7	23300	****	23011	****	2787	****	3041	882	18	6	84	11	159	235
8	14195	2572	****	127	10	14389	****	27817	****	9006	****	945	820	28	5	103	10	646	226
9	14189	2423	****	143	9	13878	****	27203	****	8755	****	1023	768	26	5	117	12	599	214
10	14186	2522	****	162	10	14492	****	27283	****	8989	****	934	726	39	7	101	11	622	205
11	14192	2634	****	166	11	14510	****	27595	****	9084	****	904	692	42	8	106	11	608	197
12	14191	2530	****	146	11	14229	****	27665	****	8901	****	896	662	27	7	90	11	620	190
13	14195	2575	****	163	11	14533	****	27383	****	8929	****	939	634	25	7	94	10	574	182
14	14198	2512	****	166	12	14732	****	27359	****	9119	****	932	611	37	7	95	10	623	176
15	14195	2557	****	142	11	14450	****	27575	****	9150	****	977	589	31	7	122	11	616	171
16	14202	2768	****	142	11	14626	****	27399	****	8949	****	822	571	25	7	103	11	453	167
17	14196	3955	****	175	12	28852	****	20042	****	1404	****	12818	****	23	7	85	11	440	163
18	14197	2601	****	151	12	14514	****	27829	****	8911	****	924	****	24	7	101	11	602	159
19	14201	2544	****	146	12	14279	****	27529	****	8917	****	946	****	22	7	111	11	614	156
20	14204	2548	****	150	12	14505	****	26995	****	9026	****	958	****	31	7	110	11	619	152

LINES DELETED: 4 7 16 17

AVE. BEAM CURRENT/SEC = 710

DATA REDUCED USING $B-AL: #GL9M

ON SPECIMEN: T241-5 JB-BS-14

$B-AL VERSION 1.0

OXIDE FORM.	WEIGHT% (OXIDE)	STD.DEV. (%)	HOMO. INDEX	FORMULA	K-RATIO	UNKN PEAK (COUNTS)	UNKN BKGD (COUNTS)	COUNTING TIME(SEC)	STD PEAK (COUNTS)	STD BKGD (COUNTS)	COUNTING TIME(SEC)	STANDARD FILENAME
NA2O	4.141	2.93	1.585	0.000	1.07342	2573.5	50.4	20.00	2400.2	49.7	20.00	ZRGSC
MGO	0.024	114.09	0.822	0.000	0.00637	151.2	136.4	20.00	2469.5	136.9	20.00	ZRGSC
AL2O3	12.649	1.20	2.006	0.000	0.96559	14449.3	247.4	20.00	14955.9	247.8	20.00	Z5831
SIO2	75.509	0.95	1.403	0.000	1.02277	27479.0	53.8	20.00	26968.4	53.9	20.00	Z5831
K2O	4.5[illegible]7	1.63	1.352	0.000	1.24944	8987.4	144.7	20.00	7230.1	152.8	20.00	ZRGSC
CAO	0.540	4.51	1.516	0.000	0.10559	954.0	179.2	20.00	7528.9	191.2	20.00	ZRGSC
TIO2	0.059	64.51	1.095	0.000	0.00054	29.0	18.4	20.00	19938.2	26.6	20.00	ZTIO2
MNO	0.069	33.36	0.957	0.000	0.00069	103.4	64.5	20.00	56342.7	119.9	20.00	ZMN2O
FEO	0.984	5.58	0.737	0.000	0.15375	612.4	105.6	20.00	3409.3	112.6	20.00	ZRGSC

TOTAL 98.530 NO. OXYGENS = 0 NO. ITERS. = 2 AVE. ATOMIC NO. = 11.16

21-OCT-91 15:00:19

Listing of 25 closest matches for COMP. NO. 2641 for elements: Na, Al, Si, K , Ca, Fe Date of Update: 06/18/92

	C.No	Sample Number	Date	SiO2	Al2O3	Fe2O3	MgO	MnO	CaO	TiO2	Na2O	K2O	Total,R	Sim. Co
1	2641	JB-BS-14 T241-5	10/21/91	76.55	12.82	1.11	0.02	0.07	0.55	0.06	4.20	4.62	100.00	1.0000
2	2637	JB-BS-9 T241-1	10/21/91	76.42	12.92	1.10	0.01	0.08	0.55	0.05	4.22	4.65	100.00	0.9951
3	1409	KRL 82182 (A1) (599) T112-1	10/22/85	76.60	12.87	1.11	0.04	0.04	0.55	0.06	4.08	4.65	100.00	0.9934
4	2639	JB-BS-12 T241-3	10/21/91	76.51	12.85	1.11	0.03	0.08	0.54	0.05	4.16	4.67	100.00	0.9931
5	2638	JB-BS-11 T241-2	10/21/91	76.55	12.80	1.10	0.02	0.08	0.54	0.06	4.16	4.68	99.99	0.9915
6	2642	JB-BS-15 T241-6	10/21/91	76.59	12.83	1.08	0.03	0.07	0.54	0.04	4.23	4.59	100.00	0.9900
7	571	KRL91982F, T56-5	07/01/83	76.61	12.89	1.14	0.03	0.05	0.55	0.05	4.12	4.56	100.00	0.9892
8	1240	WL 4-2 3.29m T93-9	5/2/85	76.75	12.79	1.13	0.03	0.04	0.55	0.05	4.02	4.64	100.00	0.9884
9	2060	FLV-64-CS T170-7	9/3/88	76.71	12.87	1.11	0.02	0.04	0.54	0.04	4.02	4.64	99.99	0.9881
10	2682	JB-BS-9 T241-1	10/21/91	76.15	13.07	1.11	0.01	0.08	0.56	0.05	4.27	4.70	100.00	0.9874
11	2645	JB-WA-1 T242-1	10/21/91	76.77	12.70	1.09	0.02	0.07	0.53	0.06	4.19	4.57	100.00	0.9867
12	431	YOS-1, T13-1		76.61	12.93	1.12	0.03	0.05	0.54	0.07	4.03	4.64	100.02	0.9865
13	2640	JB-BS-13 T241-4	10/21/91	76.49	12.83	1.08	0.03	0.08	0.53	0.06	4.26	4.64	100.00	0.9861
14	783	GS-27		76.74	12.92	1.12	0.03	0.05	0.55	0.07	3.91	4.61	100.00	0.9849
15	2717	FLV-201-TO T249-5	1/30/92	76.85	12.77	1.10	0.02	0.04	0.54	0.04	3.99	4.65	100.00	0.9848
16	760	BO-16		76.59	12.92	1.11	0.03	0.03	0.54	0.07	4.00	4.71	100.00	0.9845
17	435	3-30-82-1, T43-3		76.62	12.93	1.06	0.02	0.05	0.54	0.07	4.13	4.59	100.01	0.9840
18	1418	BL-RSA-4 T112-9	10/23/85	76.83	12.79	1.08	0.04	0.04	0.55	0.06	3.96	4.65	100.00	0.9839
19	2716	FLV-200-LC T249-4	1/30/92	76.77	12.80	1.11	0.02	0.04	0.53	0.06	4.01	4.67	100.01	0.9839
20	758	BO-11		76.35	13.11	1.12	0.03	0.04	0.55	0.09	4.00	4.70	99.99	0.9836
21	1223	WL CORE G 180cm T92-6	5/2/85	76.64	12.88	1.11	0.04	0.05	0.57	0.06	3.99	4.67	100.01	0.9831
22	1684	SCHURE-1 T134-6	11/25/86	77.01	12.64	1.09	0.03	0.05	0.55	0.05	3.94	4.64	100.00	0.9826
23	1224	WL CORE G 370cm T92-7	5/2/85	76.83	12.82	1.09	0.04	0.04	0.54	0.05	3.95	4.65	100.01	0.9824
24	788	GS-32		76.58	12.90	1.13	0.03	0.04	0.56	0.06	4.00	4.70	100.00	0.9822
25	2708	FLV-193-BC T246-2	12/12/91	76.75	12.61	1.16	0.04	0.06	0.56	0.06	4.11	4.65	100.00	0.9820

Listing of 50 closest matches for COMP. NO. 2642 for elements: Na, Al, Si, K, Ca, Fe Date of Update: 10/22/91

C.No		Sample Number	Date	[illegible]	Al2O3	Fe2O3	MgO	MnO	CaO	TiO2	Na2O	K2O	Total	[illegible]
1	2642	JB-BS-14 T241-5	10/21/91	76.55	12.82	1.11	0.02	0.07	0.55	0.06	4.20	4.62	100.00	1.0000
2	2638	JB-BS-9 T241-1	10/21/91	76.42	12.92	1.10	0.01	0.08	0.55	0.05	4.22	4.65	100.00	0.9951
3	1439	KRL #2182 (A1) (599) T112-1	10/22/85	76.60	12.87	1.11	0.04	0.04	0.55	0.06	4.08	4.65	100.00	0.9934
4	2640	JB-BS-12 T241-3	10/21/91	76.51	12.85	1.11	0.03	0.08	0.54	0.05	4.16	4.67	100.00	0.9931
5	2639	JB-BS-11 T241-2	10/21/91	76.55	12.80	1.10	0.02	0.08	0.54	0.06	4.18	4.68	99.99	0.9912
6	2643	JB-BS-15 T241-6	10/21/91	76.59	12.83	1.08	0.03	0.07	0.54	0.04	4.23	4.59	100.00	0.9900
7	571	KRL91982F, T56-5	07/01/83	76.61	12.89	1.14	0.03	0.05	0.55	0.05	4.12	4.56	100.00	0.9892
8	1260	WL 4-2 3.29m T93-9	5/2/85	76.75	12.79	1.13	0.03	0.04	0.55	0.05	4.02	4.64	100.01	0.9884
9	2060	FLV-64-CS T170-7	9/3/88	76.71	12.87	1.11	0.02	0.04	0.54	0.04	4.02	4.64	99.99	0.9881
10	2646	JB-WA-1 T242-1	10/21/91	76.77	12.70	1.09	0.02	0.07	0.53	0.06	4.15	4.57	100.00	0.9867
11	431	YDS-1, T13-1		76.61	12.93	1.12	0.03	0.05	0.54	0.07	4.03	4.64	100.02	0.9865
12	2641	JB-BS-13 T241-4	10/21/91	76.49	12.83	1.08	0.03	0.08	0.53	0.06	4.26	4.64	100.00	0.9861
13	783	GS-27		76.74	12.92	1.12	0.03	0.05	0.55	0.07	3.91	4.61	100.00	0.9845
14	760	BD-16		76.59	12.92	1.11	0.03	0.03	0.54	0.07	4.00	4.71	100.00	0.9845
15	435	3-30-82-1, T43-3		76.62	12.93	1.06	0.02	0.05	0.54	0.07	4.13	4.59	100.01	0.9840
16	1418	BL-RSA-4 T112-9	10/23/85	76.83	12.79	1.08	0.04	0.04	0.55	0.06	3.96	4.65	100.00	0.9835
17	758	BD-11		76.35	13.11	1.12	0.03	0.04	0.55	0.09	4.00	4.70	99.99	0.9834
18	1223	WL CORE G 180cm T92-6	5/2/85	76.64	12.88	1.11	0.04	0.05	0.57	0.06	3.95	4.67	100.01	0.9831
19	1684	SCHURZ-1 T134-6	11/25/86	77.01	12.64	1.09	0.03	0.05	0.55	0.05	3.94	4.64	100.00	0.9826
20	1224	WL CORE G 370cm T92-7	5/2/85	76.83	12.82	1.09	0.04	0.04	0.54	0.05	3.95	4.65	100.01	0.9824
21	788	GS-32		76.58	12.90	1.13	0.03	0.04	0.56	0.06	4.00	4.70	100.00	0.9822
22	681	KRL-91882A*, T66-8	10/25/83	76.79	12.83	1.10	0.03	0.06	0.54	0.07	3.91	4.67	100.00	0.9815
23	2236	SL-103 T186-2	2/28/89	76.68	12.95	1.10	0.03	0.04	0.55	0.07	3.88	4.69	99.99	0.9814
24	1241	WL 4-2 3.31m T93-10	5/2/85	76.69	12.91	1.14	0.04	0.04	0.55	0.06	3.92	4.67	100.02	0.9813
25	2559	SS-91-1-SU T232-1	8/6/91	76.74	12.86	1.09	0.04	0.04	0.54	0.05	3.95	4.68	99.99	0.9810
26	1416	BL-RSA-2 T112-7	10/23/85	76.78	12.85	1.12	0.04	0.03	0.54	0.06	3.90	4.68	100.00	0.9806
27	2494	FLV-156-SS T219-3	12/20/90	76.64	13.06	1.09	0.03	0.04	0.54	0.05	3.94	4.62	100.01	0.9804
28	1291	WL 8-1B 192-194cm T99-3	07/01/85	76.95	12.70	1.11	0.03	0.06	0.56	0.07	3.86	4.64	99.98	0.9804
29	1245	WL 8-3A ASH B 59.5-64.0cm T93-	5/2/85	77.00	12.70	1.10	0.03	0.06	0.56	0.04	3.85	4.61	99.99	0.9803
30	1417	BL-RSA-3 T112-8	10/23/85	76.83	12.80	1.15	0.04	0.05	0.55	0.05	3.65	4.64	100.00	0.9803
31	2571	JB-BS-7 T227-4	6/13/91	76.73	12.89	1.10	0.03	0.05	0.54	0.06	3.91	4.69	100.00	0.9802
32	2558	SS-91-1-1 T232-2	6/8/91	76.57	12.92	1.07	0.02	0.04	0.54	0.06	4.05	4.72	99.99	0.9801
33	1244	WL 8-3A ASH A 64-66cm T93-13	5/2/85	76.97	12.80	1.08	0.03	0.05	0.55	0.05	3.86	4.60	99.99	0.9801
34	2170	KRL-82982-KP T178-5	12/6/88	76.70	13.01	1.11	0.02	0.06	0.55	0.06	3.81	4.67	99.99	0.9800
35	1872	WL-4-5B (144.77m) T164-1	5/21/88	76.73	12.71	1.15	0.00	0.03	0.54	0.12	4.02	4.69	99.99	0.9797
36	557	KRL91882-K-1, T64-13	09/06/83	76.93	12.82	1.11	0.01	0.05	0.53	0.07	3.88	4.60	100.00	0.9797
37	1680	KRL 860922 A T134-2	11/25/86	76.94	12.75	1.07	0.03	0.04	0.55	0.06	3.91	4.65	100.00	0.9797
38	2563	SS-91-1-5 T232-6	8/7/91	76.97	12.65	1.08	0.03	0.04	0.54	0.07	3.98	4.65	100.01	0.9795
39	1227	WL 8-2A 61-5-70.0cm T92-11	5/2/85	77.09	12.70	1.11	0.03	0.05	0.55	0.04	3.78	4.65	100.00	0.9795
40	1225	WL CORE G 380cm T92-8	5/2/85	76.82	12.79	1.06	0.04	0.04	0.56	0.06	4.00	4.65	100.02	0.9795
41	1290	WL 8-1B 92-94cm T99-1	07/01/85	76.99	12.72	1.11	0.02	0.06	0.54	0.07	3.84	4.65	100.00	0.9794
42	2569	JB-BS-5 T227-2	6/13/91	76.69	12.91	1.08	0.02	0.05	0.55	0.09	3.90	4.70	99.99	0.9793
43	1621	BD-18 JOD	09/12/86	76.98	12.70	1.10	0.03	0.05	0.55	0.07	3.83	4.68	99.99	0.9792
44	1969	WL-4-4B (12.00M) T162-3	5/14/88	76.93	12.81	1.13	0.03	0.05	0.55	0.05	3.75	4.64	99.98	0.9791
45	1672	KRL 82182 (A-1) T117-3	3/6/86	76.80	12.75	1.10	0.03	0.04	0.55	0.07	3.87	4.77	99.98	0.9787
46	2497	FLV-159-CH T219-6	12/20/90	77.01	12.76	1.08	0.03	0.03	0.54	0.05	3.94	4.57	100.01	0.9786
47	561	KRL82282A, T66-5	10/25/83	76.71	12.88	1.12	0.04	0.05	0.52	0.06	3.98	4.65	100.01	0.9785
48	791	LD-12		76.94	12.72	1.12	0.03	0.07	0.53	0.07	3.91	4.61	100.00	0.9784
49	1229	WL 8-3A 14.5-20cm T92-13	5/2/85	77.03	12.78	1.09	0.03	0.04	0.55	0.06	3.78	4.63	99.99	0.9784
50	2644	JB-BS-16 T241-7	10/21/91	76.97	12.59	1.04	0.02	0.08	0.54	0.05	4.13	4.58	100.00	0.9783

SAMPLE ID: JB-BS-14 T241-5 Date of Analysis: 10/21/91

Raw Probe Data		Raw Probe Data (FeO to Fe2O3)		Recalculated to 100%	
SiO2	75.508			SiO2	76.55
Al2O3	12.643			Al2O3	12.82
FeO	0.984*1.1113=Fe2O3		1.094	Fe2O3	1.11
MgO	0.024			MgO	0.02
MnO	0.069			MnO	0.07
CaO	0.540			CaO	0.55
TiO2	0.059			TiO2	0.06
Na2o	4.141			Na2o	4.20
K2O	4.557			K2O	4.62
TOTAL(O)	98.530	TOTAL(N)	98.640	TOTAL(R)	100.00

20 Best Matches:

1	0.9951	10/21/91	JB-BS-9 T241-1
2	0.9934	10/22/85	KRL 82182 (A1) (599) T112-1
3	0.9931	10/21/91	JB-BS-12 T241-3
4	0.9915	10/21/91	JB-BS-11 T241-2
5	0.9892	07/01/83	KRL91982F, T56-5
6	0.9884	5/2/85	WL 4-2 3.29m T93-9
7	0.9881	9/3/88	FLV-64-CS T170-7
8	0.9865		YOS-1, T13-1
9	0.9861	10/21/91	JB-BS-13 T241-4
10	0.9849		GS-27
11	0.9845		BO-16
12	0.9840		3-30-82-1, T43-3
13	0.9839	10/23/85	BL-RSA-4 T112-9
14	0.9836		BO-11
15	0.9831	5/2/85	WL CORE G 180cm T92-6
16	0.9826	11/25/86	SCHURZ-1 T134-6
17	0.9824	5/2/85	WL CORE G 370cm T92-7
18	0.9822		GS-32
19	0.9815	10/25/83	KRL-91882A", T66-8
20	0.9814	2/28/89	SL-103 T186-2

Elements used in the calculation are:

Na2o
Al2O3
SiO2
K2O
CaO
FeO

***** This sample has been added to the data base *****

SAMPLE: T2[illegible] JB-BS-15

PT	BEAM COUNTS	NA COUNTS	9 SD	MG COUNTS	8 SD	AL COUNTS	3 SD	SI COUNTS	7 SD	K COUNTS	2 SD	CA COUNTS	6 SD	TI COUNTS	5 SD	MN COUNTS	1 SD	FE COUNTS	4 SD
1	14205	2623	51	147	12	14711	121	26991	164	9059	95	945	31	26	5	98	10	611	25
2	14207	2660	26	155	6	14756	32	26852	98	8770	204	924	15	25	1	96	1	562	35
3	14207	52	****	132	12	524	****	38205	****	129	****	153	451	17	5	91	4	83	292
4	14214	2554	****	149	10	14167	****	27756	****	9043	****	931	390	26	4	107	7	611	257
5	14220	2539	****	143	9	14801	****	27766	****	9113	****	902	346	25	4	106	7	655	238
6	14209	2521	****	134	9	14463	****	27516	****	9011	****	935	316	38	7	80	10	610	217
7	14210	2509	953	133	9	14300	****	27878	****	8977	****	936	293	34	7	100	9	603	201
8	14215	2593	892	169	13	14319	****	28139	****	8873	****	940	275	23	6	118	11	609	188
9	14214	2662	846	142	12	14733	****	27420	****	9041	****	946	260	22	6	106	11	650	179
10	14214	2796	812	147	11	14590	****	27570	****	8830	****	1014	251	23	6	96	10	594	169
11	14211	2801	783	147	11	14704	****	27802	****	8546	****	1053	245	24	6	112	10	511	161
12	14204	2627	749	153	10	14383	****	27102	****	9077	****	967	235	26	5	109	10	567	154
13	14206	29	975	142	10	463	****	37844	****	137	****	169	300	17	6	78	12	100	194
14	14215	2515	940	142	10	14312	****	27596	****	9006	****	949	290	30	6	116	12	607	188
15	14219	2630	911	161	10	14520	****	27580	****	9029	****	932	281	35	6	102	12	593	182
16	14217	2581	884	161	10	14481	****	27986	****	8921	****	955	273	25	6	109	11	621	177
17	14222	2496	857	166	11	14727	****	27564	****	9047	****	859	264	26	6	110	11	645	173
18	14223	2525	833	167	12	14449	****	27831	****	9147	****	937	257	24	5	116	11	625	169
19	14218	2546	811	141	11	14266	****	27547	****	8988	****	983	231	21	5	96	11	758	172
20	14239	2626	792	166	12	14266	****	27820	****	8861	****	936	245	18	6	99	11	580	167

LINES DELETED: 3 13 19

AVE. BEAM CURRENT/SEC = 711

DATA REDUCED USING $B-AL: #GL9M

ON SPECIMEN: T241-6 JB-BS-15

$B-AL VERSION 1.0

OXIDE FORM.	WEIGHT% (OXIDE)	STD.DEV. (%)	HOMO. INDEX	FORMULA	K-RATIO	UNKN PEAK (COUNTS)	UNKN BKGD (COUNTS)	COUNTING TIME(SEC)	STD PEAK (COUNTS)	STD BKGD (COUNTS)	COUNTING TIME(SEC)	STANDARD FILENAME
NA2O	4.184	2.92	1.789	0.000	1.08616	2603.4	50.4	20.00	2400.2	49.7	20.00	%RGSC
MGO	0.025	108.44	0.927	0.000	0.00672	152.0	136.4	20.00	2469.5	136.9	20.00	%RGSC
AL2O3	12.698	1.20	1.669	0.000	0.96976	14510.7	247.5	20.00	14955.9	247.8	20.00	%5831
SIO2	75.829	0.86	2.091	0.000	1.02722	27598.2	53.8	20.00	26868.4	53.9	20.00	%5831
K2O	4.545	1.63	1.577	0.000	1.24582	8961.9	144.8	20.00	7230.1	152.8	20.00	%RGSC
CAO	0.534	4.54	1.350	0.000	0.10432	944.8	179.3	20.00	7528.9	191.2	20.00	%RGSC
TIO2	0.043	84.59	0.982	0.000	0.00040	26.3	18.4	20.00	19938.2	26.6	20.00	%TIO2
MNO	0.072	32.24	0.914	0.000	0.00072	104.9	64.6	20.00	56342.7	119.9	20.00	%MN2O
FEO	0.966	5.65	1.435	0.000	0.15093	603.2	105.6	20.00	3409.3	112.6	20.00	%RGSC

TOTAL 98.896 NO. OXYGENS = 0 NO. ITERS. = 2 AVE. ATOMIC NO. = 11.17

21-OCT-91 15:15:07

Listing of 25 closest matches for COMP. NO. 2642 for elements: Na, Al, Si, K , Ca, Fe Date of Update: 06/18/92

	C.No	Sample Number	Date	SiO2	Al2O3	Fe2O3	MgO	MnO	CaO	TiO2	Na2O	K2O	Total,R	Sim. Co
1	2642	JB-BS-15 T241-6	10/21/91	76.59	12.83	1.08	0.03	0.07	0.54	0.04	4.23	4.59	100.00	1.0000
2	2640	JB-BS-13 T241-4	10/21/91	76.49	12.83	1.08	0.03	0.08	0.53	0.06	4.26	4.64	100.00	0.9937
3	435	3-30-82-1, T43-3		76.62	12.93	1.06	0.02	0.05	0.54	0.07	4.13	4.59	100.01	0.9916
4	2645	JB-WA-1 T242-1	10/21/91	76.77	12.70	1.09	0.02	0.07	0.53	0.06	4.19	4.57	100.00	0.9910
5	2638	JB-BS-11 T241-2	10/21/91	76.55	12.80	1.10	0.02	0.08	0.54	0.06	4.16	4.68	99.99	0.9905
6	2641	JB-BS-14 T241-5	10/21/91	76.55	12.82	1.11	0.02	0.07	0.55	0.06	4.20	4.62	100.00	0.9900
7	2637	JB-BS-9 T241-1	10/21/91	76.42	12.92	1.10	0.01	0.08	0.55	0.05	4.22	4.65	100.00	0.9899
8	2639	JB-BS-12 T241-3	10/21/91	76.51	12.85	1.11	0.03	0.08	0.54	0.05	4.16	4.67	100.00	0.9894
9	2496	FLV-159-CH T219-6	12/20/90	77.01	12.76	1.08	0.03	0.03	0.54	0.05	3.94	4.57	100.01	0.9860
10	2643	JB-BS-16 T241-7	10/21/91	76.97	12.59	1.04	0.02	0.08	0.54	0.05	4.13	4.58	100.00	0.9856
11	2557	SS-91-1-1 T232-2	6/8/91	76.57	12.92	1.07	0.02	0.04	0.54	0.06	4.05	4.72	99.99	0.9856
12	2562	SS-91-1-5 T232-6	8/7/91	76.97	12.65	1.08	0.03	0.04	0.54	0.07	3.98	4.65	100.01	0.9848
13	2707	FLV-192-BC T246-1	12/12/91	77.01	12.55	1.05	0.03	0.05	0.53	0.05	4.18	4.56	100.01	0.9847
14	2060	FLV-64-CS T170-7	9/3/88	76.71	12.87	1.11	0.02	0.04	0.54	0.04	4.02	4.64	99.99	0.9846
15	1224	WL CORE G 370cm T92-7	5/2/85	76.83	12.82	1.09	0.04	0.04	0.54	0.05	3.95	4.65	100.01	0.9846
16	2717	FLV-201-TO T249-5	1/30/92	76.85	12.77	1.10	0.02	0.04	0.54	0.04	3.99	4.65	100.00	0.9840
17	1409	KRL 82182 (A1) (599) T112-1	10/22/85	76.60	12.87	1.11	0.04	0.04	0.55	0.06	4.08	4.65	100.00	0.9839
18	2558	SS-91-1-SU T232-1	8/6/91	76.74	12.86	1.09	0.04	0.04	0.54	0.05	3.95	4.68	99.99	0.9835
19	1418	BL-RSA-4 T112-9	10/23/85	76.83	12.79	1.08	0.04	0.04	0.55	0.06	3.96	4.65	100.00	0.9831
20	431	YOS-1, T13-1		76.61	12.93	1.12	0.03	0.05	0.54	0.07	4.03	4.64	100.02	0.9830
21	2493	FLV-156-SS T219-3	12/20/90	76.64	13.06	1.09	0.03	0.04	0.54	0.05	3.94	4.62	100.01	0.9829
22	1186	WALKER LAKE CORE G 380CM t89-1	2/28/85	76.98	12.79	1.08	0.02	0.05	0.54	0.05	3.86	4.64	100.01	0.9823
23	571	KRL91982F, T56-5	07/01/83	76.61	12.89	1.14	0.03	0.05	0.55	0.05	4.12	4.56	100.00	0.9820
24	681	KRL-91882A', T66-8	10/25/83	76.79	12.83	1.10	0.03	0.06	0.54	0.07	3.91	4.67	100.00	0.9811
25	760	BO-16		76.59	12.92	1.11	0.03	0.03	0.54	0.07	4.00	4.71	100.00	0.9810

Listing of 50 closest matches for COMP. NO. 2643 elements: Na, Al, Si, K , Ca, Fe Date of Update: 10/22/91

No	Sample Number	Date	[illegible]	Al2O3	Fe2O3	MgO	MnO	CaO	TiO2	Na2O	K2O	Total	m. Co
1	2643 JB-BS-15 T241-6	10/21/91	76.59	12.83	1.08	0.03	0.07	0.54	0.04	4.23	4.59	100.00	1.0000
2	2641 JB-BS-13 T241-4	10/21/91	76.49	12.83	1.08	0.03	0.08	0.53	0.06	4.26	4.64	100.00	0.9937
3	435 3-30-82-1, T43-3		76.62	12.93	1.06	0.02	0.05	0.54	0.07	4.13	4.59	100.01	0.9916
4	2646 JB-WA-1 T242-1	10/21/91	76.77	12.70	1.09	0.02	0.07	0.53	0.06	4.19	4.57	100.00	0.9910
5	2639 JB-BS-11 T241-2	10/21/91	76.55	12.80	1.10	0.02	0.08	0.54	0.06	4.16	4.68	99.99	0.9905
6	2642 JB-BS-14 T241-5	10/21/91	76.55	12.82	1.11	0.02	0.07	0.55	0.06	4.20	4.62	100.00	0.9904
7	2638 JB-BS-9 T241-1	10/21/91	76.42	12.92	1.10	0.01	0.08	0.55	0.05	4.22	4.65	100.00	0.9895
8	2640 JB-BS-12 T241-3	10/21/91	76.51	12.85	1.11	0.03	0.08	0.54	0.05	4.16	4.67	100.00	0.9854
9	2497 FLV-159-CH T219-6	12/20/90	77.01	12.76	1.08	0.03	0.03	0.54	0.05	3.94	4.57	100.01	0.9860
10	2644 JB-BS-16 T241-7	10/21/91	76.97	12.59	1.04	0.02	0.08	0.54	0.05	4.13	4.58	100.00	0.9856
11	2558 SS-91-1-1 T232-2	6/8/91	76.57	12.92	1.07	0.02	0.04	0.54	0.06	4.05	4.72	99.99	0.9856
12	2563 SS-91-1-5 T232-6	8/7/91	76.97	12.65	1.08	0.03	0.04	0.54	0.07	3.98	4.65	100.01	0.9846
13	2050 FLV-64-CS T170-7	9/3/88	76.71	12.87	1.11	0.02	0.04	0.54	0.04	4.02	4.64	99.99	0.9846
14	1224 WL CORE G 370cm T92-7	5/2/85	76.83	12.82	1.09	0.04	0.04	0.54	0.05	3.99	4.65	100.01	0.9846
15	1439 KRL 82182 (A1) (599) T112-1	10/22/85	76.60	12.87	1.11	0.04	0.04	0.55	0.06	4.08	4.65	100.00	0.9835
16	2559 SS-91-1-SU T232-1	8/6/91	76.74	12.86	1.09	0.04	0.04	0.54	0.05	3.99	4.68	99.99	0.9835
17	1418 BL-RSA-4 T112-9	10/23/85	76.83	12.79	1.08	0.04	0.04	0.55	0.06	3.96	4.65	100.00	0.9831
18	431 YOS-1, T13-1		76.61	12.93	1.12	0.03	0.05	0.54	0.07	4.03	4.64	100.02	0.9830
19	2494 FLV-156-SS T219-3	12/20/90	76.64	13.06	1.09	0.03	0.04	0.54	0.05	3.94	4.62	100.01	0.9825
20	1186 WALKER LAKE CORE G 380CM t89-1	2/28/85	76.98	12.79	1.08	0.02	0.05	0.54	0.05	3.86	4.64	100.01	0.9823
21	571 KRL91982F, T56-5	07/01/83	76.61	12.89	1.14	0.03	0.05	0.55	0.05	4.12	4.56	100.00	0.9820
22	681 KRL-91882A*, T66-8	10/25/83	76.79	12.83	1.10	0.03	0.06	0.54	0.07	3.91	4.67	100.00	0.9813
23	750 80-16		76.59	12.92	1.11	0.03	0.03	0.54	0.07	4.00	4.71	100.00	0.9810
24	1244 WL 8-3A ASH A 64-66cm T93-13	5/2/85	76.97	12.80	1.08	0.03	0.05	0.55	0.05	3.86	4.60	99.99	0.9808
25	570 KRL91982D, T66-10	xx/xx/83	76.81	12.89	1.08	0.03	0.05	0.53	0.06	3.90	4.65	100.00	0.9805
26	564 KRL82782A, T64-11	09/06/83	76.99	12.75	1.09	0.01	0.06	0.53	0.08	3.90	4.59	100.00	0.9805
27	2562 SS-91-1-4 T323-5	8/7/91	77.02	12.63	1.06	0.02	0.04	0.53	0.06	4.00	4.63	99.99	0.9798
28	2571 JB-BS-7 T227-4	6/13/91	76.73	12.89	1.10	0.03	0.05	0.54	0.06	3.91	4.69	100.00	0.9797
29	682 KRL-91882G, T66-11	10/25/83	76.91	12.76	1.07	0.03	0.06	0.54	0.07	3.87	4.68	99.99	0.9795
30	1680 KRL 860922 A T134-2	11/25/86	76.94	12.75	1.07	0.03	0.04	0.55	0.06	3.91	4.65	100.00	0.9789
31	1684 SCHURZ-1 T134-6	11/25/86	77.01	12.64	1.09	0.03	0.05	0.55	0.05	3.94	4.64	100.00	0.9788
32	2569 JB-BS-5 T227-2	6/13/91	76.69	12.91	1.08	0.02	0.05	0.55	0.09	3.90	4.70	99.99	0.9788
33	1225 WL CORE G 380cm T92-8	5/2/85	76.82	12.79	1.06	0.04	0.04	0.56	0.06	4.00	4.65	100.02	0.9787
34	1240 WL 4-2 3.29m T93-9	5/2/85	76.75	12.79	1.13	0.03	0.04	0.55	0.05	4.02	4.64	100.00	0.9787
35	1025 KRL-71082C (590) T58-1	6/22/84	76.91	12.71	1.08	0.02	0.00	0.53	0.05	3.95	4.74	99.99	0.9784
36	567 KRL91882-K-1, T64-13	09/06/83	76.93	12.82	1.11	0.01	0.05	0.53	0.07	3.68	4.60	100.00	0.9774
37	1419 BL-RSA-5 T112-10	10/23/85	76.98	12.65	1.09	0.04	0.04	0.53	0.05	3.93	4.68	99.99	0.9772
38	1416 BL-RSA-2 T112-7	10/23/85	76.78	12.85	1.12	0.04	0.03	0.54	0.06	3.90	4.68	100.00	0.9772
39	566 KRL91882B, T64-12	09/06/83	76.81	12.82	1.10	0.01	0.05	0.53	0.08	3.93	4.69	100.00	0.9771
40	562 KRL82282A(P), T66-6	xx/xx/83	76.86	12.85	1.05	0.03	0.06	0.54	0.05	3.87	4.70	100.01	0.9764
41	679 KRL-82182(A-4), T66-3	10/25/83	76.89	12.82	1.02	0.02	0.05	0.52	0.04	4.08	4.55	99.99	0.9764
42	2490 FLV-155-CH T218-10	11/19/90	76.77	13.06	1.08	0.03	0.05	0.54	0.06	3.76	4.64	99.99	0.9764
43	2561 SS-91-1-3 t232-4	8/7/91	77.08	12.64	1.06	0.02	0.05	0.53	0.06	3.92	4.64	100.00	0.9763
44	1142 WL-2-3-2.14M T85-2	12/4/84	76.97	12.69	1.06	0.03	0.05	0.56	0.06	3.96	4.63	100.01	0.9762
45	783 GS-27		76.74	12.92	1.12	0.03	0.05	0.55	0.07	3.91	4.61	100.00	0.9762
46	1228 WL 8-2B 130-134cm T92-12	5/2/85	77.03	12.81	1.08	0.04	0.04	0.55	0.04	3.77	4.63	99.99	0.9762
47	1972 WL-4-58 (144.77m) T164-1	5/21/88	76.73	12.71	1.15	0.00	0.03	0.54	0.12	4.02	4.69	99.99	0.9762
48	680 KRL-82282B, T54-4	xx//xx/x	76.99	12.71	1.08	0.02	0.06	0.53	0.04	3.86	4.70	99.99	0.9760
49	1948 WL-4-4 (12.25M) T162-2	5/14/88	76.87	12.86	1.09	0.02	0.05	0.54	0.06	3.80	4.72	100.01	0.9755
50	554 KRL82182(A-3), T56-4	07/01/83	76.97	12.82	1.02	0.03	0.03	0.55	0.04	4.05	4.44	99.99	0.9758

SAMPLE ID: J8-8S-15 T241-6 D[illegible] of Analysis: 10/21/91

Raw Probe Data		Raw Probe Data (FeO to Fe2O3)		Recalculated to 100%	
SiO2	75.829			SiO2	76.59
Al2O3	12.698			Al2O3	12.83
FeO	0.966*1.1113=Fe2O3		1.074	Fe2O3	1.08
MgO	0.025			MgO	0.03
MnO	0.072			MnO	0.07
CaO	0.534			CaO	0.54
TiO2	0.043			TiO2	0.04
Na2o	4.184			Na2o	4.23
K2O	4.545			K2O	4.59
TOTAL(O)	98.896	TOTAL(N)	99.004	TOTAL(R)	100.00

20 Best Matches:

1	0.9937	10/21/91	J8-8S-13 T241-4
2	0.9916		3-30-82-1, T43-3
3	0.9905	10/21/91	J8-8S-11 T241-2
4	0.9900	10/21/91	J8-8S-14 T241-5
5	0.9899	10/21/91	J8-8S-9 T241-1
6	0.9894	10/21/91	J8-8S-12 T241-3
7	0.9860	12/20/90	FLV-159-CH T219-6
8	0.9856	6/8/91	SS-91-1-1 T232-2
9	0.9848	8/7/91	SS-91-1-5 T232-6
10	0.9846	9/3/88	FLV-64-CS T170-7
11	0.9846	5/2/85	WL CORE G 370cm T92-7
12	0.9839	10/22/85	KRL 82182 (A1) (599) T112-1
13	0.9835	8/6/91	SS-91-1-SU T232-1
14	0.9831	10/23/85	BL-RSA-4 T112-9
15	0.9830		YOS-1, T13-1
16	0.9829	12/20/90	FLV-156-SS T219-3
17	0.9823	2/28/85	WALKER LAKE CORE G 380CM t89-1
18	0.9820	07/01/83	KRL91982F, T56-5
19	0.9811	10/25/83	KRL-91882A', T66-8
20	0.9810		80-16

Elements used in the calculation are:

Na2o
Al2O3
SiO2
K2O
CaO
FeO

***** This sample has been added to the data base *****

SAMPLE: T2 JB-BS-16

	BEAM	NA	9	MG	8	AL	3	SI	7	K	2	CA	6	TI	5	MN	1	FE	4
PT	COUNTS	COUNTS	SD	COUNTS	SD	COUNTS	SD	COUNTS	SD	COUNTS	SD	COUNTS	SD	COUNTS	SD	COUNTS	SD	COUNTS	SD
1	14240	2454	50	133	12	13989	118	26211	162	8717	93	870	30	23	5	108	10	569	24
2	14239	1453	707	162	20	14104	81	26394	129	12027	####	1152	199	32	6	117	6	529	28
3	14244	6062	####	128	18	25166	####	21905	####	2418	####	5342	####	23	5	70	25	174	218
4	14247	2544	####	148	15	14468	####	27311	####	9083	####	894	####	23	4	102	20	572	193
5	14249	2576	####	142	13	14281	####	28190	####	8741	####	886	####	26	4	106	18	560	173
6	14243	2722	####	162	14	14706	####	26942	####	9230	####	933	####	29	4	101	16	343	164
7	14244	2471	####	141	13	14185	####	27899	####	8685	####	940	####	30	4	104	15	600	159
8	14244	2564	####	177	16	14438	####	27765	####	8842	####	934	####	30	4	110	14	603	154
9	14249	2537	####	153	15	14179	####	28110	####	8951	####	994	####	29	3	100	13	594	148
10	14249	2537	####	126	16	14233	####	27957	####	9206	####	878	####	20	4	104	12	854	178
11	14252	2412	####	149	16	13543	####	26921	####	8712	####	945	####	33	4	104	12	596	169
12	14252	2437	####	151	15	13843	####	26999	####	8499	####	1000	####	24	4	107	11	599	162
13	14251	2535	####	148	14	14064	####	27822	####	8887	####	931	####	18	5	120	12	566	156
14	14253	2528	####	161	14	14229	####	27947	####	8916	####	962	####	37	5	118	12	568	149
15	14252	2478	976	142	14	14170	####	26995	####	9076	####	952	####	32	5	113	12	544	144
16	14252	2552	944	135	14	14365	####	27512	####	9018	####	1005	####	27	5	114	11	590	140
17	14249	2518	914	155	13	13754	####	27108	####	8633	####	944	####	39	6	117	11	595	135
18	14251	5317	####	138	13	26697	####	21257	####	399	####	9200	####	16	6	78	13	151	163
19	14249	2531	####	171	14	14030	####	28373	####	8860	####	910	####	21	6	106	13	550	158
20	14245	2546	####	148	13	14190	####	27814	####	8815	####	920	####	31	6	113	12	556	154

LINES DELETED: 1 2 3 18

AVE. BEAM CURRENT/SEC = 712

DATA REDUCED USING $B-AL: $GL9M

ON SPECIMEN: T241-7 JB-BS-16

$B-AL VERSION 1.0

OXIDE FORM.	WEIGHT% (OXIDE)	STD.DEV. (%)	HOMO. INDEX	FORMULA	K-RATIO	UNKN PEAK (COUNTS)	UNKN BKGD (COUNTS)	COUNTING TIME(SEC)	STD PEAK (COUNTS)	STD BKGD (COUNTS)	COUNTING TIME(SEC)	STANDARD FILENAME
NA2O	4.071	2.94	1.360	0.000	1.05511	2530.4	50.4	20.00	2400.2	49.7	20.00	%RGSC
MGO	0.023	121.33	1.043	0.000	0.00598	150.3	136.4	20.00	2469.5	136.9	20.00	%RGSC
AL2O3	12.394	1.20	2.387	0.000	0.94643	14167.3	247.1	20.00	14955.9	247.8	20.00	%5831
SIO2	75.779	0.86	2.956	0.000	1.02744	27604.0	53.7	20.00	26868.4	53.9	20.00	%5831
K2O	4.505	1.63	2.176	0.000	1.23494	8884.6	144.6	20.00	7230.1	152.8	20.00	%RGSC
CAO	0.530	4.56	1.244	0.000	0.10360	939.1	179.0	20.00	7528.9	191.2	20.00	%RGSC
TIO2	0.052	71.89	1.107	0.000	0.00047	27.8	18.3	20.00	19938.2	26.6	20.00	%TIO2
MNO	0.079	29.75	0.607	0.000	0.00079	108.6	64.4	20.00	56342.7	119.9	20.00	%MN2O
FEO	0.923	5.80	3.961	0.000	0.14418	580.8	105.4	20.00	3409.3	112.6	20.00	%RGSC

TOTAL 98.355 NO. OXYGENS = 0 NO. ITERS. = 2 AVE. ATOMIC NO. = 11.15

21-OCT-91 15:29:05

Listing of 25 closest matches for COMP. NO. 2643 for elements: Na, Al, Si, K , Ca, Fe Date of Update: 06/18/92

	C.No	Sample Number	Date	SiO2	Al2O3	Fe2O3	MgO	MnO	CaO	TiO2	Na2O	K2O	Total,R	Sim. Co
1	2643	JB-BS-16 T241-7	10/21/91	76.97	12.59	1.04	0.02	0.08	0.54	0.05	4.13	4.58	100.00	1.0000
2	2707	FLV-192-BC T246-1	12/12/91	77.01	12.55	1.05	0.03	0.05	0.53	0.05	4.18	4.56	100.01	0.9920
3	435	3-30-82-1, T43-3		76.62	12.93	1.06	0.02	0.05	0.54	0.07	4.13	4.59	100.01	0.9914
4	2561	SS-91-1-4 T323-5	8/7/91	77.02	12.63	1.06	0.02	0.04	0.53	0.06	4.00	4.63	99.99	0.9861
5	2642	JB-BS-15 T241-6	10/21/91	76.59	12.83	1.08	0.03	0.07	0.54	0.04	4.23	4.59	100.00	0.9856
6	2559	SS-91-1-2 T232-3	8/7/91	77.11	12.63	1.03	0.03	0.05	0.54	0.06	3.89	4.67	100.01	0.9847
7	2645	JB-WA-1 T242-1	10/21/91	76.77	12.70	1.09	0.02	0.07	0.53	0.06	4.19	4.57	100.00	0.9846
8	2562	SS-91-1-5 T232-6	8/7/91	76.97	12.65	1.08	0.03	0.04	0.54	0.07	3.98	4.65	100.01	0.9845
9	679	KRL-82182(A-4), T66-3	10/25/83	76.89	12.82	1.02	0.02	0.05	0.52	0.04	4.08	4.55	99.99	0.9843
10	554	KRL82182(A-3), T56-4	07/01/83	76.97	12.82	1.02	0.03	0.03	0.55	0.04	4.09	4.44	99.99	0.9841
11	1141	WL-2-3-1.94M T85-1	12/4/84	76.97	12.65	1.05	0.03	0.05	0.56	0.05	4.00	4.66	100.02	0.9836
12	2496	FLV-159-CH T219-6	12/20/90	77.01	12.76	1.08	0.03	0.03	0.54	0.05	3.94	4.57	100.01	0.9835
13	1421	BL-RSA-7 T112-12	10/23/85	77.16	12.66	1.03	0.04	0.05	0.52	0.03	3.95	4.57	100.01	0.9833
14	559	KRL82182(bubble wall), T56-4	07/01/83	76.87	12.92	1.01	0.02	0.03	0.53	0.03	4.03	4.55	99.99	0.9825
15	2638	JB-BS-11 T241-2	10/21/91	76.55	12.80	1.10	0.02	0.08	0.54	0.06	4.16	4.68	99.99	0.9825
16	2560	SS-91-1-3 t232-4	8/7/91	77.08	12.64	1.06	0.02	0.05	0.53	0.06	3.92	4.64	100.00	0.9822
17	2557	SS-91-1-1 T232-2	6/8/91	76.57	12.92	1.07	0.02	0.04	0.54	0.06	4.05	4.72	99.99	0.9820
18	1142	WL-2-3-2.14M T85-2	12/4/84	76.97	12.69	1.06	0.03	0.05	0.56	0.06	3.96	4.63	100.01	0.9809
19	2567	JB-BS-4 T227-1	6/13/91	76.75	12.83	1.04	0.03	0.06	0.55	0.06	3.95	4.73	100.00	0.9808
20	2639	JB-BS-12 T241-3	10/21/91	76.51	12.85	1.11	0.03	0.08	0.54	0.05	4.16	4.67	100.00	0.9807
21	1225	WL CORE G 380cm T92-8	5/2/85	76.82	12.79	1.06	0.04	0.04	0.56	0.06	4.00	4.65	100.02	0.9802
22	2717	FLV-201-TO T249-5	1/30/92	76.85	12.77	1.10	0.02	0.04	0.54	0.04	3.99	4.65	100.00	0.9801
23	2563	SS-91-1-Adgss	8/7/91	76.73	12.85	1.04	0.03	0.05	0.53	0.07	3.95	4.74	99.99	0.9801
24	562	KRL82282A(P), T66-6	xx/xx/83	76.86	12.85	1.05	0.03	0.06	0.54	0.05	3.87	4.70	100.01	0.9801
25	2640	JB-BS-13 T241-4	10/21/91	76.49	12.83	1.08	0.03	0.08	0.53	0.06	4.26	4.64	100.00	0.9793

Listing of 50 closest matches for COMP. NO. 2644 elements: Na, Al, Si, K, Ca, Fe Date of Update: 10/22/91

	No	Sample Number	Date		Al_2O_3	Fe_2O_3	MgO	MnO	CaO	TiO_2	Na_2O	K_2O	Total	Sim. Co
1	2644	JB-BS-16 T241-7	10/21/91	76.97	12.59	1.04	0.02	0.08	0.54	0.05	4.13	4.55	100.00	1.0000
2	435	3-30-82-1, T43-3		76.62	12.93	1.06	0.02	0.05	0.54	0.07	4.13	4.53	100.01	0.9914
3	2552	SS-91-1-4 T323-5	8/7/91	77.02	12.63	1.06	0.02	0.04	0.53	0.06	4.00	4.63	99.99	0.9861
4	2643	JB-BS-15 T241-6	10/21/91	76.59	12.83	1.08	0.03	0.07	0.54	0.04	4.23	4.53	100.00	0.9856
5	2560	SS-91-1-2 T232-3	8/7/91	77.11	12.63	1.03	0.03	0.05	0.54	0.06	3.85	4.67	100.01	0.9847
6	2646	JB-WA-1 T242-1	10/21/91	76.77	12.70	1.09	0.02	0.07	0.53	0.06	4.15	4.57	100.00	0.9846
7	2553	SS-91-1-5 T232-6	8/7/91	76.97	12.65	1.08	0.03	0.04	0.54	0.07	3.98	4.65	100.01	0.9845
8	579	KRL-82182(A-4), T66-3	10/25/83	76.89	12.82	1.02	0.02	0.05	0.52	0.04	4.08	4.55	99.99	0.9843
9	554	KRL82182(A-3), T56-4	07/01/83	76.97	12.82	1.02	0.03	0.03	0.55	0.04	4.05	4.44	99.99	0.9841
10	1141	WL-2-3-1.94M T85-1	12/4/84	76.97	12.65	1.05	0.03	0.05	0.56	0.05	4.00	4.66	100.04	0.9836
11	2437	FLV-159-CH T219-6	12/20/90	77.01	12.76	1.08	0.03	0.03	0.54	0.05	3.94	4.57	100.01	0.9835
12	1421	BL-RSA-7 T112-12	10/23/85	77.16	12.66	1.03	0.04	0.05	0.52	0.03	3.95	4.57	100.01	0.9833
13	559	KRL82182(bubble wall), T56-4	07/01/83	76.87	12.92	1.01	0.02	0.03	0.53	0.03	4.03	4.55	99.99	0.9825
14	2639	JB-BS-11 T241-2	10/21/91	76.55	12.80	1.10	0.02	0.08	0.54	0.06	4.16	4.66	99.99	0.9824
15	2561	SS-91-1-3 T232-4	8/7/91	77.08	12.64	1.06	0.02	0.05	0.53	0.06	3.92	4.64	100.00	0.9822
16	2558	SS-91-1-1 T232-2	6/8/91	76.57	12.92	1.07	0.02	0.04	0.54	0.06	4.05	4.72	99.99	0.9820
17	1142	WL-2-3-2.14M T85-2	12/4/84	76.97	12.69	1.06	0.03	0.05	0.56	0.06	3.96	4.63	100.01	0.9809
18	2568	JB-BS-4 T227-1	6/13/91	76.75	12.83	1.04	0.03	0.06	0.55	0.06	3.95	4.73	100.00	0.9808
19	2640	JB-BS-12 T241-3	10/21/91	76.51	12.85	1.11	0.03	0.08	0.54	0.05	4.16	4.67	100.00	0.9807
20	1225	WL CORE G 380cm T92-8	5/2/85	76.82	12.79	1.06	0.04	0.04	0.56	0.06	4.00	4.65	100.02	0.9802
21	2564	SS-91-1-Adgss	8/7/91	76.73	12.85	1.04	0.03	0.85	0.53	0.07	3.99	4.74	99.99	0.9801
22	562	KRL82282A(P), T66-6	xx/xx/83	76.86	12.85	1.05	0.03	0.06	0.54	0.05	3.87	4.70	100.01	0.9801
23	2641	JB-BS-13 T241-4	10/21/91	76.49	12.83	1.08	0.03	0.08	0.53	0.06	4.26	4.64	100.00	0.9793
24	1224	WL CORE G 370cm T92-7	5/2/85	76.83	12.82	1.09	0.04	0.04	0.54	0.05	3.99	4.65	100.01	0.9793
25	682	KRL-91882G, T66-11	10/25/83	76.91	12.76	1.07	0.03	0.06	0.54	0.07	3.87	4.68	99.99	0.9789
26	1684	SCHURZ-1 T134-6	11/25/86	77.01	12.64	1.09	0.03	0.05	0.55	0.05	3.94	4.64	100.00	0.9788
27	1680	KRL 860922 A T134-2	11/25/86	76.94	12.75	1.07	0.03	0.04	0.55	0.06	3.91	4.65	100.00	0.9788
28	2060	FLV-64-CS T170-7	9/3/88	76.71	12.87	1.11	0.02	0.04	0.54	0.04	4.02	4.64	99.99	0.9787
29	1418	BL-RSA-4 T112-9	10/23/85	76.83	12.79	1.08	0.04	0.04	0.55	0.06	3.96	4.65	100.00	0.9785
30	2642	JB-BS-14 T241-5	10/21/91	76.55	12.82	1.11	0.02	0.07	0.55	0.06	4.20	4.62	100.00	0.9783
31	1836	OD-ML-65CM T143-7	6/24/87	76.81	12.80	1.05	0.03	0.05	0.56	0.05	3.96	4.70	100.01	0.9783
32	1156	WALKER LAKE CORE G 380CM t89-1	2/28/85	76.98	12.79	1.08	0.02	0.05	0.54	0.05	3.86	4.64	100.01	0.9781
33	1034	WL 2-2-2.64, T78-7	08/18/84	77.06	12.62	1.06	0.03	0.05	0.55	0.06	3.86	4.71	100.00	0.9777
34	2559	SS-91-1-SU T232-1	8/6/91	76.74	12.86	1.09	0.04	0.04	0.54	0.05	3.95	4.68	99.99	0.9775
35	1036	WL 2-3-2.01, T78-9	08/18/84	77.05	12.74	1.05	0.02	0.04	0.55	0.05	3.82	4.67	99.99	0.9775
36	1439	KRL 82182 (A1) (599) T112-1	10/22/85	76.60	12.87	1.11	0.04	0.04	0.55	0.06	4.08	4.65	100.00	0.9775
37	554	KRL82782A, T64-11	09/06/83	76.99	12.75	1.09	0.01	0.06	0.53	0.08	3.90	4.59	100.00	0.9775
38	2342	FLV-67-MA T195-1	7/21/89	77.02	12.94	1.05	0.02	0.06	0.54	0.06	3.72	4.59	100.00	0.9769
39	1310	WL 8-2B 172-174.5CM T99-10	7/1/85	76.90	12.74	1.05	0.02	0.05	0.56	0.07	3.91	4.71	100.01	0.9769
40	1419	BL-RSA-5 T112-10	10/23/85	76.98	12.65	1.09	0.04	0.04	0.53	0.05	3.93	4.68	99.99	0.9768
41	431	YOS-1, T13-1		76.61	12.93	1.12	0.03	0.05	0.54	0.07	4.03	4.64	100.02	0.9767
42	2385	FLV-142-TC T203-8	4/16/90	77.51	12.24	1.03	0.00	0.06	0.51	0.08	3.98	4.60	100.01	0.9766
43	571	KRL91982F, T56-5	07/01/83	76.61	12.89	1.14	0.03	0.05	0.55	0.05	4.12	4.56	100.00	0.9766
44	2494	FLV-156-SS T219-3	12/20/90	76.64	13.06	1.09	0.03	0.04	0.54	0.05	3.94	4.62	100.01	0.9765
45	1244	WL 8-3A ASH A 64-66cm T93-13	5/2/85	76.97	12.80	1.08	0.03	0.05	0.55	0.05	3.86	4.60	99.99	0.9764
46	2638	JB-BS-9 T241-1	10/21/91	76.42	12.92	1.10	0.01	0.08	0.55	0.05	4.22	4.65	100.00	0.9764
47	1025	KRL-71082C (590) T58-1	6/22/84	76.91	12.71	1.08	0.02	0.00	0.53	0.05	3.99	4.74	99.99	0.9761
48	1420	BL-RSA-6 T112-11	10/23/85	77.08	12.78	0.97	0.02	0.04	0.53	0.04	3.97	4.56	99.99	0.9758
49	1757	OD-ML-18-405 CM T139-14	5/28/87	76.99	12.77	1.05	0.03	0.06	0.53	0.09	3.80	4.69	100.01	0.9757
50	1423	BL-RSA-9 T112-14	10/23/85	77.13	12.80	1.02	0.03	0.03	0.52	0.04	3.67	4.54	99.98	0.9756

SAMPLE ID: JB-BS-16 T241-7 D[illegible] of Analysis: 10/21/91

Raw Probe Data		Raw Probe Data (FeO to Fe2O3)		[illegible]lculated to 100%	
SiO2	75.779			SiO2	76.97
Al2O3	12.394			Al2O3	12.59
FeO	0.923*1.1113=Fe2O3		1.026	Fe2O3	1.04
MgO	0.023			MgO	0.02
MnO	0.079			MnO	0.08
CaO	0.530			CaO	0.54
TiO2	0.052			TiO2	0.05
Na2o	4.071			Na2o	4.13
K2O	4.505			K2O	4.58
TOTAL(O)	98.355	TOTAL(N)	98.458	TOTAL(R)	100.00

20 Best Matches:

1	0.9914		3-30-82-1, T43-3
2	0.9861	8/7/91	SS-91-1-4 T323-5
3	0.9856	10/21/91	JB-BS-15 T241-6
4	0.9847	8/7/91	SS-91-1-2 T232-3
5	0.9845	8/7/91	SS-91-1-5 T232-6
6	0.9843	10/25/83	KRL-82182(A-4), T66-3
7	0.9841	07/01/83	KRL82182(A-3), T56-4
8	0.9836	12/4/84	WL-2-3-1.94M T85-1
9	0.9835	12/20/90	FLV-159-CH T219-6
10	0.9833	10/23/85	BL-RSA-7 T112-12
11	0.9825	07/01/83	KRL82182(bubble wall), T56-4
12	0.9825	10/21/91	JB-BS-11 T241-2
13	0.9822	8/7/91	SS-91-1-3 t232-4
14	0.9820	6/8/91	SS-91-1-1 T232-2
15	0.9809	12/4/84	WL-2-3-2.14M T85-2
16	0.9808	6/13/91	JB-BS-4 T227-1
17	0.9807	10/21/91	JB-BS-12 T241-3
18	0.9802	5/2/85	WL CORE G 380cm T92-8
19	0.9801	8/7/91	SS-91-1-Adgss
20	0.9801	xx/xx/83	KRL82282A(P), T66-6

Elements used in the calculation are:

Na2o
Al2O3
SiO2
K2O
CaO
FeO

***** This sample has been added to the data base *****

SAMPLE: T2[illegible]8 JR-RS-17

PT	BEAM COUNTS	NA 9 COUNTS	SD	MG 8 COUNTS	SD	AL 3 COUNTS	SD	SI 7 COUNTS	SD	K 2 COUNTS	SD	CA 6 COUNTS	SD	TI 5 COUNTS	SD	MN 1 COUNTS	SD	FE 4 COUNTS	SD
1	14263	2428	49	163	13	14186	119	26470	163	9013	95	1150	34	27	5	107	10	447	21
2	14256	2342	61	145	13	14329	101	26300	120	9092	56	1103	33	22	3	96	8	437	7
3	14256	2301	65	160	10	14196	80	26468	97	8842	128	1135	24	29	4	102	5	472	18
4	14253	2347	53	157	8	14081	102	26430	80	8711	171	1098	25	28	3	130	15	450	15
5	14253	2407	52	154	7	14427	135	25846	265	9016	155	1064	34	29	3	117	13	470	15
6	14258	2378	46	157	6	14473	153	26014	265	8618	190	1126	31	30	3	103	12	457	14
7	14258	2374	42	152	6	13878	207	26152	245	8757	180	1099	29	18	4	93	13	442	13
8	14263	2395	40	158	6	14308	194	26517	247	8802	168	1121	27	29	4	93	13	518	26
9	14259	2445	45	166	6	14277	182	25993	249	8900	158	1132	26	23	4	106	12	482	25
10	14254	2295	50	174	8	14613	208	26017	246	9195	182	1288	60	28	4	100	11	494	26
11	14262	2219	66	155	8	14182	200	26045	239	8834	174	1239	66	31	4	105	11	510	28
12	14270	2518	78	146	8	14513	203	26440	238	8840	166	1125	63	21	4	88	11	456	27
13	14267	2417	76	164	8	14124	200	26025	234	8972	161	1136	60	21	4	109	11	477	26
14	14269	2294	76	182	10	14406	195	26845	282	9488	222	1332	77	25	4	92	11	501	26
15	14260	2322	74	168	10	14234	188	26018	279	8748	219	1059	78	27	4	109	11	466	25
16	14265	2436	74	178	11	14243	182	26288	269	8837	213	1187	76	21	4	101	10	456	25
17	14264	2327	72	147	11	14574	190	26201	261	8921	206	1118	74	30	4	93	10	489	24
18	14262	2287	73	154	11	14159	187	26570	265	8766	203	1117	72	28	4	112	10	480	24
19	14266	2236	76	156	11	14334	182	25807	277	9123	204	1113	71	22	4	109	10	476	23
20	14262	2434	76	158	10	14337	178	26112	271	8744	202	1091	70	40	5	108	10	473	22

LINES DELETED: 14 7

AVE. BEAM CURRENT/SEC = 713

DATA REDUCED USING $B-AL: $GL9M

ON SPECIMEN: T241-8 JR-RS-17

$B-AL VERSION 1.0

OXIDE FORM.	WEIGHT% (OXIDE)	STD.DEV. (%)	HOMO. INDEX	FORMULA	K-RATIO	UNKN PEAK (COUNTS)	UNKN BKGD (COUNTS)	COUNTING TIME(SEC)	STD PEAK (COUNTS)	STD BKGD (COUNTS)	COUNTING TIME(SEC)	STANDARD FILENAME
NA2O	3.826	2.99	1.625	0.000	0.98383	2363.0	50.6	20.00	2400.2	49.7	20.00	%RGSC
MGO	0.036	76.75	0.722	0.000	0.00960	158.7	136.3	20.00	2469.5	136.9	20.00	%RGSC
AL2O3	12.567	1.20	1.299	0.000	0.95631	14310.6	245.2	20.00	14955.9	247.8	20.00	%5831
SIO2	72.135	0.87	1.496	0.000	0.97501	26197.8	53.3	20.00	26868.4	53.9	20.00	%5831
K2O	4.501	1.63	1.643	0.000	1.23552	8887.4	143.2	20.00	7230.1	152.8	20.00	%RGSC
CAO	0.664	3.97	1.668	0.000	0.13036	1133.4	176.9	20.00	7528.9	191.2	20.00	%RGSC
TIO2	0.047	78.16	0.920	0.000	0.00043	26.7	18.1	20.00	19938.2	26.6	20.00	%TIO2
MNO	0.074	31.52	0.937	0.000	0.00073	104.8	63.6	20.00	56342.7	119.9	20.00	%MN2O
FEO	0.716	6.76	0.979	0.000	0.11178	472.8	104.2	20.00	3409.3	112.6	20.00	%RGSC

TOTAL 94.565 NO. OXYGENS = 0 NO. ITERS. = 2 AVE. ATOMIC NO. = 11.02

21-OCT-91 15:47:59

Listing of 25 closest matches for COMP. NO. 2644 for elements: Na, Al, Si, K , Ca, Fe Date of Update: 06/18/92

	C.No	Sample Number	Date	SiO2	Al2O3	Fe2O3	MgO	MnO	CaO	TiO2	Na2O	K2O	Total,R	Sim. Co
1	2644	JB-BS-17 T241-8	10/21/91	76.22	13.28	0.84	0.04	0.08	0.70	0.05	4.04	4.76	100.01	1.0000
2	454	679-340, T31-2		76.57	13.20	0.84	0.03	0.03	0.70	0.07	3.84	4.71	99.99	0.9882
3	2569	JB-BS-6 T227-3	6/13/91	76.39	13.29	0.83	0.04	0.06	0.71	0.06	3.88	4.74	100.00	0.9879
4	183	KRL7982-19B, T45-4		76.37	13.29	0.83	0.04	0.02	0.71	0.07	3.88	4.79	100.00	0.9876
5	1982	WL-5-13 (64.49m) T164-11	5/22/88	76.59	13.19	0.83	0.03	0.05	0.70	0.07	3.73	4.80	99.99	0.9819
6	1979	WL-5-12 (61.28m) T164-8	5/22/88	76.51	13.26	0.87	0.04	0.05	0.70	0.07	3.76	4.75	100.01	0.9815
7	182	KRL7982-16, T45-3		76.66	13.17	0.83	0.03	0.02	0.68	0.07	3.91	4.64	100.01	0.9814
8	2709	FLV-194-BC T246-3	12/12/91	76.50	12.97	0.88	0.05	0.05	0.72	0.06	4.00	4.75	99.98	0.9813
9	495	IIB, T32-1		76.58	13.16	0.87	0.03	0.06	0.71	0.05	3.87	4.68	100.01	0.9798
10	695	RSCS1		76.82	12.90	0.85	0.01	0.00	0.66	0.05	4.00	4.70	99.99	0.9787
11	1243	WL 4-26 66.40m T93-12	5/2/85	76.71	13.12	0.83	0.05	0.04	0.71	0.06	3.70	4.78	100.00	0.9779
12	756	BO-5		76.29	13.42	0.90	0.04	0.06	0.70	0.08	3.80	4.71	100.00	0.9753
13	545	KRL7982-17, T50-4	02/01/83	76.61	13.14	0.87	0.03	0.04	0.68	0.05	3.77	4.79	99.98	0.9747
14	1242	WL 4-26 66.33m T93-11	5/2/85	76.65	13.16	0.87	0.05	0.04	0.71	0.05	3.69	4.78	100.00	0.9743
15	1958	WL-4-17 (39.81M) T162-12	5/15/88	76.91	12.98	0.84	0.04	0.05	0.72	0.05	3.70	4.70	99.99	0.9740
16	572	KRL91982J, T64-14	09/06/83	76.90	12.98	0.83	0.02	0.05	0.67	0.06	3.85	4.65	100.01	0.9739
17	1963	WL-4-26 (66.50M) T163-7	5/15/88	76.67	13.24	0.84	0.04	0.04	0.73	0.07	3.66	4.70	99.99	0.9739
18	1974	WL-5-5 (36.93m) T164-3	5/21/88	76.69	13.09	0.83	0.03	0.05	0.66	0.06	3.79	4.82	100.02	0.9727
19	1975	WL-5-6 (39.31m) T164-4	5/21/88	76.69	13.10	0.82	0.04	0.05	0.66	0.07	3.79	4.78	100.00	0.9722
20	549	KRL71082F, T55-5	11/25/83	76.59	13.26	0.86	0.05	0.05	0.71	0.07	3.59	4.82	100.00	0.9721
21	1976	WL-5-6 (40.08m) T164-5	5/21/88	76.68	13.08	0.82	0.03	0.05	0.66	0.06	3.81	4.82	100.01	0.9714
22	2711	FLV-196-BC T246-5	12/12/91	76.65	12.88	0.90	0.05	0.04	0.67	0.08	3.95	4.78	100.00	0.9714
23	1045	DSDP 36-10-2 SSA, T78-5	07/18/84	76.90	12.80	0.85	0.04	0.04	0.72	0.09	3.73	4.83	100.00	0.9707
24	1136	WL-5-13-1.11M T84-12	12/3/84	76.59	13.09	0.89	0.04	0.06	0.71	0.07	3.74	4.82	100.01	0.9706
25	1569	WLC-85-2 (10.65M) T127-14	8/18/86	76.61	13.40	0.87	0.03	0.06	0.70	0.05	3.52	4.76	100.00	0.9705

Listing of 50 closest matches for COMP. NO. 2645 (... elements: Na, Al, Si, K, Ca, Fe Date of Update: 10/22/91

	.No	Sample Number	Date		Al2O3	Fe2O3	MgO	MnO	CaO	TiO2	Na2O	K2O	Total	s. Co
1	2645	J8-85-17 T241-8	10/21/91	76.22	13.28	0.84	0.04	0.08	0.70	0.05	4.04	4.70	100.01	1.0000
2	454	679-340, T31-2		76.57	13.20	0.84	0.03	0.03	0.70	0.07	3.84	4.71	99.99	0.9882
3	2570	J8-85-6 T227-3	6/13/91	76.39	13.29	0.83	0.04	0.06	0.71	0.06	3.88	4.74	100.00	0.9875
4	193	KRL7982-198, T45-4		76.37	13.29	0.83	0.04	0.02	0.71	0.07	3.88	4.79	100.00	0.9876
5	1932	WL-5-13 (64.49m) T164-11	5/22/88	76.59	13.19	0.83	0.03	0.05	0.70	0.07	3.73	4.80	99.99	0.9815
6	1979	WL-5-12 (61.28m) T164-8	5/22/88	76.51	13.26	0.87	0.04	0.05	0.70	0.07	3.76	4.75	100.01	0.9815
7	182	KRL7982-16, T45-3		76.66	13.17	0.83	0.03	0.02	0.68	0.07	3.91	4.64	100.01	0.9814
8	495	II8, T32-1		76.58	13.16	0.87	0.03	0.06	0.71	0.05	3.87	4.68	100.01	0.9798
9	635	RSCS1		76.82	12.90	0.85	0.01	0.00	0.66	0.05	4.00	4.70	99.99	0.9787
10	1243	WL 4-26 66.40m T93-12	5/2/85	76.71	13.12	0.83	0.05	0.04	0.71	0.06	3.70	4.76	100.00	0.9779
11	756	80-5		76.29	13.42	0.90	0.04	0.06	0.70	0.08	3.80	4.71	100.00	0.9753
12	545	KRL7982-17, T50-4	02/01/83	76.61	13.14	0.87	0.03	0.04	0.68	0.05	3.77	4.79	99.98	0.9747
13	1242	WL 4-26 66.33m T93-11	5/2/85	76.65	13.16	0.87	0.05	0.04	0.71	0.05	3.69	4.78	100.00	0.9743
14	1958	WL-4-17 (39.81M) T162-12	5/15/88	76.91	12.98	0.84	0.04	0.05	0.72	0.05	3.70	4.70	99.99	0.9740
15	572	KRL91982J, T64-14	09/06/83	76.90	12.98	0.83	0.02	0.05	0.67	0.06	3.85	4.65	100.01	0.9735
16	1953	WL-4-26 (66.50M) T163-7	5/15/88	76.67	13.24	0.84	0.04	0.04	0.73	0.07	3.66	4.70	99.99	0.9735
17	1974	WL-5-5 (36.93m) T164-3	5/21/88	76.69	13.09	0.83	0.03	0.05	0.66	0.06	3.79	4.82	100.02	0.9727
18	1975	WL-5-6 (39.31m) T164-4	5/21/88	76.69	13.10	0.82	0.04	0.05	0.66	0.07	3.79	4.76	100.00	0.9722
19	569	KRL71082F, T55-5	11/25/83	76.59	13.26	0.86	0.05	0.05	0.71	0.07	3.59	4.82	100.00	0.9721
20	1976	WL-5-6 (40.08m) T164-5	5/21/88	76.68	13.08	0.82	0.03	0.05	0.66	0.06	3.81	4.82	100.01	0.9714
21	1045	DSDP 36-10-2 SSA, T78-5	07/18/84	76.90	12.80	0.85	0.04	0.04	0.72	0.09	3.73	4.83	100.00	0.9707
22	1136	WL-5-13-1.11M T84-12	12/3/84	76.59	13.09	0.89	0.04	0.06	0.71	0.07	3.74	4.82	100.01	0.9706
23	1569	WLC-85-2 (10.65M) T127-14	8/18/86	76.61	13.40	0.87	0.03	0.06	0.70	0.05	3.52	4.76	100.00	0.9705
24	2566	SS-91-1 high Ca SS	8/7/91	77.12	12.77	0.83	0.03	0.05	0.67	0.05	3.75	4.67	99.98	0.9691
25	1033	KRL-71082 (II-4) (593) T58-4	6/22/84	76.44	13.18	0.88	0.05	0.00	0.70	0.07	3.65	4.98	99.99	0.9685
26	1258	*WL 4-26 66.79m t95-5	5/29/85	76.94	12.84	0.81	0.05	0.04	0.73	0.07	3.77	4.75	100.00	0.9686
27	574	KRL92082-A, T53-3	03/25/83	76.12	13.32	0.94	0.04	0.04	0.67	0.06	3.95	4.86	100.00	0.9673
28	455	679-409-6, T31-1		76.71	13.04	0.88	0.03	0.03	0.66	0.07	3.78	4.80	100.00	0.9667
29	191	LD-10, T40-2		76.71	13.04	0.91	0.04	0.03	0.68	0.07	3.80	4.71	99.99	0.9667
30	1959	WL-4-18 (43.53M) T162-13	5/15/88	77.01	12.97	0.82	0.04	0.04	0.67	0.06	3.63	4.77	100.01	0.9660
31	1257	*WL 4-26 66.68m	5/29/85	76.78	12.82	0.88	0.05	0.05	0.75	0.07	3.86	4.73	99.99	0.9658
32	588	PMR-1, T54-12	07/xx/83	77.00	12.77	0.86	0.13	0.07	0.72	0.13	3.88	4.44	100.00	0.9656
33	1259	*WL 4-26 66.87m t95-6	5/29/85	77.01	12.69	0.88	0.04	0.04	0.73	0.09	3.81	4.71	100.00	0.9652
34	1250	*WL 4-26 6a7.04m t95-7	5/29/85	77.27	12.59	0.84	0.04	0.05	0.74	0.06	3.73	4.70	100.02	0.9652
35	1983	WL-5-16 (73.40m) T164-12	5/22/88	76.37	13.29	0.81	0.05	0.04	0.75	0.10	3.70	4.89	100.00	0.9640
36	1964	WL-4-27 (68.59M) T163-8	5/15/88	76.85	13.06	0.85	0.04	0.06	0.75	0.06	3.64	4.69	100.00	0.9636
37	1962	WL-4-25 (62.76M) T164-6	5/15/88	76.91	12.91	0.79	0.05	0.05	0.70	0.09	3.62	4.87	99.99	0.9626
38	1039	WL 4-26-3.06, T78-12	08/16/84	76.97	12.78	0.86	0.04	0.05	0.73	0.06	3.65	4.87	100.01	0.9615
39	1238	WL 2-7 21.02m T93-7	5/1/85	76.85	13.15	0.89	0.05	0.04	0.71	0.05	3.48	4.78	100.00	0.9615
40	1978	WL-5-7 (51.83m) T164-7	5/21/88	75.54	13.66	0.98	0.07	0.05	0.68	0.14	4.01	4.87	100.00	0.9603
41	573	KRL91982-K, T64-15	09/06/83	76.84	13.01	0.90	0.02	0.05	0.66	0.06	3.70	4.75	99.99	0.9603
42	1570	WLC-85-2 (11.34M) T128-1	8/18/86	76.89	12.97	0.84	0.04	0.05	0.75	0.08	3.54	4.85	100.01	0.9598
43	1047	DSDP 36-10-2 SSA3, T78-5	07/18/84	77.04	13.17	0.81	0.02	0.06	0.67	0.03	3.50	4.69	99.99	0.9590
44	2596	EL-1-M T230-5	7/2/91	76.61	13.14	0.85	0.06	0.04	0.79	0.08	3.64	4.79	100.00	0.9585
45	1480	6VI84-1-5.5M T117-13	3/6/86	76.73	13.08	0.87	0.06	0.05	0.74	0.08	3.59	4.85	100.01	0.9583
46	1056	WL-4-13 (33.32M) T162-10	5/15/88	76.98	12.91	0.86	0.04	0.04	0.65	0.06	3.60	4.85	99.99	0.9567
47	1998	WL-5-57 (144.18m) T165-13	5/22/88	77.70	11.93	0.88	0.05	0.08	0.71	0.09	3.76	4.82	100.02	0.9563
48	2376	KRL880-604B T201-5	10/12/89	76.67	13.17	0.93	0.02	0.03	0.66	0.04	3.69	4.80	100.01	0.9562
49	180	KRL7982-11L, T44-8		76.76	13.01	0.92	0.02	0.03	0.63	0.04	3.89	4.70	100.00	0.9560
50	1985	WL-5-16 (73.62m) T164-14	5/22/88	76.34	13.31	0.83	0.06	0.03	0.73	0.10	3.47	5.13	100.00	0.9550

SAMPLE ID: JB-85-17 T241-8 Date of Analysis: 10/21/91

Raw Probe Data		Raw Probe Data (FeO to Fe2O3)		Recalculated to 100%	
SiO2	72.135			SiO2	76.22
Al2O3	12.567			Al2O3	13.28
FeO	0.716*1.1113=Fe2O3		0.796	Fe2O3	0.84
MgO	0.036			MgO	0.04
MnO	0.074			MnO	0.08
CaO	0.664			CaO	0.70
TiO2	0.047			TiO2	0.05
Na2o	3.826			Na2o	4.04
K2O	4.501			K2O	4.76
TOTAL(O)	94.565	TOTAL(N)	94.645	TOTAL(R)	100.01

20 Best Matches:

1	0.9882		679-340, T31-2
2	0.9879	6/13/91	JB-85-6 T227-3
3	0.9876		KRL7982-198, T45-4
4	0.9819	5/22/88	WL-5-13 (64.49m) T164-11
5	0.9815	5/22/88	WL-5-12 (61.28m) T164-8
6	0.9814		KRL7982-16, T45-3
7	0.9798		II8, T32-1
8	0.9787		RSCS1
9	0.9779	5/2/85	WL 4-26 66.40m T93-12
10	0.9753		BO-5
11	0.9747	02/01/83	KRL7982-17, T50-4
12	0.9743	5/2/85	WL 4-26 66.33m T93-11
13	0.9740	5/15/88	WL-4-17 (39.81M) T162-12
14	0.9739	09/06/83	KRL91982J, T64-14
15	0.9739	5/15/88	WL-4-26 (66.50M) T163-7
16	0.9727	5/21/88	WL-5-5 (36.93m) T164-3
17	0.9722	5/21/88	WL-5-6 (39.31m) T164-4
18	0.9721	11/25/83	KRL71082F, T55-5
19	0.9714	5/21/88	WL-5-6 (40.08m) T164-5
20	0.9707	07/18/84	DSDP 36-10-2 SSA, T78-5

Elements used in the calculation are:

Na2o
Al2O3
SiO2
K2O
CaO
FeO

***** This sample has been added to the data base *****

SAMPLE: T2 JB-WA-1

	BEAM	NA	9	MG	8	AL	3	SI	7	K	2	CA	6	TI	5	MN	1	FE	4
PT	COUNTS	COUNTS	SD	COUNTS	SD	COUNTS	SD	COUNTS	SD	COUNTS	SD	COUNTS	SD	COUNTS	SD	COUNTS	SD	COUNTS	SD
1	14276	2659	52	157	13	14569	121	27309	165	9014	95	895	30	27	5	108	10	627	25
2	14264	2653	5	185	20	14507	44	26973	238	8987	19	911	11	27	0	104	3	656	21
3	14274	2669	9	154	17	14522	32	27862	449	9035	24	844	35	27	0	107	2	493	87
4	14278	2506	77	136	20	14492	33	27821	428	9007	20	905	31	33	3	124	9	607	71
5	14270	2516	82	156	18	13725	358	26101	724	8357	293	908	28	31	3	99	9	577	62
6	14269	2388	114	141	17	13936	365	27063	650	8601	286	925	28	23	3	97	9	564	57
7	14265	2656	109	151	16	13907	363	27553	609	8856	261	909	26	23	4	109	9	568	52
8	14261	2464	109	149	15	14116	339	26927	575	8689	247	942	29	29	3	110	8	609	49
9	14258	2556	102	167	15	14177	317	28007	601	8722	233	949	30	31	3	106	8	581	46
10	14274	2478	100	143	14	14345	302	27126	569	8837	220	910	29	43	6	83	10	590	44
11	14278	2461	99	148	14	13407	379	26957	548	8361	249	945	29	21	6	108	10	660	47
12	14270	2566	94	157	13	14129	361	27485	527	8659	240	918	28	31	6	97	10	587	45
13	14268	2626	93	122	15	14491	358	27608	514	8975	237	948	28	29	6	111	10	639	45
14	14273	2363	103	142	15	13535	385	26505	537	8612	232	924	27	18	6	86	10	606	43
15	14276	2530	99	157	15	14242	372	27845	540	8794	224	969	30	23	6	108	10	604	41
16	14279	2372	105	153	14	13552	388	26504	557	8594	220	922	29	31	6	106	10	566	41
17	14269	2451	103	144	14	13801	383	27193	539	8822	214	899	28	25	6	105	9	549	41
18	14273	2585	101	142	13	14359	377	27322	523	8873	209	916	27	38	6	105	9	638	41
19	14283	2616	100	155	13	14707	392	27437	511	8673	204	941	27	26	6	108	9	641	41
20	14283	2558	98	156	13	14564	394	27897	518	9346	238	944	27	31	6	102	9	598	40

LINES DELETED: 5 6

AVE. BEAM CURRENT/SEC = 714

DATA REDUCED USING $B-AL: $DL9M

ON SPECIMEN: T242-1 JB-WA-1

$B-AL VERSION 1.0

OXIDE FORM.	WEIGHT% (OXIDE)	STD.DEV. (%)	HOMO. INDEX	FORMULA	K-RATIO	UNKN PEAK (COUNTS)	UNKN BKGD (COUNTS)	COUNTING TIME(SEC)	STD PEAK (COUNTS)	STD BKGD (COUNTS)	COUNTING TIME(SEC)	STANDARD FILENAME
NA2O	4.097	2.93	1.915	0.000	1.06034	2542.8	50.5	20.00	2400.2	49.7	20.00	ZRGSC
MGO	0.024	115.74	1.082	0.000	0.00628	151.0	136.4	20.00	2469.5	136.9	20.00	ZRGSC
AL2O3	12.428	1.20	3.338	0.000	0.94799	14190.0	246.9	20.00	14955.9	247.8	20.00	Z5831
SIO2	75.144	0.86	2.774	0.000	1.01803	27351.8	53.7	20.00	26868.4	53.9	20.00	Z5831
K2O	4.474	1.63	2.354	0.000	1.22660	8825.4	144.4	20.00	7230.1	152.8	20.00	ZRGSC
CAO	0.517	4.62	0.931	0.000	0.10126	921.7	178.7	20.00	7528.9	191.2	20.00	ZRGSC
TIO2	0.055	68.83	1.131	0.000	0.00050	28.2	18.3	20.00	19938.2	26.6	20.00	ZTIO2
MNO	0.072	32.24	0.877	0.000	0.00072	104.6	64.3	20.00	56342.7	119.9	20.00	ZMN2O
FEO	0.962	5.66	1.689	0.000	0.15036	601.0	105.3	20.00	3409.3	112.6	20.00	ZRGSC

TOTAL 97.773 NO. OXYGENS = 0 NO. ITERS. = 2 AVE. ATOMIC NO. = 11.13

21-OCT-91 16:09:31

SAMPLE ID: JB-WA-1 T242-1 D... of Analysis: 10/21/91

Raw Probe Data		Raw Probe Data (FeO to Fe2O3)		Recalculated to 100%	
SiO2	75.144			SiO2	76.77
Al2O3	12.428			Al2O3	12.70
FeO	0.962*1.1113=Fe2O3		1.069	Fe2O3	1.09
MgO	0.024			MgO	0.02
MnO	0.072			MnO	0.07
CaO	0.517			CaO	0.53
TiO2	0.055			TiO2	0.06
Na2o	4.097			Na2o	4.19
K2O	4.474			K2O	4.57
TOTAL(O)	97.773	TOTAL(N)	97.880	TOTAL(R)	100.00

20 Best Matches:

1	0.9910	10/21/91	JB-BS-15 T241-6
2	0.9909	10/21/91	JB-BS-13 T241-4
3	0.9885	10/21/91	JB-BS-11 T241-2
4	0.9867	10/21/91	JB-BS-14 T241-5
5	0.9866	10/21/91	JB-BS-12 T241-3
6	0.9866	09/06/83	KRL82782A, T64-11
7	0.9859		3-30-82-1, T43-3
8	0.9848	10/21/91	JB-BS-9 T241-1
9	0.9846	10/21/91	JB-BS-16 T241-7
10	0.9846	10/23/85	BL-RSA-5 T112-10
11	0.9842	8/7/91	SS-91-1-4 T323-5
12	0.9841	12/20/90	FLV-159-CH T219-6
13	0.9831	8/7/91	SS-91-1-5 T232-6
14	0.9828	5/2/85	WL CORE G 370cm T92-7
15	0.9825	6/22/84	KRL-71082C (590) T58-1
16	0.9823		LD-12
17	0.9823	9/3/88	FLV-64-CS T170-7
18	0.9817	09/06/83	KRL91882-K-1, T64-13
19	0.9815	xx/xx/83	KRL91982D, T66-10
20	0.9815		LD-12, T3,4

Elements used in the calculation are:

Na2o
Al2O3
SiO2
K2O
CaO
FeO

***** This sample has been added to the data base *****

Listing of 50 closest matches for COMP. NO. 2646 [illegible] elements: Na, Al, Si, K , Ca, Fe Date of Update: 10/22/91

No	Sample Number	Date	[illegible]	Al2O3	Fe2O3	MgO	MnO	CaO	TiO2	Na2O	K2O	Total	S. Co
1	2646 JB-WA-1 T242-1	10/21/91	76.77	12.70	1.03	0.02	0.07	0.53	0.06	4.15	4.57	100.00	1.0000
2	2643 JB-BS-15 T241-6	10/21/91	76.59	12.83	1.08	0.03	0.07	0.54	0.04	4.23	4.59	100.00	0.9916
3	2641 JB-BS-13 T241-4	10/21/91	76.49	12.83	1.08	0.03	0.08	0.53	0.06	4.26	4.64	100.00	0.9905
4	2639 JB-BS-11 T241-2	10/21/91	76.55	12.80	1.10	0.02	0.08	0.54	0.06	4.16	4.68	99.99	0.9883
5	2642 JB-BS-14 T241-5	10/21/91	76.55	12.82	1.11	0.02	0.07	0.55	0.06	4.20	4.62	100.00	0.9867
6	2640 JB-BS-12 T241-3	10/21/91	76.51	12.85	1.11	0.03	0.08	0.54	0.05	4.16	4.67	100.00	0.9866
7	564 KRL82782A, T64-11	09/06/83	76.99	12.75	1.09	0.01	0.06	0.53	0.08	3.90	4.59	100.00	0.9866
8	435 3-30-82-1, T43-3		76.62	12.93	1.06	0.02	0.05	0.54	0.07	4.13	4.59	100.01	0.9855
9	2638 JB-BS-9 T241-1	10/21/91	76.42	12.92	1.10	0.01	0.08	0.55	0.05	4.22	4.65	100.00	0.9848
10	2644 JB-BS-16 T241-7	10/21/91	76.97	12.59	1.04	0.02	0.08	0.54	0.05	4.13	4.58	100.00	0.9846
11	1419 BL-RSA-5 T112-10	10/23/85	76.98	12.65	1.09	0.04	0.04	0.53	0.05	3.93	4.68	99.99	0.9846
12	2552 SS-91-1-4 T323-5	8/7/91	77.02	12.63	1.06	0.02	0.04	0.53	0.06	4.00	4.63	99.99	0.9842
13	2497 FLV-159-CH T219-6	12/20/90	77.01	12.76	1.08	0.03	0.03	0.54	0.05	3.94	4.57	100.01	0.9841
14	2563 SS-91-1-5 T232-6	8/7/91	76.97	12.65	1.08	0.03	0.04	0.54	0.07	3.98	4.65	100.01	0.9831
15	1224 WL CORE G 370cm T92-7	5/2/85	76.83	12.82	1.09	0.04	0.04	0.54	0.05	3.99	4.65	100.01	0.9828
16	1025 KRL-71082C (590) T58-1	6/22/84	76.91	12.71	1.08	0.02	0.00	0.53	0.05	3.95	4.74	99.99	0.9825
17	701 LD-12		76.94	12.72	1.12	0.03	0.07	0.53	0.07	3.91	4.61	100.00	0.9823
18	2060 FLV-64-CS T170-7	9/3/88	76.71	12.87	1.11	0.02	0.04	0.54	0.04	4.02	4.64	99.99	0.9823
19	567 KRL91882-K-1, T64-13	09/06/83	76.93	12.82	1.11	0.01	0.05	0.53	0.07	3.88	4.60	100.00	0.9817
20	570 KRL91982D, T66-10	xx/xx/83	76.81	12.89	1.08	0.03	0.05	0.53	0.06	3.90	4.65	100.00	0.9815
21	192 LD-12, T3,4		76.94	12.70	1.12	0.03	0.07	0.53	0.07	3.91	4.64	100.01	0.9815
22	566 KRL91882B, T64-12	09/06/83	76.81	12.82	1.10	0.01	0.05	0.53	0.08	3.91	4.69	100.00	0.9814
23	2559 SS-91-1-SU T232-1	8/6/91	76.74	12.86	1.09	0.04	0.04	0.54	0.05	3.95	4.68	99.99	0.9813
24	1439 KRL 82182 (A1) (599) T112-1	10/22/85	76.60	12.87	1.11	0.04	0.04	0.55	0.06	4.08	4.65	100.00	0.9811
25	739 S-20		76.83	12.90	1.09	0.03	0.07	0.51	0.06	4.00	4.50	99.99	0.9809
26	2561 SS-91-1-3 t232-4	8/7/91	77.08	12.64	1.06	0.02	0.05	0.53	0.06	3.92	4.64	100.00	0.9807
27	571 KRL91982F, T56-5	07/01/83	76.61	12.89	1.14	0.03	0.05	0.55	0.05	4.12	4.56	100.00	0.9807
28	2494 FLV-156-SS T219-3	12/20/90	76.64	13.06	1.09	0.03	0.04	0.54	0.05	3.94	4.62	100.01	0.9803
29	431 YOS-1, T13-1		76.61	12.93	1.12	0.03	0.05	0.54	0.07	4.03	4.64	100.02	0.9803
30	1694 SCHURZ-1 T134-6	11/25/86	77.01	12.64	1.09	0.03	0.05	0.55	0.05	3.94	4.64	100.00	0.9802
31	680 KRL-822828, T54-4	xx//xx/x	76.99	12.71	1.08	0.02	0.06	0.53	0.04	3.86	4.70	99.99	0.9801
32	2558 SS-91-1-1 T232-2	6/8/91	76.57	12.92	1.07	0.02	0.04	0.54	0.06	4.09	4.72	99.99	0.9797
33	679 KRL-82182(A-4), T66-3	10/25/83	76.89	12.82	1.02	0.02	0.05	0.52	0.04	4.08	4.55	99.99	0.9792
34	1418 BL-RSA-4 T112-9	10/23/85	76.83	12.79	1.08	0.04	0.04	0.55	0.06	3.96	4.65	100.00	0.9791
35	684 KRL--92082D, T66-12	10/25/83	77.02	12.69	1.09	0.02	0.05	0.51	0.04	3.92	4.66	100.00	0.9791
36	681 KRL-91882A", T66-8	10/25/83	76.79	12.83	1.10	0.03	0.06	0.54	0.07	3.91	4.67	100.00	0.9790
37	551 KRL82282A, T66-5	10/25/83	76.71	12.88	1.12	0.04	0.05	0.52	0.06	3.98	4.65	100.01	0.9787
38	760 BD-16		76.59	12.92	1.11	0.03	0.03	0.54	0.07	4.00	4.71	100.00	0.9782
39	1136 WALKER LAKE CORE G 380CM t89-1	2/20/85	76.98	12.79	1.08	0.02	0.05	0.54	0.05	3.86	4.64	100.01	0.9781
40	559 KRL82182(bubble wall), T56-4	07/01/83	76.87	12.92	1.01	0.02	0.03	0.53	0.03	4.03	4.55	99.99	0.9776
41	1240 WL 4-2 3.29m T93-9	5/2/85	76.75	12.79	1.13	0.03	0.04	0.55	0.05	4.02	4.64	100.00	0.9775
42	2571 JB-BS-7 T227-4	6/13/91	76.73	12.89	1.10	0.03	0.05	0.54	0.06	3.91	4.69	100.00	0.9775
43	437 6A, T35-7		75.81	12.97	1.11	0.03	0.03	0.52	0.06	3.92	4.56	99.01	0.9772
44	1872 WL-4-58 (144.77m) T164-1	5/21/88	76.73	12.71	1.15	0.00	0.03	0.54	0.12	4.02	4.69	99.99	0.9770
45	1421 BL-RSA-7 T112-12	10/23/85	77.16	12.66	1.03	0.04	0.05	0.52	0.03	3.95	4.57	100.01	0.9768
46	1760 DD-ML-6-135 CM T139-11	5/20/87	77.17	12.73	1.09	0.05	0.05	0.54	0.08	3.72	4.58	100.01	0.9766
47	1244 WL 8-3A ASH A 64-66cm T93-13	5/2/85	76.97	12.80	1.08	0.03	0.05	0.55	0.05	3.86	4.60	99.99	0.9765
48	1764 DD-QWP-34 CM T139-7	5/20/87	77.27	12.64	1.07	0.04	0.05	0.53	0.08	3.74	4.59	100.01	0.9765
49	1230 WL 8-1B 92-94cm T99-1	07/01/85	76.99	12.72	1.11	0.02	0.06	0.54	0.07	3.84	4.65	100.00	0.9764
50	2599 FLV-163-LC T230-8	7/2/91	77.28	12.61	1.08	0.02	0.04	0.51	0.06	3.94	4.47	100.01	0.9763

Appendix C

Paper and Field Guide Presented at Geological Society of Nevada Symposium on Walker Lane dc106

GEOLOGICAL SOCIETY OF NEVADA

WALKER LANE SYMPOSIUM

1992 SPRING FIELD TRIP #1 GUIDEBOOK

HAWTHORNE AREA-NORTHERN WALKER LANE

STRUCTURE AND TECTONICS

Northern Wassuk Range Faults

Walker Lake Area - Pine Nut Fault Zone

Santa Fe Mine - Isabella Tectonic Setting

Bettles Well Graben Tectonics

Cedar Mountain Fault Zone

Dicalite Summit Detachment Fault

Sheep Canyon Fault

SPECIAL PUBLICATION #14

April 25-26, 1992

Luning Thrust ∴ Benton Springs f. z. displ. dies to S.

50.7 Approximate trace of the northwest-trending Betties Well strike-slip fault, which apparently merges with the Petrified Spring fault to the north. Together, these faults truncate the east end of the Betties Well Valley half-graben and displace the east end of the graben about 3 km right-laterally to the southeast. This amount of displacement is equal to that of displaced Mesozoic structures across this fault.

52.3 Summit, elevation 6439', microwave tower to north.

53.1 Fork in road at power line, take right fork heading east into the southern Stewart Valley.

55.0 To the left of the road (east) and about 200 yards down the broad drainageway are fault scarps produced during the 1932 Cedar Mountain earthquake (Molinari, 1984, and references therein).

56.7 Water trough near cattle guard in fence. Looking to the west and south is an overview of the geology of the eastern Pilot Mountains. Of importance is the southerly displaced continuation of the Betties Well half-graben now exposed at the Gun Metal mine. The half-graben has been displaced about 3 km south by the Betties Well fault system. The eastern extent of the half-graben is obscured by range-front faults along the eastern Pilot Mountains. Scarps in alluvium can be seen in the valley fill east of the prominent pre-Tertiary exposures.

In the southeastern part of the Pilot Mountains, a large skarn tungsten deposit, the Gunmetal mine, was extensively explored and developed by Duval Corporation in the late 1970s. The original Gunmetal mine produced tungsten during WW II from generally low grade ores, which locally averaged 1% WO_3. An extensive exploration effort was conducted by Union Carbide in late 1970s-early 1980s (Grabher, 1984).

56.8 Fork in road, stay right and drive south.

58.4 Take track on left (east) to small hill with white trench dumps.

58.7 STOP 11 - Craig dePolo, Figure 18. Examine features of the 1932 Cedar Mountain earthquake where Trench #8 exposes upturned tuffaceous sediments.

The Stewart-Monte Cristo fault zone, along which the 1932 Cedar Mountain earthquake occurred, is more than a kilometer wide in this area. The fault zone is dominantly right-lateral strike slip in nature. About 1 m of right-lateral displacement occurred in this area in 1932. The small hill at this location is a "pressure ridge" formed by compression at a left step in the fault zone (restraining bend). Due to a small amount of contraction, Tertiary sedimentary rocks with a veneer of Quaternary alluvium are pushed up forming the topographic high. Trench 8 was dug across a subtle scarp on the southern side of the hill (see figure 18 for faults and trench locations) and confirmed the contractional nature of the fault zone at this location.

The northern half of the trench revealed steeply to vertically tilted Tertiary sedimentary rocks cut by several reverse faults. The southern end of the trench exposes Quaternary gravels deposited by streams running along the southern edge of the pressure ridge, roughly perpendicular to the trench. These gravels are faulted and deformed towards the contact with the Tertiary sediments. The contact between the gravels and the Tertiary sediments is a fault zone with several episodes of movement represented. Most of the Tertiary units in the fault zone have been highly sheared and jumbled. Several reverse faults are present in the rest of the trench particularly in the hanging wall of the main (contact) fault zone, three of which offset the section exposed in the trench. Movement in 1932 may have occurred along the southernmost fault in the trench, and along two of the reverse faults cutting the Tertiary sediments. The southernmost fault deforms gravels very near the surface. In all cases the movement would have been minor. A simplified trench log is given in Figure 19.

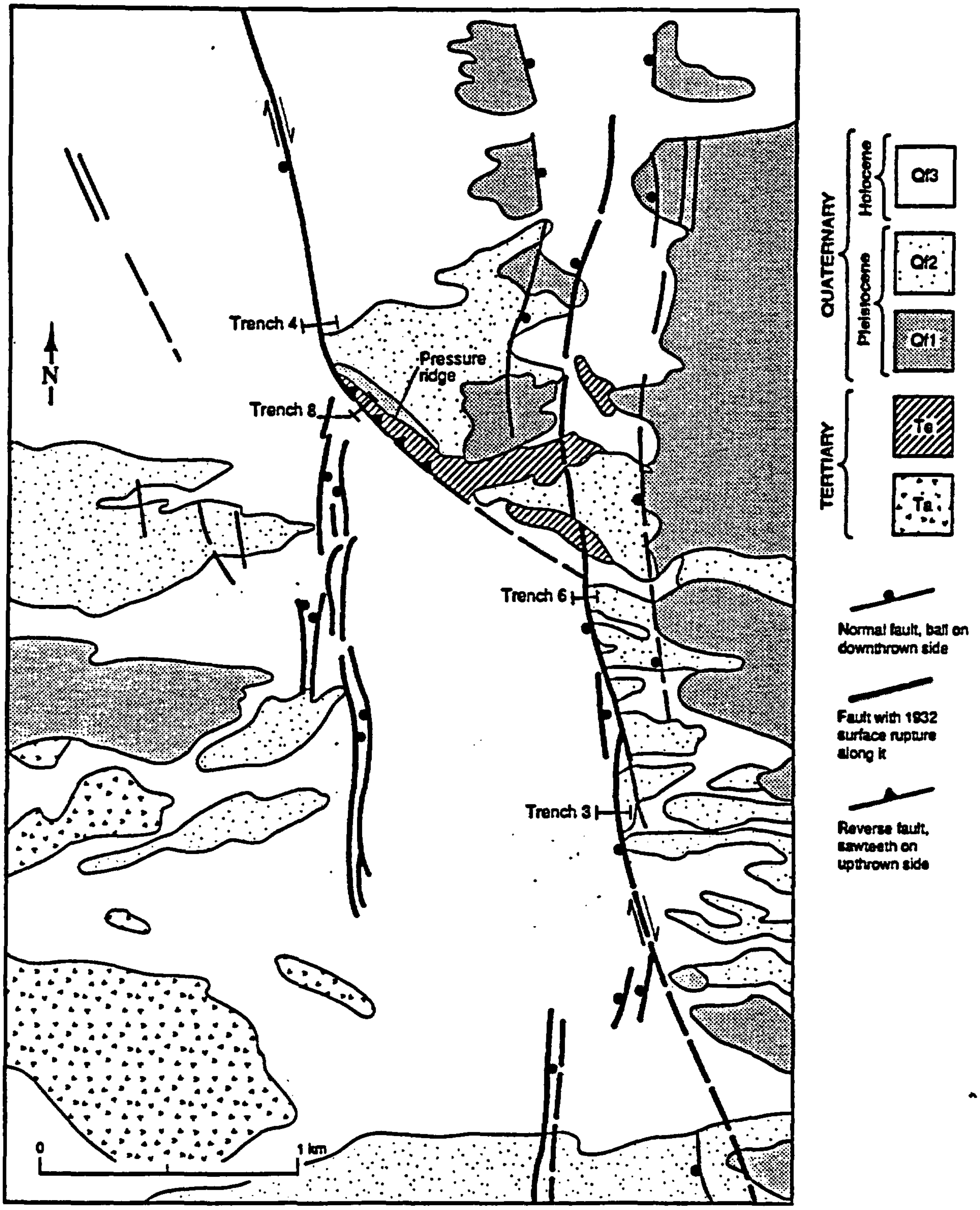

Surface geology of Monte Cristo Valley.

Figure 18.

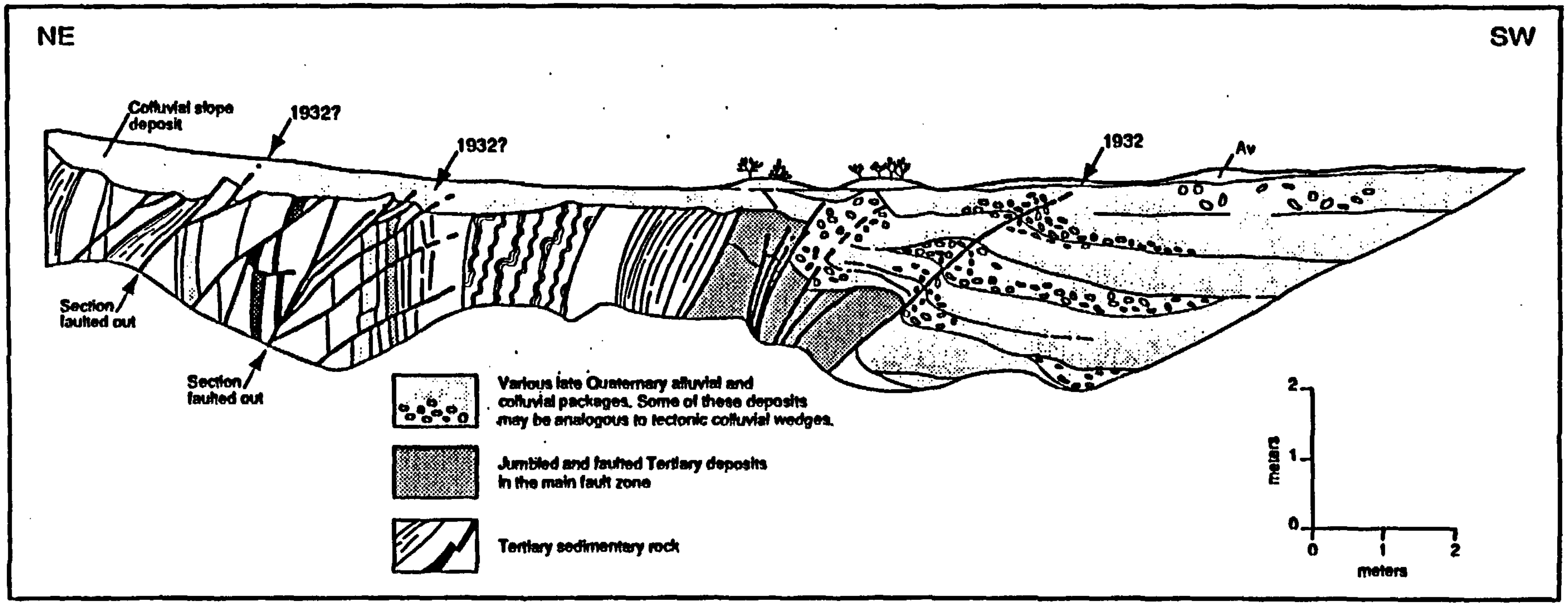

Trench 8, east wall.

Figure 19.

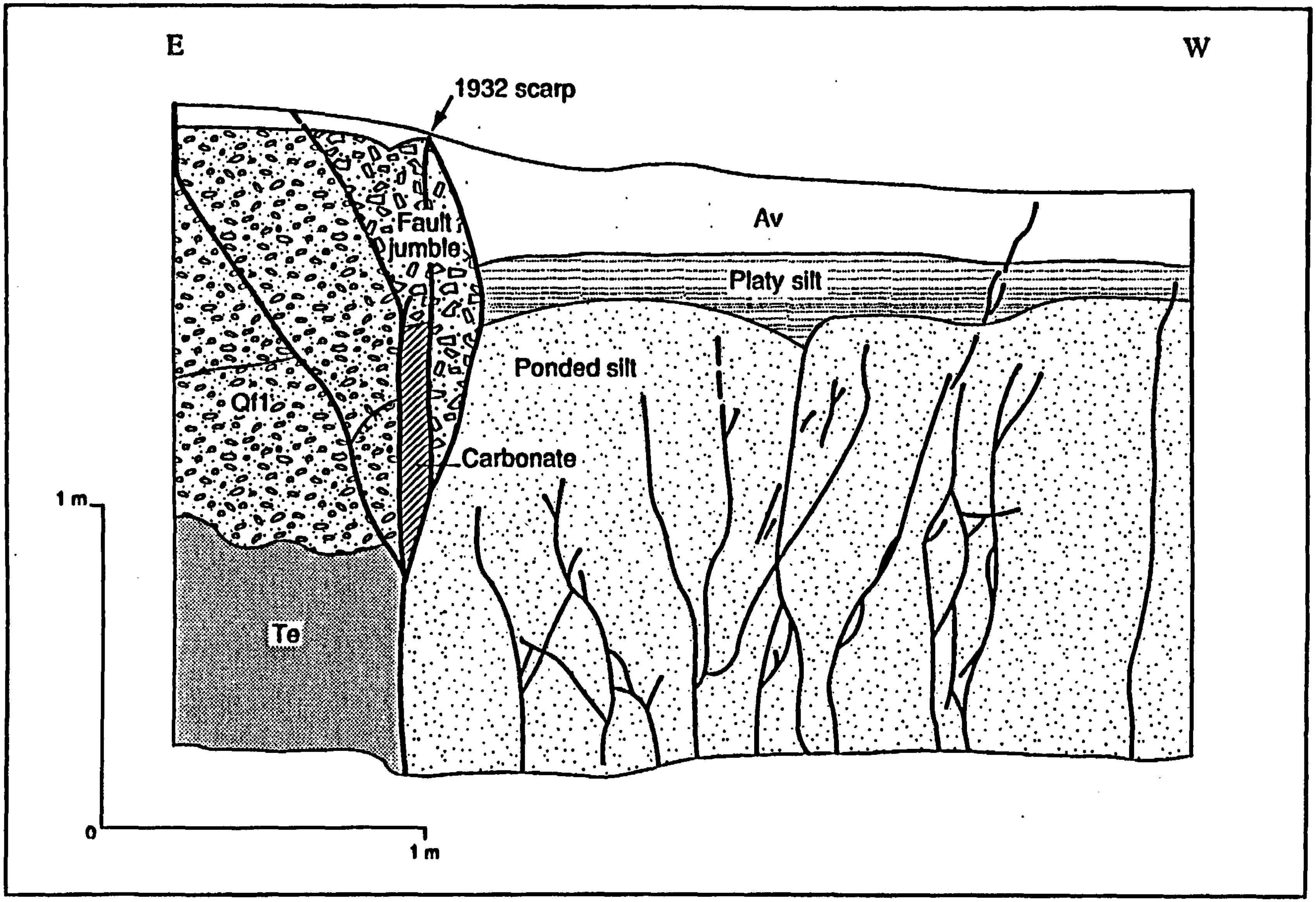

Partial log of Cedar Mountain Trench 3A, cut back 80 cm from original face on south wall.

Figure 20.

58.9 Return to main road and turn left (south).

60.1 Turn left on track and drive east to trenches.

60.6 **STOP 12 - Craig dePolo, Figure 18. Examine fault escarpment and Trench #3. Don't fall in!**

This is one of the first trenches dug by the Nevada Bureau of Mines and Geology in the study of the 1932 Cedar Mountain earthquake. Originally a single trench, Trench 3 was expanded into an "H" shape to better establish stratigraphic relationships. One to two meters of right-lateral strike-slip displacement occurred at this location in 1932. The 30-cm high surface scarp from this event is still well preserved and can be traced out in either direction. **To preserve these ruptures for others to examine and for potential future scientific studies, please avoid walking on the scarp; this is especially important for large groups of people or when the ground is wet.**

Trench 3 exposes a vertical main fault that commonly splays into a flower structure near the surface, and several secondary faults on the "downthrown" side (see Figure 20). The backfacing nature of this scarp with respect to topography has ponded younger sediments against the fault. In some cases these packages of ponded alluvium appear to represent individual earthquake events.

The east side of the trench reveals ponded late Quaternary silts and gravels. The west side consists of tilted tertiary sediments, overlain by mid-Quaternary gravels (ash within these gravels has been identified as Bishop-aged ash; 0.7-1 Ma). The fault zone, especially in the flower structure, contains jumbled and sheared units from both sides of the fault. Carbonate has been deposited in a small mass in the fault zone, a fairly common occurrence along youthful faults in the Basin and Range province. Slickensides from the main fault plunge 6 to 9 degrees to the north supporting a large component of right-lateral strike-slip motion along this north-striking fault.

The stream to the immediate south of the trench has a right-lateral offset at the fault zone. The 1932 stream-offset can be seen, but is difficult to measure. The overall right-lateral jog in the stream is due to several late Pleistocene and Holocene offsets. This is a rare, well-developed lateral offset of a stream channel. Most streams have straightened their channels across the rupture. The particular example south of the trench appears to be well developed due to a limited catchment basin and significant lateral offsets per event.

61.1 Retrace route to main road and turn right (north) back to fork in road at mile 58.1.

63.9 Turn hard right at the road fork and proceed southeast and east across the southern Stewart Valley to the southern Cedar Mountains and Dicalite Summit area.

64.6 Crossing trace of Quaternary fault scarp from Stop 12.

64.9 Fork in road, bear left.

66.8 Cross main Stewart Valley wash.

70.8 Old bulldozer cut, trending east from the main Dicalite summit road, claim post and workings west of road.

The hills to the east are composed of Tertiary ash-flow tuff units that overlie locally discontinuous intermediate composition lavas (about 30 Ma) that thicken to the south (Whitebread and Hardyman, 1987).

dePolo

Geological Society of Nevada
Structure, Tectonics and Mineralization of the Walker Lane
A Short Symposium

April 24, 25, 26, 1992

AGENDA

CORPORATE SPONSORS

ABSTRACTS

1991-1992 Officers

President	Eric Seedorff - Magma Copper Co.
Vice President	Steve Craig - Kennecott Exploration Co.
Secretary	Opal Adams - Independence Mining Co.
Treasurer	Eric Ruud - Cone Geochemical Inc.
Membership Chairman	Bob Felder - Santa Fe Pacific Mining Co.

Geological Society of Nevada
Laxalt Mineral Research Center, Room 266
Mackay School of Mines
University of Nevada, Reno

Geological Society of Nevada
P.O. Box 12021
Reno, Nevada 89510
(702) 323-3500
FAX (702) 784-1766

The 1932 Cedar Mountain Earthquake: An Example of Active Tectonism in the Walker Lane

Craig M. dePolo, Nevada Bureau of Mines and Geology, University of Nevada-Reno, Reno, NV 89557

The 1932 Cedar Mountain earthquake (surface-wave magnitude 7.2) has an important bearing on the neotectonics of the western Great Basin because the event is the largest historical earthquake in the Walker Lane, had an unusually wide distribution of surface ruptures, consisted of multiple events, and precipitated the notion of the Walker Lane. Gianella and Callaghan (1934a) were the first to discuss the significance of the Cedar Mountain earthquake, strike-slip faulting in the western Great Basin, and topographic aspects associated with the Walker Lane.

The main shock of the 1932 earthquake occurred at 0610 UTC (2210 PST) on December 21 and had a felt area of 850,0000 km^2 (Coffman and von Hake, 1973). Considering the location of the epicenter in southern Gabbs Valley (Byerly, 1935) and the extension of surface ruptures for roughly 60 km to the south of the epicenter, it seems clear that this earthquake propagated to the south. Seismological studies conducted by Doser (1988) suggest the Cedar Mountain earthquake was a complicated, multiple event. Doser studied and modeled the teleseismic P-waves from this earthquake using seismograms recorded worldwide and found that it was comprised of at least two subevents. For the preferred northerly-striking nodal planes, both subevents were dominated by right-lateral strike-slip displacement and were subparallel to the Walker Lane. Doser noted that the better located aftershocks from the 1932 event cluster in two major areas, Gabbs Valley and northern Monte Cristo Valley, possibly highlighting the areas of the two major subevents.

The earthquake appears to have involved at least two major faults and many minor faults in the region. The two major faults involved are the Stewart-Monte Cristo Valley fault zone (Molinari, 1984) and an unmapped, subsurface fault below northern Stewart and Gabbs Valleys. Both of these ruptures were right-lateral strike-slip in nature. Other faults that were involved in the 1932 earthquake include normal faults on the west flank of Cedar Mountain, strike-slip faults in Stewart Valley, and normal faults in southern Gabbs Valley. The Stewart-Monte Cristo Valley fault zone is the easternmost member of the group of strike-slip faults in the central Walker Lane.

The zone of surface ruptures from the Cedar Mountain earthquake is approximately 60 km in length (end-to-end measurement) and 6 to 14 km wide (Gianella and Callaghan, 1934b). Surface ruptures were not confined to a mountain front or a single topographic feature, but rather were distributed broadly across three valleys and along short parts of adjacent mountain fronts. The longest and most continuous surface faulting was about 17 km in length and occurred along the Stewart-Monte Cristo Valley fault zone in northern Monte Cristo Valley. Right-lateral displacements along this fault zone ranged from a few centimeters to 2 m, and vertical displacements were as much as 0.5 m. Small-scale geomorphic features formed during the surface rupture include fault scarps, grabens, moletracks, swells and depressions, warped scarps (small surficial monoclines), and echelon-stepping breaks.

Trenching and Quaternary stratigraphic studies in Monte Cristo Valley have been conducted by the Nevada Bureau of Mines and Geology to determine the structural nature of the surface faulting and the paleoseismic history of the Stewart-Monte Cristo Valley fault zone. In trench exposures where significant lateral slip occurred, the fault planes are vertical and small scale (1 to 2 m) flower structures commonly exist near the surface. These structures, consisting of upward splaying fault traces and small reverse faults, appear to underlie surface expressions such as warped or ramped scarps, moletracks, and swells.

The ages of surfaces and deposits in Monte Cristo Valley have been estimated using tephrochronology, rock varnish radiocarbon dating, and soil development. From these ages and crosscutting relations of the surfaces and deposits with the faults, normal-right slip rates for the Stewart-Monte Cristo Valley fault zone of 0.2-0.5 mm/yr are estimated for the late Quaternary. The lateral to vertical displacement ratio ranges from 3:1 to 6:1 (dePolo and others, 1987). Studies thus far indicate that the most recent paleoseismic event prior to the 1932 earthquake probably occurred in early Holocene.

The 1932 Cedar Mountain earthquake underscores the importance of considering multiple source models when analyzing faults for seismic hazards in the Basin and Range province. It demonstrates the potential for small surface faults to reflect an earthquake larger than an analysis of a single fault would suggest, and for the potential involvement of subsurface faults that lack clear surface expression. Although many of the widely distributed surface ruptures from the 1932 event were probably secondary or sympathetic in nature, displacements ranged from a few centimeters to a decimeter or more at the surface, which can be a significant amount for some engineering projects. In southern Gabbs Valley, surface ruptures occurred along a group of subparallel northeast-striking normal faults, whereas the main subsurface rupture below appears to have been a northerly striking right-lateral fault. The complex nature of this event illustrates the need for considering such complexities when analyzing earthquake hazards in the Basin and Range province, especially for critical engineering facilities.

TASK 3: EVALUATION OF MINERAL RESOURCE POTENTIAL, CALDERA GEOLOGY, AND VOLCANO-TECTONIC FRAMEWORK AT AND NEAR YUCCA MOUNTAIN

REPORT FOR OCTOBER, 1991 - SEPTEMBER, 1992

Steven I. Weiss,[1] Donald C. Noble,[2] and Lawrence T. Larson[2]

Department of Geological Sciences, Mackay School of Mines, University of Nevada, Reno

[1] Research Associate
[2] Co-principal Investigators and Professors of Geology

INTRODUCTION

This report summarizes the results of Task 3 work initially discussed in our monthly reports for the period October 1, 1991 through September 30, 1992, and contained in our various papers and abstracts, both published and currently in press or review (see appendices). Our work during this period has involved a) the continuation of studies begun prior to October, 1991, focussed mainly on aspects of the caldera geology, volcanic stratigraphy, magmatic activity, hydrothermal mineralization and extensional tectonics of the western and northwestern parts of the southwestern Nevada volcanic field (SWNVF), and b) new studies of the alteration and trace-metal geochemistry of subsurface rocks of Yucca Mountain utilizing drill hole samples obtained in late 1991 and early 1992.

UPDATE ON THE NATURE AND DISTRIBUTION OF SUBSURFACE ALTERATION IN YUCCA MOUNTAIN

During the past year, we have continued to investigate the nature and distribution of alteration in the subsurface of Yucca Mountain. This has been accomplished by the visual examination of intervals of core that were not previously inspected by our group, coupled with initial hand-specimen, polished-section and thin-section petrographic studies of core samples obtained primarily for chemical analyses. A graphical summary of alteration features is presented in Figure 1, which has been modified from our 1991 report based on our observations made during the period of this report.

Distribution, nature and origin of pyrite in tuffs and lavas of Yucca Mountain

One of our principal concerns has been to address questions about the distribution, nature, and origin of pyrite observed in various intervals of drill core from the volcanic rocks of Yucca Mountain by personnel Task 3, by Stephen B. Castor and the Nevada Bureau of Mines group, and by several previous workers of the U.S. Geological Survey and the national laboratories. In the volcanic rocks, pyrite is unevenly distributed in pyroclastic rocks, mainly occurring in the unwelded to partially welded, lithic-rich parts of the Tram Member of the Crater Flat Tuff and the Lithic Ridge Tuff, and in intercalated silicic lavas (Figure 1). Our view has been that the pyrite is simply one product of hydrothermal activity and its uneven distribution reflects the flow paths of fluids that had activities of reduced sulphur species sufficient to sulphidize iron-rich phases in the rock mass (Weiss et al., 1991). Castor et al. (1991; in review) believe most, or all, of the pyrite in the pyroclastic rocks is lithic material, and therefore consider the pyrite to *predate* deposition of the pyroclastic host rocks. Their hypothesis is that the "lithic" pyrite originated by hydrothermal alteration of rocks in the vent area(s) of the Tram Member and the Lithic Ridge Tuff. They speculate that during the eruptions of these pyroclastic rocks, pyrite and pyritic altered rock fragments were ripped from the vent walls and incorporated in the tuffs. Castor et al. (1991; in review) therefore propose that the pyrite in the pyroclastic rocks does not reflect *in situ* alteration within Yucca Mountain. Based on a number of lines of textural evidence and the near magmatic temperatures of the eruption, transport, deposition and initial cooling of the ash-flow sheets, we strongly disagree with the proposition that no *in-situ* addition of sulphur has occurred, although hydrothermally altered and pyritic rock fragments could provide evidence for earlier hydrothermal events.

In the subsurface of Yucca Mountain pyrite is most common and most widely distributed in the Tram Member of the Crater Flat Tuff (Figure 1), where it is present as disseminated grains composing <1% of the groundmass and as disseminated grains and veins in lithic fragments. Some lithic fragments contain as much as about 10% pyrite, and many are partly to completely replaced by varying proportions of albite, adularia, quartz and clay. Pyrite is also present both in lithic fragments and in the groundmass of the Lithic Ridge Tuff, although it is apparently less widely distributed (Figure 1) and less abundant. In lithic fragments and the groundmass of both ash-flow sheets, the disseminated pyrite consists of anhedral to subhedral, generally pitted and wormy to seived, or skeletal(?), individual crystals and granular aggregates of ~5 μm - 300 μm in maximum dimension (Figures 2 and 3). In some grains pits and ophitic texture appear to result from the presence of numerous inclusions of altered groundmass, while other grains, mainly those smaller than about 10 μm in diameter, are not uncommonly subhedral in shape and free of pits. Propylitically altered silicic lavas in USW-G2 contain disseminated pyrite grains having textures and morphology indistinguishable from those of the pyrite in the tuffs (Figure 4). Fractures, not uncommon in granular pyrite in the tuffs, are present in pyrite grains in the altered lavas as well. These observations demonstrate that the fragmentation and degassing processes of ash-flow eruptions are not required to produce the textures and morphology of the pyrite in the tuffs, since the pyrite in the lavas is clearly not lithic material. Instead, as is the case in the altered lavas, the observed pyrite textures in the tuffs more likely stem from precipitation and growth (± partial dissolution ?) from hydrothermal solutions.

Further textural evidence in support of the above argument includes the presence of partly sulphidized phenocrystic biotite in the Lithic Ridge Tuff (Figure 5a), and pyritic clay-altered pumice in the Tram Member (Figure 5b). It is difficult to imagine that this pyrite predated and survived the eruptions of each ash-flow unit. The features shown in Figure 5 were found only with careful examination of an initial, small number of sections that had been impregnated with epoxy prior to polishing, and, though not abundant, they may be more common than would be inferred from inspection of unpolished core or unimpregnated polished sections.

Another significant line of evidence arguing that the pyrite in tuff in Yucca Mountain is the result of *in situ* growth involves the similarity in texture and morphology of the pyrite in Yucca Mountain tuffs to that found in obviously hydrothermally altered porous ash-flow tuffs elsewhere. For example, in the Divide mining district the early Miocene Tonopah Summit Member of the Fraction Tuff contains as much as 1 - 3% pyrite where the unit has been affected by propylitic and phyllic alteration (Bonham and Garside, 1979). This pyrite has been considered by Bonham and Garside (1979) to comprise a common component of the hydrothermal mineral assemblage in the Divide district. Examination of samples from partially welded, pyritic ash-flow tuff of the Tonopah Summit Member shows that this hydrothermal pyrite is essentially identical in texture and morphology to the pyrite in volcanic rocks in Yucca Mountain (Figure 6), and in some hand-specimens tends to be more abundant in lithic fragments than in the groundmass. It should be noted that pyrite has not been described as a component of unaltered rocks of the Tonopah Summit Member (Bonham and Garside, 1979). Similarly, in areas of little or no alteration, pyrite has not been described as a component of the Lithic Ridge Tuff or members of the Crater Flat Tuff (e.g., Carr et al., 1986). We intend to obtain additional specimens of pyritic, porous ash-flow tuff from other paleohydrothermal systems (e.g., Round Mountain, NV) for comparison of pyrite textures with those of Yucca Mountain.

Finally, although traces of magmatic pyrrhotite, cubanite chalcopyrite, and Fe-Ni sulphides are not uncommon in volcanic rocks, they are found *only* as blebby inclusions in phenocrysts and dense glassy rock (vitrophyre) where they have been sufficiently encapsulated to prevent degassing of sulphur during eruption and primary cooling (e.g., Hildreth, 1977; Drexler, 1982; Whitney and Stormer, 1983; Keith et al., 1991). At the near magmatic temperatures associated with the eruption, deposition and primary cooling of the Yucca Mountain tuffs, "lithic" pyrite gains ripped from vent walls would have been rapidly heated and would have lost most or all of their sulphur. Although pyrite enclosed within altered rock fragments might retain their sulphur, it seems highly unlikely that unprotected pyrite grains only 5 μm to few 100's of μm in maximum dimension would survive such heating. Evidence for such degassing would include partial or total conversion of pyrite grains to iron oxides. Iron oxide coatings or rims are absent from much of the groundmass pyrite in the Yucca Mountain tuffs, arguing strongly against the idea that these grains are but remnants of originally larger, partially degassed "lithic" grains.

Within both the Lithic Ridge Tuff and the Tram Member of the Crater Flat Tuff of drill holes USW-G3, USW-G1and USW-G2, many lithic fragments are more strongly altered than the enclosing ash-flow tuff. Much of the groundmass of the tuffs consists of glass shards and small pumice fragments that have been altered to mixtures of clay, zeolites and opaline silica. The stronger alteration of many lithic fragments, the lack of observable pyrite veins cutting the matrix of tuffs, the truncation of quartz and pyrite veins by the margins of the lithic fragments, and the relatively rare presence of pyrite in clay-altered pumice clasts have led Castor et al. (1991; in review) to argue that essentially *all* pyrite, including that in the groundmass, originated by hydrothermal alteration of rocks in the vent area(s) of these two ash-flow units. Disseminated pyrite is also present in the pre-Lithic Ridge tuffs of UE25p-1 (S. I. Weiss, unpublished data, 1992), and in the lower parts of the Prow Pass and Bullfrog members in USW-G2 (Caporuscio et al., 1982). Are we to believe that this pyrite is of a "lithic" origin as well, in units not particularly rich in lithics, when its presence can be more easily explained by the passage of sulphidic fluids through the more permeable areas of the rock mass? There can be little doubt that altered lithic fragments provide important evidence for pre-Lithic Ridge and pre-Tram hydrothermal events. However, the *later* addition of pyrite is strongly supported by the textural, distribution and temperature considerations discussed above.

Other observations concerning the nature and distribution of subsurface rock alteration

Petrographic work on samples from the Yucca Mountain drill core is currently getting under way and systematic studies have not yet been carried out, but several observations merit discussion in this report. In USW G1 propylitic alteration of the pre-Tram silicic lavas was verified. Beneath these lavas, the alteration gap composed of unaltered Lithic Ridge Tuff, previously inferred from published reports (Figure 1) was confirmed. Another gap is present in USW G3 where the presence of unaltered tuffs beneath the Lithic Ridge was verified. These areas of apparently fresh rocks demonstrate, not surprisingly, that alteration and hydrothermal fluid flow were not vertically or laterally continuous over the depths and wide spacing of the drill holes.

Cursory examination of a small number of thin sections indicates that many of the lithic fragments in the Tram Member and the Lithic Ridge Tuff of drill holes UE25b-1H, USW G1 and USW G3 are more strongly altered than the enclosing tuffs. In the few sections of these units examined to date, sanidine, plagioclase and mafic phenocrysts are mainly unaltered, in contrast to the replacement of lithic fragments by combinations of albite, adularia, quartz, calcite and clay.

In USW G2, pyritic propylitic(?) alteration in the lower part of the Prow Pass Member of the Crater Flat Tuff dies out upward into weak argillic alteration, defined by the presence of clay-replaced feldspar phenocrysts, associated with a zone of breccia veins at depths from 2873' to about 2975'. The breccia veins are irregular, anastomosing to planar structures filled with a mixture of cm- to mm-sized rock fragments, rock flour, very fine-grained silica and reddish to black iron and manganese oxides. Jigsaw textures, irregular pinchouts and the ranges of fragment size and shapes, and associated bleaching and argillic alteration of the welded tuff, suggest that the veins are hydrothermal in origin. Very similar breccia veins containing a matrix of extremely fine-grained iron-oxide, silica and fluorite (Figure 7) are present in iron-oxide stained, brecciated, moderately to densely welded, devitrified ash-flow tuff of the Crater Flat Tuff in drill holes UE25 C1, UE25 C2 and UE25 C3. Multiple stages of cross-cutting quartz, fluorite, and iron-manganese oxide veinlets are present within and cutting through the breccia veins. Fluorite also fills small cavities and is intergrown with montmorillonite in other small, irregular cavities. Spengler and Rosenbaum (1991) recognized that the brecciated rocks of the Crater Flat Tuff in the UE25 C holes form a tabular, shallowly west-dipping body of hydrologic significance, through which aqueous fluids have passed. Analyses of 7 samples from these brecciated rocks show the presence of anomalous concentrations of Mo, Sb, Bi and As (see below), demonstrating that such fluids have included metal-bearing solutions.

TRACE-METAL CHEMISTRY OF ROCKS FROM THE SUBSURFACE OF YUCCA MOUNTAIN

Samples from 41 intervals of core and rotary cuttings were analysed for precious metals and a broad suite of elements generally considered useful in indicating the presence of hydrothermal mineralization. These analyses were carried out to investigate the possible presence of metal and trace-element enrichments in the subsurface of Yucca Mountain that might be associated with undiscovered, potentially economic mineralization.

Methods

Samples were analyzed by highly sensitive inductively-coupled plasma emission spectrography (ICP-ES), graphite-furnace atomic absorption (GFAA) and hydride-generator atomic absorption (AA) methods carried out at MB Associates and the Nevada Mining Analytical Laboratory (Hg); the results are listed in Table 2. Blind duplicate analyses carried out in this and other studies indicate acceptable levels of precision for all of the elements determined (Table 2). In all but a few samples, ICP-ES measurements gave higher Hg values than were determined by AA measurements. Previous experience has shown that at low levels the AA determinations of Hg are more precise and probably more accurate than ICP-ES determinations (Weiss et al., 1991).

Special care was taken to avoid contamination of samples during preparation for the analyses. First, with the core enclosed in 50 mil plastic bags, representative fragments totalling about 60-100 grams were broken from each core interval using a clean, acid-treated hammer. Where veins or filled fractures were observed, selected fragments contained more wall-rock than vein material. Core fragments were inspected visually to avoid macroscopically visible drill-tool rubs, drilling lubricant and paint. Each core fragment was then scrubbed and rinsed with distilled water, using a nylon brush, to mechanically remove potential microscopic surface contaminants. After air drying, samples were crushed and pulverized to -200 mesh powders using carefully cleaned, small volume equipment not normally used for processing ores. Ceramic plates were used on a small rotary pulverizer. In addition to an initial mechanical and acid cleaning, both the crusher and pulverizer were cleaned between each sample using an abrasion flux of fresh, unmineralized, densely welded tuff of the Tiva Canyon Member having extremely low trace metal concentrations (e.g. Table 4 of Weiss et al., 1991; Table 2, sample 3SW-589 of this report). Sample powders were split and sealed in clean plastic and glass vials.

Rotary cuttings were inspected under a binocular microscope for the possible presence of drill-tool fragments, lubricants and other foreign material. Due to the small amounts of cuttings available for study (<50 grams for each 10' interval) and the sand-sized nature of most of the cuttings, some contamination with drill-tool and lubricant particles could not be avoided. Samples containing visible foreign material are noted in Table 2. As will be discussed below, the effects of this contamination on measured precious- and trace-metal contents are not likely to be significant. Cuttings were also pulverized to -200 mesh powders using ceramic plates and sealed in clean plastic and glass vials.

Results

Elemental abundances measured for fresh specimens of the Bullfrog Member of the Crater Flat Tuff and the Tiva Canyon Member of the Paintbrush Tuff ("fresh tuff reference samples", Table 2), together with analyses by similar methods of unaltered tuff given by

Castor et al. (1989), Connors et al. (1991a; in review), Weiss et al. (1991) and Castor and Weiss (1992) provide a limited, but useful indication of precious- and associated trace-metal contents to be expected in unaltered, silicic volcanic rocks in Yucca Mountain. Silicic rocks that have undergone cooling-related (primary) devitrification and weathering tend to have slightly larger contents of As and Au than those found in glassy rocks, but overall, precious- and associated trace-metal contents are extremely low. Based on the sources mentioned above, and our prior exploration experience, we expect concentrations in fresh silicic volcanic rocks to be approximately as follows:

Au	<1 ppb (most <0.3 ppb
Ag	<0.10 ppm
As	<6 ppm (most <2 ppm)
Bi	<0.10 ppm
Hg	<30 ppb (most <15 ppb)
Sb	<0.20 ppm
Se	<0.10 ppm
Te	<0.10 ppm
Mo	<2.0 ppm (most <1.0 ppm)
Tl	<0.50 ppm

In east-central Yucca Mountain, rotary cuttings from four 10' intervals of mineralized carbonate sedimentary rocks of drill hole UE25p-1 assigned to the Silurian Lone Mountain and Roberts Mountain formations (Carr et al., 1986), and containing disseminated pyrite and fragments of pyrite, quartz and fluorite veins were analysed. Sample 16963, from a depth of 5530'-5540' contains highly anomalous concentrations of Hg, Sb, Mo, Pb and Zn, and modestly anomalous concentrations of As, Bi, and Tl (Table 2). Gold and Ag are modestly enriched in 16963 with respect to the other three intervals of Silurian sedimentary rocks (Table 2), but are still relatively low in absolute value. Analysis of powder made from a second split from this interval (16963B) confirmed the first analysis and indicates that within this interval, the cuttings are not chemically homogenous. The data are inconsistent with contamination by drill-tool fragments and(or) lubricant owing to the clearly elevated *suite* of trace metals. Rather, the chemical data, together with the vein fragments in this interval, provide unequivocal evidence for the passage of metal-bearing, epithermal-type fluids through pre-Cenozoic rocks beneath Yucca Mountain. Although the anomalous metals in these sedimentary rocks could have been introduced prior to deposition of the overlying Miocene volcanic rocks, significantly elevated As (~14-63 ppm), Zn (125 ppm) and Sb (~1-2 ppm), and weakly elevated Mo (~2-3 ppm) and Hg (~50-135 ppb) are also present in several scattered intervals from tuffs of stratigraphic unit Tot of UE25p-1 (Table 2).

To the northwest of drill hole UE25p-1, an unusual association of modestly to very highly elevated Mo (as high as ~200 ppm) ± elevated Sb, As and Bi, is present in brecciated rocks of the Crater Flat Tuff in drill holes UE25 C2, UE25 C3, and probably in UE25 C1 as well (Table 2). Three lines of evidence indicate that the elevated Mo concentrations are unlikely to result from contamination by drilling tools, cutting tools or lubricants. First, sample 20069B (109 ppm Mo) was composed entirely of fragments broken from the interior of the core and having no surfaces cut by drilling or splitting tools. Second, the elevated Mo values are associated with elevated Sb, As and Bi contents, which are not likely to result from such contamination. Finally, the presence of drusy fluorite, and breccia veins with a matrix rich in iron oxide, provide direct evidence for the passage of fluoride- and metal-bearing fluids. These fluids passed through the tuffs after compaction, and apparently caused some or all of the brecciation, but their origin remains unclear.

Further to the north, significantly elevated concentrations of As (39-85 ppm) and Hg (~120-150 ppb) are found in strongly propylitically altered lavas of stratigraphic unit Tr1 in drill hole USW-G2 (Table 2). In the same drill hole, between 3420' and 3421' (sample 16871), a 0.5-2 mm thick fracture filled with manganese oxide and adjacent fresh, but iron-oxide stained tuff of the Bullfrog Member of the Crater Flat Tuff contains less As (18 ppm), but much greater amounts of Hg (~0.7 ppm) and Sb (~5 ppm).

As discussed previously, drill holes USW-G3, UE25B-1H, USW-G1 and USW-G2 encountered deep, but aerially widespread pyritic alteration in units of the Crater Flat Tuff and the Lithic Ridge Tuff. In drill holes USW-G1 and UE25B-1H nine samples from these pyritic rocks contain no distinctly elevated Au, Ag, Sb and Tl (Table 2). Arsenic concentrations are only 2-5 ppm higher than concentrations found in weathered devitrified rhyolitic ash-flow tuff. Modest Hg enrichment (~106 ppb) is present in only one of these 9 samples (sample 16860), but 8 samples contain marked enrichments of Bi, Se and Te. Further to the south in USW-G3, where less pyrite is present in the Lithic Ridge Tuff than is found in the Tram Member to the north, the pyritic rocks apparently contain less Bi, Se and Te, and slightly more Hg (Table 2). Selenium is a common element in many volcanic-hosted epithermal precious-metal deposits. Bismuth and Te are associated with magmatic-hydrothermal systems (i.e. porphyry and skarn deposits) and various types of epithermal vein systems. Trace amounts of these metals are commonly attributed to the input of magmatic fluids into hydrothermal systems.

From textural and temperature considerations discussed earlier, we believe that much or all of the pyrite formed after deposition of the tuffs by partial hydrothermal sulfidation of iron-bearing phenocrysts and other iron-bearing phases in the groundmass and lithic fragments. This pyritic alteration, or sulfidation, clearly represents a major enrichment of sulphur relative to fresh rhyolitic tuffs.

The chemical data given above, in combination with presently available information on subsurface alteration, veining, pyrite distribution, etc., are consistent with the passage of hydrothermal fluids through parts of Yucca Mountain and the movement and local, generally low-level accumulation of various combinations of elements (including As, Sb, Hg, Bi, Se, Te, Mo, Pb, Zn and Tl) commonly associated with hydrothermal mineralization. In many volcanic-hosted epithermal ore deposits, mineralization and associated trace-metal halos are restricted to narrow areas of high permeability that channeled large volumes of fluid flow. Commonly, rocks a few meters outside these channelways show little, if any, metal enrichments. This is true not only in vein systems, but in disseminated deposits as well. For example, in porous ash-flow tuff of the Round Mountain gold deposit, mineralizing fluids were guided in part by primary permeability enhanced and preserved by original vapor-phase crystallization, and fluid flow was restricted by lower permeability in porous glassy zones (Sander, 1990). Many of our sample are from porous, previously largely glassy tuff units which, upon alteration of shards and pumice to clays and zeolites, probably became relatively impermeable and conducted only small amounts of fluid flow. Therefore, many of our analyses may reflect the chemistry of zones of relatively small fluid flow. Our data do not rule out, or demonstrate the presence of, possible epithermal precious-metal mineralization between the widely spaced drill holes in Yucca Mountain.

MAJOR-ELEMENT CHEMISTRY OF THE MOUNT JACKSON DOME FIELD

In our 1990-1991 report (Weiss et al., 1991) we presented radiometric age data demonstrating that rhyolite domes of the Mount Jackson dome field were emplaced from about 6.8 Ma to 2.9 Ma. We have considered most rocks of the domes to be rhyolitic in composition, except for the intermediate composition, lower lava of Mount Jackson, based on field examination and reconnaissance-level hand-specimen and thin-section petrography (McKee et al., 1989; Noble et al., 1991a). During the period of this report we have obtained major- and minor-element chemical data from splits of the rocks used for the radiometric age determinations (Table 3 and Figure 8). These data show that chemically, the capping lavas are indeed high- to medium-silica subalkaline rhyolites, confirming our previous classification of these rocks. Two samples of the basal, less silicic lavas exposed on the west and southeast sides of Mount Jackson (samples MJ-W and MJ-SE, Table 3) have chemical compositions of trachydacite (Le Bas et al., 1986) or rhyodacite. Many of the rhyolites are highly evolved as shown by Rb/Sr ratios of >15 and low barium contents.

The linear alignments of the domes (Figure 8) and similarities in chemistry, petrography, and general morphology suggest that the entire dome field was produced by eruptions from a linear, high-angle fault controlled array of vents that were probably fed by a single magmatic system. If this is the case, the geometry and remarkably long-lived nature of the system (minimum of about 4 Ma) may reflect the influence of deep-seated faults or zones of weakness during a period of tectonic stability within the Goldfield segment of the Walker Lane belt.

PROGRESS IN RADIOMETRIC DATING STUDIES

Timing of Au-Ag mineralization, northern Bare Mountain

Much of the presently known Au-Ag mineralization in northern and eastern Bare Mountain is spatially associated with the silicic porphyry dikes of Bare Mountain and resulted from hydrothermal activity that occured at about 12.9 - 12.5 Ma during the main magmatic stage of the SWNVF (Noble et al., 1989; 1991a). This interpretation is based on age determinations of hydrothermal minerals from the Goldspar and Telluride mine areas and from the fact that the *ca.* 13.9 Ma silicic dikes are in most places strongly altered, locally contain elevated gold concentrations (e.g., Sterling mine area, Jackson, 1988) and host gold mineralization at the Mother Lode mine (Noble et al., 1989; Castor and Weiss, 1992).

Altered porphyry dikes have not been identified within or near the presently subeconomic Secret Pass disseminated gold deposit, but stratigraphic and structural relations permit a similar timing for gold mineralization there. Mineralization at Secret Pass is hosted by the Bullfrog Member of the Crater Flat Tuff and is truncated by the underlying Fluorspar Canyon - Tate's Wash fault (Greybeck and Wallace, 1991). Alteration affects rocks of the Bullfrog Member and the porous lower portion of the overlying Topopah Spring Member of the Paintbrush Tuff (Castor and Weiss, 1992), which has a radiometric age of about 12.8 Ma (cf. Marvin et al., 1970; Sawyer et al., 1990). Movement on the Fluorspar Canyon - Tate's Wash fault accomodated tilting of the hanging-wall section at Secret Pass after deposition of the Tiva Canyon Member of the Paintbrush Tuff, but prior to the deposition of nearby, flat-lying rocks of the 11.6 Ma Rainier Member of the Timber Mountain Tuff (Monsen et al., 1990). A strong argument can be made, therefore, that hydrothermal activity and mineralization at Secret Pass took place between about 12.9 Ma and 11.6 Ma.

The feasibilty of direct dating of the timing of hydrothermal activity at the Mother Lode mine remains under investigation. At the Mother Lode mine ore-grade disseminated Au-Ag mineralization is present within argillically altered porphyry dike rocks and adjacent tuffaceous sedimentary rocks (Noble et al. 1989; Castor and Weiss, 1992). Mineralized and altered dike and sedimentary rock samples containing abundant illitic mica (modestly-ordered interstratified illite-montmorillonite) have been sent to Los Alamos National Laboratory for evaluation for possible K-Ar dating.

PRIMARY LOW-LEVEL GOLD CONTENTS OF SILICIC VOLCANIC ROCKS: APPLICATIONS TO STUDIES OF YUCCA MOUNTAIN

A short journal paper summarizing the results of K.A. Connors work on the initial gold contents of silicic volcanic rocks was prepared and submitted to *Geology*. The principal points of the paper, entitled *The initial gold contents of silicic volcanic rocks* (Appendix A), are contained in the abstract as follows:

> Fresh silicic volcanic rocks have markedly lower initial gold contents than would be inferred from much of the geochemical literature. The great majority of 129 carefully selected glassy silicic volcanic rocks analyzed contain less than 1.0 ppb, and many contain only $\leq$ 0.1 to 0.3 ppb Au. Nonperalkaline rhyolites contain <0.1 to 0.7 ppb, mean 0.22 ppb Au; of these, highly evolved, high-silica subalkaline and peraluminous rhyolites have the lowest Au contents. Peralkaline and iron-rich subalkaline rhyolites have higher gold contents of 0.2 to 4.5 ppb, mean about 1 ppb. The mean of 23 relatively silicic intermediate rocks is 0.54 ppb Au, with tholeiitic andesites (icelandites) generally higher in gold than calc-alkalic types. Fundamental controls on the initial gold content of silicic volcanic rocks appear to be melt structure and petrologic affinity; regional setting is less important. High-silica, nonperalkaline rhyolite melts apparently do not readily accomodate gold, whereas crystal fractionation appears to increase the gold concentration in less-polymerized peral-

kaline melts. Bulk composition and melt structure, and the amount and timing of separation of vapor, mineral, and sulfide or metal melt phases, may largely determine the gold content of silicic magmas on eruption. Silicic and intermediate volcanic rocks, particularly high-silica nonperalkaline rhyolites, appear to be less favorable sources of gold for hydrothermal mineral deposits than crystallizing magmatic bodies or other, more gold-rich rock types. Although iron-rich rhyolites may have contributed to development of certain deposits, factors other than associated volcanic rock type appear to be more important in determining gold availability to hydrothermal systems.

A longer paper is presently being prepared for *Economic Geology* to more fully discuss the data, inferences and interpretive conclusions outlined above and in the text of Connors et al. (*in review*; Appendix A). Clearly, rocks and alluvium in silicic volcanic terranes such as Yucca Mountain should be very sensitive to the addition of small amounts of gold by groundwater and hydrothermal solutions owing to the very low initial gold contents of most rhyolites. Existing and future gold analytical data from Yucca Mountain must be evaluated and interpreted in the context of Connors' results, rather than average crustal abundance values or average volcanic rock values found in much of the geochemical literature. Low-level anomalies have the potential to delineate structural features and other paleohydrologic flow paths along which post-depositional addition of gold may have taken place.

UPDATE ON THE MIOCENE VOLCANIC STRATIGRAPHY AND STRUCTURAL GEOLOGY OF THE GOLD MOUNTAIN - SLATE RIDGE AREA

Most of our knowledge of the volcano-tectonic evolution of the Gold Mountain-Slate Ridge area (GMSR) has been outlined in abstracts and papers included with previous yearly reports (e.g., McKee et al., 1990; Noble et al., 1991a; 1991b; Worthington et al., 1991). During the past year Ted Worthington has nearly completed his masters thesis on the GMSR. In addition, we have obtained a new K-Ar age determination of 16.8 ± 0.5 Ma on biotite from the Tuff of Mount Dunfee, the stratigraphically oldest ash-flow unit recognized in the Gold Mountain-Slate Ridge area. This age determination confirms a previous age determination of 16.7 ± 0.4 Ma on biotite from the same unit in another locality (E.H. McKee, D.C. Noble and J. E. Worthington, unpublished data 1991-1992). Based on our past work in the GMSR and in collaboration with E. H. McKee and M. C. Reheis of the U.S. Geological Survey, we are currently preparing to lead a field trip entitled *Neogene Tectonism from the Southwestern Nevada Volcanic Field to the White Mountains, California* for the 1993 joint Cordilleran-Rocky Mountain Section meeting of the Geological Society of America.

UPDATE ON MINING AND MINERAL EXPLORATION

Even though precious metals prices have been relatively weak during the past year, strong exploration and mining efforts continued in the Beatty area of the SWNVF. Heap leaching continued at the presently closed Mother Lode gold mine. Considerable refractory gold mineralization remains at the Mother Lode mine, but is subeconomic at current gold prices. Exploratory drilling by U. S. Precious Metals continued near the mine and north of

Tarantula Canyon in eastern Bare Mountain. Further south in Bare Mountain, gold production continues at the Sterling mine, which is situated adjacent to Crater Flat. A new area of subsurface gold mineralization has reportedly been identified between the Sterling and Goldspar mines (J. Marr, pers. communication, 1992).

Gold production at the Lac Gold Bullfrog mine is projected to substantially exceed the 240,000 oz planned for 1992 due to better than expected grades in the open-pit mining area. Underground production is running just under the planned rate of 1000 tons per day from the decline at the north end of the open-pit. The decline encountered hot water (approx. 42° C), which is slowing underground production and requires pumping at a rate of about 15 gallons per minute. Lac Minerals Ltd is presently conducting exploratory drilling a short distance north of the mine.

Exploration for precious metals continued in the northern Bullfrog Hills. Pathfinder Resources began an exploratory drilling program in the Pioneer mine area and has completed a detailed geologic map of the northern Bullfrog Hills. This map is based primarily on lithology and does not incorporate the regional stratigraphic units recognized by Task 3 (Weiss and Connors, unpublished mapping, 1989-1990) or previous U.S. Geological Survey investigators such as Ransome et al. (1910), Cornwall and Kleinhampl (1964), and Maldonado and Hausback (1990).

HG Mining Inc. of Beatty, NV. continues production of cut stone products from ash-flow tuffs quarried in the Transvaal Hills and upper Oasis Valley area. Although conventional models predict little or no hydrocarbon resource potential, rigging began in June, 1992, for an attempt to re-enter and deepen the Coffer #1 wildcat oil well, which was originally drilled in Oasis Valley to a depth of 3880 feet in 1991.

REVIEWS, PRESENTATIONS AND PUBLICATIONS

Presentations

Noble presented to the Nevada Commission for Nuclear Projects an overview of Task 3's efforts and hypotheses to address the issue of undiscovered potential mineral resources in and near Yucca Mountain.

Publications

The following abstracts and articles resulting from Task 3 studies were produced and(or) published during the period covered by this report, and are contained in the appendices as follows:

Appendix A:

Connors, K., A., Noble, D. C., Bussey, S., D., and Weiss, S. I., (*in review*), The initial gold contents of silicic volcanic rocks, manuscript submitted to *Geology*, 1992, 14 p.

Appendix B:

Castor, S. B., and Weiss, S. I., 1992, Contrasting styles of epithermal precious-metal mineralization in the southwestern Nevada volcanic field, USA: *Ore Geology Reviews*, v. 7, p. 193-223.

SUMMARY OF CONCLUSIONS AND RECOMMENDATIONS

The veins and disseminated pyrite present in altered lithic fragments suggest that hydrothermally altered rocks may have been present in the vent area(s) of the Lithic Ridge Tuff and the Tram Member of the Crater Flat Tuff. The locations of these vents are not known, but geophysical and other information has been used to propose that they may in part lie beneath northwestern Yucca Mountain (Carr et al., 1986). If this is correct, the lithic fragments may provide direct evidence for one or more previously unrecognized periods of hydrothermal activity in or very near Yucca Mountain. A more basic problem is to confidently determine if there has been, as we strongly suspect, a later *in-situ* addition of sulphur to rocks in Yucca Mountain. Sulphidic solutions are common in hydrothermal systems in volcanic rocks and have the capacity to transport significant quantities of precious metals. We believe that the groundmass pyrite in the tuffs, with its similarity in texture and morphology to that present in the pre-Lithic Ridge silicic lavas and other hydrothermally altered ash-flow tuff elsewhere, provides evidence for such a post-depositional addition of sulphur. Clearly, this process has affected the pre-Lithic Ridge silicic lavas in drill hole USW G2, the lowermost part of the pre-Lithic Ridge tuffs in drill hole UE25p-1 and the pre-Cenozoic carbonate rocks in UE25p-1. In the Lithic Ridge Tuff and portions of the Crater Flat Tuff this sulphidation may have been from the passage of fluids, perhaps at low water to rock ratios, that had little effect on the tuffs other than the destruction of glass and the weak development of laterally and vertically discontinuous propylitic assemblages. The uneven and discontinuous distribution of pyrite and veins and cavity in-fillings of quartz, calcite, fluorite and barite in Yucca Mountain would be consistent with irregular, highly channelized paleohydrology, a phenomena that is not uncommon in fossil hydrothermal systems known elsewhere. Much basic petrographic work is planned to better determine the identity and distribution of alteration minerals, and to ascertain that previous investigators did not confuse altered lithic material with primary, magmatic components of the ash-flow units. Also, as mentioned previously, further comparisons will be made between pyrite textures of Yucca Mountain tuffs and those of pyrite in hydrothermally altered, porous ash-flow tuffs elsewhere.

With regard to the chemical data in Table 2, it should be emphasized that the analysed samples were selected to test, on a reconnaissance basis, the trace-element and precious-metal contents of various types of alteration and paleo-fluid channelways, and represent only a few, widely spaced drill hole intervals. The current data set provides only a minimal glimpse of the nature of fluids that may have included cold as well as heated meteoric water. Although no significant Au or Ag concentrations were found, there can be little doubt that various combinations of trace-elements and metals, including Hg, As, Sb, Mo, Se, Te, Bi, Pb, Zn and Tl, are locally elevated relative to fresh rock concentrations. The remarkable Mo concentrations in rocks of the UE25 C holes (Table 2) are associated with breccia veins, fluorite, quartz and Fe-Mn oxide veinlets, and less enriched, but still highly elevated Sb, As and Bi. These accumulations reflect the movement of metal-bearing fluids and are sufficiently dispersed in the rock mass of Yucca Mountain to be detected by the few samples analyzed. In particular, mineralogic and chemical data from the pre-Cenozoic rocks of

UE25p-1 suggest the possible presence of deep base-metal and(or) precious-metal mineralization in the vicinity of the drill hole. Additional samples from UE25p-1, particularly those intervals adjacent to sample #16963, should be obtained for chemical analyses to better bracket the vertical extent of the highly anomalous metal and trace-element concentrations. Further geochemical work is clearly warranted and we intend to obtain additional analyses.

Another area of research planned for the coming year will be to investigate the precious-metals and trace-element contents of hydrothermally altered, but unmineralized, rocks from several silicic tuff-hosted epithermal mineral deposts. This would involve the same types of low-level, multi-element analyses reported in Table 2. If possible, we will obtain specimens from a number of deposits, including Round Mountain, Secret Pass, Rawhide, Paradise Peak and Wonder, Nevada, and perhaps Castle Mountain, California.

REFERENCES CITED AND OTHER PERTINENT LITERATURE

The following references were selected because of their direct bearing on the Cenozoic volcanic stratigraphy and caldera geology, hydrothermal activity, and mineral potential of Yucca Mountain and the surrounding region of the southwestern Nevada volcanic field. Additional pertinent references on mineral potential, and particularly unpublished data in files of the Nevada Bureau of Mines and Geology, are given by Bell and Larson (1982b). A compendium of information from the U.S. Geological Survey's Mineral Resource Data System is given by Bergquist and McKee (1991).

Ahern, R., and Corn, R.M., 1981, Mineralization related to the volcanic center at Beatty, Nevada: Arizona Geological Society Digest, v. XIV, p. 283-286.

Albers, J. P., and Stewart, J. H., 1972, Geology and mineral deposits of Esmeralda County, Nevada, Nevada Bur. Mines and Geol. Bull. 78, 80 p.

Ander, H.D., and Byers, F.M., 1984, Nevada Test Site field trip guidebook; Reno, Nevada, University of Nevada-Reno, Department of Geological Sciences, v. 2, 1984, 35 p.

Anderson, R.E., Ekren, E.B., and Healey, D.L., 1965, Possible buried mineralized areas in Nye and Esmeraldo Counties, Nevada: U.S. Geological Survey Professional Paper 525-D, p. D144-D150.

Anonymous, 1928, One strike of real importance made at Nevada's new camp: Engineering and Mining Journal, v. 125, no. 1, p. 457.

Aronson, J.L., and Bish, D.L., 1987, Distribution, K/Ar dates, and origin of illite/smectite in tuffs from cores USW G-1 and G-2, Yucca Mountain, Nevada, a potential high-level radioactive waste repository: Abstract of presentation at Clay Minerals Society Meeting, Socorro, NM, 1987.

Armstrong, R. L., Ekren, E. B., McKee, E. H., and Noble, D. C., 1969, Space-time relations of Cenozoic silicic volcanism in the Great Basin of the western United States: Am. Jour. Sci., v. 267, p. 478-490.

Bailey, E.H., and Phoenix, D.A., 1944, Quicksilver deposits in Nevada: Nevada Bureau of Mines and Geology Bulletin 41.

Barton, C.C., Tectonic significance of fractures in welded tuff, Yucca Mountain, Southwest Nevada: Geological Society of America, Abstracts with Programs, v. 16, 1984, p. 437.

Bath, G.D., and Jahren, C.E., 1984, Interpretations of magnetic anomalies at repository site proposed for Yucca Mountain area, Nevada Test Site: U.S. Geological Survey Open-File Report 84-120, 40 p.

Bath, G.D., and Jahren, C.E., 1985, Investigation of an aeromagnetic anomaly on west side of Yucca Mountain, Nye County, Nevada: U.S. Geological Survey Open-File Report 85-459, 24 p.

Beck, B. A., 1984, Geologic and gravity studies of the structures of the northern Bullfrog Hills, Nye County, Nevada: California State University at Long Beach, unpublished MSc Thesis, 86 p.

Bedinger, M.S., Sargent, K.A., and Langer, W.H., 1984, Studies of geology and hydrology in the Basin and Range Province, Southwestern United States, for isolation of high-level radioactive waste; characterization of the Death Valley region, Nevada and California: U.S. Geological Survey Open-File Report 84-743, 173 p.

Bedinger, M.S., Sargent, K.A., and Langer, W.H., 1984, Studies of geology and hydrology in the Basin and Range Province, Southwestern United States, for isolation of high- level radioactive waste; evaluation of the regions: U.S. Geological Survey Open-File Report 84-745, 195 p.

Bell, E.J., and Larson, L.T., 1982a, Overview of energy and mineral resources of the Nevada Nuclear Waste Storage Investigations, Nevada Test Site, Nye County, Nevada: U.S. Department of Energy Report NVO-250 (DE83001418), 64 p. plus maps.

Bell, E.J., and Larson, L.T., 1982b, Annotated bibliography, Overview of energy and mineral resources for the Nevada Nuclear Waste Storage Investigations, Nevada Test Site, Nye County, Nevada: U.S. Department of Energy Report NVO-251 (DE83001263), 30 p.

Benson, L.V. and McKinley, P.W., 1985, Chemical composition of the ground water in the Yucca Mountain area, Nevada: U.S. Geological Survey Open-File Report 85-484, 10 p.

Bentley, C.B., 1984, Geohydrologic data for test well USW G-4, Yucca Mountain area, Nye County, Nevada: U.S. Geological Survey Open-File Report 84-63, 67 p.

Bergquist, J. R., and McKee, E. H., 1991, Mines, prospects and mineral occurrences in Esmeralda and Nye Counties, Nevada, nera Yucca Mountain: U.S. Geological Survey Administrative Report to the Department of Energy, Yucca Mountain Project, 385 p.

Bish, D.L., 1987, Evaluation of past and future alteration in tuff at Yucca Mountain, Nevada based on clay mineralogy of drill cores USW G-1, G-2, and G-3: Los Alamos, New Mexico, Los Alamos National Laboratory Report LA-10667-MS, 42 p.

Bonham, H. F., Jr., and Garside, L. J., 1979, Geology of the Tonopah, Lone Mountain, Klondike and northern Mud Lake Quadrangles, Nevada: Nevada Bureau of Mines and Geology Bulletin 92, 142 p., 1:48,000.

Booth, M., 1988, Dallhold finalizes plans for huge Nevada mine: The Denver Business Journal, April 4, 1988, p. 10.

Boyle, R. W., 1979, The geochemistry of gold and its deposits: Geological Survey of Canada Bulletin 280, 584 p.

Boyle, R.W., and Jonasson, I.R., 1973, The geochemistry of arsenic and its use as an indicator element in geochemical prospecting: Journal of Geochemical Exploration, v. 2, p. 251-296.

Broxton, D. E., Vaniman, D., Caporuscio, F., Arney, B., and Heiken, G., 1982, Detailed petrographic descriptions and microprobe data fro drill holes USW-G2 and UE25b-1H, Yucca Mountain, Nevada: Los Alamos, New Mexico, Los Alamos National Laboratory Report LA-10802-MS, 168 p.

Broxton, D.E., Byers, F.M., Warren, R.G. and Scott, R.B., 1985, Trends in phenocryst chemistry in the Timber Mountain-Oasis Valley volcanic field, SW Nevada; evidence for isotopic injection of primitive magma into an evolving magma system: Geological Society of America, Abstracts with Programs, v. 17, p. 345.

Broxton, D. E., Warren, R. G., and Byers, F. M., Jr., 1989, Chemical and mineralogic trends within the Timber Mountain-Oasis Valley caldera complex, Nevada: Evidence for multiple cycles of chemical evolution in a long-lived silicic magma system: Jour. Geophys. Res., v. 94, p. 5961-5985.

Broxton, D.E., Warren, R.G., Byers, F.M., Jr., Scott, R.B., and Farner, G.L., 1986, Petrochemical trends in the Timber Mountain-Oasis Valley caldera complex, SW Nevada: EOS (American Geophysical Union Transactions), v. 67, p. 1260.

Broxton, D.E., Warren, R.G., Hagan, R.C. and Luedemann, G.,1986, Chemistry of diagenetically altered tuffs at a potential nuclear waste repository, Yucca Mountain, Nye County, Nevada: Los Alamos, New Mexico, Los Alamos National Laboratory Report LA-10802-MS, 160 p.

Byers, F. M., Jr., Carr, W. J., and Orkild, P. P., 1989, Volcanic centers of southwestern Nevada: evolution of understanding, 1960-1988: Jour. Geophys. Res., v.94, p. 5908-5924.

Byers, F.M., Jr., Carr, W.J., and Orkild, P.P., 1986, Calderas of southwestern Nevada-Evolution of understanding, 1960-1986: EOS (American Geophysical Union Transactions), v. 67, p. 1260.

Byers, F.M., Jr., Carr, W.J., Orkild, P.P., Quinlivan, W.D. and Sargent, K.A., 1976a, Volcanic Suites and related cauldrons of Timber Mountain-Oasis Valley caldera complex: U.S. Geological Survey Professional Paper 919, 70 p.

Byers, F.M., Jr., Carr, W.J., Christiansen, R.L., Lipman, P.W., Orkild, P.P., and Quinlivan, W.D., 1976b, Geologic map of the Timber Mountain Caldera area, Nye County, Nevada: U.S. Geological Survey Miscellaneous Investigations Series, I-891, sections, 1:48,000 scale.

Byers, F.M., Jr., Orkild, P.P, Carr, W. J., and Quinlivan, W.D., 1968, Timber Mountain Tuff, southern Nevada, and its relation to cauldron subsidence: Geological Society of America Memoir 110, p. 87-97.

Caporuscio, F., Vaniman, D.T., Bish, D.L., Broxton, D.E., Arney, D., Heiken, G., Byers, F.M., and Gooley, R., 1982, Petrologic studies of drill cores USW-G2 and UE25b-1H,Yucca Mountain, Nevada: Los Alamos, New Mexico, Los Alamos National Laboratory Report LA-9255-MS, 114 p.

Carr, M.D., and Monsen, S.E., 1988, A field trip guide to the geology of Bare Mountain: Geological Society of America Field Trip Guidebook, Cordilleran Section Meeting, Las Vegas, Nevada, p. 50-57.

Carr, M.D., Waddell, S.J., Vick, G.S., Stock, J.M., and Monsen, S.A., Harris, A.G., Cork, B.W., and Byers, F.M., Jr., 1986, Geology of drill hole UE25p-1: A test hole into pre-Tertiary rocks near Yucca Mountain, southern Nevada: U.S. Geological Survey Open File Report 86-175.

Carr, W.J., 1964, Structure of part of the Timber Mountain dome and caldera, Nye County, Nevada: U.S. Geological Survey Professional Paper 501-B, p. B16-B20.

Carr, W.J., 1974, Summary of tectonic and structural evidence for stress orientation at the NTS: U.S. Geological Survey Open-File Report 74-176, 53 p.

Carr, W.J., 1982, Volcano-tectonic history of Crater Flat, southwestern Nevada, as suggested by new evidence from drill hole USW-VH-1 and vicinity: U.S. Geological Survey Open-File Report 82-457, 23 p.

Carr, W.J., 1984a, Regional structural setting of Yucca Mountain, southwestern Nevada, and late Cenozoic rates of tectonic activity in part of the southwestern Great Basin, Nevada and California: U.S. Geological Survey Open-File Report 84-0854, 114 p.

Carr, W.J., 1984b, Timing and style of tectonism and localization of volcanism in the Walker Lane belt of southwestern Nevada: Geological Society of America, Abstracts with Programs, v. 16, p. 464.

Carr, W.J., 1988a, Styles of extension in the Nevada Test Site region, southern Walker Lane Belt: an integration of volcano-tectonic and detachment fault models: Geological Society of America, Abstracts with Programs, v. 20, p. 148.

Carr, W. J., 1988b, Volcano-tectonic setting of Yucca Mountain and Crater Flat, *in* Carr, M. D., and Yount, J. C., eds., Geologic and hydrologic investigations of a potential nuclear waste disposal site at Yucca Mountain, southern Nevada: U.S. Geol. Survey Bull. 1790, p. 35-49.

Carr, W.J., and Quinlivan, W.D., 1966, Geologic map of the Timber Mountain quadrangle, Nye County, Nevada: U.S. Geological Survey Geologic Quadrangle Map GQ-503, 1:24,000 scale, sections.

Carr, W.J., and Quinlivan, W.D., 1968, Structure of Timber Mountain resurgent dome, Nevada Test Site: Geological Society of America Memoir 110, p. 99-108.

Carr, W.J. and Parrish, L.D., 1985, Geology of drill hole USW VH-2, and structure of Crater Flat, southwestern Nevada: U.S. Geological Survey Open-File Report 85-475, 41 p.

Carr, W.J., Byers, F.M., and Orkild, P.P., 1984, Stratigraphic and volcano-tectonic relations of Crater Flat Tuff and some older volcanic units, Nye County, Nevada: U.S. Geological Survey Open-File Report 84-114, 97 p.

Carr, W.J., Byers, F.M., and Orkild, P.P., 1986, Stratigraphic and volcano-tectonic relations of Crater Flat Tuff and some older volcanic units, Nye County, Nevada: U.S. Geological Survey Professional Paper 1323, 28p.

Castor, S. B., and Weiss, S. I., 1992, Contrasting styles of epithermal precious-metal mineralization in the southwestern Nevada volcanic field, USA: Ore Geology Reviews, v. 7, p. 193-223.

Castor, Feldman and Tingley, 1989, Mineral evaluation of the Yucca Mountain Addition, Nye County, Nevada: Nevada Bureau of Mines and Geology, Open-file Report 90-4, 80 pp.

Castor, Feldman and Tingley, 1990, Mineral potential report for the U.S. Department of Energy, Serial No. N-50250: Nevada Bureau of Mines and Geology, University of Nevada, Reno, 24 pp.

Castor, S. B., Tingley, J. V., and Bonham, H. F., Jr., 1991, Yucca Mountain Addition subsurface mineral resource analysis: unpub. proposal to Science Applications International Corp., 10 p.

Castor, S. B., Tingley, J. V., and Bonham, H. F., Jr., (*in review*), Pyritic ash-flow tuff in Yucca Mountain: manuscript submitted in 1992 to Geology.

Christiansen, R.L., and Lipman, P.W., 1965, Geologic map of the Topopah Spring NW quadrangle, Nye County, Nevada: U.S. Geological Survey Geologic Quadrangle Map GQ-444, 1:24,000 scale, sections.

Christiansen, R.L., Lipman, P.W., Carr, W.J., Byers, F.M., Jr., Orkild, P.P., and Sargent, K.A., 1977: Timber Mountain-Oasis Valley caldera complex of southern Nevada: Geological Society of America Bulletin, v. 88, p. 943-959.

Christiansen, R.L., Lipman, P.W., Orkild, P.P., and Byers, F.M., Jr., 1965, Structure of the Timber Mountain caldera, southern Nevada, and its relation to basin-range structure: U.S. Geological Survey Professional Paper 525-B, p. B43-B48.

Connors, K. A., Studies in silicic volcanic geology: Part I: Compositional controls on the initial gold contents of silicic volcanic rocks; Part II: Geology of the western margin of the Timber Mountain caldera complex and post-Timber Mountain volcanism in the Bullfrog Hills: unpublished PhD dissertation, University of Nevada, Reno, (*in preparation*).

Connors, K.A., Weiss, S.I., Noble, D.C., and Bussey, S.D., 1990, Primary gold contents of some silicic and intermediate tuffs and lavas: evaluation of possible igneous sources of gold: Geological Society of America Abst. with Programs, v. 22, p. A135.

Connors, K.A., Noble, D.C., Weiss, S.I., and Bussey, S.D., 1991a, Compositional controls on the gold contents of silicic volcanic rocks: 15th International Geochemical Exploration Symposium Program with Abstracts, p. 43.

Connors, K. A., McKee, E. H., Noble, D. C., and Weiss, S. I., 1991, Ash-flow volcanism of Ammonia Tanks age in the Oasis Valley area, SW Nevada: Bearing on the evolution of the Timber Mountain calderas and the timing of formation of the Timber Mountain II resurgent dome: EOS, Trans. Am. Geophys. Union., v. 72, p. 570.

Connors, K., A., Noble, D. C., Bussey, S., D., and Weiss, S. I., (*in review*), The initial gold contents of silicic volcanic rocks, unpublished manuscript submitted to Geology, 1992, 14 p.

Cornwall, H.R., 1962, Calderas and associated volcanic rocks near Beatty, Nye County, Nevada: Geological Society of America, Petrologic Studies, A.F. Buddington Volume, p. 357-371.

Cornwall, H.R., 1972, Geology and mineral deposits of southern Nye County, Nevada: Nevada Bureau of Mines and Geology Bulletin 77, p. 49.

Cornwall, H.R., and Kleinhampl, F.J., 1961, Geology of the Bare Mountain quadrangle, Nevada: U.S. Geological Survey Geologic Quadrangle Map GQ-157, 1:62,500 scale.

Cornwall, H.R., and Kleinhampl, F.J., 1964, Geology of the Bullfrog quadrangle and ore deposits related to the Bullfrog Hills caldera, Nye County, Nevada, and Inyo County, California: U.S. Geological Survey Professional Paper 454-J, 25 p.

Cornwall, H.R., and Norberg, J.R., 1978, Mineral Resources of the Nellis Air Force Base and the Nellis Bombing and Gunnery Range, Clark, Lincoln, and Nye Counties, Nevada: U.S. Bureau of Mines Unpublished Administrative Report, 118 p.

Craig, R.W. and Robinson, J.H., 1984, Geohydrology of rocks penetrated by test well UE-25p#1, Yucca Mountain area, Nye County, Nevada, U.S. Geological Survey Water-Resources Investigations 84-4248, 57 p.

Craig, R.W., Reed, R.L., and Spengler, R.W., 1983, Geohydrologic data for test well USW H-6, Yucca Mountain area, Nye County, Nevada: U.S. Geological Survey Open-File Report 83-856, 52 p.

Crowe, B.M., 1980, Disruptive event analysis: Volcanism and igneous intrusion: Batelle Pacific Northwest Laboratory Report PNL-2822, 28 p.

Crowe, B.M., and Carr, W.J., 1980, Preliminary assessment of the risk of volcanism at a proposed nuclear waste repository in the southern Great Basin: U.S. Geological Survey Open-File Report 80-357, 15 p.

Crowe, B.M., Johnson, M.E., and Beckman, R.J., 1982, Calculation of probability of volcanic disruption of a high-level radioactive waste repository within southern Nevada, USA: Radioactive Waste Management and the Nuclear Fuel Cycle, v. 3, p. 167-190.

Crowe, B.M., Vaniman, D.J., and Carr, W.J., 1983b, status of volcanic hazard studies for the Nevada nuclear waste storage investigations: Los Alamos, New Mexico, Los Alamos National Laboratory Report LA-9325-MS.

Deino, A.L., Hausback, B.P., Turrin, B.T., and McKee, E.H., 1989, New $^{40}Ar/^{39}Ar$ ages for the Spearhead and Civet Cat Canyon Members of the of Stonewall Flat Tuff, Nye County, Nevada: EOS, Trans. American Geopphysical Union, v. 70, p. 1409.

Drexler, J. W., 1982, Mineralogy and geochemistry of Miocene volcanic rocks related to the Julcani Ag-Au-Cu-Bi deposit, Peru: Physiochemical conditions of a productive magma body: unpublished PhD dissertation, Houghton, Michigan Technical University, 250 p.

Eckel, E.B., ed., 1968, Nevada Test Site: Geological Society of America Memoir 110, 290 p.

Ekren, E.B., and Sargent, K.A., 1965, Geologic map of Skull Mountain quadrangle at the Nevada Test Site, Nye County, Nevada: U.S. Geological Survey Geologic Quadrangle Map GQ-387.

Ekren, E.B., Anderson, R.E., Rodgers, C.L., and Noble, D.C., 1971, Geology of northern Nellis Air Force Base Bombing and Gunnery Range, Nye County, Nevada: U.S. Geological Survey Professional Paper 651, 91 p.

Feitler, S., 1940, Welded tuff resembling vitrophyre and pitchstone at Bare Mountain, Nevada: Geological Society of America Bulletin, v. 51, p. 1957.

Flood, T.P., and Schuraytz, B.C., 1986, Evolution of a magmatic system. Part II: Geochemistry and mineralogy of glassy pumices from the Pah Canyon, Yucca Mountain, and Tiva Canyon Members of the Paintbrush Tuff, southern Nevada: EOS Trans. American Geophysical Union, v. 67, p. 1261.

Foley, D., 1978, The geology of the Stonewall Mountain volcanic center, Nye County, Nevada: Ohio State University, Columbus Ohio, unpublished PhD Dissertation, 139 p.

Fouty, S.C., 1984, Index to published geologic maps in the region around the potential Yucca Mountain Nuclear Waste Repository site, southern Nye County, Nevada: U.S. Geological Survey Open-File Report 84-524, 31 p.

Frischknecht, F.C. and Raab, P.V., 1984, Time-domain electromagnetic soundings at the Nevada Test Site, Nevada, Geophysics, v. 49, p. 981-992.

Frizzell, Virgil, and Shulters, Jacqueline, 1986, Geologic map of the Nevada Test Site: EOS Trans. American Geophysical Union, v. 67, p. 1260.

Frizzell, Virgil, and Shulters, Jacqueline, 1990, Geologic map of the Nevada Test Site: U.S. Geological Survey Misc. Invest. Map I-2046, 1:100,000.

Gans, P. B., Mahood, G. A., and Schermer, E., 1989, Synextensional magmatism in the Basin and Range province; A case study from the eastern Great Basin: Geological Society of America Spec. Paper 233, 53 p.

Garside L.J. and Schilling, J.H., 1979, Thermal waters of Nevada: Nevada Bureau of Mines and Geology, Bulletin 91, 163 p.

Geehan, R.W., 1946, Exploration of the Crowell fluorspar mine, Nye County, Nevada: U.S. Bureau of Mines Report of Investigations 3954, 9 p.

Greybeck, J. D., and Wallace, A. B., 1991, Gold mineralization at Fluorspar Canyon near Beatty, Nye County, Nevada: *in* Raines, G. L., Lisle,R. E., Shafer, R. W., and Wilkinson, W. W., eds., Geology and ore deposits of the Great Basin: Symposium Proceedings, Geol. Soc. of Nevada, sp. 935-946.

Hagstrum, J.T., Daniels, J.J., and Scott, J.H., 1980, Interpretation of geophysical well-log measurements in drill hole UE 25a-1, NTS, Radioactive Waste Program: U.S. Geological Survey Open-File Report 80-941, 32 p.

Hall, R.B., 1978, World nonbauxite aluminum resources--Alunite: U.S. Geological Survey Professional Paper 1076-A, 35 p.

Hamilton, W. B., 1988, Detachment faulting in the Death Valley region, California and Nevada, *in* Carr, M. D., and Yount, J. C., eds., Geologic and hydrologic investigations of a potential nuclear waste disposal site at Yucca Mountain, southern Nevada: U.S. Geol. Survey Bull. 1790, p. 51-86.

Hausback, B. P., and Frizzell, V. A. Jr., 1987, Late Miocene syntectonic volcanism of the Stonewall Flat Tuff, Nye County, Nevada [abs.]: Geological Society of America Abst. with Programs, v. 19, p. 696.

Hausback, B.P., Deino, A.L., Turrin, B.T., McKee, E.H., Frizzell, V.A., Noble, D.C., and Weiss, S.I., 1990, New $^{40}Ar/^{39}Ar$ ages for the Spearhead and Civet Cat Canyon Members of the Stonewall Flat Tuff, Nye County, Nevada: Evidence for systematic errors in standard K-Ar age determinations on sanidine: Isochron/West, No. 56, p. 3-7.

Harris, R.N., and Oliver, H.W., 1986, Structural implications of an isostatic residual gravity map of the Nevada Test Site, Nevada: EOS (American Geophysical Union Transactions), v. 67, p. 1262.

Heald, P., Foley, N.K., and Hayba, D.O., 1987, Comparative anatomy of volcanic-hosted epithermal deposits: acid-sulfate and adularia-sericite types: Economic Geology, v. 82, no. 1, p. 1-26.

Heikes, V.C., 1931, Gold, silver, copper, lead and zinc in Nevada--Mine report, in Mineral Resources of the U.S., 1928: U.S. Department of commerce, Bureau of Mines, pt. 1, p. 441-478.

Hildreth, E. W., 1977, The magma chamber of the Bishop Tuff: Gradients in temperature, pressure and composition: unpublished PhD dissertation, Univ. California-Berkely, 328 p.

Hill, J.M., 1912, The mining districts of the western U.S.: U.S. Geological Survey Bulletin 507, 309 p.

Holmes, G.H., Jr., 1965, Mercury in Nevada, in Mercury potential of the United States: U.S. Bureau of Mines I.C., 8252, p. 215-300.

Hoover, D.L., Eckel, E.B., and Ohl, J.P., 1978, Potential sites for a spent unreprocessed fuel facility (SUREF), southwest part of the NTS: U.S. Geological Survey Open-File Report 78-269, 18 p.

Hoover, D. B., Chornack, M. P., Nervick, K. H., and Broker, M. M., 1982, Electrical studies at the proposed Wahmonie and Calico Hills Nuclear Waste Sites, Nye County, Nevada: U.S. Geol. Survey Open-File Rept. 82-466, 45 p.

Hudson, M. R., 1992, Paleomagnetic data bearing on the origin of arcuate structures in the Frenchman Peak - Massachusetts Mountain area of southern Nevada: Bull. Geol. Soc. Am., v. 104, p. 581-594.

Jackson, M. J., 1988, The Timber Mountain magmato-thermal event: an intense widespread culmination of magmatic and hydrothermal activity at the southwestern Nevada volcanic field: University of Nevada, Reno - Mackay School of Mines, Reno, Nevada, unpublished MSc Thesis.

Jackson, M.R., Noble, D.C., Weiss, S.I., Larson, L.T., and McKee, E.H., 1988, Timber Mountain magmato-thermal event: an intense widespread culmination of magmatic and hydrothermal activity at the SW Nevada volcanic field, Geol. Soc. Am. Abstr. Programs, v. 20, p. 171.

Jorgensen, D. K., Rankin, J. W., and Wilkins, J., Jr., 1989, The geology, alteration and mineralogy of the Bullfrog gold deposit, Nye County, Nevada: Soc. Mining Eng. Preprint 89-135, 13 p.

Kane, M.F., and Bracken, R.E., 1983, Aeromagnetic map of Yucca Mountain and surrounding regions, southwest Nevada: U.S. Geological Survey Open-File Report 83-616, 19 p.

Kane, M.F., Webring, M.W., and Bhattacharyya, B.K., 1981, A preliminary analysis of gravity and aeromagnetic surveys of the Timber Mountain areas, southern Nevada: U.S. Geological Survey Open-File Report 81-189, 40 p.

Keith, J. D., Dallmeyer, R. D., Kim, Choon-Sik, and Kowallis, B. J., 1991, The volcanic history and magmatic sulfide mineralogy of latites of the central East Tintic Mountains, Utah: *in* Raines, G. L., Lisle,R. E., Shafer, R. W., and Wilkinson, W. W., eds., Geology and ore deposits of the Great Basin: Symposium Proceedings, Geol. Soc. of Nevada, p. 461-483.

Kistler, R.W., 1968, Potassium-argon ages of volcanic rocks on Nye and Esmeralda Counties, Nevada: Geological Society of America Memoir 110, P. 251-263.

Knopf, A., 1915, Some cinnabar deposits in western Nevada: U.S. Geological Survey Bulletin 620-D, p. 59-68.

Kral, V.E., 1951, Mineral resources of Nye County, Nevada: University of Nevada Bulletin, v. 45, no. 3, Geological and Mining Series 50, 223 p..

Lahoud, R.G., Lobmeyer, D.H. and Whitfield, M.S., 1984, Geohydrology of volcanic tuff penetrated by test well UE-25b#1, Yucca Mountain, Nye County, Nevada: U.S. Geological Survey Water-Resources Investigations 84-4253, 49 p.

Larson, L. T., Noble, D. C., and Weiss, S. I., 1988, Task 3 report for January, 1987 - June, 1988: Volcanic geology and evaluation of potential mineral and hydrocarbon resources of the Yucca Mountain area: unpublished report to the Nevada Nuclear Waste Project Office, Carson City, Nevada.

Le Bas, M. J., Le Maitre, R. W., Streckheisen, A., and Zenettin, B., 1986, A chemical classification of volcanic rocks based on the total alkali-silica diagram: Journal of Petrology, v. 27, p. 745-750.

Lincoln, F.C., 1923, Mining districts and mineral resources of Nevada: Reno, Nevada, Nevada Newsletter Publishing Co., Reno, 295 p.

Lipman, P.W., Christiansen, R.L., and O'Connor, J.T., 1966, A compositionally zoned ash-flow sheet in southern Nevada: U.S. Geological Survey Professional Paper 524-F, p. F1-F47.

Lipman, P.W., and McKay, E.J., 1965, Geologic map of the Topopah Spring SW quadrangle, Nevada: U.S. Geological Survey Geologic Quadrangle Map GQ-439, 1:24,000 scale.

Lipman, P.W., Quinlivan, W.D., Carr, W.J., and Anderson, R.E., 1966, Geologic map of the Thirsty Canyon SE quadrangle, Nye County, Nevada: U.S. Geological Survey Geologic Quadrangle Map GQ-489, 1:24,000 scale.

Lobmeyer, D.H., Whitfield, M.S., Lahoud, R.G., and Bruckheimer, L., 1983, Geohydrologic data for test well UE-25bH, Nevada Test Site, Nye County, Nevada: U.S. Geological Survey Open-File Report 83-855, 54 p.

Luedke, R.G., and Smith, R.L., 1981, Map showing distribution, composition, and age of late Cenozoic volcanic centers in California and Nevada: U.S. Geological Survey Miscellaneous Investigation Series, I-1091-C, 2 sheets.

Maldonado, F., 1985, Late Tertiary detachment faults in the Bullfrog Hills, southwestern Nevada: Geol. Soc. Am. Abstr. Programs, 17, p. 651.

Maldonado, F., 1988, Geometry of normal faults in the upper plate of a detachment fault zone, Bullfrog Hills, southern Nevada: Geological Society of America, Abstracts with Programs, v. 20, P. 178.

Maldonado, F, 1990, Structural geology of the upper plate of the Bullfrog Hills detachment fault system, southern Nevada: Geological Society of America Bulletin, v. 102, p. 992-1006.

Maldonado, F, and Hausback, B.P., 1990, Geologic map of the northeastern quarter of the Bullfrog 15-minute quadrangle, Nye County, Nevada: U.S. Geological Survey Misc. Investigations Series Map I-2049, 1:24,000.

Maldonado, F, and Koether, S.L., 1983, Stratigraphy, structure, and some petrographic features of Tertiary volcanic rocks at the USW G-2 drill hole, Yucca Mountain, Nye County, Nevada: U.S. Geological Survey Open-File Report 83-732, 83 p.

Maldonado, F, Muller, D.C., and Morrison, J.N., 1979, Preliminary geologic and geophysical data of the UE25a-3 exploratory drill hole, Nevada Test Site, Nevada: U.S. Geological Survey Report, USGS-1543-6, 47 p.; available only from U.S. Department of Commerce, National Technical Information Service, Springfield, VA 22161.

Maldonado, Florian, Muller, D.C., and Morrison, J.N., 1979, Preliminary geologic and geophysical data of the UE25a-3 exploratory drill hole, Nevada Test Site, Nevada: U.S. Geological Survey Open-File Report 81-522.

Mapa, M.R., 1990 Geology and mineralization of the Mother Lode mine, Nye County, Nevada, *in* Hillmeyer, F., Wolverson, N., and Drobeck, P., 1990 spring fieldtrip guidebook, Volcanic-hosted gold deposits and structural setting of the Mohave region: Reno, Geol. Soc. Nevada, 4 p.

Marvin, R.F., Byers, F.M., Mehnert, H.H., Orkild, P.P, and Stern, T.W., 1970, Radiometric ages and stratigraphic sequence of volcanic and plutonic rocks, southern Nye and western Lincoln Counties, Nevada: Geological Society of America Bulletin, v. 81, p. 2657-2676.

Marvin, R. F., and Cole, J. C., 1978, Radiometric ages: Compilation A, U.S. Geological Survey: Isochron/West, no. 22, p. 3-14.

Marvin, R. F., Mehnert, H. H., and Naeser, C. W., 1989, U.S. Geologic Survey radiometric ages - compilation "C", part 3: California and Nevada: Isochron/West, no. 52, p. 3-11.

McKague, H.L. and Orkild, P.P., 1984, Geologic Framework of the Nevada Test Site: Geological Society of America, Abstracts with Programs, v. 16, p. 589.

McKay, E.J., 1963, Hydrothermal alteration in the Calico Hills, Jackass Flats quadrangle, Nevada Test Site: U.S. Geological Survey Technical Letter NTS-43, 6 p.

McKay, E.J., and Sargent, K.A., 1970, Geologic map of the Lathrop Wells quadrangle, Nye County, Nevada: U.S. Geological Survey Geologic Quadrangle Map GQ-883, 1:24,000 scale.

McKay, E.J., and Williams, W.P., 1964, Geology of Jackass Flats quadrangle, Nevada Test Site, Nevada: U.S. Geological Survey Geologic Quadrangle Map GQ-368, 1:24,000 scale.

McKee, E.H., 1983, Reset K-Ar ages: evidence for three metamorphic core complexes, western Nevada: Isocron/West, no.38, p 17-20.

McKee, E. H., Noble, D. C., and Weiss, S. I., 1989, Very young silicic volcanism in the southwestern Great Basin: The late Pliocene Mount Jackson dome field, SE Esmeralda County, Nevada: EOS, Trans. Am. Geophys. Union., v. 70, p. 1420.

McKee, E. H., Noble, D. C., and Weiss, S. I., 1990, Late Neogene volcanism and tectonism in the Goldfield segment of the Walker Lane belt: Geological Society of America Abstracts with Programs, v. 22, p. 66.

Miller, D.C. and Kibler, J.E., 1984, Preliminary analysis of geological logs from drill hole UE-25p#1, Yucca Mountain, Nye County, Nevada: U.S. Geological Survey Open-File Report 84-649, 17 p.

Mills, J.G., Jr., and Rose, T.P., 1986, Geochemistry of glassy pumices from the Timber Mountain Tuff, southwestern Nevada: EOS (American Geophysical Union Transactions), v. 67, p. 1262.

Monsen, S.A., Carr, M.D., Reheis, M.C., and Orkild, P.P., 1990, Geologic map of Bare Mountain, Nye County Nevada: U.S. Geological Survey Open-file Report 90-25, 1:24,000.

Morton, J. L., Silberman, M. L., Bonham, H. F., Garside, L. J., and Noble, D. C., 1977, K-Ar ages of volcanic rocks, plutonic rocks, and ore deposits in Nevada and eastern California - Determinations run under the USGS-NBMG cooperative program: Isochron/West, n. 20, p. 19-29.

Noble, D. C., and Christiansen, R. L., 1974, Black Mountain volcanic center, in Guidebook to the geology of four Tertiary volcanic centers in central Nevada: Nevada Bur. Mines Geol. Rept. 19, p. 22-26.

Noble, D. C., McKee, E. H., and Weiss, S. I., 1988, Nature and timing of pyroclastic and hydrothermal activity and mineralization at the Stonewall Mountain volcanic center, southwestern Nevada: Isochron/West, No. 51, p. 25-28.

Noble, D. C., Weiss, S. I., and Green, S. M., 1989, High-salinity fluid inclusions suggest that Miocene gold deposits of the Bare Mtn. district, NV, are related to a large buried rare-metal rich magmatic system: Geological Society of America Abs. with Programs, v. 21, p. 123.

Noble, D. C., Weiss, S. I., and McKee, E. H., 1990a, Style, timing, distribution, and direction of Neogene extension within and adjacent to the Goldfield section of the Walker Lane structural belt: EOS, Trans. American Geophysical Union, v. 71, p. 618-619.

Noble, D. C., Weiss, S. I., and McKee, E. H., 1990b, Magmatic and hydrothermal activity, caldera geology and regional extension in the western part of the southwestern Nevada volcanic field: Great Basin Symposium, Program with Abstracts, Geology and ore deposits of the Great Basin, Geol. Soc. of Nevada, Reno, p. 77.

Noble, D. C., Weiss, S. I., and McKee, E. H., 1991a, Magmatic and hydrothermal activity, caldera geology, and regional extension in the western part of the southwestern Nevada volcanic field: *in* Raines, G. L., Lisle,R. E., Shafer, R. W., and Wilkinson, W. W., eds., Geology and ore deposits of the Great Basin: Symposium Proceedings, Geol. Soc. of Nevada, p. 913-934.

Noble, D. C., Worthington, J. E., and McKee, E. H., 1991b, Geologic and tectonic setting and Miocene volcanic stratigraphy of the Gold Mountain-Slate Ridge area, southwestern Nevada: Geol. Soc. America Abstr. with Prog., v. 23, p. A247.

Noble, D. C., Sargent, K. A., Ekren, E. B., Mehnert, H. H., and Byers, F. M., Jr., 1968, Silent Canyon volcanic center, Nye County, Nevada: Geological Society of America Spec. Paper 101, p. 412-413.

Noble, D.C., Vogel, T. A., Weiss, S.I., Erwin, J.W., McKee, E.H., and Younker, L.W., 1984, Stratigraphic relations and source areas of ash-flow sheets of the Black Mountain and Stonewall Mountain volcanic centers, Nevada: Journal of Geophysical Research, v. 89, p. 8593-8602.

Norberg, J.R., 1977, Mineral Resources in the vicinity of the Nellis Air Force Base and the Nellis Bombing and Gunnery Range, Clark, Lincoln, and Nye Counties, Nevada: U.S. Bureau of Mines Unpublished Report, 112 p.

Orkild, P.P., 1968, Geologic map of the Mine Mountain quadrangle, Nye County, Nevada: U.S. Geological Survey Geologic Quadrangle Map GQ-746, 1:24,000 scale.

Orkild, P.P., and O'Connor, J.T., 1970, Geologic map of the Topopah Springs quadrangle, Nye County, Nevada: U.S. Geological Geologic Quadrangle Map GQ-849, 1:24,000 scale.

Odt, D. A., 1983, Geology and geochemistry of the Sterling gold deposit, Nye County, Nevada: Unpub. M.S. thesis, Univ. Nevada-Reno, 91 p.

Papike, J. J., Keith, T. E. C., Spilde, M. N., Galbreath, K. C., Shearer, C. K., and Laul, J. C., 1991, Geochemistry and mineralogy of fumarolic deposits, Valley of Ten Thousand Smokes, Alaska: bulk chemical and mineralogical evolution of dacite-rich protolith: American Mineralogist, v. 76, p. 1662-1673.

Papke, K.G., 1979, Fluorspar in Nevada: Nevada Bureau of Mines and Geology, Bulletin 93, 77 p.

Ponce, D.A., 1981, Preliminary gravity investigations of the Wahmonie site, Nevada Test Site, Nye County, Nevada: U.S. Geological Survey Open-File Report 81-522, 64 p.

Ponce, D.A., 1984, Gravity and magnetic evidence for a granitic intrusion near Wahmonie site, Nevada Test Site, Nevada, Journal of Geophysical Research, v. 89, p. 9401-9413.

Ponce, D.A., Wu, S.S. and Speilman, J.B., 1985, Comparison of survey and photogrammetry methods to positive gravity data, Yucca Mountain, Nevada: U.S. Geological Survey Open-File Report 85-36, 11 p.

Poole, F.G., 1965, Geologic map of the Frenchman Flat quadrangle, Nye, Lincoln, and Clark Counties, Nevada: U.S. Geological Survey Geological Quadrangle Map GQ-456, 1:24,000 scale.

Poole, F.G., Carr, W.J., and Elston, D.P., 1965, Salyer and Wahmonie Formations of southeastern Nye County, Nevada: U.S. Geological Survey Bulletin 1224-A, p. A44-A51.

Poole, F.G., Elston, D.P., and Carr, W.J., 1965, Geologic map of the Cane Spring quadrangle, Nye County, Nevada: U.S. Geological Survey Geological Quadrangle Map GQ-455, 1:24,000 scale.

Powers, P.S. and Healey, D.L., 1985, Free-air gradient observations in Yucca Flat, Nye County, Nevada: U.S. Geological Survey Open-File Report 85-530, 18 p.

Quade, J., and Tingley, J.V., 1983, A mineral inventory of the Nevada Test Site and portions of the Nellis Bombing and Gunnery Range, southern Nye County, Nevada: DOE/NV/10295-1, U.S. Department of Energy, Las Vegas.

Quade, J., and Tingley, J.V., 1984, A mineral inventory of the Nevada Test Site, and portions of Nellis Bombing and Gunnery Range southern Nye County, Nevada: Nevada Bureau of Mines and Geology Open File Report 82-2, 40 p. plus sample descriptions and chemical analyses.

Quade, J., and Tingley, J.V., 1986a, Mineral inventory and geochemical survey Groom Mountain Range Lincoln County, Nevada: Nevada Bureau of Mines and Geology Open File Report 86-9, 66 p. plus sample descriptions and chemical analyses.

Quade, J., and Tingley, J.V., 1986b, Mineral inventory and geochemical survey appendices F., G., & H Groom Mountain Range, Lincoln County, Nevada: Nevada Bureau of Mines and Geology Open File Report 86-10.

Quinlivan, W.D., and Byers, F.M., Jr., 1977, Chemical data and variation diagrams of igneous rock from the Timber Mountain-Oasis Valley caldera complex, southern Nevada: U.S. Geological Survey Open-File Report 77-724, 9 p.

Ramelli, A. R., Bell, J. W., and dePolo, C. M., Late Quaternary faulting at Crater Flat and Yucca Mountain, southern Nevada: Nevada Bureau of Mines and Geology (in review).

Raney, R. G., and Wetzel, N., Natural resource assessment methodologies for the proposed high-level nuclear waste repository at Yucca Mountain, Nye County, Nevada: U.S. Bureau of Mines report NRC FIN D1018, prepared for the Office of Nuclear Safety and Safeguards, U.S. Nuclear Regulatory Commission, 353 p.

Ransome, F.L., 1907, Preliminary account of Goldfield, Bullfrog, and other mining districts in southern Nevada: U.S. Geological Survey Bulletin 303, 98 p.

Ransome, F.L., Emmons, W.H., and Garrey, G.H., 1910, Geology and ore deposits of the Bullfrog district, Nevada: U.S. Geological Survey Bulletin 407, 130 p.

Reno Gazette-Journal, June 19, 1988, Gold report is favorable: Business page, Gold, J., Business editor.

Robinson, G.D., 1985, Structure of pre-Cenozoic rocks in the vicinity of Yucca Mountain, Nye County, Nevada; a potential nuclear-waste disposal site: U.S. Geological Survey Bulletin 1647, 22 p.

Rowe, J. J., and Simon, F. O., 1968, The determination of gold in geologic materials by neutron-activation analysis using fire assay for the radiochemical separations: U. S. Geological Survey Circular 559, 4 p.

Rush, F.E., Thordason, William, and Bruckheimer, Laura, 1983, Geohydrologic and drill-hole data for test well USW-H1, adjacent to Nevada Test Site, Nye County, Nevada: U.S. Geological Survey Open-File Report 83-141, 38 p.

Sander, M. V., (1990), The Round Mountain gold-silver deposit, Nye County, Nevada: Geol. Soc. Nevada Symposium, Geology and Ore Deposits of the Great Basin, Field Trip Guidebook # 11, p. 108-121.

Sawyer, D. A., and Sargent, K. A., 1989, Petrologic evolution of divergent peralkaline magmas from the Silent Canyon caldera complex, southwestern Nevada volcanic field: Jour. Geophys. Res., v. 94, p. 6021-6040.

Sawyer, D. A., Fleck, R. J., Lanphere, M. A., Warren, R. G., and Broxton, D. E., 1990, Episodic volcanism in the southwest Nevada volcanic field: new $^{40}Ar/^{39}Ar$ geochronologic results: EOS, Transactions of the American Geophysical Union, v. 71, p. 1296.

Schoen, R., White, D.E., and Hemley, J.J., 1974, Argillization by decending acid at Steamboat Springs, Nevada: Clays and Clay Minerals, v. 22, p. 1-22.

Schneider, R. and Trask, N.J., 1984, U.S. Geological Survey research in radioactive waste disposal; fiscal year 1982: U.S. Geological Survey Water-Resource Investigation 84-4205, 116 p.

Schuraytz, B.C., Vogel, T.A., and Younker, L.W., 1986, Evolution of a magmatic system. Part I: Geochemistry and mineralogy of the Topopah Spring Member of the Paintbrush Tuff, southern Nevada: EOS, Transactions of the American Geophysical Union, v. 67, p. 1261.

Scott, R.B., 1984, Internal deformation of blocks bounded by basin-and-range-style faults: Geological Society of America, Abstracts with Programs, v. 16, p. 649.

Scott, R.B., 1986a, Rare-earth element evidence for changes in chemical evolution of silicic magmas, southwest Nevada: Transactions of the American Geophysical Union, v. 67, p. 1261.

Scott, R. B., 1986b, Extensional tectonics at Yucca Mountain, southern Nevada [abs.]: Geological Society of America Abs. with Programs, v. 18, p. 411.

Scott, R.B., 1988, Tectonic setting of Yucca Mountain, southwest Nevada: Geological Society of America, Abstracts with Programs, v. 20, p. 229.

Scott, R.B. and Bonk, J., 1984, Preliminary geologic map of Yucca Mountain, Nye County, Nevada, with geologic sections: U.S. Geological Survey Open-File Report 84-494, scale 1:12,000, plus 10 p.

Scott, R.B. and Castellanos, Mayra, 1984, Stratigraphic and structural relations of volcanic rocks in drill holes USW GU-3 and USW G3, Yucca Mountain, Nye County, Nevada: U.S. Geological Survey Open-File Report 84-491, 121 p.

Scott, R. B., and Whitney, J. W., 1987, The upper crustal detachment system at Yucca Mountain, SW Nevada [abs.]: Geological Society of America Abs. with Programs, v. 19, p. 332-333.

Scott, R.B., Byers, F.M. and Warren, R.G., 1984, Evolution of magma below clustered calderas, Southwest Nevada volcanic field [abstr.], EOS, Transactions of the American Geophysical Union, v.65, p. 1126-1127.

Scott, R.B., Spengler, R.W., Lappin, A.R., and Chornack, M.P., 1982, Structure and intra-cooling unit zonation in welded tuffs of the unsaturated zone, Yucca Mountain, Nevada, a potential nuclear waste repository: EOS, Transactions of the American Geophysical Union, v. 63, no. 18, p. 330.

Scott, R.B., Spengler, R.W., Diehl, S., Lappin, A.R., and Chornack, M.P., 1983, Geologic character of tuffs in the unsaturated zone at Yucca Mountain, southern Nevada: in Mercer, J.M., Rao, P.C. and Marine, W., eds., Role of the unsaturated zone in radioactive and hazardous waste disposal: Ann Arbor press, Ann Arbor, Michigan, p. 289-335.

Scott, R.B., Bath, G.D., Flanigan, V.J., Hoover, D.B., Rosenbaum, J.G., and Spengler, R.W., 1984, Geological and geophysical evidence of structures in northwest-trending washes, Yucca Mountain, southern Nevada, and their possible significance to a nuclear waste repository in the unsaturated zone: U.S. Geological Survey Open-File Report 84-567, 25 p.

Selner, G.I. and Taylor, R.B., 1988, GSDRAW and GSMAP version 5.0: prototype programs, level 5, for the IBM PC and compatible microcomputers, to assist compilation and publication of geologic maps and illustrations: U.S. Geological Survey Open File Report #88-295A (documentation), 130 p. and #88-295B (executable program disks).

Selner, G.I., Smith, C.L., and Taylor, R.B., 1988, GSDIG: a program to determine latitude/longitude locations using a microcomputer (IBM PC or compatible) and digitizer: U.S. Geological Survey Open File Report #88-014A (documentation) 16 p. and #88-014B (executable program disk).

Smith, C., Ross, H.P., and Edquist, R., 1981, Interpreted resistivity and IP section line W1 Wahmonie area, Nevada Test Site, Nevada: U.S. Geological Survey Open-File Report 81-1350, 14 p.

Smith, R.C., and Bailey, R.A., 1968, Resurgent Cauldrons: Geological Society of America Memoir 116, p. 613-662.

Smith, R.M., 1977, Map showing mineral exploration potential in the Death Valley quadrangle, California and Nevada: U.S. Geological Survey Miscellaneous Field Investigation Map MF-873, 1:250,000 scale.

Snyder, D.B., and Oliver, H.W., 1981, Preliminary results of gravity investigations of the Calico Hills, Nevada Test Site, Nye County, Nevada: U.S. Geological Survey Open-File Report 81-101, 42 p.

Snyder, D.B., and Carr, W.J., 1982, Preliminary results of gravity investigations at Yucca Mountain and vicinity, southern Nye County, Nevada: U.S. Geological Survey Open-File Report 82-701, 36 p.

Snyder, D.B. and Carr, W.J., 1984, Interpretation of gravity data in a complex volcano-tectonic setting, southwestern Nevada: Journal of Geophysical Research. B, v. 89, p. 10,193-10,206.

Spengler, R.W., Byers, F.M., Jr., and Warner, J.B., 1981, Stratigraphy and structure of volcanic rocks in drill hole USW-G1, Yucca Mountain, Nye County, Nevada: U.S. Geological Survey Open-File Report 82-1338, 264 p.

Spengler, R.W. and Chornack, M.P., 1984, Stratigraphic and structural characteristics of volcanic rocks in core hole USW G-4, Yucca Mountain, Nye County, Nevada: U.S. Geological Survey Open-File Report 84-789, 82 p.

Spengler, R.W., Muller, D.C., and Livermore, R.B., 1979, Preliminary report on the geology of drill hole UE25a-1, Yucca Mountain, Nevada Test Site: U.S. Geological Survey Open-File Report 79-1244, 43 p.

Spengler, R.W., and Rosenbaum, J.G., 1980, Preliminary interpretations of geologic results obtained from boreholes UE25a-4, -5, -6, and -7, Yucca Mountain, Nevada Test Site: U.S. Geological Survey Open-File Report 80-929, 35 p.

Spengler, R.W., and Rosenbaum, J.G., 1991, A low-angle breccia zone of hydrologic significance at Yucca Mountain, Nevada: Geological Society of America, Abstracts with Programs, v. 23, p. A119.

Stewart, J. H., 1988, Tectonics of the Walker Lane belt, western Great Basin-Mesozoic and Cenozoic deformation in a zone of shear, *in* Ernst, W. G., ed., Metamorphism and crustal evolution of the western United States, Rubey Vol. VII: Englewood Cliffs, New Jersey, Prentice Hall, p. 683-713.

Stuckless, J. S., Peterman, Z. E. and Muhs, D. R., 1991, U and Sr isotopes in groundwater and calcite, Yucca Mountain, Nevada: evidence against upwelling water: Science, v. 254, p. 551-554.

Sutton, V.D., 1984, Data report for the 1983 seismic-refraction experiment at Yucca Mountain, Beatty, and vicinity, southwestern Nevada: U.S. Geological Survey Open-File Report 84-661, 62 p.

Swadley, W.C., Hoover, D.L. and Rosholt, J.N., 1984, Preliminary report on late Cenozoic faulting and stratigraphy in the vicinity of Yucca Mountain, Nye County, Nevada: U.S. Geological Survey Open-File Report 84-788, 44 p.

Swolfs, H.S. and Savage, W.Z., 1985, Topography, stresses and stability at Yucca Mountain, Nevada, Proceedings - Symposium on Rock Mechanics: Research and engineering applications in rock masses, 26, p. 1121-1129.

Szabo, B.J. and Kyser, T.K., 1985, Uranium, thorium isotopic analyses and uranium-series ages of calcite and opal, and stable isotopic compositions of calcite from drill cores UE25a 1, USW G-2 and USW G-3/GU-3, Yucca Mountain, Nevada: U.S. Geological Survey Open-File 85-224, 30 p.

Szabo, B. J., and Kyser, T. K., 1990, Ages and stable-isotope compositions of secondary calcite and opal in drill cores from Tertiary volcanic rocks of the Yucca Mountain area, Nevada: Geological Society of America Bulletin, v. 102, p. 1714-1719.

Szabo, B.J. and O'Malley, P.A., 1985, Uranium-series dating of secondary carbonate and silica precipitates relating to fault movements in the Nevada Test Site region and of caliche and travertine samples from the Amargosa Desert: U.S. Geological Survey Open-File Report 85-0047, 17 p.

Taylor, E.M., and Huckins, H.E., 1986, Carbonate and opaline silica fault-filling in the Bow Ridge Fault, Yucca Mountain, Nevada -- deposition from pedogenic processes of upwelling ground water: Geological Society of America, Abstracts with Programs, v. 18, no. 5, p. 418.

Thordarson, William, Rush, F.E. , Spengler, R.W. and Waddell, S.J., 1984, Geohydrologic and drill-hole data for test well USW H-3, Yucca Mountain, Nye County, Nevada: U.S. Geological Survey Open-File Report 84-0149, 54 p.

Tingley, J.V., 1984, Trace element associations in mineral deposits, Bare Mountain (Fluorine) mining district, southern Nye County, Nevada: Nevada Bureau of Mines and Geology Report 39, 28 p.

Turrin, B. D., Champion, D., and Fleck, R. J., 1991, $^{40}Ar/^{39}Ar$ age of the Lathrop Wells volcanic center, Yucca Mountain Nevada: Science, v. 253, p. 654-657.

U.S. Department of Energy, 1986, Environmental Assessment Yucca Mountain Site, Nevada Research and Development Area, Nevada, v. 1: Washington, DC, Office of Civilian Radioactive Waste Management.

U.S. Department of Energy, 1988a, Consultation Draft Site Characterization Plan, Yucca Mountain Site, Nevada Research and Development Area, Nevada: Washington, DC,Office of Civilian Radioactive Waste Management, 347 p.

U.S. Department of Energy, 1988b, Site Characterization Plan, Yucca Mountain Site, Nevada Research and Development Area, Nevada: Washington, DC,Office of Civilian Radioactive Waste Management.

U.S. Geologic Survey, 1984, A summary of geologic studies through January 1, 1983 of a potential high-level radioactive waste repository site at Yucca Mountain, southern Nye County, Nevada: U.S. Geological Survey Open-File Report 84-792, 164 p.

Vaniman, D. T., 1991, Calcite, opal, sepiolite, ooids, pellets, and plant/fungal traces in laminar-fabric fault fillings at Yucca Mountain Nevada: Geological Society of America, Abstracts with Programs, v. 23, p. 117.

Vaniman, D.T., and Crowe, B.M., 1981, Geology and petrology of the basalts of Crater Flat: Applications to volcanic risk assessment for the Nevada nuclear waste storage investigations: Los Alamos, New Mexico, Los Alamos National Laboratory Report, LA-8845-MS, 67 p.

Vaniman, D.T., Crowe, B.M., and Gladney, E.S., 1982, Petrology and geochemistry of Hawaiite lavas from Crater Flat, Nevada: Contributions to Mineralogy and Petrology, v. 80, p. 341-357.

Vaniman, D.T., Bish, D.L., and Chipera, S., 1988, A preliminary comparison of mineral deposits in faults near Yucca Mountain, Nevada, with possible analogs: Los Alamos, New Mexico, Los Alamos National Laboratory Report LA-11298-MS, UC-70, 54 p.

Vaniman, D.T., Bish, D., Broxton, D., Byers, F., Heiken, G., Carlos, B., Semarge, E., Caporuscio, F., and Gooley, R., 1984, Variations in authigenic mineralogy and sorptive zeolite abundance at Yucca Mountain, Nevada, based on studies of drill cores USW GU-3 and G-3.

Vogel, T. A., Noble, D. C., and Younker, L. W., 1989, Evolution of a chemically zoned magma body: Black Mountain volcanic center, southwestern Nevada: Jour. Geophys. Res., v. 94, p. 6041-6058.

Vogel, T.A., Ryerson, R.A., Noble, D.C., and Younker, L.W., 1987, Constrains on magma mixing in a silicic magma body: disequilibrium phenocrysts in pumices from a chemically zoned ash-flow sheet: Journal of Geology, v. 95, in press.

Waddell, R.J., 1984, Geohydrologic and drill-hole data for test wells UE-29a#1 and UE-29a#2, Fortymile Canyon, Nevada Test Site: U.S. Geological Survey Open-File Report 84-0142, 25 p.

Wang, J.S.Y., and Narasimhan, T.N., 1985, Hydrologic mechanisms governing fluid flow in partially saturated, fractured, porous tuff at Yucca Mountain: University of California Lawrence Berkeley Laboratory Report SAND84-7202 (LBL-18473), 46 p.

Warren, R.G., and Broxton, D.E., 1986, Mixing of silcic and basaltic magmas in the Wahmonie Formation, southwestern Nevada volcanic field, Nevada: EOS (American Geophysical Union Transactions), v. 67, p. 1261.

Warren, R.G., Byers, F.M., and Caporuscio, F.A., 1984, Petrography and mineral chemistry of units of the Topopah Springs, Calico Hills and Crater Flat Tuffs, and some older volcanic units, with emphasis on samples from drill hole USW G-1, Yucca Mountain, Nevada Test site: Los Alamos, New Mexico, Los alamos National Laboratory Report LA-10003-MS.

Warren, R.G., Nealey, L.D., Byers, F.M., Jr., and Freeman, S.H., 1986, Magmatic components of the Rainier Mesa Member of the Timber Mountain Tuff, Timber Mountain-Oasis Valley Caldera Complex: EOS (American Geophysical Union Transactions), v. 67, p. 1260.

Warren, R. G., Byers, F. M., Jr., Broxton, D. E., Freeman, S. H., and Hagan, R. C., 1989, Phenocryst abundances and glass and phenocryst compositions as indicators of magmatic environments of large-volume ash flow sheets in southwestern Nevada: Jour. Geophys. Res., v. 94, p. 5987-6020.

Warren, R.G., McDowell, F.W., Byers, F.M., Broxton, D.E., Carr, W.J., and Orkild, P.P., 1988, Eposodic leaks from Timber Mountain caldera: new evidence from rhyolite lavas of Fortymile Canyon, southwestern Nevada Volcanic Field: Geological Society of America, Abstracts with Programs, v. 20, p. 241.

Weiss, S.I., 1987, Geologic and Paleomagnetic studies of the Stonewall and Black Mountain volcanic centers, southern Nevada: University of Nevada, Reno-Mackay School of Mines, Reno, Nevada, unpublished MSc Thesis, 67 p.

Weiss, S.I., and Noble, D.C., 1989, Stonewall Mountain volcanic center, southern Nevada: stratigraphic, structural and facies relations of outflow sheets, near-vent tuffs, and intracaldera units: Journal of Geophysical Research, v. 94, 6059-6074.

Weiss, S.I., Noble, D.C., and Mckee, E.H.,1984, Inclusions of basaltic magma in near-vent facies of the Stonewall Flat Tuff: product of explosive magma mixing: Geological Society of America, Abstracts with Programs, v. 16, p. 689.

Weiss, S. I., Noble, D. C., and McKee, E. H., 1988, Volcanic and tectonic significance of the presence of late Miocene Stonewall Flat Tuff in the vicinity of Beatty, Nevada: Geological Society of America Abs. with Programs, v. 20, p. A399.

Weiss, S. I., Noble, D. C., and McKee, E. H., 1989, Paleomagnetic and cooling constraints on the duration of the Pahute Mesa-Trail Ridge eruptive event and associated magmatic evolution, Black Mountain volcanic center, southwestern Nevada: Jour. Geophys. Res., v. 94, p. 6075-6084.

Weiss, S. I., Noble, D. C., and Larson, L. T., 1989, Task 3: Evaluation of mineral resource potential, caldera geology and volcano-tectonic framework at and near Yucca Mountain; report for July, 1988 - September, 1989: Center for Neotectonic Studies, University of Nevad-Reno, 38 p. plus appendices.

Weiss, S. I., Noble, D. C., and Larson, L. T., 1990, Task 3: Evaluation of mineral resource potential, caldera geology and volcano-tectonic framework at and near Yucca Mountain; report for October, 1989 - September, 1990: Center for Neotectonic Studies, University of Nevad-Reno, 29 p. plus appendices.

Weiss, S. I., Noble, D. C., and Larson, L. T., 1991, Task 3: Evaluation of mineral resource potential, caldera geology and volcano-tectonic framework at and near Yucca Mountain; report for October, 1990 - September, 1991: Center for Neotectonic Studies, University of Nevad-Reno, 37 p. plus appendices.

Weiss, S. I., Connors. K. A., Noble, D. C., and McKee, E. H., 1990, Coeval crustal extension and magmatic activity in the Bullfrog Hills during the latter phases of Timber Mountain volcanism: Geological Society of America Abstracts with Programs, v. 22, p. 92-93.

Weiss, S. I., McKee, E. H., Noble, D. C., Connors, K. A., and Jackson, M. R., 1991, Multiple episodes of Au-Ag mineralization in the Bullfrog Hills, SW Nevada, and their relation to coeval extension and volcanism: Geological Society of America Abstracts with Programs, v. 23, p. A246.

Wernicke, B. P., Christiansen, R. L., England, P. C., and Sonder, L. J., 1987, Tectonomagmatic evolution of Cenozoic extension of the North America Cordillera, *in* Coward, M. P., Dewey, J. F., and Hancock, P. L., eds., Continental extensional tectonics: Geol. Soc. London Spec. Pub. 28, p. 203-222.

White, A.F., 1979, Geochemistry of ground water associated with tuffaceous rocks, Oasis valley, Nevada: U.S. Geological Survey Professional Paper 712-E.

Whitney, J. A., and Stormer, J. C., Jr., 1983, Igneous sulfides in the Fish Canyon Tuff and the role of sulfur in calc-alkaline magmas: Geology, v. 11., p. 99-102.

Whitfield, M.S., Eshom, E.P., Thordarson, W., and Schaefer, D.H., 1985, Geohydrology of rocks penetrated in test well USW H-4, Yucca Mountain, Nye County, Nevada: U.S. Geological Survey Water-Resources Investigations Reports, 1985, 33 p.

Whitfield, M.S., Thordarson, W. and Eshom, E.P., 1984, Geohydrologic and drill-hole data for test well USW H-4, Yucca Mountain, Nye County, Nevada: U.S. Geological ts

Worthington, J. E., Noble, D. C., and Weiss, S. I., 1991, Structural geology and Neogene extensional tectonics of the Gold Mountain-Slate Ridge area, southwestern Nevada: Geol. Soc. America Abstr. with Prog., v. 23, p. A247.

Wu, S.S., 1985, Topographic Maps of Yucca Mountain area, Nye County, Nevada, 6 oversize sheets, scale 1:5,000: U.S. Geological Survey Open-File Report 85-0620.

Zartman, R. E., and Kwak, L. M., 1991, Lead isotopes in the carbonate-silica veins of Trench 14, Yucca Mountain, Nevada: Geological Society of America, Abstracts with Programs, v. 23, p. 117.

Table 1. List of Core and Rotary Cuttings Samples from the Subsurface of Yucca Mountain Received by Task 3

Hole #	SMFSpecID	Depth Top	Depth Bot	Unit	Type	Alt?Type	Py?	Vns?	comments
UE25B-1H	16937	2110.0	2120.0	Tcp	chips	?			
UE25B-1H	16938	2130.0	2140.0	Tcp	chips	?			
UE25B-1H	16939	2140.0	2150.0	Tcp	chips	?			
UE25B-1H	16940	2240.0	2250.0	Tcp	chips	?			
UE25B-1H	16941	2280.0	2290.0	Tcp	chips	?			
UE25B-1H	17755	3184.7	3185.5	Tct	core		N	Y	cal ±? vns
UE25B-1H	17756	3195.3	3196.2	Tct	core			N	
UE25B-1H	17757	3208.3	3209.0	Tct	core			Y	cal vns
UE25B-1H	17758	3214.0	3214.7	Tct	core		N	N	
UE25B-1H	16847	3550.0	3550.8	Tct	core	Y	Y	N	
UE25B-1H	16848	3555.2	3556.0	Tct	core	Y	Y	Y	cal? vns
UE25B-1H	16849	3659.5	3660.2	Tct	core	Y	Y	Y	cal vns
UE25B-1H	16850	3675.0	3676.0	Tct	core	Y	Y	N	
UE25B-1H	16851	3695.0	3695.6	Tct	core	Y	Y	N	
UE25B-1H	16852	3771.2	3772.0	Tct	core	Y	Y	N	lithology similar to Round Mtn type II ore
UE25B-1H	16854	3773.0	3773.5	Tct	core	Y	Y	N	lithology similar to Round Mtn type II ore; photos of gdass py ??
UE25B-1H	16855	3786.0	3786.8	Tct	core	Y	Y	N	
UE25B-1H	16856	3796.2	3796.7	Tct	core	Y	Y	Y	cal vns
UE25B-1H	16857	3821.8	3822.4	Tct	core	Y	Y	Y	dissem py in gdmass+py in lithics; minor py in cal vn.
UE25B-1H	16859	3825.0	3825.7	Tct	core	Y	Y	Y	good green fluor? + cal vein, poss. fluid incls.
UE25B-1H	16860	3935.9	3936.5	Tct??	core	?	N	Y	no py seen; cal±? vn
UE25B-1H	16961	3959.9	3960.6	Tlr	core	Y?	?	N	
UE25B-1H	16862	3985.7	3986.3	Tlr	core	Y, arg?	N	Y	cal vn
UE25B-1H	16863	3999.8	4000.6	Tlr	core	Y	N	N	
UE25 P1	16948	880.0	890.0	Tpt	chips	N	N	?	
UE25 P1	16949	900.0	910.0	Tpt	chips	N	N	?	
UE25 P1	16950	920.0	930.0	Tpt	chips	N	N	?	
UE25 P1	16951	940.0	950.0	Tpt	chips	N	N	?	
UE25 P1	16952	2870.0	2880.0	Tct?	chips	?	N	?	
UE25 P1	16953	3120.0	3130.0	Tlr	chips	?	N	?	
UE25 P1	16954	3870.0	3880.0	Tot	chips	?	N	?	
UE25 P1	16955	3890.0	3900.0	Tot	chips	?	Y	?	alt volc frags, some w/py
UE25 P1	16956	3920.0	3930.0	Tot	chips	?	N	?	contam w/drill tool frags
UE25 P1	16957	3930.0	3940.0	Tot	chips	?	N	?	
UE25 P1	16958	4060.0	4070.0	Tot/Slm	chips	?	Y	?	mixed Tot/Slm
UE25 P1	16959	4080.0	4090.0	Tot+Pz	chips	?	Y	Y	mixed Tot(±py) + carb frags, occais. qtz, py vein frags.
UE25 P1	16960	4210.0	4220.0	Tot/Slm	chips	?	Y	?	mixed, 90% Tot w/sparse py
UE25 P1	16961	5490.0	5500.0	Slm	chips	?	N	Y	cal + fluor? vns
UE25 P1	16962	5510.0	5520.0	Srm	chips	?	N	Y	cal, fluor, qtz vn frags
UE25 P1	16963	5530.0	5540.0	Srm	chips	?	Y	Y	contam. w/drill frags; py vn/vug frags; fluor, qtz, cal vn frags
UE25 P1	16964	5550.0	5560.0	Srm	chips	?	Y?	Y	contam w/drill tool frags; dissem py; qtz, cal, fluor vn frags
USW G1	16898	3216.0	3217.0	Tct	core	?	Y	N	py in lithics only??
USW G1	16899	3219.5	3220.5	Tct	core	Y	Y	N	
USW G1	16900	3236.3	3237.1	Tct	core	Y	Y	N	
USW G1	16901	3250.3	3250.6	Tct	core	Y	Y	N	
USW G1	16903	3324.0	3224.9	Tct	core	Y	Y	N	
USW G1	16904	3368.2	3368.8	Tct	core	Y?	Y	N	
USW G1	16905	3372.0	3372.4	Tct	core	Y?	Y	Y	clear qtz vn, pyritic lithics + gdmss.
USW G1	16906	3384.0	3385.0	Tct	core	Y?	Y	N	
USW G1	16907	3392.3	3393.0	Tct	core	Y?	Y	N	py in gdmss too?, good one for TS
USW G1	16897	3393.0	3393.8	Tct	core	Y	Y	N	
USW G1	16908	3477.0	3478.0	Tct	core	Y?	Y	N	
USW G1	16909	3493.0	3494.0	Tct	core	Y?	Y	N	
USW G1	16910	3515.3	3516.0	Tct	core	Y?	Y	N	
USW G1	16911	5775.4	5776.4	Tot	core	Y?	N	N	good spec. for TS to check out alt.
USW G1	16912	5790.0	5791.0	Tot	core	Y?	N	N	

Table 1, continued

Hole #	SMFSpecID	Depth Top	Depth Bot	Unit	Type	Alt?Type	Py?	Vns?	comments
USW G1	16913	5823.0	5824.0	Tot	core	Y?	N	N	
USW G1	16914	5846.7	5847.7	Tot	core	Y?	N	N	xtal-rich, milky fldsp- get TS for alt check
USW G1	16915	5860.0	5861.0	Tot	core	Y?	N	N	
USW G1	16916	5879.8	5880.6	Tot	core	Y?	N	N	
USW G2	16864	1674.1	1675.1	Tpt	core	Y?	N	N	incipient alt?? in vit ??
USW G2	16865	1690.2	1690.8	Tpt	core	?	N	N	incipient argillic alt.??
USW G2	16866	1700.0	1700.6	Tpt	core	?	N	N	incipient arg. alt.?
USW G2	16867	2280.2	2280.8	Trc	core	?	N	Y	silica vns
USW G2	16868	2306.3	2307.2	Trc	core	?	N	N	
USW G2	16869	3105.0	3105.9	Tcp	core	?	N	Y	silica vns
USW G2	16870	3313.0	3313.5	Tcb	core	N	N	N	fresh? dense Tcb- possible baseline gc
USW G2	16871	3420.0	3421.0	Tcb	core	?	N	Y	Mnox-filled fracture/vein
USW G2	16872	3445.9	3447.1	Tcb	core	?	N	N	
USW G2	16873	3935.0	3935.7	Tct	core	Y	N	N	
USW G2	16874	3949.8	3950.5	Tct	core	Y?	N	N	
USW G2	16875	3968.0	3968.8	Tct	core	Y	N	N	
USW G2	16876	3985.0	3986.0	Tct	core	Y	N	N	arg. alt?, dark, pheno-rich subunit, lower Tct
USW G2	16877	3991.4	3992.4	Tct	core	Y?	N	N	arg. alt? propylitic?
USW G2	16878	4188.3	4189.0	Tr2	core	Y?	N	N	propylitic? alt. welded tuff
USW G2	16879	4198.4	4199.0	Tlr	core	?	N	Y?	clay/FeOx shear? bands, prev. glassy?
USW G2	16880	4202.0	4202.7	Tlr	core	?	N	N	prop. alt? prev. glssy dense ash-flow tuff
USW G2	16881	4204.4	4205.2	Tlr	core	?	N	N	propylitic alt?
USW G2	16882	4219.0	4219.7	Tlr	core	Y?	N	N	propylitic alt?
USW G2	16883	4277.3	4278.0	Tlr	core	Y?	N	N	propylitic alt?, py??
USW G2	16884	4291.3	4292.0	Tlr	core	Y?	N	N	
USW G2	16885	4305.0	4306.0	Tlr	core	Y?	N	N	
USW G2	16886	5207.0	5207.7	Trl	core	Y?	Y?	N	
USW G2	16887	5232.9	5233.7	Trl	core	Y	Y	Y	cal-silica-chlor vns, hydraulic/hydrothermal? brecc vns; sparse py
USW G2	16888	5254.0	5255.0	Trl	core	Y	Y?	Y	
USW G2	16889	5260.0	5260.6	Trl	core	Y	Y	Y	propyl. alt, cal-chlor-silica vns., sparse py
USW G2	16890	5263.0	5264.0	Trl	core	Y,prop	N?	Y	fault shear surfaces,sheared cal+grnclay? vn
USW G2	16891	5644.0	5645.0	Trltuff	core	Y?prop	N	N	propylitic? alt welded tuff
USW G2	16892	5664.0	5665.0	Trltuff	core	Y?prop	N	N	propylitic? alt. welded tuff
USW G2	16893	5670.5	5671.3	Trl	core	Y?prop	N	N	propylitic alt? lava
USW G2	16894	5684.3	5685.3	Trl	core	Y?prop	N	Y	propylitic alt? lava; cal vns
USW G2	16895	5697.0	5698.0	Trl	core	Y?prop	N	Y	cal vns
USW G2	16896	5711.9	5712.7	Trl	core	Y?prop	N	Y	cal vns
USW G3	16930	4652.9	4654.5	Tlr	core	Y?prop	N	N	
USW G3	16932	4754.7	4755.5	Tlr	core	Y?prop	Y	N	py in lithics and gdes
USW G3	16933	4790.0	4790.7	Tlr	core	Y?prop	Y	N	v. sparse py in a few lithics; good match for Round Mtn type II ore
USW G3	16934	4805.0	4805.7	Tlr	core	Y?prop	Y	N	v. sparse py in a few lithics; good match for Round Mtn type II ore
USW G3	16935	4816.7	4817.1	Tlr	core	Y?prop	Y	N	v. sparse py in a few lithics; good match for Round Mtn type II ore
USW G3	16936	4828.0	4828.7	Tlr	core	Y?prop	?	N	
USW GU3	16924	1041.0	1041.7	Tpt	core	N	N	Y	cal vns
USW GU3	16927	1185.6	1186.2	Tpt	core	N	N	N	did not receive part of core interval with vein
USW GU3	16929	1229.4	1230.4	Tpt	core	N	N	N	fresh Tpt vit for possible baseline gc
USW H3	16942	3340.0	3350.0	??Tc?	chips	N	N	N	
USW H3	16943	3990.0	4000.0	??Tc?	chips	N	N	N	
UE25 A1	16917	2115.3	2115.9	Tcp	core	Y?	N	Y	yellow-green fracture coating; SEM-EDI shows no As, U or trace metals
UE25 A1	16918	2116.8	2117.2	Tcp	core	Y?	N	N	not what we requested, incipient alt. vit??
UE25 A1	16919	2123.0	2123.7	Tcp	core	Y?	N	Y	arg alt?; similar to Rawhide oxide ore; silica vns
UE25 A1	16920	2133.5	2134.0	Tcp	core	Y?	N	Y?	arg alt+clay-zeol-wad fracture filling; similar to Rawhide oxide ore
UE25 A1	16921	2187.4	2188.1	Tcb	core	Y?	N	N	silicified? glassy tuff??
UE25 A1	16922	2478.1	2478.7	Tcb	core	Y?	N	N	wk arg. alt plag, bio v. ox; strong v.p.??
UE25 A1	16923	2495.5	2496.1	Tcb	core	Y?	N	N	arg. alt? v.p., fault surfaces
UE25 A4	16944	359.4	360.2	Tpt	core	N	N	N	delicate carb xtals lining relict v.p. pues

Table 1, continued

Hole #	SMFSpecID	Depth Top	Depth Bot	Unit	Type	Alt?Type	Py?	Vns?	comments
UE25 A4	16945	366.3	366.7	Tpt	core	N	N	N	caliche in relict v.p. pums; contam w/coppery metallic drill lube
UE25 A4	16946	386.1	386.5	Tpt	core	N	N	N	fresh devit+v.p.; minor caliche
UE25 A4	16947	398.2	399.0	Tpt	core	N	N	Y	drusy cal vn and cal-cemented brecc, fault surface
UE25 C1	20064	2783.0	2784.0	Tc	core	arg?+Feox	N	Y	rubble zone frags containing hydraulic/hydrothermal? breccia veins
UE25 C2	20065	2688.1	2688.5	Tc	core	arg?+Feox	N	N	strong reddish Feox stain
UE25 C2	20066	2830.0	2840.0	Tc	chips	arg?	N	Y	bleached, Feox hydraulic/hydrothermal? breccia vns
UE25 C2	20067	2900.0	2910.0	Tc	chips	arg?	N	Y	breccia veins as in 20064; bleached, bio fresh
UE25 C3	20068	2900.1	2900.5	Tc	core	arg?+Feox	N	Y	breccia veins, clear calcite and dark grey calcite veins
UE25 C3	20069	2902.2	2903.0	Tc	core	arg?+Feox	N	Y	breccia vns, fluor cubes lining cavities, vfg qtz+fl? vns, no efferv.
UE25 C3	20070	2821.3	2821.6	Tc	core	arg?+Feox	N	N	bleached to mustard color

SMFSpecID = sample identification number assigned to each interval by staff of the Sample Management Facility, Area 25, Nevada Test Site.

Depth top and Depth Bot refer to the depth in feet from the surface to the top and bottom of each sample interval.

Srm = Roberts Mountain Formation, Slm = Lone Mountain Dolomite; Tot = pre-Lithic Ridge sequence of ash-flow and bedded tuffs, Tr1 = pre-Lithic Ridge silicic lavas, Tlr = Lithic Ridge Tuff; Tct, Tcb and Tcp = Tram, Bullfrog and Prow Pass members of the Crater Flat Tuff, respectively; Tc = Crater Flat Tuff undivided,; Tpc = Tiva Canyon Member of the Paintbrush Tuff.

py = pyrite, fluor = fluorite, cal = calcite, qtz = quartz, vns = veins, alt = altered, mod = moderately, dissem = disseminated, gdmss = groundmass, arg = argillic, carb = carbonate, v.p. = vapor phase, pums = pumice(s), brecc = breccia.

Table 2. Precious Metals and Indicator-Element Abundances in Core and Rotary Cuttings Samples from the Subsurface of Yucca Mountain

Ag and Au values given in ppb, all others given in ppm

Hole #	SMF ID#	Unit	Py?	Vns?	Comments	Ag	Au	As	Bi	Cd	Hg	HgAA	Sb	Se	Te	Cu	Mo	Pb	Zn	Tl
UE25B-1H	16854	Tct	Y	N	lithology similar to Round Mountain type II ore.	38.0	0.492	4.2	0.451	0.202	0.066	0.023	<0.05	0.355	0.208	2.8	0.38	13.5	37.4	<0.492
UE25B-1H	16855	Tct	Y	N		34.5	0.233	4.8	0.554	0.132	0.063	0.022	0.22	0.456	0.413	3.3	0.47	17.0	37.0	<0.500
UE25B-1H	16856	Tct	Y	Y	cal vns.	37.9	<0.200	7.8	0.442	0.118	0.068	0.037	0.23	0.416	0.428	3.5	0.33	15.8	38.4	<0.500
UE25B-1H	16857	Tct	Y	Y	cal vns; dissem py in groundmass and in lithics; minor py in cal vn.	33.7	0.230	5.2	0.450	0.196	0.078	0.021	<0.05	0.556	0.268	3.2	0.69	14.1	38.2	<0.493
UE25B-1H	16859	Tct	Y	Y	cal + green to clear fluor?? vein, possible fluid inclusions.	34.1	0.596	7.9	0.445	0.118	0.080	0.024	<0.05	0.464	0.202	3.1	0.27	16.5	39.7	<0.496
UE25B-1H	16860	Tct?	N	Y	cal + green phase in vn; no py seen.	33.3	0.324	0.7	0.182	0.324	0.153	0.106	<0.05	<0.243	<0.049	5.8	0.23	7.7	54.1	<0.486
	YMX-2				(blind duplicate 16860)	40.1	1.10	<0.75	0.167	0.355	0.142	nd	<0.15	<0.753	<0.151	6.5	0.41	7.9	53.2	<1.51
UE25B-1H	16861	Tlr	?	N		28.6	<0.200	0.5	0.183	0.082	0.060	0.040	0.14	<0.250	0.112	2.4	0.23	8.7	41.4	<0.500
UE25B-1H	16862	Tlr	N	Y	cal vn.	33.6	0.230	0.3	0.057	0.037	<0.020	<0.010	<0.05	<0.246	<0.049	0.9	<0.02	8.0	36.4	<0.493
UE25 P1	16954	Tot	N	?		41.1	0.360	5.2	0.156	0.320	0.140	0.120	<0.07	<0.338	<0.068	1.7	1.18	14.9	30.8	<0.675
UE25 P1	16955	Tot	Y	?	alt volc frags, some w/py.	27.1	<0.198	2.7	0.154	0.089	0.053	0.038	0.42	<0.248	0.085	2.6	0.79	22.6	125	<0.495
UE25 P1	16956	Tot	N	?	alt Tot, no py seen, contains drill tool fragments.	29.6	<0.197	3.4	0.105	0.082	0.039	0.022	0.52	<0.247	0.062	1.7	0.62	14.1	21	<0.493
UE25 P1	16958	Tot	Y	?	mixed Tot/Slm.	54.0	0.519	47.8	0.123	0.127	0.092	0.061	1.84	<0.243	0.055	1.6	2.86	11.7	29.4	<0.487
UE25 P1	16959	fault?	?	?		93.0	2.13	63.2	0.051	0.253	0.129	0.136	0.39	<0.242	<0.048	1.4	1.32	5.6	42.5	<0.484
UE25 P1	16960	Tot/Slm	Y	?	mixed Tot/Slm, 90% Tot fragments contain sparse py.	29.8	<0.198	14.3	0.164	0.107	0.060	0.027	1.14	<0.247	0.157	1.4	0.82	13.0	21.5	<0.494
UE25 P1	16961	Slm	N	Y	cal + fluor? vns.	91.3	0.794	9.7	<0.050	0.035	0.056	0.046	1.35	0.268	<0.050	1.1	2.19	1.9	12.8	<0.496
UE25 P1	16962	Srm	N	Y	cal+fluor?+qtz? vn fragments.	51.3	<0.196	3.7	<0.049	0.030	0.025	0.031	0.77	0.363	<0.049	0.8	1.92	2.3	11.7	<0.489
	YMH-X5				(blind dup. 16962).	54.7	<0.199	3.9	<0.050	0.031	0.031	nd	0.86	0.318	0.065	0.9	1.78	2.3	11.8	<0.498
UE25 P1	16963	Srm	Y	Y	contains drill tool fragments; py and fluor vn or vug fragments.	139.0	4.83	25.9	1.92	0.469	0.585	nd	12.7	0.687	0.091	38.6	208	900	227	2.44
	16963B*				(powder from 2nd split of chips; 5 gram GXPL).	173.0	7	38.2	1.65	0.208	0.815	0.714	20.1	1.38	<0.526	64.9	286	1358	304	3.05
UE25 P1	16964	Srm	Y	Y	qtz, py, fluor? vns + dissem py , contains drill tool fragments.	49.2	0.328	4.5	0.053	0.037	0.051	0.051	1.23	<0.246	<0.049	1.6	16.2	9.7	15	<0.492
USW G1	16904	Tct	Y	N		41.8	<0.196	8.0	0.340	0.079	0.073	0.023	0.15	0.404	0.439	4.3	0.37	16.1	21.2	<0.491
USW G1	16905	Tct	Y	Y	clear qtz vn; pyritic lithics and groundmass.	39.1	2.72	6.8	0.427	0.173	0.070	0.023	<0.05	0.526	0.206	3.9	0.64	18.3	37.9	<0.486
USW G1	16907	Tct	Y	N	pyritic lithics and groundmass.	36.7	0.396	8.4	0.381	0.224	0.069	0.016	<0.05	0.687	0.325	4.7	0.68	15.0	37.4	<0.495
USW G1	16914	Tot	N	N	xtal-rich, milky feldspar phenocrysts.	33.3	0.327	2.6	0.070	0.045	0.054	<0.010	<0.05	<0.245	<0.049	2.0	<0.02	10.1	57.3	<0.490
USW G2	16871	Tcb	N	Y	Mn-ox filled fracture.	14.8	1.47	18	<0.049	0.416	0.649	0.786	5.31	<0.246	<0.049	1.7	0.46	9.5	36.8	<0.491
	16871				(second split of original powder)							0.681								
USW G2	16887	Tr1	Y	Y	propylitic alt, cal-chlor-silica vns., albitized feldspar phenos.	28.4	0.332	68.8	<0.050	0.100	0.192	0.118	<0.05	<0.249	<0.050	3.9	0.59	12.1	50.1	<0.498
USW G2	16888	Tr1	N	Y	as above	26.2	<0.197	85.2	0.064	0.119	0.220	0.152	0.40	<0.247	0.073	3.5	1.16	17.2	81.9	<0.493
USW G2	16889	Tr1	Y	Y	as above	28.7	0.232	47.1	0.081	0.126	0.220	0.123	<0.05	<0.248	<0.050	3.1	2.05	16.9	52	<0.497
	YMX-1				(blind duplicate 16889)	34.9	1.14	50	<0.132	0.132	0.188	nd	<0.132	<0.66	<0.132	3.5	2.2	16.5	51.8	<1.32
USW-G2	16890	Tr1	N	Y	fault surfaces, sheared cal+green clay? vn.	27.9	<0.198	38.6	<0.050	0.163	0.081	0.037	0.34	<0.248	0.067	3.7	0.18	22.3	86.8	<0.496
USW G2	16895	Tr1	N	Y	cal vns.	43.0	0.360	1.6	<0.049	0.092	0.061	0.016	0.17	<0.246	0.067	12.6	0.18	9.3	76.8	<0.491
USW G2	16896	Tr1	N	Y	cal vns.	38.6	<0.197	0.5	<0.049	0.100	0.178	0.021	<0.25	<0.246	<0.049	11.2	<0.02	7.2	78.8	<0.492
USW G3	16932	Tlr	Y	N	py in lithics and groundmass.	36.7	<0.198	1.5	0.196	0.153	0.078	0.046	<0.05	<0.248	<0.050	1.8	0.13	9.3	12.7	<0.496
	X-1				(blind duplicate 16932 for Hg by AA)							0.050								
USW G3	16933	Tlr	Y	N	very sparse py in few lithics; lithology similar to Round Mtn type II.	36.7	<0.194	1.3	0.152	0.071	0.091	0.063	0.11	<0.243	0.130	1.0	0.30	10.5	32.8	<0.486
USW G3	16934	Tlr	Y	N	v. sparse py in few lithics; good match for RM typeII ore.	40.2	0.328	1.2	0.268	0.215	0.110	0.079	<0.05	<0.246	<0.049	1.7	0.15	10.6	31.7	<0.492
USW G3	16935	Tlr	Y	N	v. sparse py in few lithics; good match for RM typeII ore.	41.3	0.329	1.1	0.177	0.144	0.111	0.066	<0.05	<0.247	<0.049	1.6	0.12	10.8	29.8	<0.493
USW G3	16936	Tlr	?	N		34.4	<0.199	1.1	0.179	0.077	0.053	0.046	0.24	<0.249	0.115	1.7	0.29	14.8	27.7	<0.498
UE25 C1	20064	Tc	N	Y	rubble zone fragments w/breccia veins.	8.5	<0.198	18.1	0.106	0.119	0.042	0.033	15.1	<0.247	<0.049	0.8	1.25	9.9	40.6	<0.494
UE25 C2	20065	Tc	N	N	strong reddish Feox stain.	6.5	0.295	5.5	1.110	0.050	<0.020	0.017	<0.05	<0.246	0.083	0.5	<0.02	13.9	17.0	<0.491
UE25 C2	20066	Tc	N	Y	bleached, Feox breccia vns.	12.4	<0.225	22.4	0.122	0.057	0.026	0.018	3.72	<0.282	<0.056	0.6	8.83	6.2	9.3	<0.563
UE25 C2	20067	Tc	N	Y	bleached, breccia veins as in 20064; biotite fresh.	10.1	0.276	20.4	0.277	0.120	0.050	0.021	0.47	<0.345	<0.069	0.8	12.5	6.5	27.3	<0.689
UE25 C3	20068	Tc	N	Y	breccia veins, clear calcite+dark grey calcite veins.	12.5	0.328	77.4	0.163	0.292	0.075	0.062	1.49	<0.246	<0.049	0.6	0.98	10.9	39.1	<0.491
UE25 C3	20069	Tc	N	Y	breccia vns; fluor+montmorill. in cavities; vfg qtz+fluor? vns, no cal.	21.1	0.395	34.3	1.970	0.083	0.153	0.045	3.37	<0.247	0.134	0.5	193	11.1	20.8	<0.494
	20069R				(2nd analysis of powder from original split of 20069)	10.0	<0.199	37.7	1.240	0.092	0.113	0.045	3.67	<0.249	0.188	0.7	207	11.3	23.6	<0.499
	X-2				(blind duplicate 20069 for Hg by AA)							0.050								
	20069B				(powder from second split of 20069 excluding cut surfaces)	9.9	<0.199	23	0.674	0.067	0.065	0.030	2.35	<0.248	0.090	0.4	110	9.2	19.3	<0.497
	YMH-X4				(blind duplicate 20069B)	10.4	<0.198	22.7	0.744	0.066	0.064	0.045	2.3	<0.248	0.107	0.6	109	9.0	19.1	<0.496
UE25 C3	20070	Tc	N	N	bleached to mustard color.	4.5	0.261	35.3	<0.049	0.063	0.041	0.058	4.67	<0.244	<0.049	0.7	0.29	2.8	12.8	<0.489
	Fresh tuff reference samples																			
BMCF-D		Tcb			mod. welded, devit; S end Yucca Mtn NW of Lathrop Wells cinder cone.	10.1	<0.199	5.3	<0.050	0.062	0.024	0.013	0.26	<0.249	0.055	1.0	1.36	2.0	47.9	<0.497
3SW-589		Tpc			fresh, dense, devit, minor caliche in lithophys.; Exile Hill.	9.7	0.265	2.7	<0.050	0.037	<0.020	0.015	<0.05	<0.249	<0.050	1.4	0.89	4.9	49.0	<0.497
YMH-X3					(blind duplicate 3SW-589)	13.1	<0.198	2.6	<0.049	0.044	0.023	0.014	0.12	<0.247	0.053	1.2	0.64	4.5	50.5	<0.495
X-3					(blind duplicate 3SW-589 for Hg by AA)							0.012								

Analyses by MB Associates, North Highland, CA, using inductively-coupled plasma emission spectrography for all elements except Au which was carried out by graphite furnace - atomic absorption spectrometry; * = 5 gram digestion, all other analyses used 15 gram digestion. Values as reported by MB Associates except Ag rounded to nearest ppb, As, Sb and Cu rounded to nearest 0.1 ppm, and Mo to nearest 0.01 ppm. Number of significant figure does not indicate precision or accuracy of analyses.

HgAA = analyses carried out by the Nevada Mining Analytical Laboratory using hydride-generator type atomic absorption methods, M. O. Desilets, analyst.

nd = not determined.

SMF ID # denotes sample identification assigned to each interval by staff of Sample Management Facility, Area 25, Nevada Test Site; ID numbers beginning with YM and X were assigned by Task 3 to denote blind duplicates.

Srm = Roberts Mountain Formation, Slm = Lone Mountain Dolomite; Tot = pre-Lithic Ridge sequence of ash-flow and bedded tuffs, Tr1 = pre-Lithic Ridge silicic lavas, Tlr = Lithic Ridge Tuff; Tct, Tcb and Tcp = Tram, Bullfrog and Prow Pass members of the Crater Flat Tuff, respectively; Tc = Crater Flat Tuff undivided,; Tpc = Tiva Canyon Member of the Paintbrush Tuff.

py = pyrite, fluor = fluorite, cal = calcite, qtz = quartz, vns = veins, alt = altered, mod = moderately, dissem = disseminated.

Table 3. X-Ray Fluorescence Analyses of Rocks of the Mount Jackson Dome Field
major elements given in weight percent, minor elements in ppm

Sample #	383A	383A*	383B	385	387	387*	MJ-SE	MJ-W	DWLJ-1
SiO_2	75.6	72.9	74.4	74.5	72.6	72.8	67.0	65.6	74.6
Al_2O_3	12.6	12.2	12.4	12.1	12.7	12.7	14.4	15.2	12.8
MgO	0.20	0.24	0.23	0.18	0.19	0.18	0.72	0.87	0.11
CaO	0.66	1.52	0.79	0.82	0.76	0.85	2.49	2.92	0.70
Na_2O	4.26	4.03	4.08	4.06	4.05	4.06	3.70	4.14	3.74
K_2O	4.48	4.53	4.56	4.25	4.85	4.83	4.16	3.77	4.55
P_2O_5	0.02	0.04	0.03	0.03	0.02	0.02	0.11	0.12	0.02
TiO_2	0.161	0.141	0.145	0.131	0.135	0.127	0.380	0.367	0.118
MnO	0.08	0.08	0.08	0.08	0.08	0.08	0.06	0.06	0.07
Fe_2O_3	0.97	0.83	0.87	0.84	0.92	0.87	2.13	2.30	0.58
Cr	-10	13	-10	-10	-10	-10	-10	-10	-10
Rb	172	189	187	316	157	159	138	95	237
Sr	-10	-10	-10	19	13	21	715	977	-10
Y	27	34	28	42	-10	16	14	-10	14
Zr	119	112	114	100	129	102	162	130	93
Nb	35	50	47	73	32	53	39	30	40
Ba	31	57	63	91	77	72	1230	1650	41
LOI(%)	0.85	2.65	2.10	2.80	2.95	3.00	2.90	2.95	2.20
SUM(%)	99.9	99.2	99.7	99.9	99.3	99.6	98.3	98.6	99.5

Analyses Recalculated "Anhydrous"

Sample #	383A	383A*	383B	385	387	387*	MJ-SE	MJ-W	DWLJ-1
SiO_2	76.2	74.9	76.0	76.6	74.8	75.1	69.0	67.6	76.3
Al_2O_3	12.7	12.5	12.7	12.4	13.1	13.1	14.8	15.7	13.1
MgO	0.20	0.25	0.23	0.19	0.20	0.19	0.74	0.90	0.11
CaO	0.67	1.56	0.81	0.84	0.78	0.88	2.57	3.01	0.72
Na_2O	4.30	4.14	4.17	4.18	4.17	4.19	3.81	4.27	3.82
K_2O	4.52	4.65	4.66	4.37	5.00	4.98	4.29	3.89	4.65
P_2O_5	0.02	0.04	0.03	0.03	0.02	0.02	0.11	0.12	0.02
TiO_2	0.162	0.145	0.148	0.135	0.139	0.131	0.392	0.378	0.121
MnO	0.08	0.08	0.08	0.08	0.08	0.08	0.06	0.06	0.07
Fe_2O_3	0.98	0.85	0.89	0.86	0.95	0.90	2.19	2.37	0.59
Cr	-10	13	-10	-10	-10	-10	-10	-10	-10
Rb	173	194	191	325	162	164	142	98	242
Sr	-10	-10	-10	20	13	22	737	1007	-10
Y	27	35	29	43	-10	16	14	0	14
Zr	120	115	116	103	133	105	167	134	95
Nb	35	51	48	75	33	55	40	31	41
Ba	31	59	64	94	79	74	1267	1701	42

See Figure 7 for sample locations. All samples contained small amounts of secondary carbonate minerals (caliche). To minimize the CaO contributed by caliche, most samples were crushed to -20 mesh and leached for 10 minutes with 5% acetic acid in a sonic cleaner. * indicates samples not leached in 5% acetic acid. Total iron as Fe_2O_3.

Analyses carried out by XRAL Ltd., using fused disk (lithium metaborate flux) X-ray fluorescence methods.

HYDROTHERMAL ALTERATION IN DRILL HOLES IN YUCCA MOUNTAIN

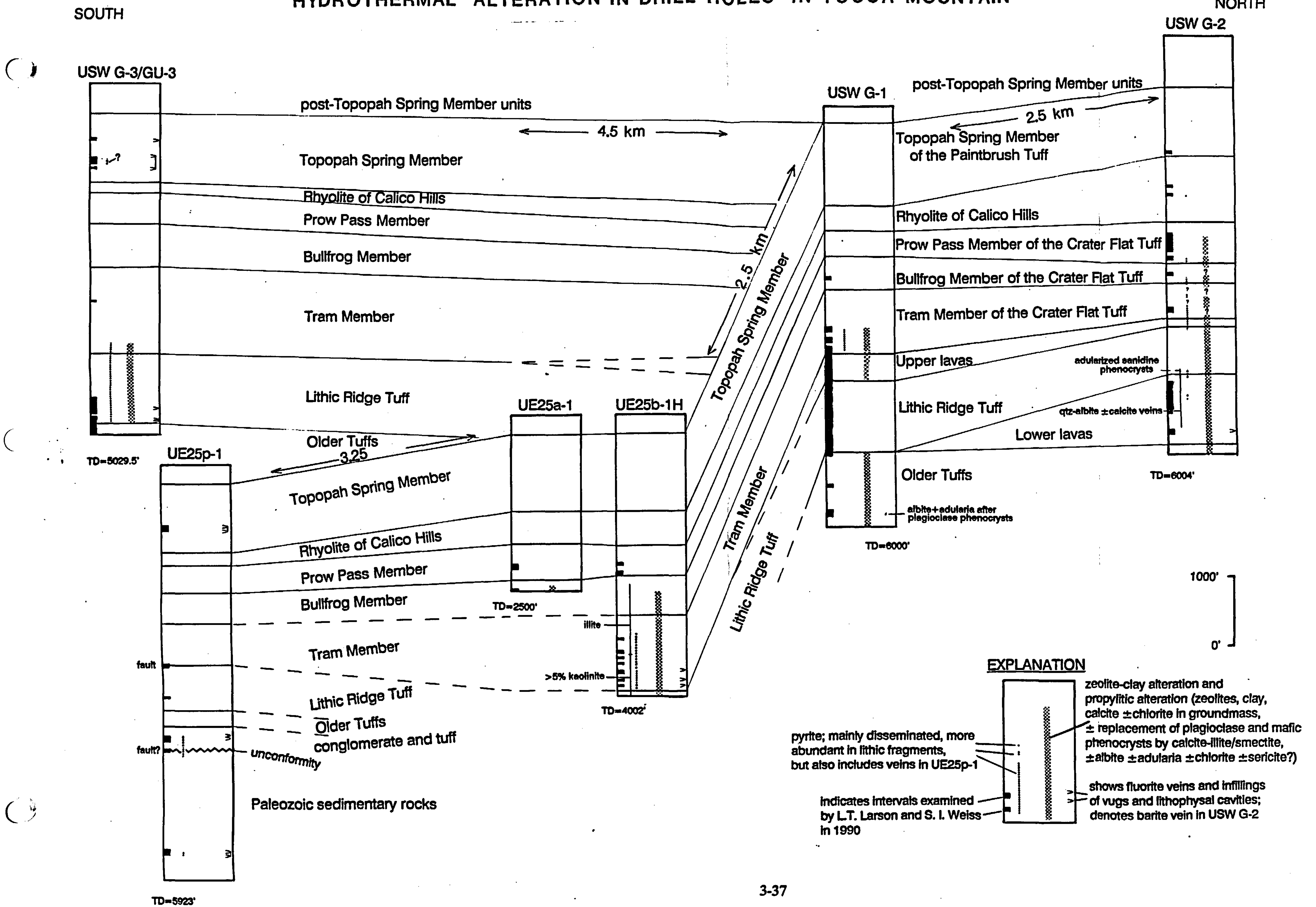

Figure 1. Subsurface stratigraphy and hydrothermal alteration features of deep drill holes in Yucca Mountain. Data from direct visual inspection by Task 3 and numerous published reports of the U. S. Geological Survey and the Los Alamos National Laboratory.

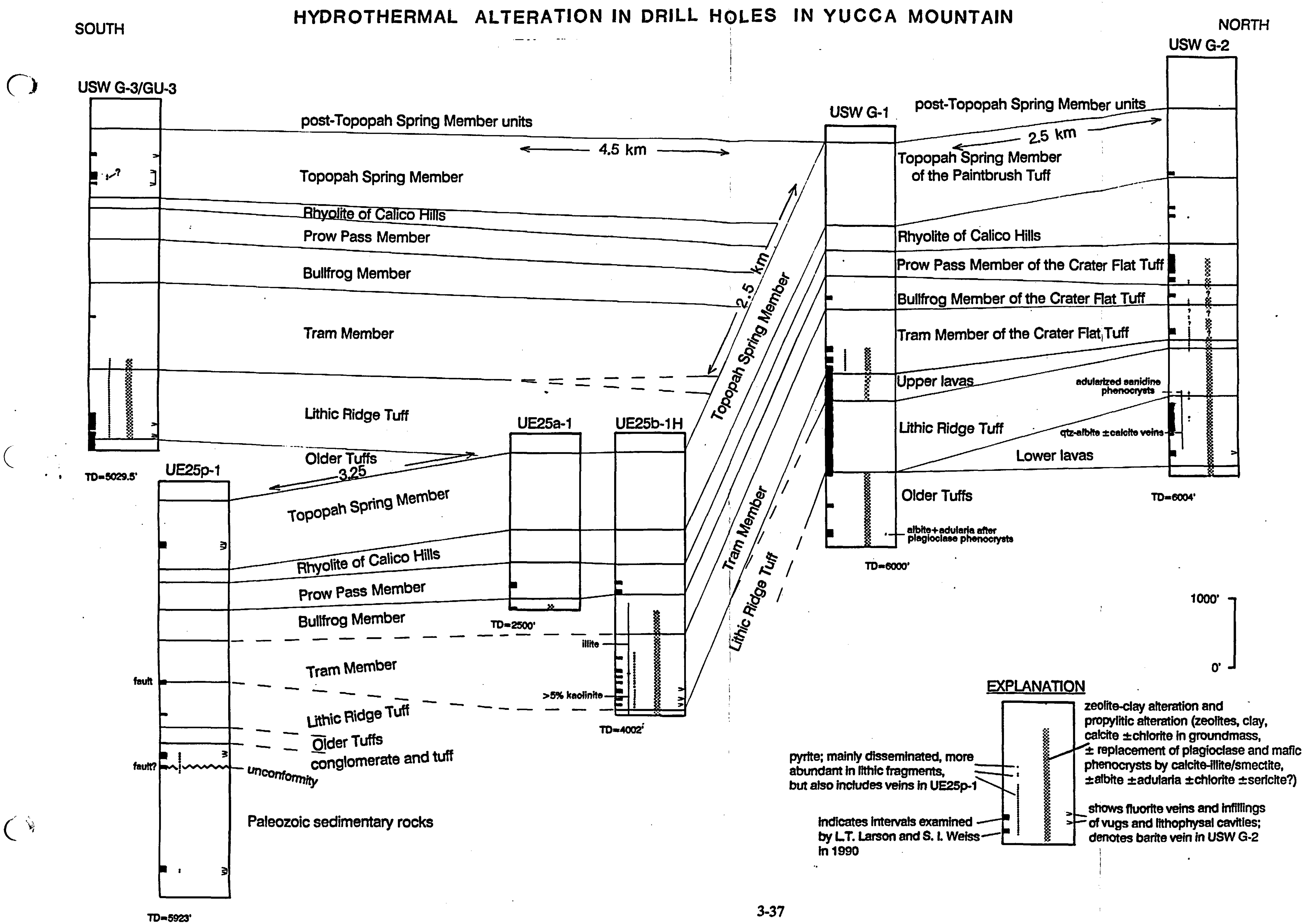

Figure 1. Subsurface stratigraphy and hydrothermal alteration features of deep drill holes in Yucca Mountain. Data from direct visual inspection by Task 3 and numerous published reports of the U. S. Geological Survey and the Los Alamos National Laboratory.

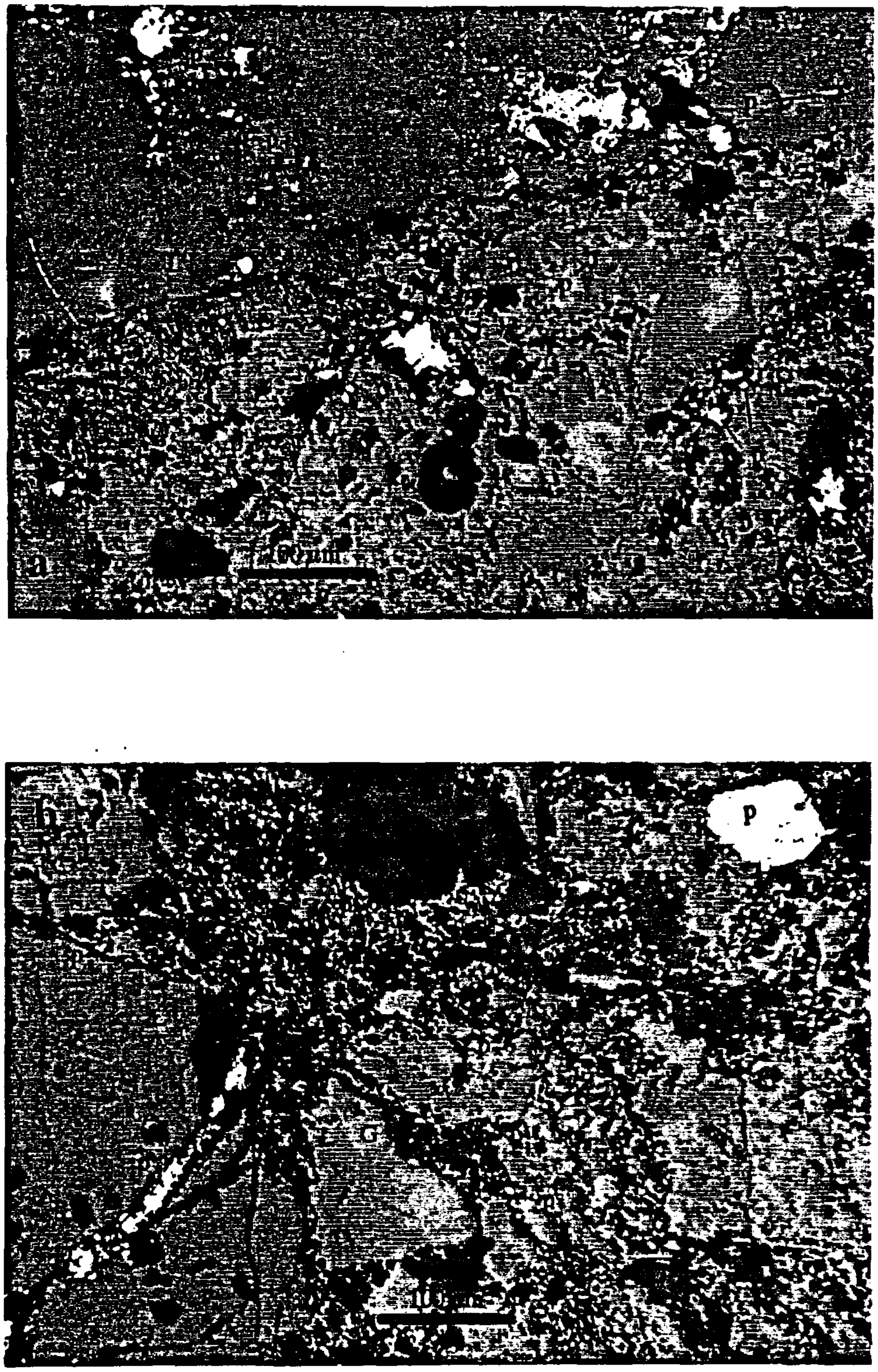

Figure 2. Pyrite in lithic fragments and groundmass of the Tram Member of the Crater Flat Tuff from drill hole UE25-B1H, SMF sample # 16954, including both disseminated and vein pyrite. p = pyrite, G = groundmass, L = lithic fragment.

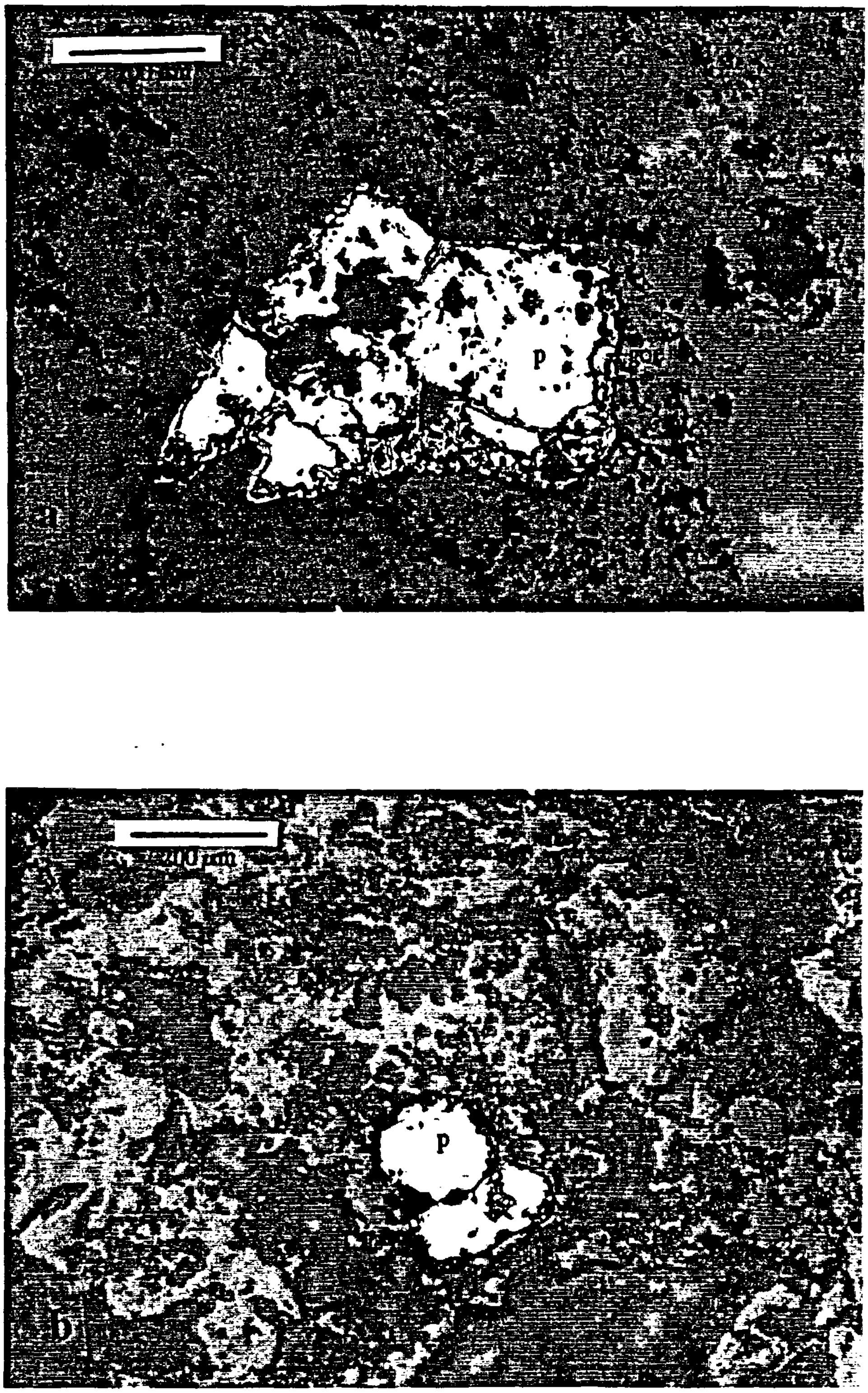

Figure 3. Poorly formed pyrite in the groundmass of the Lithic Ridge Tuff from drill hole USW-G3.
a) SMF sample # 16935. b) SMF sample # 16932. p = pyrite, goe = goethite.

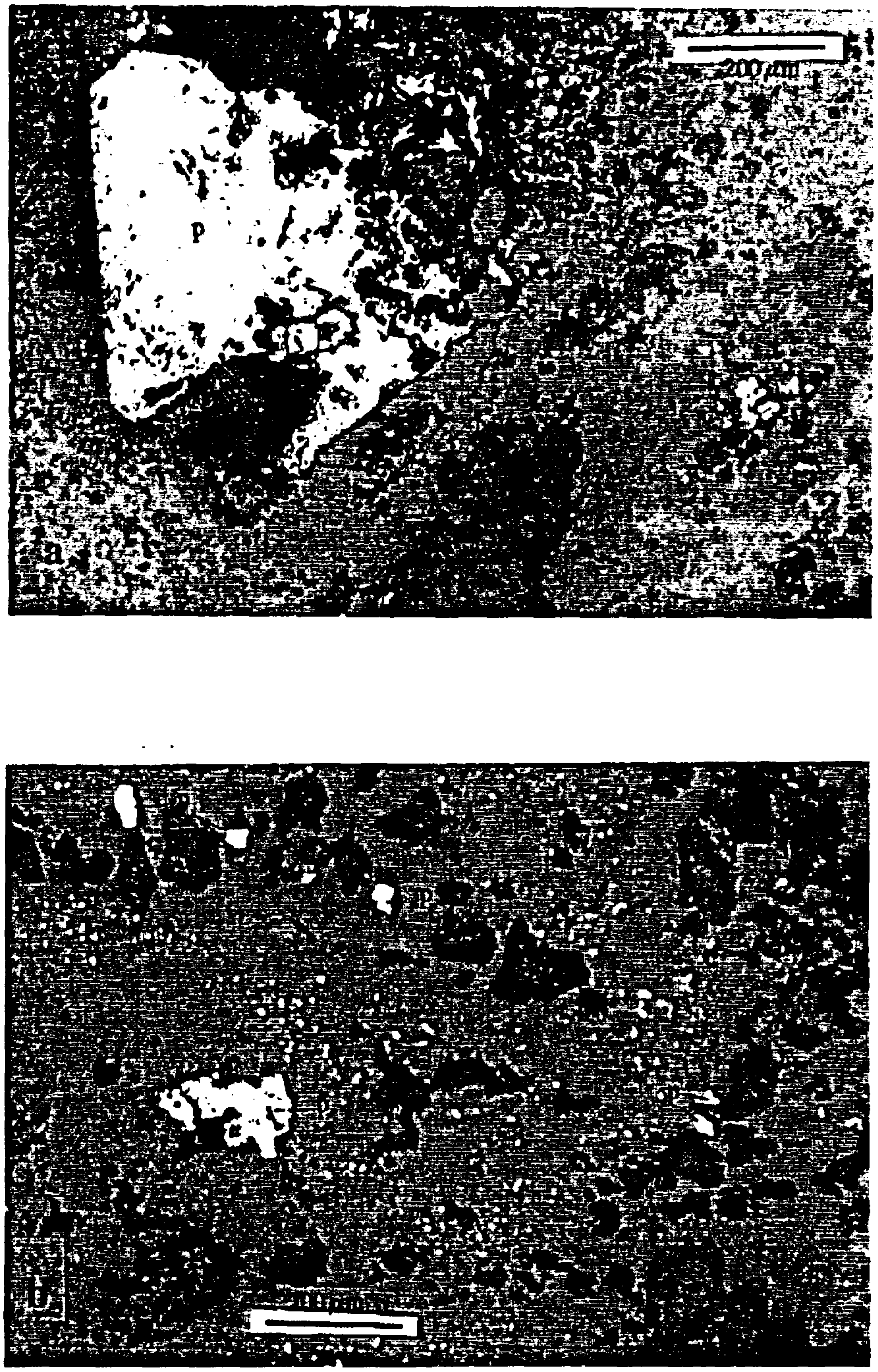

Figure 4. Disseminated pyrite in altered silicic lava from drill hole USW-G2, SMF sample # 16887. a) large, inclusion-bearing, pitted to seived, subhedral pyrite grain. b) small subhedral pyrite grains and larger, anhedral skeletal grain. p = pyrite

Figure 5. a) Partial sulphidation of biotite phenocryst in the Lithic Ridge Tuff from drill hole USW-G3, SMF sample # 16932. b) pyrite rimming and within clay altered pumice fragment in the Tram Member of the Crater Flat Tuff from drill hole UE25-B1H, SMF sample #16859. p = pyrite.

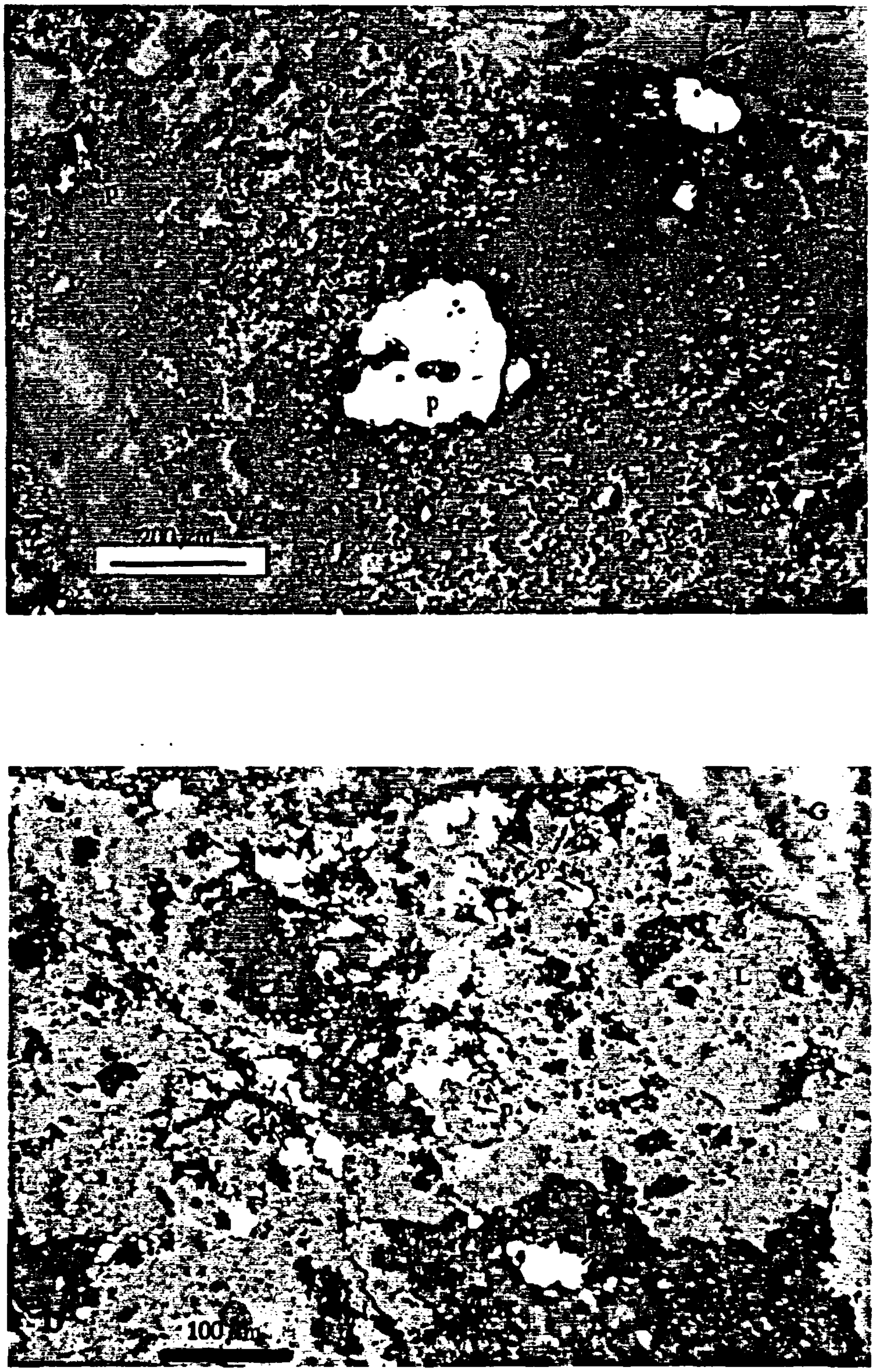

Figure 6. Pyrite in groundmass (a) and porous lithic fragment (b) of the Tonopah Summit Member of the Fraction Tuff (Bonham and Garside, 1979) from the Belcher Divide mine, Divide mining district, Esmeralda County, Nevada. Note anhedral, pitted and ophitic to wormy morphology of the pyrite. p = pyrite, G = groundmass, L = lithic fragment.

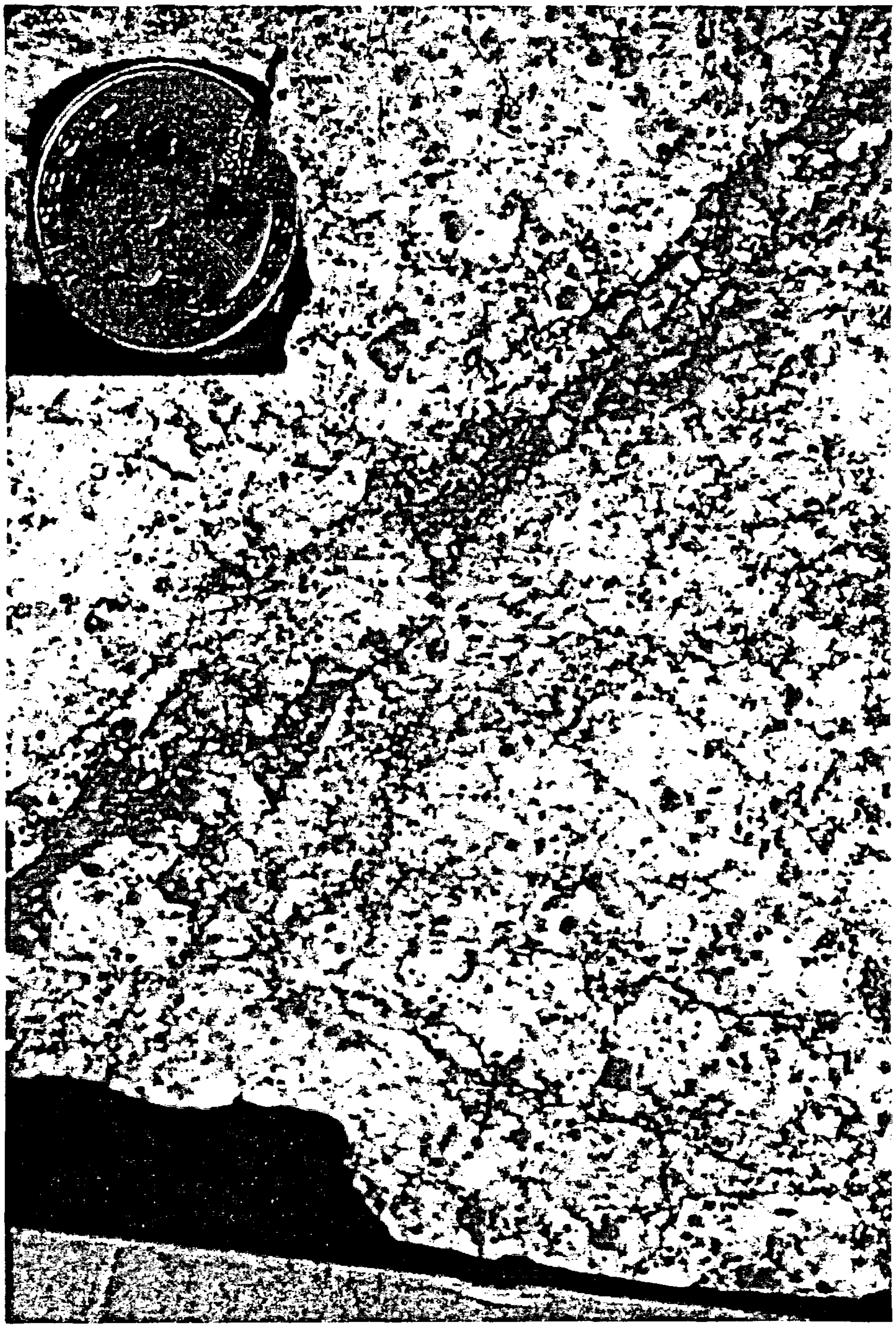

Figure 7. Oxidized Crater Flat Tuff with iron-oxide cemented breccia vein, SMF sample # 20069, drill hole UE25-C3.

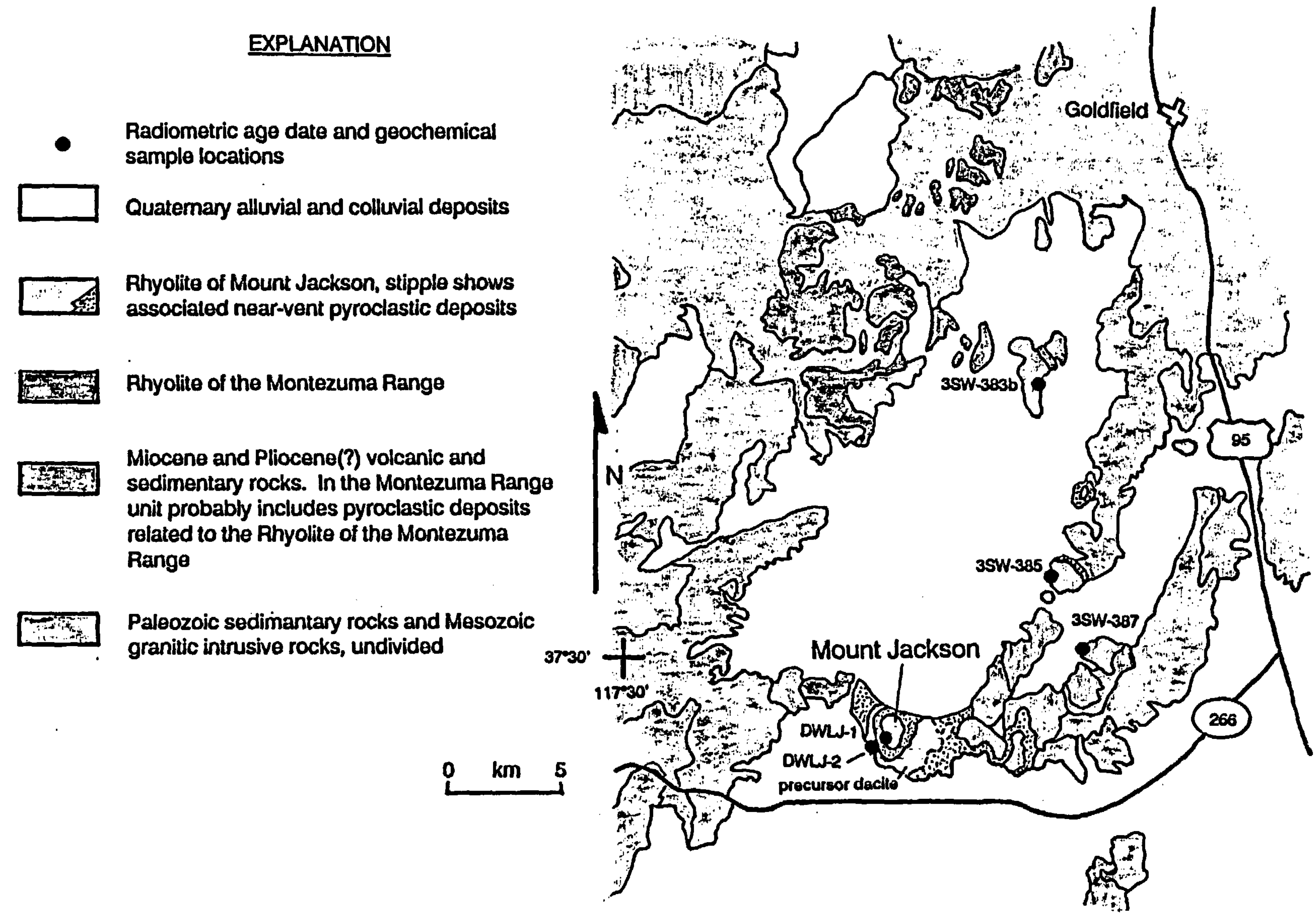

Figure 8. Simplified geologic map of the Mount Jackson dome field. Modified from Albers and Stewart (1972)

APPENDIX A

The initial gold contents of silicic volcanic rocks

Katherine A. Connors, Donald C. Noble,
Mackay School of Mines, University of Nevada-Reno, Reno, NV 89557
Steven D. Bussey
Western Mining Corp., (USA), 240 S. Rock Blvd., Suite 137, Reno, NV 89502
Steven I. Weiss
Mackay School of Mines, University of Nevada-Reno, Reno, NV 89557

ABSTRACT

Fresh silicic volcanic rocks have markedly lower initial gold contents than would be inferred from much of the geochemical literature. The great majority of 129 carefully selected glassy silicic volcanic rocks analyzed contain less than 1.0 ppb, and many contain only $\leq$ 0.1 to 0.3 ppb Au. Nonperalkaline rhyolites contain <0.1 to 0.7 ppb, mean 0.22 ppb Au; of these, highly evolved, high-silica subalkaline and peraluminous rhyolites have the lowest Au contents. Peralkaline and iron-rich subalkaline rhyolites have higher gold contents of 0.2 to 4.5 ppb, mean about 1 ppb. The mean of 23 relatively silicic intermediate rocks is 0.54 ppb Au, with tholeiitic andesites (icelandites) generally higher in gold than calc-alkalic types. Fundamental controls on the initial gold content of silicic volcanic rocks appear to be melt structure and petrologic affinity; regional setting is less important. High-silica nonperalkaline rhyolite melts apparently do not readily accommodate gold, whereas crystal fractionation appears to increase the gold concentration in less-polymerized peralkaline melts. Bulk composition and melt structure, and the amount and timing of separation of vapor, mineral, and sulfide or metal melt phases, may largely determine the gold content of silicic magmas on eruption. Silicic and intermediate volcanic rocks, particularly high-silica nonperalkaline rhyolites, appear to be less favorable sources of gold for hydrothermal mineral deposits than crystallizing magmatic bodies or other, more gold-rich, rock types. Although iron-rich rhyolites may have contributed to development of certain deposits, factors other than associated volcanic rock type appear to be more important in determining gold availability to hydrothermal systems.

INTRODUCTION

There are remarkably few reliable data on the gold contents of fresh volcanic rocks in view of the importance of gold in the mineral industry, the intimate association of several types of gold deposits with high-level magmatic activity, the fact that many precious metal deposits are hosted by volcanic rocks, and the availability of analytical techniques for determining very low concentrations of gold. We have measured the gold contents of a variety of fresh, glassy volcanic rocks, most of silicic composition, with the principal objectives being to: 1) better define the range of initial gold contents, 2) determine if gold content is related to petrochemical type and degree of differentiation/evolution and, 3) determine if rocks of areas with different geologic setting and history have significantly different gold contents. Our findings bear on problems of geochemical exploration, the genesis of hydrothermal precious-metal deposits, and more general petrologic and geochemical questions.

The average gold content of felsic volcanic rocks is commonly given as between 2 and 4 ppb (Table 1). Work by Gottfried et al. (1972) and Bornhorst et al. (1986) suggests considerably lower values, of about 0.1 to 2.0 ppb, for generally fresh silicic and intermediate volcanic rocks. Our ongoing studies (Connors et al., 1990, 1991) have produced a body of data showing that rocks careful selected to represent *initial* gold contents typically contain less than 1 ppb Au, and in many cases 0.1 ppb or less.

Crocket (1991), who gives an average of 1.55 ppb for silicic volcanic rocks, based in large part on data sets that include numerous individual values much higher than any observed in the above studies, notes that "the lowest gold contents in felsic volcanics are from the western US localities (Gottfried et al., 1972), where averages of <1 ppb apply". Interestingly, these values of <1 ppb were common in the one study that carefully documents preparation and analysis. All other felsic volcanic suites included by Crocket are of pre-Cenozoic age, from the former Soviet Union, and give averages of >1 ppb Au. Indeed, rocks from one region have an average value of 9.6 ppb with a range of 1.5 to 22.5 ppb. Crocket (1991) suggests that the low gold contents found in the western U.S. may reflect regional variation or analytical bias at these very low gold concentrations. We believe that the average of 1.55 ppb given by Crocket (1991) is strongly influenced by the relatively high averages for suites of samples to which gold has been added by groundwater and/or hydrothermal solutions.

Sample Selection, Preparation and Analysis

Many factors influence the initial gold content of volcanic rocks. These include: 1) gold content of the original source material(s), 2) degree of partial melting and other aspects of magma generation, 3) magma differentiation, mixing and assimilation, and 4) magmatic outgassing at depth and on eruption with possible fractionation of gold into the vapor phase. These factors are presently difficult to quantify. Careful sample selection can, however, minimize or eliminate changes resulting from loss, migration, and/or addition of gold during primary crystallization, or later by circulating hydrothermal fluid or groundwater.

Glassy volcanic rocks, unlike plutonic and crystallized (devitrified) volcanic rocks, are essentially unaffected by circulating fluids during crystallization and cooling, and therefore more closely represent the composition of the magma upon eruption. Halogens and many other elements may be lost from silicic melts and volcanic rocks before, during or shortly after primary crystallization (e.g., Noble et al., 1967; Haffty and Noble, 1972; Stuart et al., 1983; Webster and Duffield, 1991). Studies of fumarolic gases and precipitates (e.g., Symonds et al., 1987; Anderson, 1991) suggest that gold and many other metals may be removed, transported by high-temperature magmatic gases, and concentrated in fumarolic encrustations, including those of "rootless" systems such as the hot pyroclastic flows of the Valley of Ten Thousand Smokes (Zies, 1929; Papike et al., 1991). Keays and Scott (1976) demonstrated that gold is largely lost from fresh, crystallized interiors of ocean-ridge basalt pillows relative to their glassy rims, suggesting crystallization makes gold readily available to solution mobilization. Moreover, devitrified and vapor-phase crystallized silicic volcanic rocks are more readily subject to the addition of various elements, presumably including gold, both during crystallization and from groundwater after crystallization, because of their porosity, the great surface area of the finely crystalline groundmass material and the presence of iron oxides, etc.

For these reasons we have used glassy rocks in preference to primarily crystallized (devitrified) specimens to minimize the effects of possible post-eruption loss and addition of gold. Nonhydrated glassy specimens, which have behaved as completely closed systems since cooling (Rosholt et al., 1971), were used wherever possible. Where such materials were not available, dense hydrated glassy rocks (vitrophyres) free of observable alteration were analyzed. Because of the ubiquity of gold in the home and laboratory, special care was taken to avoid contamination during sample collection and preparation.

Gold contents were determined by XRAL Activation Services, Inc. using procedures similar to those of Rowe and Simon (1968). Neutron activation was done prior to fire-assay collection of gold to eliminate contamination during the fire-assay procedure. Two grams of sample, instead of one as generally used, were analyzed to decrease the effects of sample inhomogeneity and to slightly lower the nominal detection limit of 0.1 ppb. Analyses of a single split of U.S.G.S. standard RGM-1 gave values of 0.61 and 0.67 ppb Au; these agree well with values of from 0.4 to 0.8, mean 0.6 ± 0.05 ppb for three runs on each of six splits of RGM-1 reported by Gottfried et al. (1972). Ten samples were run twice, and most results agreed within 0.1 ppb. A nonhydrated comendite glass analyzed 14 times between August, 1990, and January, 1992, yielded values of from 0.9 to 1.1 ppb Au. Petrochemical affinity was inferred from petrologic and major and minor element data.

RESULTS

A total of 129 samples of tuff and lava, largely from the Great Basin of the western United States, were analyzed. Most were from various centers in southern and northwestern Nevada. Samples also include rocks from the Long Valley and Little Walker volcanic centers, and various centers in the eastern Great Basin, as well as specimens from other regions, including Idaho, Colorado, Ethiopia, Mexico, Peru, and Japan.

Our data indicate that the great majority of silicic volcanic rocks have very low original gold contents (Fig. 1). Most contain considerably less than 1 ppb gold and many, particularly very highly evolved, high-silica subalkaline and peraluminous rhyolites, contain 0.1 ppb or less. Subalkaline high-Si rhyolites, which have low Ca and Fe, have extremely low gold contents, most between <0.1 and 0.3 ppb (Figs. 1A, 2A). The mean and median of 23 samples are about 0.2 ppb and the maximum is 0.6 ppb. Eight peraluminous (S-type and topaz) rhyolites also have uniformly very low gold contents of <0.1 to 0.5 ppb with mean and median values of 0.15 and 0.1 ppb, respectively (Fig. 1A, 2A). This suite includes samples from Spor Mountain and the Honeycomb Hills in west-central Utah (Christiansen et al., 1986) and aluminosilicate-bearing ash-flow tuff and Macusani glass from southeastern Perú (Noble et al., 1984), which contain very high contents of such elements as Li, Rb, Cs, F, Ta, and Nb, but only 0.1-0.2 ppb Au. Low- to medium-silica subalkaline rhyolites, which are less evolved and have higher Fe and Ca have only slightly higher gold contents of from <0.1 to 0.8, mean 0.26 ppb (Fig. 1B, 2B). Iron-rich subalkaline rhyolites (tholeiitic or ferrorhyolites - filled symbols on Fig. 1B) have generally higher gold contents of from 0.4 to 0.8 ppb.

Peralkaline rhyolites contain appreciably more gold. A suite of 37 samples ranges from 0.2 to 4.5, average 1.0 ppb Au (Fig. 1C). However, there is no obvious correlation between *degree* of peralkalinity and gold content. The highest gold values (4.5 and 3.2 ppb) obtained are from slightly peralkaline comendites, whereas pantellerite glasses from Ethiopia and southern Nevada, the highly peralkaline samples, contain only 0.2 ppb and 0.6 ppb Au, respectively.

The silicic rocks can be divided into distinct high- and low-gold groups (Fig. 3). The low-gold group includes subalkaline and peraluminous rhyolites with various silica contents and degrees of evolution (Fig. 3A), which have from <0.1 to 0.7 ppb, average 0.22 ppb Au. The high-gold group includes the peralkaline rhyolites and the iron-rich, nonperalkaline rhyolites and dacites, with Au contents between 0.2 and 4.5 ppb. More than 30 percent of the peralkaline rhyolites have gold contents of 1.0 to 4.5 ppb and 70 percent have 0.6 ppb or more Au. Even the average for the high-gold group of 0.96 ppb Au is much lower than the commonly cited average gold content of silicic volcanic rocks of 3-4 ppb. It should be specifically pointed out that our sampling has markedly overemphasized peralkaline rocks relative to their abundance in nature, and unweighted averaging of our entire data set would produce an overestimation of the average initial gold contents of salic volcanic rocks.

The mean and median of 0.54 and 0.4 ppb Au respectively for 23 relatively silicic intermediate rocks (Fig. 1D), are slightly higher than those for subalkaline and peraluminous silicic rocks. The higher gold concentrations are generally found in rocks with tholeiitic affinity, with iron-rich tholeiitic andesites (icelandites) being somewhat higher in gold than calc-alkalic types (Fig. 1D). Five specimens of icelandite from the McDermitt caldera complex (Wallace et al., 1980) and three specimens from the High Rock Canyon icelandite-ferrodacite field, northwestern Nevada, have a mean value of 0.8 ppb. Similar relatively high gold contents have been found in the Fe-rich differentiates of Tertiary basalts in Iceland (Zentilli et al., 1985).

Correlation Between Petrochemistry and Gold Content:

There is a general trend of increasing gold with increasing iron but iron content alone does not allow prediction of the gold content of a rock. A better correlation is obtained when both Ca and Fe are used. Figure 2 is the same type of plot used by Warshaw and Smith (1988), but with logarithmic axes to better display samples with low Fe and Ca. The diagrams show a distinct division between rock types, with a general increase in gold content with increasing FeO/CaO. The subalkaline and peraluminous rhyolites plot in the lower portion of the diagram, and the peralkaline rocks in the upper left, reflecting their higher iron contents and higher Fe/Ca ratios. Warshaw and Smith (1988) demonstrated a general trend of decreasing fO_2 with increasing FeO/CaO; the importance of low fO_2 in stabilizing gold in melts can be inferred from the higher gold contents of the peralkaline and tholeiitic subalkaline rocks. When evaluated in detail, relations may prove more complicated. For example, the compositionally complex Summit Lake Tuff in NW Nevada (Noble et al., 1970) shows no simple relationship between major element chemistry and gold content.

Regional Variations in Initial Gold Content

The gold contents of the silicic volcanic rocks analyzed in this study are consistently low, irrespective of geographical location. The gold contents of specimens from Colorado (0.5 and 0.1 ppb), Mexico (0.08 and 0.16 ppb), Peru (9 rocks with Au from 0.1 to 1.2, avg. 0.4 ppb), Japan (0.36 ppb) and Ethiopia (0.2 ppb) correspond well with samples of similar composition from the western U.S. (both this study and Gottfried et al., 1972). The data give no indication that the low gold concentrations seen in the western United States are a regional phenomena as suggested by Crocket (1991).

Sample suites from northwest Nevada and the Southwest Nevada volcanic field provide a measure of the influence of differences in regional geology on gold contents. Sr and Nd isotope data suggest that volcanic rocks in northwest Nevada have little or no crustal component (Tegtmeyer and Farmer, 1987) whereas volcanic rocks in southwest Nevada show evidence of a considerable crustal component (Farmer et al., 1991). The major differences between the average gold contents of rocks from the two regions (Fig. 4) are largely explained by the much higher ratio of peralkaline to nonperalkaline rhyolite in northwestern Nevada. We conclude that although regional setting may exert some subtle influence on gold content, the most important control appears to be petrologic affinity. Even in the NW Great Basin, where Neogene silicic volcanic rocks are closely associated in space and time, and probably genetically, with large volumes of continental flood basalts, which as a group appear to have higher gold contents than other basalts (Gottfried et al., 1973; Bird et al., 1991), four nonperalkaline rhyolites have gold contents of only 0.1, 0.2, 0.25, and 0.36 ppb. In our suite of silicic rocks, variations with regional setting are evident only in the dominance of particular petrologic types.

Controls on gold content

Our data suggest that the elevated gold contents of many peralkaline rocks is largely a function of the compatible behavior of gold in peralkaline melts, although mixing and perhaps wall rock assimilation may account for the higher than average gold concentrations of some samples. That significant amounts of gold can be carried in slightly peralkaline rhyolite melts is demonstrated by 15 specimens of aphyric, nonhydrated comendite obsidian from northwestern and southern Nevada that contain from 0.6 to 4.5 ppb Au. Also, densely welded, phenocryst-rich glassy tuff from the Soldier Meadow Tuff, NW Nevada (Korringa, 1973), contains 0.6 ppb Au, whereas nonhydrated glassy groundmass material from the rock contains 0.9 ppb Au.

The relatively high gold contents of the peralkaline rhyolites may reasonably be explained by retention of gold in the residual liquid during phenocryst separation in a manner similar to that generally accepted for the elevated Fe, Zr, REE, Nb, etc., contents of such rocks (e.g., Noble, 1968; Mahood and Hildreth, 1983). Zentilli et al. (1985) show that Au correlates positively with Y, Zr and other indicators of differentiation, and suggest that Au has been systematically partitioned into the evolving melt. Conversely, the extremely low gold contents of many high-silica nonperalkaline rhyolites would appear to require removal of the gold during differentiation (Tilling et al., 1973), and/or during degassing.

A fundamental control of the different gold contents of these two types of silicic rocks therefore appears to be melt structure. High-silica rhyolites, containing small amounts of Ca and Fe, are highly polymerized and a wide range of minor elements, apparently including gold, are not accommodated. Higher contents of network-modifying cations, particularly iron and alkalies in excess of that required to balance the aluminum present, as well as water and halogens, depolymerize silicate melts. This markedly reduces the partition coefficients of minor elements between the melt and the separating crystal (Drexler et al., 1983; Mahood and Hildreth, 1983) and presumably also immiscible melt phases. Gold content will be controlled by the amount and timing of separation of mineral phases capable of siting gold, such as Fe oxides, and of sulfide melt and perhaps liquid metal phases (Bornhorst and Rose, 1986; Bird et al., 1991), as well as by the degree to which gold is accommodated within the melt. Another major control may be volatile loss, which would effectively remove gold and other metals strongly partitioned into the vapor phase (e.g., Symonds et al., 1987; Lowenstern et al., 1991).

DISCUSSION AND CONCLUSIONS

Initial gold contents of silicic volcanic rocks, irrespective of geographical location, are lower than indicated in much of the geochemical literature. Fresh, glassy volcanic rocks typically have original gold contents much lower than the 4 ppb commonly quoted for igneous rocks. Average values range from about 0.15 ppb for peraluminous rhyolites to about 1.0 ppb for peralkaline rhyolites. Our results are much lower than those reported in the Russian literature (e.g., Korobeynikov, 1989) and average values given in geochemical texts and reviews (Table 1). These higher values reflect, we believe, the addition of small but significant amounts of gold to older and probably altered rocks. Indeed, it is likely that some of the Cenozoic silicic volcanic rocks analyzed by Gottfried et. al (1973) contain gold added by post-depositional processes.

Original gold content of silicic volcanic rocks appear to depend more on petrochemical type and degree of differentiation/evolution than on regional setting. Rocks with high Fe contents and Fe/Ca ratios have generally higher gold contents than rocks of more calc-alkalic character (Fig. 2). We speculate that this is largely due to differences in melt structure and fO_2 and the amount and timing of separation of crystal, liquid sulfide and metal (?), and volatile phases.

High-silica subalkaline rhyolites appear to be poor sources of gold for the formation of gold deposits. Very large volumes of rock would have to be leached by hydrothermal solutions.

Economic epithermal deposits in subalkaline silicic terranes would appear to require contributions of gold from other, more gold rich, igneous or sedimentary rocks and/or from known or inferred intrusive bodies that drove the hydrothermal systems.

Peralkaline silicic rocks, other iron-rich silicic and intermediate rocks, and mafic rocks (Gottfried et al., 1973) are more viable potential sources of gold. Mafic rocks and magmas are the only possible source material in deposits such as those on Lihir Island, Papua New Guinea (Moyle et al., 1990), and are attractive sources in continental areas with coeval large-volume basaltic magmatism (Noble et al., 1988). Certain deposits, for example Hog Ranch in northwestern Nevada, and prospects in the Challis volcanic field, Idaho, are associated in time and space with peralkaline rhyolite and ferrorhyolite (Harvey et al., 1986; Hardyman and Fisher, 1985; Hardyman and Noble, 1989). However, even the relatively gold-rich peralkaline rocks analyzed in this study contain very modest absolute concentrations of gold. The lack of an obvious preferential association of gold mineralization with volcanic fields dominated by peralkaline and subalkaline Fe-rich volcanic rocks, combined with the close association of Au$\pm$Ag mineralization with high-level magmatic (porphyry) systems, argues that factors such as contents of halogens, sulfur, water, etc., higher initial gold, and fO_2 conditions of magmas, are more important than volcanic rock type in controlling gold availability to hydrothermal systems in volcanic terranes. The common association of pronounced gold anomalies with intrusive related hydrothermal systems, the occurrence of hypogene porphyry ores containing $\geq$ 0.3 ppm Au, and evidence for the existence of metal-rich salic melts (e.g., Wilson 1978) all suggest the existence of atypical silicic to intermediate magmas with much higher gold contents. Indeed, silicic magmas may, in general, initially contain much higher concentrations of gold than observed in volcanic rocks, with a large fraction of this gold being removed, transported and possibly reconcentrated by magmatic degassing during and/or prior to eruption.

The very low initial gold content of most rhyolites make rocks and alluvium in silicic volcanic terranes very sensitive to the addition of small amounts of gold by groundwater as well as by hydrothermal solutions. Such terranes will be particularly amenable to ultra-low detection limit soil and rock geochemical surveys. Low-level anomalies have the potential to delineate structural features that may have controlled addition of gold by post-depositional processes that include upward migration as volatile complexes during primary cooling, and migration in surface and groundwater as well as by hydrothermal activity.

REFERENCES CITED

Allman, R., and Crocket, J.H., 1978, Gold, *in* Wedepohl, K.H., ed., Handbook of geochemistry: New York, Springer-Verlag, section 79, p. A1-O1.

Anderson, A.T., 1992, Subvolcanic degassing of magma: Extended abstracts, Japan-U.S. Seminar on Magmatic Contributions to Hydrothermal Systems: Geological Survey of Japan Report 279 (in press).

Bird, D.K., Brooks, C.K., Gannicott, R.A., and Turner, P.A., 1991, A gold-bearing horizon in the Skaergaard intrusion, East Greenland: Economic Geology, v. 86, p. 1083-1092.

Boyle, R.W., 1979, The geochemistry of gold and its deposits (together with a chapter on geochemical prospecting for the element): Geological Survey of Canada Bulletin 280, 584 p.

Bornhorst, T.J., and Rose, W.I., Jr., 1986, Partitioning of gold in young calc-alkalic volcanic rocks from Guatemala: Journal of Geology, v. 94, p. 412-418.

Christiansen, E.H., Sheridan, M.F., and Burt, D.M., 1986, The geology and geochemistry of Cenozoic topaz rhyolites from the western United States: Geological Society of America Special Paper 205, 82 p.

Connors, K.A., Weiss, S.I., Noble, D.C., and Bussey, S.D., 1990, Primary gold contents of some silicic and intermediate tuffs and lavas: Evaluation of possible igneous sources of gold: Geological Society of America Abstracts with Programs, v. 22, n. 7, p. 135.

Connors, K.A., Noble, D.C., Weiss, S.I., and Bussey, S.D., 1991, Compositional controls on the gold contents of silicic volcanic rocks: Association of Exploration Geochemists, 15th International Geochemical Exploration Symposium, Abstracts with Programs, p. 43.

Crocket, J.H., 1991, Distribution of gold in the earth's crust, *in* Foster, R.P., ed., Gold metallogeny and exploration: Blackie, Glasgow and London, p. 1-36.

Drexler, J.W., Bornhorst, T.J., and Noble, D.C., 1983, Trace-element sanadine/glass distribution coefficients for peralkaline silicic rocks and their implications for peralkaline petrogenesis: Lithos, v. 16, p. 265-271.

Farmer, G.L., Broxton, D.E., Warren, R.G., and Pickthorn, W., 1991, Nd, Sr, and O isotopic variations in metaluminous ash-flow tuffs and related volcanic rocks at the Timber Mountain/Oasis Valley Caldera, Complex, SW Nevada: implications for the origin and evolution of large-volume silicic magma bodies: Contributions to Mineralogy and Petrology, v. 109, p. 53-68.

Gottfried, David, Rowe, J.J., and Tilling, R.I., 1972, Distribution of gold in igneous rocks: U.S. Geological Survey Professional Paper 727, 42 p.

Hardyman, R.F. and Fisher, F.S., 1985, Rhyolite intrusions and associated mineral deposits in the Challis volcanic field, Challis quadrangle, *in* McIntyre, D.H., ed., Symposium on the geology and mineral deposits of the Challis 1°x2°quadrangle, Idaho: U.S. Geological Survey Bulletin 1658 A-S, p. 167-179.

Hardyman, R.F., and Noble, D.C., 1989, Late iron-rich pyroxene±fayalitic olivine bearing silicic tuffs, lavas, and intrusions of the Eocene Challis volcanic field, central Idaho [abs.]: Geological Society of America Abstracts with Programs, v. 21, p. 90.

Harvey, D.S., Noble, D.C., and McKee, E.H., 1986, Hog Ranch gold property, northwest Nevada: age and genetic relation of hydrothermal mineralization to coeval peralkaline silicic and associated basaltic magmatism: Isochron/West, n. 47, p. 9-11.

Haffty, J., and Noble, D.C., 1972, Release and migration of molybdenum during primary crystallization of peralkaline silicic volcanic rocks: Economic Geology, v. 67, p. 768-775.

Keays, R.R., and Scott, R.B., 1976, Precious metals in ocean-ridge basalts: Implications for basalts as source rocks for gold mineralization: Economic Geology, v. 71, n. 4, p. 705-720.

Korobeynikov, A.F., 1989, Gold in volcanic rocks: Geochemistry International, v. 26, n. 6, p. 74-82. (translated from Geokhimiya, n. 11, p. 1618-1626, 1988)

Korringa, M.K., 1973, Linear vent area of the Soldier Meadow Tuff, an ash-flow sheet in northwestern Nevada: Geological Society of America, Bulletin, v. 84, p. 3849-3866.

Levinson, A.A., 1980, Introduction to exploration geochemistry, 2nd edition: Wilmette, Illinois, Applied Publishing, Ltd., 924 p.

Lowenstern, J.B., Mahood, G.A., Rivers, M.L., and Sutton, S.R., 1991, Evidence for extreme partitioning of copper into a magmatic vapor phase: Science, V. 252, p. 1405-1409.

Mahood, Gail, Hildreth, Wes, 1983, Large partition coefficients for trace elements in high-silica rhyolites: Geochimica et Cosmochimica Acta, v. 47, p. 11-30.

Moyle, A.J., Doyle, B.J., Hoogvliet, H., and Ware, A.R., 1990, Ladolam gold deposit, Lihir Island, *in* Hughes, F.E., ed., Geology of the mineral deposits of Australia and Papua New Guinea: Australian Institute of Mining and Metallurgy, Melbourne, p. 1793-1805.

Noble, D.C., 1968, Systematic variation of major elements in comendite and pantellerite glasses: Earth and Planetary Science Letters, v. 4, p. 167-172.

Noble, D.C., McCormack, J.K., McKee, E.H., Silberman, M.L., and Wallace, A.B., 1988, Time of mineralization in the evolution of the McDermitt caldera complex, Oregon-Nevada, and the relation of middle Miocene mineralization in the northern Great Basin to coeval regional basaltic magmatic activity: Economic Geology, v. 83, p. 859-863.

Noble, D.C., McKee, E.H., Smith, J.G., and Korringa, M.K., 1970, Stratigraphy and geochronology of Miocene volcanic rocks in northwestern Nevada: U.S. Geological Survey Professional Paper 700-D, p. 23-32.

Noble, D.C., Smith, V.C., and Peck, L.C., 1967, Loss of halogens from crystallized and glassy silicic volcanic rocks: Geochimica et Cosmochimica Acta, v. 31, p. 215-223.

Noble, D.C., Vogel, T.A., Peterson, P.S., Landis, G.P., Grant, N.K., Jezek, P.A., and McKee, E.H., 1984, Rare-element-enriched, S-type ash-flow tuffs containing phenocrysts of muscovite, andalusite, and sillimanite, southeastern Peru: Geology, v. 12, p. 3539.

Papike, J.J., Keith, T.E.C., Spilde, M.N., Galbreath, K.C., Shearer, C.K., and Laul, J.C., 1991, Geochemistry and mineralogy of fumarolic deposits, Valley of Ten Thousand Smokes, Alaska: Bulk chemical and mineralogical evolution of dacite-rich protolith: American Mineralogist, v. 76, p. 1662-1673.

Romberger, S.B., 1988, Geochemistry of gold in hydrothermal deposits: Geology and resources of gold in the United States, Chapter A, Introduction to geology and sources of gold, and geochemistry of gold: U.S. Geological Survey Bulletin 1857, p. A9-A25.

Rose, A.W., Hawkes, H.E., and Webb, J.S., 1979, Geochemistry in mineral exploration: London, Academic Press, 657 p.

Rosholt, J.N., Prihana, and Noble, D.C., 1971, Mobility of uranium and thorium in glassy and crystallized silicic volcanic rocks: Economic Geology, v. 66, p. 1061-1069.

Rowe, J.J., and Simon, F.O., 1968, The determination of gold in geologic materials by neutron-activation analysis using fire assay for the radiochemical separations: U.S. Geological Survey Circular 599, 4 p.

Stuart, E.J., Bornhorst, T.J., Rose, W.I., Jr., and Noble, D.C., 1983, Distribution and mobility of uranium and thorium in the peralkaline Soldier Meadow Tuff, northwestern Nevada: Economic Geology, v. 78, p. 353-358.

Symonds, R.B., Rose, W.I., Reed, M. H., Lichte, F.E., and Finnegan, D.L., 1987, Volatilization, transport and sublimation of metallic and non-metallic elements in high temperature gases at Merapi Volcano, Indonesia: Geochimica et Cosmochimica Acta, v. 51, p. 2083-2101.

Tegtmeyer, K., and Farmer, G.L., 1987, Nd evidence for the origin of late Tertiary metaluminous and peralkaline rhyolite in the Great Basin: Eos, v. 68, p. 1512.

Tilling, R.I. Gottfried, D., and Rowe, J.J., 1973, Gold abundance in igneous rocks: Bearing on gold mineralization: Economic Geology, v. 68, p. 168-186.

Wallace, A.B., Drexler, J.W., Grant, N.K., and Noble, D.C., 1980, Icelandite and aenigmatite-bearing pantellerite from the McDermitt caldera complex, Nevada-Oregon: Geology, v. 8, p. 380-384.

Warshaw, C.M., and Smith, R.L., 1988, Pyroxenes and fayalites in the Bandelier Tuff, New Mexico: Temperatures and comparison with other rhyolites: American Mineralogist, v. 73, p. 1025-1037.

Webster, J.D. and Duffield, W.A., 1991, Volatiles and lithophile elements in Taylor Creek Rhyolite: Constraints from glass inclusion analysis: American Mineralogist, v. 76, p. 1628-1645.

Wilson, J.C., 1978, Ore fluid-magma relationships in vesicular quartz latite porphyry dike at Bingham, Utah: Economic Geology, v. 73, p. 1287-1307.

Zentilli, M., Brooks, R.R., Helgason, J., Ryan, D.E., and Zang, H., 1985, The distribution of gold in volcanic rocks of eastern Iceland: Chemical Geology, v. 28, p. 17-28.

Zies, E.G., 1929, The Valley of Ten Thousand Smokes: I. The fumarolic incrustations and their bearing on ore deposition. II. The acid gases contributed to the sea during volcanic activity: National Geographic Society, Contributed Technical Papers, Katmai Series, v. 4, p. 1-79.

ACKNOWLEDGEMENTS

Various aspects of this study were supported by the Geological Society of America, Mackay Minerals Research Institute, WAIIME, Nevada Nuclear Waste Project Office, and the U. S. Geological Survey Reno Field Office. Western Mining Corporation allowed access to samples and data from the Hog Ranch Mine, Eric Christiansen and Jeff Keith guided in sampling topaz rhyolites in west-central Utah, and Paul Lechler assisted with major-element analyses.

FIGURE CAPTIONS

Figure 1. Cumulative plots showing distribution of gold contents for different rock types. A: subalkaline high-silica rhyolite and peraluminous rhyolite (solid symbols), B: subalkaline low- to medium-silica rhyolite, C: peralkaline rhyolite, and D: rocks of intermediate composition. Solid symbols in 1B and 1D indicate iron-rich (tholeiitic) specimens.

Figure 2. Gold content as a function of Ca and Fe. A: high-silica rhyolites and peraluminous rhyolite, B: low- to medium-silica rhyolite and, C: peralkaline rhyolite.

Figure 3. Histograms of samples from the 'low gold' and 'high-gold' groups of silicic volcanic rocks. A: low-Fe subaluminous and peraluminous rhyolite, B: peralkaline rhyolite, ferrorhyolite and ferrodacite.

Figure 4. Cumulative frequency diagram for all samples from northwest and southwest Nevada, showing a comparison of the distribution of gold contents for the two regions. Solid symbols indicate peralkaline samples, symbols with cross-bars represent intermediate composition samples.

Table 1 -- Average Gold Contents of Silicic Volcanic Rocks Given in Review Papers and Texts

TABLE 1. AVERAGE GOLD CONTENTS OF SILICIC VOLCANIC ROCKS GIVEN IN REVIEW PAPERS AND TEXTS

Source and date	Rock Type/Suite	Au range, ppb	Au avg., ppb	No. of samples
Allman and Crocket (1978)	silicic volcanic rocks from various regions and averaged from various sources	1.0-3.5	1.8	11
		none given	1.79	2
		0.1-2.8	0.6	21
		0.4-5.5	2.3	4
Rose et al. (1979)	granitic	none given	2.3	??
Boyle (1979)	rhyolite, obsidian, etc.	0.1-113.0	3.7	372
Levinson (1980)	felsic igneous	none given	4.0	??
Romberger (1988)	rhyolite	0.5-3.5	1.5	188
Crocket (1991)	felsic volcanic rocks	none given	1.55	??

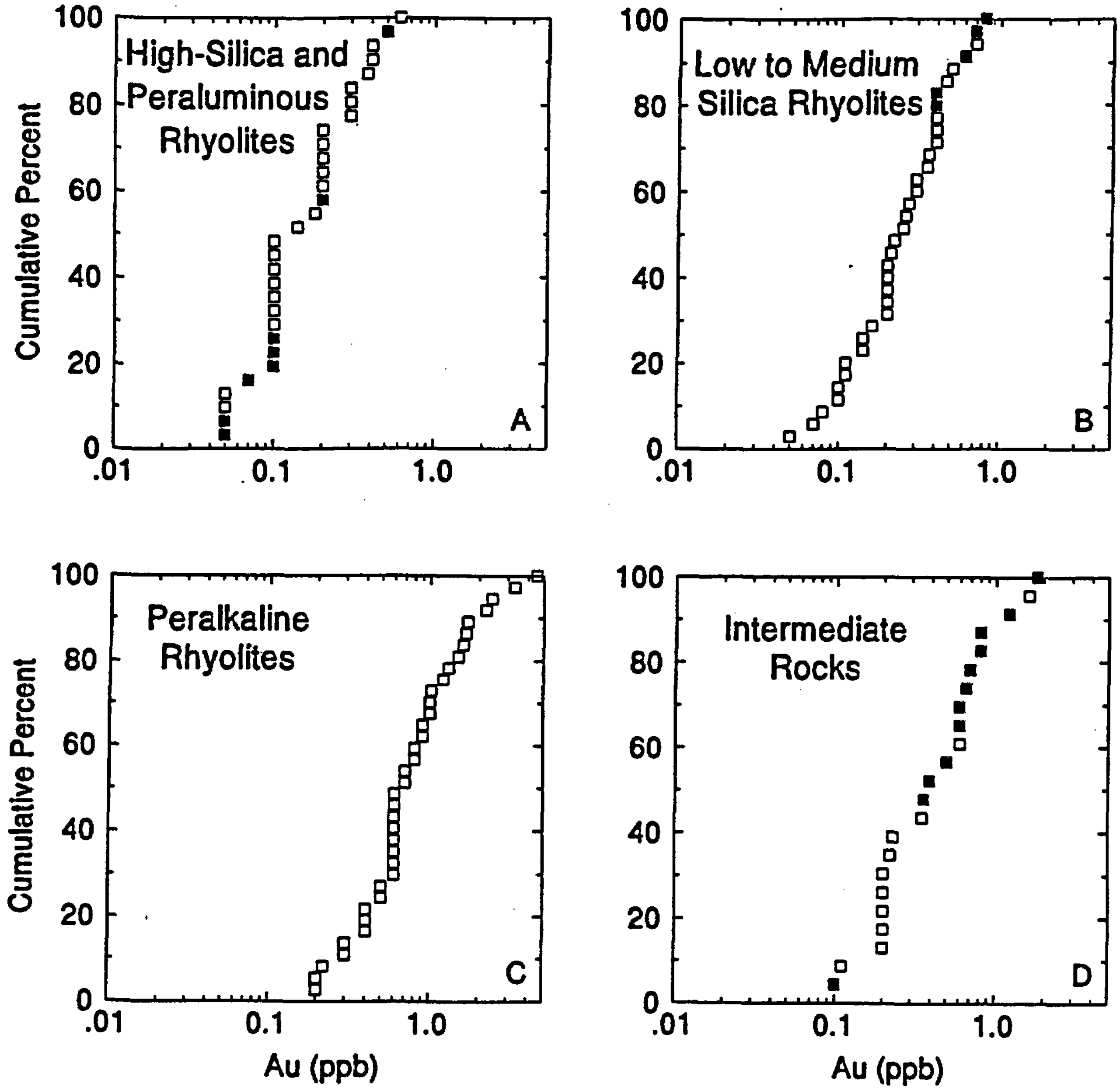

High-Silica and Peraluminous Rhyolites
A
Low to Medium Silica Rhyolites
B
Peralkaline Rhyolites
C
Intermediate Rocks
D
Cumulative Percent
Au (ppb)
0
20
40
60
80
100
.01
0.1
1.0

Figure 1.

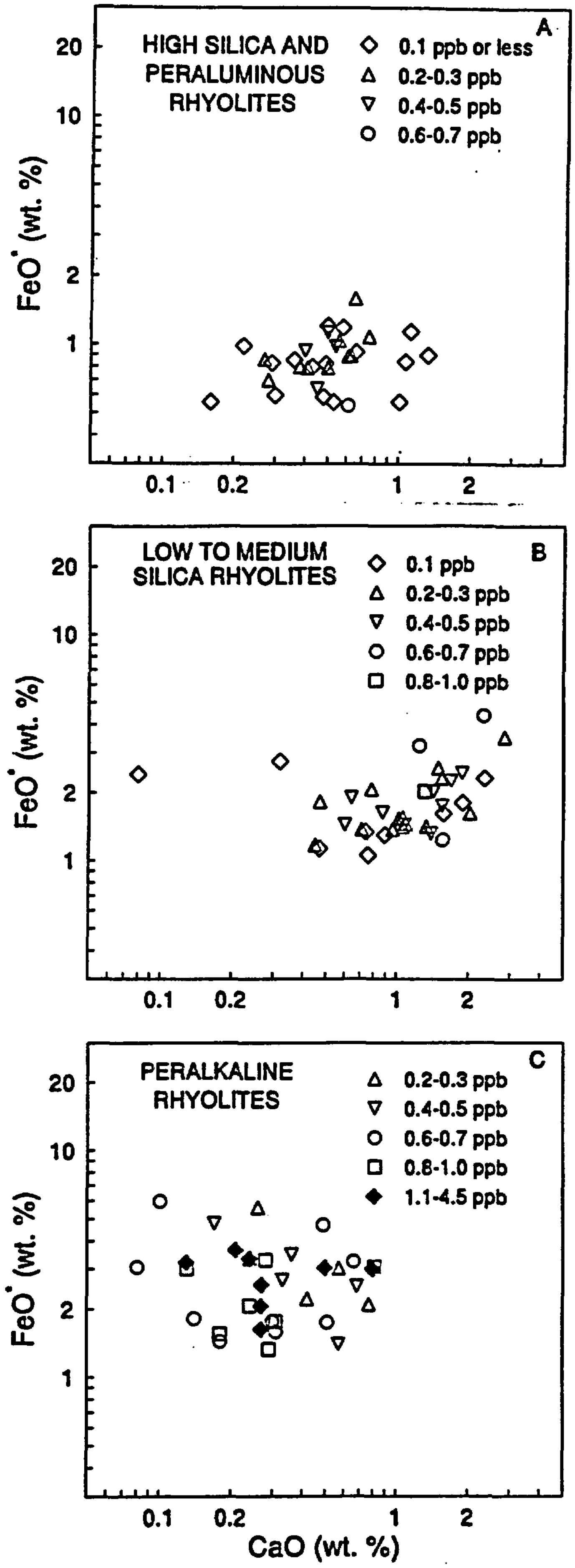
A
HIGH SILICA AND PERALUMINOUS RHYOLITES
0.1 ppb or less
0.2-0.3 ppb
0.4-0.5 ppb
0.6-0.7 ppb
FeO* (wt. %)
20
10
2
1
0.1
0.2
1
2
B
LOW TO MEDIUM SILICA RHYOLITES
0.1 ppb
0.2-0.3 ppb
0.4-0.5 ppb
0.6-0.7 ppb
0.8-1.0 ppb
C
PERALKALINE RHYOLITES
0.2-0.3 ppb
0.4-0.5 ppb
0.6-0.7 ppb
0.8-1.0 ppb
1.1-4.5 ppb
CaO (wt. %)

Figure 2.

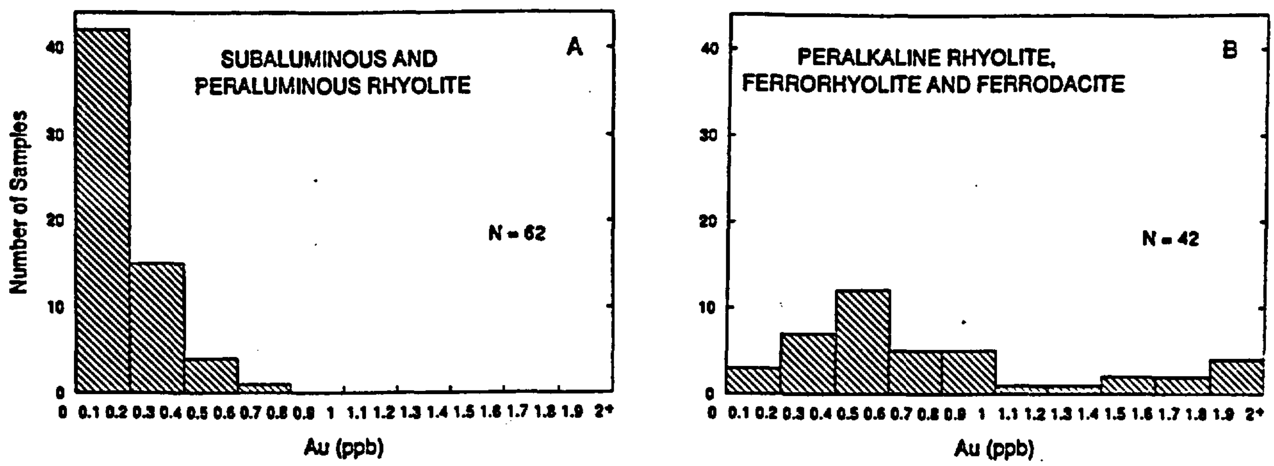

Figure 3.

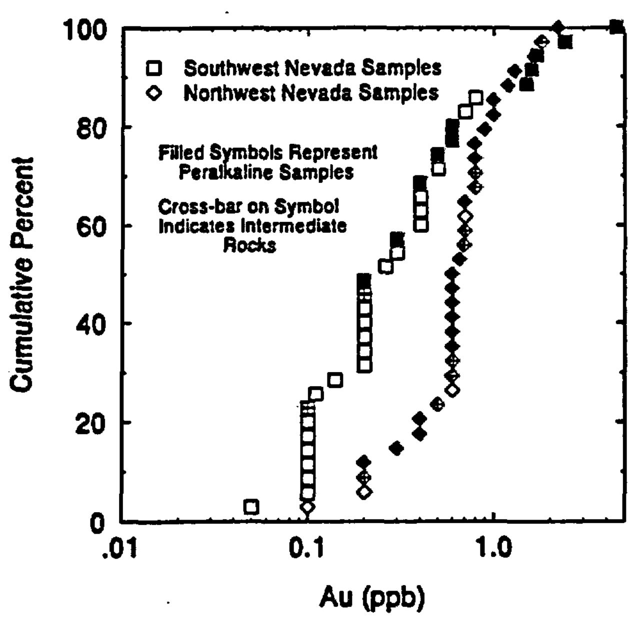

Figure 4.

APPENDIX B

Ore Geology Reviews, 7 (1992) 193–223
Elsevier Science Publishers B.V., Amsterdam — Printed in The Netherlands

Contrasting styles of epithermal precious-metal mineralization in the southwestern Nevada volcanic field, USA

Stephen B. Castor[a] and Steven I. Weiss[b]
[a]*Nevada Bureau of Mines and Geology, Mackay School of Mines, University of Nevada, Reno, NV 89557, USA*
[b]*Department of Geological Sciences, Mackay School of Mines, University of Nevada, Reno, NV 89557, USA*

(Received August 27, 1991; accepted after revision January 27, 1992)

ABSTRACT

Castor, S.B. and Weiss, S.I., 1992. Contrasting styles of epithermal precious-metal mineralization in the southwestern Nevada volcanic field, USA. *Ore Geol. Rev.*, 7: 193–223.

The southwestern Nevada volcanic field contains epithermal precious-metal deposits hosted by Miocene volcanic rocks and pre-Tertiary sedimentary rocks with production + reserves greater than 60 t of gold and 150 t of silver. The volcanic rocks consist predominantly of ash-flow tuffs erupted between 15 and 7 Ma during three major magmatic stages: the main stage (ca. 15–13 Ma); the Timber Mountain stage (ca. 13–9 Ma); and the late stage (ca. 9–7 Ma). Hydrothermal activity and precious-metal mineralization in the southern part of the field took place between ca. 13 and 8.5 Ma, coinciding with portions of all three magmatic stages. Regional extension during this period produced imbricate normal and detachment faulting that provided structural control for some of the mineralization.

Contrasts in the style and geochemistry of mineralization, together with stratigraphic and radiometric age data and differences in geologic setting reflect the variable nature of hydrothermal activity during development of the southwestern Nevada volcanic field. During the main magmatic stage, silver-rich vein mineralization of the adularia-sericite type occurred in an intermediate volcanic center at Wahmonie. Secondary high-salinity fluid inclusions in felsic subvolcanic intrusions, a trace element suite that includes bismuth and tellurium, and geophysical data support the presence of a buried porphyry-type magmatic system at Wahmonie.

Hydrothermal activity at Bare Mountain took place during the main magmatic stage, and may have continued into the Timber Mountain magmatic stage. Bare Mountain contains gold-rich, disseminated Carlin-type deposits with high arsenic, antimony, mercury and fluorine in sedimentary and igneous rocks. In northern and eastern Bare Mountain, mineralization is associated with felsic porphyry dikes that contain secondary high-salinity fluid inclusions. A genetic relationship between porphyry magmatism and shallow Carlin-type gold deposits seems likely at Bare Mountain.

Sedimentary-rock-hosted mineralization at Mine Mountain is spatially associated with a thrust fault and was apparently deposited, in part, by a hydrothermal system active during the Timber Mountain magmatic stage. The silver:gold ratio is high and base-metal, arsenic, antimony, mercury and selenium contents are very high. Mine Mountain mineralization shares features with vein and disseminated silver deposits at Candelaria, Nevada.

Gold-silver deposits in the areally extensive Bullfrog district comprise the largest known precious-metal resource in the volcanic field. They are mainly quartz-carbonate ± adularia veins with alteration and mineralization styles similar to other adularia-sericite-type deposits in the Great Basin. Deposits in the Rhyolite area and at the Gold Bar mine have very low contents of arsenic and mercury compared to other epithermal deposits in the Great Basin, although copper and antimony are locally elevated. Similarities in mineralization style and assemblages, which include two occurrences of the rare gold-silver sulfide uytenbogaardtite, indicate deposition under similar conditions in different parts of the district. Hydrothermal activity in the Bullfrog district was coeval with extensional tectonism and may have continued from the Timber Mountain stage into the late magmatic stage. Mineralization at some deposits in the Bullfrog and Bare Mountain districts is spatially associated with, and, in part, structurally controlled by a regional detachment fault system. However, significant differences in age, mineralization style and geochemistry indicate that mineralization in the two districts is unrelated.

Correspondence to: S.B. Castor, Nevada Bureau of Mines and Geology, Mackay School of Mines, University of Nevada, Reno, NV 89557, USA.

0169-1368/92/$05.00

Introduction

The southwestern Nevada volcanic field (SWNVF) consists of middle- to late-Miocene volcanic rocks that once covered an area of more than 10,000 km^2 (Byers et al., 1989), centered about 150 km northwest of Las Vegas (Fig. 1). The southern part of the SWNVF contains precious-metal deposits that have been exploited intermittently from the mid 19th century to the present. These deposits are hosted by volcanic rocks of the SWNVF and underlying pre-Tertiary sedimentary rocks.

In the course of more than three decades of geologic investigations, conducted mainly in support of nuclear weapons testing and proposed nuclear-waste storage programs, the SWNVF has become one of the most studied intracontinental volcanic fields in the world. Considerable efforts have been directed toward understanding the intense, long-lived history of magmatic and volcanic activity, caldera geology, volcano-tectonic evolution, and Neogene structural setting of the SWNVF. Investigations of hydrothermal activity and mineralization in the SWNVF have mostly been limited to reports on individual ore deposits and mineralized districts (e.g., Ransome et al., 1910; Cornwall and Kleinhampl, 1964; Tingley, 1984; Jorgensen et al., 1989) or to mineral inventories of large areas that include parts of the SWNVF (e.g., Cornwall, 1972; Quade et al., 1984). Jackson (1988) summarized time–space patterns of hydrothermal activity and mineralization, and proposed that hydrothermal activity and epithermal mineralization in the southern part of the SWNVF were related to magmatic and volcanic activity at major volcanic centers. More recently, Noble et al. (1991) proposed that hydrothermal activity and mineralization were associated with specific magmatic stages in the development of the SWNVF. However, comparisons of geologic and geochemical features of precious-metal deposits for the SWNVF as a whole are lacking.

In this paper we compare geologic settings, geochemical characteristics, mineralization and alteration assemblages, and general styles

Stephen Castor graduated from the University of California, Riverside (1965) and obtained a Ph.D. from the University of Nevada, Reno (1972). He has worked for more than twenty years as an economic geologist, studying deposits of a wide variety of mineral commodities. Current research interests include the geology of rare metal, industrial mineral and gold deposits.

Steven Weiss graduated from The Colorado College (1978) and obtained an M.Sc. degree from the University of Nevada, Reno (1987). He has worked as an economic geologist for 11 years, primarily on mineral deposits in volcanic terranes. Current research includes precious-metals hydrothermal systems associated with silicic volcanic centers, caldera geology and large-volume pyroclastic volcanism, and the interaction of high-level silicic magmatic-volcanic activity with detachment-style extenional faulting.

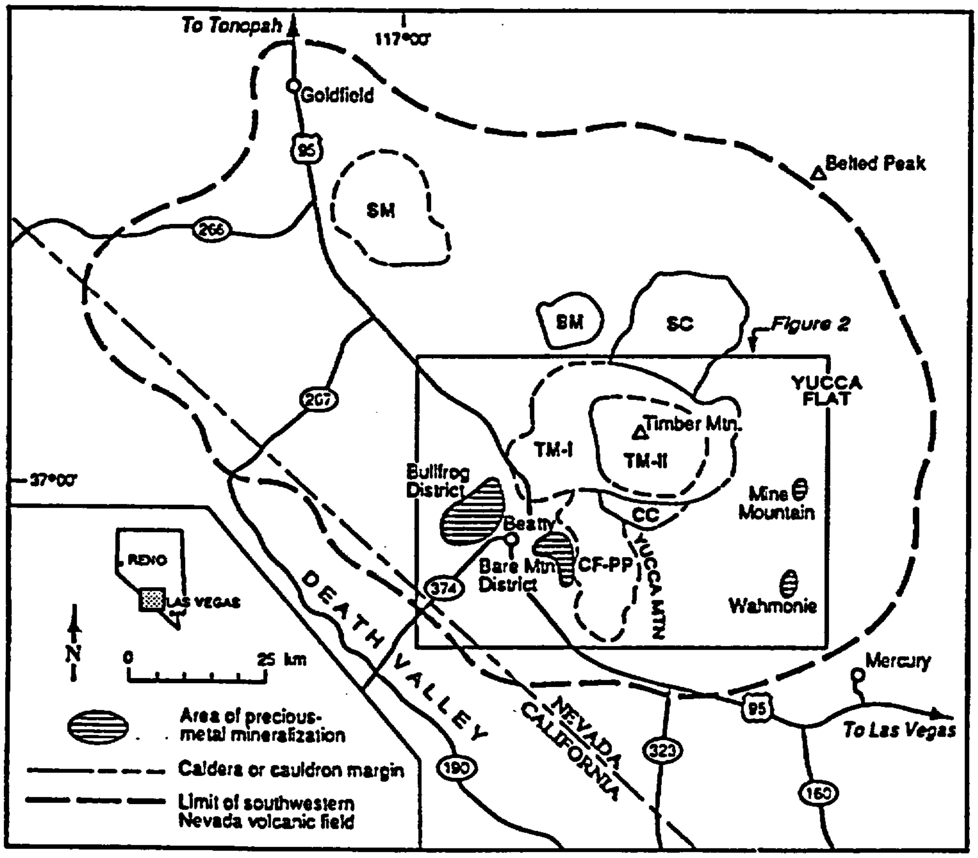

Fig. 1. Map of the southwestern Nevada volcanic field showing major volcanic centers and mineralized areas. (Modified from Noble et al., 1991; and Byers et al., 1989.) *BM*=Black Mountain caldera, *CF-PP*=Inferred Crater Flat–Prospector Pass caldera complex, *CC*=Claim Canyon cauldron, *SC*=Silent Canyon caldera, *SM*=Stonewall Mountain volcanic center, *TM-I*=Timber Mountain caldera complex I, *TM-II*=Timber Mountain caldera complex II. Heavy dashed line is approximate limit of SWNVF.

of mineralization of four selected areas in the southern part of the SWNVF: the Bullfrog district; northern and eastern Bare Mountain; the Wahmonie district; and Mine Mountain. Contrasts between these four mineralized areas illustrate the diverse nature of hydrothermal systems associated with the development of the SWNVF.

Geology of the SWNVF

The SWNVF is composed predominantly of silicic ash-flow tuff, including twelve sheets of regional extent, along with related surge and air-fall deposits and subordinate silicic to mafic lavas and intrusions. These rocks overlie complexly deformed and locally metamorphosed late Precambrian and Paleozoic miogeoclinal sedimentary rocks. Rocks of the SWNVF are distinctly younger than late Oligocene to early Miocene volcanic rocks exposed to the north (such as the volcanic rocks of the Goldfield district). Most rocks of the SWNVF were erupted between 15 and 10 Ma during the development of a large central complex of nested and overlapping volcanic centers of the collapse caldera type (Fig. 1). From about 9 to 7 Ma, volcanism in the SWNVF shifted to volcanic centers in the northwestern part of the field. Table 1 summarizes the stratigraphy and

TABLE 1

Generalized stratigraphy and geochronology of the southwestern Nevada volcanic field

Modified from Byers et al. (1989), Noble et al. (1991) and sources therein; additional age data from Hausback et al. (1990) and Sawyer et al. (1990); ages corrected for modern constants.

Formation	Member	Ma (approx.)	Volcanic Center
Late Magmatic Stage			
Stonewall Flat Tuff	Civet Cat Canyon	7.5	Stonewall Mountain caldera complex
	Spearhead	7.6	
Thirsty Canyon Tuff	Gold Flat	8.0	Black Mountain caldera complex
	Trail Ridge		
	Pahute Mesa		
	Rocket Wash	9.4	
Timber Mountain Magmatic Stage			
Rhyolite of Shoshone Mtn., Tuffs and lavas of the Bullfrog Hills		9-11	Periphery of Timber Mountain caldera complex
Mafic lavas		9-10	Timber Mountain caldera complex
Timber Mountain Tuff	Tuffs of Fleur de Lis Ranch	11.4	Timber Mountain caldera complex
	Ammonia Tanks	11.4	Timber Mtn. caldera complex - II
	Rainier Mesa	11.6	Timber Mtn. caldera complex - I
Rhyolite lavas of Fortymile Cyn.; pre-Rainier rhyolites		11-13	Timber Mountain caldera
Main Magmatic Stage			
Paintbrush Tuff	Tiva Canyon	12.7	Claim Canyon cauldron
	Yucca Mountain		Other members from area of
	Pah Canyon		Timber Mountain caldera complex
	Topopah Spring	13	
Rhyolite of Calico Hills		13	Calico Hills
Wahmonie & Salyer Fms.		13	Wahmonie
Crater Flat Tuff	Prow Pass		All members from Crater Flat—Prospector Pass caldera complex (?)
	Bullfrog	13.1	
	Tram		
Belted Range Tuff	Grouse Canyon	13.6	Silent Canyon caldera
Dacite lavas & breccias		14	Periphery of Crater Flat
Lithic Ridge Tuff		13.8	uncertain
Belted Range Tuff	Tub Spring	14.9	Silent Canyon caldera
"Older" tuffs			uncertain
Sanidine-rich tuff			uncertain
Tuff of Yucca Flat		15	uncertain
Redrock Valley Tuff		15.1	uncertain

geochronology of the three major magmatic stages of the SWNVF proposed by Noble et al. (1991): the 15.2–12.7-Ma main stage; the 11.6–9-Ma Timber Mountain stage; and the 9–7-Ma late stage.

Although the SWNVF is located within the Walker Lane structural belt, northwest-trending right-lateral faults and shear zones that characterize other parts of the belt are poorly developed in the SWNVF (Stewart, 1988). Instead, the majority of structural features within the SWNVF are attributed to magmatic and volcanic processes, including magmatic tumescence, caldera collapse and resurgent doming (Christiansen et al., 1977), and to middle- to late-Miocene regional extension that resulted in imbricate normal faulting and detachment faulting. In the southwestern part of the SWNVF, much extension appears to have been accommodated along the Original Bullfrog–Fluorspar Canyon (OB–FC) detachment fault system (Fig. 2), which is part of a regional fault system that continues southwest into Death Valley (Carr and Monsen, 1988; Hamilton, 1988).

Analytical methods

Chemical analyses were performed by Geochemical Services Inc., Rocklin, California, using inductively-coupled plasma emission spectroscopy (ICP-ES). Blind repeat analyses of sample pulps showed good reproducibility of results for all elements; but analyses on duplicate rock specimens show some differences (particularly for moderate- to high-level gold analyses) that are probably due to the "nugget effect". Comparative analyses done at the Nevada Bureau of Mines and Geology (NBMG) using atomic absorption for arsenic, bismuth, mercury and antimony showed excellent agreement for background-level samples collected from the SWNVF (Castor et al., 1990). Comparative analyses for gold, silver, arsenic and antimony performed by Bondar-Clegg, Inc., by instrumental neutron activation methods showed good agreement with the ICP-ES values for samples that ranged from background to highly mineralized. In addition, a comparison of Geochemical Services Inc., gold and silver values for NBMG standards (Lechler and Desilets, 1991) showed good agreement at high levels with recommended values obtained by averaging analyses by a number of commercial laboratories.

Mineral identifications were made using standard petrographic techniques, X-ray diffraction, and scanning electron microscope (SEM) analyses. Mineral compositions were obtained during SEM examination by energy dispersive X-ray (EDX) techniques using pure metal standards at the U.S. Bureau of Mines Western Research Center, Reno, Nevada. Mineral compositions reported are as molecular contents (rather than by weight percent). Descriptions of vein textures are based on a formal classification of the textures of vein quartz developed by Dowling and Morrison (1989).

Mineralized areas

Although records are sparse, we estimate that early gold production from the southern part of the SWNVF was about 3 t (100,000 oz) until significant operations ceased in the 1940s; silver production was of about the same magnitude. However, extensive exploration and development have taken place since the mid-1970s, and production and reserves for the SWNVF now total over 60 t (2 million oz) of gold and 150 t (5 million oz) of silver.

In connection with studies of mineral potential at the proposed nuclear waste site at Yucca Mountain, we obtained multi-element analyses of 150 vein and altered wall-rock samples from areas with precious-metal mineralization in the SWNVF. Our results (Table 2), together with data from the literature, show significant variations in trace-element suites for different mineralized areas in the SWNVF. For comparative purposes, analyses of unaltered volcanic

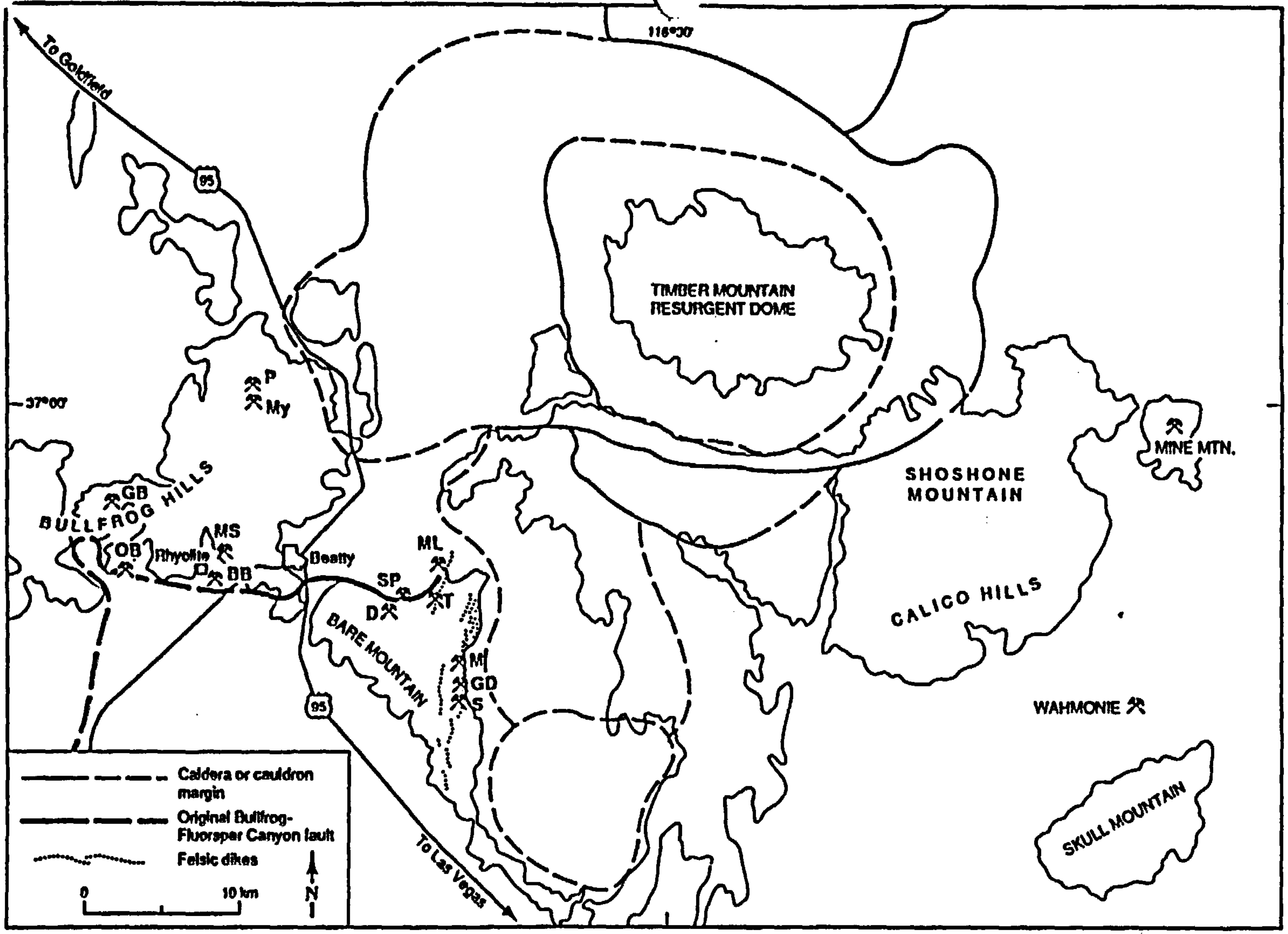

Fig. 2. Map of the south part of the southwestern Nevada volcanic field showing caldera margins, mineral deposits, and other features discussed in the text. (Modified from Noble et al., 1991.) *BB*=Lac Bullfrog mine, *D*=Daisy mine, *GB*=Gold Bar mine, *GD*=Goldspar mine, *M*=Mary mine, *ML*=Mother Lode mine, *MS*=Montgomery-Shoshone mine, *My*=Mayflower mine, *P*=Pioneer mine, *S*=Sterling mine, *SP*=Secret Pass deposit, *T*=Telluride mines. Heavy dashed line shows approximate surface trace of the Original Bullfrog–Fluorspar Canyon detachment fault system.

TABLE 2

Median, maximum and minimum trace-element contents of mineralized and altered samples from areas of precious-metal mineralization in the southwest Nevada volcanic field

Analyses by Geochemical Services, Inc.; all values in ppm, except Ag/Au; number of analyzed samples in parentheses.

	Ag			As			Au			Bi		
	Median	High	Low	Median	High	Low	Median	High	Low	Median	High	Low
Original Bullfrog (13)	1.79	1100	<.015	11.7	355	1.16	0.07	117	<.0005	<0.25	19.1	<0.25
Gold Bar (15)	0.39	30.8	0.05	3.02	8.7	1.05	0.07	3.76	0.006	<0.25	<0.25	<0.25
Rhyolite (42)	0.67	21000	<.015	6.8	88.2	<1.00	0.17	9223	<.0005	<0.25	0.52	<0.25
Mother Lode (36)	0.17	3.87	<.015	83.9	3874	1.63	0.05	7.47	0.001	<0.25	1.68	<0.25
Wahmonie (26)	0.48	3741	0.04	21.7	360	<1.00	0.01	383	<.0005	1.10	211	<0.25
Mine Mountain (21)	0.87	77.9	0.03	315	11200	<1.00	0.02	0.58	<.0005	<0.25	1.22	<0.25

	Cd			Cu			Ga			Hg		
	Median	High	Low	Median	High	Low	Median	High	Low	Median	High	Low
Original Bullfrog (13)	<0.10	1.42	<0.10	60.8	5160	21.8	<0.50	10.3	<0.50	<0.10	0.18	<0.10
Gold Bar (15)	<0.10	0.13	<0.10	24.4	47.8	2.48	0.96	5.11	<0.50	<0.10	0.46	<0.10
Rhyolite (42)	<0.10	0.42	<0.10	3.31	4413	0.92	0.53	2.2	<0.50	<0.10	1.22	<0.10
Mother Lode (36)	<0.10	1.03	<0.10	4.6	41.5	1.04	0.75	20	<0.50	0.25	5.87	<0.10
Wahmonie (26)	<0.10	0.27	<0.10	18.7	2434	2.24	0.51	1.66	<0.50	0.16	59.6	<0.10
Mine Mountain (21)	6.34	864	<0.10	35.6	531	2.31	0.88	9.23	<0.50	8.28	624	0.21

	Mo			Pb			Sb			Se		
	Median	High	Low	Median	High	Low	Median	High	Low	Median	High	Low
Original Bullfrog (13)	3.2	8.5	1.8	9	91.3	2.3	2.2	494	0.3	<1.0	<1.0	<1.0
Gold Bar (15)	2.1	3.7	0.5	9.2	17.6	1.3	0.5	1.0	<0.25	<1.0	<1.0	<1.0
Rhyolite (42)	4.4	429	1.2	8.6	381	0.6	0.7	296	<0.25	<1.0	173	<1.0
Mother Lode (36)	3.8	45.2	0.4	6.9	93.7	0.6	6.3	2077	<0.25	<1.0	8.3	<1.0
Wahmonie (26)	3.5	16.4	0.5	7.7	205	1.1	1.3	9.9	<0.25	<1.0	3.7	<1.0
Mine Mountain (21)	4.6	324	0.3	268	23k	1.9	181	2920	<0.25	<1.0	34.7	<1.0

	Te			Tl			Zn			Ag/Au		
	Median	High	Low	Median	High	Low	Median	High	Low	Median	High	Low
Original Bullfrog (13)	<0.5	5.0	<0.5	<0.5	4.5	0.5	24.7	125	2.1	22.7	216	6.4
Gold Bar (15)	<0.5	<0.5	<0.5	<0.5	<0.5	<0.5	19.3	34.4	2.8	8.19	33.1	1.0
Rhyolite (42)	<0.5	12	<0.5	<0.5	4.5	<0.5	15.8	179	2.7	2.3	87	0.37
Mother Lode (36)	<0.5	5.2	<0.5	<0.5	5.2	<0.5	11.6	261	<1.0	1.67	220	0.1
Wahmonie (26)	1.5	90.4	<0.5	<0.5	2.7	<0.5	7.1	61.5	<1.0	37.5	227	2.86
Mine Mountain (21)	<0.5	0.8	<0.5	<0.5	1.5	<0.5	705	146k	1.5	17.4	30k	2.73

TABLE 3

Trace-element analyses of background samples from the southwestern Nevada volcanic field

Analyses by Geochemical Services, Inc.; all values in ppm, except for Au which is in ppb; no data reported for Hg, Bi, Tl, and tellurium, which are below detection levels of 0.1, 0.25, 0.5, and 0.5 ppm, respectively.

SAMPLE	Ag	As	Au	Cu	Mo	Pb	Sb	Zn	Cd	Ga	Se
Glassy tuff											
SC 12	0.023	<1.0	1.0	5.3	0.6	4.9	<0.25	24.9	0.26	<0.50	<1.0
SC 16	0.021	<1.0	<0.5	5.6	0.7	2.8	<0.25	20.0	0.10	0.5	<1.0
SC 93	<0.015	<1.0	1.0	1.0	0.2	2.4	<0.25	17.6	<0.10	1.0	<1.0
SC 46A	0.017	<1.0	1.0	4.5	0.4	4.9	<0.25	12.0	0.16	<0.50	<1.0
BH 34G	0.044	1.9	<0.5	2.2	1.2	5.1	<0.25	11.4	<0.10	1.5	<1.0
BH 40	0.037	1.5	<0.5	1.0	0.8	5.7	<0.25	6.6	<0.10	1.2	<1.0
BH 43	0.034	2.4	<0.5	0.9	1.1	6.7	<0.25	8.2	<0.10	1.6	<1.0
Devitrified tuff											
SC 11	0.021	1.1	<0.5	14.3	1.7	5.1	<0.25	29.9	<0.10	<0.50	<1.0
SC 15	0.028	2.6	1.0	10.1	1.4	9.1	<0.25	35.2	<0.10	<0.50	<1.0
SC 23	0.034	1.4	2.0	15.5	1.8	5.1	<0.25	27.8	<0.10	<0.50	<1.0
SC 48C	0.027	1.3	1.0	10.2	1.2	1.2	<0.25	30.7	<0.10	1.0	<1.0
SC 58	0.029	2.8	<0.5	11.8	1.4	2.9	<0.25	20.5	<0.10	0.8	<1.0
SC 64	0.021	2.2	<0.5	12.3	1.3	9.2	<0.25	19.1	<0.10	0.8	<1.0
SC 80	0.028	2.2	<0.5	2.5	1.7	2.0	1.5	31.9	0.14	0.8	<1.0
DD 42	0.020	2.2	<0.5	1.6	1.2	1.7	<0.25	30.2	<0.10	<0.50	<1.0
DD 54	0.027	1.6	1.0	3.9	1.6	4.4	<0.25	12.2	<0.10	1.0	<1.0
DD 55 A	0.018	6.2	<0.5	3.5	1.0	2.0	<0.25	28.5	0.13	0.6	<1.0
DD 55 B	<0.015	1.3	1.0	3.9	1.1	1.8	<0.25	7.4	<0.10	0.6	<1.0
BH 34	0.035	3.9	<0.5	1.5	1.0	9.9	<0.25	33.7	<0.10	1.5	<1.0
BH 35	0.053	9.2	<0.5	1.8	1.1	8.4	<0.25	19.6	<0.10	2.0	<1.0
BH 41	0.052	3.9	<0.5	1.8	1.9	6.6	<0.25	10.8	<0.10	1.4	<1.0
BH 32	0.031	2.7	1.0	2.2	0.7	8.0	<0.25	26.7	0.15	2.5	1.1
BH 33	0.037	2.9	1.0	2.2	1.2	12.0	<0.25	9.5	<0.10	1.5	<1.0
GEXA 50	0.032	2.2	3.0	28.6	2.8	4.8	0.42	38.1	<0.10	3.2	<1.0
Volcanic sediment											
GEXA 20	0.025	14.0	2.0	5.4	1.2	17.7	<0.25	32.2	0.05	<0.50	<1.0

Glassy tuff	
SC 12	Orange glassy ash-flow tuff, bedded tuff unit, Yucca Mtn.
SC 16	Gray glassy ash-flow tuff, bedded tuff unit, Yucca Mtn.
SC 93	Gray glassy ash-flow tuff, bedded tuff unit, Yucca Mtn.
SC 46A	Black vitrophyre, Tiva Canyon Mbr., Yucca Mtn.
BH 34G	Brown glassy ash-flow tuff, Tiva Canyon Mbr., Bullfrog Mtn.
BH 40	Brown and black vitrophyre, Rainier Mesa Mbr., Bullfrog Mtn.
BH 43	Brown vitrophyre, Ammonia Tanks Mbr., Paradise Mtn.
Devitrified tuff	
SC 11	Lithophysal ash-flow tuff, Topopah Spring Mbr., Yucca Mtn.
SC 15	Clinkstone ash-flow tuff, Tiva Canyon Mbr., Yucca Mtn.
SC 23	Columnar ash-flow tuff, Tiva Cyn. Mbr., Yucca Mtn.
SC 48C	Brown biotitic ash-flow tuff, Topopah Spring Mbr., Yucca Mtn.
SC 58	Lithophysal ash-flow tuff, Topopah Spring Mbr., Yucca Mtn.
SC 64	Crystal-rich ash-flow tuff, Rainier Mesa Mbr., Yucca Mtn.
SC 80	Red-brown ash-flow tuff, Topopah Spr. Mbr., Yucca Mtn.
DD 42	Lithophysal ash-flow tuff, Tiva Canyon Mbr., Yucca Mtn.
DD 54	Crystal-rich ash-flow tuff, Rainier Mesa Mbr., Yucca Mtn.
DD 55 A	Crystal-rich ash-flow tuff, Rainier Mesa Mbr., Yucca Mtn.
DD 55 B	Air-fall tuff below Rainer Mesa Mbr., Yucca Mtn.
BH 34	Pinkish-grey ash-flow tuff, Tiva Canyon Mbr., Bullfrog Mtn.
BH 35	Pink ash-flow tuff, Crater Flat Tuff, Bullfrog Mtn.
BH 41	Brown ash-flow tuff, Rainier Mesa Mbr., Bullfrog Mtn.
BH 32	Light gray air-fall(?) tuff, Rainier Mesa Mbr., Bullfrog Mtn.
BH 33	Light gray air-fall(?) tuff, Rainier Mesa Mbr., Bullfrog Mtn.
GEXA 50	Flow(?) rock, rocks of Joshua Hollow, E of Mother Lode mine
Volcanic sediment	
GEXA 20	Fine sandstone, rocks of Joshua Hollow, SE of Mother Lode mine

MOTHER LODE MINE

	Ag	As	Au	Bi	Cd	Cu	Ge	Hg	Mo	Pb	Sb	Se	Te	Tl	Zn
Ag	1.00														
As	0.62√	1.00													
Au	0.72√	0.62√	1.00												
Bi	-0.28	-0.04	-0.01	1.00											
Cd	0.48√	0.43√	0.27	-0.14	1.00										
Cu	0.48√	0.67√	0.52√	-0.13	0.37	1.00									
Ge	-0.16	0.17	-0.07	0.17	-0.16	-0.12	1.00								
Hg	0.29	0.43√	0.34	0.18	0.39	0.40√	-0.22	1.00							
Mo	-0.08	0.04	-0.14	0.14	0.27	0.30	-0.09	0.27	1.00						
Pb	0.59√	0.67√	0.50√	0.17	0.24	0.47√	0.20	0.28	0.05	1.00					
Sb	0.63√	0.88√	0.65√	0.00	0.52√	0.61√	0.08	0.51√	0.10	0.71√	1.00				
Se	0.22	0.54√	0.25	0.23	0.42√	0.40√	0.25	0.26	0.35	0.47√	0.43√	1.00			
Te	0.62√	0.54√	0.58√	-0.10	0.40√	0.33	0.18	0.34	0.07	0.54√	0.66√	0.22	1.00		
Tl	0.61√	0.51√	0.56√	-0.08	0.31	0.35	0.16	0.30	-0.02	0.51√	0.62√	0.05	0.40√	1.00	
Zn	0.44√	0.65√	0.28	-0.28	0.69√	0.64√	-0.04	0.46√	0.30	0.37√	0.64√	0.41√	0.33	0.49√	1.00

ORIGINAL BULLFROG MINE

	Ag	As	Au	Bi	Cd	Cu	Ge	Hg	Mo	Pb	Sb	Se	Te	Tl	Zn
Ag	1.00														
As	0.33	1.00													
Au	0.88√	0.29	1.00												
Bi	0.59	0.51	0.42	1.00											
Cd	0.61	0.89√	0.53	0.54	1.00										
Cu	0.82√	0.34	0.54	0.74√	0.63	1.00									
Ge	0.59	-0.42	-0.59	-0.58	-0.18	-0.86√	1.00								
Hg	-0.51	-0.06	-0.47	-0.47	-0.11	-0.85√	0.80√	1.00							
Mo	0.23	0.56	0.12	0.47	0.57	0.34	-0.18	-0.05	1.00						
Pb	0.14	0.76√	0.00	0.49	0.62	0.24	0.30	0.25	0.35	1.00					
Sb	0.92√	0.50	0.91√	0.21	0.71√	0.78√	-0.45	-0.50	0.21	0.24	1.00				
Se												1.00			
Te	0.08	0.00	-0.14	0.08	0.08	0.08	-0.25	-0.16	0.46	-0.23	-0.16		1.00		
Tl	-0.23	0.10	-0.30	0.09	0.07	-0.13	0.08	0.22	0.76√	0.02	-0.27		0.41	1.00	
Zn	-0.42	0.57	-0.44	-0.19	0.32	-0.21	0.63	0.50	0.42	0.58	-0.21		-0.08	0.38	1.00

WAHMONIE DISTRICT

	Ag	As	Au	Bi	Cd	Cu	Ge	Hg	Mo	Pb	Sb	Se	Te	Tl	Zn
Ag	1.00														
As	0.11	1.00													
Au	0.84√	0.20	1.00												
Bi	0.51√	0.32	0.47√	1.00											
Cd	0.49√	0.41	0.38	0.22	1.00										
Cu	0.21	0.24	0.07	0.47√	0.22	1.00									
Ge	-0.23	0.51√	0.09	0.03	-0.10	0.08	1.00								
Hg	0.69√	0.04	0.62√	0.43	0.51√	0.29	-0.14	1.00							
Mo	-0.16	0.16	-0.02	-0.02	-0.16	0.05	0.50√	0.14	1.00						
Pb	0.07	0.44	0.06	0.70√	0.18	0.34	0.25	0.13	0.18	1.00					
Sb	-0.01	0.70√	0.15	0.12	0.24	0.23	0.25	0.10	0.17	0.30	1.00				
Se	-0.16	0.46√	-0.16	0.19	-0.05	-0.06	0.32	-0.10	0.24	0.38	0.14	1.00			
Te	0.72√	0.38	0.58√	0.75√	0.30	0.32	-0.04	0.58√	-0.03	0.49√	0.28	0.03	1.00		
Tl	0.33	0.31	0.33	0.28	0.41	0.28	0.30	0.35	0.33	0.28	0.31	0.13	0.34	1.00	
Zn	0.25	0.32	0.32	0.15	0.52√	0.28	0.12	0.40	-0.06	0.26	0.43	-0.32	0.42	0.33	1.00

GOLD BAR MINE

	Ag	As	Au	Bi	Cd	Cu	Ge	Hg	Mo	Pb	Sb	Se	Te	Tl	Zn
Ag	1.00														
As	-0.26	1.00													
Au	0.68√	0.29	1.00												
Bi				1.00											
Cd	-0.37	-0.25	-0.25		1.00										
Cu	0.31	0.41	0.63√		-0.25	1.00									
Ge	-0.06	0.31	0.31		0.31	0.22	1.00								
Hg	-0.09	0.77	0.48		-0.18	0.71√	0.30	1.00							
Mo	0.09	0.29	0.22		-0.37	0.37	-0.31	0.40	1.00						
Pb	-0.30	0.65√	0.08		-0.22	0.20	-0.17	0.66√	0.72√	1.00					
Sb	-0.19	0.43	0.29		0.22	0.25	0.50	0.49	0.04	0.30	1.00				
Se												1.00			
Te													1.00		
Tl														1.00	
Zn	-0.69√	0.48	-0.26		0.40	-0.21	0.69√	0.13	-0.24	0.13	0.35				1.00

MINE MOUNTAIN

	Ag	As	Au	Bi	Cd	Cu	Ge	Hg	Mo	Pb	Sb	Se	Te	Tl	Zn
Ag	1.00														
As	0.65√	1.00													
Au	0.55√	0.78√	1.00												
Bi	-0.13	-0.10	-0.04	1.00											
Cd	0.90√	0.68√	0.52√	-0.20	1.00										
Cu	0.47	0.45	0.38√	0.00	0.52√	1.00									
Ge	-0.22	0.00	0.03	-0.03	-0.28	-0.21	1.00								
Hg	0.90√	0.66√	0.43	-0.70	0.85√	0.44	-0.19	1.00							
Mo	0.23	0.16	0.06	-0.19	0.09	-0.22	0.17	0.23	1.00						
Pb	0.93√	0.72√	0.56√	-0.10	0.88√	0.40	-0.29	0.86√	0.26	1.00					
Sb	0.83√	0.68√	0.54√	-0.08	0.79√	0.29	-0.18	0.74√	0.33	0.92√	1.00				
Se	0.42	0.72√	0.66√	0.04	0.46	0.45	0.03	0.37	0.03	0.45	0.45	1.00			
Te	0.13	0.19	-0.02	-0.10	0.13	-0.14	0.47	0.12	0.22	0.10	0.07	0.23	1.00		
Tl	-0.04	0.19	0.03	-0.16	-0.14	-0.37	0.34	-0.01	0.38	0.02	-0.15	0.06	0.33	1.00	
Zn	0.70√	0.65√	0.37	-0.20	0.92√	0.44	-0.22	0.81√	0.10	0.79√	0.85√	0.47	0.33	0.05	1.00

√ Correlation coefficient significant at 99% confidence level

RHYOLITE AREA

	Ag	As	Au	Bi	Cd	Cu	Ge	Hg	Mo	Pb	Sb	Se	Te	Tl	Zn
Ag	1.00														
As	0.05	1.00													
Au	0.76√	0.09	1.00												
Bi	0.27	-0.01	0.22	1.00											
Cd	0.22	0.21	0.01	0.12	1.00										
Cu	0.47√	0.38√	0.37√	0.24	0.26	1.00									
Ge	0.35	0.52√	-0.29	-0.30	-0.24	-0.06	1.00								
Hg	0.20	0.09	0.21	-0.10	-0.06	-0.02	0.14	1.00							
Mo	0.26	-0.07	0.02	0.17	0.34	-0.19	-0.31	-0.05	1.00						
Pb	-0.12	0.41√	-0.17	0.18	0.25	0.19	0.10	-0.13	-0.06	1.00					
Sb	0.20	0.65√	0.10	0.20	0.28	0.48√	0.19	0.00	0.02	0.25	1.00				
Se	0.37√	0.29	0.38√	0.20	0.30	0.25	-0.03	0.05	0.20	0.06	0.21	1.00			
Te	0.42√	-0.06	0.44√	0.40√	0.22	0.27	-0.21	0.17	0.01	0.29	-0.02	0.40√	1.00		
Tl	0.31	-0.17	0.11	0.43√	0.51√	0.18	-0.46√	-0.15	0.34	-0.01	0.22	0.25	0.17	1.00	
Zn	-0.08	0.58√	-0.16	-0.05	0.47√	0.10	0.36√	0.06	0.14	0.32	0.34	0.10	0.06	0.07	1.00

√ Correlation coefficient significant at 99% confidence level

Fig. 3. Spearman correlation coefficients for trace-element analyses in samples from mineralized areas in the southwestern Nevada volcanic field.

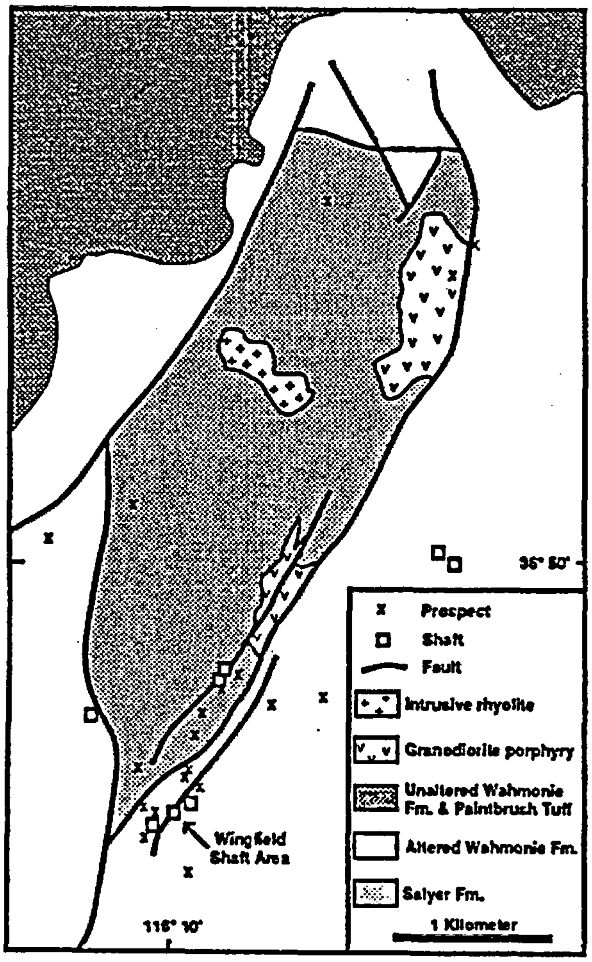

Fig. 4. Map showing mine workings and generalized geology for part of the Wahmonie district. (Modified from Ekren and Sargent, 1965.)

rocks from the SWNVF are also reported (Table 3). Correlation coefficients between trace-element contents for each area represented by thirteen or more samples are shown in Fig. 3.

We have not separated the chemical data reported in this study (Table 2) by sample type (e.g., vein versus wall rock) because few samples composed exclusively of vein or wall-rock material were analyzed. Most samples consisted of variable proportions of mixed vein and altered wall-rock material, or of disseminated mineralization containing little or no vein material. In addition, analyses of the few pure vein and wall-rock samples showed little difference in trace-element assemblage other than overall metal concentration. Most of the samples collected during this study are partially to completely oxidized. In a few cases where unoxidized samples could be compared with oxidized samples from the same locality, trace-element signatures were not found to be significantly different. The data presented here reflect differences in trace-element signatures between mineralized areas that are more significant than differences within areas.

Wahmonie district

The earliest mining activity in rocks of the SWNVF took place in the Wahmonie mining district (Figs. 2 and 4) where near-surface ores are thought to have been worked as early as 1853 (Quade et al., 1984). Discoveries of high-grade silver-gold ore in 1928 resulted in considerable development, including the 150-m-deep Wingfield shaft, but little ore was shipped. In 1940, the Wahmonie district was withdrawn from mineral entry when it was included within the Tonopah Bombing and Gunnery Range. This area later became part of the Nevada Test Site of the U.S. Department of Energy and remains excluded from civilian development.

Precious-metal mineralization in the Wahmonie district lies in a northeast-trending 8 km by 4 km elliptical area underlain by intensely altered andesitic to latitic lavas, tuffs and breccias of the Wahmonie Formation (Ekren and Sargent, 1965). The altered area includes a central northeast-trending 3 km by 1 km horst, containing weakly to strongly altered rhyodacitic volcanic rocks assigned to the Salyer Formation (Ekren and Sargent, 1965), that are cut by intermediate to silicic subvolcanic intrusions (Fig. 4). The intermediate to felsic igneous rocks at Wahmonie probably comprise the eroded remnants of a central volcano or dome and flow field. K/Ar ages (recalculated to current constants) indicate that rocks comprising this center, informally termed the

Wahmonie–Salyer volcanic center, were emplaced between about 13.2 and 12.8 Ma (Kistler, 1968). They are overlain by units of the Paintbrush Tuff (Ekren and Sargent, 1965), which have similar to slightly younger ages of about 13.0 to 12.7 Ma (Sawyer et al., 1990).

The area of the most intense prospecting and development, which includes the Wingfield shaft (Fig. 4), is a northeast-trending zone of abundant quartz veins, about 1 km long in strongly altered rock along the southeastern side of the central horst. Near-vein alteration in this area is dominated by silicification and adularization with some argillic minerals. Feldspar phenocrysts are replaced by granular adularia with illite+sericite±kaolinite or by single crystals of secondary potash feldspar with mottled extinction. According to Jackson (1988), near-vein adularia+sericite+silica alteration grades outward to kaolinite-bearing rock. Alunite was reported to occur in strongly altered rock and in quartz veins (Ekren and Sargent, 1965; Quade et al., 1984), but no alunite was found by the authors during petrographic and X-ray diffraction analyses. Sulfide-rich silicified rock on mine dumps in the Wingfield shaft area, and widespread limonite indicate that significant amounts of pyrite were previously present in altered wall rock. Propylitic alteration consisting of chlorite± albite ±calcite±pyrite is widespread in the central horst. Argillic alteration, potassic alteration (with secondary biotite), and tourmaline veinlets are locally present in, or adjacent to, central horst intrusions.

Precious-metal-bearing veins consist mainly of fine comb quartz±calcite with minor adularia. They carry free gold, cerargyrite, hessite, iron and manganese oxides, acanthite and other sulfides (Quade et al., 1984). Very finely granular quartz veins with anomalously high precious-metal contents (as much as 0.4 ppm gold and 3.5 ppm silver) are exposed in the vicinity of the Wingfield shaft. Stockworks of fine comb to granular quartz veinlets with adularia rhombs are also present.

SEM/EDX studies of highly mineralized rock from Wahmonie disclosed electrum ($Au_{77}Ag_{23}$) occurring as irregular threads or flakes in cerargyrite, and hessite (Ag_2Te) occurring as colloform bands in cerargyrite. Iron tellurite containing minor gold and manganese (possibly mackayite, $Fe_2(TeO)_3 \cdot x\,H_2O$) was found in cerargyrite. Frohbergite ($FeTe_2$) and hedleyite ($BiTe_2$) were also tentatively identified, and cinnabar was found in cavities as micron-size granules on cerargyrite (J. Sjoberg and J. Quade, pers. commun., 1991).

Vein samples analyzed during this study contain as much as 3.7 kg silver and 0.4 kg gold per ton, but samples carrying as much as 38.7 kg silver and 1.7 kg gold per ton have been reported previously (Quade et al., 1984). Mineralized and altered samples from the Wahmonie district have relatively high silver:gold ratios (Table 2) and bismuth, mercury and tellurium correlate well with gold (Figs. 3 and 5). Copper, lead and antimony are locally high, but do not correlate with gold. Base-metal contents are low in mineralized samples from Wahmonie, with the exception of a single vein sample with secondary copper minerals that is enriched in copper and lead, but poor in silver and gold. Arsenic content is generally low (Table 2), but pyrite-rich silicified rock with 360 ppm arsenic was collected from a dump near the Wingfield shaft.

Rock with high precious-metal and tellurium contents in the Wahmonie district is not restricted to the Wingfield shaft area, and may occur widely in the district. Hessite-bearing comb quartz from a small dump in the central horst, 1 km northeast of the Wingfield shaft, contains 748 ppm silver, 11 ppm gold and 90 ppm tellurium. Granodiorite, altered to a mixture of quartz and illite (4 km northeast of the Wingfield shaft), also has elevated gold and tellurium contents (Quade et al., 1984).

Adularia from altered rocks with abundant silica-adularia veins in the Wahmonie district gave K/Ar ages of 12.6±0.4 and 12.9±0.4 Ma (Jackson, 1988). These ages indicate that hy-

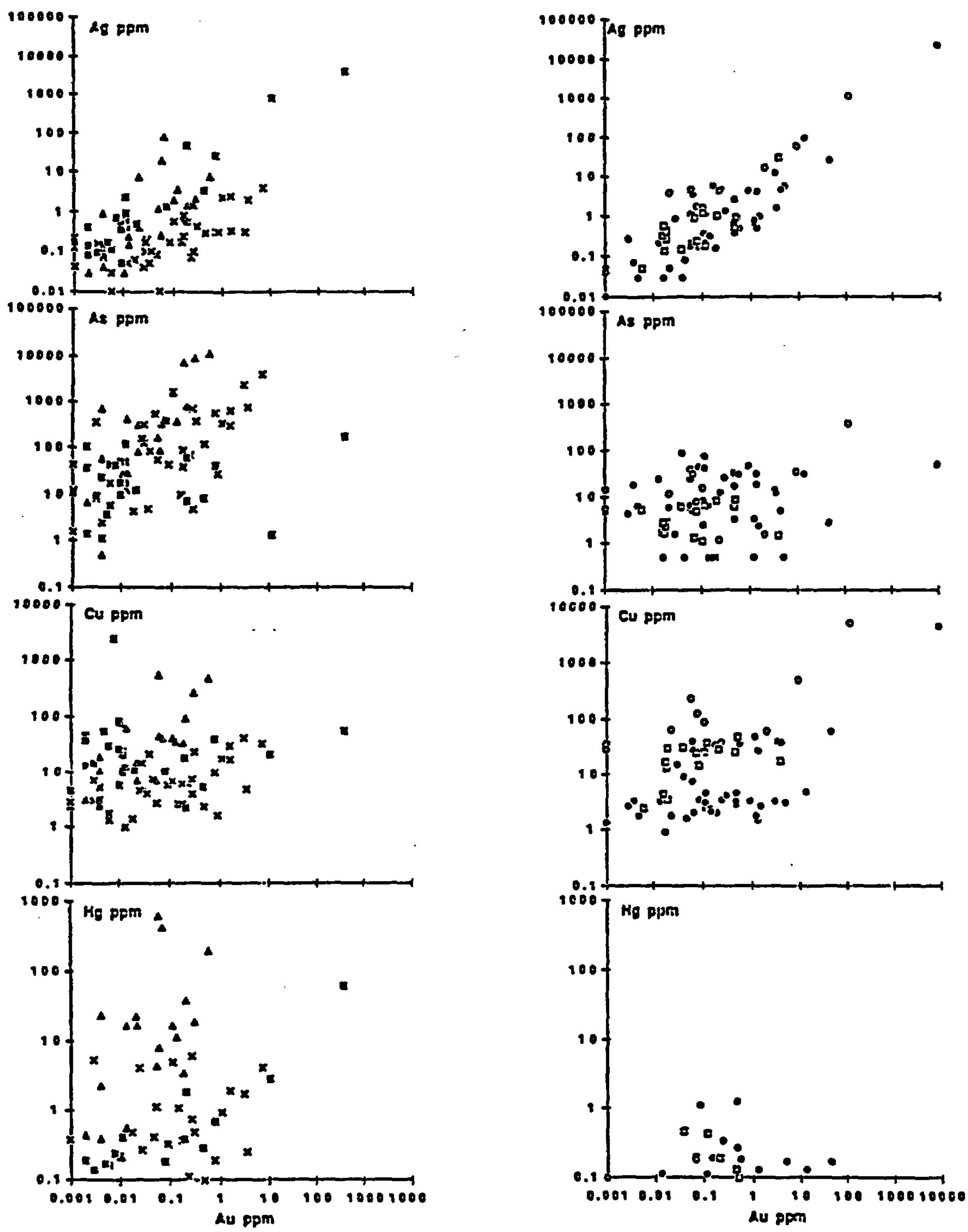

Fig. 5. Plots of Ag, As, Hg and Cu against Au in samples from mineralized areas in the southwestern Nevada volcanic field. Plots on the left represent samples from Wahmonie (■) Bare Mountain (×), and Mine Mountain (△). Plots on the right are of samples from the Bullfrog mining district: Original Bullfrog mine (○); Gold Bar mine (□); and Rhyolite area (●).

drothermal activity and mineralization closely followed magmatic and volcanic activity of the main magmatic stage of the SWNVF at Wahmonie.

On the basis of a positive residual gravity anomaly centered about 1 km southwest of the mineralized area at Wahmonie and associated magnetic highs, Ponce (1981) inferred the presence of a large buried felsic intrusive mass similar to and contiguous with granodiorite exposures in the central horst. The highest portions of this intrusive body appear to be along the east side of the central horst, coincident with the area of precious-metal mineralization. As pointed out by Hoover et al. (1982), the edges of the inferred intrusion correspond approximately with alteration in the Wahmonie district. Relatively high resistivity in the inferred intrusion indicates high porosity due to fracturing, faulting, alteration and possibly mineralization. Induced polarization data indicate that 2% or more sulfides are present below the water table at Wahmonie (Hoover et al., 1982).

Alteration and veining in granodioritic porphyry intrusions in the central horst, along with high bismuth and tellurium support the presence of a porphyry magmatic–hydrothermal system at Wahmonie. In addition, quartz phenocrysts containing hypersaline secondary fluid inclusions, which are indicative of magmatic hydrothermal fluids, occur in samples with secondary biotite (D.C. Noble, pers. commun., 1990).

Bare Mountain area

Between initial discovery in 1905 and the late 1970s, small amounts of gold and mercury were produced intermittently from deposits in northern and eastern Bare Mountain, including the Panama-Sterling gold mine and the Telluride gold-mercury camp (Fig. 2). Fluorspar was produced more-or-less continuously from the same area between 1918 and 1989 from the Daisy, Goldspar and Mary mines. Approximately 2.5 t (80,000 oz) of gold were produced from disseminated deposits at the Sterling and Mother Lode mines between 1983 and 1990 (Bonham and Hess, 1991). Additional, currently subeconomic disseminated gold deposits are present at the Daisy mine, Secret Pass, Goldspar mine, and near the Mother Lode mine (J. Marr, pers. commun., 1987; Greybeck and Wallace, 1991).

Bare Mountain consists predominantly of weakly metamorphosed late Proterozoic through late Paleozoic sedimentary rocks of the Cordilleran miogeocline that underwent Mesozoic folding and thrust-faulting and Tertiary low- to high-angle normal and strike-slip faulting (Cornwall and Kleinhampl, 1961; Monsen et al., 1990). In northern Bare Mountain, these rocks are separated from overlying, imbricately faulted volcanic rocks of the SWNVF by the north-dipping, low- to moderate-angle Fluorspar Canyon fault (Cornwall and Kleinhampl, 1961) which is considered by recent workers to be the eastern continuation of the Original Bullfrog fault (e.g., Carr and Monsen, 1988). In contrast to the Bullfrog Hills, where major faulting and tilting post-dated deposition of the 11.4 Ma Ammonia Tanks Member, deformation in northeastern Bare Mountain had mostly ceased by 11.6 Ma, as indicated by strong angular discordance between the flat-lying, 11.6-Ma Rainier Mesa Member of the Timber Mountain Tuff and underlying tilted units of the SWNVF (Carr, 1984; Carr and Monsen, 1988; Monsen et al., 1990; Weiss et al., 1990).

A swarm of north-trending felsic porphyry dikes intrudes the pre-Cenozoic rocks in eastern and northern Bare Mountain. The dike rocks typically have coarsely granophyric groundmass and have been affected by variable degrees of potassium-feldspar, sericitic and argillic alteration. Secondary hypersaline fluid inclusions that are present in quartz phenocrysts reflect the passage of an early high-salinity hydrothermal fluid (Noble et al., 1989). The dikes were emplaced during the main magmatic stage of the SWNVF, as demonstrated by radiometric age determinations ranging between 14.9±0.5 and 13.8±0.2 Ma (Marvin et al., 1989; Monsen et al., 1990; Noble et al., 1991). Most mineral deposits along the east flank of Bare Mountain are spatially associated with, and post-date or are nearly contemporaneous with the emplacement of, these dikes.

Several base-metal±gold occurrences, generally associated with quartz veins in Precambrian and Cambrian rocks, have been reported along the west flank of Bare Mountain (Cornwall, 1972; Tingley, 1984). However, most of the mineral deposits in Bare Mountain are located in its northern and eastern flanks.

At the Sterling mine (Fig. 2), sediment-hosted disseminated gold-silver mineralization is controlled by the intersection of normal faults with a thrust fault that juxtaposes clastic rocks of the late Proterozoic to early Cambrian Wood Canyon Formation over carbonate rocks of the middle Cambrian Bonanza King Formation (Odt, 1983). This mineralization is associated with alteration assemblages that include kaolinite, illite, sericite, jarosite and alunite, and with very little introduction or removal of silica and iron (Odt, 1983). Stibnite, cinnabar and fluorite are present in ore and in nearby exposures of hydrothermal breccia (Tingley, 1984). Hydrothermally altered porphyry dikes are abundant in the Sterling Mine area, and locally have elevated gold contents (Odt, 1983; Tingley, 1984; Jackson, 1988).

North of the Sterling mine, a zone of argillic alteration and bleaching accompanies the porphyry dikes and locally contains fluorite and disseminated gold mineralization in Paleozoic carbonate rocks (Tingley, 1984; D. Odt, pers. comm., 1987). At the Goldspar mine (Fig. 2), fluorite replaces brecciated and sheared carbonate rocks of the Nopah Formation and fills fractures in altered dike rock (Papke, 1979; Tingley, 1984; Jackson, 1988). Similar fluorite mineralization and alteration is present in Silurian dolomite at the Mary mine.

The Goldspar deposit has been interpreted as a high-level breccia pipe (e.g., Tingley, 1984). Altered clasts of Tertiary volcanic rocks in the breccia (Jackson, 1988) are unlikely to have been transported from below the Cambrian host rocks. This suggests that the breccia was open to much higher stratigraphic levels at the time of hydrothermal activity.

In the Telluride mine area (Fig. 2), gold mineralization is present with quartz, opal, alunite and pyrite along the Fluorspar Canyon fault (Jackson, 1988) and occurs in altered porphyry dikes that intrude carbonate rocks in the footwall of the fault. Mercury was mined from pipe-like breccia bodies and also occurs as disseminated cinnabar with fluorite, calcite, opal and alunite at the Telluride mine (Tingley, 1984).

The Mother Lode gold mine is situated immediately to the north of the Telluride mine area, near the northeasternmost exposure of the Fluorspar Canyon fault segment of the OB-FC fault system (Fig. 2). Disseminated gold mineralization is present in felsic porphyry dikes, sills and extrusive(?) rocks and in adjacent interbedded sandstone, siltstone and limestone. Mapa (1990) considered the sedimentary host rocks to be part of the Mississippian Eleana Formation, whereas others (e.g., S. Ristorcelli, pers. commun., 1990) interpret them as belonging to the early(?) to middle Miocene rocks of Joshua Hollow of Monsen et al. (1990). Alteration is primarily argillic, with pyrite in unoxidized rocks and jarosite in oxidized rocks. Altered rock is mostly composed of quartz and illite, and feldspar phenocrysts are generally completely replaced by illite±calcite, but some samples contain sanidine that is apparently unaltered. Mafic minerals are replaced by sericite±illite±calcite ±rutile. Sooty remobilized carbon is abundant locally in the sedimentary rocks. Very sparse, irregular veins containing fine to medium drusy quartz+ manganese oxide±opal occur in oxidized ore, and calcite veins cut limestone. About 150 m west of the mine, glassy bedded tuff that is considered to lie stratigraphically between the Paintbrush and Timber Mountain Tuffs (Monsen et al., 1990) contains very fine-grained alunite. In addition, chalcedony replaces conglomerate and opal replaces bedded tuff in the same unit about 600 m northwest of the mine.

Three mineralized zones, containing a total of 12.3 Mt that average 0.81 g/t of gold (13.5 Mst at 0.026 oz/st), have been delineated in Fluorspar Canyon 3–5 km southwest of the Mother Lode mine (Greybeck and Wallace, 1991). In this area, two disseminated gold deposits associated with fluorite mineralization are present within Cambrian rocks of the Nopah, Bonanza King and Carrara Formations in and near the Daisy fluorite mine (Fig. 2) (Papke, 1979; Tingley, 1984; Greybeck and Wallace, 1991). These deposits, which are situated beneath the Fluorspar Canyon fault (Fig. 2), are associated with alteration that ranges from subtle decalcification to intense silicification (Greybeck and Wallace, 1991). Cinnabar commonly accompanies fluorite in the Daisy mine.

The nearby volcanic-hosted Secret Pass deposit (Fig. 2) contains disseminated gold in altered ash-flow tuff of the Bullfrog Member of the Crater Flat Tuff. The deposit is bounded by the underlying Fluorspar Canyon fault (Greybeck and Wallace, 1991). An alteration assemblage including quartz, adularia, calcite and pyrite, with generally weak silicification, is associated with gold mineralization (Greybeck and Wallace, 1991). Although precious-metal mineralization is confined to the Crater Flat Tuff, adularia- and illite(?)-bearing alteration assemblages continue up into the overlying ca. 13-Ma Topopah Spring Member of the Paintbrush Tuff. In addition, chalcedonic veins that may be related to this mineralization are present in the 12.7-Ma Tiva Canyon Member.

Altered and mineralized samples from the Bare Mountain area collected during this study include twenty samples from the Mother Lode orebody and sixteen samples from workings and outcrops within 1 km south and west of the mine. These samples generally have high arsenic and antimony contents, and gold correlates strongly with these two elements (Figs. 2 and 5). Gold is also correlative with copper, lead, mercury, tellurium and thallium, although the contents of these metals are not highly anomalous. The median silver:gold ratio for all 36 samples is about 2:1. In general, Mother Lode mine samples with the highest gold contents contain drusy quartz ± opal along with manganese oxide. Pyritic ore contains gold contents similar to adjacent oxidized ore (W. Hickinbotham, pers. commun., 1990). Gold-bearing phases could not be found using reflected light and scanning electron microscopy in samples containing as much as 7 ppm gold.

The mineralized areas in Fluorspar Canyon southwest of the Mother Lode mine have similar trace-element abundances and correlations between gold and other trace elements, particularly antimony, thallium, and molybdenum (Greybeck and Wallace, 1991). Arsenic, mercury and base metals are also correlative with gold, but not in all three deposits. Silver:gold ratios are generally low.

Gold-rich samples from the Sterling mine area have high arsenic, antimony, mercury and thallium contents (Odt, 1983; Hill et al., 1986). Tingley (1984) reported high arsenic, antimony and molybdenum contents in samples from the Telluride, Sterling, and Daisy mine areas, and high lead and zinc from the latter two areas.

The presence of hydrothermal alteration, fluorite, and locally elevated gold concentrations in porphyry dikes indicates that much, or all, of the mineralization in Bare Mountain postdates emplacement of the dikes. K/Ar and Ar/Ar ages of about 12.9 Ma have been obtained on hydrothermal potassium feldspar that replaces groundmass and phenocrysts of igneous potassium feldspar in altered dike rock at the Goldspar mine, indicating that hydrothermal activity took place there during the main magmatic stage of the SWNVF (Noble et al., 1991). Close similarities in mineralization style and trace-element signatures support a similar timing for gold mineralization in pre-Cenozoic rocks in the vicinity of the Daisy mine. At the nearby Secret Pass deposit, hydrothermal alteration extends into the ca. 13-Ma Topopah Spring Member of the Paintbrush Tuff, but not into adjacent exposures of the 11.6-Ma Rainier Mesa Member of the Timber Mountain Tuff. In the Telluride mine area, alunite occurs in altered gravel in the hanging wall of the Fluorspar Canyon fault and in hydrothermal breccia in the footwall of the fault. Samples of this alunite were dated at 12.2±0.4 Ma and 11.2±0.3 Ma, respectively, by K/Ar methods (Jackson, 1988). Alunitic alteration is also found near the Mother Lode mine in bedded tuff between the Paintbrush Tuff and Rainier Mesa Member of the Timber Mountain Tuff.

The dated alunite is fine grained, suggesting either a supergene origin or a vapor-dominated depositional environment (e.g., Thompson, 1991), and the dates, therefore, may represent minimum ages for mineralization. If the alunite was deposited by hypogene fluids, the ages suggest the possibility of more than one period of activity or that hydrothermal activity in the Telluride–Mother Lode area was of long duration.

A number of lines of evidence suggest a shallow or high-level environment for mineralization in Bare Mountain. Hydrothermal breccia in the Sterling, Goldspar and Telluride mine areas is suggestive of a high-level environment. The altered Tertiary volcanic rocks present in fluoritized breccia at the Goldspar mine include clasts of the Paintbrush Tuff. The most reasonable interpretation is that the volcanic rock fragments fell into the breccia prior to, or during, hydrothermal activity. Because the age of hydrothermal activity is essentially the same as the age of the Paintbrush Tuff, the deposit was probably open to the paleosurface. Cinnabar and high mercury concentrations are widespread in northern and eastern Bare Mountain and alunite±opal is present in several mineralized areas. Such mineral associations are considered indicative of a shallow hydrothermal environment, although it is possible that the alunite is not entirely hypogene.

Noble et al. (1989) inferred the presence of a buried, granite-type porphyry molybdenum system in Bare Mountain from the presence of porphyry-style crystallization textures and hypersaline fluid inclusions in the felsic dikes, the spatial association of mineralization with the dikes, and the fluorite-molybdenum component of the trace-element assemblage of the mineralization in Bare Mountain. Gold-silver-mercury-fluorite mineralization in Bare Mountain may represent the distal, near-surface expression of hydrothermal activity related to a deeper porphyry molybdenum system (Noble et al., 1989).

Mine Mountain

Mine Mountain, in the southeast part of the SWNVF (Fig. 1), was the site of mercury, base-metal, and precious-metal prospecting in the 1920s, but was subsequently included in the Nevada Test Site and withdrawn from mineral entry. A 2-km-long northeast-trending area along the crest of Mine Mountain contains quartz±calcite±barite±sulfides in veins, hydrothermal breccia, and silicified areas (Quade et al., 1984; L.T. Larson and S.I. Weiss, unpubl. mapping, 1989). Mineralization is closely associated with the flat-lying Mine Mountain thrust fault, which separates underlying Mississippian clastic rocks from Devonian carbonate rocks in the upper plate (Orkild, 1968). The mineralization occurs both above and below the thrust fault, but appears to be most strongly developed within a few tens of meters above the fault in highly brecciated rock (L.T. Larson and S.I. Weiss, unpubl. mapping, 1989).

Above the Mine Mountain thrust, mineralization is closely associated with moderate- to high-angle northeasterly-striking faults and fractures, and north- to northwest-striking high-angle fractures. Subhorizontal slickensides on these structures indicate lateral slip, probably related to movements along the nearby, northeast-trending, left-slip Mine Mountain fault zone of Carr (1984). Locally, quartz-barite veins both crosscut and are offset by faults with subhorizontal slickensides, indicating that mineralization was coeval with strike-slip movement.

In the lower plate of the Mine Mountain thrust, quartz- and calcite-cemented fault and hydrothermal breccia comprise narrow veins that trend NW to nearly E–W and can be traced for as much as 1 km in clastic rocks of the Eleana Formation. Samples of these veins, which yielded the highest gold analyses of any rocks from Mine Mountain, contain very finely granular to chalcedonic quartz along with alunite and cinnabar. SEM/EDX examination of a breccia-vein sample with 0.6 ppm gold and very high arsenic and lead contents shows an arsenate, iodide and selenide assemblage including mimetite ($3Pb_3(AsO_4)_2 \cdot PbCl_2$), conichalcite ($8(Cu,Ca)As_2O_3 \cdot 3H_2O$), tocornalite (HgAgI), and tiemannite (HgSe). Trace amounts of pyrite and arsenopyrite are also present.

Alteration mineralogy at Mine Mountain is dominated by fine-grained silicification. In massive carbonate rocks in the upper plate, silicification includes variable amounts of chalcedonic replacement (jasperoid) and millimeter- to centimeter-wide sheeted or stockwork quartz veins. White calcite veins are abundant in carbonate rocks surrounding the area of silicification. Vein quartz has fine- to medium-granular or fine comb textures, and clear drusy quartz is also present. Barite, calcite, galena, sphalerite and anglesite have been identified in veins and silicified rocks. Cinnabar is present in veins and is also disseminated in leached, decalcified and silicified carbonate rocks. Small amounts of gossan are associated with massive white calcite and barite-rich hydrothermal breccia.

Samples from Mine Mountain have high base-metal contents, along with an epithermal precious-metal suite that includes arsenic, antimony and mercury (Table 2). Lead, zinc, selenium, cadmium, antimony and mercury contents are very high relative to other mineralized areas in the SWNVF. The gold and silver correlation with base metals is strong at Mine Mountain (Fig. 3). The correlation between gold and selenium is particularly striking, but silver correlates much more strongly with cadmium, mercury and base metals than does gold. The gold–silver correlation is weaker at Mine Mountain than it is in other mineralized areas in the SWNVF (Fig. 3).

The timing of hydrothermal activity at Mine Mountain is constrained by indirect stratigraphic and structural relations. Based on the presence of argillic and alunitic alteration in tuffs as young as the Ammonia Tanks Member of the Timber Mountain Tuff on the south flank of Mine Mountain, Jackson (1988) inferred the mineralization to be approximately contemporaneous with Timber Mountain magmatic activity. Alunite from an outcrop of the altered Ammonia Tanks Member has given a K/Ar age of 11.1 ± 0.3 Ma (E.H. McKee, S.I. Weiss and L.T. Larson, unpubl. data, 1989), consistent with alteration shortly after deposition of the 11.4-Ma Ammonia Tanks Member. Alteration has not been traced from the dated outcrop directly into the main mineralized area. However, if syn-mineralization lateral slip movements on fault surfaces along the crest of Mine Mountain were associated with deformation along the Mine Mountain strike-slip fault system, which offsets both units of the Timber Mountain Tuff (Orkild, 1968; Carr, 1984), then mineralization occurred after 11.4 Ma as well, consistent with the K/Ar age of the alunitic alteration.

The geochemical data at Mine Mountain are consistent with mineralization from more than one hydrothermal system. Base-metal and silver vein or replacement mineralization in Paleozoic sedimentary rocks may have been remobilized and overprinted by later epithermal metallization during magmatic activity of the Timber Mountain stage of the SWNVF.

Bullfrog district

The Bullfrog district in the Bullfrog Hills west of the town of Beatty (Fig. 1) has been the most important source of precious metals in the SWNVF. The district contains gold-silver vein deposits that are scattered within large areas underlain by hydrothermally altered rock, particularly in the southern part of the Bullfrog Hills (Fig. 2).

The Original Bullfrog mine in the southwest corner of the Bullfrog district was discovered in 1904, but most early production came from the Montgomery–Shoshone mine 6.5 km to the east (Fig. 2). By 1940, the Bullfrog district had recorded precious-metals production totalling about $3 million (Couch and Carpenter, 1943). Minor precious-metal production came from the Gold Bar mine and from several mines near the town of Rhyolite. The Mayflower and Pioneer mines, about 12 km north of Rhyolite, also had minor early production. Renewed exploration in the district since the mid-1970s resulted in open-pit mining for three years at the Gold Bar mine, the delineation of open-pit mineable reserves at the Montgomery–Shoshone mine, and the discovery and development of the Lac Bullfrog mine (Fig. 2), an entirely new deposit on the east side of Ladd Mountain that is expected to produce at least 61 t (1.8 million oz) of gold.

The Bullfrog Hills consist of an imbricately normal-faulted allochthon, composed mostly of Miocene volcanic and sedimentary rocks, that is separated from underlying Paleozoic and Proterozoic sedimentary and metamorphic rocks by a low-angle fault first recognized by Ransome et al. (1910). This structure is the Original Bullfrog segment of the regional OB-FC detachment fault system (Fig. 2) (Carr and Monsen, 1988; Maldonado, 1990a). Upper-plate rocks consist chiefly of silicic ash-flow sheets including units of the Crater Flat, Paintbrush and Timber Mountain Tuffs that were erupted from the central caldera complex of the SWNVF between about 15 and 11.4 Ma (Table 1). Lesser volumes of lava flows, domes and local tuffs of silicic composition, and relatively minor amounts of mafic and intermediate composition lava flows are intercalated with the regional ash-flow sheets. Units of tuffaceous sandstone, conglomerate, shale and lacustrine limestone are present mainly in the lower part of the volcanic section. Lying with angular discordance upon the Timber Mountain Tuff and older ash-flow sheets, is a local sequence of interbedded rhyolitic flows, domes and associated pyroclastic deposits which are capped by latite flows. These post-Timber Mountain Tuff rocks were erupted prior to about 10 Ma (Marvin et al., 1989; Noble et al., 1991).

Throughout much of the Bullfrog Hills, upper-plate rocks are cut by numerous west-dipping normal faults, many of listric geometry, that mostly strike north to northeast. This deformation has long been recognized as the result of WNW–ESE-directed upper crustal extension, and estimates of the amount of extension range from about 25% (Ransome et al., 1910) to more than 100% (Maldonado, 1990a). Most of the faulting and tilting began after about 11.4 Ma, as demonstrated by conformable and paraconformable relations between the Ammonia Tanks Member of the Timber Mountain Tuff and underlying ash-flow sheets in the southern Bullfrog Hills. Major tilting and faulting ceased before deposition of the flat-lying, 7.6-Ma Spearhead Member of the Stonewall Flat Tuff and local late Miocene conglomeratic deposits (Weiss et al., 1990).

Original Bullfrog mine

The Original Bullfrog mine was developed in a complex, shallowly north-dipping vein that is approximately 10 m thick. The vein is a shattered mass of banded crustiform quartz, calcite and silicified breccia that lies along the Original Bullfrog fault (Ransome et al., 1910). This fault, which appears to truncate the vein material against underlying, strongly sheared Paleozoic clastic and carbonate rocks that contain only minor veining, is part of the Bullfrog detachment fault system of Maldonado (1990a, b). The main vein grades upwards into sheeted veins within moderately east-dipping silicified ash-flow tuff of the 13.85-Ma Lithic Ridge Tuff (Carr et al., 1986; Sawyer et al., 1990). Adularia and albite replace feldspar phenocrysts and groundmass potash-feldspar and locally, between closely spaced veins, the tuff has been pervasively adularized. This alteration grades laterally and up-section into quartz-illite and sericite-albite-calcite assemblages, and at greater distances, into weak illite-calcite$\pm$albite alteration.

Vein quartz ranges from white, yellow and grey, banded fine granular or chalcedonic material to white, clear or amethystine, fine to medium comb quartz. Calcite occurs as coarsely crystalline masses intergrown with comb quartz, as inwardly-growing crystals along the walls of veins that were subsequently filled with comb quartz, or as irregular drusy veins with little or no quartz.

In addition to quartz and calcite, the main vein carries visible gold that is associated with limonite, malachite, chrysocolla and sulfide. SEM/EDX examinations of high-grade ore show that gold occurs in irregular electrum grains up to 1 mm in diameter with compositions that range between $Au_{52}Ag_{48}$ and $Au_{42}Ag_{58}$. Gold also occurs in mixed grains of native metal ($Au_{80}Ag_{20}$) and uytenbogaardtite (Ag_3AuS_2) (Fig. 6A). Silver is also present as acanthite, which occurs as irregular grains in quartz, and as mixed grains with uytenbogaardtite and gold. Textural relations indicate a complex paragenetic sequence. In ore containing visible gold, early calcite was followed by white comb quartz with sulfide and electrum, and lastly by vein-filling grey to amethystine quartz. The calcite is locally replaced by malachite and chrysocolla, which also occur in irregular masses surrounding gold and sulfide, and in late veinlets with sulfide and limonite. Textural relationships indicate that electrum is the earliest ore mineral, followed by acanthite, uytenbogaardtite and gold.

Samples from the Original Bullfrog mine have relatively high average silver:gold when compared to other mineralized areas in the Bullfrog district (Table 2). In addition, Original Bullfrog samples have strong copper, antimony and bismuth correlations with gold (Figs. 3 and 5).

Adularia from altered Lithic Ridge Tuff adjacent to the main vein has a K/Ar age of 8.7$\pm$0.3 Ma (Jackson, 1988) indicating that hydrothermal activity took place about 1–1.5 million years after the end of volcanic activity in the Bullfrog Hills. This age, along with shattering of the vein and apparent truncation of the vein by the underlying Original Bullfrog fault, is consistent with mineralization during the major period of detachment-style faulting in the region between 11.4 and 7.6 Ma.

Gold Bar mine

At the Gold Bar mine in the northwest corner of the Bullfrog district (Fig. 2), silver-gold mineralization is present in quartz-calcite veins and quartz-calcite-cemented breccia along a northeast-trending, west-dipping normal fault system cutting units of the Crater Flat and Paintbrush Tuff and minor basaltic rocks. The main area of mineralization lies about 2 km from the surface trace of the Bullfrog detachment fault system (Maldonado, 1990a). Veins consist of banded crustiform intergrowths of calcite and fine granular and comb quartz, commonly with drusy quartz and calcite and minor amethystine comb quartz. Late calcite veins are also present. Pyrite is the only sulfide mineral reported in vein material at the Gold Bar mine (Ransome et al., 1910). Wall-rock alteration appears to be similar to that at the Original Bullfrog mine. Variable albitization and adularization of feldspar phenocrysts and

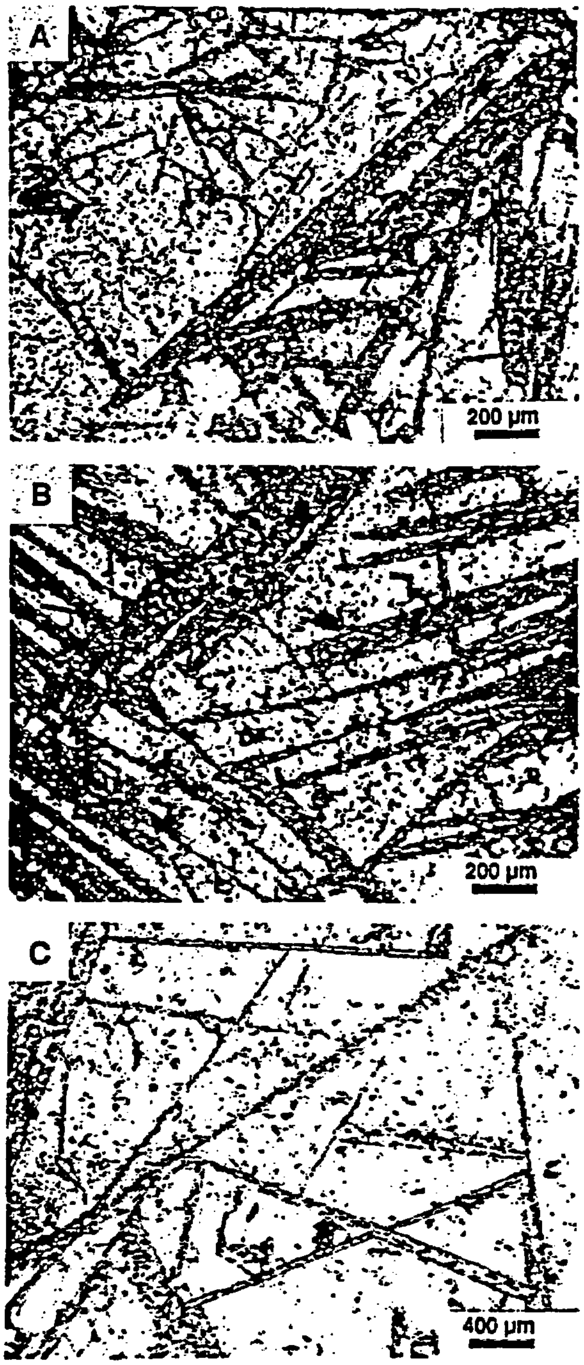

Fig. 7. Finely bladed calcite (dark) in quartz from (A) Gold Bar, (B) Lac-Bullfrog, and (C) Mayflower mines. Photomicrographs A and B, reflected light; photomicrograph C, transmitted light.

mineralization in the other deposits (see below).

Rhyolite area

The Rhyolite area contains the largest and highest grade known gold-silver ore reserves in the SWNVF. It includes vein systems at the Montgomery–Shoshone mine, the Lac Bullfrog mine and several small mines near the town of Rhyolite (Fig. 2). Most of the reserves are in the Lac Bullfrog deposit where Jorgensen et al. (1989) reported 13.0 Mt of ore averaging 3.77 g/t (14.3 Mst at 0.110 oz/st) prior to the start of production. By the end of 1991, 16.4 t (480,000 oz) of gold had been produced from this deposit, and reserves were estimated at 48 t (1.4 million oz) of economically mineable gold (D. McClure, pers. commun., 1991). Most of the historic gold and silver production in the Bullfrog district came from the Montgomery–Shoshone mine, about 1.5 km northeast of Rhyolite (Couch and Carpenter, 1943), which has reserves of 2.8 Mt of gold ore at an average grade of 2.5 g/t (3.1 Mst at 0.072 oz/st) as reported by Jorgensen et al. (1989). Host rocks for veins in the Rhyolite area are predominantly densely welded, devitrified portions of ash-flow sheets of the Paintbrush and Timber Mountain Tuffs.

At the Lac Bullfrog mine gold-silver ore is mined from a moderately west-dipping vein system that lies along a normal fault ("middle-plate fault" of Jorgensen et al., 1989) at the eastern foot of Ladd Mountain. Ore comprises a central zone, as much as 70 m thick, of complexly cross-cutting veins, hydrothermal breccia and silicified volcanic rock, that lies within the vein system. Closely spaced veins in the ore zone form stockworks and sheeted vein swarms. More widely spaced veins also form stockworks above and below the ore zone (Jorgensen et al., 1989). Well developed faults that have been the locus of significant displacement bound the ore zone in most places and are accompanied by gold-rich hydrothermal breccia (B. Claybourn, pers. commun., 1991). The hanging-wall rocks are well exposed on Ladd Mountain, an east-tilted fault-block that is composed mainly of a pervasively altered section of the Timber Mountain Tuff, a thin basaltic flow or sill, and underlying units of the Paintbrush Tuff and Crater Flat Tuff (Maldonado and Hausback, 1990). Exposed footwall rocks include strongly altered rocks probably belonging to the Crater Flat Tuff and an underlying unit of dacitic to rhyodacitic lava that is widely exposed beneath the Crater Flat and Lithic Ridge Tuffs elsewhere in the Bullfrog Hills (c.f., Maldonado and Hausback, 1990).

Vein material consists mostly of crustiform fine granular and comb quartz (locally amethystine) ± intergrown calcite of anhedral to finely bladed habit (Fig. 7B). Bands and veins of very finely granular to chalcedonic quartz and moderately coarse comb quartz are also present, and bands of fine adularia occur in minor amounts. Fluorite and barite have also been reported (Jorgensen et al., 1989). Fragments of wall rock are included in the veins and have been partly to nearly completely replaced by fine-grained quartz and adularia.

Multiple generations of cross-cutting quartz ± calcite veins, open space infillings, and fragments of vein material surrounded by later stages of quartz ± calcite provide evidence for a multi-stage paragenesis and for fracturing and brecciation concurrent with vein deposition. Much of the vein material is highly fractured, and faults generally form the margins of the main ore zone. These features suggest that the latest movements on the host fault postdate the last stages of vein deposition.

The style of mineralization at the Montgomery–Shoshone mine is similar to that at the Lac Bullfrog deposit (Jorgensen et al., 1989). Most of the gold-silver ore came from veins and breccia along a major, northeast-trending high-angle fault that juxtaposes unmineralized and unaltered, to very weakly altered, post-Timber Mountain rhyolitic to latitic rocks on the north against strongly altered rocks, mainly of the Ammonia Tanks Member of the Timber Mountain Tuff, to the south.

Mineralization extends southward for as much as 0.5 km in and along several north-trending quartz-calcite veins that occupy fractures and minor faults (Jorgensen et al., 1989; Maldonado and Hausback, 1990). Faults and fractures that control mineralization are part of the imbricate fault system associated with extension above the OB-FC fault (Maldonado, 1990a).

A number of smaller gold-silver bearing quartz and quartz-calcite veins similar to those of the Lac Bullfrog and Montgomery–Shoshone deposits were mined in the immediate vicinity of Rhyolite. The most notable workings include those of the National Bank mine, where sheeted and stockwork veins of fine granular quartz cut silicified and adularized tuffs of the Paintbrush Tuff and the Rainier Mesa Member of the Timber Mountain Tuff. At the Denver–Tramp mine these units host a system of subparallel steeply dipping north–south-trending quartz-carbonate veins up to 8 m wide that carry visible gold. The Denver–Tramp veins contain banded, very finely granular to fine comb quartz that is locally amethystine, and pockets of calcite that has been partially leached, leaving dark earthy manganese and iron oxides.

In addition to local silicification, mineralization in the Rhyolite area is associated with locally pervasive adularia flooding and more widespread adularia and albite replacement of feldspar phenocrysts. Thin veins within the Rainier Mesa Member on Ladd Mountain west of the Lac Bullfrog mine have adularized envelopes up to 1 cm thick, and sheeted veins at the National Bank mine occur in hard rock composed almost completely of adularia. In the Lac Bullfrog, Montgomery–Shoshone, National Bank, and Denver–Tramp mines, near-vein alteration consists of replacement of feldspar phenocrysts with adularia ± albite (Fig. 8) and probable adularization of groundmass feldspar. Small amounts of illite are present,

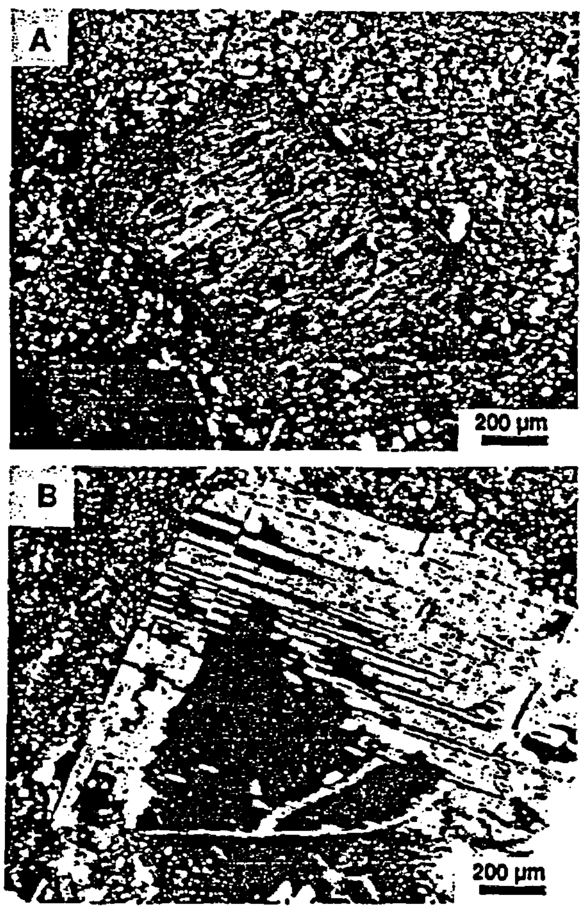

Fig. 8. Photomicrographs in cross-polarized transmitted light of (A) adularized, and (B) albitized feldspar phenocrysts in near-vein altered rhyolite tuff from the Lac Bullfrog mine. Identical alteration is present at the Original Bullfrog, Montgomery–Shoshone, Gold Bar, Mayflower, and Pioneer mines.

generally intergrown with secondary K-feldspar and quartz. Strong phyllosilicate alteration is uncommon in the Rhyolite area, except locally at the Montgomery–Shoshone mine. Primary biotite is commonly preserved, even in strongly altered rocks, reflecting the high activity of K^+ needed to produce adularia. At the Bold Gold Bullfrog mine pseudomorphs of limonite after pyrite are present in oxidized rock, and unoxidized rocks contain 1–2% disseminated pyrite.

Near-vein alteration described above grades outward from mineralized structures to much more subtle, but nevertheless pervasive and widespread illite-calcite ± quartz ± albite assemblages that could be considered propylitic in character (e.g., Sander and Einaudi, 1990). Chlorite- and carbonate-bearing assemblages have been reported only from sedimentary and metamorphic rocks beneath the Original Bullfrog–Fluorspar Canyon fault (Jorgensen et al., 1989).

All of the gold identified visually in samples from the Rhyolite area was found in fine granular and comb quartz. Very fine granular vein quartz is generally present in gold ore, but was not seen to contain gold. Finely bladed calcite intergrown with quartz in vein material from the Lac Bullfrog mine is similar to that observed in vein material from the Gold Bar mine. Acanthite is a major silver-bearing phase in some ore at the Lac Bullfrog mine and minor amounts of chalcopyrite, galena and sphalerite have also been reported (Jorgenson et al., 1989). Cerargyrite was reported at the Montgomery–Shoshone mine by Ransome et al. (1910). Secondary copper minerals are locally associated with gold at depth in the Lac-Bullfrog mine (B.W. Claybourn, pers. commun., 1991) and tetrahedrite has also been identified (D. Brosnahan, pers. commun., 1991). This mineral association is similar to that at the Original Bullfrog mine.

Ransome et al. (1910) reported that gold in the Bullfrog district characteristically occurs as electrum in limonitic specks that represent oxidized pyrite crystals. Electrum of this type is present at the Lac Bullfrog mine as well (Fig. 6B). We found other types of gold in the district. Electrum occurs as contorted flakes between quartz grains (Fig. 6C) at the Lac Bullfrog and Denver–Tramp mines. SEM/EDX analysis shows that electrum in this form from the Lac Bullfrog mine has a composition of $Au_{44}Ag_{56}$. In addition, electrum and gold are present in irregular lenses composed of quartz, limonite, chrysocolla, acanthite and uytenbogaardtite, that are similar to mineralization described above at the Original Bullfrog mine.

The electrum ($Au_{57}Ag_{43}$ to $Au_{51}Ag_{49}$) is in irregular grains up to 1 mm in maximum dimension, and gold ($Au_{72}Ag_{28}$) is present as narrow borders on electrum. The uytenbogaardtite is intergrown with gold ($Au_{72}Ag_{28}$ to $Au_{77}Ag_{23}$) and acanthite, and appears to replace electrum (Fig. 6D).

Most samples of veins and altered volcanic rocks from the Rhyolite area contain elevated gold and silver contents relative to unaltered silicic volcanic rocks, but have low contents of other trace elements (Table 2). A sample of unusually rich ore containing 9223 ppm gold and 2.1% silver from the Lac Bullfrog mine is an exception, containing high copper, lead, antimony, zinc, selenium and tellurium. A few samples contain anomalous molybdenum or tellurium, but copper is the only trace element that correlates well with precious metals (Fig. 3). Copper reportedly increases in abundance with depth at the Lac Bullfrog mine (Jorgenson et al., 1989) Arsenic is remarkably low; maximum arsenic content in samples that we obtained from the Rhyolite area is 88 ppm, and arsenic values are not correlative with gold (Figs. 3 and 5).

Alteration and mineralization in the Rhyolite area postdate deposition of the 11.4-Ma Ammonia Tanks Member of the Timber Mountain Tuff and are structurally controlled by faults and fractures that formed in the upper plate of the Bullfrog detachment system during the period of regional extensional faulting between 11.4 and 7.6 Ma. A K/Ar age of 9.5±0.2 Ma on adularia from the Montgomery–Shoshone mine (Morton et al., 1977) indicates that mineralization took place there during this period. Fault relationships and quartz-healed brecciation in the Lac Bullfrog vein are consistent with mineralization that took place during faulting and prior to the last movements along the controlling structure. The similarities in structural control, mineralogy, style of veins, and alteration lead us to infer that mineralization throughout the Rhyolite area took place at about the same time as that at the Montgomery–Shoshone mine.

Mayflower–Pioneer area

The Mayflower and Pioneer mines, about 12 km north of Rhyolite, were developed between 1905 and the early 1920s, but little production was recorded (Ransome et al., 1910; Cornwall, 1972). The original gold strike at the Pioneer mine consisted of mineralized gouge and breccia along a steeply southwest-dipping shear zone (unpubl. inf., NBMG mining district files). At the Mayflower mine, gold ore was found in a southwest-dipping fracture zone with sheeted to irregular quartz-calcite veins (Ransome et al., 1910). Both mines are in rocks containing adularia-albite-illite alteration and quartz-calcite veining similar to that in the Rhyolite area. Host rocks include the Crater Flat Tuff as well as overlying coarse volcaniclastic and megabreccia deposits consisting of debris that includes pre-Tertiary rock and ash-flow units as young as the 11.4-Ma Tuffs of Fleur de Lis Ranch (S. Weiss and K. Connors, unpubl. mapping, 1990). The coarse clastic rocks are overlain by rhyolitic tuffs and lavas erupted by about 10 Ma (Marvin et al., 1989; Noble et al., 1991).

Analyses of a small number of mineralized and altered samples reported gold values as high as 15.3 ppm along with high mercury and antimony, but relatively low arsenic. A vein sample from the Mayflower mine was found to contain fine grey comb quartz with finely bladed calcite (Fig. 7C) similar to that found in gold-rich veins in the Rhyolite area and at the Gold Bar mine. Veins in the Mayflower mine contain electrum in limonite and as contorted flakes similar to occurrences in the Rhyolite area (c.f., Figs. 6B and C).

Adularia from mineralized rock at the Mayflower mine has a K/Ar age of 10.0±0.3 Ma (Jackson, 1988), consistent with stratigraphic constraints. This date overlaps, within analytical uncertainty, the adularia age-date for the Montgomery–Shoshone mine, but is appreciably older than the date reported for adularia from the Original Bullfrog mine.

Discussion

Hydrothermal activity and precious-metal mineralization in the southern part of the SWNVF took place over a period of approximately 4.5 million years that overlapped with episodes of magmatic activity. Although all of the mineralization is epithermal in nature, its style and geochemistry vary significantly from area to area (Table 4).

Silver-gold mineralization in the Wahmonie district differs from mineralization in other parts of the SWNVF in that it is situated in the eroded remnants of a volcanic center dominated by rocks of intermediate composition. K/Ar ages indicate that hydrothermal activity at Wahmonie occurred during the main magmatic stage of the SWNVF, and coincided with, or closely followed, the end of magmatic and volcanic activity at the Wahmonie–Salyer volcanic center. Based on mineral assemblages in ore, vein, and wall rock alteration, type of host rocks, and available geochemical data, mineralization at Wahmonie comprises an epithermal precious-metal system of the adularia-sericite type of Heald et al. (1987) or the low sulfur type of Bonham (1989).

Available data show that base metals, arsenic, antimony and mercury at Wahmonie are relatively low compared to high base-metal, adularia-sericite type deposits (e.g., Creede, Colorado, Heald et al., 1987), and suggest kinship with high silver:gold ratio, relatively base-metal-poor deposits such as Tonopah, Nevada (e.g., Bonham, 1989). However, the high bismuth and tellurium concentrations of the Wahmonie district are not typical of adularia-sericite type precious-metal deposits; these elements are more commonly associated with

TABLE 4

Summary of precious-metal mineralized areas in the southern part of the southwestern Nevada volcanic field

District	Host Rocks	Mineralization Style	Mineralization Age (Ma)	Trace Element Assemblage	Structural Setting
Wahmonie	andesitic to rhyodacitic volcanic and intrusive rocks ca. 13 Ma	adularia-sericite type; quartz-calcite veins, sheeted veins	13-12.5	Ag+Au+Te+Bi+Hg ±Sb; moderate to high Ag:Au	normal faults
Bare Mountain (Sterling, Daisy, and Mother Lode mines; Secret Pass, Goldspar, and Telluride deposits)	Precambrian + Paleozoic clastic and carbonate sedimentary rocks; felsic intrusives and tuffs ca. 13-11.4 Ma	mostly disseminated; minor quartz-adularia veinlets; fluorite veins	13-11.2(?)	Au+Ag+Sb+As+F ±Hg±Te±Tl±Mo ±Cu±Pb; low Ag:Au	thrust fault; low- to high angle normal faults in part associated with detachment
Mine Mountain	Devonian carbonate rocks and Mississippian clastic rocks	veins, hydrothermal breccia, jasperoid	<11.4	Ag+Au+Pb+Zn+Sb +As+Hg+Cd±Se; very high Ag:Au	thrust fault; high-angle normal and strike-slip faults
Bullfrog (Original Bullfrog, Gold Bar, Mayflower, and Pioneers mines; Rhyolite area: Lac Bullfrog and Montgomery-Shoshone mines)	mainly rhyolitic ash-flow tuff units ca. 14-11 Ma	adularia-sericite type; quartz-calcite veins, sheeted veins and stockworks	9-10	Au+Ag±Cu±Sb; other trace elements generally low; low to moderate Ag:Au	low- to high-angle normal faults associated with detachment

porphyry-related gold deposits such as the Top deposit at Bald Mountain and the Fortitude and McCoy deposits in Nevada (e.g., Bonham, 1989; Brooks et al., 1991). Two other characteristics of the Wahmonie area suggest that exposed and near-surface mineralization may be associated with an underlying porphyry system. First, subvolcanic stocks and rhyolite dikes exposed in the central horst as well as geophysical evidence for a pluton beneath the district are consistent with the presence of a buried, perhaps composite, porphyry intrusion. Secondly, the presence of hypersaline fluid inclusions in quartz phenocrysts and biotite ± tourmaline veins within the porphyritic granodiorite argue strongly for at least some porphyry-type magmatic-hydrothermal activity.

Precious-metal mineralization in the Bare Mountain district, although apparently similar in age to that at Wahmonie, occupies an entirely different geologic setting. Mineral assemblages, chemistry, and style of Bare Mountain mineralization and alteration are also markedly different from the Wahmonie district. Stratigraphic, structural and radiometric age relations indicate that gold-silver ± mercury ± fluorite mineralization in Bare Mountain took place during the main magmatic stage of the SWNVF subsequent to the emplacement of the felsic dike swarm. With the exception of the Secret Pass deposit, areas of gold-silver mineralization in northern and eastern Bare Mountain have geochemical and geologic characteristics of Carlin-type, sedimentary rock-hosted disseminated deposits (e.g., Radtke, 1985, Percival et al., 1988). Gold deposits in Bare Mountain consists of disseminated mineralization in sedimentary, hypabyssal, and extrusive rocks with only minor quartz veining, little or no silicification, and common fluorite and cinnabar. Alteration is mainly illitic to kaolinitic with decalcification ± silica replacement of sedimentary rocks. Remobilized carbon is conspicuous at the Mother Lode deposit. High contents of arsenic, antimony, mercury and molybdenum as well as anomalous thallium are associated with mineralization in the north and east parts of Bare Mountain, and base metals are locally high. Silver contents, however, are generally low, and silver:gold ratios are distinctly lower than in other areas of precious-metal mineralization in the southern part of the SWNVF.

The Secret Pass deposit differs from the sediment-hosted deposits in host-rock lithology, alteration assemblage, and in having lower thallium contents. Although veining and silicification are reported to be weakly developed at Secret Pass (Greybeck and Wallace, 1991), the alteration assemblage, perhaps strongly influenced by host lithology, best fits that of the adularia-sericite type of epithermal precious-metal system. Similarities in trace-element signatures between the Secret Pass deposit and other Bare Mountain deposits show that host-rock lithology does not play a major role in controlling trace-element assemblages.

Gold-silver mineralization in Bare Mountain is clearly epithermal in nature, and has features strongly suggestive of a shallow level of emplacement; nevertheless, it is similar in several respects to Carlin-type disseminated deposits. As Noble et al. (1989) proposed, the presence of a buried, granite-type porphyry molybdenum system in Bare Mountain is likely on the basis of geologic, geochemical, and fluid-inclusion data. Following Noble et al., we propose that most of the gold-silver deposits in Bare Mountain provide examples of distal disseminated sediment-hosted deposits genetically related to magmatic-hydrothermal systems (e.g., Sillitoe and Bonham, 1990) such as deposits in the Bau District, Sarawak (Percival et al., 1990), Purisima Concepcion, Peru (Alvarez and Noble, 1988) and Barney's Canyon, Utah (Sillitoe and Bonham, 1990).

Sediment-hosted precious-metal mineralization is also present within the SWNVF at Mine Mountain. Structural relations and the K/Ar age of alunitic alteration at Mine Mountain indicate that hydrothermal activity and mineralization were, at least in part, concurrent with magmatic and volcanic activity of the Timber Mountain magmatic stage of the SWNVF as first proposed by Jackson (1988). The hydrothermal breccia veins, cinnabar and chalcedonic quartz at Mine Mountain, along with abundant mercury, arsenic and antimony (Table 2), are indicative of epithermal mineralization. Mine Mountain also possesses characteristics common to Carlin-type disseminated gold deposits, including association with a thrust fault, occurrence in sedimentary rocks that are variably decalcified, veined, silicified (including jasperoid) and cut by hydrothermal breccia, and the presence of barite veins. However, the high lead and zinc contents, low thallium contents, high silver:gold ratio, and abundance of quartz in veins at Mine Mountain are not typical of Carlin-type deposits (e.g., Radtke, 1985).

On the basis of geology and trace-element chemistry, Mine Mountain is similar to the Candelaria silver district approximately 150 km northwest of Mine Mountain. At Candelaria, disseminated silver ore is associated with thrust faults and intrusions cutting Mesozoic sedimentary and igneous rocks (Moeller, 1988). Carbonate-quartz veins mined for silver, gold, lead, zinc and antimony are present as well (Page, 1959). Candelaria veins have lead, zinc, arsenic, antimony and cadmium contents similar to the Mine Mountain veins and also carry anomalously high mercury (Hill et al., 1986), though not as high as at Mine Mountain. Alternatively, geochemical and geologic data at Mine Mountain are consistent with more than one period of hydrothermal activity that may, in part, have preceded development of the SWNVF.

A distinctly younger episode of mineralization is present in the Bullfrog district. Hydrothermal activity in the district, at about 9 to 11 Ma, occurred during the latter part of the Timber Mountain magmatic stage and may have extended into the late magmatic stage of the SWNVF as proposed by Jackson (1988). The age of mineralization in the Bullfrog district overlaps with a period of intense extensional tectonism in the Bullfrog Hills that provided structural preparation for mineralization, and may also have displaced mineralized rock.

Vein and alteration mineral assemblages, along with mineralization style, show that mineralization in the Bullfrog district was the result of adularia-sericite (low sulfur)-type hydrothermal activity. Wall-rock alteration in the Bullfrog district, which includes large volumes of rock with subtle adularia and albite replacement of feldspar phenocrysts, is similar to alteration described at Round Mountain, Nevada (e.g., Sander and Einaudi, 1990). Precious-metal mineralization in the Bullfrog district is mainly restricted to several quartz-carbonate vein deposits that are similar to each other in texture and mineralogy (Figs. 6 and 7).

The low content of precious-metal-related trace elements serves to distinguish the Rhyolite area from other areas that contain economic gold and silver mineralization in adularia-sericite systems. In comparison with such systems elsewhere in the Great Basin (e.g., Round Mountain, Tingley and Berger, 1985; Sleeper, Nash et al., 1990; Hollister, Bartlett et al., 1991; Rawhide, Black et al., 1991; and Hart Mountain, Capps and Moore, 1991), altered and mineralized rock from the Rhyolite area has the lowest overall contents of precious-metal pathfinder elements, particularly arsenic, antimony and mercury. Most, but not all, of the samples collected during this study came from the oxidized zone, and low metal contents might be the result of supergene leaching; however, most of the data from the other systems listed above are also from analyses of oxidized material. Rhyolite area mineralization took place in an areally extensive hydrothermal system from which typical epithermal and base-metal elements may have been flushed by late-stage fluids. The uytenbogaardtite that appears to replace electrum in the Lac Bullfrog mine (Fig. 6d) in association with acanthite may be evidence of such a process, because uytenbogaardtite can only occur in equilibrium with acanthite at temperatures below 113°C (Barton et al., 1978). Alternatively, Rhyolite area mineralization may simply have been introduced by fluids with lower base-metal and pathfinder element budgets than those responsible for other volcanic-hosted precious-metal deposits.

The Gold Bar mine in the northwest part of the Bullfrog district has a similar lack of trace elements to mineralized rock at Rhyolite. In comparison, available trace-element data show that the Original Bullfrog and Mayflower mines have higher trace-element contents. The style of veining and occurrence of uytenbogaardtite in both the Original Bullfrog and Lac Bullfrog deposits (Fig. 6) indicates that physical conditions were similar during precious-metal mineralization in widely separated parts of the Bullfrog district, despite differences in trace-element geochemistry.

Precious-metal deposits in the Gold Bar mine, Original Bullfrog mine, Rhyolite area, Daisy mine–Secret Pass area, and Mother Lode mine are located within 2 km of the trace of the OB-FC detachment fault (Fig. 2). Jorgensen et al. (1989) implied that deposits in the Bullfrog district and Fluorspar Canyon resulted from the same hydrothermal system. We believe that this is not the case. Mineralized rock in the Bare Mountain district contains a consistent suite of trace elements that contrasts with the trace-element suite in the Bullfrog district (with the possible exception of the Mayflower–Pioneer area), and the age of hydrothermal activity in the Bullfrog district is significantly younger than in the Bare Mountain area. Moreover, the quartz-carbonate-adularia veins and style of wall-rock alteration that are typical of the Bullfrog district are uncommon in the Bare Mountain area, and large areas of unaltered rock separate the two districts.

Conclusions

Strong differences in ore and gangue mineralogy, style of mineralization, wall-rock alteration assemblages, and trace-element chemistry between areas of precious-metal mineralization reflect the variable geologic settings and chemical diversity of hydrothermal systems active during the development of the SWNVF. These systems were active over a period of about 4.5 million years that spanned portions of the three magmatic stages of the field and gave rise to a broad spectrum of deposit types. The presence of intrusive porphyry, trace-element suites associated with porphyry-related mineralization, and evidence for the passage of high-salinity fluids suggest that mineralization, during the main magmatic stage of the SWNVF at Bare Mountain and Wahmonie was associated with porphyry-type magmatic systems. At Wahmonie silver-rich vein mineralization of the adularia-sericite type is hosted by an intermediate volcanic center, and is temporally and spatially associated with subvolcanic intrusions. At Bare Mountain, a genetic relationship between porphyry magmatism and shallow Carlin-type gold deposits seems likely.

The relatively base-metal- and silver-rich system at Mine Mountain was apparently active during the Timber Mountain stage of SWNVF volcanism. It shares features with vein and disseminated silver mineralization at Candelaria, Nevada, and may be the result of mineralization from more than one hydrothermal system.

The style of mineralization and alteration in the Bullfrog district is similar to other quartz-adularia precious-metal deposits in the Great Basin. The district contains gold-rich deposits that are largely devoid of epithermal elements and base metals. Hydrothermal activity was coeval with strong extensional tectonism and may have continued into the late magmatic stage of the SWNVF. Mineralization in the Bullfrog district and some deposits in the Bare

Mountain district were structurally controlled by the OB-FC detachment fault system. However, differences in age, mineralization style and geochemistry indicate that mineralization in the two districts is unrelated.

Acknowledgements

Our studies have been partially supported by funds provided by the Nevada Nuclear Waste Project Office through the Center for Neotectonic Studies (to Weiss) and by the U.S. Department of Energy and Science Applications International Corporation (to Castor). J.J. Sjoberg, U.S. Bureau of Mines Western Research Center, Reno, Nevada, is gratefully acknowledged for providing SEM/EDX analyses. We thank M.O. Desilets of the NBMG for calculation of correlation coefficients for the chemical analyses. J.V. Tingley and H.F. Bonham of the NBMG, and L.T. Larson and D.C. Noble of the Mackay School of Mines, University of Nevada, Reno, contributed useful comments and discussion on data and ideas reported herein. J. Quade kindly provided unpublished data on the Wahmonie mining district. We are grateful to the staff of Lac Bullfrog, Inc., GEXA Gold Corp., U.S. Precious Metals, Ltd., and Angst, Inc. for allowing access to their properties, as well as discussions on the geology of their deposits. We thank J.S. Cline and A.B. Wallace for constructive reviews of the manuscript.

References

Alvarez, A.A. and Noble, D.C., 1988. Sedimentary rock-hosted disseminated precious metal mineralization at Purisima Concepcion, Yauricocha district, central Peru. Econ. Geol., 83: 1368–1378.

Bartlett, M.W., Enders, M.S. and Hruska, D.C., 1991. Geology of the Hollister gold deposit, Ivanhoe district, Elko County, Nevada. In: G.L. Raines, R.E. Lisle, R.W. Schafer and W.H. Wilkinson (Editors), Geology and Ore Deposits of the Great Basin, Vol. II. Geol. Soc. Nev., pp. 957–978.

Barton, M.D., Kieft, C., Burke, E.A.J. and Oen, I.S., 1978. Uytenbogaardtite, a new silver-gold sulfide. Can. Mineral., 16: 651–657.

Black, J.E., Mancuso, T.K. and Gant, J.L., 1991. Geology and mineralization at the Rawhide Au–Ag deposit, Mineral County, Nevada. In: G.L. Raines, R.E. Lisle, R.W. Schafer and W.H. Wilkinson (Editors), Geology and Ore Deposits of the Great Basin, Vol. II. Geol. Soc. Nev., pp. 1123–1144.

Bonham, H.F., Jr., 1989. Bulk mineable gold deposits of the western United States. In: R.R. Keays, R.H. Ramsay and D.I. Groves (Editors), The Geology of Gold Deposits: The Perspective in 1988. Econ. Geol. Monogr., 6: 193–207.

Bonham, H.F., Jr. and Hess, R.H., 1991. Bulk-mineable precious-metal deposits. In: The Nevada Mineral Industry—1990. Nev. Bur. Min. Geol., Spec. Publ., MI-1990: 19–26.

Brooks, J.W., Meinert, L.D., Kuyper, B.A. and Lane, M.L., 1991. Petrology and geochemistry of the McCoy gold skarn, Lander County, Nevada. In: G.L. Raines, R.E. Lisle, R.W. Schafer and W.H. Wilkinson (Editors), Geology and Ore Deposits of the Great Basin, Vol. II. Geol. Soc. Nev., pp. 419–442.

Byers, F.M., Jr., Carr, W.J. and Orkild, P.P., 1976. Volcanic suites and cauldrons of Timber Mountain–Oasis Valley Caldera Complex, Southern Nevada. U.S. Geol. Surv. Prof. Pap., 919, 70 pp.

Byers, F.M., Jr., Carr, W.J. and Orkild, P.P., 1989. Volcanic centers of southwestern Nevada: evolution of understanding, 1960–1988. J. Geophys. Res., 94 (B5): 5908–5924.

Capps, R.C. and Moore, J.A., 1991. Geologic setting of mid-Miocene gold deposits in the Castle Mountains, San Bernardino County, California and Clark County, Nevada. In: G.L. Raines, R.E. Lisle, R.W. Schafer and W.H. Wilkinson (Editors), Geology and Ore Deposits of the Great Basin, Vol. II. Geol. Soc. Nev., pp. 1195–1219.

Carr, M.D. and Monsen, S.A., 1988. A field trip guide to the geology of Bare Mountain. In: D.L. Wide and M.L. Faber (Editors), This Extended Land—Geological Journeys in the Southern Basin and Range. Geol. Soc. Am., Cordilleran Section, Field Trip Guidebook. pp. 50–57.

Carr, W.J., 1984. Regional structural setting of Yucca Mountain, southwestern Nevada, and late Cenozoic rates of tectonic activity in part of the southwestern Great Basin, Nevada and California. U.S. Geol. Surv., Open-File Rep., 84-854, 114 pp.

Carr, W.J., Byers, F.M. and Orkild, P.P., 1986. Stratigraphic and volcano-tectonic relations of Crater Flat Tuff and some older volcanic units, Nye County, Nevada. U.S. Geol. Surv. Prof. Pap., 1323, 23 pp.

Castor, S.B., Feldman, S.C. and Tingley, J.V., 1990. Mineral evaluation of the Yucca Mountain Addition, Nye County, Nevada. Nev. Bur. Min. Geol., Open-File Rep., 90-4, 107 pp.

Christiansen, R.L., Lipman, P.W., Carr, W.J., Byers, F.M., Jr., Orkild, P.P. and Sargent, K.A., 1977. Timber Mountain–Oasis Valley caldera complex of southern Nevada. Geol. Soc. Am. Bull., 88: 943–959.

Cornwall, H.R., 1972. Geology and mineral deposits of southern Nye County, Nevada. Nev. Bur. Min. Geol. Bull., 77, 49 pp.

Cornwall, H.R. and Kleinhampl, F.J., 1961. Geology of the Bare Mountain quadrangle. U.S. Geol. Surv. Map GQ-157, 1:62,500 scale.

Cornwall, H.R. and Kleinhampl, F.J., 1964. Geology of the Bullfrog quadrangle and ore deposits related to the Bullfrog Hills caldera, Nye County, Nevada, and Inyo County, California. U.S. Geol. Surv. Prof. Pap., 454-J, 25 pp.

Couch, B.F. and Carpenter, J.A., 1943. Nevada's metal and mineral production. Nev. Bur. Min. Geol. Bull., 38, 159 pp.

Dowling, K. and Morrison, G., 1989. Application of quartz textures to the classification of gold deposits using North Queensland examples. In: R.R. Keays, R.H. Ramsay and D.I. Groves (Editors), The Geology of Gold Deposits: The Perspective in 1988. Econ. Geol. Monogr., 6: 342–355.

Ekren, E.B. and Sargent, K.A., 1965. Geologic map of the Skull Mountain quadrangle, Nye County, Nevada. U.S. Geol. Surv. Map GQ-387, 1:24,000 scale.

Greybeck, J.D. and Wallace, A.B., 1991. Gold mineralization at Fluorspar Canyon near Beatty, Nye County, Nevada. In: G.L. Raines, R.E. Lisle, R.W. Schafer and W.H. Wilkinson (Editors), Geology and Ore Deposits of the Great basin, Vol. II. Geol. Soc. Nev., pp. 935–946.

Hamilton, W.B., 1988. Detachment faulting in the Death Valley region. California and Nevada. U.S. Geol. Surv. Bull., (1790): 51–85.

Hausback, B.P., Deino, A.L., Turrin, B.T., McKee, E.H., Frizzell, V.A., Noble, D.C. and Weiss, S.I., 1990. New $^{40}Ar/^{39}Ar$ ages for the Spearhead and Civet Cat Canyon Members of the Stonewall Flat Tuff, Nye County, Nevada: Evidence for systematic errors in standard K-Ar age determinations on sanidine. Isochron/West, 56: 3–7.

Heald, P., Foley, J.K. and Hayba, D.O., 1987. Comparative anatomy of volcanic-hosted epithermal deposits: acid-sulfate and adularia-sericite types. Econ. Geol., 82: 1–26.

Hill, R.H., Adrian, B.M., Bagby, W.C., Bailey, E.A., Goldfarb, R.J. and Pickthorn, W.J., 1986. Geochemical data for rock samples collected from selected sediment-hosted disseminated precious-metal deposits in Nevada. U.S. Geol. Surv. Open-File Rep. 86-107, 30 pp.

Hoover, D.B., Chornack, M.P., Nervick, K.H. and Broker, M.M., 1982. Electrical studies at the proposed Wahmonie and Calico Hills nuclear waste sites, Nevada Test Site, Nye County, Nevada. U.S. Geol. Surv. Open-File Rep., 82-466, 45 pp.

Jackson, M.R., Jr., 1988. The Timber Mountain magmato-thermal event: an intense widespread culmination of magmatic and hydrothermal activity at the southwestern Nevada volcanic field. Unpubl. MSc thesis, Univ. Nevada, Reno, Nev., 46 pp.

Jorgensen, D.K., Rankin, J.W. and Wilkins, J., Jr., 1989. The geology, alteration, and mineralogy of the Bullfrog gold deposit, Nye County, Nevada. Soc. Min. Eng., Preprint 89-135, 13 pp.

Kistler, R.W., 1968. Potassium-argon ages of volcanic rocks in Nye and Esmeralda Counties, Nevada. Geol. Soc. Am. Mem., 110: 251–263.

Lechler, P.L. and Desilets, M.O., 1991. The NBMG standard reference material project. Nev. Geol., 10: 1–2.

Maldonado, F., 1990a. Structural geology of the upper plate of the Bullfrog Hills detachment fault system, southern Nevada. Geol. Soc. Am. Bull., 102: 992–1006.

Maldonado, F., 1990b. Geologic map of the northwest quarter of the Bullfrog 15-minute quadrangle, Nye County, Nevada. U.S. Geol. Surv. Map I-1985, 1:24,000 scale.

Maldonado, F. and Hausback, B.P., 1990. Geologic map of the northeast quarter of the Bullfrog 15-minute quadrangle, Nye County, Nevada. U.S. Geol. Surv. Map I-2049, 1:24,000 scale.

Mapa, M.R., 1990. Geology and mineralization of the Mother Lode mine, Nye County, Nevada. In: R.H. Buffa and A.R. Coyner (Editors), Geology and Ore Deposits of the Great Basin Symposium, April 1990; Field Trip Guidebook Compendium. Geol. Soc. Nev., pp. 1076–1077.

Marvin, R.F., Mehnert, H.H. and Naeser, C.W., 1989. U.S. Geological Survey radiometric ages—compilation "C", part 3: California and Nevada. Isochron/West, 52: 3–11.

Moeller, S.A., 1988. Geology and mineralization in the Candelaria district. Mineral County, Nevada. In: R.W. Schafer, J.J. Cooper and P.G. Vikre (Editors), Bulk Mineable Precious Metal Deposits of the Western United States. Symp. Proc., Geol. Soc. Nev., pp. 135–158.

Monsen, S.A., Carr, M.D., Reheis, M.C. and Orkild, P.P., 1990. Geologic map of Bare Mountain, Nye County, Nevada. U.S. Geol. Surv. Open-File Rep. 90-25, 17 pp.

Morton, J.L., Silberman, M.L., Bonham, H.F., Garside, L.J. and Noble, D.C., 1977. K-Ar ages of volcanic rocks, plutonic rocks, and ore deposits in Nevada and eastern California. Isochron/West, 20: 19–29.

Nash, J.T., Frey, D.L., Motooka, J.M. and Siems, D.F., 1990. Geochemical analyses of ore and host rocks, Sleeper gold-silver deposit, Humboldt County, Nevada. U.S. Geol. Surv. Open-File Rep., 90-702A, 69 pp.

Noble, D.C., Weiss, S.I. and Green, S.M., 1989. High-salinity fluid inclusions suggest that Miocene gold deposits of the Bare Mtn. district, NV, are related to a large buried rare-metal rich magmatic system. Geol. Soc. Am., Abstr. with Progr., 20(3): 123.

Noble, D.C., Weiss, S.I. and McKee, E.H., 1991. Magmatic and hydrothermal activity, caldera geology, and regional extension in the western part of the southwestern Nevada volcanic field. In: G.L. Raines, R.E. Lisle, R.W. Schafer and W.H. Wilkinson (Editors), Geology and Ore Deposits of the Great Basin, Vol. II. Geol. Soc. Nev., pp. 913–934.

Odt, D.A., 1983. Geology and geochemistry of the Sterling gold deposit, Nye County, Nevada. Unpubl. M.Sc. thesis, Univ. Nevada, Reno—Mackay School of Mines, Reno, Nev., 100 pp.

Orkild, P.P., 1968. Geologic map of the Mine Mountain Quadrangle, Nye County, Nevada. U.S. Geol. Surv., Map GQ-746, 1:24,000 scale.

Page, B.M., 1959. Geology of the Candelaria mining district, Mineral County, Nevada. Nev. Bur. Mines Geol. Bull., 56, 67 pp.

Papke, K.G., 1979. Fluorspar in Nevada. Nev. Bur. Mines Geol. Bull., 93: 40–47.

Percival, T.J., Bagby, W.C. and Radtke, A.S., 1988. Physical and chemical features of precious metal deposits hosted by sedimentary rocks in the western United States. In: R.W. Schafer, J.J. Cooper and P.G. Vikre (Editors), Bulk Mineable Precious Metal Deposits of the Western United States. Symp. Proc., Geol. Soc. Nev., pp. 11–34.

Percival, T.J., Radtke, A.S. and Bagby, W.C., 1990. Relationships among carbonate-replacement gold deposits, gold skarns and intrusive rocks, Bau mining district, Sarawak, Malaysia. Min. Geol., 40: 1–16.

Ponce, D.A., 1981. Preliminary gravity investigations of the Wahmonie site, Nevada Test Site, Nye County, Nevada. U.S. Geol. Surv. Open-File Rep. 81-522, 64 pp.

Quade, J., Tingley, J.V., Bentz, J.L. and Smith, P.L., 1984. A mineral inventory of the Nevada Test Site and portions of Nellis Bombing and Gunnery Range, southern Nye County, Nevada. Nev. Bur. Mines Geol. Open-File Rep. 84-2, 68 pp.

Radtke, A.S., 1985. Geology of the Carlin gold deposit, Nevada. U.S. Geol. Surv., Prof. Pap., 1262, 124 pp.

Ransome, F.L., Emmons, W.H. and Garrey, G.H., 1910. Geology and ore deposits of the Bullfrog district, Nevada. U.S. Geol. Surv. Bull. 407, 129 pp.

Sander, M.V. and Einaudi, M.T., 1990. Epithermal deposition of gold during transition from propylitic to potassic alteration at Round Mountain, Nevada. Econ. Geol., 85: 285–311.

Sawyer, D.A., Fleck, R.J., Lanphere, M.A., Warren, R.G. and Broxton, D.E., 1990. Episodic volcanism in the southwestern Nevada volcanic field: new $^{40}Ar/^{39}Ar$ geochronologic results (abstract). EOS, Trans. Am. Geophys. Union, 71: 1296.

Silitoe, R.H. and Bonham, H.F., Jr., 1990. Sediment-hosted gold deposits: distal products of magmatic-hydrothermal systems. Geology, 18: 157–161.

Stewart, J.H., 1988. Tectonics of the Walker Lane belt, western Great Basin—Mesozoic and Cenozoic deformation in a zone of shear. In: W.G. Ernst (Editor), Metamorphism and Crustal Evolution of the Western United States. Rubey Vol. VII. Prentice-Hall, Englewood Cliffs, NJ., pp. 683–713.

Thompson, A.J.B., 1991. Characteristics of acid-sulfate alteration in the Marysvale—Pioche mineral belt: a guide to gold mineralization. Utah Geol. Miner. Surv. Misc. Publ., 9-12, 29 pp.

Tingley, J.V., 1984. Trace element associations in mineral deposits, Bare Mountain (fluorine) mining district, Southern Nye County, Nevada. Nev. Bur. Mines Geol. Rep. 39, 28 pp.

Tingley, J.V. and Berger, B.R., 1985. Lode gold deposits of Round Mountain, Nevada. Nev. Bur. Mines Geol. Bull., 100, 62 pp.

Weiss, S.I., Connors, K.A., Noble, D.C. and McKee, E.H., 1990. Coeval crustal extension and magmatic activity in the Bullfrog Hills during the latter phases of Timber Mountain volcanism. Geol. Soc. Am. Abstr. with Progr., 22: 92–93.

YEARLY REPORT

YUCCA MOUNTAIN PROJECT

TASK 4

October 1, 1991 to Sept 30, 1992

James N. Brune

SUMMARY OF PROPOSED ACTIVITIES: We proposed to (1) Develop our data logging and analysis equipment and techniques for analyzing seismic data from the Southern Great Basin Seismic Network (SGBSN), (2) Investigate the SGBSN data for evidence of seismicity patterns, depth distribution patterns, and correlations with geologic features (3) Repair and maintain our three broad band downhole digital seismograph stations at Nelson, Nevada, Troy Canyon, Nevada, and Deep Springs, California (4) Install, operate, and log data from a super sensitive microearthquake array at Yucca Mountain (5) Analyze data from micro-earthquakes relative to seismic hazard at Yucca Mtn.

SUMMARY OF ACTIVITIES

(1) Continued activities to upgrade the CUSP data logging for eventual use on Yucca Mountain data.

(2) Maintained 3 broadband stations. Re-installed seismometers. Sent Nelson control unit to England for external repairs (after vault flooding). Received digitally recorded data.

(3) Continued to operate the 4-station microearthquake array at Yucca Mountain.

(4) Continued analysis of the Szymansky and Archambeau-Price reports.

(5) Attended workshops on seismic hazard in Santiago Chile and Mexico City.

(6) Began work on a system to estimate magnitudes from microearthquake data.

(7) Received and analyzed paper by Gomberg on the strain pattern in southern Nevada.

(8) Visited Univ. of California, San Diego, to discuss use of digital seismic arrays for seismic hazard and seismic source mechanism studies. Consulted with colleagues about future of proposed strain meter installation at Yucca Mountain.

(9) Attended meetings of Seismological Society of America, Santa Fe. Presented paper on precarious rocks at Yucca Mtn.

(10) Published paper on microearthquakes at Yucca Mountain, Nevada (see attached reprint).

(11) Investigated possible causes for bias in magnitude between Northern Nevada Network and SGBSN.

(12) Filtered selected SGBSN stations to duplicate Yucca Mtn. microearthquake response in order to check high frequency noise level of SGBSN stations.

(13) Made repairs on Nellis Boundary microearthquake station.

(14) Copied selected microearthquake records from Yucca Mtn. region.

(15) Studied microearthquakes triggered in southern Nevada region by Landers, CA, (see attached abstracts).

(16) Studied micro-earthquakes associated with Little Skull Mtn. earthquake.

(17) Studied rocks dislodged by Little Skull Mtn. earthquake.

PUBLICATIONS

Microearthquakes at Yucca Mountain, Nevada, James N. Brune, Walter Nicks, and Arturo Aburto, Bull. Seismol. Soc. Am., vol. 82, no. 1, 164-174, 1992.

Real Time Analog and Digital Data Acquisition through CUSP, William A. Peppin, Seis. Res. Lett., submitted 1991.

1992 AGU Abstracts:

Distribution of Precariously Balanced Rocks in Nevada and California: Correlation with Probability Maps for Strong Ground Motion by J. Brune.

Seismicity in Nevada Apparently Triggered by the Landers, California Earthquake, June 28, 1992 by J.G. Anderson, J. Louie, J. Brune, D. dePolo, M. Savage and G. Yu.

Remote Seismicity Triggered by the M 7.5 Landers, California, Earthquake of June 28, 1992 by J. Brune et al.

MEETINGS, WORKSHOPS

Gave invited papers at Santiago, Chile and Mexico City.

Seismicity in Nevada Apparently Triggered by the Landers, California Earthquake, June 28, 1992

John G. Anderson, John Louie, James N. Brune, Diane dePolo, Martha Savage, and Guang Yu (Seismological Laboratory, University of Nevada, Reno, NV 89557; 702-784-4975)

Within 24 hours after the Landers earthquake, there were 3 magnitude 3.4+ events in western Nevada and a general increase in the rate of small events. Based on the previous 25 year combined catalog for northern and southern Nevada, this level of widely scattered seismicity appeared quite unusual. Using a quantitative model that assumes statistical independence of these regions, the probability of this happening in a 24 hour period by random chance is less than ~2×10^{-4}. Therefore, we conclude that there is a very high probability that these were triggered by the Landers event. The principal events that occurred were: Mina, 500 kilometers from Landers, M4.0, 36 minutes after Landers; Smith Valley, 590 kilometers from Landers, M3.4, 56 minutes after Landers; Little Skull Mountain, 280 kilometers from Landers, M5.6, 22.3 hours after Landers. These events are not associated with known volcanic activity or ongoing aftershock sequences. The evidence for triggering is particularly strong in the case of the Little Skull Mountain event, where an increased rate of microseismicity was evident as soon as small events could be identified in the coda of the Landers earthquake. Earthquakes have been triggered in southern Nevada before, by nuclear testing and by filling of Lake Mead.

We speculate that these events are triggered by the dynamic low-frequency stress associated with surface waves propagating from the Landers earthquake. The distance dependence of static strain changes decrease as R^{-3}, which is much too rapid to cause a significant static strain change at the distances of the above events. Body wave amplitudes decrease more rapidly than surface waves with distance, so that the high-frequency strains associated with the body waves from the Landers earthquake would probably have been exceeded by other more local sources during the prior year. The above reasoning suggests that the cause of the distant triggering is the high amplitude, relatively longer period surface waves. Surface waves of a few seconds period have relatively high strains extending to a depth of more than 10 km. This mechanism for triggering satisfies the criterion of being a relatively rare phenomenon, since it is likely to occur only when a large surface wave is radiated into an area where strain has been building slowly toward the point where faults are unstable.

1. 1992 Fall Meeting

2. 001311692

3. Corresponding address:
John G. Anderson
Seismological Laboratory
University of Nevada
Reno, NV 89557

3b (702) 784-4265

3c (702) 784-1766

4. S

5a S07

5b 7230 Seismicity
8165 Crustal Mechanics

6

7 0

8 Invoice $70.00 to attached LPO 828908 at UNR, Controller's Office/124, Reno, NV 89557-0025

9 C (contributed)

10 Schedule in session with P. Reasenberg et al.

11

Remote Seismicity Triggered by the M7.5 Landers, California, Earthquake of June 28, 1992

Paul A. Reasenberg, D.P. Hill, A.J. Michael, R.W. Simpson, W.L. Ellsworth, S. Walter and M. Johnston (U.S. Geological Survey, Menlo Park, CA 94025); R. Smith, S.J. Nava, W.J. Arabasz, J.C. Pechmann (University of Utah, Salt Lake City, UT 84112); J. Gomberg (U.S. Geological Survey, Denver, CO 80225); J.N. Brune, D. DePolo (University of Nevada, Reno, NV 89557); G. Beroza (Stanford University, Stanford, CA 94305); S.D. Davis; J. Zollweg (Boise State University, Boise, ID 83725)

An intense, widespread and sudden increase in seismicity, which began within minutes after the Landers earthquake at numerous remote sites in western United States, plainly establishes seismic triggering at distances up to 1250 km (17 rupture lengths) from the Landers earthquake. The most intense triggering occurred along the western and southern margins of the Great Basin. The largest triggered earthquake (*M*5.6) was located near Yucca Mountain, Nevada. All of these sites have a history of persistent seismicity and most are characterized by recent volcanism and geothermal activity. At some sites triggered earthquakes began within 40 seconds after the local arrival of the Landers S wave (see next abstract). Postseismic compressional strain recorded by the dilatometer at Devils Postpile closely resembles the seismicity rate at nearby Long Valley. Historically, the 1906 (*M*8¼) earthquake on the San Andreas fault may have remotely triggered several earthquakes at regional distances, including a *M*6.2 event in the Imperial Valley (700 km distance) 11 hours after the main shock. Because predicted static stress changes for the Landers earthquake at distances greater than about 300 km are smaller than daily tidal stress fluctuations, they seem an unlikely explanation for all of the triggering. Other mechanisms under consideration involve the dynamic stresses associated with the passage of seismic waves, either acting directly (and nonlinearly) on faults, or nonlinearly interacting with pore fluids (pump action) or magma (liberating gas bubbles).

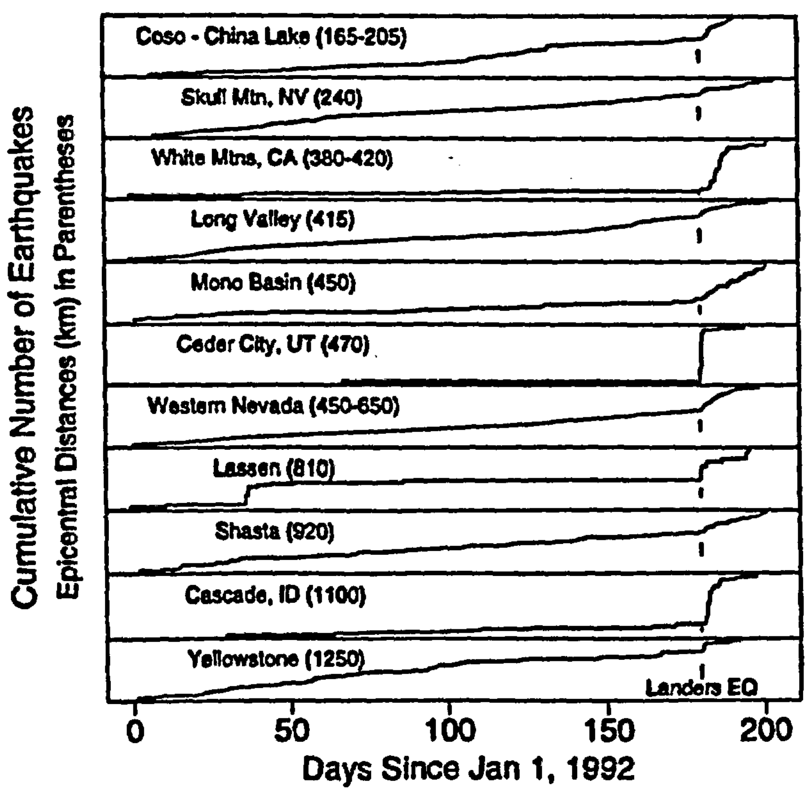

1. 1992 Fall Meeting

2. 001485672

3a. Corresponding address:

Paul A. Reasenberg
U.S.G.S., MS/977
345 Middlefield Rd.
Menlo Park, CA 94025

3b. 415-329-5002

3c. 415-329-5163

4. Joint S/T/G

5a. S07

5b. 7230 Seismicity
8165 Crustal Mechanics

6.

7. 0%

8. P.O. to follow
USGS - National Center
Mail Stop 904
Reston, VA 22092

9. C

10. Schedule immediately before A. Michael

11. no

Bulletin of the Seismological Society of America, Vol. 82, No. 1, pp. 164–174, February 1992

MICROEARTHQUAKES AT YUCCA MOUNTAIN, NEVADA

By James N. Brune, Walter Nicks, and Arturo Aburto

Abstract

We operated a microearthquake array in the neighborhood of the proposed high-level nuclear waste repository at Yucca Mountain, Nevada. The array consists of four high-gain (up to 34 million), narrow band (25 Hz) telemetered stations.

Based on approximate magnitude calibration of the array we expect during quiet periods, for distances less than 15 km, complete recording of events at Yucca Mt. for $M \geq -1$. We have operated the four stations for 12-hour periods overnight between August and October 1990 and intermittently afterward, until April 1991, when we began more or less continuous operation.

The pattern of microearthquake activity confirms the existence of a zone of seismic quiescence in the vicinity of proposed repository. We recorded only about 10 events with *S-P* times of less than 3 sec ($D < 24$ km). Most events had *S-P* times between 3 and 6.5 sec, consistent with the higher seismic activity at distances between 24 and 52 km observed by Rogers *et al.* (1987) and Gomberg (1991). Oliver *et al.* (1966) found, contrary to what has been observed by us for Yucca Mountain, that in seismically active areas most of the events had *S-P* times of less than 3 sec. We confirmed this expectation for four microearthquake stations near Mammoth Lakes, where we observed microearthquake rates of over 100 per day, most with *S-P* times of less than 3 sec. Extrapolation of seismicity data from the Southern Great Basin Seismic Network confirms the low microearthquake activity in the immediate vicinity of Yucca Mountain.

Introduction

The proposed high-level waste nuclear repository at Yucca Mountain, Nevada, would be one of the largest and most important construction projects ever undertaken by humankind. Tectonic stability is a crucial issue because the facility must be engineered to specifications for 10,000 years in the future. There are many questions that need to be answered concerning earthquakes, volcanic activity, and the response of the facility to excavation and thermal stressing from the 70,000 tons of high-level radioactive material expected to be stored at the site. There are unanswered questions relating to the interaction of the tectonic stress field and the hydrologic regime of the region. Hydrofracture experiments have been interpreted to indicate possible incipient normal faulting (Stock *et al.*, 1985). (Important questions and uncertainties about the site are expected to be answered by the Site Characterization Plan, which will last at least several years (USDE, 1988).) Because of the critical importance of understanding all tectonic, geological, and geophysical aspects of the site, we undertook extended microearthquake monitoring there.

Previous Studies

Previous seismicity studies of the region have been based primarily on data from the Southern Great Basin Seismic Network (SGBSN), currently consisting of 55 stations operated by the USGS (Rogers *et al.*, 1987; Gomberg, 1991). The station spacing is denser (a few km spacing) in the immediate neighborhood of

Yucca Mountain. Gomberg (1991) has estimated that the detection threshold of the array is about $M_L = 0.1-0.3$, but there is considerable uncertainty in this because magnitudes are determined based on both the Richter M_L scale and on a duration scale, and many smaller local events are recorded at only a few stations near the epicenter, while larger events may saturate the records.

Several features of the spatial seismicity pattern are discussed in the Rogers *et al.* (1987) and Gomberg (1991) studies. There is a concentration of seismicity in regions of previous nuclear testing, at a distance of several tens of kilometers from the Yucca Mountain site, but it is unclear how much of this is directly connected with nuclear testing. Of most importance to this study is the almost complete lack of seismicity near Yucca Mountain. It is not known whether this is simply a result of statistical temporal and spatial variations in seismicity or whether it is closely connected with some aspect of the strain field. Gomberg (1991) suggests that the "gap" in seismicity may be either a gap ready to be filled by a large event, or simply a region where shear strain is not accumulating. Parsons and Thompson (1991) suggested that volcanic magma pressure could temporarily lock up faults in a region of active volcanism. They suggested that this might be the case for the region of low seismicity at Yucca Mountain. Continued monitoring of seismicity should help to answer some of these questions, especially if coupled with accurate measurements of the strain field.

Microearthquake surveys have been made in several areas of Nevada and California. Oliver *et al.* (1966) recorded microearthquake rates in northern Nevada ranging from several per day to over two hundred per day (magnitudes mostly less than zero), with highest rates observed in areas of recent faulting. Rates at all sites were considerably higher than in aseismic areas. Molnar *et al.* (1969) operated high-gain microearthquake seismographs for several weeks before and after the nuclear explosion Benham (at nearby sites in Nevada and California). Although a pronounced increase in seismic activity was observed in the immediate vicinity of the explosion, no significant increase in activity was observed near (< 25 km) any of the microearthquake recording sites, indicating no far-field triggering of microearthquakes by either the dynamic or static change in strain field associated with the explosion. An average of about one event per day was detected by the experiment, considerably less than observed by Oliver *et al.* (1966). This could in part be a result of different instrumentation, but it was also probably due to the lower level of tectonic activity in southern Nevada as compared to the northern and central Nevada sites occupied in the Oliver *et al.* (1966) study.

Brune and Allen (1967) carried out a microearthquake study along the San Andreas Fault System in southern California and found that short-term activity is not necessarily positively correlated with long-term activity and seismic hazard, even though in this study and others there is a general similarity between microearthquake activity and macroseismicity. Observed microearthquake activity varied from more than 75 events per day in Imperial Valley to virtually nil along the central section of the San Andreas fault (near Palmdale and Lake Hughes). The area of minimal microearthquake activity along the central segment of the San Andreas fault, the very segment that broke in the great 1857 earthquake, is a particularly dramatic example of a lack of correlation between microseismicity and long-term fault activity. In a related study, Wesnousky (1990) has suggested that seismic productivity (in terms of small earthquakes) of a fault zone is related to the maturity of the fault system. Fault systems with hundreds of kilometers of displacement tend to have low rates of small earthquake activity, whereas faults with less cumulative slip had higher rates (in each case normalized to the long-term slip rate). This is consistent with the microearthquake rates observed by Brune and Allen (1967) for the site of the 1857 earthquake.

INSTRUMENTATION

Most of the previously discussed microearthquake studies were carried out with portable seismographs. However, we felt that because of the importance of the site, microearthquakes should be monitored as close to continuously as possible. Therefore we decided to test more or less permanent sites and transmit data continuously back to the Seismological Laboratory at the University of Nevada, Reno. This was accomplished via radio links to a nearby microwave relay station (see Fig. 1). Four sites were selected, two on Yucca Mountain near the Solitario Canyon fault (YNB and YYM), one abut 5 km to the west in Crater Flat (YCF), and one still further west on Black Cone (YBC) near the center of Crater Flat. The YBC station on Black Cone is important for monitoring any microseismicity which might be associated with the relatively young volcanic activity in Crater Flat. The instrumentation and telemetry setup is illustrated in the block diagram in Figure 2. Because we are using a full radio channel bandwidth for each station (single vertical component) we have higher dynamic range, and associated signal to noise ratio, than is possible for the usual situation of placing several channels on one radio band. The seismometers we are using are Geotech GS-13 instruments. The amplifiers and band-pass filters peak the system response near 25 Hz to help give high gain and relatively low noise level. Of special interest and importance to the experiment is the high dynamic range digital chart recorder, an Astro-Med Inc. DASH IV. Because true microearthquake signals are often difficult to detect in the presence of noise, we wished to have continuous recording at as high a gain as possible. The digital chart recorder format allows a high dynamic range and continuous recording, because the trace does not saturate or become faint or nonlinear at high amplitudes. Since the signal is relatively narrow band, there is little need for actual storage of the bits of digital information. The four signals from the four stations are recorded continuously on four traces of the recorder paper going in one direction, and four traces in the other direction, giving two days of recording on each roll of paper. In the initial part of the study in August through October, we ran at approximately twice this chart speed, and only recorded at night, except for special occasions.

The response of our system with recording sensitivity set at 1 volt full scale is compared with the USGS, Yucca Mountain S13Y system as given in Rogers *et al.* (1987) in Figure 3. Of course, the actual useful sensitivity of the system depends on the trace noise level at each setting. We found that we could operate the system as shown in Figure 3 with less than 1-mm noise trace amplitude during quiet nights with little wind. We could occasionally record with twice the sensitivity for short periods of time. During windy periods we often reduced the sensitivity because the trace noise level exceeded (sometimes greatly) 1 mm. The chart recorder automatically records the gain settings of each channel along with the approximate time. The response curve shown in Figure 3 suggests that during the quietest periods of operation we should be able to detect events 1 to 2 magnitude units lower than the USGS stations.

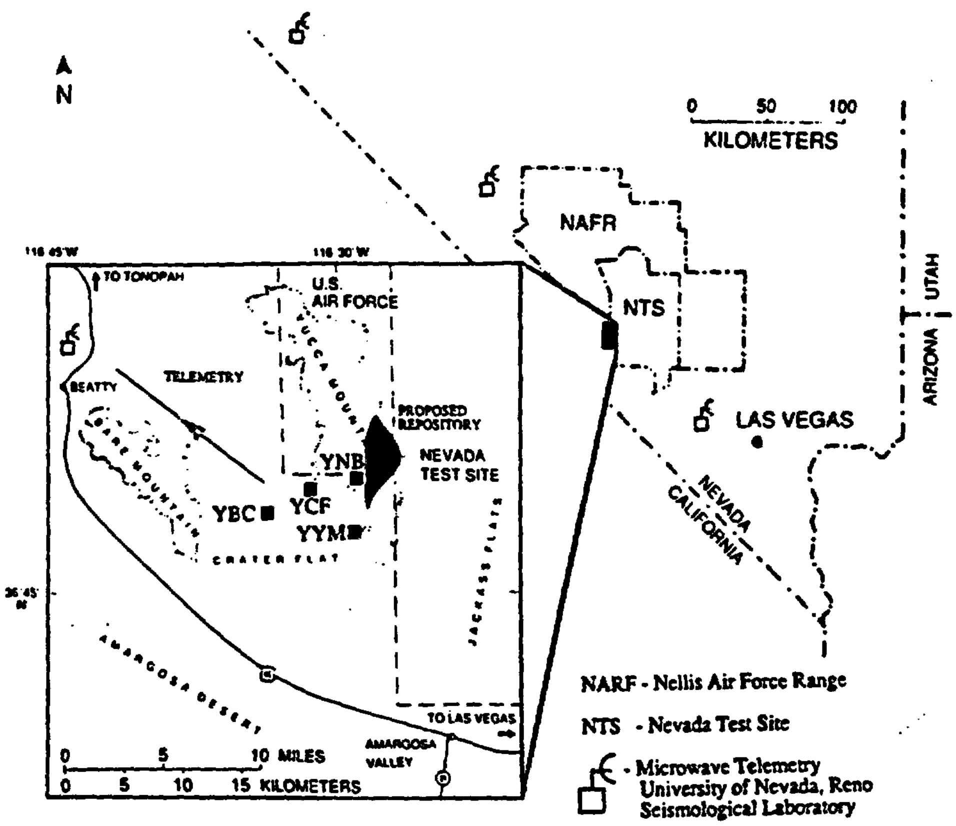

FIG. 1. Map showing location and configuration of the Yucca Mountain telemetered microearthquake array.

SEISMOGRAMS

Typical records are shown in Figures 4a and b. Figure 4a shows an event arriving from the west (first at YBC) with an *S-P* time of about 2 sec at YBC. This event did not trigger the USGS automated system. Figure 4b shows a more distant event (about 15-sec *S-P* time) along with an explosive sonic that could be confused with an earthquake if four recording stations had not been available. The use of four stations is critical for identifying small events when the noise level is relatively high, because sonic events always show a slow moveout (slow sonic velocity), whereas earthquakes appear to arrive nearly simultaneously at the stations, and a trained observer quickly learns to distinguish earthquakes from sonic bursts and other noise.

Figure 5 shows typical events with short *S-P* times at the Yucca Mountain microearthquake array. None of these events triggered the USGS automated recording. These events are relatively rare and only a few were recorded during the first three months of operation. The magnitudes are estimated to be about 0 to −1 (see later section). This qualitative observation confirms a very low rate of microearthquake activity at Yucca Mountain, consistent with the low seismicity for higher magnitudes observed by Rogers *et al.* (1987) and Gomberg (1991). Of particular note is the lack of events with short *S-P* times, less than 3

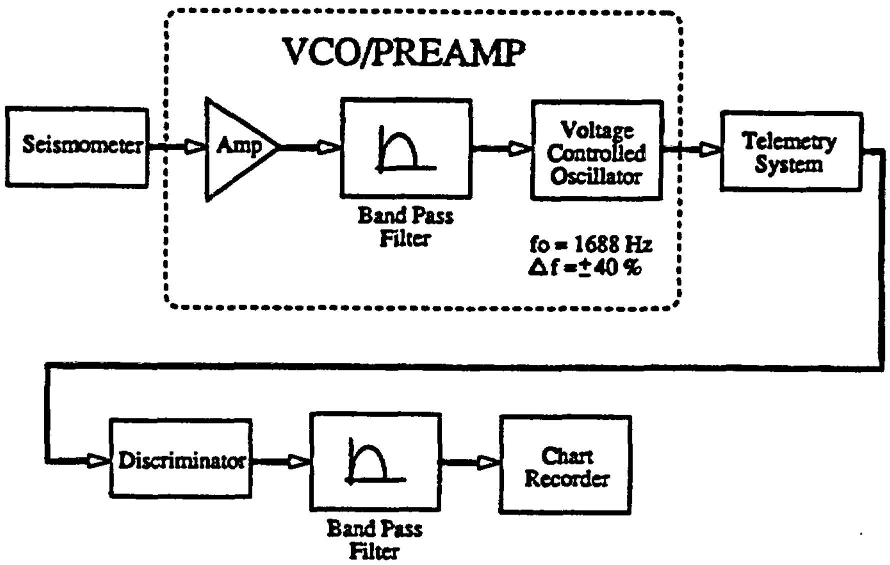

FIG. 2. Schematic block diagram for the Yucca Mountain telemetered microearthquake stations.

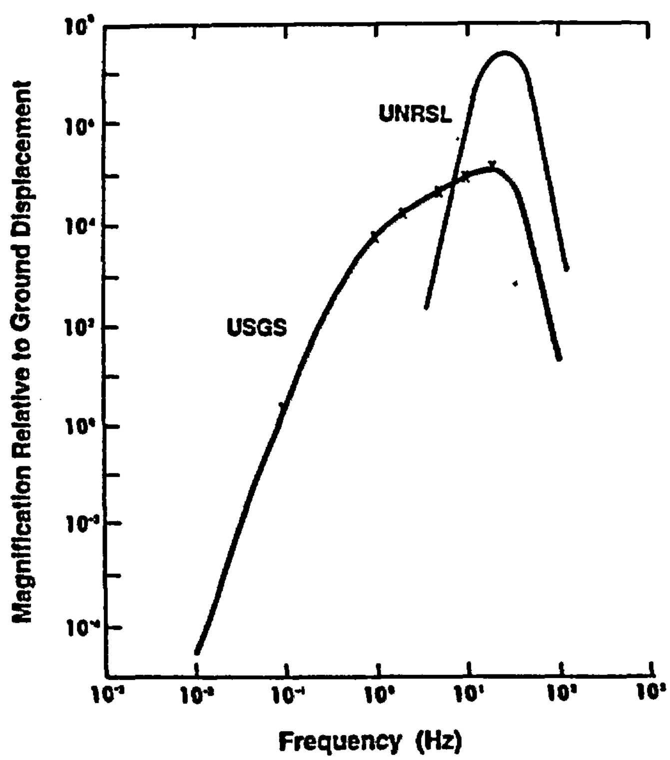

FIG. 3. Response of USGS, Yucca Mountain S13Y system into a helicorder with amplifier gain of 84 dB compared with UNRSL narrow band, high-frequency microearthquake array at Yucca Mountain, Nevada.

4A

4B

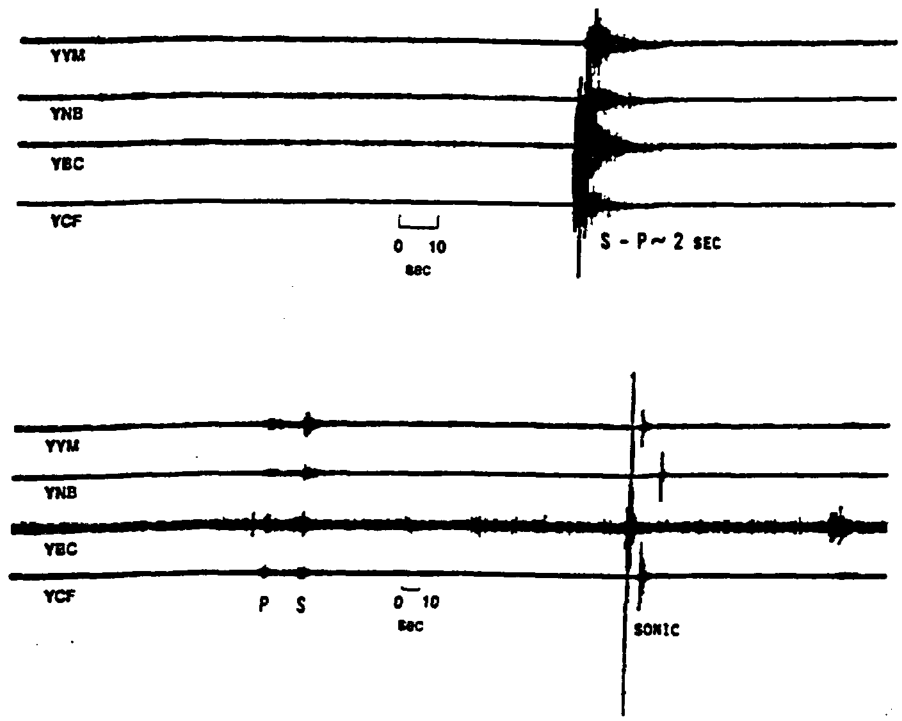

FIG. 4. Examples of microearthquake recordings and noise, including a sonic, at two different chart speeds.

sec (see dashed curve, Fig. 7). Oliver *et al.* (1966) found that in seismically active areas, most events had *S-P* times of less than 3 sec, as might be expected because of the rapid attenuation with distance of 30-Hz energy. This qualitative observation of few events with short *S-P* times further emphasizes the relatively low microearthquake activity in the immediate vicinity of the microearthquake stations at Yucca Mountain.

Because we wished to validate the operation of our systems, and the qualitative arguments given above, we temporarily transferred the recording to four stations in the Mammoth Lakes region (Red Slate Mountain, Casa Diablo Hot Springs, Deadman Pass, and Montgomery Pass), with filters applied to give approximately the same response shape as the Yucca Mountain stations. Typical seismograms from the Mammoth region are shown in Figure 6. As expected from this highly active area the great majority of events has *S-P* times of less than 3 sec (Fig. 7), and microearthquake rates were orders of magnitude higher than at Yucca Mountain, over 100 events per day.

DISTRIBUTION OF *S-P* TIMES

A careful count of all events with short *S-P* times was made from the Yucca Mountain recordings and compared with results from the Mammoth Lakes region. Results are shown in Figure 7. The dashed line histogram indicates the results from Yucca Mountain for 600 hours (25 cumulative days) of low noise recording. Most of the events recorded have *S-P* times between 4 and 10 sec, with a peak at about 6.5 sec. The relatively few events recorded with *S-P* times

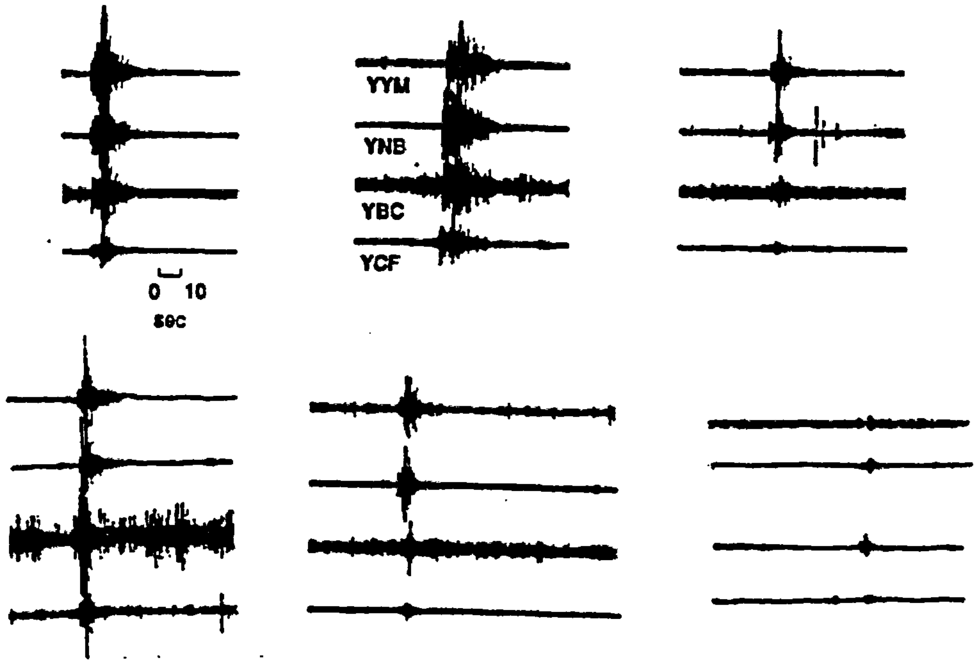

FIG. 5. Examples of recordings of the relatively rare events in the neighborhood of Yucca Mountain (S-P times of less than about 5 sec).

of less than 3 sec confirms the relatively low microearthquake activity in the immediate vicinity of Yucca Mountain. The overall microearthquake rates with S-P times of less than 10 sec (distances less than about 80 km) was about five events per day, but the number of events per day with S-P times of less than 3 sec was less than one event per 5 days. In contrast, the events from the Mammoth region almost all had S-P times of less than 3 sec (solid line, Fig. 7) and the overall rates were over 100 events per day.

ATTENUATION AND MAGNITUDE DETERMINATION

In order to approximately calibrate our system with respect to SGBSN magnitudes, we estimated an amplitude versus distance attenuation curve for a magnitude zero earthquake (as inferred from the SGBSN). We obtained a number of on-scale recordings of events that were given magnitudes from the SGBSN. In some cases, the gain was considerably lower than shown in Figure 3, so that recordings were on scale for events large enough to trigger the SGBSN. We then plotted, as a function of distance, the following quantity:

$$\text{Log } A_0(x) = \text{Log } A(x) - M,$$

where A_0 is the estimate of the amplitude of a magnitude zero event at a distance x, A is the trace amplitude (zero to peak) recorded on our system, corrected to a recorder sensitivity of 1 volt per millimeter, and M is the SGBSN magnitude.

The results are shown in Figure 8. The black dots are individual estimates of Log A_0. The solid curve is an approximate fit to the data based on theoretical

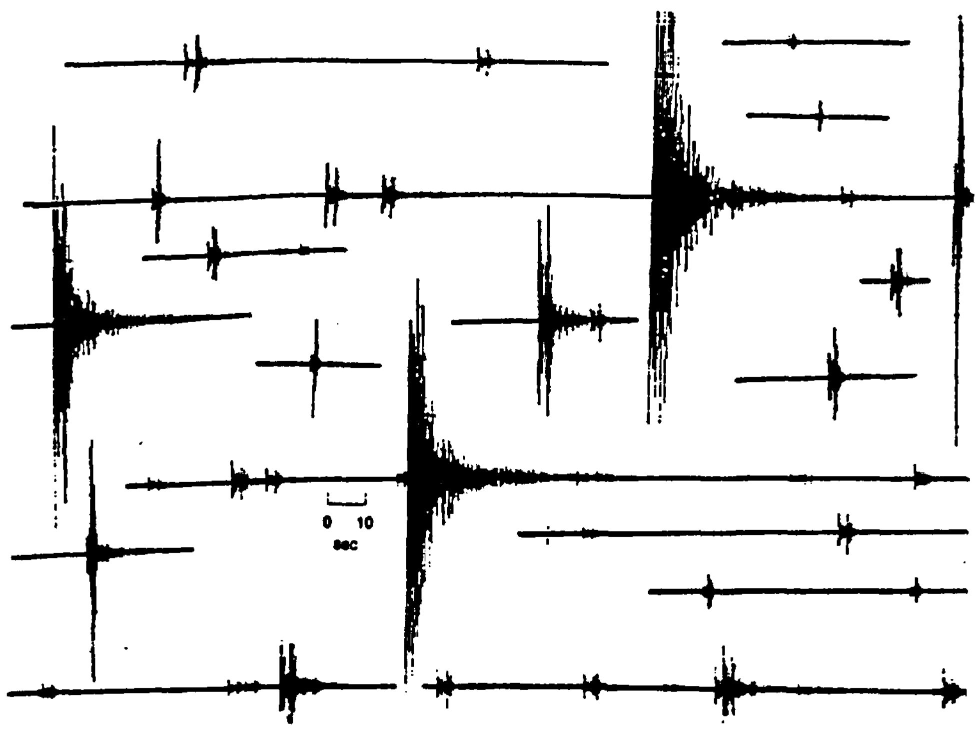

FIG. 6. Examples of microearthquake recordings at station RSM in the Mammoth Lakes-Long Valley Caldera region.

attenuation curves forced to pass through the mean of the data near a distance of 50 km. Beyond 50 km, the theoretical curve has a shape corresponding to geometrical spreading proportional to the inverse square root of distance and a Q (at 20 Hz) of 800 (with a small correction for scattering and dispersion). For distances less than 50 km, the theoretical curve corresponds to geometrical spreading proportional to the inverse distance and a Q of 400, corresponding to a lower Q, and to inverse distance spreading, as might be expected at shorter distances. For the purpose of this study, the derivation of the theoretical curves is not important, as they were constrained to have parameters giving an approximate fit to the data in order to define a curve to be used in the approximate definition of magnitude. As a further comparison, the curve obtained by Frankel *et al.* (1990) from narrow-band filtering (at 30 Hz) of records from the ANZA seismic array is shown (forced to go through the same point at a distance of 50 km). At short distances we would expect the attenuation at ANZA to be similar to that at Yucca Mountain since at close distances the attenuation due to differences in Q will be minimized. Because of the low microseismicity at Yucca Mountain, and consequent lack of data points at near distances, we wanted an independent estimate of the shape of the attenuation curve. This is provided by the results of Frankel *et al.* (1990) since they made observations with a narrow-band system similar to that used by us.

If we accept the solid curve in Figure 8 as our definition of magnitude, it indicates that we should be able to record events down to magnitude about -1.5 at distances of about 10 km (with amplitudes of >1 mm). If we take the

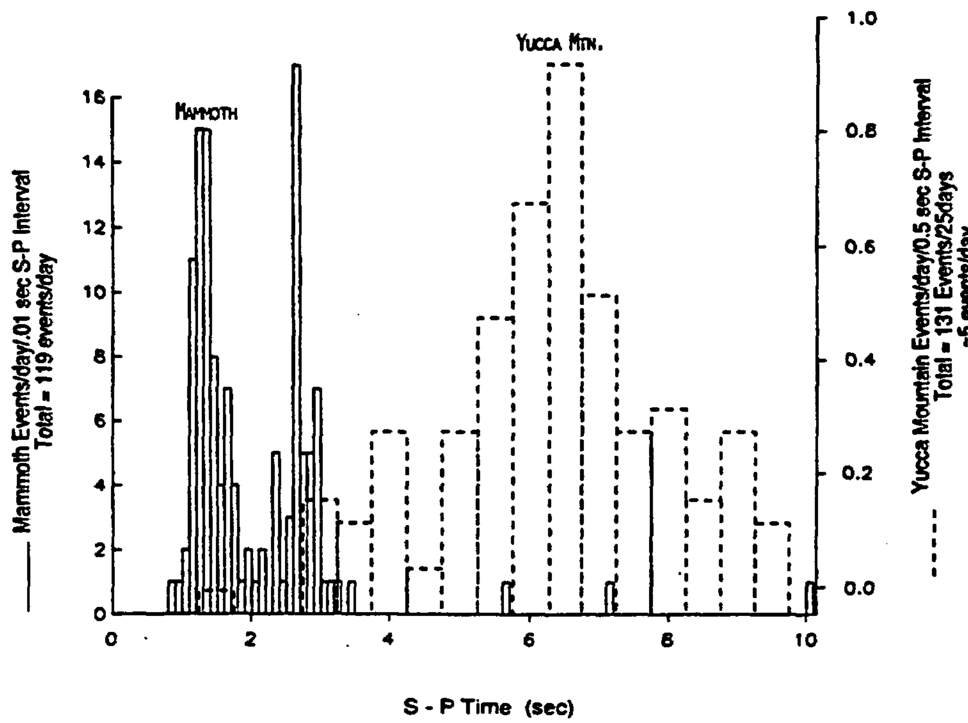

FIG. 7. Distribution of *S-P* times at Yucca Mountain and Mammoth Lakes region.

Frankel *et al.* (1990) curve, the estimated magnitude of an event with 1-mm trace amplitude is less than -2. These results are consistent with the relative magnification curves for the Yucca Mountain and SGBSN stations shown in Figure 3. We conclude that, if many events with magnitudes greater than -1 were occurring at Yucca Mountain, we should have easily observed them.

B VALUES AND ESTIMATED MICROEARTHQUAKE RATES

Gomberg (1991) estimated the seismicity distribution for the SGBSN using the Gutenberg-Richter relationship (Gutenberg and Richter, 1941, 1954):

$$\log N(M) = a - bM,$$

where $N(M)$ is the number of earthquakes with magnitude M, and a and b are two constants derived from the seismicity distribution. This equation can be extrapolated to estimate the number of earthquakes occurring in a magnitude range not covered by the SGBSN data. Gomberg fits two curves to the SGBSN data. The curve which predicts the lowest number of events near magnitude zero has constants $a = 4.56$ and $b = 1.27$ (for magnitude intervals of 0.1 magnitude units). Correcting the area covered by the SGBSN to a region of hypocentral distance equal to 24 km (*S-P* time equal or less than 3 sec), and correcting from the time period of the SGBSN data set (7 years) to the time of quiet operation in our data set (25 days) gives an estimate of 89 events with magnitude greater than -0.5, which should have been observed by us if the seismicity level at Yucca Mountain were the same as the average seismicity

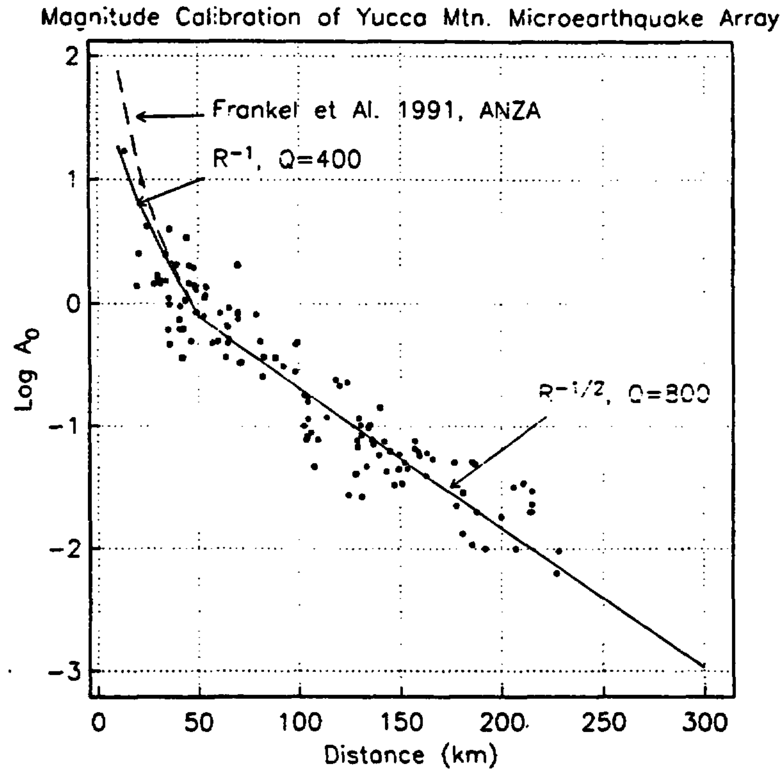

FIG. 8. Data and magnitude calibration curve for the Yucca Mountain microearthquake array.

over the whole SGBSN for 7 years. If we extend the magnitude range to -1.5 (which should have been detected by us, see above), the estimated number of events would be over several hundred. Since we only observe a few events with *S-P* times of less than 3 sec, this calculation confirms that the current microearthquake rate in the immediate vicinity of Yucca Mountain is much lower than the average for the SGBSN region.

CONCLUSION

We have operated a sensitive, narrow-band, four-station telemetered microearthquake array in the immediate vicinity of the proposed high level nuclear waste repository at Yucca Mountain, Nevada. Microearthquake rates were found to be very low, lower than for tectonically active areas in northern Nevada, lower than most sites in southern California, and lower than the average microearthquake rates for the whole region of southern Nevada monitored by the Southern Great Basin Seismic Network. The existence of a region of very low microearthquake activity in the immediate vicinity of the Yucca Mountain site is consistent with the low rate of macroseismicity observed in the same region by Rogers *et al.* (1987) and Gomberg (1991). Explanations suggested for the low rate of activity have ranged from low shear strain accumulation, to a possible seismic gap related to a future large earthquake (Gomberg, 1991), or possible magmatic locking by a build up of magma pressure in the Crater Flat region (Parsons and Thompson, 1991). The lack of microearthquake activity has potential importance relative to the suggestion that the region is near incipient normal faulting, as suggested by some hydrofracture measurements (Stock *et al.*, 1985). No matter what the explanation for the current low rate of microearthquake activity, it is very important to continue monitoring the site to establish a base line of activity from which to judge the effects of future mining activity and thermal loading from radioactive decay.

Acknowledgments

This experiment was funded by the Nevada Nuclear Waste Projects Office through the Center For Neotectonics of the University of Nevada, Reno.

References

Brune, J. N. and C. R. Allen (1967). A micro-earthquake survey of the San Andreas fault system in southern California, *Bull. Seism. Soc. Am.* **57**, 277-296.

Frankel, A., A. McGarr, J. Bicknell, J. Mori, L. Seeber, and E. Cranswick. (1990). Attenuation of high-frequency shear waves in the crust: measurements from New York State, South Africa, and southern California, *J. Geophys. Res.* **95**, 17,441-17,458.

Gomberg, J. (1991). Seismicity and detection/location threshold in the southern Great Basin Seismic Network, *J. Geophys. Res.* **96**, 16, 40-46, 414.

Gutenberg, B. and C. F. Richter (1941). Seismicity of the earth, *Geol. Soc. Am. Spec. Pap.* **34**, 1-133.

Gutenberg, B. and C. F. Richter (1954). *Seismicity of the Earth and Associated Phenomena*, 2nd ed., 310 pp, Princeton University Press, Princeton, New Jersey.

Molnar, P., K. Jacob, and L. R. Sykes (1969). Microearthquake activity in eastern Nevada and Death Valley California before and after the nuclear explosion Benham, *Bull. Seism. Soc. Am.* **59**, 2177-2184.

Oliver, J., A. Ryall, J. N. Brune, and D. B. Slemmons (1966). Microearthquake activity recorded by portable seismographs of high sensitivity, *Bull. Seism. Soc. Am.* **56**, 899-924.

Parsons, T. and G. A. Thompson (1991). The role of magma overpressure in suppressing earthquakes and topography: worldwide examples, *Science* **253**, 1399-1402.

Rogers, A. M., S. C. Harmsen, M. E. Meremonte (1987). Evaluation of the seismicity of the southern Great Basin and its relationship to the tectonic framework of the region, *U.S. Geol. Surv. Open-File Rept. 87-408.*

Stock, J. M., J. H. Healy, S. H. Hickman, and M. D. Zoback (1985). Hydraulic fracturing stress measurements at Yucca Mountain, Nevada, and relationship to the regional stress field, *J. Geophys. Res.* **90**, 8691-8706.

U.S. Department of Energy (1988). Site characterization plan, Yucca Mountain site, Nevada Research and Development Area, Nevada, USDOE Report DOE/RW-0199, December.

Wesnousky, S. G. (1990). Seismicity as a function of cumulative geologic offset: some observations from southern California, *Bull. Seism. Soc. Am.* **80**, 1374-1381.

Seismological Laboratory
University of Nevada, Reno
Reno, Nevada 89557-0141

Manuscript received 24 May 1991

PROGRESS REPORT--OCTOBER 1, 1991 TO SEPTEMBER 30, 1992

TASK 5 Tectonic and Neotectonic framework of the Yucca Mountain Region

Personnel

Principal Investigator: Richard A. Schweickert

Research Associate: Mary M. Lahren, October 1, 1991 to March 31, 1991

Graduate Research Assistants:

a. Zhang, Y.--October, 1991-September, 1992

Part I. Highlights of major research accomplishments

a. Structural studies in Grapevine Mountains, Bullfrog Hills, and Bare Mountain

b. Acceptance for publication of manuscript submitted to Tectonics on Mesozoic thrust belt by S.J. Caskey and R. A. Schweickert

c. Publication of one abstract based upon research funded under Task 5: Zhang and Schweickert (1992).

d. Recognition of significance of pre-Middle Miocene normal and strike-slip faulting at Bare Mountain (Yang Zhang)

e. Compilation of map of Quaternary faulting in southern Amargosa Valley (M.M. Lahren)

f. Preliminary paleomagnetic analysis of Paleozoic and Cenozoic units at Bare Mountain (Yang Zhang, S. Gillette, and R. Karlin).

Part II. Research projects

This section highlights the research projects conducted by Task 5 personnel.

1. *Regional overview of structure and geometry of Mesozoic thrust faults and folds in the area around Yucca Mountain*; R. A. Schweickert.

The purpose of this study is to provide information about the deep structural geometry of Paleozoic units and their bounding faults, which is necessary both for understanding of Tertiary faults and for the correct formulation of regional hydrologic models. It has also provided evidence for a previously unknown strike-slip fault beneath Crater Flat, and for the existence of major pre-Middle Miocene extension in the NTS region. The study involves new field work in selected areas and a synthesis of structural relations in areas both east and west of Yucca Mountain, including the CP Hills-Mine Mountain area to the east, and Bare Mountain-Bullfrog Hills-Grapevine Mountains to the west.

2. *Kinematic analysis of low and high angle normal faults and strike-slip faults in the Bare Mountain area, study of metamorphic rocks, and comparison of structures with the Grapevine Mountains* Y. Zhang and R. Schweickert

The purpose of this study is to determine the timing and slip directions of high and low-angle normal faults exposed at Bare Mountain, which is a direct analogue of the deep structure beneath Yucca Mountain. This will provide better constraints on the displacement histories of the faults. In addition, metamorphic fabrics are being studied in metamorphic rocks in the northern parts of the mountain and traced to lower grade rocks in the southern part of the mountain. Finally, the development of these structures is compared with possible analogues in the Grapevine Mountains and the CP Hills to develop firm constraints on the deep structure beneath the Yucca Mountain area.

3. *Evaluation of pre-Middle Miocene structure of Grapevine Mountains and its relation to Bare Mountain.* R. Schweickert and M.M. Lahren

The goal of this project is to establish the Mesozoic and Cenozoic structural geometry and timing of deformation in the Grapevine Mountains, which developed in close proximity to the Bullfrog Hills and Bare Mountain areas, prior to post-10 Ma displacement on the Bullfrog Hills-Boundary Canyon detachment fault. This study is clarifying the significance of pre-Middle Miocene and possibly pre-Tertiary extension and detachment faulting on crustal structure in the area between the NTS and Death Valley, and beneath Yucca Mountain.

4. *Evaluation of paleomagnetic character of Tertiary and pre-Tertiary units in the Yucca Mountain region, as tests of the Crater Flat shear zone hypothesis and the concept of oroclinal bending.* S. Gillett, R. Karlin, Y. Zhang, and R. A. Schweickert.

Paleomagnetic data from various volcanic units at Yucca Mountain show that up to 30° of progressive north-to-south clockwise rotation has occurred since mid-Miocene. These studies are geographically relatively limited; one of the goals of this study is to expand the data base to various Paleozoic and Mesozoic units to understand the regional variations of magnitude and timing of rotations.

5. *Late Quaternary fault patterns in southern Amargosa Valley, Stewart Valley, and Pahrump Valley.* M.M. Lahren and R.S. Schweickert.

This project involves the compilation of all available data on the distribution and style of late Quaternary faults in the region, primarily from mapping by Donovan and Hoffard (M.S. Theses completed under Task 5) and USGS mapping. This compilation will reveal the nature of the late Quaternary structural setting of Yucca Mountain. Field checking of certain key areas is required.

6. *Tectonics and Neotectonics of the Pahranagat shear zone, Lincoln County, Nevada;* (R. Elwood and T. Reynolds, formerly supported here, have both left UNR but still plan to complete their studies).

The rationale for this study has been that the Pahranagat shear zone lies on trend with the Spotted Range - Mine Mountain structural zone, which is composed of seismically active, ENE-striking, sinistral faults, and which lies immediately south of Yucca Mountain. Studies of the Pahranagat shear zone have been undertaken to evaluate whether the two zones are parts of a related zone of crustal weakness that may be active.

In addition, the Pahranagat shear zone shows clear evidence that shortening occurs within the Basin and Range province. Such shortening may be manifest as thrust earthquakes and (or) as shortening through aseismic folding. Elwood's part of this project was completed in 1991, and her thesis report is in progress.

Part III.

Brief summaries of research results during FY 1992

This section presents a summary of progress to date. Because these projects are long-term and field-intensive, the results are still preliminary, and should not be quoted without permission. Many of our interpretations are speculative.

1. Quaternary fault patterns and basin history of Pahrump and Stewart Valleys, Nevada and California. (See attached map, Figure 1).

Our map is preliminary and requires field checking in a number of areas, but it clearly indicates that Late Quaternary faults at Yucca Mountain (area A, Figure 1) lie along strike with an 80+ km-long, continuous zone of NNW-striking late Quaternary strike-slip and normal faults (B, Figure 1) in the southeastern part of Amargosa Valley and in Stewart and Pahrump Valleys, that represents the principal zone of late Quaternary fault movements in the area east of Death Valley. These faults are distinctly east of, and are not connected to, the Death Valley-Furnace Creek fault zone. These facts indicate that the fault patterns at Yucca Mountain are a manifestation of a regional strain pattern involving NW-trending strike-slip displacements and associated NS-striking normal faults. A 10-mile wide gap exists in this zone of surface faults between the southern end of Yucca Mountain and the southeastern end of Amargosa Valley (C, Figure 1), and this coincides with the area of late Holocene outwash from Forty-Mile Canyon to the northeast.

Near the northern end of the zone of faulting in southern Amargosa Valley (D, Figure 1), northeast-striking faults apparently related to the Rock Valley fault zone to the northeast (E, Figure 1), occur in association with north and northwest-striking faults. The interaction of northeast- and northwest-striking faults is not understood.

Our preliminary tectonic model is that normal faults in Crater Flat and at Yucca Mountain are related to a major late Quaternary pull-apart zone in the northwest-striking strike-slip system (see Figure 2).

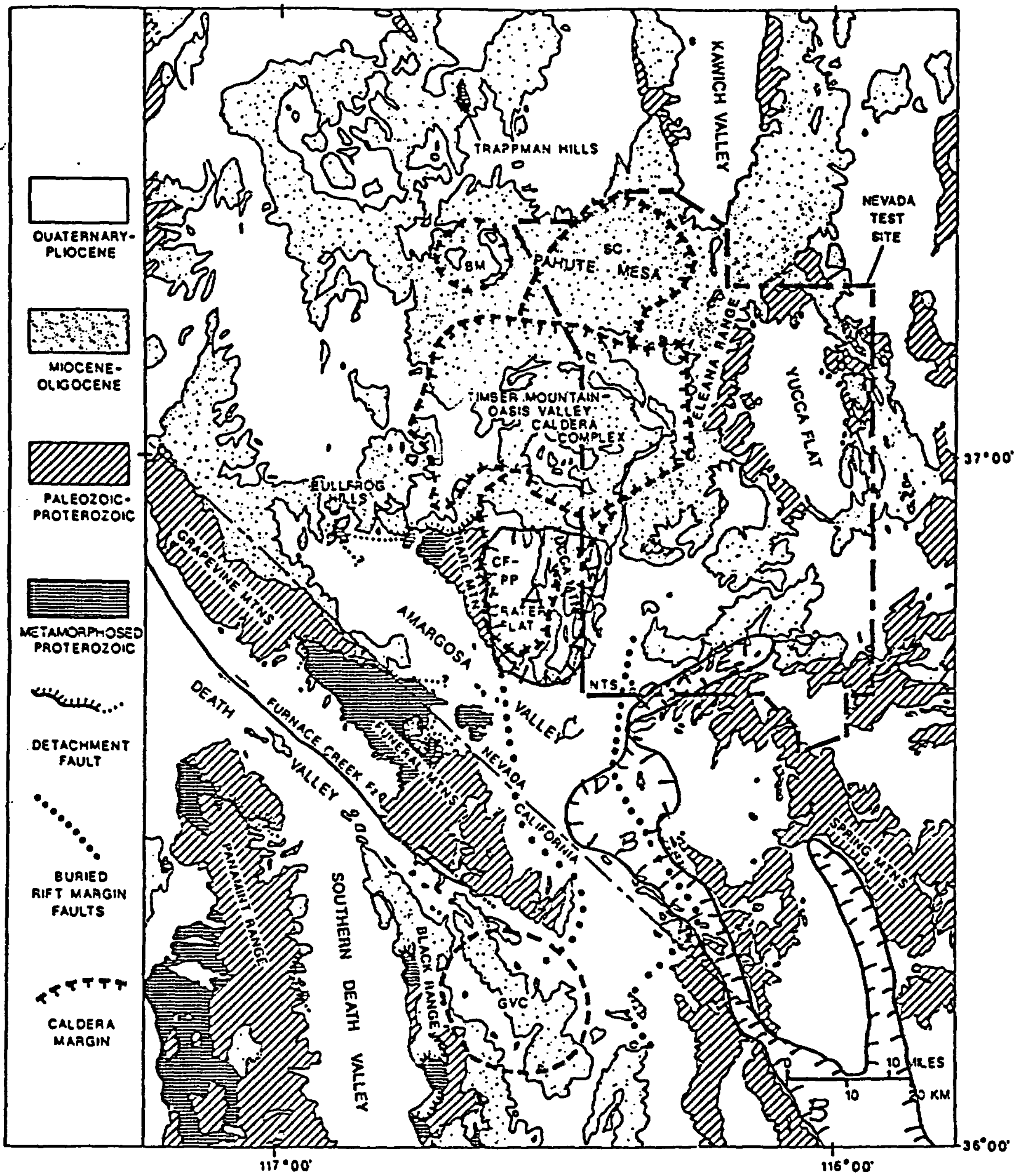

Generalized geologic map of the Nevada Test Site region, showing relation of caldera complexes, Greenwater volcanic center, and rift zone to metamorphic rocks and detachment structures. BM—Black Mountain caldera; SC—Silent Canyon caldera; CF-PP—Crater Flat-Prospector Pass caldera complex; GVC—Greenwater volcanic center. Buried rift margin faults shown are based on presence of steep, linear gravity gradients.

Figure 1. Modified from Carr (1990). Zones of late Quaternary normal and strike slip faulting (A, B, D, and E) are outlined.

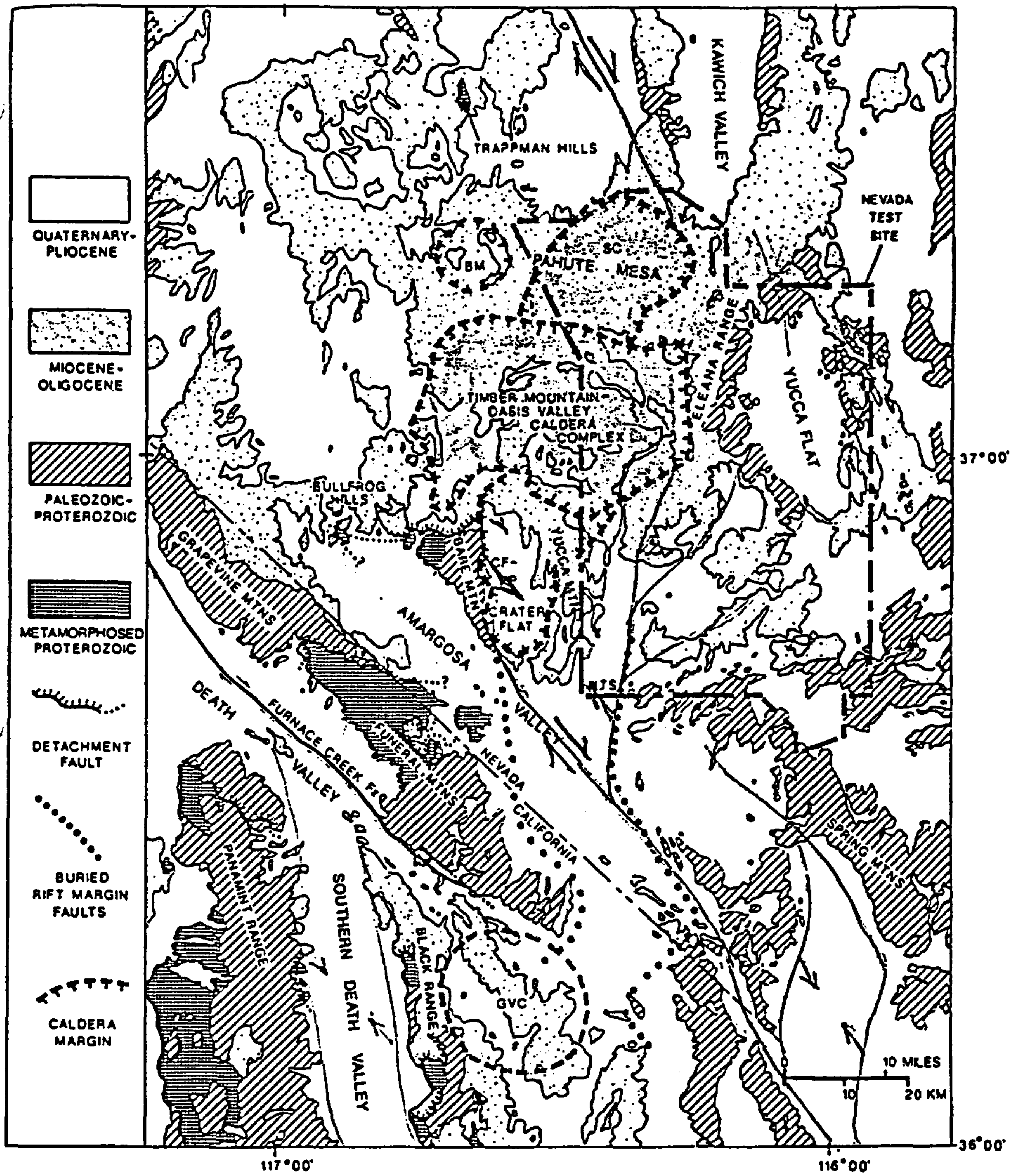

Figure 2. Modified from Carr (1990). Tectonic model of late Quaternary faulting in the Pahrump Valley-Yucca Mountain region. Yucca Mountain and Crater Flat are viewed as lying within a large right-step pullapart zone in a northwest-trending zone of right-lateral faulting. These features evolved since Middle Miocene time and are currently active.

2. Regional overview of structure and geometry of Mesozoic thrust faults and folds in the area around Yucca Mountain. R. A. Schweickert.

(See preprint by Caskey and Schweickert; Appendix 1).

3. Evaluation of pre-Middle Miocene structure of Grapevine Mountains and its relation to Bare Mountain. R. Schweickert and M.M. Lahren. (see Figure 3).

New field work and map-scale structural analysis has confirmed that the Oligocene Titus Canyon Formation unconformably overlaps a major detachment fault system related to the Titus Canyon fault (as mapped by Reynolds (1969))(Figure 3). We documented four localities in Titanothere and Titus Canyons and south of Daylight Pass in which conglomerate and sandstone of the Titus Canyon Formation lies in unmoved depositional contact on Cambrian rocks in upper and lower plate positions relative to the Titus Canyon fault. The basal conglomerate commonly contains highly polished 1-3m boulders of Zabriskie Quartzite in a sandy conglomerate matrix, all resting on Cambrian rocks. We also recorded kinematic indicators on several segments of the Titus Canyon fault that indicate top to the east displacements. Finally, in the lower part of Titus Canyon, we discovered that the Miocene Hall Canyon fault is a high-angle fault that cuts across the trace of the older, low-angle Titus Canyon fault.

As noted previously, the Titus Canyon fault (Figure 3) is a detachment fault that excises the upright limb of a major Mesozoic recumbent fold, the Titus Canyon anticline, and has a structural relation similar to that of the Wildcat Peak normal fault at the southern end of Bare Mountain, and the Conejo Canyon fault at the north end of Bare Mountain. The former excises the upright limb of a large recumbent anticline in the hangingwall of the Panama thrust (as mapped by Monsen and others (1990)).

The Titus Canyon fault is undated, but is pre-Titus Canyon Formation, and could even be of Late Cretaceous age. Existing data suggests that the Late Miocene Fluorspar Canyon-Bullfrog-Boundary Canyon detachment system (Figure 3) pulled apart and exposed elements of a much older detachment system, which includes the Titus Canyon fault, the lower detachment fault in the Bullfrog Hills, and the Conejo Canyon and Wildcat Peak faults at Bare Mountain. New work at Bare Mountain by Y. Zhang indicates that this older detachment system was largely

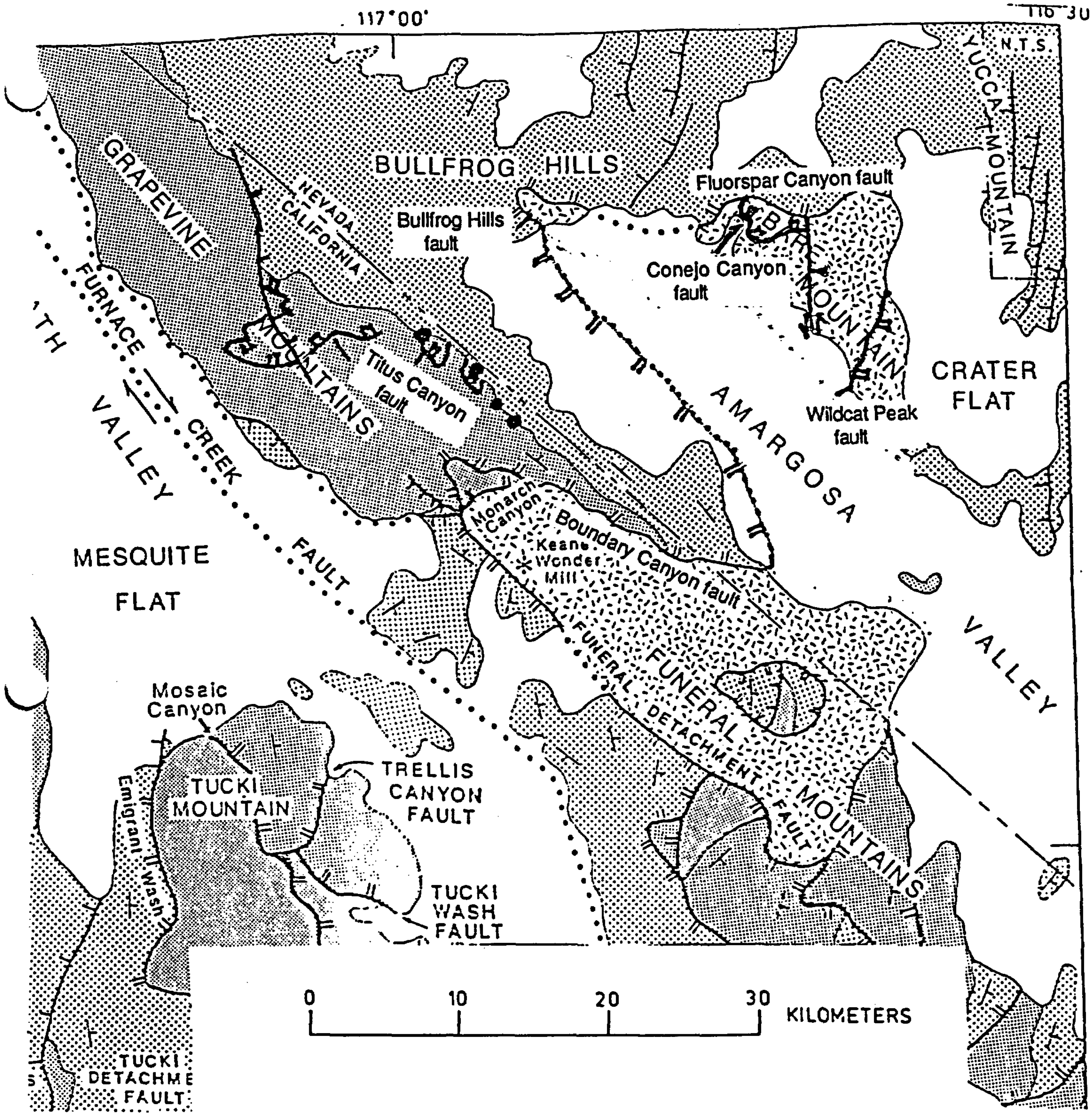

Figure 3. Modified from Hamilton (1988). Map showing post-10 Ma Boundary Canyon-Bullfrog Hills-Fluorspar Canyon detachment fault and remnants of Oligocene or older detachments, including Titus Canyon fault, Conejo Canyon fault, and Wildcat Peak fault. If the post-10 Ma detachment system were restored, the Titus Canyon fault would be located immediately west of Bare Mountain, and in close proximity to the Conejo Canyon and Wildcat Peak faults.

responsible for the exhumation of deep metamorphic rocks at northern Bare Mountain, Bullfrog Hills, and the Funeral Mountains, and that these metamorphic rocks were already exposed at high structural levels when ash flow tuffs of the Southwest Nevada Volcanic Field were erupted.

Structural relations in the western part of the Bullfrog Hills suggest that a portion of the Grapevine thrust is exposed where Ordovician carbonates rest upon Mississippian clastic rocks. To account for this segment of the Grapevine thrust, displacement on pre-Middle Miocene faults like the Titus Canyon fault must be invoked.

Implications of this study for Yucca Mountain are that pre-Middle Miocene detachment faults are very likely to occur beneath the volcanic section, and have probably disrupted and extended the Paleozoic section at depth. The combination of Mesozoic thrusts, pre-Middle Miocene detachment faults, and post-13 Ma faults at Yucca Mountain most likely indicates the impossibility of constructing accurate cross-sections of Paleozoic aquifers and aquitards beneath Yucca Mountain.

4. Kinematic analysis of low and high angle normal faults in the Bare Mountain area, and comparison of structures with the Grapevine Mountains Y. Zhang. (see Figure 4)(also see attached abstract by Zhang and Schweickert; Appendix 1).

A complete section of upper Precambrian through Mississippian sedimentary strata is well exposed at Bare Mountain. These rocks are involved in numerous folds, low- and high-angle faults, and strike-slip faults. Field relations indicate that many of these structures are pre-Middle Miocene in age. Thus, Bare Mountain provides an important window into the deep structures of Paleozoic rocks that lie beneath Yucca Mountain.

Research Activity

Two periods were spent in the field at Bare Mountain and vicinity, January 7 - 18 and June 1 - 7, 1992, respectively.

Structural mapping of fault-related structures at Bare Mountain was performed at a scale 1:24,000, incorporating published geologic maps of Bare Mountain. The northern part of Bare Mountain, which exposes complex structures, was selected as a key area for detailed mapping at scale of 1:12,000.

Field work also included reconnaissance in the Grapevine Mountains

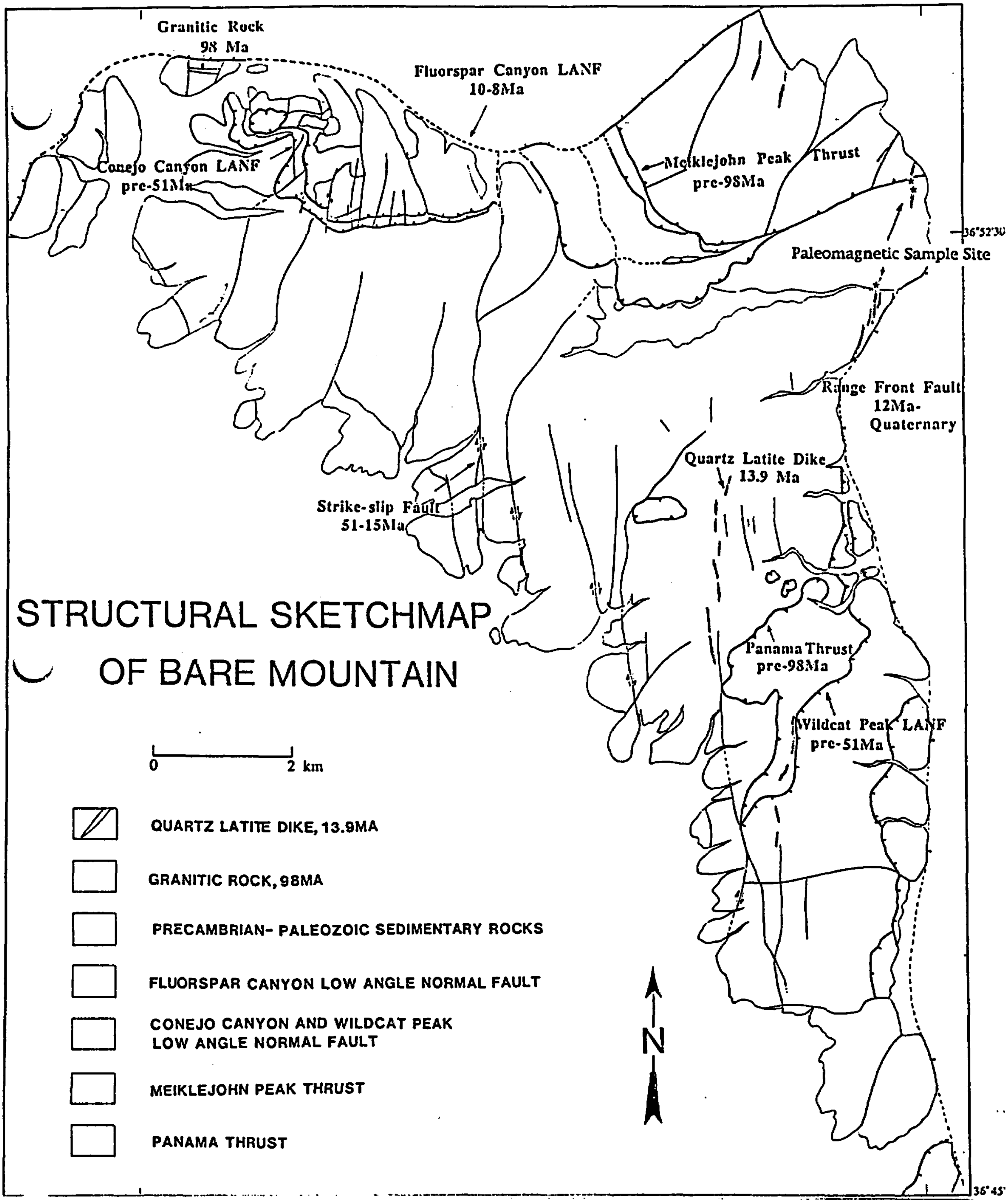

Figure 4. Structural sketchmap of Bare Mountain showing fault types, timing of faults and relations of various structures recognized at Bare Mountain.

of the Death Valley region with R.A. Schweickert and M.M. Lahren.

Samples of metamorphic rocks and fault rocks were collected for micro-structural analyses. Thin sections were made and were investigated for deformation styles. Both brittle and ductile deformation have been documented in various faults at Bare Mountain.

Samples also were collected from metamorphic rocks and diorite dikes that intruded Precambrian and Cambrian metasedimentary rocks for U-Pb and Ar-Ar geochronologic dating. Unfortunately, the sample of diorite cannot be dated by the U-Pb method because of a lack of zircon in the rocks. Other options will be tried with the sample.

Geologic map compilations and cross-section constructions on the basis of field data and air-photo information are approximately half complete. These maps and sections will show the structural patterns and Mesozoic and Cenozoic geologic history of Bare Mountain. Preliminary results are:

Summary

On the basis of structural studies at Bare Mountain, my main conclusions are listed below.

1. Pre-Tertiary thrusts exist at Bare Mountain (Figure 4), as shown by Monsen and others (1990). The Panama thrust is north-vergent and the Meiklejohn Peak thrust is south-vergent. North-vergent large scale folds occurring throughout the footwall of the Panama thrust and south-vergent folds in the footwall of the Meiklejohn Peak thrust are compatible with north-south shortening that resulted from Mesozoic deformation.

2. Two different ages of detachment faults have been distinguished at Bare Mountain. An older detachment fault (Conejo Canyon detachment fault) is exposed in the footwall of the Fluorspar Canyon detachment fault (7.5 - 10 Ma) in the northern part of Bare Mountain. The Conejo Canyon detachment fault was responsible for the denudation of amphibolite-facies metamorphic rocks at the northwestern end of Bare Mountain. Kinematic and structural data indicate that the Conejo Canyon detachment fault roots to the south. Still earlier high-angle faults, some possibly strike-slip faults, predate the Conejo Canyon fault. Published K-Ar ages from metamorphic rocks in the footwall of the Conejo Canyon detachment fault suggest that the unroofing and detachment faulting occurred in pre-Miocene times.

3. North-south striking and east-dipping oblique-slip faults became

active with most right oblique displacement prior to 14 Ma. Minor younger displacement has cut the 14 Ma dikes. These faults truncated both the Mesozoic thrust faults and the pre-Miocene detachment faults. Kinematic indicators indicate east-side-down oblique displacement on the larger faults, which further implies that rocks in the central part of Bare Mountain have been downdropped from the upper plate of the Conejo Canyon fault. If so, the Conejo Canyon fault roots at depth beneath the southern parts of Bare Mountain and the Wildcat Peak fault lies structurally above the Conejo Canyon fault. Some east-dipping faults are overlapped by 15 Ma volcanic rocks at the north end of Bare Mountain.

5. Evaluation of paleomagnetic character of Tertiary and pre-Tertiary units in the Yucca Mountain region, as tests of the Crater Flat shear zone hypothesis and the concept of oroclinal bending. S. Gillett, R. Karlin, Y. Zhang, and R. A. Schweickert.

Knowledge of the amount and sense of structural rotations is important for constraining kinematic models of tectonic deformation. Paleomagnetism is a powerful tool for identifying rotations about both horizontal axes (tilts) and vertical axes (oroclinal bending). Previous work at Bare Mountain (Monsen and others, 1990) revealed that north-south trending vertical quartz latite dikes (13.9 Ma) cut, or are cut by, a set of east-dipping faults that are dominant structures in the central part of Bare Mountain. The quartz latite dikes intruded Paleozoic rocks in various structural domains along the north - south extent of the range. Paleomagnetic study of the dikes is intended to constrain the sense of tilting and/or rotation of the domains separated by low angle faults.

Paleomagnetic data (Rosenbaum et al., 1991) from ash flow tuffs at Yucca Mountain demonstrated about 30 degrees of vertical axis rotation (clockwise) over the 25 km north-south extent of Yucca Mountain since emplacement of the Tiva Canyon member (about 13 Ma) of the Paintbrush Tuff. Paleomagnetic data from 13.9 Ma quartz latite dikes at Bare Mountain can provide a test of the oroclinal bending hypothesis.

Method and measurement

In January, 1991, paleomagnetic sampling of the following units was completed: the Lower Cambrian Carrara Formation at Carrara Canyon and Gold Ace Canyon at Bare Mountain, and in Striped Hills; Devonian rocks of Tarantula Canyon in Tarantula Canyon, at north end of Bare Mountain; 14 Ma dacite dikes at Tarantula Canyon; and the Middle Jurassic Sylvania pluton at Slate Ridge. All samples were collected with a portable rock drill and oriented with a brunton compass. In the laboratory, each sample was separated into 2 or 3 specimens (A,B, and C). NRM's have been measured on all samples of the quartz latite dikes. Specimen A was subjected to progressive alternating field demagnetization (measurements for AF demagnetization have not been completed). Specimen B was thermally demagnetized over Curie temperatures of the minerals or to 700° C. Specimen C from some of the samples was subjected to both AF and thermal demagnetization in order to compare the results from specimens A and B.

Specimens with strong magnetism were measured on a spinner magnetometer (usually for natural remanence and several early steps of demagnetization). Most of the specimens were measured on a cryogenic magnetometer.

Discussion

Demagnetization indicates magnetite and hematite carry most of the remanence in the dikes. A few samples contain pyrrhotite that loses magnetism at a low temperature range from 310° C to 330° C. Samples containing magnetite have blocking temperatures of about 580° C. A few samples have blocking temperatures as high as 620° C. This phenomenon probably indicates maghemite is the remanence carrier. Hematite is the dominant carrier of magnetization in the dikes. Blocking temperature in these samples is about 685° C.

Most samples have a remanence that comprises two or more components. On equal-area projections of directions, two concentrations are recognized, one a reversed direction in the west and another, also reversed, in the south portions, respectively. Two stable reversed Tertiary field has been recognized and have the potential to constrain structural movements. Remanences of the overprinting field with low blocking temperature are not difficult to differentiate from primary components and viscous components. Further measurements and analyses of the paleomagnetism of the dikes are continuing. This work will hopefully provide quantitative constraints on the timing and mode of deformation since 13.9 Ma at Bare Mountain.

6. Geology of Black Marble butte

Existing geologic maps show a NNW-striking high-angle fault along the eastern edge of Black Marble butte, at the southern tip of Bare Mountain, which separates Cambrian Bonanza King Formation on the west from the Timber Mountain Tuff to the east. If present, this fault could represent a NNW-striking strike-slip fault or a southern continuation of the Bare Mountain fault. However, our field studies suggest no fault is present in this location.

Near the southeastern end of Black Marble butte, a section of poorly indurated Cenozoic sandstones and crystal tuffs strikes northwest, dips northeast, and appears to lie unconformably upon Cambrian Bonanza King Formation. These strata dip eastward beneath basalts that underlie the Timber Mountain Tuff. If so, the Bonanza King represents either basement or large slide blocks in the pre-13 Ma stratigraphic section. If no fault is present in this location, the southern continuation of the Bare Mountain fault would have to pass west of Black Marble butte, through Steves Pass.

Part IV. Other activities of Task 5 personnel

1. Technical review of reports for the Center

None formally assigned; reviewed new publications by Snow (1992) and Wernicke (in press):

Snow, J.K., 1992, Large-magnitude Permian shortening and continental-margin tectonics in the southern Cordillera: Geol. Soc. America Bull., v. 104, p. 80-105.

Wernicke, B., 1991, Cenozoic extensional tectonics of the U.S. Cordillera, in Burchfiel, B.C., Lipman, P.W., and Zoback, M.L., eds., The Cordilleran orogen; Coterminus United States: Boulder, Colorado, Geol. Soc. America, The Geolopgy of North America, v. G3, in press.

2. Meetings attended in relation to the Yucca Mountain Project and the Center for Neotectonic Studies

a. Geological Society of America, National Meeting, San Diego, California, October, 21-24,1991 (attended by Schweickert, Lahren, and Zhang; see abstract by Zhang and Schweickert)

b. Premeeting fieldtrip, attended by Schweickert, October 17-20, 1991, to Chicago Pass, Death Valley, southern Nopah Range, Kingston Range, Winters Pass in the Mesquite Mountains, Providence Mountains, Soda Mountains, Marble Mountains, and Little Piute Mountains, southeastern California.

3. **Field work**
   a. Structural mapping in Bare Mountain, Y. Zhang, January 7-10, June 1-7, 1992; Schweickert, Lahren, and Zhang, January, 11-14, 1992
   b. Geologic mapping and structural analysis in Grapevine Mts., Bullfrog Hills, Bare Mountain, and Black Marble--Schweickert, Lahren, and Zhang, January, 14-17, 1992

4. **Professional reports provided to NWPO**
   a. None

5. **Abstracts published**
   a. Zhang, Y., and Schweickert, R.A., 1991, Structural analysis of Bare Mountain, southern Nevada (abs.): Geol. Soc. America Abs. with Programs, v. 23, p. A185-A186.

6. **Papers accepted for publication in peer-reviewed literature**

   a. Caskey, S.J., and Schweickert, R.A., Mesozoic deformation in the Nevada Test Site region: Implications for the structural framework of the Cordilleran fold and thrust belt and Tertiary extension north of Las Vegas Valley: Tectonics; accepted for publication, 2/92.

7. **Graduate theses supported by NWPO**
   a. Zhang, Y., in progress, Structural and kinematic analysis of Mesozoic and Cenozoic structures at Bare Mountain, Nye County, Nevada

Appendix I.
Abstracts and published papers

1. Caskey, S.J., and Schweickert, R.A., Mesozoic deformation in the Nevada Test Site region: Implications for the structural framework of the Cordilleran fold and thrust belt and Tertiary extension north of Las Vegas Valley: Tectonics, accepted for publication, 2/92. (preprint)

2. Zhang, Y., and Schweickert, R.A., 1991, Structural analysis of Bare Mountain, Southern Nevada (abs.): Geol. Soc. America Abs. with Programs, v. 23, p. A185.

2/21/92
In press
Tectonics

MESOZOIC DEFORMATION IN THE NEVADA TEST SITE REGION: IMPLICATIONS FOR THE STRUCTURAL FRAMEWORK OF THE CORDILLERAN FOLD AND THRUST BELT AND TERTIARY EXTENSION NORTH OF LAS VEGAS VALLEY

S. John Caskey and Richard A. Schweickert

Center for Neotectonic Studies

Department of Geological Sciences

University of Nevada, Reno

Reno, Nevada 89557

MESOZOIC DEFORMATION IN THE NEVADA TEST SITE AND VICINITY: IMPLICATIONS FOR STRUCTURAL FRAMEWORK OF THE CORDILLERAN FOLD AND THRUST BELT AND TERTIARY EXTENSION NORTH OF LAS VEGAS VALLEY

S. John Caskey and Richard A. Schweickert *Center for Neotectonic Studies Department of Geological Sciences University of Nevada, Reno Reno, Nevada 89557*

ABSTRACT

Detailed studies in the CP Hills and Mine Mountain area of the Nevada Test Site (NTS), together with analysis of published maps and cross sections and a reconnaissance of regional structural relations, indicate that the CP thrust of Barnes and Poole (1968) actually comprises two separate, oppositely verging Mesozoic thrust systems: 1) the west-vergent CP thrust which is well exposed in the CP Hills and at Mine Mountain; and 2) the east-vergent Belted Range thrust located northwest of Yucca Flat. Regional structural relations indicate that the CP thrust forms part of a narrow sigmoidal belt of west-vergent folding and thrusting traceable for over 180 km along strike. The Belted Range thrust represents earlier Mesozoic deformation that was probably related to the Last Chance thrust system in southeastern California, as suggested by earlier workers. A reconstruction of the pre-Tertiary geometry of the Cordilleran fold and thrust belt in the region between the NTS and the Las Vegas Range bears a close resemblance to other regions of the Cordillera and suggests that west-vergent deformation developed in the hinterland of a part of the Sevier fold and thrust belt characterized by substantial structural relief. Reconstruction

of the fold and thrust belt also suggests that previous estimates of upper crustal Tertiary extension north of the Las Vegas Valley shear zone (e.g. 80% (Guth, 1981)) are two or three times too large.

INTRODUCTION

The Nevada Test Site (NTS) (fig.1) of the southern Great Basin lies within the dominantly east-vergent Mesozoic Cordilleran thrust belt near one of the thickest known parts of the Paleozoic Cordilleran miogeocline. In this region, Barnes and Poole (1968) and Hinrichs (1968) interpreted several thrust faults that place upper Precambrian and lower Paleozoic rocks over upper Paleozoic rocks as remnants of a single, regional, east- to southeast-vergent thrust system. They named this thrust system the CP thrust for exposures in the Control Point (CP) Hills, south of Yucca Flat (fig. 1). Subsequent work on the Mesozoic structure in the region has been hampered by the general inaccessibility of the NTS and surrounding regions. Later discussions of the regional structural setting of the NTS and vicinity (e.g. Carr, 1984; Wernicke et al., 1988a, 1988b) have therefore relied on these earlier interpretations.

Our detailed studies in the CP Hills and Mine Mountain area (figs. 1 and 4), together with published maps and cross sections by Orkild (1968) and McKeown et al. (1976) and a reconnaissance of regional structural relations, indicate that the CP thrust of Barnes and Poole (1968) actually comprises parts of two separate, oppositely verging thrust systems: 1) the west-vergent CP thrust, which is well exposed in the CP Hills and at Mine Mountain (figs. 1 and 4), and 2) the southeast-vergent Belted Range thrust, located northwest of Yucca Flat (fig. 1).

Herein, we redefine the CP thrust of Barnes and Poole (1968) and suggest a revision of nomenclature for thrusts in the NTS region. We also present modifications of previous interpretations of Mesozoic structures of surrounding regions to develop a coherent synthesis of the pre-Tertiary structural framework.

GEOLOGIC SETTING

The NTS lies within the late(?) Mesozoic Sevier orogenic belt (Armstrong, 1968; Fleck, 1970). However, alluviated extensional basins and Tertiary volcanic and sedimentary rocks (fig. 1) obscure many structural details of the fold and thrust belt. Throughout most of the NTS region, the Mesozoic structural framework has been disrupted by at least two episodes of Tertiary extensional faulting (Ekren et al., 1968; Schweickert and Caskey, 1990), further hindering our understanding of the pre-Tertiary regional tectonic framework. Fortunately, all seven systems of the Paleozoic Cordilleran miogeocline are represented in the NTS region and these together with Precambrian strata form a generally conformable stratigraphic section over 38,000 feet (nearly 12,000 m) thick (fig. 2). (e.g. Cornwall, 1972; Ekren, 1968; Longwell et al., 1965; Stewart and Poole, 1972). This stratigraphy is essential to unravelling locally complicated Mesozoic and Tertiary structure and for piecing together upper crustal blocks that have been separated as a result of large-scale Tertiary extension.

The area surrounding Yucca Flat (fig. 1) offers the most extensive exposures of upper Proterozoic and Paleozoic rocks within the NTS. Mesozoic thrusts and folds have been mapped northwest of Yucca Flat (Gibbons et al., 1963; Barnes and Poole, 1968), at the southwest end of Yucca Flat in the CP Hills and Mine Mountain area (Barnes and Poole, 1968; McKeown et al., 1976; and Orkild, 1968), and also just east of the NTS in the Spotted Range (Barnes and Poole, 1968; Barnes et al., 1982; Cornwall, 1972; Longwell et al., 1965; Tschanz and Pampeyan, 1970). An understanding of the Mesozoic structure of the NTS region, as well as other neighboring regions, is critical to evaluating the regional pre-Tertiary structural framework of the Cordilleran fold and thrust belt at this latitude, the magnitude and style of Tertiary extension, and to interpreting the deep structure beneath Southwest Nevada volcanic field (fig. 1).

In the following section, we outline the major structural elements of Mesozoic thrusts and folds that occur in the NTS region. We then discuss a regional structural section and a preliminary pre-Tertiary palinspastic reconstruction to illustrate the tectonic framework of the Mesozoic Cordilleran fold and thrust belt at this latitude.

MESOZOIC STRUCTURE

CP thrust

The CP thrust, in the CP Hills (figs. 3 and 4), places uppermost Precambrian and Cambrian rocks above Mississippian through Pennsylvanian strata. Recent studies in the CP Hills and Mine Mountain areas indicate that the CP thust is a major west-vergent Mesozoic structure

(Caskey, 1991). While this interpretation is consistent with published maps and cross sections of McKeown et al. (1976), other workers have interpreted the CP thrust, where exposed in the CP Hills, as an east- to southeast-vergent structure (e.g. Barnes and Poole, 1968; Carr, 1984; Hinrichs, 1968; Wernicke et al., 1988a, 1988b; Snow, 1992). Two independent lines of evidence support the west-vergent interpretation: 1) large-scale west-facing, nearly recumbent folds occur in both the hanging wall and footwall of the CP thrust (figs. 4 and 5); and 2) the CP thrust ramps upsection through hanging wall strata toward the northwest.

A north-trending, west-facing recumbent syncline in the footwall of the CP thrust is exposed in an erosional window through upper plate strata in the southern part of the CP Hills (figs. 4 and 5). The recumbent footwall syncline involves at least Upper Mississippian through Pennsylvanian strata and can be traced for several kilometers along strike.

Rocks in the upper plate of the CP thrust are imbricately faulted, highly folded, and locally are overturned to the west. In the eastern and northeastern part of the CP Hills (fig. 4), a north-trending, west-facing, nearly recumbent fold pair in the upper plate involves a minimum of 2000 m of Lower through Upper Cambrian strata. These folds are similar in scale to the footwall syncline (fig. 5).

Strata of the CP allochthon young progressively to the northwest, from uppermost Precambrian and Cambrian strata in the southeastern part of the CP Hills, through upper Cambrian and Ordovician strata at the north end of the CP Hills. Farther northwest, in the Mine

Mountain area, sequentially younger Silurian and Devonian carbonates structurally overlie Carboniferous strata beneath the Mine Mountain "thrust" (Orkild, 1968) (fig. 4). Tertiary low-angle normal faults and minor strike-slip faults between Mine Mountain the CP Hills (see fig. 4) complicate the correlation of these Silurian and Devonian strata with rocks of the CP allochthon in the CP HIlls, but arguments presented below favor general stratigraphic order in this area.

Carr (1984) interpreted the Mine Mountain thrust as a Tertiary "landslide" surface (or low-angle normal fault). Although Tertiary displacement along this surface probably occurred, the older-over-younger relationship at Mine Mountain is probably a consequence of Mesozoic thrusting. Silurian and Devonian strata above the Mine Mountain "thrust" occupy the same structural level (relative to Carboniferous units) as the CP thrust plate in the southeastern part of the CP Hills. Similar styles of folds (with west-vergence) also occur in Carboniferous strata beneath both the Mine Mountain and CP Hills thrusts (Caskey and Nitchman, unpub. data). In addition, only minor omissions of stratigraphic units occur along an otherwise complete and generally sequential section of upper Precambrian through Devonian strata from the southern part of the CP Hills to Mine Mountain (discussed above). We suggest therefore that the northwest younging of strata along this transect is also a remnant Mesozoic structural feature. These relations indicate that the CP thrust and the Mine Mountain thrust are correlative west-vergent structures, and these faults are herein collectively referred to as the CP thrust.

Net displacement along the CP thrust is poorly constrained. However, in the CP Hills, the uppermost Precambrian to Lower Cambrian Wood Canyon Formation is thrust over the Pennsylvanian and Permian Tippipah Limestone. This juxtaposition requires a stratigraphic throw of approximately 8.5 km (see fig. 2). The facts that the CP thrust appears to cut obliquely through strata in the footwall and does not appear to exhibit a simple hanging wall ramp geometry (i.e. the CP thrust locally cuts open folds within the CP allochthon (see fig. 5)), both suggest that net displacement is greater than 8.5 km.

Belted Range thrust

Northwest of Yucca Flat, published maps and subsurface drill hole data (Gibbons et al., 1963) indicate the presence of a major east-vergent thrust system largely concealed beneath Tertiary volcanic rocks (figs. 1 and 3). In this region, upper Precambrian strata have been thrust over Silurian and Devonian rocks that have in turn been thrust over Mississippian rocks. The Mississippian strata of the footwall are locally folded into a large, southeast-facing recumbent syncline indicating that southeast-directed displacement occurred along this thrust system (Gibbons et al., 1963). Carboniferous rocks within the footwall of the thrust can be traced southward to the Mine Mountain area where they also form the footwall to the CP thrust. Although the Belted Range and CP thrust share a common parautochthon, the fact that they have opposite vergence clearly indicates that these are different thrust systems. However, because

Barnes and Poole (1968) interpreted the CP thrust (in the CP Hills) as an east-vergent thrust (see also Hinrichs, 1968), they correlated the two thrust systems and collectively termed them the CP thrust. This is clearly a misnomer for the east-vergent thrust northwest of Yucca Flat. We propose the name *Belted Range thrust* for the fault northwest of Yucca Flat, since the major exposures of this east-vergent thrust occur at the southern end of the Belted Range (fig. 1) (Gibbons et al., 1963).

Net displacement along the Belted Range thrust system is poorly constrained. However, a stratigraphic throw similar to that of the CP thrust (>8.5 km) is required. Net displacement along the Belted Range thrust is possibly much greater than this, as discussed below.

Spotted Range thrust

The Spotted Range thrust, located in the Spotted Range (figs. 1 and 3) about 30 km southeast of the CP Hills, places Middle Cambrian strata above Upper Devonian and Mississippian rocks that are deformed into a sequence of tight to isoclinal folds overturned to the southeast (Barnes et al., 1982). The sense of vergence of these footwall folds indicates that southeast-directed displacement occurred along the Spotted Range thrust. This precludes correlation of the Spotted Range thrust with the west-vergent CP thrust in the CP Hills as proposed by Barnes and Poole (1968). A minor west-vergent syncline which involves Devonian and Mississippian strata occurs northwest of the thrust klippen exposed at the southwest end of the Spotted Range (Barnes et al., 1982; Johnson and Hibbard, 1957) but it is unclear how this west-vergent fold is related to surrounding Mesozoic structures.

The Spotted Range thrust plate is preserved as a series of erosional remnants, or klippen, traceable for over 50 km along the north-to-northeast striking hinge surface trace of a broad regional syncline (Barnes et al., 1982), herein called the Spotted Range syncline (fig. 3). This relation strongly implies that a folding event post-dated emplacement of the Spotted Range thrust sheet (discussed later). The root zone for the Spotted Range thrust is problematic. However, structural relations discussed below suggest that the lower plate of the Spotted Range thrust is continuous with the upper plate of the west-vergent CP thrust.

At the southwest end of the Spotted Range, Ordovician strata in the lower plate of the Spotted Range thrust crop out almost continuously around the nose of the northeast-plunging Spotted Range syncline and continue northward along the northwestern limb (Barnes et al., 1982; Longwell et al., 1965; Poole, 1965; Tschanz and Pampeyan, 1970). Scattered exposures of Ordovician strata can be tracked discontinuously from there to the east edge of Yucca Flat where they occur in stratigraphic continuity with older rocks at Pahute Ridge and Banded Mountain (figs. 1 and 3) (Barnes et al., 1963, 1965; Byers and Barnes, 1967; Hinrichs and McKay, 1965). Strata at Banded Mountain form the steeply dipping western limb of a prominent, northwest-trending, asymmetric anticline involving upper Precambrian through Upper Cambrian strata (Barnes et al., 1963, 1965) which we interpret as the northern continuation of the overturned anticline in the CP thrust plate. Therefore, we equate the lower plate of the Spotted Range thrust with the upper plate of the CP thrust, meaning that the Spotted Range thrust klippen must lie structurally above the CP thrust plate (fig. 6).

The apparent continuity of strata in the footwall of the east-vergent Spotted Range thrust from the Spotted Range to the northeast edge of Yucca Flat suggests that the Spotted Range thrust must root farther to the west, and west of the CP thrust. We believe that the Spotted Range thrust correlates with the Belted Range thrust. Barnes and Poole (1968) also suggested that the Spotted Range thrust had a root zone northwest of Yucca Flat. Klippen of the Spotted Range thrust presently lie more than 50 km southeast of the trace of the Belted Range thrust. Even if large-magnitude Tertiary extension (e.g. 100%) occurred in the region between the Belted Range and the Spotted Range (which is possible), this would still indicate that more than 25 km of displacement occurred along the Belted Range/Spotted Range thrust system.

If we are correct in correlating the Belted and Spotted Range thrusts, map relations require that the thrust plate was translated eastward across a Mississippian facies boundary separating dominantly siliciclastic rocks, minor carbonates, shales, and orthoquartzites in the Eleana Range (Poole et al., 1961) from calcareous shale and carbonate strata in the Spotted Range (Barnes et al., 1982). The Belted Range thrust apparently rode along a decollement within Mississippian and/or younger strata between the Belted Range and the Spotted Range and was translated across the CP Hills area (fig. 1). Caskey (1991) reported that strata in the footwall of the

CP thrust were probably affected by an episode of east-vergent deformation prior to emplacement of the west-vergent CP thrust. This east-vergent deformation may have been related to emplacement of the Belted Range/Spotted Range thrust sheet across the CP Hills area.

A potential problem for the correlation of the Belted Range and Spotted Range thrusts is that it may require that the Belted Range/Spotted Range thrust system locally cut down stratigraphic section within its footwall between the CP Hills and the Spotted Range (i.e. down from Pennsylvanian to Mississippian strata). However, Barnes et al. (1982) showed that the Spotted Range thrust cuts several large, tight folds within its footwall so that it locally cuts both up and down stratigraphic section, indicating that a similar relationship is possible on a regional scale. Guth (1990) suggested that the tight footwall folds beneath the Spotted Range thrust klippen require a local footwall ramp (i.e. root zone) for the Spotted Range thrust. This is precluded by the continuity of Ordovician strata in the footwall around the klippen of the Spotted Range thrust (as described earlier). We suggest instead that upper level decollement-style folds (e.g. Jamison, 1987, p. 207, fig. 1c) and/or minor fault-propagation folds within the lower plate may have initially developed forward of, or beneath, the eastward-propagating Belted Range/Spotted Range thrust sheet. Guth (1990) also reported Tertiary modification of the Spotted Range thrust, so it is possible that important Mesozoic structural details have been lost through subsequent deformation.

Figure 6 illustrates our interpretation of the structural relations between the east-vergent Belted Range-Spotted Range thrust and the west-vergent CP thrust. Other structural elements shown in figure 6, together with relative timing and cross-cutting relationships (implied in figure) are discussed below.

Gass Peak thrust

East of the Spotted Range, no major thrust faults surface until the Gass Peak thrust in the Las Vegas Range (figs. 1 and 3). The Gass Peak thrust is a regionally extensive east-vergent structure that places Precambrian strata over highly folded and locally overturned Pennsylvanian and Permian carbonates (Longwell, 1965; Guth, 1981). Wernicke et al. (1984) and Guth (1980, 1990) interpreted the Gass Peak allochthon as a major structural plate of the Sevier orogenic belt characterized by decollement hanging wall geometry. This is supported by published cross sections (Longwell et al., 1965; Guth, 1981, 1990) indicating that the Gass Peak thrust has hanging wall flat and footwall ramp geometry in the Las Vegas Range. Net horizontal displacement along the Gass Peak thrust is believed to have been 30 km or more (Guth, 1980, 1981).

A minor thrust or reverse fault occurs along the west side of the Pintwater Range (fig. 3) (Longwell et al., 1965; the "Pintwater thrust" of Guth, 1990). This fault has probably been modified by Tertiary extensional faults because it exhibits both older-on-younger and younger-on-older age relationships (Guth, 1990), and appears to be of little regional importance because it is only traceable for a short distance. Because no major thrusts occur between the Gass Peak thrust and the klippen of the Spotted Range thrust, the lower plate to the Spotted Range thrust (inferred previously to be the CP allochthon) and the Gass Peak allochthon essentially constitute the same (pre-extensional) structural plate (figs. 3 and 6).

Pintwater anticline/Spotted Range syncline

Aside from the klippen of the Spotted Range thrust (inferred above to be part of the Belted Range thrust plate), the most important Mesozoic structures preserved between the west-vergent CP thrust and the east-vergent Gass Peak thrust are the Pintwater anticline (Longwell, 1945) and the Spotted Range syncline (Barnes et al., 1982) (figs. 3 and 6). These structures both occur within the same structural plate (CP-Gass Peak allochthon) (figs. 3 and 6), and together they constitute a north-trending and plunging regional fold pair that is traceable for nearly 100 km along strike and whose width now spans four mountain ranges (i.e. the Sheep, Desert, Pintwater, and Spotted Ranges) and . Longwell (1945), who was the first to recognize the Pintwater anticline, noted that the north ends of the Pintwater Range (the western limb) and the Desert Range (the eastern limb) unite to form the plunging nose of a great fold. As discussed earlier, strata at the southwest end of the Spotted Range (Longwell et al., 1965; Cornwall, 1972; Barnes et al., 1982) form the nose of the Spotted Range syncline to complete the regional fold pair.

The full significance of the regional fold pair is difficult to assess because the late Tertiary Sheep Range detachment system (Wernicke et al., 1984, Guth et al., 1988, Guth, 1990) strongly disrupts rocks in the region between the Sheep and Spotted Ranges (i.e. the CP/Gass Peak allochthon). According to Guth et al. (1988, p. 240, fig. 1 and table 1) Tertiary basin deposits show that major fault blocks of the Sheep Range detachment system have been rotated about 30 degrees to the east during Tertiary extension.

A structural section oriented NW-SE (fig. 7a) which extends from the Belted Range to the Las Vegas Range illustrates the complex Tertiary extensional overprint and the present structural disposition of pre-Tertiary strata. Extensive Miocene volcanic rocks (fig. 1) postdate and conceal much of the evidence for earlier Tertiary extension west of the Spotted Range (Schweickert and Caskey, 1990); the structural interpretations west of the Spotted Range are therefore regarded as conceptual but are supported by available data.

A preliminary palinspastic reconstruction of this NW-SE section (fig. 7b) was prepared by restoring Proterozoic and Paleozoic stratal cutoffs across normal faults (making some assumpions about normal fault geometry at depth), and by simultaneously restoring major fault blocks to pre-tilt orientations using published dip data on Tertiary sedimentary and volcanic deposits (Ekren et al., 1977; Guth et al., 1988; Longwell et al., 1965; and Tschanz and Pampeyan, 1970) that depositionally overlie Paleozoic strata. For simplicity, we assumed that Tertiary deposits were originally horizontal.

In the restored section NW-SE (fig. 7b), the Pintwater anticline-Spotted Range syncline fold pair take on a substantially different pre-Tertiary geometry. The east limb of the Pintwater anticline in the Desert Range block, when back-rotated 30 degrees to the west, acquires a gentle east dip. The west limb of the anticline restored approximately 30 degrees to the west becomes steeply west dipping. In addition, our preliminary restoration indicates that, prior to Tertiary extension, the Pintwater anticline and the Spotted Range syncline were a broad regional fold pair with structural relief possibly as great as 7 km. We suggest that structural thickening by duplex stacking (e.g. Boyer and Elliot, 1982) and/or folding of the Eocambrian clastic wedge beneath the Pintwater "anticlinorium" (shown schematically in fig. 7b) was probably responsible for this structural relief (e.g. may be required for balance).

Guth (1990) also recognized that structural relations must be complex under the Pintwater Range. In a generalized restoration of the Sevier thrust belt, Guth (1990, p. 46, fig. 6) modelled the Pintwater anticline as a fault-bend fold (e.g. Suppe, 1983) that developed above a large, but simple ramp in the footwall of the Gass Peak thrust. He showed about 5 km of structural relief. However, a problem with Guth's (1990) restoration arises because the Gass Peak thrust was shown ramping up through 5 km of Eocambrian and Cambrian strata beneath the Pintwater anticline. Equivalent strata within a hanging wall flat above an upper ramp of the Gass Peak thrust are nearly 3 km thinner (Guth, 1990, fig. 7). Guth alluded to this space problem by suggesting that thinning of strata between the Las Vegas and Desert Ranges may be "tectonic or original."

Although he did not state his preference, his reconstruction implies the thinning is tectonic. Our reconstruction also assumes tectonic thinning in this area, however studies on the exact nature of the thinning of strata are required before cross sections can be balanced across this region.

Our interpretations of the Pintwater anticline differ from those of Guth (1990) in that our reconstruction suggests a broader geometry for the Pintwater "anticlinorium" with greater structural relief and more complex subsurface structures (i.e. east-vergent folds and imbrications within Eocambrian rocks). These interpretations, though derived independently, agree with previous interpretations of structures in the northwest Spring Mountains (Burchfiel, 1974) (discussed below) that have been correlated to the Pintwater anticline (Burchfiel, 1983).

REGIONAL EXTENT OF THRUSTS AND RELATED DEFORMATION

Structures related to the CP thrust

Regional structural relations suggest that west-vergent structures likely related to the CP thrust can be traced along strike throughout the highly extended terrain of the southern Great Basin (see also discussion by Snow and Wernicke (1990)). However, in the region between the southern part of the Las Vegas Range and Bare Mountain (fig. 1 and 3), generally north-trending Tertiary structural blocks and Mesozoic structural trends, typical of the southern Great Basin, have been rotated clockwise as much as 90 degrees about a vertical axis. This phenomenon has been attributed to regional oroflexural bending within the Walker Lane belt (Albers, 1967; Stewart et al., 1968; Stewart, 1988), and also to right-lateral drag associated with the Las Vegas Valley shear zone and related structures (Longwell, 1960). In the region of maximum "bending," previously northerly-trending, west-vergent structures are presently east-trending and north-vergent.

At Bare Mountain (figs. 1 and 3), 50 km west of the CP Hills, major recumbent folds are associated with the north-vergent Panama thrust (Cornwall and Kleinhampl, 1961; Carr and Monsen, 1988; Monsen et al., 1990). The north-vergent folds appear to be tight and involve a several-kilometer-thick package of upper Precambrian through Upper Cambrian strata. It is difficult to provide a realistic estimate of net displacement along the Panama thrust. Lower and Middle Cambrian strata that structurally overlie Mississippian rocks at the north end of Bare Mountain occupy the same structural position as the Panama thrust at the south end of the range (fig. 3) (Carr and Monsen, 1988; and Monsen, et al., 1990). However, complex Tertiary overprinting has occurred at the north end of Bare Mountain (Monsen et al., 1990), thus making it difficult to interpret the Mesozoic structural framework. If these Middle Cambrian rocks at the north end of Bare Mountain belong to the north-vergent Panama thrust plate (fig. 3), displacement along the Panama thrust would be comparable to that along the CP thrust in the CP Hills. We interpret the north-vergent structures at Bare Mountain as being broadly correlative with the CP thrust, as defined in this paper.

West of Bare Mountain, in the Grapevine Mountains (figs. 1 and 3), a map-scale, west-vergent recumbent fold pair (e.g. the Titus Canyon anticline and the Corkscrew syncline (fig. 3)) occurs in the upper plate of the Boundary Canyon normal fault (Reynolds, 1969). These structures have been correlated with the Panama thrust at Bare Mountain and with west-vergent backfolds farther west in the Cottonwood Mountains (Wernicke et al., 1988a, 1988b; Snow and Wernicke, 1989). However, because large-scale north-vergent folds occur in both the upper and lower plates of the Panama thrust at Bare Mountain (Monsen et al., 1990), we are uncertain about the structural levels represented by the west-vergent folds in the Grapevine Mountains relative to those to the east (fig. 3).

In the Specter Range (fig. 1), a very large north-vergent anticline occurs whose overturned northern limb, involving a 4.5 km thickness of Lower Cambrian to Devonian strata, is well-exposed in the Striped Hills (Sargent et al., 1970; Sargent and Stewart, 1971; Schweickert, 1989). The scale of the fold, together with the rarity of hinterland-verging structures within the fold belt, suggest that this structure may correlate with recumbent north-vergent structures at Bare Mountain (Schweickert, 1989). If so, this north-vergent structure may have been displaced by a concealed dextral strike-slip fault beneath Crater Flat, east of Bare Mountain. The proposed dextral fault may be a northern continuation of the dextral Stewart Valley-Stateline fault southeast of the Amargosa Desert (fig. 3) (Schweickert, 1989).

Reconnaissance mapping in the Calico Hills (fig. 1) in the NTS has delineated large-scale north-vergent folds beneath overthrust Devonian carbonates (Caskey and Nitchman, upubl. data). In this area, lower plate folds involve Upper Mississippian orthoquartzites, shales and carbonate rocks lithologically identical to Mississippian units beneath the CP thrust in the CP

Hills. Published cross sections also indicate north-directed displacement occurred along thrust(s) in this area (McKay and Williams, 1964; Orkild and O'Connor, 1970). Approximately 20 km separate Devonian rocks in the Calico Hills from those in the Striped Hills to the south. Although this could be interpreted to mean that an extensive zone of north-vergent folds and thrusts exists in this area, we believe it is more likely that these are upper crustal blocks that have been separated by large-magnitude, northwest-directed extension near the southern and southeastern portions of the Southwest Nevada volcanic field (Schweickert and Caskey, 1990).

North of Yucca Flat, a west-facing, overturned syncline northwest of Oak Spring Butte (figs. 1 and 3) involves at least 1.2 km of Ordovician through Devonian strata (Rodgers and Noble, 1969). This syncline, which is truncated by the Tertiary Butte (normal) fault to the east (fig. 3), probably is a continuation of the west-vergent structures in the CP Hills. Middle Cambrian strata exposed on the downdropped eastern side of the Butte fault lie on trend with and are are probably continuous with Middle Cambrian strata at Banded Mountain to the south. As previously discussed, the rocks at Banded Mountain form the western limb of a very large, asymmetric, west-facing anticline which is best interpreted as part of the upper plate of the CP thrust. Johnson and Hibbard (1957) also argued that all the lower Paleozoic rocks in the Yucca Flat region east of Mine Mountain and the Butte fault comprise a major thrust plate, although they were unsure of its sense of displacement. The zone of west-vergent deformation is difficult to trace north of the NTS area because of extensive Tertiary volcanic cover and Tertiary deformation. However, this zone probably extends at least as far north as the Egan Range where major west-vergent folds have been previously mapped (Brokaw and Barosh, 1968).

In summary, regional structural correlations indicate that hinterland-vergent structures probably can be traced for at least 180 km along strike in southwest Nevada and eastern California (fig. 3). These structures form a z-shaped sigmoidal pattern which essentially parallels oroflexural bends recognized by Albers (1967) within a "mobile belt" east of the Sierra Nevada. The sigmoidal pattern is disrupted in a right-lateral sense by a possible northward projection of the Stewart Valley-Stateline fault in Crater Flat (fig. 1) and also is disrupted in the northern part of the Amargosa Desert (fig. 3). Apparent dextral offset of the west-vergent structures across the Amargosa Desert is probably a result of northwest-directed translation of the Titus Canyon anticline-Corkscrew syncline above the Bare Mountain-Bullfrog Hills-Boundary Canyon detachment system (Carr and Monsen, 1988) (fig. 3). In any case, east-trending, north-verging structures at Bare Mountain appear to curve sharply westward to become north-trending and west-verging in the Grapevine Mountains, completing the sigmoidal "z" pattern.

Regional extent of other structures

Structurally complicated Tertiary overprinting in areas such as Bare Mountain, extensive volcanic cover, and the fact that thrusts eventually die out along strike all compound the difficulties of correlating thrust faults in this region. Nevertheless, the southeast-vergent Belted Range thrust, as described here, has previously been correlated to the Meiklejohn Peak thrust at the north end of Bare Mountain and with the Last Chance thrust in eastern California (Burchfiel et al., 1970; Wernicke et al., 1988a, 1988b). This correlation is reasonable, based on the position of both thrusts relative to the west-vergent fold and thrust system, but is not altogether compelling. At the northeast corner of Bare Mountain, exposures of highly sheared and folded Mississippian strata (Monsen et al., 1990), presumably in the upper plate of the Meiklejohn Peak thrust, suggest the presence of a structurally higher, south-vergent thrust concealed beneath Tertiary volcanic rocks to the north. It is conceivable that the Belted Range thrust may correlate with such a postulated higher thrust and that the Meiklejohn Peak thrust either terminates along strike or represents a thrust imbrication structurally beneath the Belted Range thrust (see Gibbons et al., 1963) (also inferred by Snow, 1992, fig. 12, p. 92).

As previously mentioned, the klippen of the Spotted Range thrust probably belong to the once extensive Belted Range thrust plate and can be traced for more than 50 km along the hinge zone of the Spotted Range syncline. The northernmost klippe occurs at Chert Ridge, in the northern part of the Spotted Range (figs. 1 and 3) (Tschanz and Pampeyan, 1970; Jayko, 1990). Cambrian strata near the south end of the Spotted Range mapped by Barnes et al. (1982) and Cornwall (1972) appear to represent the southernmost extent of thrust klippen. An east-trending, south-vergent thrust in the Specter Range (figs. 1 and 3) (Burchfiel, 1965; Sargent and Stewart, 1971) has previously been correlated with the Spotted Range thrust (Wernicke et al., 1988a, 1988b), but this thrust exhibits considerably less stratigraphic throw (i.e. Lower Cambrian over

Ordovician strata) than the Spotted Range thrust and appears to us to lie within the lower plate of the Spotted Range thrust. We agree with Burchfiel (1965), who argued that strata in the northern part of the Specter Range, including rocks in the upper plate of the thrust in the Specter Range, are continuous with strata in the lower plate of the Spotted Range thrust to the east. He postulated that the thrust in the Specter Range had no counterpart in the Spotted Range and that it may have resulted from late Tertiary contraction that accommodated the northwest termination of the right-lateral Las Vegas Valley shear zone (fig. 3).

The Gass Peak thrust is a regionally extensive structure that can be traced for at least 140 km in southern Nevada, from at least the east side of the northern part of the Sheep Range (Longwell, 1965), through the Las Vegas Range to the south, and across the Las Vegas Valley shear zone as the Wheeler Pass thrust (Burchfiel, 1965; Fleck, 1970) in the northwestern part of the Spring Mountains (figs. 1 and 3). Wernicke et al. (1988a, 1988b) correlated structures as far west as the Slate Range in eastern California with the Wheeler Pass-Gass Peak thrust system.

The extent of regional folds related to the Pintwater anticline and Spotted Range syncline is uncertain. North of the study area, extensive Tertiary deformation and volcanic cover (Jayko, 1990; Tschanz and Pampeyan, 1970) make ambiguous any correlations of these structures. Although extreme bending and attenuation of Mesozoic structures has occurred to the south along the northern terminus of the Las Vegas Valley shear zone (fig. 3), Burchfiel et al. (1983) argued that a large, recumbent, east-vergent anticline-syncline pair in the northwestern Spring

Mountains (figs. 1 and 3) involving Precambrian Johnnie Formation and Stirling Quartzite correlated with the east-trending Pintwater anticline at the southern end of the Spotted Range. In Burchfiel's (1965, fig. 4, p. 184) interpretation of the structure of the Spring Mountains, he showed that the recumbent fold pair cores a large anticlinorium (with a structural relief in excess of 6 km) within the Wheeler Pass allochthon. Because these structural relations are consistent with those proposed herein for the Pintwater anticlinorium, we support Burchfiel's (1983) correlation and suggest that the magnitude and style of east-vergent structural thickening beneath the anticlinorium in the Spring Mountains Burchfiel, 1974, 1983) are also required farther northeast along strike in our reconstruction (fig. 7b).

Contrasts with previous thrust correlations in the NTS

Recently, much attention has been given to regional correlations of Mesozoic thrusts for the purpose of palinspastic reconstructions of the highly extended southern Great Basin (Levy and Christie-Blick, 1989; Wernicke et al., 1988a, 1988b). Wernicke et al. (1988b, fig. 5, p. 1743) and Snow (1992, fig. 12, p. 92) inferred that five structural levels bounded by major thrust faults identified in the Death Valley region project through the NTS region. Although the Wernicke et al. (1988b) estimates of Neogene extension may not be compromised by incorrect details in these particular thrust correlations, we suggest that some of the correlations of Wernicke et al. (1988b) and Snow (1992) are inconsistent with details of the geology in the NTS region.

Our studies indicate that only three principal structural levels exist in the NTS region (figs. 3 and 6): 1) strata structurally above the east-vergent Belted Range thrust system (including klippen of the Spotted Range thrust), 2) strata structurally below both the east-vergent Belted Range thrust and the west-vergent CP thrust system, and 3) strata above both the west-vergent CP thrust and the east-vergent Gass Peak thrust.

We agree in general with the Belted Range thrust-Meiklejohn Peak thrust correlation and the Mine Mountain thrust-Panama thrust correlation proposed by Wernicke et al. (1988a, 1988b), although as noted earlier, other possibilities exist for correlations of the Belted Range thrust (also inferred by Snow, 1992). However, no geologic evidence exists for projection of the east-vergent Schwaub Peak thrust system (fig. 3) through the southern part of the CP Hills and across the Halfpint Range to the northeast, as proposed by Wernicke et al. (1988a, 1988b). Snow (1992) subsequently correlated the Schwab Peak thrust with the thrust in the Specter Range (fig. 3) and also with thrust klippen in the Spotted Range. The Schwaub Peak-Specter Range thrust correlation is plausible; however, as previously discussed, stratigraphic and structural relations indicate that the thrust in the Specter Range has no counterpart in the Spotted Range (Burchfiel, 1965).

The eastward projection of the Clery thrust system (fig. 3) as shown by Wernicke et al. (1988a, 1988b) erroneously transects nearly continuous stratigraphy along the west limb of the Spotted Range syncline at Frenchman Flat. Snow (1992) correlated the Clery thrust with a recumbent fold pair in the northwestern part of the Spring Mountains (fig. 3) and also with the Pintwater thrust of Guth (1990). This contrasts sharply with Burchfiel's (1983) and our correlation of the recumbent fold pair with the Pintwater anticline of Longwell (1945) (previouly discussed). Furthermore, a possible concealed, north-trending strike-slip fault east of Bare Mountain (Schweickert, 1989), as well as an alternative option of a Tertiary origin for the Specter Range thrust (Burchfiel, 1965), as previouly discussed, may complicate the correlations of the Clery thrust with structures to the east by Wernicke et al. (1988a, 1988b), and similarly, correlations of the Schwab Peak and Clery thrusts as depicted by Snow (1992). For these reasons we are presently uncertain of correlations of the Clery and Schwaub Peak thrusts to the east (fig. 3).

TIMING OF STRUCTURAL EVENTS

Evidence for relative timing

Several lines of indirect evidence indicate that the west-vergent CP thrust and the regional fold pair to the east postdate emplacement of the east-vergent Belted Range/Spotted Range thrust plate.

1) Two generations of small-scale folds (both west- and east- vergent) have been recognized in rocks beneath the CP thrust in the CP Hills (Caskey, 1991). Where determinable, west-vergent folds related to the CP thrust overprint earlier east-vergent folds. In contrast, in the upper plate of the CP thrust, only one generation of (west-vergent) folds has been recognized which suggests that prior to movement on the CP thrust, these stratigraphically deeper rocks may

have been removed from the effects of earlier east-vergent deformation in the CP Hills. These relations suggest that deformation related to the west-vergent CP thrust occurred after emplacement of the Belted Range/Spotted Range thrust plate (see fig. 6a and b).

2) Klippen of the Spotted Range thrust are only preserved in a narrow belt along the hinge zone of the Spotted Range syncline. This relation implies that emplacement of the thrust predated the formation of the Pintwater anticline/Spotted Range syncline fold pair. Nowhere is the thrust plate, which largely consists of resistant Bonanza King dolomite, preserved on the limbs of the syncline, suggesting it was removed during uplift related to subsequent folding.

There are presently no direct constraints on relative timing between folding related to the Pintwater anticline-Spotted Range syncline and the west-vergent CP thrust to the west. However, the parallelism of the CP thrust, the regional fold pair, and the Gass Peak thrust, as well as arguments discussed later, suggest that they were all genetically related.

Constraints on the absolute age of structural events

The timing of thrust faulting and folding in the NTS region is only widely bracketed between Early Permian (age of the youngest rocks involved in thrusting) and early Tertiary (the inferred age of sedimentary deposits that overlie the Spotted Range thrust (Tschanz and Pampeyan, 1970) and are not folded by the Spotted Range syncline). North of Yucca Flat, 93 Ma quartz monzonite of the Climax Stock (Marvin et al., 1970) intrudes complexly folded Ordovician strata (Houser and Poole, 1960) and places a tighter upper age limit on local deformation. Better age constraints on thrusting must be inferred from thrust correlations and age relations established elsewhere in the thrust belt.

In eastern California, Mesozoic thrusts of the Last Chance thrust system (Burchfiel et al., 1970; Dunne et al., 1978, 1983; Dunne, 1986; Corbett et al., 1988) have been shown to predate emplacement of the 167-185 Ma Hunter Mountain batholith (Dunne et al., 1978), and have been interpreted as being Late Triassic to Early Jurassic in age. Corbett et al. (1988) interpreted this thrust system as a manifestation of the Permo-Triassic Sonoma orogeny. More recently, Snow (1990) suggested that the Last Chance thrust system predates the 228$\pm$2 Ma White Top stock in the Cottonwood Mountains. If correlations of the Belted Range thrust to the Last Chance thrust system (as previously discussed) are correct, then the Belted Range thrust may be pre- latest Middle Triassic. Based on relative timing constraints (discussed above), the age of west-vergent deformation related to the CP thrust can be refined only as post-Belted Range thrust and pre- early late Cretaceous (age of the Climax stock).

The age of the Gass Peak/Wheeler Pass thrust system is poorly constrained. However, easternmost thrusts of the Sevier orogenic belt have deformed rocks as young as early Late Cretaceous in the Muddy Mountains (i.e. the Glendale/Muddy Mountain thrust system) (Fleck, 1970) and latest Early Cretaceous (~99Ma) in the Spring Mountains (i.e. the Keystone/Contact thrust system) (Fleck and Carr, 1990). Fleck (1970) contended that because the tectonic style is consistent throughout the Sevier orogenic belt, all thrusting represents a single, regional tectonic event. However, an earlier Mesozoic age for the Gass Peak/Wheeler Pass thrust system cannot be ruled out.

SUMMARY

The recognition of an important west-vergent thrust system in the NTS region has led to an improved understanding of the pre-Tertiary structural framework of the region. Despite large-magnitude Tertiary extension, regionally extensive volcanic cover, and probable strike-slip faults concealed beneath alluviated valleys, hinterland-vergent deformation related to the CP thrust can be traced along strike for at least 180 km in southwest Nevada and eastern California (see also discussions in Wernicke et al. (1988a, 1988b)). The along-strike sigmoidal "z" pattern of the zone of west-vergent deformation parallels regional curvilinear trends of major folds and the Gass Peak thrust to the east, as well as major structural and stratigraphic trends to the northwest (Albers, 1967).

Structural relations in the NTS region indicate at least two major episodes of Mesozoic deformation occurred. The first is represented by the east-vergent Belted Range/Spotted Range thrust system. The second episode of Mesozoic deformation is represented by major hinterland-vergent folds and thrusts related to the CP thrust system. Timing relations of the Pintwater anticline-Spotted Range syncline fold pair to the CP thrust to the west are uncertain, although we speculate that the CP thrust and the regional fold pair are genetically related (discussed below).

DISCUSSION

Implications for the development of hinterland-vergent structures

The structural geometry of the region between the west-vergent CP thrust and the east-vergent Gass Peak thrust (fig. 7b) bears a close resemblance to the large scale, wedge-like, bivergent geometry recognized elsewhere in the Cordilleran fold and thrust belt (Elison, 1987; Price, 1981). Snow and Wernicke (1989) also compared hinterland-vergent deformation in the Death Valley region to structures in the Cordilleran orogen near Calgary, Alberta (Price, 1981). They compared a west-vergent backfold in the Death Valley region to a west-facing monocline developed structurally above east-vergent, blind imbricate thrusts within the westward-thickening Eocambrian clastic wedge (Price, 1981, p. 429, fig. 2) . However, the reconstruction of the Cordilleran orogenic belt by Wernicke et al. (1988a, 1988b) and Snow and Wernicke (1989) showed only a simple backfold developed above an east-vergent thrust ramp with no direct or indirect evidence for imbricate thrusting or duplexing of the Eocambrian clastic wedge.

Elison (1987) suggested that the location of major thrust belts in north-central Nevada was strongly influenced by slopes or inclinations in the regional stratigraphic and structural framework. The west-vergent CP thrust lies above one of the thickest known sections of the Cordilleran miogeocline (Ekren, 1968; Stewart and Poole, 1972). Since maximum subsidence due to sediment loading would be expected in this region, a westward inclination in the layering of the miogeoclinal prism may have once existed. Tectonic loading from earlier thrusting to the west (e.g. the Last Chance thrust system) together with the development of substantial structural relief associated with the formation of the Pintwater anticlinorium to the east would have further promoted a westward slope in the miogeocline between these regions. In Price's (1981) structural section (fig. 2, p. 429) strata lying in the region between the Purcell anticlinorium to the west and the large anticlinorium associated with an inferred (blind) hinterland-dipping duplex structure (e.g. Boyer and Elliot, 1982) to the east exhibit a pronounced westward inclination and correspond to an area of intense west-vergent folds and thrusts. The anticlinorium associated with the duplex structure in Price's section, exhibits structural relief comparable to or greater than that of the (pre-Tertiary) Pintwater anticlinorium (fig. 7b). It is reasonable to infer that regional horizontal compressional stresses, applied to mechanically anisotropic west-dipping layering within the miogeocline, resulted in west-vergent folds and thrusts in both regions. We agree with Snow and Wernicke (1989) that close similarities exist between the structural development and geometry in these two regions of the Cordilleran fold and thrust belt. However, we believe that the magnitude and complexity of the west-vergent structures in the NTS and vicinity are greater than those described in the Death Valley region by Snow and Wernicke.

Implications for the amount of extension north of the Las Vegas Valley shear zone

Although a complete discussion of regional Tertiary extension is beyond the scope of this paper, we believe that an improved understanding of the Cordilleran fold and thrust belt in the NTS and surrounding regions may provide insight into the magnitude of Tertiary extension north of the Las Vegas Valley shear zone (LVVSZ) (Fig. 3). Guth (1981) estimated the amount of extension using a "tilted block model" (Morton and Black, 1975) which assumes that Paleozoic sedimentary layering in this region was horizontal at the close of Mesozoic thrusting (Armstrong, 1968). Our preliminary reconstruction (fig. 7b) as well as a comparison with Paleozoic rocks south of the LVVSZ in the northwest Spring Mountains (fig. 1) where Tertiary extension has been minimal (Burchfiel, 1965) indicates that this assumption is invalid and has led to estimates of extension that are too high.

Using the Morton and Black (1975) model, Guth (1981) suggested that between 44% and 58% extension occurred between the Sheep Range and the west side of the Desert Range and that extension increased progressively toward the west. Our preliminary reconstruction of the fold and thrust belt (fig. 7b) indicates that only about 27% extension occurred between the Gass Peak thrust and the Desert Range. We suggest that overall extension between the Gass Peak thrust and the Spotted Range may have been as little as 15% and, in contrast with Guth (1981), that extension decreased progressively within the Sheep Range detachment system toward the west.

As another approach to estimating the amount of regional extension, Guth (1981) compared the relative spacing of correlative Mesozoic structures north and south of the LVVSZ.

He noted that north of the LVVSZ the distance (measured perpendicular to strike) between the Gass Peak thrust and the mapped trace of the Pintwater anticline (fig. 3) was about 42 km. South of the LVVSZ the distance between the Wheeler Pass thrust and the anticline in the northwest Spring Mountains is only 25 km. Guth concluded that 80% extension was required between the Gass Peak thrust and the Pintwater anticline (although his measurements support only about 70% extension).

A consequence of our preliminary reconstruction is that the mapped trace of the Pintwater anticline (fig. 7a) and the crest of the pre-Tertiary Pintwater anticlinorium (fig. 7b) do not coincide. Instead, the crest of the Pintwater anticlinorium (fig 7b) lies approximately 26 km from the Gass Peak thrust, essentially identical to the distance between correlative structures south of the LVVSZ (discussed above). We feel that this coincidence supports our preliminary reconstruction of the Pintwater anticlinorium and suggests that only about 24% extension has occurred between the Gass Peak thrust and the mapped trace of the Pintwater anticline. Furthermore, Guth (1990) interpreted the Pintwater anticline as a ramp anticline developed above a simple thrust ramp (as previously discussed) which was reactivated by the Tertiary Dog Bone Lake (normal) fault. Based on this interpretation, restoration of the Pintwater anticline (hinge surface trace) (Guth, 1990, p. 246, fig. 7) is constrained to a location above this concealed and interpreted ramp. A restoration of the geometry shown by Guth (1990) would result in a maximum of only about 45% extension between the Pintwater anticline and the Gass Peak thrust.

We therefore believe that Guth's (1981) estimate of 80% extension across this same area is too large, possibly by a factor of three based on our reconstruction.

CONCLUSIONS

1. The CP thrust of Barnes and Poole (1968) actually comprises two separate, oppositely verging Mesozoic thrust systems; 1) the west-vergent (hinterland-vergent) CP thrust which is well exposed in the CP Hills and at Mine Mountain, and 2) the east-vergent Belted Range thrust located northwest of Yucca Flat.

2. The CP thrust represents part of an important west-vergent Mesozoic fold and thrust system traceable for over 180 km along strike in southwestern Nevada and eastern California. The zone of west-vergent deformation is difficult to trace north of the NTS but probably continues at least as far north as the Egan Range where major west-vergent folds have been previously mapped (Brokaw and Barosh, 1968).

3. Klippen of the Spotted Range thrust are probably erosional remnants of a once areally extensive east-vergent Belted Range thrust sheet whose emplacement preceded the west-vergent CP thrust and regional folds between the NTS and the Sheep Range.

4. Prior to Tertiary extension, the Pintwater anticline of Longwell (1945) may have been a great anticlinorium with as much as 7 km of structural relief. This interpretation is consistent with

structural interpretations of a correlative structure in the northwest part of the Spring Mountains (Burchfiel, 1965).

5. A region or zone of significant westward inclination within the Cordilleran miogeoclinal framework may have influenced the location and development of the belt of west-vergent folding and thrusting.

6. Previous estimates of Tertiary extension north of the Las Vegas Valley shear zone are too large. A preliminary reconstruction of the fold and thrust belt suggests about 27% extension between the Desert Range and the Gass Peak thrust compared to earlier estimates ranging from 44 to 80% in this area. Overall extension between the Spotted Range and the Las Vegas Range may have been as little as 15%, although much greater extension certainly occurred locally.

ACKNOWLEDGMENTS

This project was supported by the State of Nevada Nuclear Waste Projects Office. We thank S.P. Nitchman, P. Goldstrand, and K.P. Corbett for reviews of drafts. We also thank J.M. Bartley whose thorough review for *Tectonics* substantially improved the manuscript. Special thanks go out to the kind and helpful folks at the NTS, especially those at the USGS office and Chuck Rosenbury and associates at RAMATROL. Center for Neotectonic Studies contribution number 8.

REFERENCES CITED

Albers, J.P., 1967, Belt of sigmoidal bending and right-lateral faulting in the western Great Basin: Geological Society of America Bulletin, v. 78, p. 143-156.

Armstrong, R.L., 1968, Sevier orogenic belt in Nevada and Utah: Geological Society of America Bulletin: v. 79, p. 429-458.

Barnes, H., Houser, F.N., and Poole, F.G., 1963, Geology of the Oak Spring quadrangle, Nye County, Nevada: U.S. Geological Survey Quadrangle Map GQ-214.

Barnes, H., Christiansen, R.L., and Byers, F. M. Jr., 1965, Geologic map of the Jangle Ridge quadrangle, Nye County, Nevada: U.S. Geological Survey Quadrangle Map GQ-363.

Barnes, H., and Poole, F.G., 1968, Regional thrust-fault system in Nevada Test Site and vicinity: *in* Nevada Test Site, Eckel, E. G., ed., Geological Society of America Memoir 110, p. 233-238.

Barnes, H., Ekren, E.B., Rodgers, C. L., and Hedland, D. C., 1982, Geologic and tectonic maps of the Mercury quadrangle, Nye and Clark Counties, Nevada: U.S. Geological Survey Miscellaneous Investigations Map I-1197.

Boyer, S. E., and Elliott, D., 1982, Thrust systems: American Association of Petroleum Geologists, v. 66, p. 1196-1230.

Brokaw, A.L, and Barosh, P.J., 1968, Geologic map of the Riepetown Quadrangle, White Pine County, Nevada: U.S. Geological Survey Quadrangle Map GQ-758.

Burchfiel, B.C., 1965, Structural geology of the Specter Range quadrangle, Nevada, and its regional significance: Geological Society of America Bulletin, v. 76, p. 175-192.

Burchfiel, B.C., Fleck, R.J., Secor, D.T., Vincelette, R.R., and Davis, G.A., 1974, Geology of the Spring Mountains, Nevada: Geological Society of America Bulletin, v. 85, p. 1013-1022.

Burchfiel, B.C., Hamill, G.S., and Wilhelms, D.E. IV, 1983, Structural Geology of the Montgomery Mountains and the northern half of the Nopah and Resting Springs Ranges, Nevada and California: Geological Society of America Bulletin, v. 94, p. 1359-1376.

Burchfiel, B.C., Pelton, P.J., and Sutter, J., 1970, An early Mesozoic deformation belt in south-central Nevada - southeastern California: Geological Society of America Bulletin, v. 81, p. 211-215.

Byers, F.M. Jr., and Barnes, H., 1967, Geologic map of the Paiute Ridge quadrangle, Nye and Lincoln Counties, Nevada: U.S. Geological Survey Quadrangle Map GQ-577.

Carr, M.D., and Monsen, S.A., 1988, A field trip guide to the geology of Bare Mountain, *in* Weide, D. L., and Faber, M. L., eds., This extended land, geological journeys in the southern Great Basin: Geological Society of America Cordilleran Section Field Trip Guide, p. 50-57.

Carr, W.J., 1984, Regional structural setting of Yucca Mountain, southern Nevada, and late Cenozoic rates of tectonic activity in part of the southwestern Great Basin, Nevada and California: U.S. Geological Survey Open File Report 84-854, 109 p.

Caskey, S.J., and Schweickert, R.A., 1989, Mesozoic west-vergent thrust in the CP Hills, Nevada Test Site, Nye County, Nevada: Geological Society of America Abstracts with Programs, v. 21, no. 5, p. 64.

Caskey, S.J., 1991, Mesozoic and Cenozoic structural geology of the CP Hills, Nevada Test Site, Nye County, Nevada: M.S. thesis, University of Nevada, Reno, Reno, Nevada, 153 p.

Corbett, K.P., Wrucke, C.T., and Nelson, C.A., 1988, Structure and tectonic history of the Last Chance thrust system, Inyo Mountains and Last Chance Range, California, *in* Weide, D. L., and Faber, M. L., eds., This extended land, geological journeys in the southern Great Basin: Geological Society of America Cordilleran Section Field Trip GUide, p. 269-292.

Cornwall, H.R., 1972, Geology and mineral deposits of southern Nye County, Nevada: Nevada Bureau of Mines and Geology Bulletin 77, 49 p.

Cornwall, H.R., and Kleinhampl, F.J., 1961, Geologic map of the Bare Mountain quadrangle, Nevada: U.S. Geological Survey Quadrangle Map GQ-157.

Dunne, G.C., 1986, Mesozoic evolution of southern Inyo, Argus, and Slate Ranges; *in* Mesozoic and Cenozoic structural evolution of selected areas, east-central California: Cordilleran Section, Geological Society of America Guidebook and Volume, fieldtrips 2 and 14, p. 3-22.

Dunne, G.C., Gulliver, R.M., and Sylvester, A.G., 1978, Mesozoic evolution of rocks of the White, Inyo-Argus, and Slate Ranges, eastern California: *in* Mesozoic paleogeography of the western United States, Howell, D. G., and McDougall, K. A., eds., Pacific Section Society of Economic Paleontologists and Mineralogists, Pacific Coast Paleography Symposium 2, p. 189-208.

Dunne, G.C., Moore, S.C., Gulliver, R.M., and Fowler, J., 1983, East Sierra thrust system: Geological Society of America Abstrats with Programs, v. 15, p. 322.

Ekren, E.B., 1968, Geologic setting of Nevada Test Site and Nellis Air Force Range: *in* Nevada Test Site, Eckel, E. G., ed., Geological Society of America Memoir 110, p. 11-20.

Ekren, E.B., Rodgers, C.L., Anderson, R.E., and Orkild, P.P., 1968, Age of Basin and Range faults in Nevada Test Site and Nellis Air Force Range, Nevada: *in* Nevada Test Site, Eckel, E.G., ed., Geological Society of America Memoir 110, p. 247-250.

Ekren, E.B., Orkild, P.P., Sargent, K.A., and Dixon, G.L., 1977, Geologic map of Tertiary rocks, Lincoln County, Nevada: U.S. Geological Survey Miscellaneous Investigations Map I-1041.

Elison, M.W., 1987, Structural geology and tectonic implications of the East Range, Nevada [Ph. D. thesis]: Evanston, Illinois, Northwestern University, 308 p.

Fleck, R.J., 1970, Tectonic style, magnitude and age of of deformation in the Sevier orogenic belt in southern Nevada and eastern California: Geological Society of America Bulletin, v. 81, p. 1705-1720.

Fleck, R.J., and Carr, M.D., 1990, The age of the Keystone thrust: laser fusion 40Ar/39Ar dating of foreland basin deposits, southern Spring Mountains, Nevada: Tectonics, v. 9, no. 3, p. 467-476.

Gibbons, A.B., Hinrichs, E.N., Hansen, W.R., and Lemke, R.W., 1963, Geology of the Ranier Mesa quadrangle, Nye County, Nevada: U.S. Geological Survey Quadrangle Map GQ-215.

Guth, P.L., 1981, Tertiary extension north of the Las Vegas Valley shear zone, Sheep and Desert Ranges, Clark County, Nevada: Geological Society of America Bulletin, v. 92, p. 763-771.

Guth, P.L., 1990, Superimposed Mesozoic and Cenozoic deformation, northwestern Clark County, Nevada: *in* Wernicke, B., ed., Basin and Range extensional tectonics near the latitude of Las Vegas, Nevada: Geological Society of America Memoir 176, p. 237-249.

Guth, P.L., Schmidt, D.L., Deibert, J., and Yount, J.C., 1988, Tertiarty extensional basins of northwestern Clark County, Nevada: *in* Weide, D.L., and Faber, M.L., eds., This extended land, geological journeys in the souther Great Basin: Geological Society of America Cordilleran Section Field Trip Guide, p. 239-253.

Hamilton, W., and Myers, W.B., 1966, Cenozoic tectonics of the western United States: Reviews of Geophysics, v. 4, p. 509-549.

Hinrichs, E.N., and McKay, E.J., 1965, Geolgic map of the Plutonium Valley quadrangle, Nye County, Nevada: U.S. Geological Survey Quadrangle Map GQ-384.

Hinrichs, E.N., 1968, Geologic structure of Yucca Flat area: Nevada: *in* Nevada Test Site, Eckel, E.G., ed., Geological Society of America Memoir 110, p. 239-246.

Houser, F.N., and Poole, F.G., 1960, Preliminary geologic map of the Climax Stock and vicinity, Nye County, Nevada: U.S. Geological Survey Miscellaneous Investigations Map I-328.

Jamison, W.R., Geometric analysis of fold development in overthrust terranes: Journal of Structural Geology, v. 9, no. 2, p. 207-219.

Jayko, A.S., 1990, Shallow crustal deformation in the Pahranagat 1^{o} quadrangle, southern Nevada: *in* Wernicke, B., ed., Extensional tectonics at the latitude of Las Vegas: Geological Society of America Memoir 176, p. 213-236.

Johnson, M.S., and Hibbard, D.E., 1957, Geology of the Atomic Energy Commission Nevada Proving Grounds area, Nevada: U.S. Geological Survey Bulletin 1021-K, p. 333-383.

Levy, M., and Christie-Blick, N., 1989, Pre-Mesozoic palinspastic reconstructions of the eastern Great Basin (western United States): Science, v. 245, p. 1454-1462.

Longwell, C.R., 1945, Low-angle normal faults in the Basin-and-Range Province: Transactions, American Geophysical Union, v. 26, part I., p. 107-118.

Longwell, C.R., 1960, Possible explanation of diverse structural patterns in southern Nevada: American Journal of Science, Bradley Volume, v. 258-A, p. 192-203.

Longwell, C.R., Pampeyan, E.H., Bower, B., and Roberts, R.J., 1965, Geology and mineral deposits of Clark County, Nevada: Nevada Bureau of Mines and Geology, Bulletin 62, 218 p.

Marvin, R.F., Byers, F.M. Jr., Mehnert, H.H., Orkild, P.P., and Stern, T.W., 1970, Radiometric ages and stratigraphic sequence of volcanic and plutonic rocks, southern Nye and western Lincoln Counties, Nevada: Geological Society of America Bulletin, v. 81, p. 2657-2676.

McKay, E.J., and Williams, W.P., 1964, Geology of the Jackass Flats quadrangle, Nye County, Nevada: U.S. Geological Survey Quadrangle Map GQ-368.

McKeown, F.A., Healey, D.L., and Miller, C.H., 1976, Geologic map of the Yucca Lake quadrangle, Nye County, Nevada: U.S. Geological Survey Quadrangle Map GQ- 1327.

Monsen, S.A., Carr, M.D., Reheis, M.C., and Orkild, P.P., 1990, Geologic map of Bare Mountain, Nye County, Nevada: U.S. Geological Survey Open File Report, OFR 90-25, 17 p.

Morton, W.H., and Black, R., 1975, Crustal attenuation in Afar, in Pilger, A., and Rosler, A., eds., Afar depression of Ethiopia, Inter-Union Commission on geodynamics: International symposium on the Afar region and rlated rift prblems, E. Scheizer-bart'sche Verlagsbuchhandlung, Stuttgart, Germany, Proceedings, Scientific Report No. 14, p. 55-65.

Orkild, P.P., 1968, Geologic map of the Mine Mountain quadrangle, Nye County, Nevada: U.S. Geological Survey Quadrangle Map GQ-746.

Orkild, P.P., and O'Connor, J.T., 1970, Geologic map of the Topopah Spring quadrangle, Nye County, Nevada: U.S. Geological Survey Quadrangle Map GQ-849.

Poole, F.G., 1965, Geologic map of the Frenchman Flat quadrangle, Nye, Lincoln, and Clark Counties, Nevada: U.S. Geological Survey Quadrangle Map GQ-456.

Poole, F.G., Houser, F.N., and Orkild, P.P., 1961, Eleana Formation of Nevada Test Site and vicinity, Nye County, Nevada: U.S. Geological Survey Prof. Paper 424-D, p. D104-D111.

Price, R.A., 1981, The Cordilleran foreland thrust and fold belt in the southern Canadian Rocky Mountains: *in* McClay, K. R., and Price, N. J., eds., Thrust and nappe tectonics: London, England, The Geological Society of London, p. 427-448.

Reynolds, M.W., 1969, Stratigraphy and structural geology of the Titus and Titanothere Canyons area, Death Valley, California [Ph.D. thesis]: Berkeley, California, University of California, 310 p.

Rodgers, C.L., and Noble, D.C., 1969, Geologic map of the Oak Spring Butte quadrangle, Nye County, Nevada: U.S. Geological Survey Quadrangle Map GQ-822.

Sargent, K.A., McKay, E.J., and Burchfiel, B.C., 1970, Geologic map of the Striped Hills quadrangle, Nye County, Nevada: U.S. Geological Survey Quadrangle Map GQ-882.

Sargent, K.A., and Stewart, J.H., 1971, Geologic map of the Specter Range quadrangle, Nye County, Nevada: U.S. Geological Survey Map GQ-884.

Schweickert, R.A., 1989, Evidence for a concealed dextral strike-slip fault beneath Crater Flat, Nevada: Geological Society of America Abstracts with Programs, v. 21, no. 6, p. A90.

Schweickert, R.A., and Caskey, S.J., 1990, Pre-Middle Miocene extensional history of the Nevada Test Site (NTS) region, southern Nevada: Geological Society of America Abstracts with Programs, v. 22, no. 3, p. 81.

Snow, J.K., 1990, A Permian age for the Last Chance thrust, CA and NV ?,: Geological Society of America Abstracts with Programs, v. 22, no. 3, p. 85.

Snow. J.K., 1992, Large-magnitude Permian shortening and continental-margin tectonics in the southern Cordillera: Geological Society of America Bulletin, v. 104, p. 80-105.

Snow, J.K., and Wernicke, B., 1989, Uniqueness of geological correlations: an example from the Death Valley extended terrain: Geological Society of America Bulletin, v. 101, p. 1351-1362.

Stewart, J.H., 1970, Upper Precambrian and lower Cambrian strata in the southern Great Basin, California and Nevada: U.S. Geological Survey Prof. Paper 620, 206 p.

Stewart, J.H., 1988, Tectonics of the Walker Lane belt, western Great Basin: Mesozoic and Cenozoic deformation in a zone of shear, *in* Ernst, W. G., ed., Metamorphism and crustal evolution of the western United States: Englewood Cliffs, New Jersey, Prentice-Hall, p. 683-713.

Stewart, J.H., Albers, J.P., and Poole, F.G., 1968, Summary of evidence for right-lateral displacement in the western Great Basin: Geological Society of America Bulletin, v. 79, p.1407-1414.

Stewart, J.H., Poole, F.G., 1974, Lower Paleozoic and uppermost Precambrian Cordilleran miogeocline, Great Basin, western United States: in Tectonics and Sedimentation, Dickinson, W.R., ed., SEPM Sp. Pub. No. 22, p. 28-57.

Stewart, J.H., and Carlson, J.E., 1978, Geologic Map of Nevada: prepared by the US Geological Survey in cooperation with the Nevada Bureau of Mines and Geology.

Suppe, J., 1983, Geometry and kinematics of fault-bend folding: American Journal of Science, vol. 283, p. 684-721.

Tschanz, C.M., and Pampeyan, E.H., 1970, Geology and mineral deposits of Lincoln County, Nevada: Nevada Bureau of Mines and Geology Bulletin 73, 188 p.

Wernicke, B., Spencer, J.E., Burchfiel, B.C., and Guth, P.L., 1982, Magnitude of crustal extension in the southern Great Basin: Geology, v. 10, p. 499-502.

Wernicke, B., Guth, P.L., and Axen, G.J., 1984, Tertiary extensional tectonics in the Sevier thrust belt of southern Nevada: *in* Lintz, J. P., ed., Western geological excursioins, Volume 4: Reno, Nevada, Mackay School of Mines, p. 473-510.

Wernicke, B., Snow, J.K., and Walker, J.D., 1988a, Correlation of Early Mesozoic thrusts in the southern Great Basin and their possible indication of 250-300km of Neogene crustal extension: *in* Weide, D. L., and Faber, M. L., eds., This extended land, geological journeys in the southern Great Basin: Geological Society of America Cordilleran Section Field Trip Guide, p. 255-269.

Wernicke, B., Axen, G.J., and Snow, J.K., 1988b, Basin and Range extensional tectonics at the latitude of Las Vegas, Nevada: Geological Society of America Bulletin, v. 100, p. 1738-1757.

Figure Captions

Figure 1 - Location map of the study area showing the distribution of Paleozoic, Tertiary, and Quaternary rocks. Small bodies of Mesozoic intrusive rocks are omitted for clarity (modified after Stewart and Carlson, 1978). Abbreviations: BM - Banded Mountain; CF - Crater Flat; CH - Calico Hills; CPH - CP Hills; CR - Chert Ridge; ER - Eleana Range; GR - Groom Range; MM - Mine Mountain; OSB - Oak Spring Butte; PGR - Pahranagat Range; PR - Papoose Range; PTR - Paiute Ridge; SH - Striped Hills; SR - Specter Range. Boxed areas with numbers in the lower right correspond to geologic maps (referred to in text) important to structural correlations between the Spotted and Belted Ranges: 1 - Rainier Mesa quadrangle (Gibbons et al., 1963); 2 - Jangle Ridge quadrangle (Barnes et al., 1965); 3 - Paiute Ridge quadrangle (Byers and Barnes, 1967); 4 - Plutonium Valley quadrangle (Hinrichs and McKay, 1965).

Figure 2 - Generalized stratigraphic column for upper Proterozoic and Paleozoic rocks in the Nevada Test Site region (modified after Ekren, 1968).

Figure 3 - Major Mesozoic structural features of the NTS region involving Paleozoic rocks (fig. 1). Patterns correspond to different allochthons discussed text. Abbreviations: BF - Butte fault; CS - Corksrew syncline; CT - Clery thrust; LVVSZ - Las Vegas Valley shear zone; MPT - Meiklejohn Peak thrust; MT - Montgomery thrust; PT - Pintwater thrust; PWA - Pintwater anticline; SHA - Striped Hills anticline; SPT - Schwaub Peak thrust; SRS - Spotted Range syncline; SRT - Spotted Range thrust; SVSFZ - Stewart Valley-Stateline fault zone; TCA - Titus Canyon anticline.

Figure 4 - Generalized geologic map of the CP Hills and Mine Mountain area (modified after Caskey (1991), McKeown et al. (1976), and Orkild (1968)).

Figure 5 - Simplified structural section SW-NE through the southern part of the CP Hills (see figure 4 for location) with high-angle Tertiary normal faults restored. Upper boundaries of high-angle fault blocks represent modern topography. Label on the various stratigraphic units correspond to those units shown in figure 4. Patterns do no correspond to those in figure 4.

Figure 6 - Schematic cartoon structural section which illustrates our interpretations of the relationships between the Belted Range/Spotted Range thrust, the CP thrust, the Gass Peak thrust, and the regional fold pair. a) Possible Early Mesozoic structure of the NTS region. b) Possible Late Mesozoic structural geometry of the NTS region. Patterns represent different Mesozoic structural levels; stippled - CP/Gass Peak allochthon; stippled with lines - Belted Range/Spotted Range allochthon; dark shading - CP/Belted Range parautochthon; light shading - Gass Peak parautochthon. Different thrust faults are detailed with different teeth patterns for clarity.

Figure 7 - A) Interpretive geologic cross section NW-SE (refer to fig. 3 for location). Patterns of stratigraphic units correspond to those at the lower right in figure. Structural interpretations east of the Spotted Range are based primarily on published data of Longwell et al. (1965) and interpretations of Guth (1981, 1990) and Guth et al. (1988). Structural interpretations of the Spotted Range and areas to the west are based on numerous published maps cited in text. Some structures have been projected into the section for emphasis. B) Preliminary pre-Tertiary reconstruction (section NW-SE) of the Mesozoic fold and thrust belt at the latitude of the NTS. Modern topography is shown offset along Tertiary normal faults (shown dashed). Tertiary structure shown concealed beneath Tertiary volcanic rocks between the "bend in section" and the Spotted Range (fig. 7A) is highly speculative, and therefore a reconstruction of this structure is omitted for clarity. Other detatils of the structure are discussed in text.

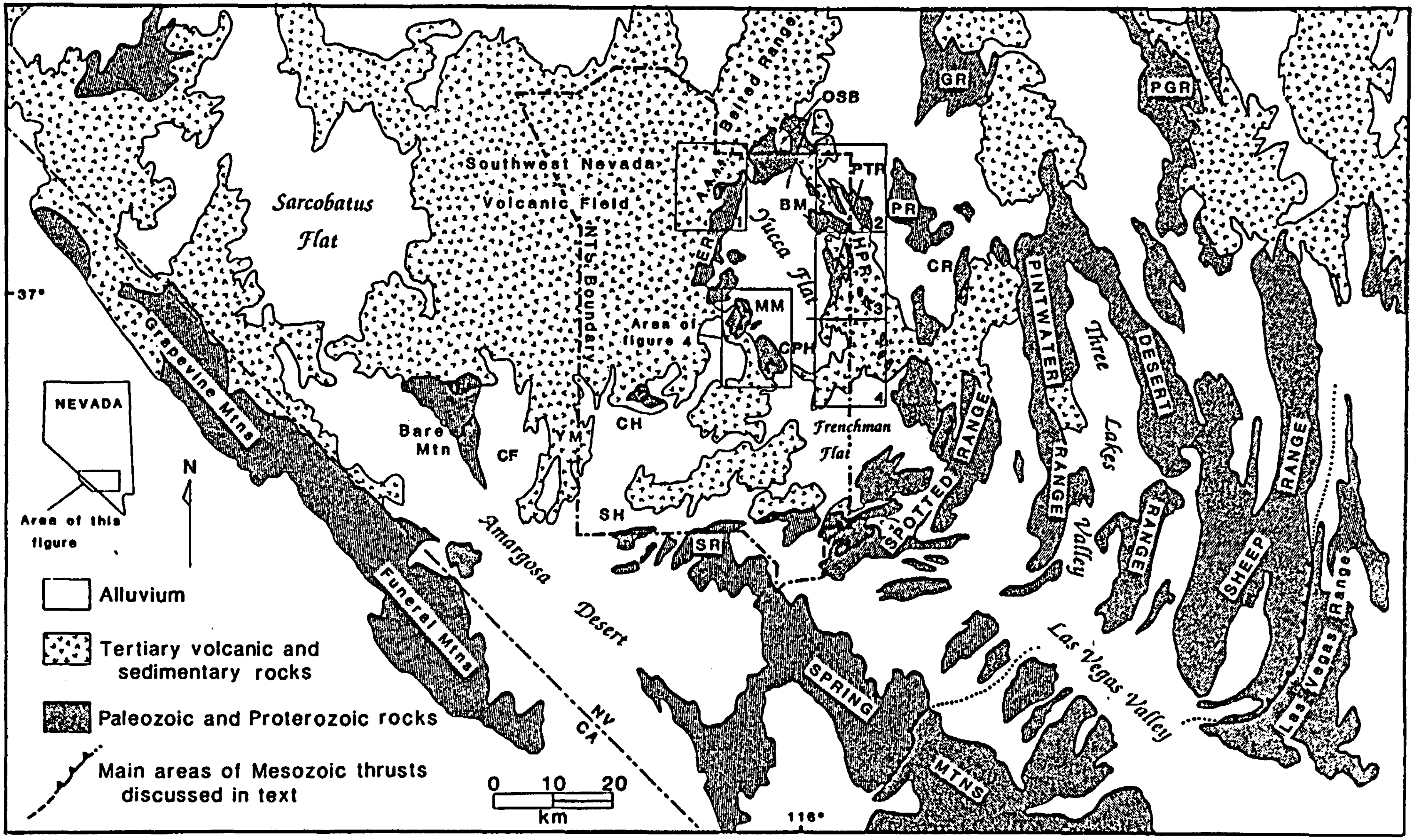
Southwest Nevada
Volcanic Field
Sarcobatus
Flat
Belted Range
OSB
GR
PGR
PTR
PR
BM
Yucca Flat
HPR
CR
MM
Area of
figure 4
CPH
NTS Boundary
PINTWATER
RANGE
Three
Lakes
Valley
DESERT
RANGE
SHEEP
RANGE
Las Vegas Range
Las Vegas Valley
Grapevine Mtns
Bare
Mtn
CF
YM
CH
Frenchman
Flat
SPOTTED
RANGE
SH
SR
Amargosa
Desert
Funeral Mtns
SPRING
MTNS
NV
CA
37°
116°
NEVADA
Area of this
figure
N
Alluvium
Tertiary volcanic and
sedimentary rocks
Paleozoic and Proterozoic rocks
Main areas of Mesozoic thrusts
discussed in text
0 10 20
km

fig. 1

113

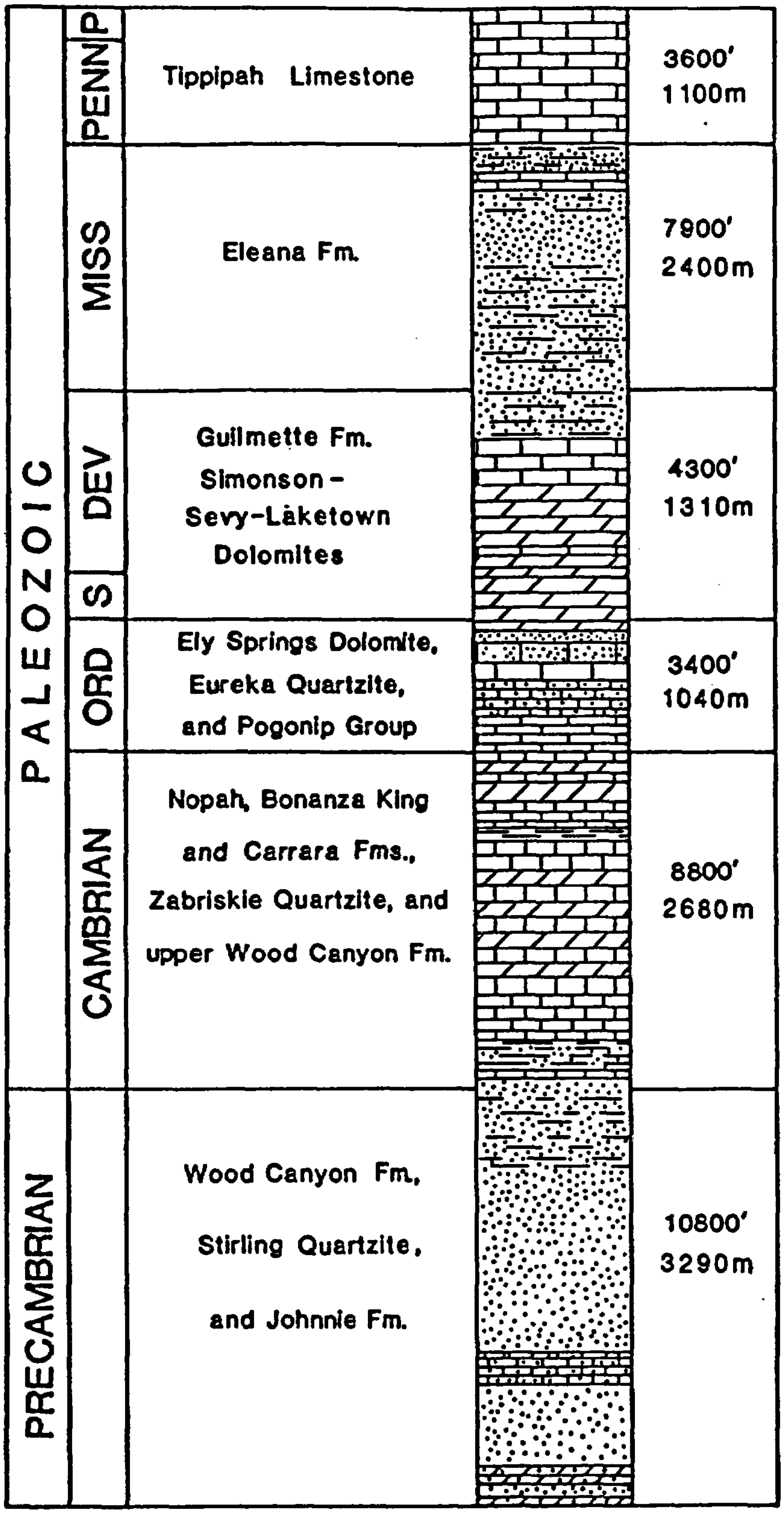
PALEOZOIC
PRECAMBRIAN
PENN
P
MISS
DEV
S
ORD
CAMBRIAN
Tippipah Limestone
3600'
1100m
Eleana Fm.
7900'
2400m
Guilmette Fm.
Simonson -
Sevy-Làketown
Dolomites
4300'
1310m
Ely Springs Dolomite,
Eureka Quartzite,
and Pogonip Group
3400'
1040m
Nopah, Bonanza King
and Carrara Fms.,
Zabriskie Quartzite, and
upper Wood Canyon Fm.
8800'
2680m
Wood Canyon Fm.,
Stirling Quartzite,
and Johnnie Fm.
10800'
3290m

Fig. 2

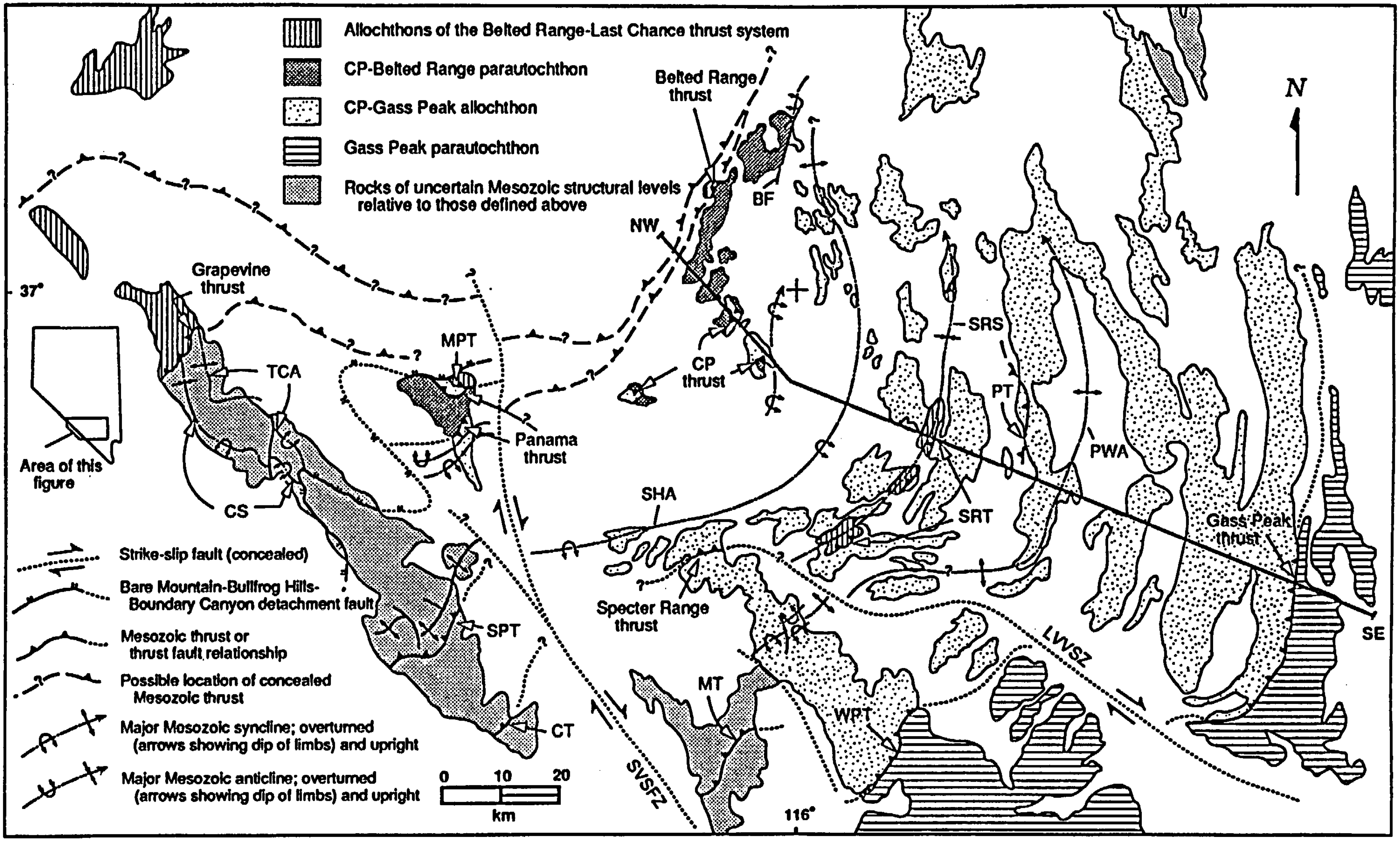
Allochthons of the Belted Range-Last Chance thrust system
CP-Belted Range parautochthon
CP-Gass Peak allochthon
Gass Peak parautochthon
Rocks of uncertain Mesozoic structural levels relative to those defined above
Belted Range thrust
BF
NW
37°
Grapevine thrust
TCA
MPT
CP thrust
Panama thrust
SRS
PT
PWA
SRT
SHA
Gass Peak thrust
SE
N
Area of this figure
CS
Strike-slip fault (concealed)
Bare Mountain-Bullfrog Hills-Boundary Canyon detachment fault
Mesozoic thrust or thrust fault relationship
Possible location of concealed Mesozoic thrust
Major Mesozoic syncline; overturned (arrows showing dip of limbs) and upright
Major Mesozoic anticline; overturned (arrows showing dip of limbs) and upright
SPT
CT
Specter Range thrust
LVVSZ
MT
WPT
SVSFZ
116°
0 10 20
km

fig. 3

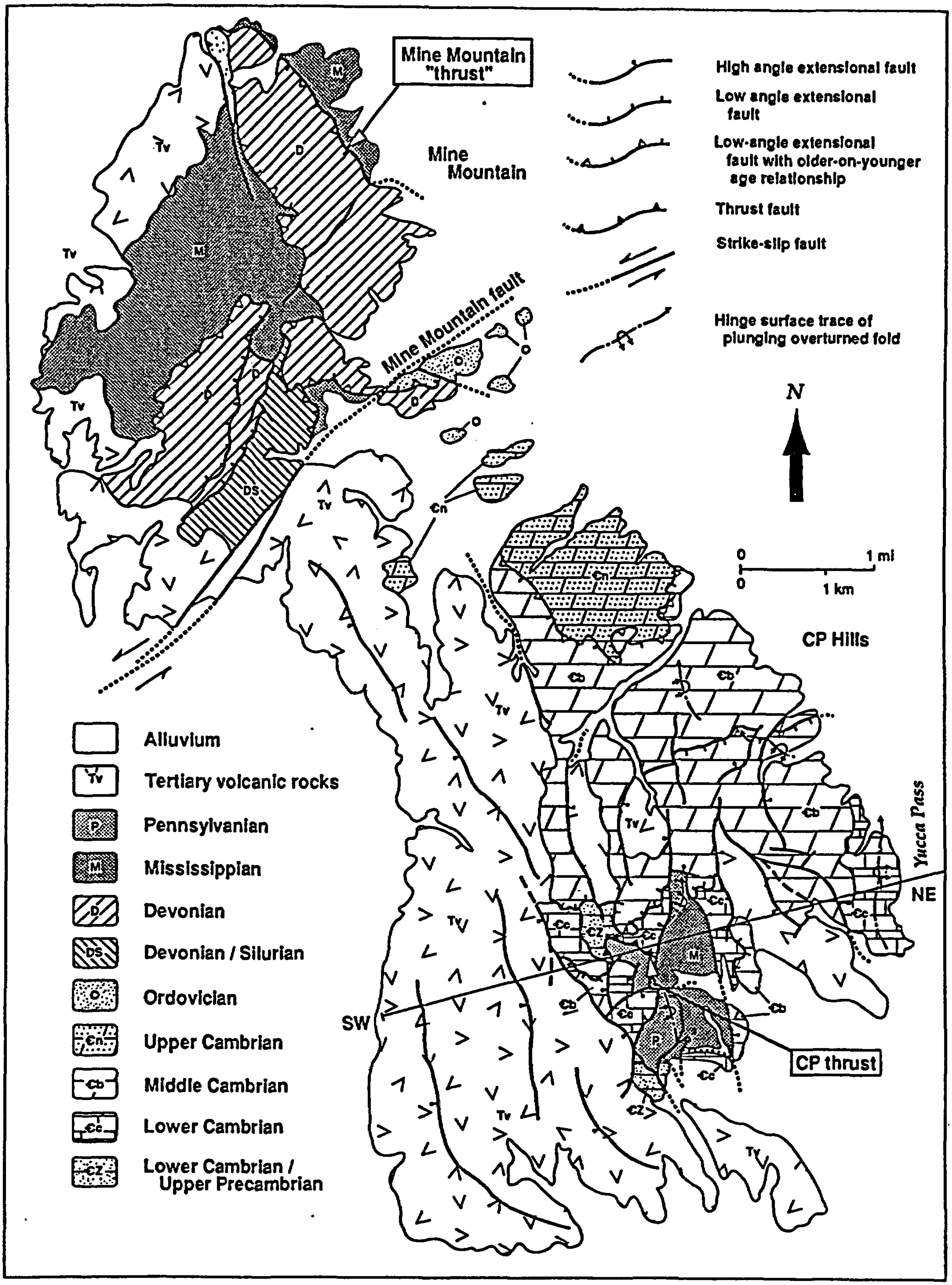

Mine Mountain "thrust"
Mine Mountain
Mine Mountain fault
High angle extensional fault
Low angle extensional fault
Low-angle extensional fault with older-on-younger age relationship
Thrust fault
Strike-slip fault
Hinge surface trace of plunging overturned fold
N
0 1 mi
0 1 km
CP Hills
Yucca Pass
NE
SW
CP thrust
Alluvium
Tertiary volcanic rocks
Pennsylvanian
Mississippian
Devonian
Devonian / Silurian
Ordovician
Upper Cambrian
Middle Cambrian
Lower Cambrian
Lower Cambrian / Upper Precambrian

fig. 4

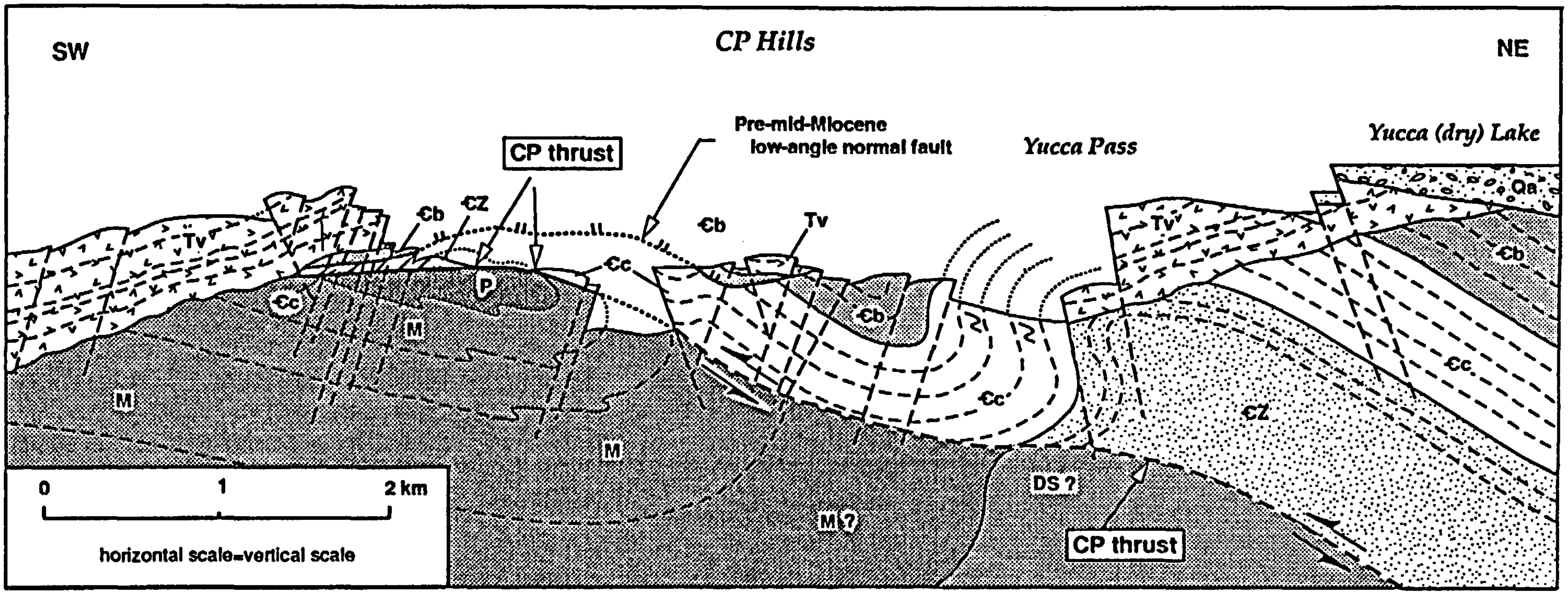
SW
CP Hills
NE
Pre-mid-Miocene
low-angle normal fault
Yucca Pass
Yucca (dry) Lake
CP thrust
Tv
€b
€Z
€c
P
M
Qa
DS ?
M ?
CP thrust
0
1
2 km
horizontal scale=vertical scale

fig. 5

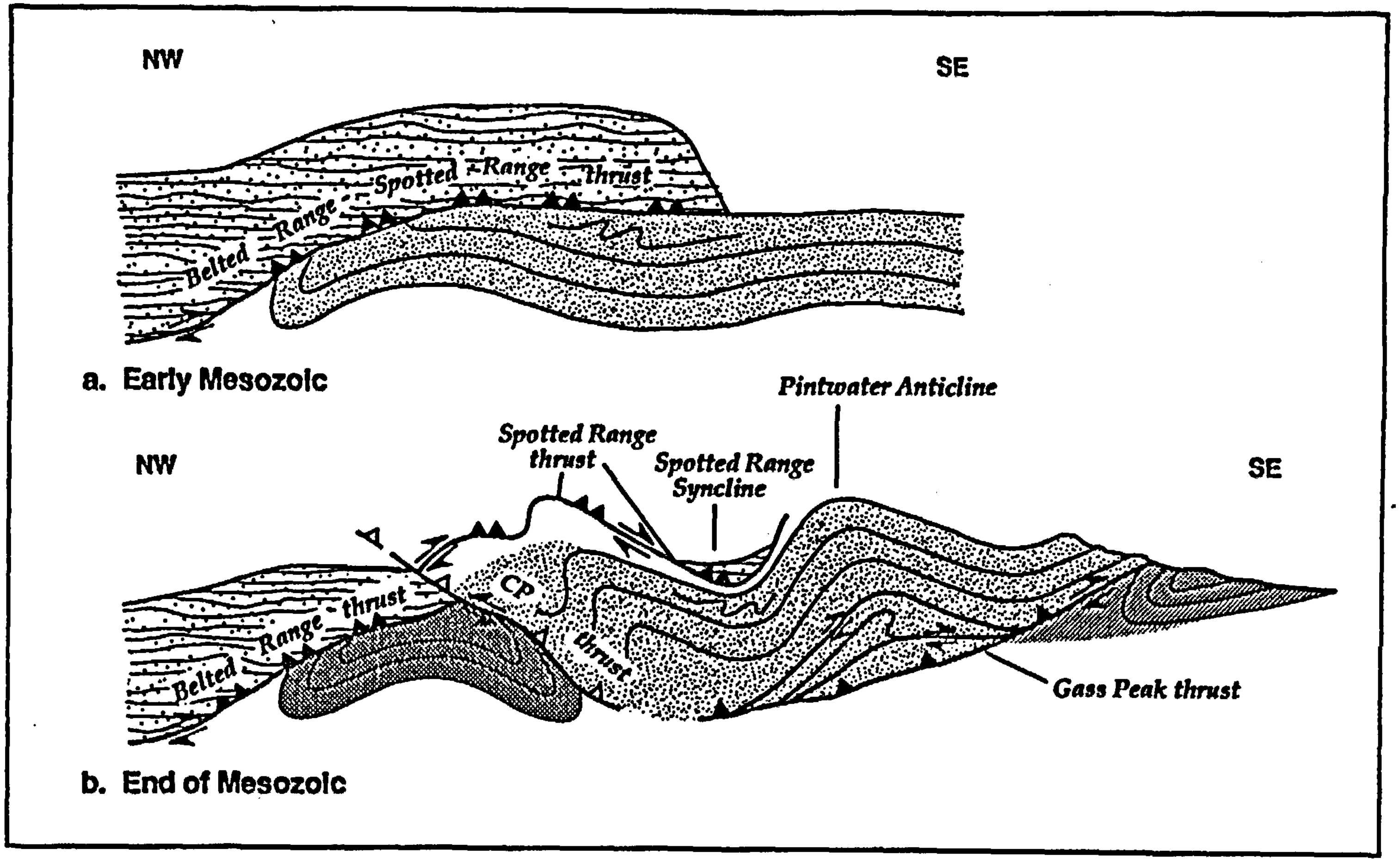

NW
SE
Belted Range Spotted Range thrust
a. Early Mesozoic
Pintwater Anticline
Spotted Range thrust
Spotted Range Syncline
NW
SE
A
CP
Belted Range thrust
thrust
Gass Peak thrust
b. End of Mesozoic

Fig. 6

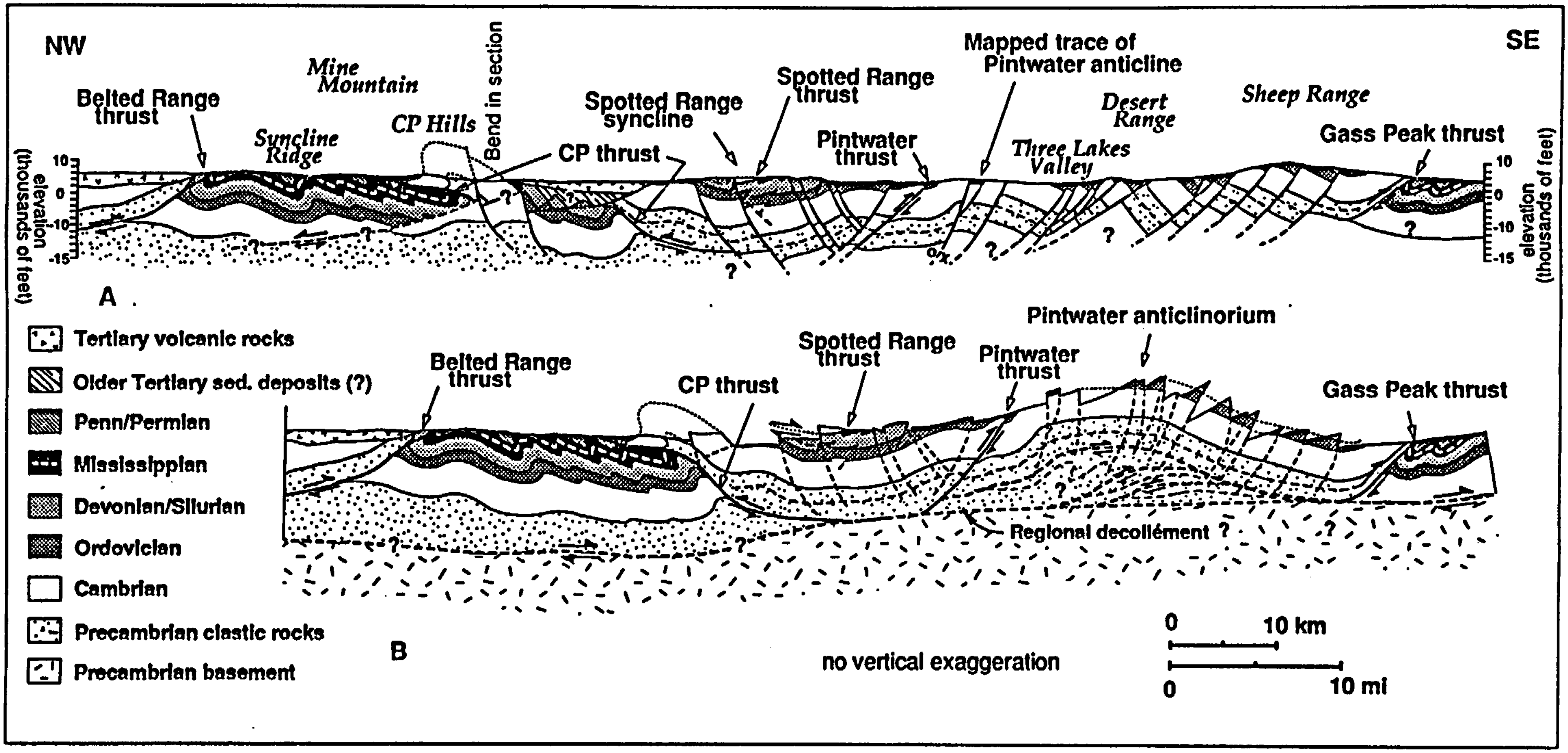

NW
SE
Belted Range thrust
Mine Mountain
Syncline Ridge
CP Hills
Bend in section
CP thrust
Spotted Range syncline
Spotted Range thrust
Pintwater thrust
Mapped trace of Pintwater anticline
Desert Range
Three Lakes Valley
Sheep Range
Gass Peak thrust
elevation (thousands of feet)
10
0
-10
-15
A
Tertiary volcanic rocks
Older Tertiary sed. deposits (?)
Penn/Permian
Mississippian
Devonian/Silurian
Ordovician
Cambrian
Precambrian clastic rocks
Precambrian basement
Pintwater anticlinorium
Regional decollément
B
no vertical exaggeration
0
10 km
10 mi

fig 7.

:astrophic, but within the Maastrichtian trends
iuct in diversity are evident. Dinosaurs
ary to the end of the Mesozoic in India and
low ersity. There is no convincing evidence
ated dinosaurs of post-Mesozoic age. At
ly in western North America can the
raphy of dinosaur extinction be documented -
statistical base of articulated specimens.

illiamson, T. E. № 22995

NOSAURS?

SON, T. E. and LUCAS, S. G., New Mexico Museum of Natural History,
Mountain Road N. W., Albuquerque, NM 87104

aleocene dinosaurs" is an oxymoron because the youngest dinosaurs n index fossils of the Late Cretaceous. Despite this, dinosaurs of ocene age have been reported from North America, South America and onstrate that a dinosaur occurrence is of Paleocene age, two criteria (1) it must be demonstrated that the dinosaur fossils are not reworked retaceous strata; and (2) it must be established that the dinosaur ectly associated or overlie autochtonous fossils of other organisms that ocene age. Extant reports of "Paleocene dinosaurs" fail to meet one or criteria, and we conclude that there are no known dinosaur fossils of e Paleocene age. Thus, "Paleocene dinosaurs" from Montana arguably fossils from Cretaceous strata, and those reported from New Mexico ly associated with Paleocene index fossils. South American and Asian inosaurs" also lack such direct association. Even if one or a few dinosaur ocene age are documented, this does not necessarily refute catastrophic of dinosaur extinction. Survival of a few individuals or populations of is possible on a global scale in any terminal Cretaceous catastrophe short rvasive that it eliminated all life on Earth.

Sullivan, Robert M. № 20061

MASS EXTINCTION: REALITY OR MYTH?

IVAN Robert M., Department of Herpetology,
an Natural History Museum, P.O. Box 1390,
an , CA 92112

sauria (inclusive of Aves [birds]) is a etic group that had its origins in the early and persists to present day. The "Dinosauria" ve of Aves) is paraphyletic, and this on has led to erroneous conclusions regarding nction of this group. Paraphyletic groups are ong modern systematists to be unnatural (i.e. not reflect phylogenetic relationships), therefore oups have no basis in reality.
ver, the supposed mass extinction of "dinosaurs" nd of the Cretaceous Period has been based solely isappearance of less than two dozen non-avian species from the latest Maastrichtian deposits of North America. Yet these "dinosaurs" account for n 7% of the 335+ valid species of non-avian s known from the Mesozoic.
strophic scenarios centering on the mass on of "dinosaurs" have, nevertheless, flourished it years. Acceptance of a Late Cretaceous mass on "event" is an erroneous assessment based on false assumptions of biostratigraphy, coupled tle understanding of phylogenetic methods.

SESSION 72, 8:00 a.m.
TUESDAY, OCTOBER 22, 1991

T 15. SCIENCE APPLICATIONS INTERNATIONAL CORPORATION (SAIC): GEOLOGY, HYDROGEOLOGY AND TECTONICS OF SOUTHERN NEVADA IN RELATION TO THE POTENTIAL STORAGE OF HIGH-LEVEL NUCLEAR WASTE (POSTERS)

SDCC: Hall B

Booth 90 Carlos, Barbara A. № 25095

FRACTURE-LINING MANGANESE OXIDE MINERALS IN SILICIC TUFF AT YUCCA MOUNTAIN, NEVADA.

CARLOS, Barbara A., BISH, David L, CHIPERA, Steve J., MS D462, Los Alamos National Laboratory, Los Alamos, NM 87545

Fracture-lining minerals are being studied as part of the characterization of mineralogy along possible transport pathways between the potential high-level nuclear waste repository at Yucca Mountain and the accessible environment. Fracture coatings were examined using petrographic and binocular microscopy, X-ray powder diffraction, electron microprobe and scanning electron microscopy. Manganese oxides are potentially important fracture minerals because of their ability to sorb some radionuclides, particularly the actinides Np and Pu, which are not strongly sorbed by the natural zeolites at Yucca Mountain. Manganese minerals are common in fractures in the devitrified intervals of the Paintbrush and Crater Flat tuffs, but their abundance varies both laterally and vertically across Yucca Mountain. The mineralogy of the manganese oxides appears to correlate with stratigraphic units rather than position with respect to the static water level. The tabular minerals lithiophorite and rancieite are the most common in the Paintbrush Tuff, and minor amounts of the tunnel structure mineral todorokite have been tentatively identified. The manganese oxide minerals in this interval occur as dendrites or crusts a few mm in diameter. Fractures in the Crater Flat Tuff contain tunnel structure manganese oxide minerals, primarily cryptomelane-hollandite with lesser amounts of pyrolusite and todorokite. Manganese oxides are not in all fractures of the devitrified Crater Flat Tuff, but where they occur, they usually form thick (0.5 to 5 mm) continuous fracture fillings. Hematite often appears to have coated the fractures prior to manganese deposition. The manganese oxide veins in the Crater Flat Tuff are mineralogically and chemically similar to manganese veins in volcanic rocks throughout the southwest US, except that there is too little manganese to be of economic interest and at Yucca Mountain they occur below the water table. The widespread distribution of manganese oxide minerals along potential flowpaths to the accessible environment suggests that they may be important in supplementing the retardation of some radionuclides at Yucca Mountain. However, the nature of the interaction between migrating fluids and fracture-lining minerals remains to be determined.

Booth 91 Zhang, Yang № 24751

STRUCTURAL ANALYSIS OF BARE MOUNTAIN, SOUTHERN NEVADA

ZHANG, Yang, and SCHWEICKERT, Richard A., Center for Neotectonic studies Mackay School of Mines, University of Nevada, Reno, NV 89557

An understanding of the structure and tectonics of Bare Mountain is very important in evaluating the risks associated with locating a nuclear waste repository at Yucca Mountain since similar upper Proterozoic through Mississippian strata exposed at Bare Mountain also underlie Cenozoic volcanic tuffs of Yucca Mountain. Thrust faults and detachment faults have recently been recognized and mapped by several geologists (Monsen, Carr, et.al., 1990). Our field reconnaissance and structural analysis provide data for kinematic interpretations of faulting at Bare Mountain. Four major structural elements are: (1) The north-vergent Panama thrust emplaced older rocks (upper p€ & €) northward over younger Pz rocks. A klippe of € rocks rests upon Miss strata, 6 km north of the thrust root zone in southern Bare Mountain. North-vergent recumbent folds occurred in hange wall and foot wall of the Panama thrust. (2) The south-vergent Meiklejohn Peak thrust consists of northward dipping of Ord-Sil rocks and are resting on a south-facing footwall syncline of Dev-Miss rocks. The syncline itself rests on a klippe of the Panama thrust. This relationship suggests the Meiklejohn Peak thrust is younger than the Panama thrust. Drag folds in the upper plate imply southward movement of the upper plate. (3) Top-to-the-south detachment faults (Conejo Canyon detachment & Wildcat Peak detachment) ruptured the entire Bare Mountain range. Faults root to south, and are arched above the middle of the range. The upper plate comprises fragmented slivers of Pz strata which are generally unmetamorphosed. Lower plate rocks are locally metamorphosed. In Conejo Canyon, lower plate rocks (upper p€ & €) are penetratively deformed and metamorphosed to amphibolite facies, and here are considered to be a metamorphic core complex. (4) The youngest detachment fault (Fluorspar Canyon fault) involved volcanic rocks as its upper plate, and truncated all

am TUE

pre-Tertiary structures at north end of the range. Bare Mountain has been domed, tilted and deeply eroded during Cenozoic extension since volcanic rocks have been stripped from the range. Large scale folding related to thrusts is compatible with N-S shortening that resulted from Mz orogenesis, probably pre-98 Ma (Monsen et.al.,1990). Detachment faulting and denudation are closely associated with Cenozoic extension in Basin and Range Province. Conejo Canyon fault and Wildcat Peak fault probably occurred pre-Miocene, and Fluorspar Canyon fault occurred between 10-8 Ma (Maldonado,1990).

Booth 92 Boak, Jeremy M. № 25913

MINERAL CHEMISTRY OF CLINOPTILOLITE AND HEULANDITE IN DIAGENETICALLY ALTERED TUFFS FROM YUCCA MOUNTAIN, NYE COUNTY, NEVADA

BOAK, Jeremy M., U. S. Dept. of Energy, Yucca Mountain Site Characterization Project, P. O. Box 98608, Las Vegas, NV 89193-8608; CLOKE, Paul, SAIC, 101 Convention Ctr. Dr., Las Vegas, NV 89109; BROXTON, David, Los Alamos National Laboratory, Los Alamos, NM 87545

Electron microprobe analyses of clinoptilolite (CPT) and heulandite (HEU) in 89 samples from the site for a potential high-level nuclear waste repository at Yucca Mountain, Nevada, define two compositional trends. The CPT trend, comprising the greatest number of the analyses, conforms to the formula $M_6Al_6Si_{30}O_{72}\cdot(12H_2O)$, where M = $(Na,K,Ca_{1/2},Mg_{1/2})$. The trend encompasses most of the Na-Ca-K compositional plane, as described previously (Broxton and others,1986). The Si/(Al+Fe) value varies between 4.0 and ~5.8, with most analyses restricted to <5.1. The formula $M_6(MAl,Si)_6Al_6Si_{24}O_{72}\cdot12H_2O$ represents the HEU trend, which is defined primarily by samples on the eastern side of Yucca Mountain, near the base of zeolite occurrences. Increasing Al substitution lies along the vector that connects silica to the other tectosilicates, rather than along a plagioclase-type substitution. For the HEU trend, Si/(Al+Fe) values vary from 5.0 to 2.7. (Ca+Mg) / (Na+K) ≥ 1 for all analyses in the trend.

Values of Si/(Al+Fe) = 4.0 (Boles, 1972) and of (Ca+Mg)/(Na+K) = 1 (Mason, 1960) have been proposed in the past to define chemical boundaries between CPT and HEU as minerals. Most Yucca Mountain compositions are assignable to one mineral type by either criterion, but *the two trends meet in a region where the two criteria give opposite names to minerals.* These data fill gaps in previously reported compositional ranges of the minerals, and suggest that the terms clinoptilolite and heulandite have greater significance with respect to compositional trends than with respect to distinctly separable minerals.

Most variation in the Yucca Mountain CPT/HEU zeolites reflects cation exchange among alkalis and alkaline earths (CPT trend), which proceeds easily and rapidly in the lab, and may reflect compositional variations of relatively moderate temperature groundwater. However, variation deeper in the section, in which Al substitution reflects differences in the framework of these zeolite minerals (HEU trend), is likely a relict of original formation during hydrothermal alteration *immediately following eruption of these tuffs (10-13 Ma).* The common disappearance of CPT along with opal-CT and other high-silica-activity phases with depth, replaced either by analcime or albite + quartz, suggests that silica activity was an important determinant of phase stability. The presence of more aluminous HEU at depth on the eastern side of Yucca Mountain is consistent with this trend. The rates of the zeolite breakdown reactions are commonly slow, and suggest that the zeolites, which would provide an important sorptive barrier to radionuclide migration, may well survive metastably for millions of years.

Booth 93 Soeder, Daniel J. № 6457

LABORATORY ANALYSIS OF POROSITY AND PERMEABILITY IN UNSATURATED TUFFS AT YUCCA MOUNTAIN, NEVADA

SOEDER, Daniel J., Foothill Engineering Consultants; FLINT, Lorraine E., Raytheon Services Nevada; and FLINT, Alan L., U.S. Geological Survey, P.O. Box 327, Mailstop 721, Mercury, Nevada 89023, U.S.A.

New laboratory techniques are needed to accurately measure the hydrologic properties of welded and non-welded tuff in the unsaturated zone at Yucca Mountain, Nevada, because these rocks contain hydrated minerals, such as clays and zeolites, which are sensitive to handling. The objectives of this study were to determine the effects of drying methods on measurements of porosity and permeability, and develop new laboratory analytical procedures to minimize sample damage and provide representative data.

Porosity and permeability measured with gas are lower on tuff samples dried to stable weight at 60°C under 45% relative humidity, than on the same samples dried in a standard oven at 105°C. Observations using a scanning electron microscope show fibrous smectite clay in the pores of the humidity-dried samples to be well-preserved, but identical samples dried in a standard oven contain damaged clay structures. Physical property and water saturation values obtained from such damaged samples are thus not representative of in situ conditions. Porosity measurements indicated that zeolitic tuffs had as much as 8 percent greater porosity for water than for other liquids or gas. This is probably due to preferential uptake of water by the zeolites in comparison to other fluids. Quantitative and statistical studies are currently underway to assess the laboratory procedures which provide the most representative data from Yucca Mountain rock samples.

Booth 94 Mattson, Steven R. № 28172

NATURAL RESOURCE ASSESSMENT OF YUCCA MOUNTAIN, NEVADA

MATTSON, Steven R., Science Applications International Corp., 101 Convention Center Drive, Las Vegas, NV 89109; Joel R. BERGQUIST, Joel R., U. S. Geological Survey, Menlo Park, CA

The natural resources of the proposed high-level nuclear waste repository at Yucca Mountain, Nevada are being assessed as a part of a larger geologic program to evaluate the suitability of the Yucca Mountain site. Mineral, energy, and water resources must be assessed in terms of their likelihood of present-day economic occurrence or likely economic occurrence in the foreseeable future. The presence of economic natural resources could induce exploration or mining activity that could compromise the waste isolation capabilities of the site directly or indirectly. Several occurrences and mines for precious metals are located in the region. However, precious and base-metal evaluations of the site have been extensive, and the potential for these resources is presently considered to be low. No economic energy resources are known to occur in the area, including oil, gas, coal, uranium, geothermal etc. These resources are presently considered to have low to very low potential, even in light of new exploration models that have been proposed (e.g., Chamberlain, 1991). Zeolites, clays, and volcanic cinders are mined in the area, but these industrial resources have a very low potential for occurrence at Yucca Mountain or they occur in such low grade and quantity as not to be considered economic now or in the foreseeable future. Good quality water is available at the site and in the region. This water is not expected to be exploited at the Yucca Mountain site because of the depth to the resource (>600 m) and lack of reasons (e.g., poor soils, no local industry, no mining) for its exploitation. Future work needed to assess the natural resource potential includes downhole, surface rock, and soil geochemical sampling, Lopatin-type paleogeothermal modeling, and comparisons of the geologic setting of the site to that of known mineral deposits in the region.

SESSION 73, 8:00 a.m. TUESDAY, OCTOBER 22, 1991

T 16. HYDROGEOLOGY DIVISION: CHARACTERIZATION AND MONITORING OF GROUND-WATER CONTAMINATION AT HAZARDOUS WASTE SITES: RESEARCH AND CASE HISTORIES

SDCC: Room 6F

08:00 a.m. Corley, Helen P. № 32132

FATE AND TRANSPORT OF BTEX COMPOUNDS THROUGH A THICK UNSATURATED ZONE IN THE CALIFORNIA DESERT; AN EXAMPLE OF THE PREFERENTIAL TRANSPORT OF TOLUENE.

CORLEY, Helen P., ERC Environmental and Energy Services Co., 5510 Morehouse Drive, San Diego, CA 92121.

The release of gasoline from an underground storage tank in Ocotillo Wells, California resulted in ground-water contamination in an unconfined aquifer located 110 feet below ground surface. Ground-water sampling and laboratory analyses have been conducted since October 1987. Dissolved aromatic hydrocarbon constituents including benzene, toluene, ethylbenzene, and xylene (BTEX) have been identified in 12 monitor wells, and public and domestic supply water wells over a ten acre area. Typically benzene is observed to be the most widespread BTEX compound in an aquifer; however, in this case toluene was the dominant BTEX compound.

Benzene has the highest solubility and lowest retardation factor of the four BTEX compounds, suggesting that its plume should be the most extensive. However, since toluene, rather than benzene, was observed to be the most dominant BTEX compound in the ground water, unsaturated zone characteristics as well as BTEX volatilities and relative percentages in gasoline were investigated. Also evaluated were the chemical mobility of BTEX compounds in the unsaturated zone and aquifer, single- and multi-phased solubilities, site-specific retardation factors, the potential for compound specific biodegredation, and the study of BTEX plume geometries and concentrations at the site over time.

These studies concluded that the high volatility of benzene coupled with the very dry and thick unsaturated zone significantly reduced the benzene proportion in the non-aqueous phase liquid that reached ground water.

University of Nevada, Reno
Center For Neotectonic Studies

Site Characterization of the Proposed Nuclear Waste Repository at Yucca Mountain

Task 8
Evaluation of Hydrocarbon Potential

Report of Investigations
Oct. 1991 through Sept. 1992

Principal Investigators:
Patricia H. Cashman
James H. Trexler, Jr.

EXECUTIVE SUMMARY

Task 8 is responsible for assessing the hydrocarbon potential of the Yucca Mountain vicinity. Our main focus is source rock stratigraphy in the NTS area in southern Nevada. (In addition, Trexler continues to work on a parallel study of source rock stratigraphy in the oil-producing region of east-central Nevada, but this work is not funded by Task 8.) As a supplement to the stratigraphic studies, we are studying the geometry and kinematics of deformation at NTS, particularly as these pertain to reconstructing Paleozoic stratigraphy and to predicting the nature of the Late Paleozoic rocks under Yucca Mountain.

Our stratigraphic studies continue to support the interpretation that rocks mapped as the "Eleana Formation" are in fact parts of two different Mississippian units. We have made significant progress in determining the basin histories of both units. These place important constraints on regional paleogeographic and tectonic reconstructions. In addition to continued work on the Eleana, we plan to look at the overlying Tippipah Limestone. Preliminary TOC and maturation data indicate that this may be another potential source rock.

We have set up a lab for extracting radiolaria and sponge spicules from siliceous rocks, and are in the process of setting up a lab to extract conodonts from calcareous rocks. This substantially improves our biostratigraphic dating capability, by increasing both the number of rock types we can date and the number of individual samples we can run. More dates tied to measured sections will allow us to refine the basin histories and will aid in regional correlation.

Our structural studies focus on understanding the distribution of Late Paleozoic rocks at NTS. The deformational history is complex, and detailed mapping is necessary to determine both the present surface distribution of Late Paleozoic sedimentary rocks and the geometry and kinematics of the various faults that offset them. Both are necessary in order to predict the subsurface distribution of potential source rocks.

INTRODUCTION

Our studies continue to concentrate on the stratigraphy of Late Devonian through Lower Pennsylvanian rocks at NTS, because these have the best potential to be hydrocarbon source rocks. Our work involves structural as well as stratigraphic studies: detailed stratigraphy will identify the extent of potential source rocks, and structural history controls both the maturation and the present structural position of these rocks.

This report summarizes new results of our stratigraphic and structural studies in southern Nevada. New to this year's report is a basin history for each unit (the 'eastern' and 'western' Eleana), and a separate section on biostratigraphy. Directions for future work are included where appropriate in each section. We conclude with a brief summary of implications of all the above for hydrocarbon potential in the NTS region.

STRATIGRAPHY

A. introduction

Our work this year supports the interpretation that rocks mapped as "Eleana Formation" at NTS are in fact two different, in part coeval, sedimentary units. The evidence for two separate units includes: (1) a fault contact wherever the two are adjacent; (2) different sandstone compositions between the two units; (3) paleocurrent directions which are internally consistent for each unit, but differ between the two units; (4) different depositional environments and basin histories; and (5) overlapping ages.

The following section will describe the internal stratigraphy of the 'eastern Eleana' and then the 'western Eleana'. These are followed by a comparison of the basin histories documented in each unit, and a discussion of the stratigraphic and structural implications of these histories.

B. Eastern Eleana

The **Internal stratigraphy** of the 'eastern' Eleana documents a two-stage depositional history. Most of the section is mud interbedded with occasional thin, craton-derived, sand sheets. These were deposited on a west-facing continental platform or slope, and may also comprise parts of the distal Mississippian foreland basin. We have so far been unable to determine whether the mud came from the craton or the Antler allochthon. The mudstone and sandstone are unconformably overlain by limestone which represents the re-establishment of a carbonate platform in the area. Exposure of the 'eastern' Eleana is poor; our surface measured section is supplemented by several cores and well logs, including one complete core through

1000m of section. There is evidence for both soft-sediment and tectonic deformation in this core, suggesting that neither original thickness nor internal stratigraphy of the mudstone section can be determined reliably.

The 'eastern Eleana' section (see Red Canyon Wash measured section, Fig.s 1,2) is predominantly thick, siliciclastic mudstone; quartz arenite and calcareous mudstone are occasionally interbedded. Strong bioturbation of some horizons indicates that the water column was well oxygenated and well mixed at the time of deposition. However, euxinic horizons in both the siliciclastic and calcareous mudstones document a restricted basin at the time these were deposited. At present, we don't know whether the degree of oxygenation varied spatially, temporally, or both ... or whether an open or a restricted basin was more characteristic during deposition of the 'eastern 'Eleana'.

Primary **sedimentary structures** are generally absent in the mudstone, with the exception of local lamination or bioturbation. The quartz arenite contains both ripple and trough cross-lamination, indicating that sands were reworked by bottom currents. Paleocurrents determined from cross-lamination are variable, ranging from SE to WNW, but generally indicate sediment transport toward the south or west.

Sandstones from the 'eastern' Eleana are uniformly quartz arenites. The few (less than 2%) sand grains that are not quartz are stable, resistant grains like zircon and epidote. Sandstone compositions, therefore, support the paleocurrent evidence that the sediments were derived from the craton; there is no petrographic evidence of derivation from the Antler allochthon.

At the top of the section, quartz arenite beds are thicker and more common, and limestone is occasionally interbedded. These compositional changes indicate that clear-water, open marine conditions were established at this point in the local depositional history. Sedimentary structures in the quartzite suggest shallow-marine currents (possibly longshore), and wave reworking. These quartzites probably correlate with the Scotty Wash sand beds associated with the Chainman Shale to the northeast. Scotty Wash sandstones are petrographically identical, are of the same age (as well as they are presently constrained) and paleocurrents indicate a linked sand distribution system.

Prior to our work, the only **dates** for these rocks were from macrofossils high in the section (i.e., in the open marine deposits described above), and even these dates have undergone a recent revision. The lower (mudstone) part of the 'eastern Eleana' is difficult to date. Spores (dated for Task 8) suggest an Osagean - Meramecian (middle Mississippian) age for much of the mudstone section, but palynology on rocks of this age is not deemed reliable by many workers. The top of the Eleana was dated as Chesterian (latest Mississippian) (Gordon and Poole, 1968). Endothyrids dated for Task 8 were also latest Chesterian (Mamet, written comm., 1990). However, the

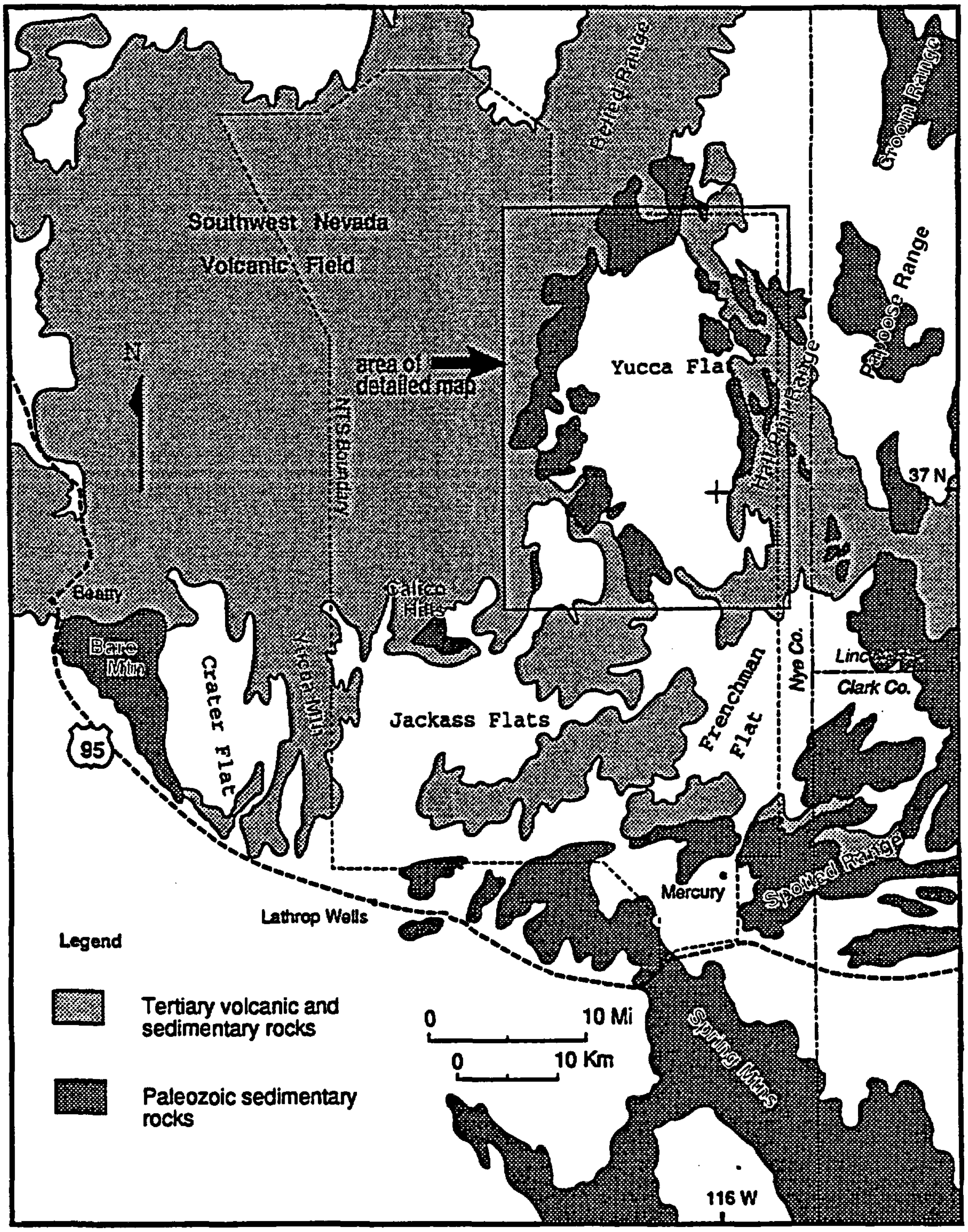

Figure 1(a): Location map, Nevada Test Site and vicinity, area of Fig. 1(b) shown.

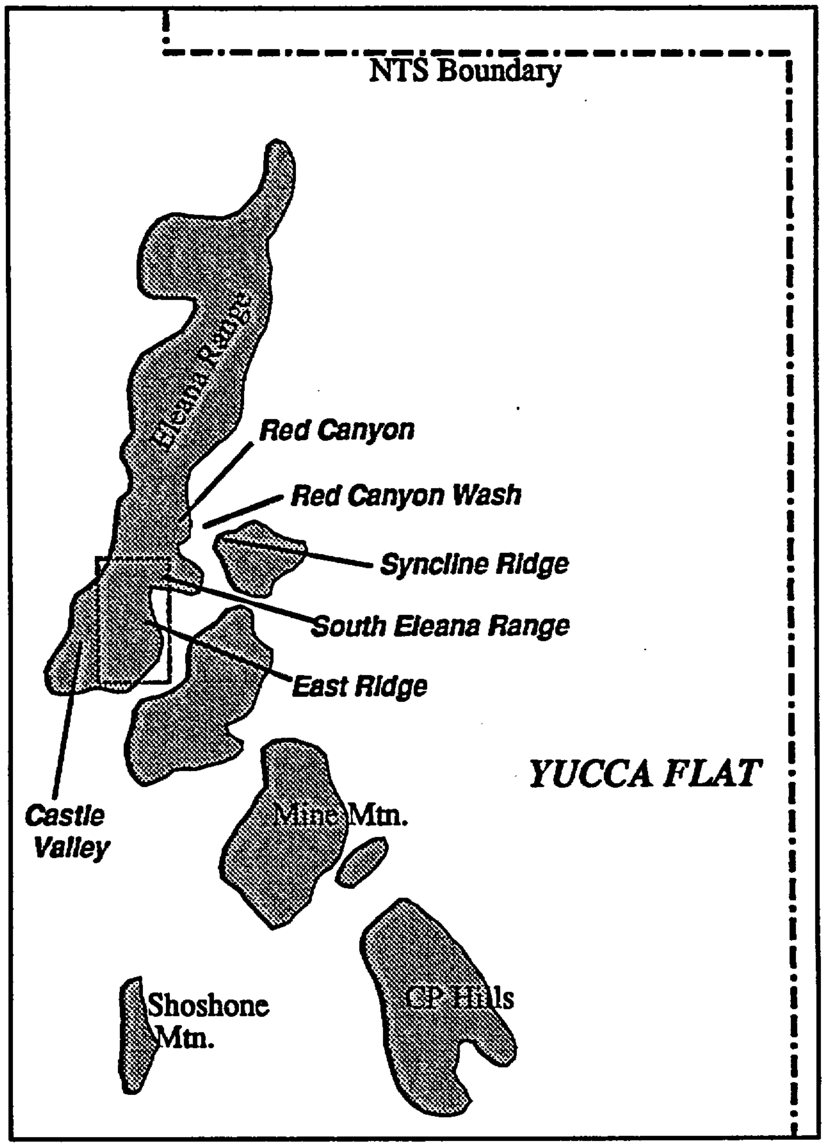

Figure 1b: Location map, Eleana Range and vicinity; area of Fig. 3 and locations of measured sections shown.

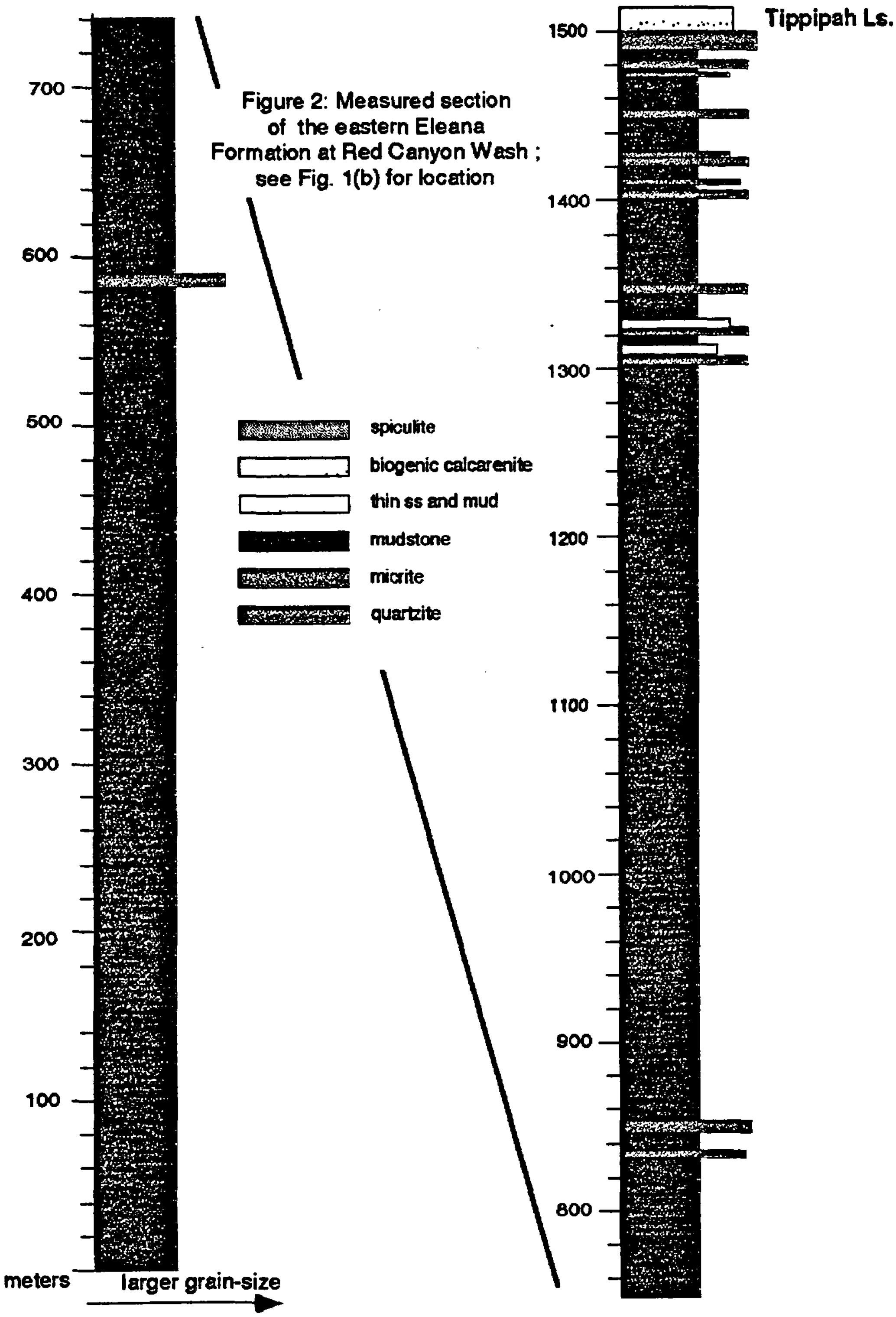

Figure 2: Measured section of the eastern Eleana Formation at Red Canyon Wash ; see Fig. 1(b) for location

ammonoid Homoceras (which defines the base of the Pennsylvanian) has recently been discovered in continuous section with upper Mississippian ammonoids within the uppermost Eleana (Titus and Manger, 1992). This moves the top of the Eleana section into the Pennsylvanian. (For a summary of all Task 8 age data see appendices 2 and 3).

The carbonate rocks of the **Tippipah Limestone** unconformably overlie the mudstone/sandstone/limestone section at the top of the 'eastern' Eleana with substantial erosional relief. For example, Titus and Manger, (1992) describe an ammonoid assemblage that occupies a 17m-thick shale section below orthoquartzites of the highest Eleana. This assemblage has been erosionally removed in similar basinal rocks just 16 km to the east. The flooding surface at the base of the Tippipah is therefore a sequence boundary, representing a transition from possibly subaerial to shallow marine conditions. Conodont dates consistently identify the base of the Tippipah as Lower Pennsylvanian (Morrowan) (Gordon and Poole, 1968). The shallow marine conditions that allowed the build-up of a Pennsylvanian carbonate platform differed from those prior to erosion in that there was a dramatic reduction in the amount of fine-grained siliciclastic detritus.

We haven't worked on the Tippipah yet, but the internal stratigraphy of the Tippipah Limestone is one of the topics we intend to investigate further in the next year. Reconnaissance has shown that chert pebble conglomerates with a carbonate matrix occur within the section. The chert pebbles clearly are reworked from older sedimentary rocks, but the depositional environment of such rocks (and the paleogeography at the time of deposition) is enigmatic. The geologic history recorded in the Tippipah is the last chapter in the 'eastern Eleana' tectonic story; in addition, maturation and TOC results on a few samples of Tippipah suggest that it may be a potential source rock.

C. Western Eleana

The **internal stratigraphy** of the 'western' Eleana also documents a two-stage tectonic and depositional history: the lower part is siliciclastic submarine fan deposits, the upper part is organic/detrital basin fill. The transition between the two is fairly abrupt, and represents an important Mississippian tectonic event. From the sections that we have measured so far, it appears that we may be seeing two different parts of the 'western Eleana' basin that have been structurally juxtaposed. This may ultimately prove very helpful in deciphering the Mississippian paleogeography as well as in improving our understanding of the 'western' Eleana.

The **submarine fan** basin fill comprises a fining-upward sequence of mid-fan to inner fan deposits. Our current interpretation of this setting is that it was a mid-fan channel complex, topographically constrained laterally and occupying an elongate trough. This is born out by the lack of dispersal of paleocurrent trends, and the general lack of fine-grained inter-channel deposits. The small and large-scale fining-thinning upward cycles observed in the measured section are consistent with channel fill and amalgamation as channels were alternately abandoned and reoccupied in the narrow fan system. Paleocurrents determined from these rocks are more consistent than those from the 'eastern' Eleana, and trend SSW to SW. These confirm a somewhat unusual fan geometry: the submarine fan may have occupied an elongate SSW-trending basin that was filled primarily by axial turbidity currents.

The **clast compositions** in the sandstones and conglomerates provide information about the source areas feeding the submarine fan. Limestone (+/- chert) and quartzite clasts were most probably derived from the older sedimentary rocks of the Paleozoic continental margin. These rocks must have been tectonically uplifted in order to be a source; paleocurrents suggest that this tectonic source was generally to the north of the 'western Eleana' basin. Vesicular basalt clasts were most probably derived from the Antler allochthon, although they could also have been derived from terranes to the west of it. At any rate, it is unlikely that these clasts were derived from the North American craton to the east. Phosphatic clasts (appendix 1) (+/- chert) were formed *in situ* or also were derived from the Antler allochthon and/or terranes to the west of it (e.g., those now in the northern Sierra); there is no known phosphatic source of pre-Mississippian age on the North American craton. We hope to be able to do more with these phosphatic clasts -- possibly finding diagnostic fossils associated with them -- to pinpoint their source.

Although the Eleana has generally been interpreted as part of the Antler foreland clastic wedge and thus correlative with the Diamond Peak and Chainman formations of central Nevada, there are no known units directly correlative to the 'western' Eleana. Identifying such unit(s) and determining their relative paleogeographic position(s) would go a long way toward resolving the obvious paleogeographic problems posed by our interpretation that rocks previously mapped as "Eleana" are in fact parts of two separate basins. As far as we know, coarse-grained rocks of the 'western Eleana' are found only at the Nevada Test Site and the adjacent Nellis Air Force Range. Finer-grained rocks of apparently similar composition (e.g., primarily chert-grain sandstones) and Mississippian age are mapped as "Eleana" at Bare Mountain and also occur in the El Paso Mountains (M. Carr, pers. comm. 1992) and in the northern Sierra (Harwood and others, 1991; M. Carr, pers. comm. 1992). At present, it is not known whether any of these are genetically related to each other or to the coarse submarine fan deposits of the 'western' Eleana; this is another direction for future work.

The **organic/detrital basin fill** depositionally overlies the submarine fan deposits, and contains a variety of rock types. The carbonates in this section are reworked bioclastic sands, often in graded beds. These sands are primarily crinoidal, but also include brachiopods, gastropods, corals, ammonoids, etc. This organic detritus comprises reworked Mississippian organisms, derived from a productive carbonate platform. The siliceous argillites and cherts contain some radiolaria, but are primarily spiculites. The sponge spicules originated in relatively shallow water (Murchey, 1990; B. Murchey, pers. comm., 1992) but are almost certainly reworked, because they occur in the graded beds. In many places, beds which contain coarse crinoid debris at the base grade up into spiculitic chert at the top, demonstrating that siliceous and carbonate reworked organic debris were transported and deposited simultaneously. Preliminary dating from the radiolaria supports a Mississippian (no older than Osage) age for these rocks (B. Murchey, pers. comm., 1992). Micrites, calcareous mudstones, and mudstones are intimately interbedded with the bioclastic limestones and cherts. Locally, these fine-grained rocks show extensive bioturbation, indicating a well-oxygenated water column.

The biogenic beds contain the **primary sedimentary structures** associated with submarine fan turbidites in an outer fan setting. Primary depositional mechanisms are turbidity flows and pelagic rain-out of suspended debris in the water column. Paleocurrent data from these rocks are limited, but suggest that transport was in part toward the east.

Sedimentary clasts (in addition to bioclastic debris) in the graded beds include chert and phosphate. The phosphatic clasts (see Appendix 1) may be primary phosphate nodules formed on a slope where upwelling currents enhanced biogenic productivity, or they may be reworked from older rocks. The chert clasts are presumably reworked material from the oceanic terranes to the west or northwest.

There are several similarities between rocks of the organic/detrital portion of the 'western' Eleana and the siliceous sedimentary rocks in the upper Paleozoic Havallah sequence of northern and central Nevada. Both contain sponge spicule-rich turbidites derived from a shallow source. Similar assemblages of radiolaria and sponge spicules occur in the two (B. Murchey, pers. comm., 1992). Several distinctive structural features in chert ("step boudins" with silica-sealed cracks, and asymmetric to overturned folds with thickening at the hinges) resemble those described in the Havallah (Snyder and Bruekner, 1983; Snyder and others, 1983; Bruekner and Snyder, 1985; Bruekner and others, 1987), and interpreted to be pre-lithification features. It is premature to propose a correlation between the two, but testing this idea will be another direction for future work. If the two units correlate, it will require significant revision of both structural and paleogeographic models!

So far, our **age control** on the 'western' Eleana is limited to the sediments from the upper (organic/detrital) part of the basin. (For a summary of all Task 8 age data see Appendices 2 and 3.) Endothyrids and calcareous algae from the lowest bioclastic limestone horizons consistently yield zone 16 (latest Meramec - earliest Chester) ages. We are provisionally using this information to date the shift from a siliciclastic-dominated sediment system to one that was fed primarily by an organically productive platform. Other potential dating methods for these rocks include radiolaria

Figure 3: Geologic map of the southern Eleana Range, showing the distribution of 'eastern' and 'western' Eleana Fm. See Fig. 1(b) for location

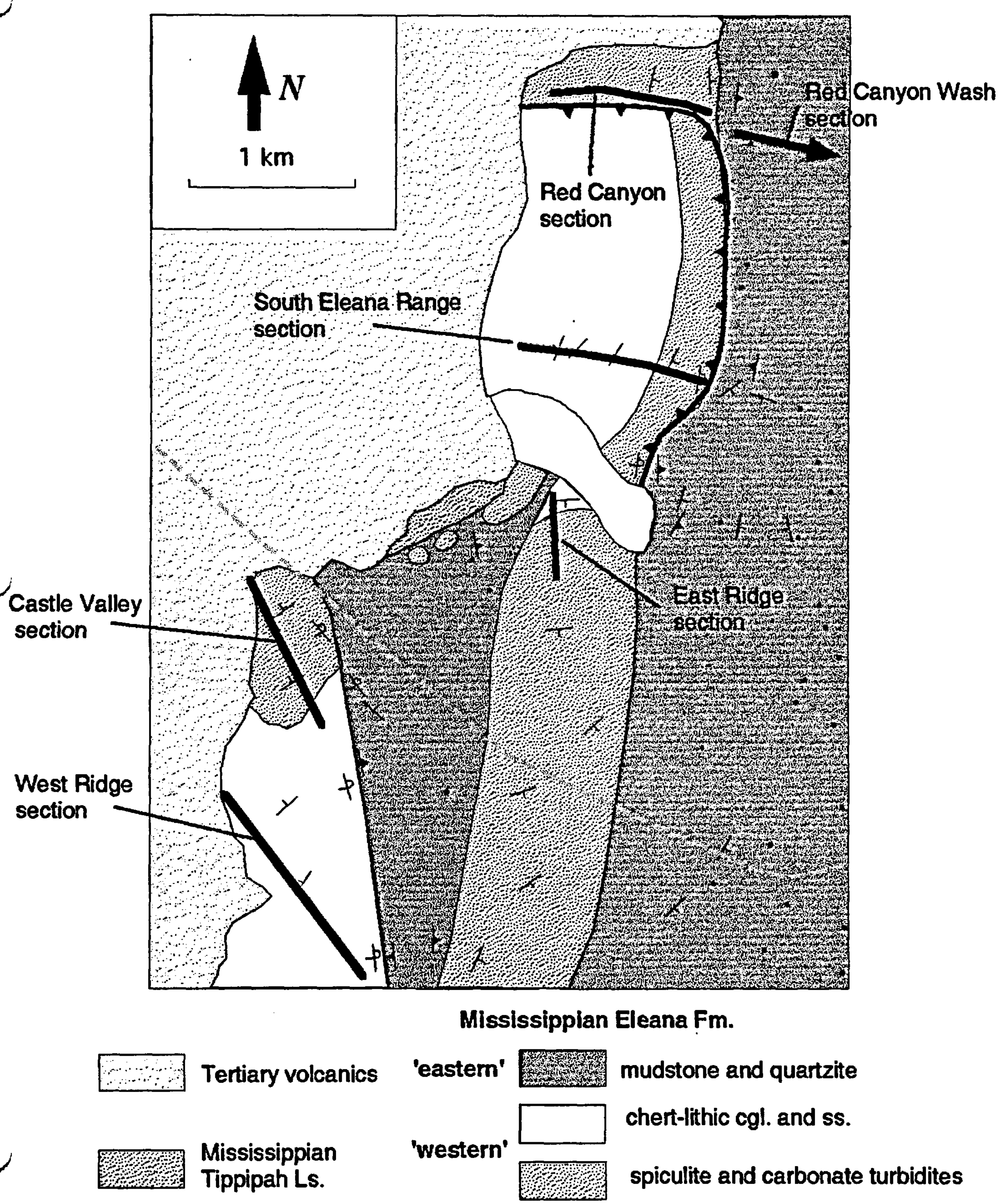

Figure 4: Measured section of the 'western' Eleana Fm. at West Ridge; see Fig.s 1(b) and 3 for location

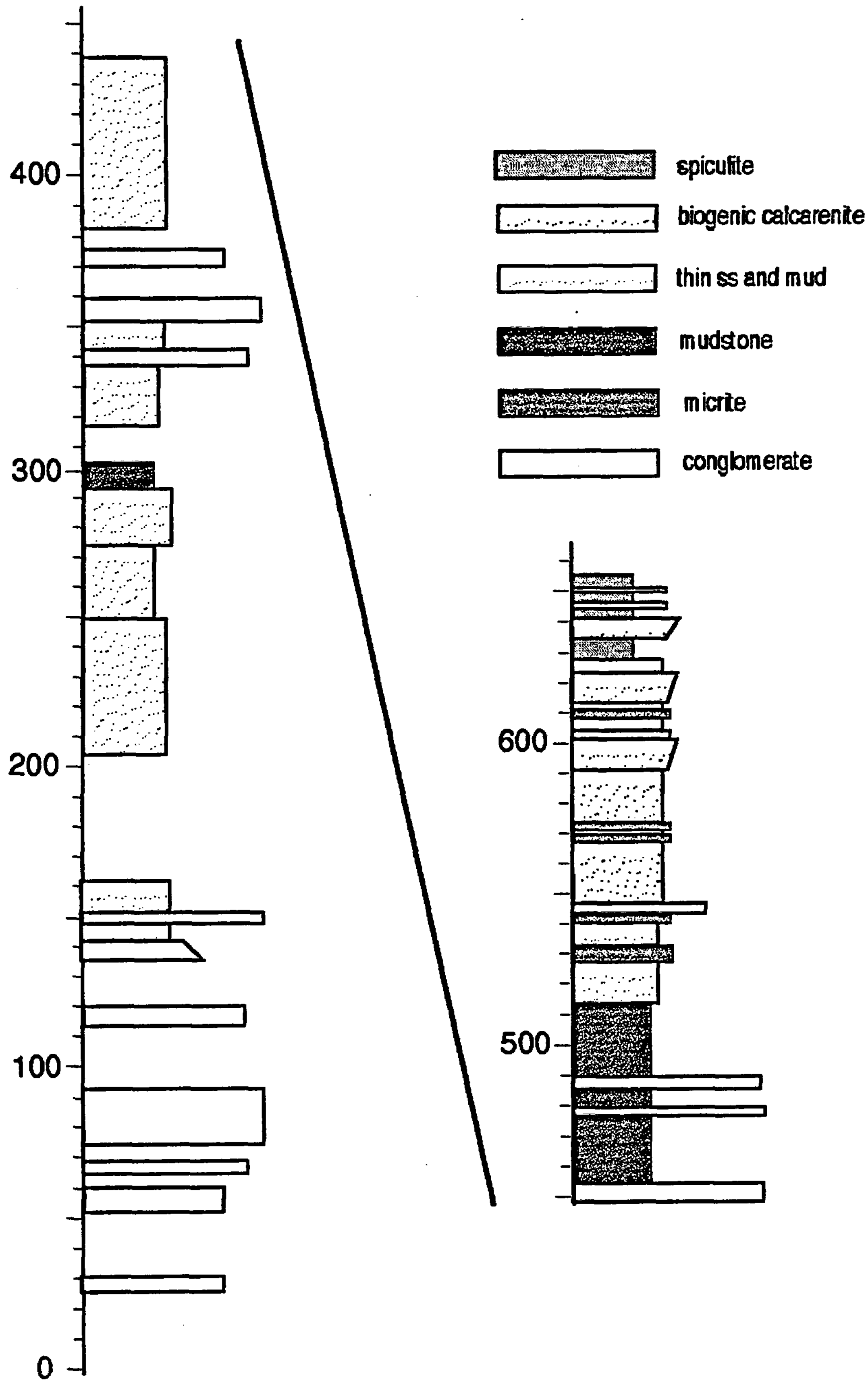

Figure 5: Measured section of the 'western' Eleana Fm. at Red Canyon; see Fig.s 1(b) and 3 for location.

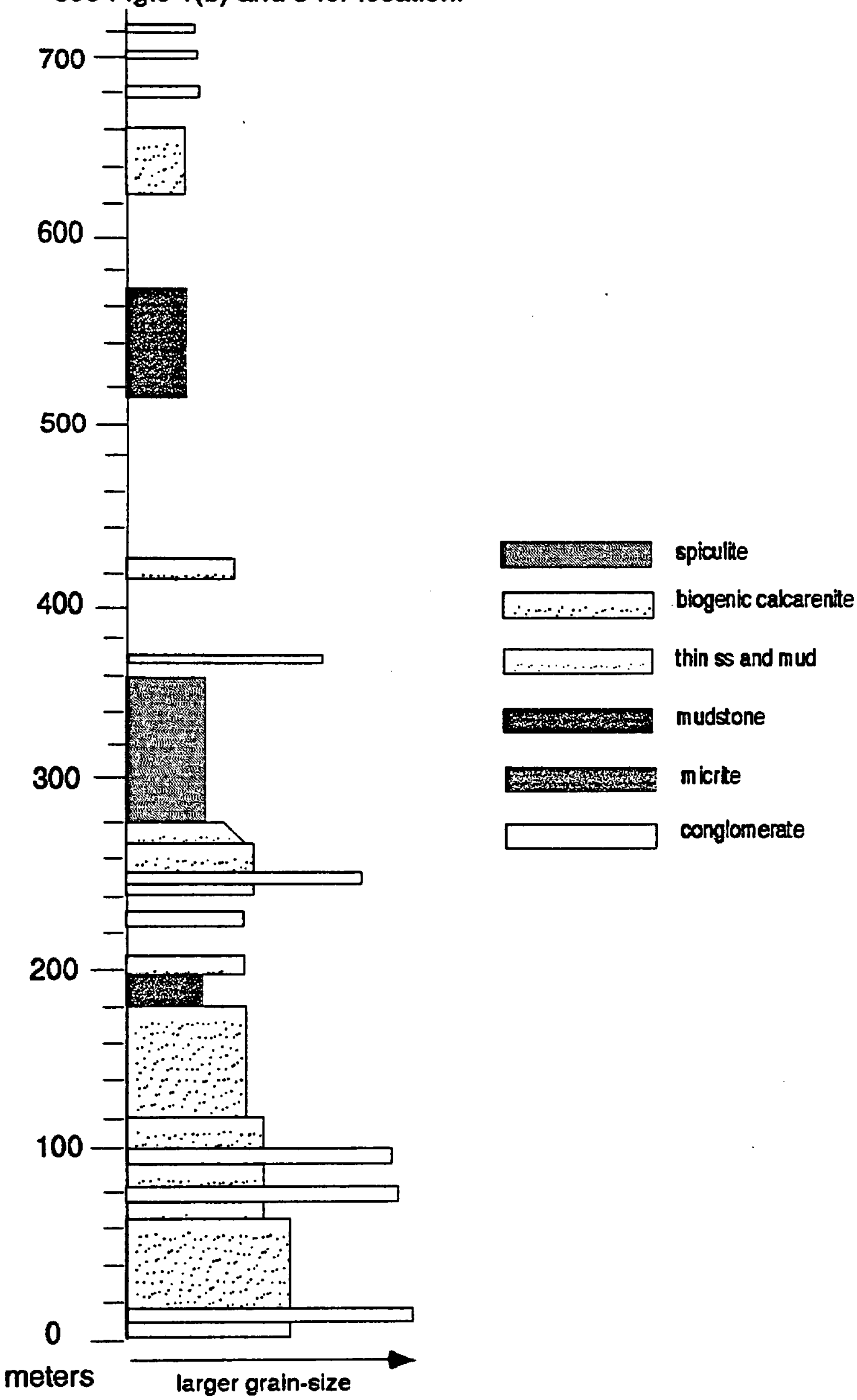

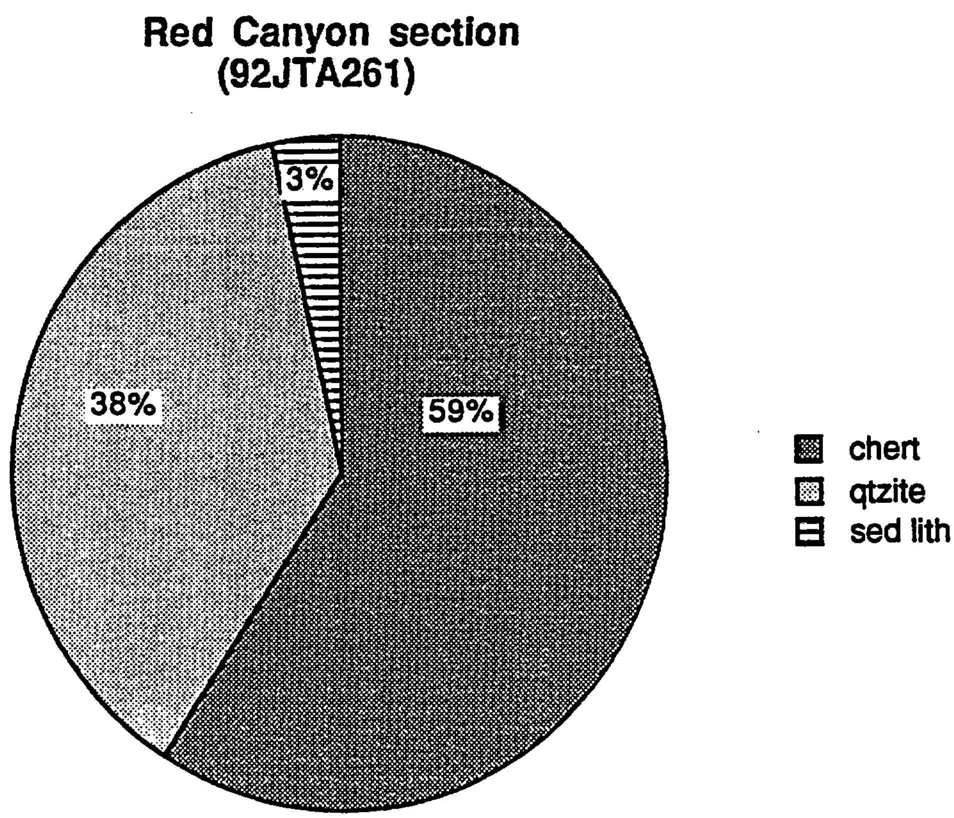

Figure 6: Pie diagram of conglomerate clast count (300 clasts) near the base of the Red Canyon measured section; "sed lith" clasts are fine-grained litharenite. Compare with Fig. 9.

Figure 7: Measured section of the 'western' Eleana Fm. in the southern Eleana Range; see Fig.s 1(b) and 3 for location.

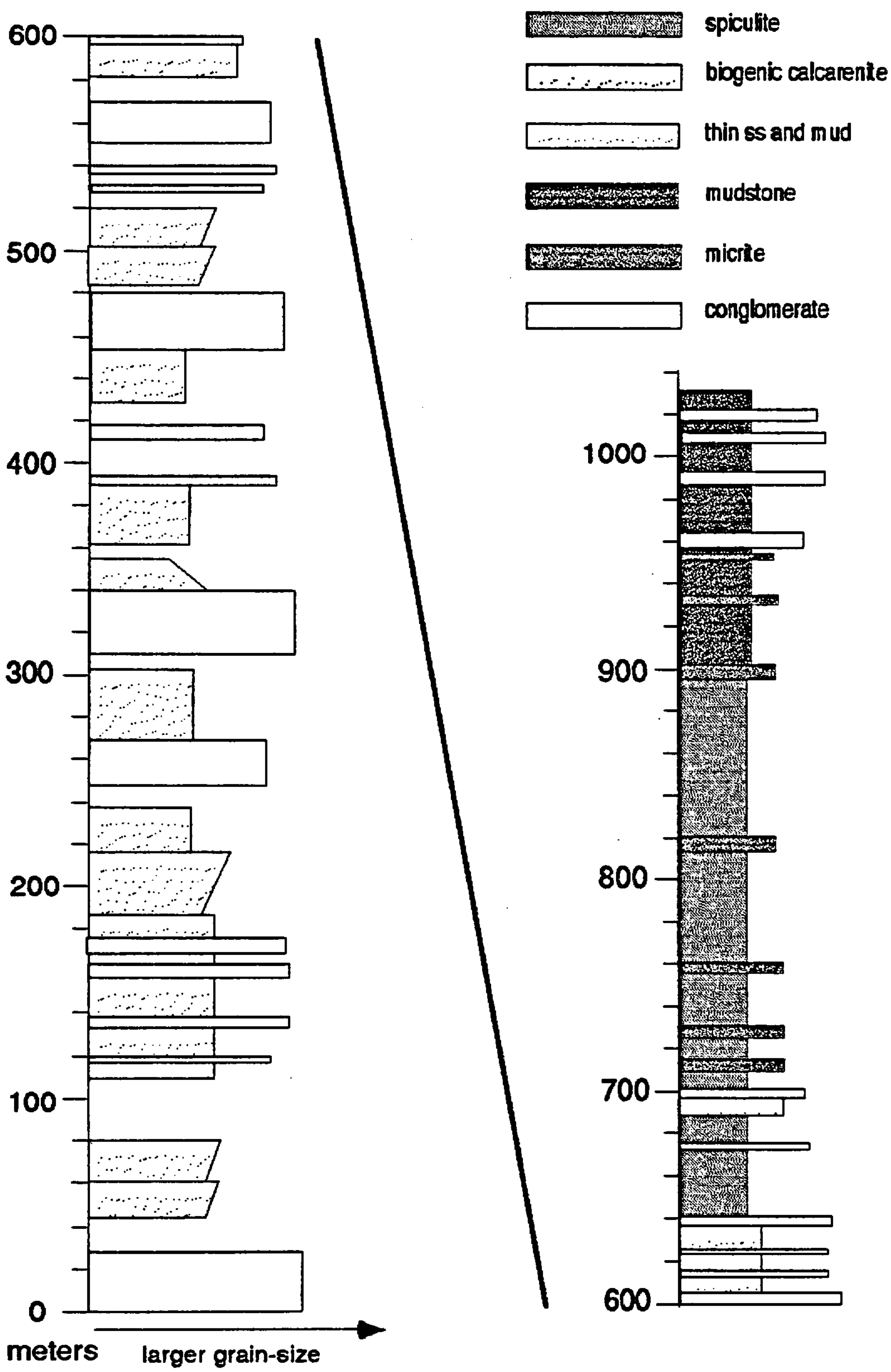

Figure 8: Measured section of the 'western' Eleana Fm. at East Ridge; see Fig.s 1(b) and 3 for location

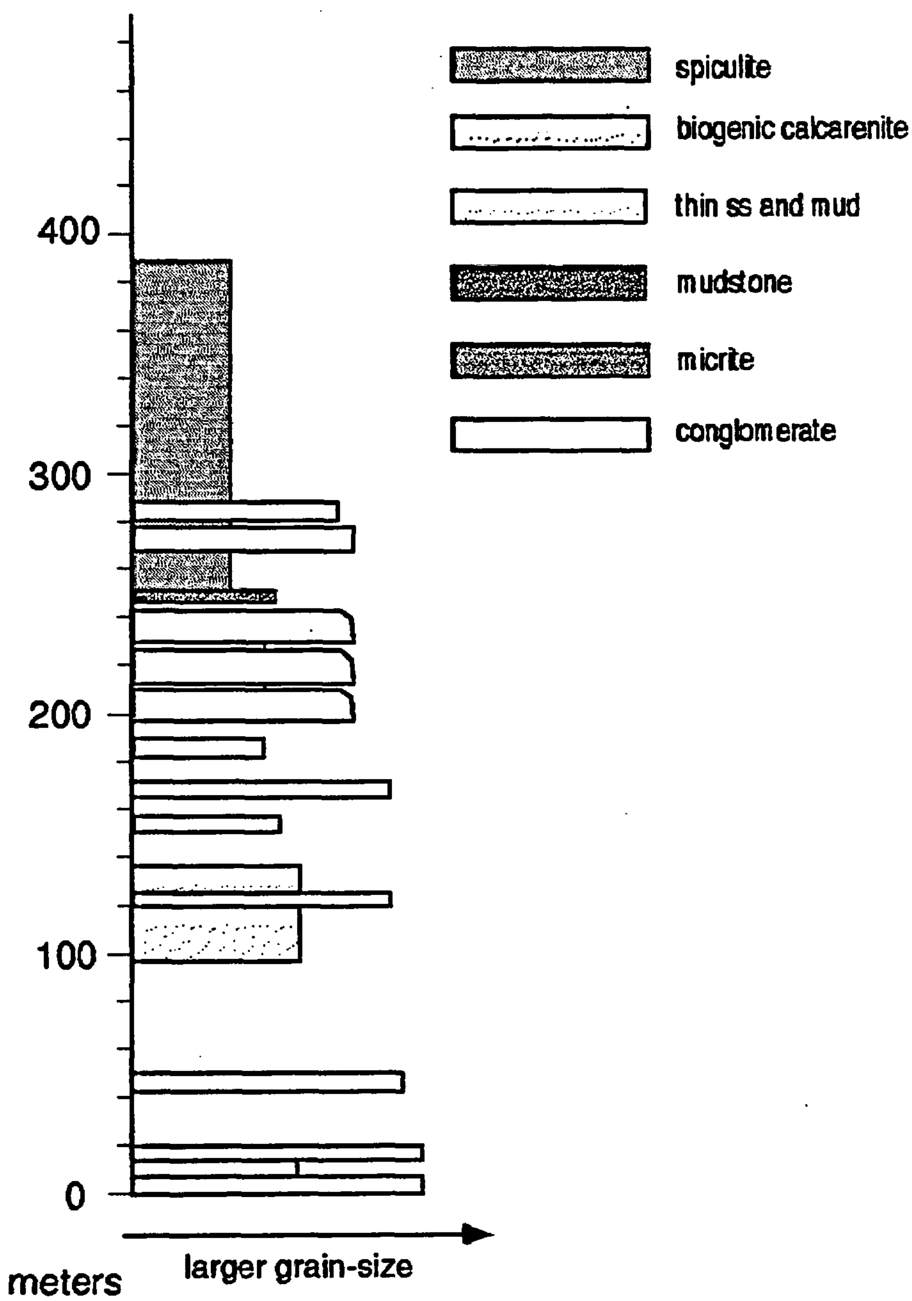

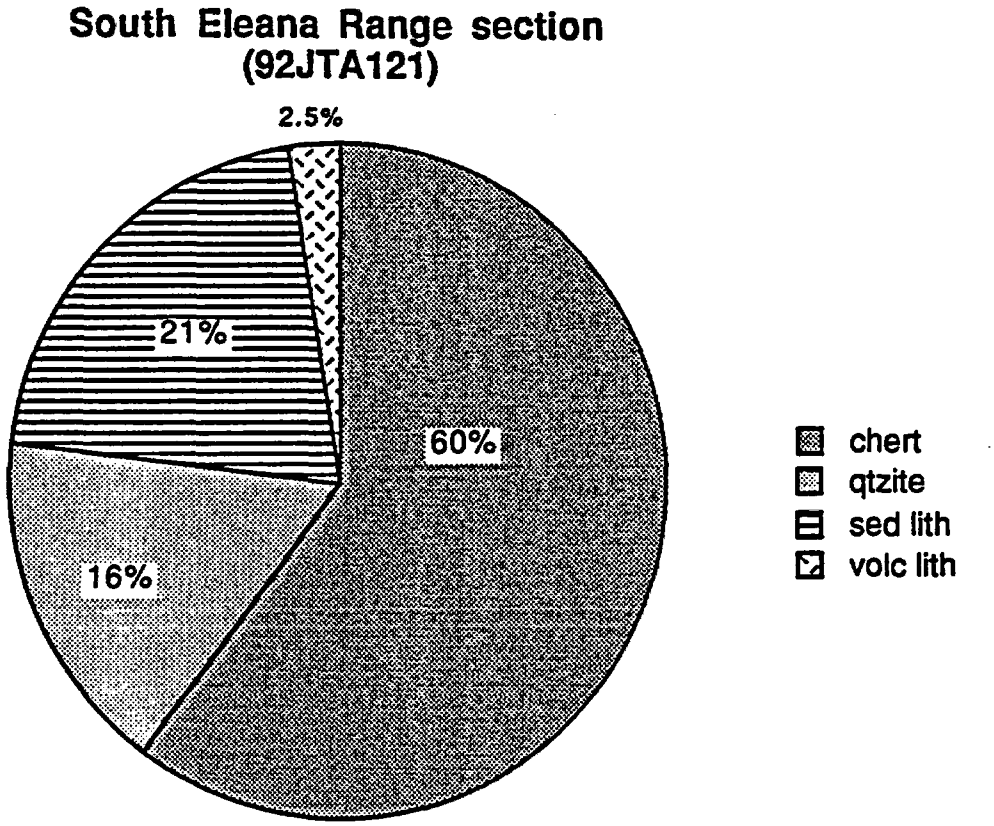

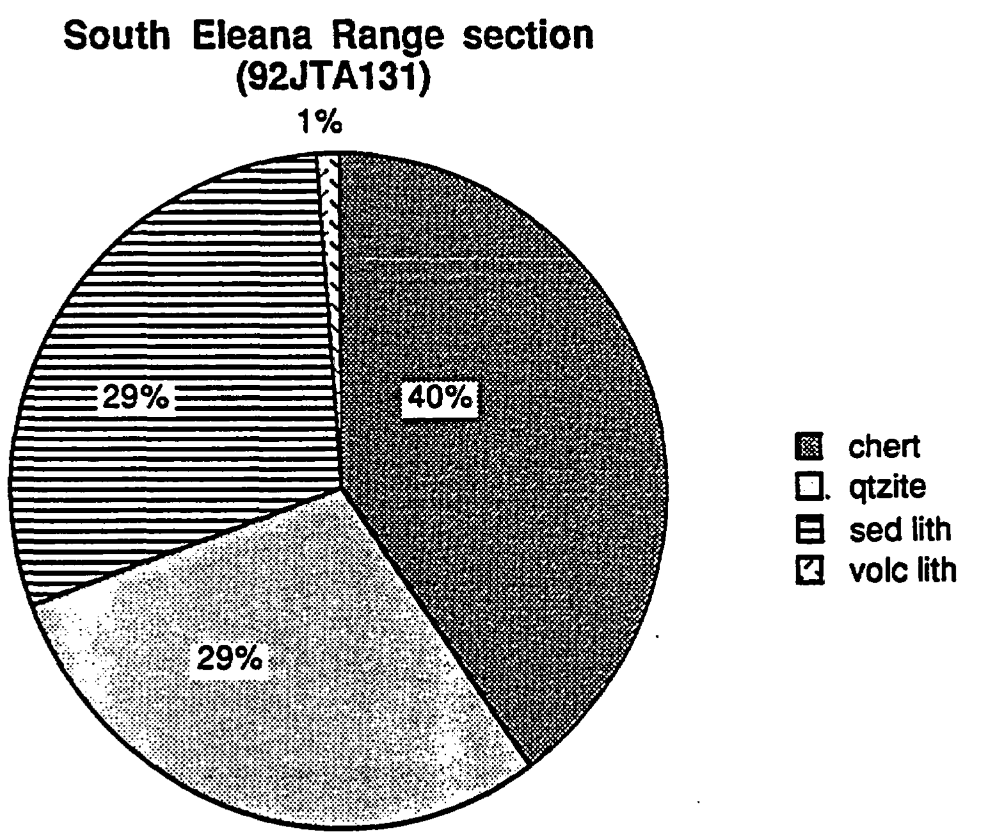

Figure 9: Pie diagrams of conglomerate clast counts (250 and 200 clasts) near the base of the Southern Eleana Range section. "sed lith" includes limestone, siltstone, and litharenite. Compare with Fig. 6.

and sponge spicules from the cherts, and conodonts from the limestones. In addition, it may be possible to date radiolaria and/or spicules from the phosphatic clasts which occur in both the submarine fan section and the organic/detrital section. Note that if the phosphatic clasts are reworked from an older oceanic terrane, ages from the phosphatic clasts would date the source terrane (and might aid in correlation), but would not date the Eleana!

The 'western Eleana' measured sections fall into two groups of similar stratigraphy. This suggests that we are seeing **two different parts of the 'western Eleana' basin**, now faulted together:

version 1: In some measured sections (e.g., West Ridge (Fig. 4) and Red Canyon (Fig. 5)), micrite and biogenic calcarenite immediately overlie the conglomerate and sandstone of the submarine fan deposits. There are at least 100 - 200m of these calcareous rocks before the appearance of siliceous sediments (chert and siliceous argillite containing radiolaria and sponge spicules). In the submarine fan deposits associated with these sections, conglomerates contain chert, quartzite and minor amounts of siliciclastic sedimentary rocks (Fig. 6).

version 2: In other measured sections, (e.g., Southern Eleana Range (Fig. 7) and East Ridge (Fig. 8)), 50m or more of siliceous sediment lies between the coarse clastics of the submarine fan and the first occurrence of micrite. In the one case we have with continuous section, there is another 120m of spiculite and occasional micrite before the first occurrence of biogenic calcarenite. In the submarine fan deposits associated with these sections, conglomerates contain chert, quartzite and siliciclastic sedimentary rocks, but also include basaltic volcanic and limestone clasts (Fig. 9).

It therefore appears that in *version 1* we are seeing a part of the basin that was relatively close to the productive Mississippian carbonate shelf, and received calcareous debris as soon as the clastic sedimentation ceased. In *version 2*, we are seeing a part of the basin that was either far from or separated from the carbonate source, and received only fine-grained material that was carried in suspension. Eventually, the coarse bioclastic material also made it to this part of the basin. The geographic separation of these two parts of the 'western' Eleana basin is also reflected in the submarine fan deposits in the lower parts of these sections: although the source terranes for the different parts of the submarine fan had many characteristics in common, the volcanic and limestone source(s) supplied only a limited part of the fan (i.e.,*version 2*).

D. Comparison of basin histories; implications

A comparison of the basin histories of the 'eastern' Eleana and 'western Eleana', as they are presently known from the measured sections (Fig. 10) and paleontologic data summarized above, shows that the Mississippian rocks at NTS do

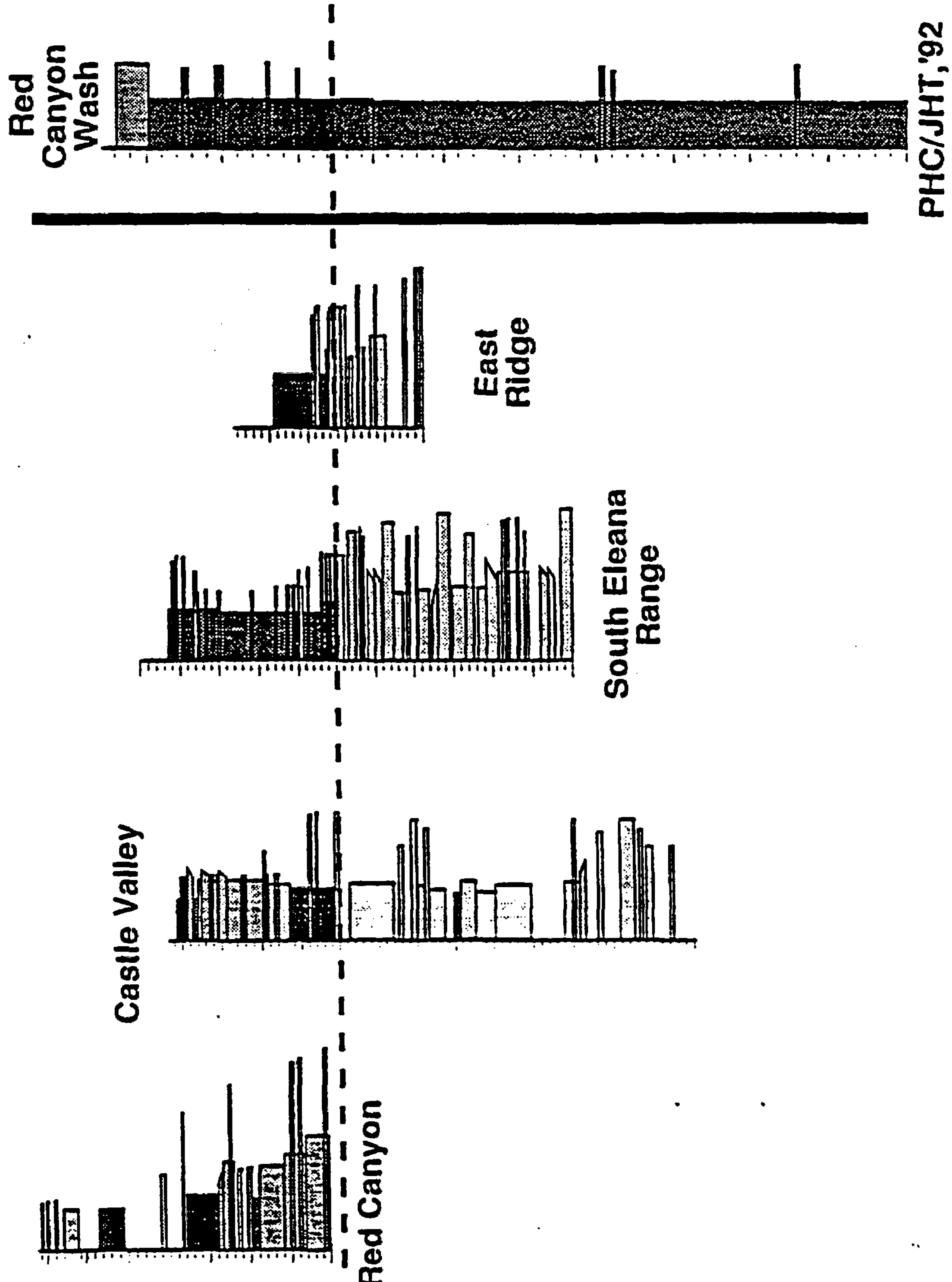

Figure 10: Comparison of measured sections. Datum (dashed) is Early Chester. Note that the 'eastern' Eleana Fm. shows no change at this time, but the 'western' Eleana sections record the change from submarine fan to pelagic, organic-detrital basin.

not reflect the evolution of a single simple basin. Rather, they record the development of two separate basins. Indirectly, this points to a poorly understood but significant structural juxtaposition of the two. The history of each basin will be summarized briefly below, followed by a discussion of the implications for tectonic/structural history.

The muddy sedimentary basin of the 'eastern' Eleana was probably established on the Devonian carbonate margin of North America. We have not found the depositional base of unequivocal 'eastern' Eleana rocks. However, we are tentatively interpreting the fine-grained mudstone and limestone unit mapped as "Ml" on the Mine Mountain 7 1/2' quadrangle (Orkild, 1968), which depositionally overlies Devonian carbonates, to represent the base of the 'eastern' Eleana. This interpretation is based on Orkild's (1968) Mississippian age*, the presence of mudstone and quartz arenite and absence of chert and other lithic clasts (like the 'eastern', and unlike the 'western', Eleana), and the fact that "Ml" has never been mapped or described anywhere except in a single, 250ft thick exposure on the flank of Shoshone Mountain, in the Mine Mountain quadrangle. Mississippian rocks in nearby areas -- within and adjacent to the Mine Mountain quadrangle -- are either chert-bearing submarine fan deposits (which we interpret to be 'western' Eleana) or mudstone and quartz arenite shelf (?) deposits (which we interpret to be 'eastern 'Eleana). It is hard to justify a new and unique unit designation ("Ml") for a single exposure, when similar rocks with an established name crop out nearby, so we suggest that this unit may represent the lower 'eastern' Eleana.

The 'eastern' Eleana basin fill consists of prograding muds which were locally calcareous, and craton-derived quartz arenite. There is no evidence so far of any sediment source other than the craton. Sand dispersal was generally toward the south and west. The quartz sand beds became thicker and more common with time; limestone is interbedded with the quartz arenite at the top of the section. The limestone at the top of the section had been dated as late Chesterian (latest Mississippian) (Gordon and Poole, 1968) and on calcareous (Mamet, written comm.. to Task 8, 1990). However, the uppermost part of the section has recently been reinterpreted as earliest Pennsylvanian (Titus and Manger, 1992). The water in the 'eastern' Eleana basin was well oxygenated at some times and restricted at others; we don't yet understand the mechanism or know which was dominant.

The siliciclastic basin fill is erosionally truncated (Titus and Manger, 1992), so we do not see the top of the section. Although there was significant erosion on this

* The map explanation -- which is the only published description of "Ml" -- notes "common, well-preserved Devonian conodonts, probably reworked from the Devil's Gate Limestone". There is no explanation of why the conodonts are thought to be reworked or why the unit is interpreted to be Mississippian rather than Devonian. If "Ml" is Devonian, it may still represent the base of the 'eastern' Eleana ... it just pushes back the inception of siliciclastic deposition into Devonian time.

surface in the NTS area, there seems to be little section missing at Syncline Ridge because lower Pennsylvanian rocks occur both above and below the unconformity. The erosional surface was flooded in earliest Morrowan (Early Pennsylvanian) time, and a carbonate platform (the Tippipah Limestone) developed.

The 'western' Eleana submarine fan also depositionally overlies Devonian carbonate. Clastic (Eleana) deposition appears to have started by Late Devonian time -- a Late Devonian conodont assemblage is described 160ft above the base of the Eleana clastic section (Rogers and Noble, 1969). We have not been allowed access to the area where the basal contact is exposed, but the stratigraphy is briefly described in the explanation on the Oak Spring Butte 7 1/2' quadrangle (Rogers and Noble, 1969). Based on this description and the coarse base of our measured sections, the submarine fan appears to have prograded quickly into the narrow foreland basin. The timing of this event is not well constrained, and the relationship of this clastic fan to the arrival of the Antler allochthon in central Nevada is not currently known. Because of the basin geometry, the direction of sediment transport, and nature of the basin fill, a simple peripheral foreland basin model such as is currently popular in central Nevada for this orogeny does not work here.

The submarine fan was active from Late Devonian to Late Mississippian (late Meramecian or early Chesterian) time. The fan appears to have developed in an elongate trough, with SSW-trending axial currents. Sediments in the fan were derived from tectonically uplifted older Paleozoic rocks, the Antler orogen, and possibly also from volcanic and/or oceanic terranes to the west of the Antler orogen. The submarine fan rocks we have observed were deposited in a channel-fill complex that is regressional overall. Submarine fan sedimentation tapered off by early Chesterian time, and slow subsidence of the basin continued without much external sedimentary input. Slow deposition of fine-grained organic debris (both calcareous and siliceous) was the dominant mode of sedimentation. The arrival of numerous bioclastic-rich turbidites signals the appearance of a significant "carbonate factory" upstream. This may be synchronous with the transgressive event suggested in central Nevada, where Diamond Peak siliciclastic sediments are overwhelmed by carbonate shelf limestone (Trexler and Cashman, 1991). Transgressive events should shut off siliciclastic sediment transport and enhance carbonate production in shelf areas. Note that the suggestion we made in an early Task 8 Progress Report -- that the change in sediment composition might be due to the emergence of the orogenic highland represented by the mid-Mississippian unconformity in the Diamond Mountains -- now appears to be incorrect, even though the two events occurred at about the same time. The unconformity in the Diamond Mountains represents uplift and emergence of marine sedimentary rocks; the change in sediment composition in the 'western Eleana' basin represents subsidence and flooding of the continental margin in the source area.

The obvious conclusion that can be drawn from these two basin histories is that the Latest Devonian and Mississippian rocks at NTS do not reflect a single, simple orogenic history (Fig. 10). Rather, they document sediment derived from different sources and deposited in different environments. Furthermore, they have been subjected to different syndepositional tectonic histories. Clastic deposition appears to have started at about the same time (Late Devonian) in both the 'eastern' and 'western' Eleana basins. A late Meramec or early Chester transgressive event is recorded in the 'western' Eleana. An Early Pennsylvanian erosion event, followed by Early Pennsylvanian flooding, is recorded in the 'eastern' Eleana.

STRUCTURAL GEOLOGY

Our work on the structure of the southern Eleana Range documents several superimposed deformations, and shows that detailed mapping is required throughout the area in order to understand the structure. Deformation events that pre-date the oldest Tertiary volcanic rocks in the area (the ca. 16 Ma Redrock Valley Tuff) include (1) possible pre-lithification (therefore Late Paleozoic) deformation in the upper part of the 'western' Eleana, (2) thrust faulting and associated overturned folding of probable Mesozoic age, and (3) the cryptic fault that juxtaposes 'eastern' and 'western' Eleana. Tertiary low-angle normal faulting obscures the earlier deformations, and makes structural reconstructions difficult. Structures typical of each of these events are described briefly below.

A possible **Late Paleozoic deformation** was pointed out to us by colleague Walt Snyder (Boise State University) when he visited NTS with us in December, 1991. Its existence is suggested by a distinctive mesoscopic deformational style that occurs locally in the upper part of the 'western Eleana'. Good examples of this deformation occur both north and south of the Pahute Mesa road where it crosses the ridge we informally call East Ridge -- between Syncline Ridge and the southern end of the Eleana Range (see Fig. 1b). Interbedded spiculitic chert, siliceous argillite and bioclastic turbidites are folded into asymmetric to overturned mesoscopic folds. Bedding thickens at some fold hinges, suggesting that the rock was not completely lithified when the folding occurred. These rocks also contain "step boudins" (or "step planes" and "solution boudins"), as described in the Havallah sequence rocks of the Golconda allochthon (Snyder and Bruekner, 1983; Snyder and others, 1983; Bruekner and Snyder, 1985; Bruekner and others, 1987). In these structures, bedding is extended by slip along multiple sub-parallel surfaces and rotation of the intervening blocks. The cracks are sealed with silica (not obvious quartz veins) that Snyder interpreted to be diagenetic (Snyder and Bruekner, 1983; Snyder and others, 1983; Bruekner and Snyder, 1985; Bruekner and others, 1987). Further documentation of this deformational event is important for two reasons: (1) If it exists, it provides another line of evidence that the rocks of the 'western' Eleana may be genetically related to the Havallah sequence of the Golconda allochthon. (2) If it exists, we must be careful not to confuse it with mesoscopic deformation produced by later structures (e.g., Mesozoic(?) thrusting).

We have mapped several structures in the southern Eleana Range that are unequivocally related to **Mesozoic(?) thrust faulting**. One of these is the large overturned fold south of Red Canyon in the lower (submarine fan) portion of the 'western' Eleana (just north of the uncolored area in Fig. 3). Overturned upper (biogenic/detrital) 'western Eleana' overlies 'eastern Eleana' along a sub-horizontal contact farther south in the Eleana Range. More mapping is needed to resolve the structural relationships between these two areas (uncolored area in Fig. 3). The geometry and extent of thrust faulting in the southern Eleana Range is particularly important to Task 8: It will constrain projections of structures toward the southwest (toward the poorly-exposed Calico Hills and then Yucca Mountain). It will also help us evaluate the applicability of "thrust play" models for creating hydrocarbon reservoirs at NTS.

The **fault juxtaposing 'eastern' and 'western' Eleana** is cryptic, and is best exposed in the southernmost Eleana Range (see the southwest quadrant of the geologic map, Fig. 3). Here, it is sub-vertical and strikes north-northwest. Several exposures farther north in the Eleana Range also indicate a north-striking, sub-vertical fault contact. It is not yet known whether this represents the original fault contact between the 'eastern' and 'western' Eleana, or a later (possibly reactivated) fault. Steep foliation characterizes the 'eastern' Eleana in the vicinity of the fault. In the 'western 'Eleana, the fault is at a relatively high angle to bedding, and a broad, overturned fold is sometimes -- but not always -- developed within 10 to 20 m of the fault. This folding suggests west-over-east reverse movement. Foliation, brecciation, and veining (quartz, calcite, or chalcedony) occur locally, adjacent to the contact. The fault juxtaposing 'eastern' and 'western' Eleana is potentially the most significant structure at NTS from a tectonic standpoint, yet the nature of this fault remains disappointingly enigmatic. Further mapping, particularly farther north along the front of the Eleana Range, may reveal better exposures of this feature.

Tertiary low-angle normal faulting is characterized by brecciation, iron staining, and polished or striated fault surfaces. Shattering -- with or without veining -- is typical near the base of the upper plate. Its distribution is irregular; it may extend tens of meters into the upper plate. Iron staining is common along the fault contact and in the lower plate in the vicinity of the contact. We have mapped low-angle faulting at several places in the southern Eleana Range; its presence has explained some anomalous map relationships (e.g., the "thrust slice" of Tippipah Limestone over Eleana mapped by Orkild (1963) in the Tippipah Spring quad (see geologic map, Fig. 3)). Jim Cole's detailed mapping at Mine Mountain (Cole and others, 1991) showed that both high- and low-angle normal faulting were active during Redrock Valley Tuff time (ca. 16 Ma). The tectonic transport due to low-angle faulting was toward the west and southwest. We don't yet know whether this is also true for the low-angle faulting in the southern Eleana Range, or how/whether Tertiary faulting in these adjacent areas might be related. Detailed mapping will be necessary to identify the low-angle faulting (let alone to determine the kinematics); it is vital that we do so, because of the potential for structural and stratigraphic misunderstandings if Tertiary faulting goes unrecognized!

BIOSTRATIGRAPHY

We have made great strides in biostratigraphic dating in the last year, increasing both the variety of techniques we can use and the number of samples we can analyze (at no increase in budget for biostratigraphic dating). In addition, we have curated all the samples -- they are now all stored, in numerical order by sample number, in the sample storage drawers in LMR 355A -- and put all sample information into a computer data base (see Appendices 2 and 3). Much of this has been possible because of student technician help.

With the recognition (in December, 1991) that the siliceous rocks in the upper 'western' Eleana were spiculites, came the possibility of getting both age and environmental information from these rocks. We have set up a lab for extracting **radiolaria and sponge spicules**, and have arranged for Bonny Murchey (USGS) to analyze the residues. She is able to date them, based primarily on radiolaria, and to make some interpretations about the depositional environment (especially paleobathymetry) based on the proportions of different kinds of sponge spicules. Preliminary results are in agreement with age determinations based on other methods. Our future sampling will be designed to take advantage of our new ability to date siliceous rocks.

We have not dated any additional samples using **endothyrids and calcareous algae**. This method has given very consistent results from the two stratigraphic horizons we have sampled extensively (the base of the organic/detrital section in the 'western' Eleana and the top of the 'eastern' Eleana). We would now like to determine how these ages compare to conodont and radiolarian ages from the same rocks.

We have not dated any additional samples using **palynology**, because we have found widespread skepticism about the accuracy of this technique among colleagues in academia. We were using this method to date the mudstones of the 'eastern' Eleana section, and we have yet to find an effective alternate dating method for these rocks. Claude Spinosa (of Boise State University) sampled 'eastern' Eleana core and processed it for conodonts in his lab, but, so far, the samples have been barren.

Ideally, we would like to have a single biostratigraphic dating tool that could be applied throughout both 'eastern' and 'western' Eleana sections; this would be the most reliable way to compare the ages of the two. The best candidate for such a tool is

conodonts, which can be found in both carbonates and mudstones. In previous years, we have gotten conodont ages from both 'eastern' and 'western' Eleana rocks, although these have only been from the carbonates in each section. We are now in the process of setting up a conodont extraction lab. This will allow us to run more (potentially barren) samples in our attempt to find datable rocks. Dora Gallegos and Claude Spinosa of Boise State University are willing to do preliminary identifications for us, but have recommended that we contact an expert on Mississippian conodonts (Anita Harris or Bruce Wardlaw of the USGS) to do the final identifications.

IMPLICATIONS FOR HYDROCARBON POTENTIAL

The 'eastern' Eleana is the only potential hydrocarbon **source rock** within the Eleana Formation, and its surface exposure is limited to the area around Yucca Flat. It can probably be traced to correlative units (Chainman Shale and Scotty Wash quartzite) to the northeast. To the southwest, it is exposed in the Calico Hills (Fig. 1(a)), where it extends to a depth of at least 2552' in drillhole UE25a-3 (Jim Cole, written comm., 1991). We have no data about the extent of the 'eastern' Eleana west of the Calico Hills. In the southern Eleana Range, 'eastern' Eleana is structurally juxtaposed against the 'western' Eleana along a cryptic fault. We must understand the geometry and kinematics of this fault in order to predict the sub-surface distribution of the 'eastern Eleana'. This distribution will be a critical factor in assessment of hydrocarbon potential near Yucca Mountain.

The other potential source rock in the area is the Tippipah limestone. This unit has received almost no attention to date, and will be a target of our investigations in the next year.

The coarse clastic 'western' Eleana is a potential hydrocarbon **reservoir**, although surface exposures suggest very low porosity and permeability. These strata do have correlatives to the west and probably project to Bare Mountain, where a section of mostly fine-grained siliciclastic sediments has been mapped as Eleana Formation. The paleotopographic control on the 'western' Eleana strongly indicates that coarse facies cannot be projected northwest or southeast, but that very likely they will extend to the southwest toward Yucca Mountain

Thermal maturation data indicate that the 'eastern' Eleana and Tippipah Limestone may have had a favorable thermal history for hydrocarbon generation, while the 'western' Eleana is overmature.

REFERENCES CITED

Bruekner, H.K. and Snyder, W.S., 1985a, Structure of the Havallah sequence allochthon, Nevada: evidence for prolonged evolution in an accretionary prism: Geol. Soc. America Bull., v. 96, p. 1113-1130.

Bruekner, H.K., Snyder, W.S., and Boudreau, M., 1987, Diagenetic controls on the structural evolution of siliceous sediments in the Golconda allochthon, Nevada, USA: Jour. Struc. Geol., v. 9, no. 4,

Cole, J.C., Wahl, R.R., and Hudson, M.R., 1991, Structural relations within the Paleozoic basement of the Mine Mountain block; implications for interpetation of gravity data in Yucca Flat, Nevada Test Site: *in* Olsen, C.L. (ed.), Proceedings of the fifth symposium on the containment of nuclear detonations: Lawrence Livermore National Laboratory Report, Conf. 89-09163, p. 431-455.

Gordon, M., Jr., and Poole, F.G., 1968, Mississippian - Pennsylvanian boundary in southwestern Nevada and southeastern California: GSA Memoir 110, 157 p.

Harwood, D. S., Yount, J.C., and Seiders, V.M., 1991, Upper Devonian and Lower Mississippian island-arc and back-arc deposits in the northern Sierra Nevada, California: *in* Cooper, J.D. and Stevens, C.H. (eds.), Paleozoic Paleogeography of the Western United States II, Pacific Section SEPM, vol. 67, p. 717-733.

Murchey, B.L., 1990, Age and depositional setting of siliceous sediments in the upper Paleozoic Havallah sequence near Battle Mountain, Nevada; *in* Harwood, D.S. and Miller, M.M. (eds.), Paleozoic and early Mesozoic paleogeographic relations; Sierra Nevada, Klamath Mountains, and related terranes: Geol. Soc. America Spec. Paper 255.

Orkild, P.P., 1963, Tippipah Spring Quadrangle: U.S.G.S. Map GQ-213, 1:24,000

Orkild, P.P., 1968, Mine Mountain Quadrangle: U.S.G.S. Map GQ-746, 1:24,000

Rogers, C.L. and Noble, D.C., 1969, Oak Spring Butte Quadrangle: U.S.G.S. Map GQ-822, 1:24,000

Snyder, W.S. and Brueckner, H.K., 1983 Tectonic evolution of the Golconda allochthon, Nevada: problems and perspectives; *in* Stevens, C.A. (ed.), Paleozoic and early Mesozoic rocks in microplates of western North America: Spec. Publs. SEPM, Pacific Section, p. 103-123.

Titus, A.L. and Manger, W.L., 1992, Mid-Carboniferous (E_{2c}-H_{1b}) ammonoid biostratigraphy, Nevada Test Site, Nye County, Nevada (abs): Geol. Soc. America Abs. with Programs, v. 24, no. 6, p. 66.

Trexler, J.H., Jr. and Cashman, P.H., 1991, Mississippian stratigraphy and tectonics of east-central Nevada: post-Antler orogenesis; *in* Cooper, J.D. and Stevens, C.H. (eds.), Paleozoic Paleogeography of the Western United States II, Pacific Section SEPM, vol. 67, p. 331-342.

APPENDICES

Appendix 1: Three analyses -- core to rim -- of a white-weathering phosphatic clast from the 'western Eleana' (sampled near the base of the Castle Valley measured section). Phosphate, silica and calcium contents vary concentrically across the clast. Analyses were done using the energy dispersive spectrometer on the SEM.

Appendix 2: Table of samples processed by Task 8.

Appendix 3: Table of sample processing in progress.

APPENDIX I

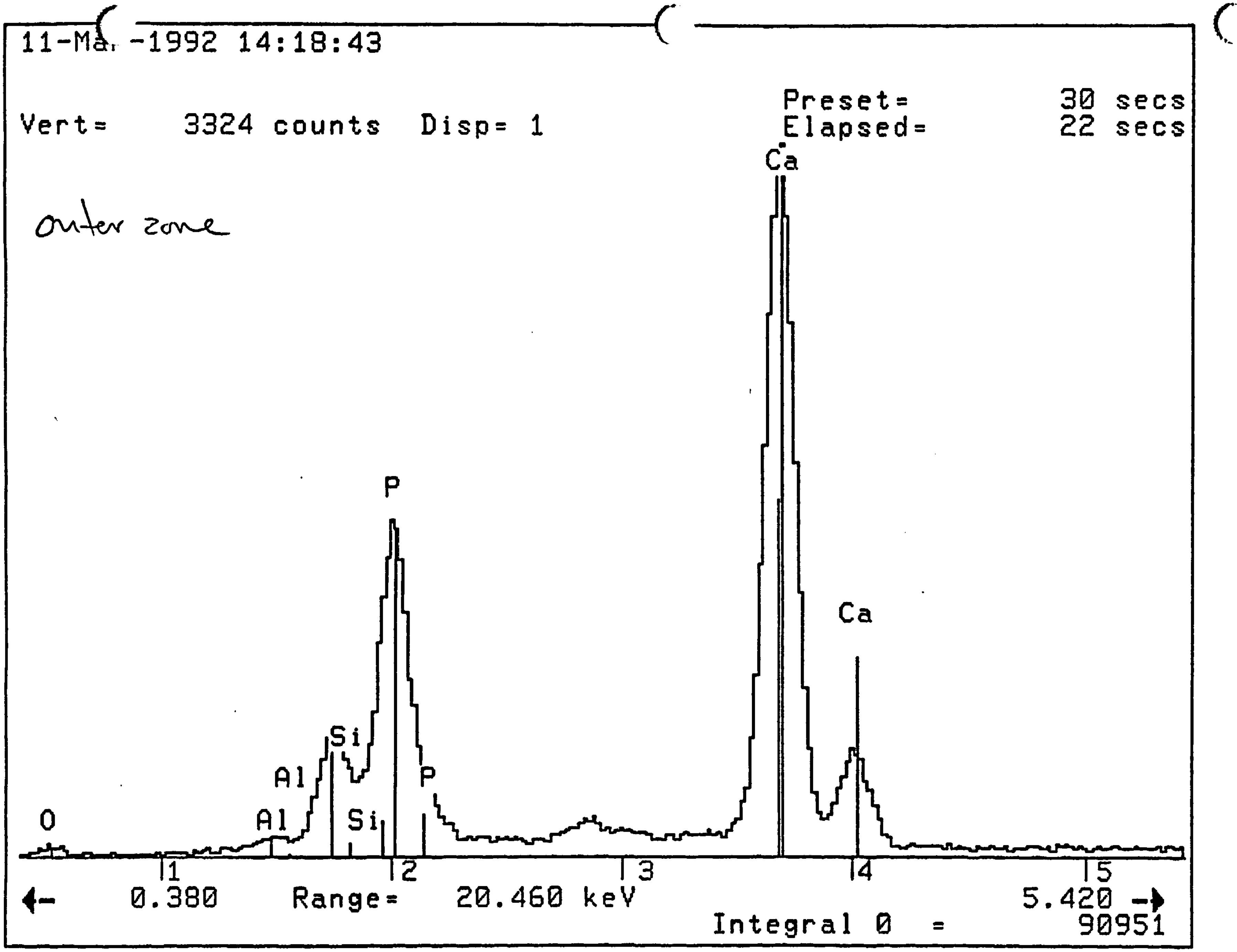

11-Mar-1992 14:18:43
Vert= 3324 counts Disp= 1
Preset= 30 secs
Elapsed= 22 secs
outer zone
Ca
P
Si
Al
P
Ca
O
Al
Si
1
2
3
4
5
0.380 Range= 20.460 keV 5.420
Integral 0 = 90951

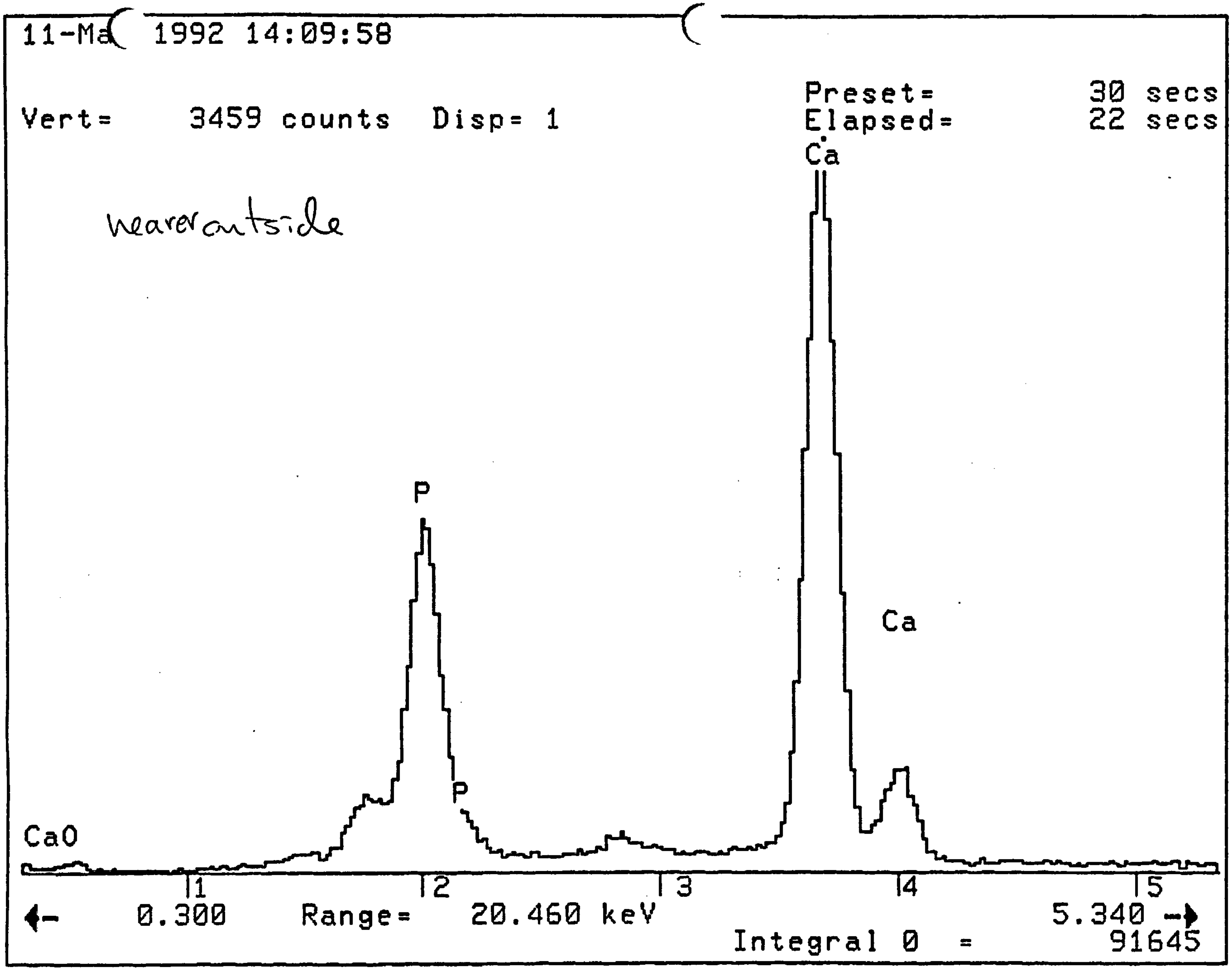
11-Ma 1992 14:09:58
Vert= 3459 counts Disp= 1
Preset= 30 secs
Elapsed= 22 secs
wearer outside
Ca
P
P
Ca
CaO
1
2
3
4
5
0.300 Range= 20.460 keV 5.340
Integral 0 = 91645

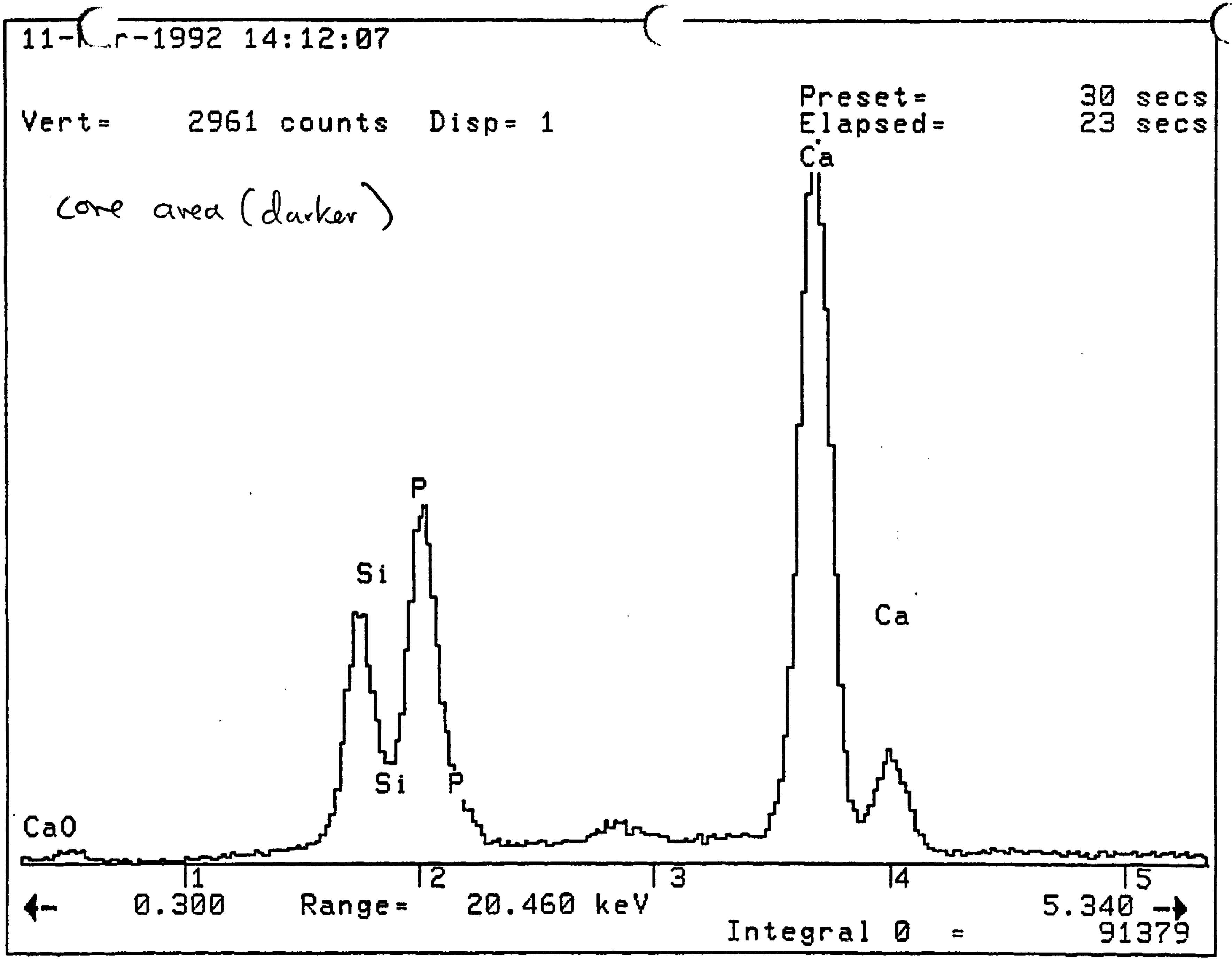

11- r-1992 14:12:07
Vert= 2961 counts Disp= 1
Preset= 30 secs
Elapsed= 23 secs
core area (darker)
Ca
P
Si
Ca
Si
P
CaO
1
2
3
4
5
0.300 Range= 20.460 keV 5.340
Integral 0 = 91379

APPENDIX II

DATED NTS SAMPLES

SAMPLE#	DATE	ROCK TYPE	STRATIGRAPHIC UNIT	PURPOSE FOR COLLECTION
89-JT-331	UNKNOWN	LS	Mdp	PALEO
89-JT-341	6/8/89	LS	TRIPON PASS FM (?)	PALEO
89-JT-402	7/9/89	LS	Mdp	PALEO
89-JT-442	7/10/89	LS	Mdp	PALEO
89-JT-446	7/10/89	LS	Mdp	PALEO
89-JT-451	7/11/89	LS	Mdp	PALEO
89-JT-454	7/11/89	LS	ELY (?)	PALEO
89-JT-455	7/11/89	LS	ELY	PALEO
89-JT-457	7/11/89	LS	ELY	PALEO
89-JT-461	7/11/89	LS	ELY	PALEO
2-89-SN-402	3/18/89	LS	MDe	PALEO
2-89-SN-402	3/18/89	LS	MDe	PALEO
2-89-SN-404	3/18/89	MICRITE	MDe	PALEO
2-89-SN-421	3/18/89	MICRITE	MDe	PALEO
2-89-SN-423	3/18/89	BLACK SH	MDe	PALEO
2-89-SN-461A	3/20/89	BCLSTC PACKSTONE	MDe	PETROG
2-89-SN-461B	3/20/89	BCLSTC PACKSTONE	MDe	PALEO
2-89-SN-601	5/20/89	DOL	DEVONIAN CARB	CAI
2-89-SN-612	5/20/89	BXTED, SLIGHTLY SLCFD BCLSTC LS	DEVONIAN CARBONATE	CAI
2-89-SN-613	5/20/89	BCLSTC LS	M ELEANA	CAI
2-89-SN-633	5/21/89	BCLSTC LS	M ELEANA	CAI
2-89-SN-642	5/21/89	MED GREY FINE-GRAINED LS	DEVONIAN	CAI
2-89-SN-643	5/22/89	DARK FETID LS	DEVONIAN	TOC
2-89-SN-651	5/22/89	FUSILINID-RICH SILTY LS	PERMIAN: BIRD SPG LS, *	CAI
2-89-SN-653	5/22/89	SANDY BCLSTC LS	M ELEANA FM	CAI
2-89-SN-662B	5/22/89	BCLSTC SILTY LS	M ELEANA	CAI
2-89-SN-671	5/22/89	BCLSTC LS	ORDOVICIAN ANTELOPE VALLEY	CAI & PALEO
2-89-SN-681	5/23/89	COARSE-GRAINED BCLSTC LS	M ELEANA	CAI/PETROG
2-89-SN-684A	5/23/89	MICRITE	PENN - PERM BIRD SPG	PALEO/CAI
2-89-SN-721	5/24/89	DOL	DEVONIAN	CAI
2-89-SN-722	5/24/89	BCLSTC LS	M ELEANA	CAI/PALEO
3-89-SN-826	6/30/89	BCLSTC LS	M ELEANA	CAI
4-89-SN-923	9/1/89	BCLSTC MICRITE	M ELEANA	PALEO & CAI

DATED NTS SAMPLES

LOCATION	MAP LOCALITY
LMR 355A	DIAMOND SPG, NV 15' SEC 6, NW 1/4, T 22 N, R 55 E
LMR 355A	DIAMOND SPG, NV 15' SEC 1, SW 1/4, T 22 N, R 54 E
LMR 355A	DIAMOND MTS, NV 15' SEC 6, T 22 N, R 55 E
LMR 355A	BUCK MT, NV 15' SEC 1-2, T 20 N, R 56 E
LMR 355A	BUCK MT, NV 15' SEC 1-2, T 20 N, R 56 E
LMR 355A	DIAMOND SPG, NV 15' SEC 6, T 22 N, R 55 E
LMR 355A	DIAMOND SPG, NV 15' SEC 6, T 22 N, R 55 E
LMR 355A	DIAMOND SPG, NV 15' SEC 31, T 23 N, R 55 E
LMR 355A	DIAMOND SPG, NV 15 ' SEC 31, T 23 N, R 55 E
LMR 355A	DIAMOND SPG, NV 15' SEC 32, T 23 N, R 55 E
LMR 355A	BEATTY MT, NV 7.5' SEC 24, T 12 S, R 47 E
LMR 355A	BEATTY MT, NV 7.5' SEC 24, T 12 S, R 47 E
LMR 355A	BEATTY MT, NV 7.5' SEC 24, T 12 S, R 47 E
LMR 355A	BEATTY MT, NV 7.5' SEC 24, T 12 S, R 47 E
LMR 355A	BEATTY MT, NV 7.5' SEC 24, T 12 S, R 47 E
LMR 355A	JACKASS FLAT, NV 7.5' SEC 30, NE 1/4, T 12 S, R 51 E
LMR 355A	JACKASS FLAT, NV 7.5' SEC 30, NE 1/4, T 12 S, R 51 E
LMR 355A	CARRARA CYN, NV SEC 29, SW 1/4, T 12 S, R 48 E
LMR 355A	BEATTY MT, NV SEC 20, NW 1/4, T 12 S, R 48 E
LMR 355A	BEATTY MT, NV SEC 20, NW 1/4, T 12 S, R 48 E
LMR 355A	BEATTY MT, NV 40.81.2 X 5.29.4
LMR 355A	RAINIER MESA, NV 41.14.6 X 5.72.5
LMR 355A	RAINIER MESA, NV 41.15.6 X 5.73.2
LMR 355A	TIPPIPAH SPG, NV 41.02.5 X 5.75.3
LMR 355A	MINE MT, NV 40.94.4 X 5.75.5
LMR 355A	MINE MT, NV 40.93.5 X 5.77.4
LMR 355A	YUCCA LAKE, NV 40.93.9 X 5.79.2
LMR 355A	YUCCA LAKE, NV 40.86.1 X 5.81.9
LMR 355A	YUCCA LAKE, NV 7.5' 40.86.1 X 5.81.9
LMR 355A	JACKASS FLAT, NV 40.80.1 X 5.60.5
LMR 355A	JACKASS FLAT (CALICO HILLS), NV 40.80.1 X 5.60.8
LMR 355A	TIPPIPAH SPG, NV 41.05 X 5.71.9
LMR 355A	TIPPIPAH SPG, NV 40.99.7 X 5.71.7

DESCRIPTIVE LOCALITY
WALTERS CYN SECTION, RIDGE BETWEEN WALTERS & HOMESTEAD CYNS; LS AT BASE OF SEGMENT III
WALTERS CYN SECTION & RIDGE BETWEEN WALTERS & HOMESTEAD CYNS; AT BASE OF SECTION
1800 m LEVEL; WALTERS CYN SECTION
152 m LEVEL; BUCK MT SECTION & S END OF BUCK MT
315 m LEVEL; BUCK MT SECTION, S END OF BUCK MT
2160 m LEVEL; WALTERS CYN SECTION
2295 m LEVEL; WALTERS CYN SECTION
2420 m LEVEL; WALTERS CYN SECTION
2570 m LEVEL; WALTERS CYN SECTION
2640 m LEVEL, TOP OF SECTION; WALTERS CYN SECTION
SECRET PASS SECTION, BARE MT; 63 m
SECRET PASS SECTION, BARE MT @ 63 m
SECRET PASS SECTION, BARE MT @ 160 m
SECRET PASS SECTION, BARE MT @ 320 m
~ 10 m N OF SPECIE SPG PASS RD, SECRET PASS @ 500 m
CALICO HILLS, S FACING ARROYO, DOWNSLOPE FROM KLIPPEN OF DEVONIAN CARBONATE
CALICO HILLS, S FACING ARROYO, DOWNSLOPE FROM KLIPPEN OF DEVONIAN CARBONATE
S END OF TARANTULA CYN RD, Eern SIDE OF BARE MT
UP PLATE OF MEIKLEJOHN THRUST ~1km N OF TOP OF TARANTULA CYN MSRD SECT
E SIDE OF BARE MT, TARANTULA CYN SECTION @ 870 m
ALONG SPECIE SPG RD ~ 0.2 km E OF SECRET PASS & SECRET PASS SECT, BARE MT & UPR PLATE PANAMA, LWR PLATE MEIKLEJOHN @ 410 m
W SIDE OF TONGUE WASH, AREA 12 NTS & UPPER PLATE OF BELTED RANGE THRUST, BETWEEN G & N RDS
W SIDE OF TONGUE WASH AREA 12 NTS ALONG NEXT RD S OF N TUNNEL RD & UPPER PLATE BELTED RANGE THRUST
N END OF SYNCLINE RIDGE, S OF PAHUTE MESA RD
W SIDE OF MINE MT, LOW SLOPES ~ 1km NW OF MINE MT SUMMIT
E SIDE OF MINE MT IN FOOTWALL OF MINE MT THRUST (C.P. THRUST)
E OF MINE MT, S SIDE OF MINE MT RD ~ 1 km W OF INTERSECTION W/ MERCURY HWY
LEDGES OF BIOCLASTIC LS @ C.P. HILLS SECTION; 54 m
C.P. HILLS MEASURED SECTION, C.P. HILLS, NTS @ 85 m
CALICO HILLS, NTS, SE OF PEAK 5015
NEAR RX SMPL #721, W/IN HINGE OF W VERGENT SYNCLINE, IMMEDIATELY BELOW UPPER PLATE OF DEVONIAN CARBONATE
S ELEANA RANGE SECTION @ 400 m
TIPPIPAH SPG SECTION, SYNCLINE RIDGE @ 30 m

OUTCROP DESCRIPTION

UNRESISTENT LS FORMS SADDLE
THIN & POORLY EXPOSED LS
RECESSIVE LS
SILTY, LEDGY LS
LEDGY LS
BIOCLASTIC WACKESTONE
MICRITE
MICRITE & WACKESTONE
PACKSTONE & WACKESTONE
CHERTY LS, WACKESTONE & MICRITE
LOW LS LEDGE IN MEASURED SECTION
LOW LS LEDGE IN MEASURED SECTION
ALONG SECRET PSS MICROWAVE TOWER RD
LOW SWITCH BACK, SECRET PASS RD
HINGE ZONE OF OVEERTURNED FOLD BELOW MEIKLEJOHN THRUST
~ 2 m THICK LEDGE OF OVERTURNED LS & MICRITE
~ 2 m THICK LEDGE OF OVERTUNED LS & MICRITE
RESISTENT CARBONATE BLUFFS ALONG S SIDE OF TARANTULA CYN RD, ~ 1 km W OF TARANTULA MEASURED
LOW OC OF BXTED & SILICIFIED BIOCLASTIC LS FROM TOP OF RIDGE
LAST (HIGHEST) RESISTENT LS LEDGE W/IN TARANTULA CYN FACIES
OLIVE GREY BIOCLASTIC LS ALONG SW SIDE OF SPECIE SPG RD
STEEP KNOB OF CARBONATE ~ 500 m W OF RAINIER MESA RD
EXPOSURES IN RDCUT ADJACENT TO THRUST CONTACT W/ MISSISSIPPIAN
LOW LEDGY BENCHES OF ORANGE WEATHERING SILTY FUSILINID LS FROM LOW ON N-FACING TIP OF SYNCLINE RIDGE
LOW OC OF LS IN A SADDLE AREA
LOW OC OF LS BELOW DEVONIAN CARBONATE OF HANGING WALL
LOW HILLS TO S OF MINE MT RD, LOW EXPOSURES OF LIGHT GREY LS
LOW LEDGES OF LS
FIRST (LOW) OCCURRENCE OF GREY FINE-GRAINED MICRITE
RESISTENT RIDGE IN UPPER PLATE OF C.P. THRUST
SMALL GULLEY EXPOSURES IN SE -FACING CYN WALL
NONE
ORANGE WEATHERING LATERALLY PERSISTENT BED OF BIOCLASTIC MICRITE

DATED NTS SAMPLES

PROCESSING & RESULTS

2/3 SAMPLE TO MICROSTRAT 7/20/89& PROB ZONE 7 OR SLIGHT YNGR (MID TOURNAISIAN, UP KINDER OR SLIGHT YNGR
1/2 SAMPLE TO MICROSTRAT 7/20/89& ZONE PRE-7, KINDERHOOKIAN, E. MINIMA MICROFACIES
1/2 SAMPLE TO MICROSTRAT 7/20/89& APPROX ZONE 16, BASAL CHESTERIAN
ENTIRE SAMPLE TO MICROSTRAT 7/20/89& APPROX ZONE 16, BASAL CHESTERIAN
ENTIRE SAMPLE TO MICROSTRAT 7/20/89& ZONE 16 OR 17, MID CHESTERIAN
ENTIRE SAMPLE TO MICROSTRAT 7/20/89& BOUNDARY BETWEEN ZONES 18 & 19, LATEST CHESTERIAN
1/2 SAMPLE TO MICROSTRAT 7/20/89& BOUNDARY BETWEEN ZONES 19 & 20, LATEST CHESTERIAN/EARLIEST PENN
ENTIRE SAMPLE TO MICROSTRAT 7/20/89& EARLIEST PENN
1/2 SAMPLE TO MICROSTRAT 7/20/89& ZONE 20, EARLY PENN, MORROWAN, PART OF THE ELY
1/2 SAMPLE TO MICROSTRAT 7/20/89& ZONE 21, PENN, BASAL ATOKAN
SENT TO MICROSTRAT 5/18/89& INDETERMINATE, REWORKED MUDFLOW
SENT TO MICROSTRAT 5/18/89& INDETERMINANT, REWORKED MUDFLOW,
TO MICROSTRAT 5/18/89& INDETERMINATE-BASINAL
TO MICROSTRAT 5/18/89: INDETERMINATE, BASINAL, VERY CALM
TO MICROSTRAT 5/18/89& INDETERMINATE- BASINAL, VERY CALM
NONE (?)& ZONE 16, CHESTERIAN OT YOUNGER
TO MICROSTRAT 5/18/89& CHESTERIAN (ZONE 16), POSSIBLE MUDFLOW
TO MICROSTRAT 5/31/89& UPPER MIDDLE DEVONIAN, ENSENSIS ZONE, CAI 5
TO MICROSTRAT 5/31/89& POSSIBLE DEVONIAN, CAI 6
TO MICROSTRAT 5/31/89& CAI 5, POST-EARLY KINDERHOOKIAN
TO MICROSTRAT 5/31/89& CAI-4.5, INDETERMINATE
TO MICROSTRAT 5/31/89& CA1-6, DEVONIAN
TO MICROSTRAT 5/31/89& TOC-0.16%
TO MICROSTRAT 5/31/89& CAI 1.5-2, * UPPER DEVONIAN : FRASNIAN, FAMENNIAN
TO MICROSTRAT 8/28/89, RTRND 10/19/89 (OR 12/3/89?)& CAI-3, EARLY MISS, PROB KINDERHOOKIAN
TO MICROSTRAT 8/28/89, RTRND 10/19/89 & 12/3/89: CHESTERIAN, CAI-4
TO MICROSTRAT 5/31/89& CAI-5.5, EARLIEST MID ORD
TO MICROSTRAT 5/31/89 & TO NBMG (TS) 7/9/89& CAI-4 & INDETERMINATE (NOT INCONSISTENT W/ MISS)
TO MICROSTRAT 8/28/89, RTRND 10/19/89 & 12/3/89& CAI-4, LOW PENN (MORROWAN)
TO MICROSTRAT 5/31/89& INDETERMINANT & BARREN OF CONODONTS
TO MICROSTRAT 5/31/89& CAI-4, MID MISS (OSAGEAN)
TO MICROSTRAT 8/28/89& RTRND 10/19/89, CAI 4.5 +, INDETERMINATE
TO MICROSTRAT 3/13/90& REPORT MSI 90-15 (5/90), PENN, CAI- 4

DATED NTS SAMPLES #2

SAMPLE#	DATE	ROCK TYPE	STRATOGRAPHIC UNIT
3-89-SN-1033	9/6/89	BCLSTC LS	M ELEANA
3-89-SN-1053	9/7/89	MICRITE	PENN BIRD SPG
4-89-SN-1113	9/9/89	BLACK SH	M ELEANA*
4-89-SN-1153	9/21/89	SILICEOUS SLTST	M ELEANA
4-89-SN-1264	9/25/89	SILICEOUS MDST	M ELEANA MID SEQUENCE (LOWER MEMBER)
5-89-SN-1452	11/4/89	CLAYSTONE	M SCOTTY WASH
90-JTA-12	6/25/90	MDST	ELEANA FM
90-JTA-21	6/25/90	CALCARNT (MAMET: MED-GRND FSL BCLST PKSTN)	ELEANA FM
90-JTA-22	6/25/90	MDRX	ELEANA FM
90-JTA-31	6/25/90	MDST	ELEANA FM
90-JTA-32	6/25/90	MDST	ELEANA FM
90-JTA-33	6/25/90	MDST	ELEANA FM
90-JTA-34	6/25/90	MDST	ELEANA FM
90-JTA-41	6/25/90	CALCARNT (MAMET: MED-GRND FSL PCKSTN)	ELEANA FM
90-JTA-42	6/26/90	MDRX	ELEANA FM
90-JTA-43	5/26/90	CALCARENITE (MAMET: FOSSIL PACKSTONE)	ELEANA FM
90-JTA-51	6/26/90	CALCARNT (MAMET: CRS-GRND FSL LUMP GRAINSTN)	ELEANA FM
91-PC-172	3/21/91	BCLSTC LS; CHERT FLOAT	ELEANA, W FACIES
91-PC-271	5/10/91	BCLSTC LS	ELEANA, UPPER PART OF W FACIES
91-PC-282	5/10/91	BCLSTC LS	ELEANA, W FACIES- UP PART
UE16d-944	3/21/91	LS	NONE
UE16d-1461	3/21/91	DARK FOSSILIFEROUS LS	NONE
88-JT-201	7/12/88	GRUNGE: TAILINGS F/ PANCAKE COAL MINE	PENN ELY LS (?)
88-JT-311	7/14/88	BCLSTC LS	Mdp
88-JT-382	8/7/88	BCLSTC LS	PENN ELY
88-JT-383	8/8/88	MUDROCK	Mc (WHITE PINE SHALE)
88-JT-402B	8/8/88	CRINOIDAL LS	Mdp
88-JT-481	8/10/88	LS	Mdp
88-JT-511	8/12/88	CALCARENITE	Mdp "LOWER SEQUENCE
88-JT-513	8/12/88	SILTY LS	Mdp
88-JT-541	8/13/88	BLACK SLTST	Mc (?) BASE OF Mdp
88-JT-542	8/13/88	CRINOIDAL LS	Mdp
88-JT-581B	9/29/88	CALCAREOUS ARENITE	Mdp; "NEWARK VALLEY SEQUENCE?"
88-SN-41	10/13/88	COARSE LS PACKSTONE	Me, ELEANA FM- UPPER SEQUENCE

DATED NTS SAMPLES #2

PURPOSE FOR COLLECTION	LOCATION	MAP LOCALITY
CAI	LMR 355A	TIPPIPAH SPG, NV 41.02 X 5.70.8
PALEO	LMR 355A	TIPPIPAH SPG, NV 41.01 X 5.73.8
TOC/PALEO	LMR 355A	TIPPIPAH SPG, NV 41.05.5 X 5.73.5
TOC	LMR 355A	MINE MT, NV 40.94.8 X 5.76.4
TOC/PALY	LMR 355A	RAINIER MESA, NV 41.09.5 X 5.74.8
TOC/PALY	LMR 355A	HANCOCK SUMMIT, NV 41.50 X 6.47.6
TOC/ ROCK EVAL	LMR 355A	TIPPIPAH SPGS, NV 7.5' 41.04.7 X 5.72.4
PALEO	LMR 355A	TIPPIPAH SPG, NV 7.5' 41.04.8 X 5.72.3
TOC/ ROCK EVAL	LMR 355A	TIPPIPAH SPG, NV 7.5' 41.04.9 X 5.71.95
TOC/ ROCK EVAL	LMR 355A	TIPPIPAH SPG, NV 7.5' 41.06.5 X 5.72
TOC/ ROCK EVAL	LMR 355A	TIPPIPAH SPGS, NV 7.5' 41.06.1 X 5.72.9
TOC/ ROCK EVAL	LMR 355A	TIPPIPAH SPG, NV 7.5' 41.05.9 X 5.73.1
TOC/ ROCK EVAL	LMR 355A	TIPPIPAH SPG, NV 7.5' 41.05.6 X 5.73.4
PALEO	LMR 355A	TIPPIPAH SPG, NV 7.5' 41.06.5 X 5.71.8
TOC/ ROCK EVAL	LMR 355A	TIPPIPAH SPG, NV 7.5' 41.06.5 X 5.71.8
PALEO	LMR 355A	TIPPIPAH SPG, NV 7.5' 41.06.5 X 5.71.6
PALEO	LMR 355A	TIPPIPAH SPRINGS, NV 7.5' 41.06.6 X 5.71.2
PALEO (ENDOTHYRIDS IN LS, RADS IN CHERT)	LMR 355A	TIPPIPAH SPRING, NV 7.5' 41.03.9 X 5.70.7
PALEO	LMR 355A	TIPPIPAH SPRING, 7.5' 41.03.4 X 5.69.4
PALEO	LMR 355A	TIPPIPAH SPRING, NV 7.5' 41.01.3 X 5.70.4
PALEO	LMR 355A	TIPPIPAH SPRING, NV 7.5' 41.03.5 X 5.74.6
PALEO	LMR 355A	TIPPAH SPRING, NV 7.5' 41.03.5 X 5.74.6
PALEO (PALY)	LMR 355A	PANCAKE SUMMIT, NV 15' SEC 28, NE 1/4, T 18 N, R 56 E
PALEO	LMR 355A	UNKNOWN
PALEO	LMR 355A	GREEN SPRINGS, NV 15' SEC 4, NW 1/4, T 14 N, R 57 E
PALEO- BRACH FAUNA	LMR 355A	GREEN SPRINGS, NV 15' SEC 4, NW 1/4, T 15 N, R 57 E
PALEO	LMR 355A	GREEN SPRINGS, NV 15' SEC 32, NW 1/4, T 16 N, R 56 E
PALEO	LMR 355A	UNKNOWN
PALEO	LMR 355A	PANCAKE SUMMIT, NV SEC 2, NW 1/4, T 19 N, R 57 E
PALEO (CRINOID SPINES & BRACHS)	LMR 355A	PANCAKE SUMMIT, NV SEC 2, NW 1/4, T 19 N, R 57 E
PALEO	LMR 355A	BUCK MT, NV SEC 12, NW 1/4, T 20 N, R 56 E
PALEO	LMR 355A	BUCK MT, NV 15' SEC 11, NE 1/4, T 20 N, R 56 E
PALEO	LMR 355A	MOODY PK, NV 15' SEC 15, NE 1/4, T 15 N, R 54 E
PALEO	LMR 355A	YUCCA LAKE, NV 7.5' SE 1/4, 5.81 X 40.86

DESCRIPTIVE LOCALITY
E GAP WASH, S ELEANA RANGE @ 150 m
SYNCLINE RIDGE @ 290 m
BOTTOM OF RED CYN WASH, WELL OUT ON THE PEDIMENT, ELEANA RANGE
MINE MT SECTION @ 15 m, INCISED PEDIMENT ~ 0.5 km N OF MINE MT RD
IN INCISED ARROYO OUT ON PEDIMENT N OF GROUSE CYN
NE END OF E PAHRANAGAT RANGE ~500 m S OF HWY 375
S ELEANA RANGE SECTION, MDST SECTION
S ELEANA RANGE SECTION, LS AT TOP OF SILIC SEQUENCE
S ELEANA RANGE SECTION, UPPER SILICICLASTIC UNIT
RED CYN SECTION, MDST SEQUENCE NEAR BASE (=SPN 1551)
RED CYN SECTION, MID OF MDST INTERVAL
RED CYN SECTION, MID OF MDST INTERVAL (=SPN 1581)
RED CYN SECTION, HIGHEST EXPOSED MDST (~SPN 1113)
RED CYN SECTION, MIDDLE OF CALC TURBIDITE SECTION (= 90-JTA-42)
RED CYN SECTION, MID OF CALC TURBIDITE SECTION (= 90-JTA-41)
RED CYN SECTION , MID OF CALC TURBIDITE SEQUNENCE
RED CANYON, LOW-MID CARBONATE TURBIDITE SECTION
STRUCTURALLY BELOW THRUST SLICE OF TIPPIPAH LS & ABOVE E FACIES ELEANA
W RIDGE OF S ELEANA RANGE, IMMEDIATELY S OF PAHUTE MESA RD
SADDLE AT JUNCTION OF W & E RIDGES OF S ELEANA RANGE JUST N OF BUCKBOARD MESA RD
W EDGE OF SYNCLINE RIDGE, IMMEDIATELY N OF PAHUTE MESA RD
W EDGE OF SYNCLINE RIDGE, IMMEDIATELY N OF PAHUTE MESA RD
COLLECTED F/ TAILING PILE NEAR ADIT, Sern MOST OF 3 COAL MINE SHAFTS IN PANCAKE COAL MINE
OLD HWY 80, CARLIN TUNNEL
TOP OF GREEN SPRINGS MESURED SECTION
BASE OF GREEN SPRINGS MEASURED SECTION; LOW HILLS E OF BASE OF SECTION, WHITE PINE RANGE
BASE OF MEASURED SECTION "PANCAKE SOUTH"
HOBSON PASS AREA, TOGININI SPRINGS MTS/MAVERICK SPRINGS RANGE
BASE OF "DRY MOUNTAIN" MEASURED SECTION
145 m, DRY MT SECTION W/IN "LOWER SEQUENCE"
IN A GULLY BOTTOM, EXPOSED BLACK FOSSILIFEROUS SLTST
PROMINENT GREY-GREY VERTICAL BLUFF BENEATH WHITE-COLORED SS
LOW BED IN THE "UPPER SEQUENCE" ABOVE ANGULAR UNCONFORMITY, "E POGUE'S STATION"
Sern FLANK C.P. HILLS

OUTCROP DESRIPTION
NONE
NONE
CUT BANK EXPOSURE OF SH & SLTST
PIT EXCAVATION
BLACK MDST EXPOSED IN INCISED ARROYO
CUT BANK ALONG DIRT RD/ARROYO
RUBBLY MDST, POOR EXPOSURE
(=SPN 826)
THIN-BEDDED MDST, SLTST & SS W/ MINOR GRIT
RUBBLY POOR EXPOSURES OF MDST & FINE SS
RUBBLE OC OF MDST
RUBBLE OC OF MDST
RUBBLE OC OF MDST
WELL-EXPOSED SILICIC MUDRX & CALC TURBIDITES
WELL-EXPOSED SILIC MUDRX & CALC TURBIDITES
CARBONATE TURBIDITE & SILIC MUDRX
WELL-BEDDED CARBONATE TURBIDITES
NONE
MED-GREY BIOCLASTIC LS INTBDD W/ BLACK SILICEOUC ARGILLITE & SLTST
ORANGE-WTHRNG DOLOMITE (?), MED GREY BIOCLASTIC LS (FETID!) & BLACK SILICEOUS ARGILLITE
CORE; 944.5-944.7' BELOW SURFACE
CORE; 1461.4-1461.7' BELOW SURFACE
LEDGY, CHERT LS; COAL DOES NOT CROP OUT AT SURFACE
OC OF LS BETWEEN CGL PACKETS
LOW RESISTANT LEDGE OF BIOCLASTIC LS OF ELY
RECESSIVE SLOPE W/ OCCASIONAL GOOG (!) EXPOSURES OF CHAINMAN MUDROCK
LOW OC AT BASE OF MEASURED SECTION
LS @ 145 m; HOBSON PASS MEASURED SECTION; TOP OF FIRST CGL PACKAGE
LOWER CGL BODY, SAMPLE F/ TOP OF CGL @ 5 m
PLATY WX BUFF LS @ TOP OF LOWER SEQUENCE
GULLY BOTTOM
STRATIFIED CRINOIDAL PACKSTONE BEDS- CRINOID GRAVEYARD
LOW BEDS IN UPPER SEQUENCE; LATERALLY PERSISTENT
LOW CO ~ 10 m UPHILL F/ LOW QZ ARENITE IN UPPER UNIT

PROCESSING & RESULTS

TO MS 3/13/90; MSI 90-14 (5/90), LT DEV, POST-FRAS, PROB CREPIDA-RHOMB ZONES & CAI-4
TO MS 3/13/90; MSI 90-15 (5/90), CHEST, YNGR ZONE 16, ENDOS & CALC ALGAE, 8 SPEC, EXT DOLOMIT & RECRYST, OPEN MARINE, RWRKD CARI
TO MS 3/13/90; MSI 90-15 (5/90): CAI=1.5, CDONT PRB PENN (MRWN), ONE SPECIES "PROB" ID
*TO MS 3/13/90; MSI 90-15 (5/90): PALY - PROB UPP DEV - UP FAM.ENVIR-MARINE. TOC = 0.68.TAI = 3+.SAMPLE CNSDRD PILOT SH FM
MS 3/13/90; MSI 90-15 (5/90): PALY- LWR M- TOURN, RSTRCT TO KINDER (PROB LWR). 4 SPEC; LWR M-TOUR JOANA FM. TOC - 0.53%. TAI
TO MS 3/13/90; REPORT MSI 90-15 (5/90): PALY- UP DEV TO MISS. MARINE. TOC- 0.79% TAI- 3-3+
TO MS 3/13/90; MSI 90-15 (5/90) PALY: UP MISS-VISEAN (RSTRCTD TO BASAL TC SPORE ZONE). TOC- 0.69%. TAI= 3-3-. LOWER CHAINMAN SH
SPLIT TO MS F/ TOC 7/20/90, PALY & TAI REQ 8/15/90; MSI 90-21 (10/90)TOC=1.09, TAI=3+ AGE= LWR MISS-UP DEV TRANS AREA. ONE SPOF
MS 7/20/90; MSI 90-21 (10/90): E CHEST~ ZONE 16. . AGE (CNDNTS): UP OSOG (ANCHORALIS-LATUS ZONE). CNDNTS MAY BE REWORKED (ENDO,
SPLIT TO MS F/ TOC (7/20/90), PALY & TAI REQ (8/15/90); MSI 90-21 (10/90): TOC=0.29, TAI=3+ , LWR M-UP D TRANS AREA, PROB RSTRCT
SPLIT TO MS 7/20/90, PALY & TAI REQ 8/15/90; TOC=0.38, TAI=3+ (AMOR KRGN, UP D-FAM (PROB RSTRCTD TO TOP D UP FAM). RARE HVY RBD
SPLIT TO MS F/ TOC 7/20/90, PALY & TAI REQ 8/15/90; MSI 90-21 (10/90)TOC=1.25, TAI=3+, UP D (PROB RSTRCD TO TOP D OF FAM. RARE WI
SPLIT TO MS F/ TOC 7/20/90, PALY & TAI REQ 8/15/90; MSI 90-21 (10/90): TOC=1.29, TAI=3+ UP D (PROB RSTRCT TO TOP D OF TOURN-FAM
SPLIT TO MS F/ TOC 7/20/90, PALY & TAI REQ 8/15/90; MSI 90-21 (10/90): TOC=0.91, TAI=3+, LWR M (PROB KNDRHK, POSS BASAL KNDRHK;
SPLIT TO MS 7/20/90; MSI 90-21 (10/90): E CHEST ~ ZONE 16. PALEOENVIRON- OPEN MARINE. PRESS SOLN.
SPLIT TO MS F/ TOC 7/20/90, PALY & TAI REQ 8/15/90; MSI 90-21 (10/90): TOC=0.28, TAI=3+, UP D-FAM (RSTRCTD TO VU-GM SPORE ZNS OF
MS 7/20/90; MSI 90-21 (10/90): E CHEST ~ ZONE 16 (F/ ENDO/CALC ALGAE). CONODONT AGE- OSAGEAN (MAY BE REWORKED). CAI=5.
M-S F/ AGE 7/20/90; MSI 90-21 (10/90): CHEST. POOR ZONATION. REWORKED. POSS TURBIDITE.
CHERT TO NORM SILBERLING & LS TO M-S (4/17/91); MSI 91-06 (5/91) RCV'D 7/26/91: AGE= (ENDO) MISS (?)
MS 5/15/91; MSI 91-06 (7/91):AGE= MISS (ENDO), LT MERAM TO E CHEST [ZONE 16?]. SIM TO 91-PC-282; BOTH F/ THE "GONIATE MARKER BE
M-S 5/15/91; MSI 91-06 (7/91): AGE= MISS, LT MERAM TO E CHEST [ZONE 16 ?].
TO MS 4/17/91; [ENDOS]MSI 91-06 (5/91-RCVD 7/91): MISS
TO MS 4/17/91; [ENDOS]MSI 91-06 (5/91-RCVD 7/91): MISS (?)
TO MS 11/4/88; UP MISS/BASAL PENN, PROB UP CHEST
TO MICROSTRAT 2/22/89; CHESTERIAN
TO MICROSTRAT 2/22/88; VERY LOW IN CHESTERIAN, APPROX ZONE 16i
TO MS 11/4/88; UP MISS/BASAL PENN, UP CHEST/MORROWAN
TO MS 11/4/88: MISS-LT CHESTERIAN-ZONE 18
TO MS 11/4/8; PROBABLY BASAL CHESTERIAN, ZONE 16 INF.
TO MICROSTRAT 2/22/89: UPPERMOST MERAMECIAN, PROBABLY ZONE 15
TO MICROSTRAT 11/4/88; MISS/PENN ?, NO ORGANIC MATTER ! (?)
TO MICROSTRAT 11/4/88; PROBABLY BASAL CHESTERIAN, ZONE 16 INF
TO MICROSTRAT 2/22/89; LOWERMOST CHESTERIAN, ZONE 16i
TO MICROSTRAT 11/4/88; PROBABLY BASAL CHESTERIAN, ZONE 16 INF

APPENDIX III

NTS Samples- Work in Progress

SAMPLE#	DATE	ROCK TYPE	PURPOSE FOR COLLECTION	LOCATION
UE17e-2995.0-2995.5	12/11/91		PALEO-CONODONT/PETROG	LMR 355A
UE17e-1943.5-1944	12/11/91		PALEO-CONODONT/PETROG	LMR 355A
UE17e- 2859.5-2860	12/11/91		PALEO-CONODONT/PETROG	LMR 355A
UE17e-71.0-71.6	12/11/91		PALEO-CONODONT/PETROG	LMR 355A
UE 17e-355.0-355.5	12/11/91		PALEO-CONODONT/PETROG	LMR 355A
UE16d-1463.0-1463.5	12/11/91		PALEO-CONODONT/PETROG	LMR 355A
UE16d-2317-2319.5	12/11/91		PALEO-CONODONT/PETROG	LMR 355A
91-PC-461	12/11/91	FINE-GRAINED CARBONATE TURBIDITE	PALEO-CONODONT/PETROG	LMR 355A
PC-91-332	11/18/91	LS "M1" AT SHOSHONE MT	PALEO	LMR 355A
91-PC-342	11/18/91	SLTST "M1" @ SHOSHONE MT	PALEO	LMR 355A
92-PC-282	3/10/92	LS INTBDD BLACK CHERT	PALEO (CONODONT/PETROG:	LMR 355A
92-PC-513	1/15/92	CGL	CLAST COMPOSITION	LMR 355A
92-PC-522	1/16/92	MICRITE	PALEO	LMR 355A
92-PC-551	1/17/92	CHERT	PALEO; RADS	LMR 355A
92-PC-522B	1/17/92	CHERT	PALEO (RADS)	LMR 355A
92-PC-554	1/17/92	MICRITE/DOL	PALEO (CONODONPETROG)	LMR 355A
92-JTA-193	4/16/92	CHERT; SPICULITES (?)	PALEO	LMR 355A
92-JTA-223	4/18/92	SPICULITE MUDSTONE	RADIALARIAN PALEO	LMR 355A
92-JTA-232	4/18/92	MDST	PALEO-RADS	LMR 355A
92-JTA-263	4/19/92	CHERT (?)	PALEO-RADS/SPICULES	LMR 355A
92-JTA-271	4/19/92	CHERT	PALEO- RADS/SPICULES	LMR 355A
92-JTA-274	4/19/92	SPICULITE	PALEO	LMR 355A

MAP LOCALITY	DESCRIPTIVE LOCALITY
TIPPIPAH SPRING, NV 7.5' 5.70.8 X 41.02.1	E RIDGE , S OF PAHUTE MESW RD
MINE MT, NV 7.5' 5.71 X 4.86	STATION 332, SHOSHONE MT
MINE MT, NV 7.5' 5.70.6 X 40.86.4	M1 @ SHOSHONE MT ~ 3/4 OF THE WAY UP IN THE SLTST SECT
TIPPIPAH SPRINGS, NV 7.5' 5.71.2 X 41.04.4	N END OF E RIDGE AT INTERSECTION OF S ELEANA RANGE
TIPPIPAH SPRINGS, NV 7.5' 5.71 X 4.03.6	E RIDGE, N OF PAHUTE MESA RD, OC AT N END OF SUMMIT
TIPPIPAH SPRING, NV 7.5' 5.71.1 X 41.03.6	E RIDGE, N OF PAHUTE MESA RD
TIPPIPAH SPRING, NV 7.5' 5.71.2 X 41.03.2	E RIDGE, N OF PAHUTE MESA RD
TIPPIPAH SPRING, NV 7.5' 5.70.9 X 41.03.1	SLOPE BETWEEN 92-PC-553 & 92-PC-533
	S ELEANA RANGE
	SE OF SYNCLINE RIDGE NEAR E-W ELEANA CONTACT
	START OF N BRANCH OF S ELEANA RANGE
	RED CANYON @145 m
	RED CANYON @172 m
	CASTLE VALLY, N END

STRATIGRAPHIC UNIT	PROCESSING & RESULTS
	TO BSU 12/91
	TO BSU 12/91
	TO BSU 12/91
	TO BSU 12/12/91 F/ BIOSTRATIGRAPHY
	TO BSU 12/12/91
	TO BSU 12/91
	TO BSU 12/91
M ELEANA, W FACIES	TO BSU 12/12/91; CLAUDE SPINOSA 1/15/92
DEPOSITIONALLY OVERLYING "Dd" BASE OF E FACIES ?	TO BSU 2/8/92 F/ BIOSTRATIGRAPHY
M1	
	CRUSHED 5/20/92
M ELEANA, W-FACIES	
M ELEANA, W-FACIES	TO BSU 2/8/92 F/ BIOSTRATIGRAPHY
M ELEANA; W-FACIES	HF ETCHING
M ELEANA, W-FACIES	HF ETCHING
M ELEANA	
CASTLE VALLEY SECTION; 178 m	CRUSHED 5/20/92
SYNCLINE RIDGE SECTION	CRUSHED 5/20/92
	CRUSHED 5/20/92
	CRUSHED 5/20/92
	CRUSHED 5/20/92
	CRUSHED 5/20/92

OUTCROP DESCRIPTION

FINE-GRAINED TURBIDITE
348/24W PARTING, PROBABLY SO. IN LIGHT GREY LS--GOOD
CONT SUBCROP ALL THE WAY TO THE Tv; NO SS LAYERS IN OC OR FLT OBSERVED

CGL FLOAT; CLASTS RESEMBLE FELSIC VOLCANICS
ORANGE-WTHRNG, FRACTURED, VEINED
BLACK CHERT
ORANGE-WTHRNG FINE-GRAINED LS W/ BIOTURBATION ON WTHRD SURFACES.
FLOAT; ORANGE WTHRNG MICRITE/DOLOMITE. BIOTURBATION REMNANTS

POSS CTS W/ MEASURED SECTION ON HILL TO N
SECTION HERE PROJECTED F/ TOP OF MAIN SECTION

EASTERN: BEDDED TAN WX SLTST W/ ABNT BUROWS; WERN: TOP TO E